WATER USE AND YIELD OF SOYBEAN AND GRAIN SORGHUM FOR BIOFUEL PRODUCTION

Report

to the Water Research Commission

by

R Kunz, J Masanganise, K Reddy, T Mabhaudhi,
L Lembede, V Naiken and S Ferrer
University of KwaZulu-Natal

Report No. 2491/1/20
ISBN 978-0-6392-0152-8

June 2020

Obtainable from:
Water Research Commission
Private Bag X03
Gezina, 0031
South Africa

orders@wrc.org.za or download from www.wrc.org.za

EXECUTIVE SUMMARY

BACKGROUND AND MOTIVATION

The research focus of this project was guided by recommendations made in the previous biofuel project (Project K5/5221), as well as by policy related to biofuel production in South Africa. For example, a policy paper released by the Department of Water and Sanitation (DWS, 2016) supports the cultivation of biofuel feedstocks under rainfed conditions. In addition, the draft Biofuel Regulatory Framework, published in 2014, highlighted soybean and sorghum as reference feedstocks to represent the production of biodiesel and bioethanol, respectively. It also strongly supported the inclusion of smallholder farmers in the biofuel value chain.

A significant expansion of agricultural production is required to meet the demands for feedstock required by biofuel manufacturers. South Africa is a water-scarce country. Thus, the greatest challenge facing the biofuel industry will be to increase crop production using less water (i.e. improve crop water use efficiency). In addition, the government is promoting the use of unproductive arable land for feedstock cultivation under rainfed conditions. Research is therefore required to assist smallholder farmers to improve crop yields, thereby increasing the efficient use of available water resources. Research is also required to facilitate the participation of smallholders in the biofuel value chain.

On 13 December 2019, Cabinet approved the draft Biofuel Regulatory Framework, which allows for the implementation of the 2007 Biofuel Industrial Strategy. The framework was amended in January and published on 7 February 2020. The research presented in this document, together with that published by the previous project, will provide government (in particular the Department of Agriculture, Land Reform and Rural Development, and the Department of Human Settlements, Water and Sanitation) with valuable information and knowledge to assist with and hopefully guide the implementation process.

PROJECT OBJECTIVE AND AIMS

More specifically, research is needed to determine the expected water use and yield of soybean and grain sorghum produced by rural farming communities, as well as to determine best agronomic practices for maximising attainable yield. To assist the government and, in particular, agricultural extension services, information on which cultivars are best suited for biofuel production in particular areas, as well as advice on how to manage fertility, weeds and pests/diseases, is also required. It is important to develop enterprise budgets to determine the profitability of feedstock cultivation.

OVERVIEW OF STRATEGIC CROPS

In January 2014, the Department of Energy selected two feedstocks as a reference for biodiesel and bioethanol production in South Africa (DoE, 2014). A review of the two reference crops (soybean and grain sorghum) is provided in this report, with particular emphasis on what is known about their water use and yield. The review highlighted that more studies have been conducted on grain sorghum than on soybean in South Africa. Based on this, this project aimed to assess the water use efficiency of these two biofuel feedstocks at both the smallholder and commercial farming scale, but with an emphasis on soybean. The knowledge gained from the field trials facilitated the development of agronomic guidelines for feedstock production, particularly for smallholder farmers, and the validation of the modelling approach to estimate the water use and yield of these two feedstocks.

PRODUCTION GUIDELINES

Agronomic requirements and production guidelines for both crops were synthesised from the available literature and supplemented with knowledge gained from the field trials. For example, the application of mulch should be considered by smallholder farmers, especially under rainfed conditions where water is a major limiting factor.

Cultivar selection

Cultivar selection aims to reduce risks by avoiding, for example, drought periods during the most critical growing stages of the plant growth, such as flowering and seed set. Many factors need to be considered when selecting a cultivar for a particular location such as the target yield, intended purpose (e.g. biofuel production), expected planting date and season length, weather conditions likely to be experienced over the growing period and seed availability. The Biofuel Regulatory Framework noted that government will promote the use of drought-resistant cultivars.

Soybean

According to the soybean cultivar recommendations published by the Grains Crop Institute of the Agricultural Research Council (ARC) for 2019/20, 26 cultivars are conventional and 144 are genetically modified. Hence, about 85% of soybean cultivars are Roundup® Ready. The reader is referred to the ARC's latest publication on cultivar recommendations, which is not duplicated in this document due to the dynamic nature of the information. For example, PAN1521R is a Roundup® Ready cultivar that is equally well suited to cool, moderate and hot growing regions.

Sorghum

There are about 23 registered grain sorghum hybrids and four open pollinated varieties. Seven of the 23 hybrids are sold by PANNAR. Bird-proof (i.e. bitter) sorghum has a high tannin content and is thus not suited to biofuel production. PANNAR supplies three grain sorghum hybrids with a low tannin content, which are suitable for ethanol production (PAN8816, PAN8906 and PAN8944).

Planting dates

Under rainfed conditions, rainfall variability is an important determinant of crop yield. Thus, planting date selection is critical to ensure that critical growth stages do not coincide with dry spells. Based on an analysis of 50 years of rainfall and temperature data for each quinary subcatchment, the first planting date:

- could not be determined for 26.2% of the quinary subcatchments, thus indicating their unsuitability for crop production;
- occurs in either November or December for the majority of quinary subcatchments; and
- occurs in October and January in a few quinary subcatchments.

Maps showing the spatial variability in planting date are presented in this report. However, weather is known to vary between growing years, affecting the selection of planting dates. Hence, it is acknowledged that planting dates should be determined using climate forecasts, rather than using historical data. Access to seasonal weather forecasts is recommended to aid farmers' management practices, planning and the selection of planting dates.

Crop management

Soybean

A review of the available literature was undertaken to determine production guidelines for each strategic feedstock. A summary of the information for soybean presented in this document is as follows:

- Approximately 85% of the soybean cultivars are Roundup® Ready. Conventional cultivars may be difficult to source from seed suppliers.
- Soybean is well suited to areas with a summer rainfall of 500-900 mm and daily maximum temperatures of 20 to 30 °C. Temperatures below 18 °C or above 35 °C reduce the plant's growth rate.
- The crop can withstand short periods of drought due to its long flowering period.
- The plant displays a medium tolerance to frost, except in the early growth stages.
- A pH range of 5.5 to 6.5 is ideal for soybean production. A pH level lower than 5.2 impedes nitrogen fixation and renders phosphorus and potassium ineffective for plant uptake.
- When grown on sandy soils with a low organic matter content, soybean yields may be adversely affected by water stress, nematode damage and low micro-nutrient levels.
- Compacted soils or those that easily form a crust should be avoided or managed properly to minimise emergence problems.
- Soybean is usually planted between mid-October and mid-November.
- Although a December planting can still produce satisfactory yields, soybean grown in January may not achieve good yields.
- Seed must be inoculated with a suitable rhizobia bacterium, then planted in moist soil up to a depth of 5 cm.
- Fertilizer must not come into direct contact with seed as it is susceptible to fertilizer burn.
- The addition of phosphorus and potassium to inoculated soybean usually results in a noticeable increase in yield.
- In order to maintain phosphorus and potassium levels in the soil, approximately 5 kg of phosphorus and 18 kg of potassium should be added to the soil per ton of harvested crop.
- In general, a planting density below 300,000 plants ha^{-1} is recommended for dryland conditions, but should be increased for later planting dates.
- Young seedlings are unable to compete with fast-growing weeds. Therefore, controlling weeds at this growth stage is vitally important.
- Soybean grown in humid (or high rainfall) areas is susceptible to rust, a fungal disease that affects the leaves and is spread rapidly by wind.
- Under rainfed conditions, surface mulch has a positive effect on the soil's hydrothermal regime, as well as crop evapotranspiration and yield.

Sorghum

A summary of the production guidelines gleaned from the literature for grain sorghum is as follows:

- Grain sorghum is well adapted to areas with a summer rainfall of 400-800 mm, daily maximum temperatures of 20 to 30 °C and a frost-free period of up to 140 days.
- The crop can withstand periods of drought and is suited to areas that are considered marginal for maize.
- Sorghum's drought and waterlogging tolerance makes the crop well suited to marginal sites and smallholder faming conditions.
- Sorghum is classified as a short-day plant (i.e. photoperiod sensitive), where the night must be longer than a critical minimum length.
- When grown on sandy soils with a low organic matter content, sorghum yields may be adversely affected by water stress and low micro-nutrient levels in the soil.

- Sorghum prefers soils with a clay content of 10-30%. Soils with a clay content exceeding 50% may adversely affect yield.
- The crop is sensitive to aluminium toxicity and should not be planted on very acid soils.
- Although sorghum is usually planted between mid-October and mid-December, it can be planted in January. In the drier areas, the best planting time is approximately mid-November.
- In general, planting density ranges from 28,600 to 75,000 plants ha^{-1} for dryland conditions. However, plant density should be increased in higher rainfall areas or when weed competition is problematic.
- Sorghum seedlings are very sensitive to weed competition. Weed control during the first six to eight weeks after planting is thus recommended.
- In order to maintain nitrogen, phosphorus and potassium levels in the soil, approximately 15 kg of nitrogen, 3 kg of phosphorus and 4 kg of potassium should be added to the soil per ton of harvested crop.
- Sorghum is susceptible to ergot, a fungal disease that attacks the panicle, and which can significantly reduce grain yield.
- Hybrids with an open-type panicle (e.g. PAN8816) are recommended for areas prone to bollworm infestation, as the panicle is easier to spray.
- Zero-tannin sorghum hybrids (e.g. PAN8816, PAN8906 and PAN8944) are highly suitable for ethanol production.
- Tannin-free sorghum is highly susceptible to bird damage.
- Intercropping of sorghum (e.g. with cowpea) is beneficial in regions with low and variable rainfall patterns as it offers a safer and more lucrative alternative to monoculture.

Best management practices

Soybean

Based on the results from the Swayimane soybean trials and other literature, the following best management practices for soybean are recommended:

- Farmers are encouraged to conduct germination tests to evaluate seed quality and viability prior to planting.
- For optimum yields, smallholder farmers are strongly encouraged to use inoculants. Farmers may need to be trained on how to use inoculants. A guide is provided in this document.
- Inoculants reduce fertilizer costs by negating the need to apply nitrogen. This implies an economic benefit associated with inoculant use.
- Research has shown that inoculation use without the application of PK fertilizers is not beneficial for growth. Furthermore, soil pH should be 5.2 to 6 for inoculants to work properly.
- Optimum application of fertilizers based on soil fertility recommendations is encouraged.
- The use of pre-emergence herbicides prior to planting would be ideal and mitigate labour demands associated with weeding under smallholder conditions.
- Smallholder farmers should consider the use of soil water conservation techniques such as mulching, especially under rainfed conditions where water is a major limiting factor. However, greater thought should be given to the selection of mulch types as there may be negative trade-offs (nitrogen mineralisation and fungal diseases) with crop yield.
- Rainwater harvesting would go some way in improving soil water availability.
- Agro-ecologies similar to Swayimane are better suited to an early-medium maturing, semi-determinant cultivar (e.g. LS6161R), compared to a medium-late maturing, indeterminant cultivar (e.g. CAPG3).
- Soybean LS6161R is better suited to biofuel production due to its higher yield potential when compared to CAPG3. In addition, both mulching and inoculation improved the seed oil content of this cultivar, which means higher biodiesel yields.

Grain sorghum

Based on results from the Swayimane trial, the following best management practices for grain sorghum are recommended:

- PAN8906 outperformed PAN8816 and Macia in terms of final yield and is thus highly recommended for biofuel production.
- The late (i.e. January) planting at Ukulinga resulted in cold and water stress and is thus not recommended in similar agro-ecologies.
- Grain yield is an important factor influencing biofuel production. PAN8906 produced more theoretical biofuel due to its higher yield.
- Macia produced a relatively high proportion of biomass to grain and may thus not be a suitable feedstock for biofuel production.

Based on results from Ukulinga, as part of another WRC project (Modi and Mabhaudhi, 2017) and other literature, the following best management practices for grain sorghum are recommended:

- For smallholder farmers, suggested and affordable strategies to help reduce runoff through improved infiltration capacity and soil transmission characteristics are low-cost mulching and low-tillage practices.
- Contour farming, ridge and mound tillage, strip farming and terrace farming are options that are suggested to reduce runoff loss, particularly when farming sorghum outside optimal planting dates, as recommended next.
- Early- and mid-season plantings are recommended for rainfed sorghum cultivation in agro-ecologies similar to Ukulinga.
- Late-season planting exposes the crop to frequent intermittent stress episodes and is thus recommended in areas where farmers have access to irrigation to supplement rainfall.
- Low-cost mulching (e.g. dry grass) should be explored by smallholder farmers. In regions that experience high wind speeds, the growing of windbreaks (and effective weed control) should be explored as a long-term strategy to help reduce evaporation loss.
- A recommended long-term strategy for water capture is rainwater harvesting for the supplementary irrigation of sorghum during dry spells and for the late planting of sorghum.

Based on the results from a scenario analysis reported by Modi and Mabhaudhi (2017) for two sorghum genotypes (PAN8816 and Ujiba) across 10 different planting dates and three agro-ecologies (Deepdale, Richards Bay and Ukulinga), the following best management practices for grain sorghum are recommended:

- Sorghum farmers in Richards Bay would benefit most from strategies that maximise transpiration (i.e. rainwater harvesting for supplemental irrigation).
- Sorghum farmers in Deepdale and Ukulinga can explore increasing planting population, together with appropriate soil fertilization mechanisms.
- Intercropping sorghum with a legume could be recommended to effectively use evaporated water in all three agro-ecologies. Ideally, the legume of choice should have low water requirements and a short growing season (≈90 days).

Based on scenario analyses conducted with the Agricultural Production Systems sIMulator (APSIM) and AquaCrop models, Modi and Mabhaudhi (2017) suggested the following best management practices for a sorghum-cowpea intercrop system:

- To achieve high water use efficiency (WUE), early planting (15 September) and late planting (15 January) in low-rainfall and high-rainfall areas, respectively, is recommended.
- The ideal plant population of sorghum should be 39,000 plants·ha^{-1} in combination with 13,000 plants·ha^{-1} of cowpea.
- When yields of both crop species are desired, increasing the cowpea plant population to 19,500 plants·ha^{-1} is recommended.

Enterprise budgets

Enterprise budgets were developed to determine the profitability of feedstock cultivation and were based on the specific agronomic requirements of each crop. The budgets present costs (both fixed and variable) and income estimates for producing a hectare of soybean at Baynesfield (a commercial farm) and grain sorghum at Swayimane (a rural farming environment). The break-even yields estimated for soybean and sorghum were 1.77 and 3.43 t ha^{-1}, respectively. For sorghum, costs were scaled up from the 2017/18 research trial to a hectare, which can potentially drastically distort the budget.

METHODOLOGY

The two main components of this research project related to fieldwork and simulation modelling. For the fieldwork component, more emphasis was placed on soybean than on sorghum. The modelling component involved the use of a crop productivity model, as well as an agro-hydrological model.

Fieldwork

Crop water use, growth and yield were measured at trials conducted over four seasons (2015/16 to 2018/19) at two locations (Swayimane and Baynesfield). A summary of the main findings from each trial are presented next.

2015/16 season

In the first season, the effects of fertilization and mulching on soybean growth and yield were assessed at Swayimane. For the fully (i.e. 100%) fertilized, non-mulched treatment, a low yield of 1.6 t ha^{-1} was measured, due partly to the lack of inoculation, a low pH value of 4.2 (aluminium toxicity) and a fungal disease that may have been transferred from the hay mulch. Neither full fertilization nor mulching significantly improved biomass production or crop yield. Soil fertility had a significant effect on soybean's Leaf Area Index (LAI), but not mulching. Although chlorophyll content and leaf number were significantly higher under mulching, there were no significant differences for stomatal conductance or plant height. However, mulching not only improved soil water content, but also reduced fluctuations in the topsoil.

2016/17 season

During the second season, the water use and yield of soybean was measured at Baynesfield as recommended by the previous biofuel project. Crop evapotranspiration was estimated using a new surface renewal method that does not require calibration. Data analysis was performed using two different methods that produced similar crop evapotranspiration accumulations of 378 and 384 mm over 125 days. From the averaged water use of 381 mm, a WUE of 1.35 kg m^{-3} was calculated from a measured yield of 5.14 t ha^{-1}. Severe lodging occurred during the season, which is evident from the combine harvested yield of 3.2 t ha^{-1}. Using an average oil seed content of 18%, a biofuel yield of 955.4 ℓ ha^{-1} was obtained, which equates to a WUE for biofuel production of 0.25 ℓ m^{-3}.

2017/18 season

In the third season, a trial was conducted at Swayimane to assess the effects of fertilization on three sorghum genotypes. Due to the late planting in January, grain yield was influenced by cold and water stress experienced towards the end of the growing season. The results showed that grain yield and starch content are important factors influencing biofuel production from grain sorghum. PAN8906 showed potential to produce greater yields, and more biofuel with less water consumption than PAN8816. Macia produced a relatively high proportion of biomass-to-grain yield and exhibited the lowest starch content. Thus, this open pollen variety may not be well suited to biofuel production. Based on these results, the crop model was partially calibrated for PAN8906 (not for PAN8816 or Macia) due to its higher biofuel production potential.

2018/19 season

The fourth trial was conducted at Swayimane to assess the effects of inoculation on three soybean cultivars. Unfortunately, one cultivar (PAN1521R) failed to germinate. Although inoculation did not significantly improve the final biomass and grain yields of two cultivars (LS6161R and CAPG3), it improved canopy cover, stomatal conductance and chlorophyll content index. Nonetheless, smallholder farmers should use inoculation as it reduces fertilization costs and can also be beneficial for rotational crops such as maize. However, the inoculant must be applied correctly and in conjunction with phosphorus and potassium application. Cultivar LS6161R is better suited to biofuel production due to its higher yield potential when compared to CAPG3. Based on these results, the crop model was partially calibrated for LS6161R (but not for CAPG3).

Model selection

The agro-hydrological model of the Agricultural Catchments Research Unit (ACRU) was selected to assess the hydrological impacts of biofuel feedstock production on downstream water availability. This model was the preferred choice in numerous other studies that assessed the impacts of land-use change on runoff response, simply because the ACRU model does not require extensive parameterisation in ungauged catchments. The AquaCrop model was selected to estimate the attainable yield of each strategic biofuel feedstock. This model is ideally suited to performing multiple seasonal simulations of crop yield.

Both models have been successfully linked to the quinary subcatchment database, which facilitates simulations at the national scale. Both models have similar climate and soil inputs, but differ in their calculation of runoff response. Although ACRU will produce more accurate estimates of runoff than AquaCrop, it cannot estimate soybean and sorghum yield (only that of sugarcane, maize and wheat).

Model inputs

Climate and soils

The quinary climate database, which comprises 50 years of daily climate data, was revised and used for the first time in this project. Errors in extreme rainfall events (daily rainfall > 400 mm) were identified and corrected. Instead of using interpolated temperature data for each quinary subcatchment, observed daily data was assigned to each quinary subcatchment, and then adjusted to account for altitudinal differences between the temperature station and the quinary subcatchment. Reference evapotranspiration was then estimated from the adjusted temperatures, assuming a fixed wind speed of 2 m s^{-1}. No changes were made to the quinary soils database.

Planting date and density

For each quinary subcatchment, the first planting date was determined in each year, from which the mean and median planting months were determined. For the majority of the quinary subcatchments, the first planting date occurs in November or December. These two months were therefore selected as fixed planting dates for modelling purposes. The day of planting was set to the beginning of the month and not mid-month. This was done because the crop model was used to generate monthly crop coefficients. Thus, the initial value was averaged from 30 days of data (not 15 days).

Typical planting densities were obtained from a literature review. For this project, a planting density of 250,000 and 300,000 plants ha^{-1} was selected for soybean. For grain sorghum, a planting density of 44,444 plants ha^{-1} was selected. As a general rule of thumb, sorghum is typically planted in areas that are considered suboptimal for maize production and at the same planting density. Based on this, a higher density of 60,000 plants ha^{-1} was selected.

Parameters for crop modelling

Soil-water balance

For the soybean trial conducted in the first season, parameter values for the soil-water balance (SWB) model were selected for soybean cultivar LS6161R and compared to those derived by Dlamini (2015) for six other soybean cultivars. Leaf Area Index was then simulated using the SWB model for the control (non-mulched, fully fertilized) treatment. Although the model oversimulated the LAI, model performance was considered adequate. The SWB was also used to simulate biomass production, with a tendency to overestimate observations. The SWB did not adequately simulate the profile water content and simulated a much drier soil profile, especially at mid-season and at harvest.

AquaCrop

A full calibration of AquaCrop was not possible using data from the field trials as they were rainfed and thus water stressed. Published model parameters for both soybean and grain sorghum were obtained from a literature review. It is clear that more studies pertain to soybean than to sorghum. Most of the soybean studies performed a partial model calibration to adjust certain cultivar-specific parameters. Hence, a similar approach was adopted in this project. For sorghum, certain crop parameter values were obtained from the literature. Model calibration was then validated by comparing simulated against observed yields.

Parameters for hydrological modelling

Parameters for the hydrological model were obtained from the literature and are similar to those used in the previous biofuel project and in other national studies involving quinary subcatchments. However, a new algorithm was used to derive the coefficient of initial abstraction that was based on rainfall seasonality and distance from the coastline. In addition, surface cover fraction was estimated from monthly crop coefficients. The fraction of active roots in the topsoil horizon was estimated from the topsoil depth. With regard to parameterisation of the hydrological model, innovative approaches adopted in this project included the derivation of monthly crop coefficients from AquaCrop output, and interception loss per rain day via a new method that requires measured LAI. Furthermore, crop coefficients representing the fallow period were measured, which is also considered innovative.

Interception loss

A new approach was adopted in this project to derive monthly values of interception loss per rain day from measurements of monthly LAI for the two selected feedstocks. Two methods were used: the Von Hoyningen-Huene equation and the variable storage Gash model.

The latter method considers rainfall intensity, as well as rainfall magnitude, and thus provides more accurate estimates of interception loss from the vegetation layer in ACRU. The advantage of this approach is the derivation of representative (i.e. site-specific) interception losses per quinary subcatchment, instead of using “constant” values for all growing areas.

Weekly measurements of LAI for soybean (LS6161R from the 2018/19 season) and sorghum (PAN8906 from the 2017/18 trial) were used to calculate monthly averages. The two methods were then used to generate mean monthly interception loss values from 50 years of daily climate input. When compared to the Von Hoyningen-Huene method, the Gash model produced higher values in the summer months, but considerably lower values in the fallow period, where the monthly LAI value was set to 0.13 m^2 m^{-2}.

Crop coefficients

Various studies have shown that ACRU is sensitive to its crop coefficient (K_C) input, which explains why considerable effort was spent on deriving suitable values for both feedstocks, as well as for the fallow period. AquaCrop's ability to simulate crop coefficients was tested against measured values derived for soybean using crop water use data obtained at Baynesfield in the 2016/17 season. Similarly, water use data obtained in the 2012/13 season at Ukulinga (as part of the previous biofuel project) was used to calculate monthly crop coefficients. Simulated K_C values obtained from AquaCrop output compared favourably to measured K_C for both crops. Hence, AquaCrop was used to obtain monthly crop coefficients for each quinary subcatchment, where irrigation (to 50% of plant available water) was used to artificially remove crop water stress. Monthly values were calculated for each of the 49 seasons, then averaged to produce a unique set of values for each quinary subcatchment. The advantage of this approach is the derivation of unique monthly values, which are deemed more representative of actual growing conditions. In the previous biofuel project, crop coefficients measured at the trial site (e.g. Ukulinga) were used for all quinary subcatchments.

Tests were performed on two quinaries (Quinary 4697 and Quinary 5325) where AquaCrop-derived crop coefficients were used as input for ACRU to estimate runoff response from sorghum, which was then compared to that generated from natural vegetation. The relative reduction in mean annual runoff (MAR) that could result from a land use change to sorghum cultivation was then calculated and compared to results obtained in the previous biofuel project. The relative reduction in MAR changed from 12.1 to 1.5% in Quinary 4697 and from 24.1 to 13.8% in Quinary 4325. Hence, the use of AquaCrop-derived crop coefficients resulted in a much lower impact of crop production on runoff generation.

Fallow period K_C

The previous biofuel project recommended the measurement of evapotranspiration during fallow conditions, from which crop coefficients could be determined for the non-growing season. Measurements were conducted at Baynesfield using the new surface renewal technique from May to October 2017, after the harvesting of soybean and maize planted in October 2016. The monthly crop coefficients decreased from 0.26 in May to 0.10 in July, and then increased to 0.22 in September. These values were adjusted to represent A-pan-equivalent crop coefficients and were below the minimum threshold of 0.20 required by ACRU. This work represents the first time that crop coefficients representing the fallow period were measured using the surface renewal method.

Parameters for biofuel modelling

For this project, equations were used to estimate theoretical biodiesel and bioethanol yield. The equations require, inter alia, crop yield, as well as the oil or starch content of the crop.

Biodiesel

Seed oil content for two soybean cultivars was measured, with LS6161R having two seasons of data. The seed oil content (range: 16.7-21.8%) was averaged (18.6%) and used to estimate biodiesel production at the national scale.

Bioethanol

Similarly, extractable starch content and fermentation efficiency was measured for three sorghum genotypes and pooled with data collected in the previous biofuel project. Hence, three seasons of data exist for PAN8816. The extractable starch contents (range: 62.5-70.2%) and fermentation efficiencies (range: 0.818-0.935) for PAN8816 and PAN8906 (Macia was excluded) were averaged (i.e. 66.1% and 0.90) and used to estimate bioethanol production at the national scale.

Spatial application of models

Although running ACRU for all 5,838 quinary subcatchments was computationally automated as part of the previous biofuel project, a national run took approximately 8.5 hours to complete. Hence, considerable effort was spent on reducing this time, with ACRU now taking just over half an hour (38 minutes) to complete a national run. A detailed explanation of the methodology developed to run ACRU at the national scale is provided in this report, which – to date – has allowed researchers working on other WRC-funded projects to implement and benefit from similar speed improvements. This means that ACRU users will spend far less time waiting for model runs to complete, which allows them to consider additional scenarios.

The use of AquaCrop to derive crop coefficients for each quinary subcatchment means that the crop model runs were completed before the ACRU runs. Hence, much effort also focused on reducing AquaCrop's run time. In the previous biofuel project, a national crop model run for soybean took 89 hours to complete, which has been reduced to 16 hours. In order to fully automate the national model runs, approximately 20,000 lines of code (written in UNIX and Fortran) were developed as part of this project.

RESULTS AND DISCUSSION

Crop yield modelling

The crop model provided estimates of crop evapotranspiration (ET), yield and WUE for each quinary catchment. Four national crop model runs were performed for each crop, i.e. for two planting dates and two planting densities. The yield maps developed from AquaCrop output clearly highlight low and high potential areas for soybean and sorghum production. Large parts of the country's interior region, especially towards the western areas, are too dry for crop cultivation under rainfed conditions. Other parts along the Drakensberg Escarpment and in the Lesotho Highlands are too cold for crop production.

The maps of WUE indicate that sorghum is more water use efficient than soybean due to higher sorghum yields. The maps also show that changing the planting date had a greater impact on crop production than changing the planting density. The higher planting density usually produced a greater crop yield, as expected. Due to the speed improvements made in running AquaCrop at the national scale, the scene is set to consider other scenarios involving different planting dates and plant populations. However, model output should support decision-making processes and not be used to derive absolute recommendations for best management.

Biofuel yield potential

Biofuel yield is sensitive to crop yield and oil or starch content. The later planting date (i.e. December) at the higher planting density produced a greater biofuel yield, due to the higher attainable crop yield. A histogram, which shows the variability in biofuel yield, showed that many quinary subcatchments are unsuited to crop production (especially sorghum), and thus produced low biofuel yields. Biofuel yields are higher for sorghum than for soybean, because one ton of sorghum produces 361 ℓ of bioethanol, compared to 192 ℓ of biodiesel from soybean.

Hydrological impacts of land use change

The ACRU model was used to assess the impact of biofuel feedstock production on downstream water availability at the catchment scale, relative to natural vegetation. As part of another WRC-funded project, an alternative hydrological baseline was developed, against which land use changes can be assessed. The Department of Water and Sanitation (DWS) recently expressed an interest in adopting the new baseline. It was thus used for the first time in this project to assess the hydrological impact of land use changes from natural vegetation to biofuel feedstock production.

With the exception of only a few quinary subcatchments, neither the cultivation of soybean nor the cultivation of grain sorghum is likely to significantly affect the quantity of water available to downstream users. Hence, these crops show little to no potential of being declared stream flow reduction activities (SFRAs). This is in contrast to results from the previous biofuel project, which showed that 2,423 and 1,348 quinaries exhibited SFRA potential for grain sorghum and soybean, respectively. Compared to the previous WRC project, the most significant change to the methodology was the derivation of monthly crop coefficients from AquaCrop simulations of crop water use for non-water stressed growing conditions. As noted earlier, this provided a unique set of K_C values for each quinary, instead of using the same set of values for all subcatchments, as was done in the previous project.

SUMMARY

This project has significantly contributed to improving the methodology typically used to assess the impacts of land use change on hydrological response using the ACRU model. To recap, the main contributions are as follows:

- Crop coefficients representing fallow conditions were measured and used in modelling the hydrological impact of crop production.
- Water use coefficients representing soybean and grain sorghum were calculated from crop model output.
- Monthly interception loss values were modelled using a new and improved technique.
- A new baseline land cover was used to assess the hydrological impact of biofuel crop production on downstream water availability.
- The time required to run AquaCrop and ACRU at the national scale has been significantly reduced.

The latter point has already benefitted other WRC-funded projects, in particular those that require many model simulations (e.g. the modelling flows project K5/2560). In addition, Prof Kienzle (Lethbridge University) incorporated some of the speed improvements in his version of ACRU that was designed to simulate snowmelt and runoff response in Alberta, Canada. He reported a 30-fold speed improvement and, for the first time, was able to run the model for more complex configurations. For example, the model was run for 6,834 hydrological response units (HRUs), instead of 1,772 HRUs.

RECOMMENDATIONS FOR FUTURE RESEARCH

The effects of fertilization and inoculation on crop yield were not significant, which was not expected. The trials should therefore be repeated in other agro-ecologies and over multiple seasons to determine if the same result is obtained. When measuring crop water use, the new surface renewal method implemented in this project should be used and not the simple water balance approach. The means the trials should be at least 80 x 80 m in size. The water use and yield of PAN1521R should be determined, as this cultivar is suited to a wide range of growing conditions.

In the future, a full crop model calibration should be performed for both soybean and sorghum. This will require irrigated trials to obtain growth and yield measurements under optimum irrigation, deficit irrigation and rainfed conditions. Four planting date options (15 October, 15 November, 15 December and 15 January) should be considered for each national model run. AquaCrop outputs canopy cover development on a daily basis, from which LAI could be estimated, and then used to derive interception loss via the modified Gash model.

The quinary climate database needs to be extended beyond 1999 to 2019 (i.e. by an additional 20 years). National assessments of hydrological and agricultural response to climate variability, based on the additional 20-year record, would provide a better assessment of risk. This is due to the anthropogenically induced changes in extreme climatological events that have occurred from 2000 onwards. In addition, the quinary soils database needs to be updated by assigning soil properties (e.g. depth and texture) to each terrain unit within a particular quinary subcatchment. From this, soil water retention parameters could be estimated, thus improving the spatial accuracy of the soils database.

ACKNOWLEDGEMENTS

The research reported here formed part of a solicited project that was initiated, funded and managed by the Water Research Commission (WRC) in Key Strategic Area 4 (Water Utilisation in Agriculture). The project team is sincerely grateful to the WRC for funding and managing the project. The project team also wishes to sincerely thank the following members of the Reference Group for their valuable contributions and guidance:

Prof S Mpandeli	Water Research Commission (Chairman)
Dr G Backeberg	Water Research Commission (2015-2019)
Dr L Nhamo	Water Research Commission
Dr A Singels	South African Sugarcane Research Institute
Dr G Ceronio	University of the Free State
Prof J Steyn	University of Pretoria
Mr M Mkhize	Department of Education (previously Department of Energy)
Ms N Fourie	Department of Human Settlements, Water and Sanitation
Mr P Fouché	PhytoEnergy

We would also like to thank the following individuals:

- Mr Vivek Naiken and Sanele Ngubane (Centre for Water Resources Research, University of KwaZulu-Natal) for their assistance with fieldwork at both Swayimane and Baynesfield Estate.
- Mr Ian Doidge (African Centre for Crop Improvement, University of KwaZulu-Natal) for his valuable advice regarding crop management.
- Prof Rob Gous (Animal and Poultry Science, University of KwaZulu-Natal) for his advice on soybean.
- Dr Vimbayi Chimonyo (Crop Science, University of KwaZulu-Natal) for assisting the postgraduate students with crop-related matters and statistical analyses.
- Mr Kyle Reddy for creating all the maps in this document.

Lastly, we are grateful for and acknowledge the financial contributions received from the uMngeni Resilience Project through Prof Mabhaudhi. In particular, the automatic weather station was upgraded at Swayimane, and four CS650 probes were installed. In addition, the uMngeni Resilience Project shared travel expenses to and from Swayimane.

TABLE OF CONTENTS

LIST OF FIGURES

LIST OF TABLES

LIST OF ABBREVIATIONS

ACRU	Agricultural Catchments Research Unit
APAN	A-pan equivalent reference evaporation
APSIM	Agricultural Production Systems sIMulator
ARC	Agricultural Research Council
AWS	Automatic Weather Station
B5	5% biodiesel blend
BIN	Binary
BNF	Biological Nitrogen Fixation
CC	Canopy Cover
CCI	Chlorophyll Content Index
CDC	Canopy Decline Coefficient
CDM	Canopy Dry Matter
CGC	Canopy Growth Coefficient
CN	Curve Number
CSIR	Council for Scientific and Industrial Research
CSIRO	Commonwealth Scientific and Industrial Research Organisation
CV	Coefficient of Variation
CWWR	Centre for Water Resources Research
DAFF	Department of Agriculture, Forestry and Fisheries (now DALRRD)
DARD	Department of Agriculture and Rural Development (now DALRRD)
DALRRD	Department of Agriculture, Land Reform and Rural Development (former DAFF)
DEM	Digital Elevation Model
DHSWS	Department of Human Settlements, Water and Sanitation (former DWS)
DIFN	Diffuse Non-interceptance
DoE	Department of Energy (now DMRE)
DM	Dry Matter
DMRE	Department of Mineral Resources and Energy (former DoE)
DT	Dissipation Theory
DWA	Department of Water Affairs (now DHSWS)
DWS	Department of Water and Sanitation (now DHSWS)
E2	2% bioethanol blend
EC	Eddy Co-variance
ERD	Effective Rooting Depth
ET	Evapotranspiration
FAO	Food and Agricultural Organisation of the United Nations
FAO56	Food and Agriculture Organisation, Paper No. 56
FC	Field Capacity
GCM	Global Climate Model

GDD	Growing Degree-day
GIS	Geographic Information System
GM	Genetically Modified
HDM	Harvestable Dry Matter
HI	Harvest Index
HRU	Hydrological Response Unit
ICRISAT	International Crop Research Institute for the Semi-arid Tropics
ISCW	Institute for Soil, Climate and Water
LAI	Leaf Area Index
LRR	Lapse Rate Region
LSD	Least Significant Difference
LUC	Land Use Change
MAE	Mean Absolute Error
MAP	Mean Annual Precipitation
MAR	Mean Annual Runoff
MAT	Mean Annual Temperature
MOST	Monin-Obukhov Similarity Theory
NRMSE	Normalised Root Mean Square Error
NSE	Nash-Sutcliffe Efficiency Index
OC	Oil Content
PAR	Photosynthetically Active Radiation
PART	Leaf-stem Partitioning Parameter
PAW	Plant Available Water
PWP	Permanent Wilting Point
REW	Readily Evaporable Water
RMSD	Root Mean Square Deviation
RMSE	Root Mean Square Error
RRMSE	Relative Root Mean Square Error
SANBI	South African National Botanical Institute
SASRI	South African Sugarcane Research Institute
SAT	Saturation
SAWS	South African Weather Service
SC	Stomatal Conductance
SDM	Stem Dry Matter
SEBS	Surface Energy Balance System
SED	Standard Error of Difference
SFRA	Stream Flow Reduction Activity
SLA	Specific Leaf Area
SPAW	Soil-Plant-Air-Water
SR	Surface Renewal

SWB	Soil-water Balance
SWC	Soil Water Content
TAW	Total Available Water
USDA	United States Department of Agriculture
UKZN	University of KwaZulu-Natal
VWC	Volumetric Water Content
WP	Water Productivity
WRC	Water Research Commission
WUE	Water Use Efficiency

LIST OF SYMBOLS

AET	Actual evapotranspiration (mm)
α_S	Soil water transmission parameter (based on soil texture)
ALTF	Altitude factor for temperature station selection (fraction)
AY	Adjusted dry crop yield with moisture content removed (t ha^{-1})
B	Accumulated biomass (g m^{-2})
A-pan	A-pan equivalent evaporation (mm)
c	Coefficient of initial abstraction (same as *COIAM* in *ACRU*)
c	Canopy cover fraction
CAY	Monthly crop coefficient (K_C)
CC	Canopy cover (%)
CC_O	Initial canopy cover at emergence (%)
CC_S	Green canopy cover reached (%)
CC_X	Maximum canopy cover reached (%)
CDC	Canopy decline coefficient (% d^{-1})
CDM	Canopy dry matter yield (kg m^{-2} or t ha^{-1})
CELRUN	Stream flow generated from the subcatchment, including the contribution from all upstream subcatchments (mm d^{-1} or mm $month^{-1}$)
CGC	Canopy growth coefficient (% d^{-1})
CN	Curve number
CO_2	Atmospheric carbon dioxide concentration (ppmv)
COFRU	Base flow recession constant (set to 0.009)
COIAM	Coefficient of initial abstraction
COLON	Monthly fraction of root colonisation of the B-horizon
CONST	Fraction of plant available water at which total evaporation is assumed to drop below maximum evaporation (i.e. the onset of plant water stress)
CORPAN	Monthly APAN adjustment factors to adjust Penman-Monteith evaporation estimates to APAN equivalent evaporation (E_p/ET_O)
CORPPT	Monthly precipitation adjustment factors (e.g. to account for differences in monthly rainfall between the selected driver station and spatially averaged estimates for the subcatchment)
d	Willmott's d Index
D	Drainage (mm)
ΔS	Change in soil water content (mm)
D_f	Drainage factor (soil input parameter)
DALT	Altitude difference between rainfall and temperature station (m)
DIST	Distance between rainfall and temperature station (minutes)
DM	Dry matter production (g m^{-2})
DSTF	Distance factor for temperature station selection (fraction)
DWR	Dry matter water ratio (Pa)
DY	Dry crop yield (t ha^{-1})

E	Soil water evaporation (mm)
E	Mean daily reference evaporation (mm)
E_c	Radiation conversion efficiency in kg MJ^{-1}
E_s	Soil water evaporation
EFRDEP	Effective soil depth for colonisation by plant roots
E_i	Evaporation of intercepted water (mm)
E_p	A-pan evaporation (mm)
ET_a	Actual crop evapotranspiration (mm day^{-1})
ET_c	Maximum crop evapotranspiration (mm day^{-1})
ET_O	Reference crop evaporation (mm)
EVTR	Determines whether transpiration and soil water evaporation are calculated as separate components (*EVTR* = 2) or combined (*EVTR* = 1)
FC	Field capacity (volume %)
G	Soil heat flux (W m^{-2} s^{-1})
γ	Psychrometric constant (kPa $°C^{-1}$)
GDD	Growing degree-days accumulated for month (°C d)
H	Sensible heat flux (W m^{-2} s^{-1})
HDM	Harvestable dry matter yield (kg m^{-2} or t ha^{-1})
HI	Harvest Index (%)
HI_O	Reference Harvest Index
H_{max}	Maximum Plant Height (m)
I	Irrigation (mm)
I_a	Initial abstraction (% or fraction)
I_a	Infiltrated water (mm; $I_a = c \cdot S$)
I_c	Interception loss (mm)
I_s	Evaporation loss from saturated canopy (mm)
I_t	Evaporation loss from stem/trunk (mm)
I_w	Interception loss during wetting phase (mm)
k	Canopy extinction coefficient
K_C	Crop coefficient
K_{CB}	Basal crop coefficient
K_{ex}	Maximum soil evaporation coefficient
K_p	Pan factor (ET_O/E_p)
K_r	Water content of upper soil layer (mm)
K_S	Water stress index
K_{PAR}	Canopy extinction coefficient for solar radiation
K_{SAT}	Hydraulic conductivity at saturation (mm d^{-1})
LAI	Leaf Area Index (m^2 m^{-2})
λ	Latent heat of vapourisation (J kg^{-1})
λE	Latent heat flux (W m^{-2} s^{-1})
N_2	Atmospheric nitrogen

NRMSE	Normalised root mean square error (%)
NSE	Nash-Sutcliffe efficiency index (fraction)
O	Observed variable (e.g. t ha^{-1})
OC	Soybean seed oil content (%)
p	Throughfall coefficient
p	Soil water depletion fraction
P	Predicted variable (e.g. t ha^{-1})
P	Precipitation (mm)
P	Soil water tension (kPa)
PART	Leaf-stem partitioning parameter
PAW	Plant available water
PCSUCO	Monthly fractions (as %) of the soil surface covered by crop residue
PE	Potential soil water evaporation (mm; $PE = PET - PT$)
PET	Potential evapotranspiration (mm; $PET = K_C * ET_O$)
P_g	Gross precipitation (mm)
P'_g	Amount of rain required to fill canopy storage (mm)
Ψ_{LW}	Leaf water potential at maximum transpiration rate (J kg^{-1})
PT	Potential transpiration (mm)
p_t	Stemflow partitioning coefficient
PWP	Permanent wilting point (volume %)
QFRESP	Storm flow response fraction for the catchment (set to 0.30)
r_s	Stomatal resistance (s m^{-1})
R	Rainfall intensity (mm h^{-1})
R	Runoff (mm)
R^2	Coefficient of determination
R_a	Extraterrestrial radiation (MJ m^{-2} d^{-1})
RANK	Temperature station ranking (1-13)
RD	Root depth (m)
RD_{max}	Maximum root depth (m)
RDM	Root dry matter (kg m^{-2})
REW	Readily available water (mm)
RGR	Root growth rate (m^2 $kg^{-0.5}$)
RH	Relative humidity (%)
RH_{ave}	Average relative humidity (%)
RH_{max}	Maximum relative humidity (%)
RH_{min}	Minimum relative humidity (%)
ROOTA	Monthly fraction of roots in the A-horizon
RMSE	Root mean square error (t ha^{-1})
R_N	Net radiation (MJ m^{-2} d^{-1})
RRMSE	Relative root mean square error (%)

R_s	Watermark sensor resistance (kΩ)
R_S	Incoming solar radiation (MJ m^{-2} d^{-1})
RUE	Radiation use efficiency (kg MJ^{-1})
RUNCO	Base flow store (mm)
S	Potential maximum storage (mm; $S = 1000/CN - 10$)
SAT	Soil water content at saturation (volume %)
S_c	Interception storage capacity (mm)
SC	Extractable starch content of sorghum (%)
S_c^{max}	Maximum storage capacity (mm)
S_e^{max}	Maximum elemental volume (mm)
SDM	Stem dry matter yield (kg m^{-2})
S_f	Stemflow (mm)
SLA	Specific leaf area (m^2 kg^{-1})
SI	Specific leaf storage (mm)
SIMSQ	Stream flow generated from the subcatchment (mm d^{-1})
SMDDEP	Effective soil depth from which storm flow generation takes place (m)
S_t	Trunk storage capacity (mm)
SWD	Soil water deficit (mm; $SWD = \theta_{FC} - \theta$)
T	Throughfall (mm)
TAW	Total available water (mm; $TAW = \theta_{FC} - \theta_{PWP}$)
T_{bse}	Base temperature (°C)
t_d	Number of days since Stage 2 soil water evaporation began
T_{dew}	Dew point temperature (°C)
T_{max}	Maximum temperature (°C)
T_{min}	Minimum temperature (°C)
Tn	Daily minimum air temperature (ºC)
Tr	Transpiration (mm)
Tr_{max}	Maximum transpiration rate (MM)
$Trans_r$	Factor determining translocation of total dry matter to roots
$Trans_g$	Factor determining translocation of stem dry matter to grain
Tx	Daily maximum air temperature (ºC)
T_s	Soil temperature (°C)
T_{upp}	Upper temperature threshold (°C)
θ	Actual soil water content (mm)
θ_{FC}	Soil water content at field capacity/drained upper limit (mm m^{-1}; volume %)
θ_{PWP}	Soil water content at permanent wilting point (mm m^{-1}; volume %)
θ_{SAT}	Soil water content at saturation/porosity in (mm m^{-1} or %)
U	Upward capillary rise (mm)
v	Raindrop volume (mm^3)
VEGINT	Monthly interception loss (mm rain d^{-1})

$WEIGHT_1$	Suitability of best temperature station (fraction)
$WEIGHT_2$	Suitability of second-best temperature station (fraction)
WP	Water productivity (kg m^{-3} or g m^{-2})
WP^*	Normalised water productivity (kg m^{-2})
WUE_C	Water use efficiency of crop production (kg m^{-3})
WUE_B	Water use efficiency of biofuel production (L m^{-3})
Y	Crop yield (kg or t ha^{-1})
Z	Effective rooting depth (m)
Zr_{eff}	Effective rooting depth (m)
Zr_{max}	Maximum rooting depth (m)
Zr_{min}	Minimum rooting depth (m)

REPOSITORY OF DATA

For details related to the project's data, please contact:

Richard Kunz (principal researcher)
Centre for Water Resources Research
School of Agricultural, Earth and Environmental Sciences
University of KwaZulu-Natal
Private Bag X01, Scottsville 3209
Pietermaritzburg, South Africa
Email: kunzr@ukzn.ac.za

This page was intentionally left blank

CHAPTER 1: INTRODUCTION

1.1 BACKGROUND AND RATIONALE

Biofuel is internationally recognised as a less carbon-intensive transport fuel. The finalised version of the Biofuel Regulatory Framework was released in February 2020 (DMRE, 2020) and noted the following potential benefits of biofuel production and use in South Africa:

- Reduction of air pollutants (especially emissions of particulate matter) in the transport sector
- Reduction of greenhouse gas emissions in the transport sector
- Reduced imports of transport fuels
- Creation of new jobs in the agricultural sector
- Preservation of existing jobs in the sugar industry

The Biofuel Regulatory Framework proposes a two-phase approach to expedite the implementation of the 2007 National Biofuel Industrial Strategy. The first phase considers a 4.5% blending of biofuel into the national fuel pool, with 2% produced using first-generation technology (i.e. from crops containing sugar, starch or vegetable oil). The Biofuel Regulatory Framework strongly supports the inclusion of new, black smallholder and commercial farmers in the biofuel value chain. In addition, soybean is selected as the reference feedstock for biodiesel production from oil seed crops. Similarly, grain sorghum is the reference for bioethanol production from starch crops. Sugarcane represents sugar crops (e.g. sugarbeet and sweet sorghum) for bioethanol production (DMRE, 2020).

Of the eight intended biofuel manufacturers, two have indicated grain sorghum as their preferred feedstock and another two manufacturers intend using soybean. It is envisaged that approximately 200,000 ha of grain sorghum will be planted to meet the 2% bioethanol demand. Similarly, around 500,000 ha of soybean is required for a 2% biodiesel blend. Hence, the biofuel industry is a major catalyst for the expansion of agricultural production in South Africa, and thus a potential major source of employment and economic development, particularly in rural areas. The number of potential jobs created is approximately 34 per hectare of agricultural expansion (DMRE, 2020).

Both the former departments of Agriculture, Forestry and Fisheries (DAFF), and Water and Sanitation (DWS) support agricultural expansion for biofuel feedstock production using currently unproductive land under rainfed conditions. This approach largely negates issues of food security or diverting resources away from food crops to fuel crops. However, the land being targeted for feedstock production exists mainly in the former homelands, which is classified as moderate to low potential, due to marginal climate and/or soil conditions. Thus, the actual feedstock area required to meet the biofuel demand may increase due to the lower feedstock yields associated with production in these marginal areas.

It is estimated that about three million hectare of fallow land exists in South Africa that is either underutilised or not in production. The majority of this land is located in communal areas in former homelands. In addition, there are vast tracts of land lying fallow in commercial farming areas. Government plans to target these areas for feedstock production. For example, this land will be used to increase annual sorghum production up to 700,000 tons under rainfed conditions (DMRE, 2020). Hence, it is generally accepted that water (and not land) is South Africa's scarcest resource.

Given that South Africa is classified as a water-stressed country, there is an urgent need to quantify the water use of feedstock required to meet the expected feedstock demand for biofuel production. The former DWS is particularly interested in the impacts of water use associated with communal land farming, as well as knowing which feedstocks may need to be declared as SFRAs. Thus, the likely impact of agricultural expansion in marginal areas on the country's constrained water resources needs to be quantified.

According to the Biofuel Regulatory Framework (DMRE, 2020), the Department of Agriculture, Land Reform and Rural Development (DALRRD) is tasked with doing the following, among others:

- Ensuring that biofuel production does not negatively impact on food security and the environment (water and biodiversity)
- Approving feedstock supply plans submitted by each biofuel manufacturer
- Approving feedstock imports (if local farmers cannot supply sufficient quantities)
- Developing and managing a farmers' support programme for new black farmers
- Providing technical support for crop and farm management
- Identifying farmers who will receive subsidies and financial support
- Providing financial assistance for initial production inputs (e.g. seed and pesticides)

The Biofuel Regulatory Framework also recognises the need to increase crop yields through research and development in collaboration with universities, as well as the Agricultural Research Council and the Council for Scientific and Industrial Research (CSIR). Hence, research is required to determine the expected water use and yield of soybean and grain sorghum produced using unproductive arable land, as well as to determine best agronomic practices for maximising attainable yield. To assist agricultural extension services, information on which cultivars are best suited for biofuel production in particular areas, as well as advice on how to manage fertility, weeds and pests/diseases, is also required. It is important to develop enterprise budgets to determine the profitability of feedstock cultivation.

In November 2014, the Centre for Water Resources Research (CWRR), based at the University of KwaZulu-Natal in Pietermaritzburg, was awarded a five-year project initiated and funded by the WRC. This project (K5/2491) was titled "Water use of strategic biofuel crops", with total funding of R4 million. The project commenced in April 2015 and terminated in March 2020. Over the five-year period, 12 reports were produced for the WRC, which have been combined and summarised to produce this final project report. The main beneficiaries of the research represented in this report are as follows:

- Department of Agriculture, Land Reform and Rural Development (a merger between the Department of Agriculture, Forestry and Fisheries and the Department of Rural Development and Land Reform)
- Department of Human Settlements, Water and Sanitation (a merger between the Department of Human Settlements and the Department of Water and Sanitation)
- Department of Mineral Resources and Energy (a merger between the Department of Mineral Resources and the Department of Energy)
- Licensed biofuel manufacturers (e.g. Mabele Fuels, Arengo 316, Rainbow Nation and Basfour)
- The Biofuels Task Team, which drives the implementation of the National Biofuel Industrial Strategy

1.2 PROJECT AIM AND OBJECTIVES

The overall aim of this project is to determine the water use of two strategic biofuel feedstocks (grain sorghum and soybean) that were selected in 2014 to represent bioethanol and biodiesel production in South Africa (DoE, 2014). The specific objectives of the project were as follows:

1. Identify potential feedstock cultivars and review their suitability for biofuel production, particularly in low potential and high potential areas.
2. Measure the water use and yield of key feedstocks grown under rainfed conditions in both commercial and traditional farm environments.
3. Parameterise an appropriate hydrological model to estimate feedstock water use and stream flow at the catchment scale for both large- and small-scale farms.
4. Parameterise and validate an appropriate crop model to estimate the attainable yield produced under different growing conditions.
5. Map areas suitable for the cultivation of the two feedstocks, particularly on under-utilised land, mainly in Limpopo, North West, Mpumalanga, KwaZulu-Natal and Eastern Cape.

6. Specify agronomic practices and associated costs for the cultivation of the two feedstocks at localities where these feedstocks can be grown.
7. Develop general guidelines for emerging farmers regarding the cultivation of the two feedstocks best suited for biofuel production.
8. Determine enterprise budgets of income and costs pertaining to feedstock cultivation.
9. Spatially model the water use and yield resulting from a land use change to feedstock cultivation under dryland conditions and to assess the impact on stream flow generation.

All but one of the above objectives (to map areas suitable for the cultivation of the two feedstocks, particularly on under-utilised land, mainly in Limpopo, North West, Mpumalanga, KwaZulu-Natal and Eastern Cape) were satisfactorily met. Although land suitability maps for soybean and sorghum were produced in the previous biofuel project (Kunz et al., 2015c) and prior to that in the biofuel scoping study, this project planned to further improve the mapping approach. Although this objective was not adequately addressed, the maps presented in this project (e.g. suitable planting date, crop yield, season length and water use efficiency) provide valuable information to assess if a location is suitable for crop production. Furthermore, other land suitability maps exist, including that developed by the Protein Research Foundation for soybean (cf. Section 15.3.2.3). A map showing areas where sorghum is grown is available in the Biofuel Regulatory Framework (DMRE, 2020).

1.3 SCOPE OF THE PROJECT

To date, the WRC has funded 13 years of research related to the water use of biofuel crops. This was subdivided into a scoping phase, a research phase and an implementation phase. The work began in 2007 with a two-year scoping study that identified 20 crops with potential for biofuel production in South Africa, and highlighted those crops that may exhibit stream flow reduction potential (Jewitt et al., 2009a). This work was followed by a six-year research phase, which, inter alia, measured and modelled the water use of potential biofuel crops not commonly grown in South Africa, such as sugarbeet and sweet sorghum (Kunz et al., 2015a). This five-year project represents the implementation phase, which developed production guidelines and best management practices for two crops (soybean and grain sorghum), as well as the enterprise budgets of income and costs. These outputs will assist with the inclusion of smallholder farmers in the biofuels supply chain.

Agronomic requirements and production guidelines for both crops were synthesised from the available literature and supplemented with knowledge gained from research trials conducted over four seasons. The field trials addressed knowledge gaps such as the response of soybean to mulching, fertilization and inoculation at the smallholder farming level. To assess the potential impact of biofuel crop production on downstream water availability, a crop yield model was partially calibrated and then used to simulate maximum evapotranspiration under non-stressed growing conditions. From this, crop coefficients were derived and used as input into a hydrological model in order to assess the potential reduction in runoff that may occur from a change in land use from natural vegetation to biofuel crop production. Maps showing the spatial variation in simulated crop yield and water use efficiency are useful in identifying areas best suited to the cultivation of soybean and grain sorghum.

1.4 STRUCTURE OF REPORT

Chapter 2 provides an overview of each strategic feedstock, which highlights the fact that the draft Biofuel Regulatory Framework published in 2014 was finally approved by Cabinet in December 2019 and published on 7 February 2020 *(*cf. Section 2.5.3). This paves the way for the implementation of the Biofuel Industrial Strategy released in 2007. The research presented in this document, together with that published by the previous biofuel project (Kunz et al., 2015a; Kunz et al., 2015b; Kunz et al., 2015c), will provide government with valuable information and knowledge to assist with and hopefully guide the implementation process.

Chapter 3 addresses four objectives of the project as shown in Table 1.1. The review of cultivars deemed suitable for biofuel projection is presented in Section 3.2. Agronomic requirements and production guidelines are given in Section 3.3 and Section 3.4, together with climatic criteria for crop growth in Appendix D, as well as a soybean inoculation guide in Appendix E. The information was mainly synthesised from the available literature and supplemented with knowledge gained from the field trials. The enterprise budgets of income and costs pertaining to soybean and sorghum cultivation are presented in Section 3.5.

Table 1.1: Guide to the chapter that addresses each project objective

Chapter	Objective	Topic
2		Feedstock overview
3	1 6 7 8	Cultivar review Agronomic requirements Production guidelines Enterprise budgets
4 **5** **6** **7** **8**	2	Feedstock water use and yield
9 **10**		Model description Model inputs
11 **12** **13**	3 4	Parameters for modelling
14		Methodology for model runs
15 **16**	5 9	Feedstock water use and yield modelling

With regard to the second objective, Chapter 4 provides definitions of water use efficiency pertaining to crop and biofuel production, as well as a discussion of factors affecting water use efficiency. Chapter 5 to Chapter 8 describe the field-based research undertaken by the project over four consecutive seasons (2015/16 to 2018/19). In accordance with the request of the project's reference group, each trial is presented in a separate chapter, each with an introduction, methodology and results section. The protocols followed for crop growth measurements are given in Appendix F. Attention is drawn to Chapter 6, where a new surface renewal method was used for the first time to estimate soybean's water (cf. Table 28 in Section 6.3.3.1), as well as evapotranspiration during fallow conditions. These measurements were used to derive crop coefficients representing the fallow period (cf. Table 9013.11 in Section 13.3.7.1).

Chapter 9 provides a summary of the process followed in selecting the appropriate hydrological and crop yield models required to meet the research objectives of this project (cf. Section 9.1), together with a brief description of each model (cf. Section 9.2), as well as a comparison of the models (cf. Section 9.3; Appendix I).

A distinction is made between model inputs and model parameters. Hence, the input datasets used to run the simulation models at the national scale are described in Chapter 10. The input climate datasets were revised for this project (cf. Section 10.1; Appendix J) and used for the first time. At the request of the project's reference group, suitable planting dates were determined for the country using relatively simple rules based on rainfall and temperature, but not photoperiod (cf. Section 10.3.3).

The equations and parameter values used to estimate theoretical biofuel yield are given in Chapter 12. Chapter 11 and Chapter 13 (including Appendix G and Appendix K) describe and list the parameters used to model crop yield and the water use of soybean and grain sorghum.

Since the crop trials were conducted under rainfed conditions, the growth and yield data collected in each season could not be used to calibrate the selected crop productivity model. Instead, a partial calibration of the model was performed for parameters related to phenological growth as described in Section 9.4.2. Default values were used for conservative crop parameters, while values for certain parameters were gleaned from an extensive literature review (cf. Appendix K). A new method was used in this project to estimate vegetation interception losses for each crop (cf. Appendix M), as well as a unique approach to derive monthly crop coefficients for unstressed conditions from crop model output (cf. Appendix N). The interception loss and crop coefficient values were then used as input for the hydrological model.

Section 9.1.3 noted that, as part of the previous biofuel project, Kunz et al. (2015b) automated the procedure to run the simulation models at the national scale. However, the process was computationally expensive, i.e. it required days to complete a crop model run. Hence, considerable effort was spent on reducing the time required to complete the model runs, which is described in detail in Chapter 14. This detailed explanation has allowed other researchers (both local and overseas) to implement and benefit from similar speed improvements. More importantly, the speed improvements facilitated multiple model runs for different scenarios as explained next.

Chapter 15 gives maps showing the spatial distribution in crop yield and water use efficiency, together with maps showing the average season length for each crop. Biofuel yield was also estimated from simulated crop yield and the oil or starch content of the crop. The crop productivity model was run for two planting dates (cf. Section 10.3) and two planting densities (cf. Section 10.4) that were deemed appropriate for soybean and sorghum production. Hence, four attainable yield and four WUE maps were developed for each crop.

Chapter 16 discusses the output from the hydrological model that was used to quantify the potential impact of biofuel crop production on downstream water availability. Results are presented in histogram format. Finally, the main findings of this study and the recommendations for future work are presented in Chapter 17.

CHAPTER 2: OVERVIEW OF STRATEGIC FEEDSTOCKS

2.1 INTRODUCTION

This project started in April 2015 and was guided by the draft version of the Biofuel Regulatory Framework released in January 2014 (DoE, 2014), which highlighted soybean and grain sorghum as strategic crops for biodiesel and bioethanol production, respectively. However, the regulatory framework was criticised for not including sugarcane to represent bioethanol production from sugar crops, which is cheaper to produce than bioethanol from starch crops. At the third reference group meeting in November 2017, a decision was made not to include sugarcane as a third strategic feedstock. Hence, only soybean and sorghum are reviewed in this chapter, with emphasis on what is known about their water use and yield, particularly in the smallholder farming environment.

2.2 SOYBEAN

Soybean *(Glycine max*) is a leguminous annual C3 plant belonging to the Fabaceae family, which is native to China and is classed as an oilseed crop (Schulze and Maharaj, 2007b). The largest producers of soybean in the world are the USA, Brazil and Argentina, where the annual production is about 77.3 (35%), 44.5 (30%) and 30.3 (27%) million tons per year, respectively (El Bassam, 2010). In Africa, soybean is a minor crop, making up less than 1% of global production. Given the right conditions and materials, increasing soybean production represents a huge opportunity for the continent's farmers (ACCI, 2018).

South Africa is one of the major soybean-producing countries. Soybean is the most important oil seed crop produced in South Africa (SAGL, 2016). Annual production of commercial soybean exceeds 1 million tons on average (Table 2.1) and occurs mainly in Mpumalanga (DAFF, 2013). In 2017/18, soybean in South Africa was mainly used for animal feed. Its production has risen due to the increase in poultry production in South Africa, which has more than doubled over the past decade (DAFF, 2018a; DAFF, 2018b). Current production, which is focused on food, is far less than the required volumes needed. According to Statistics SA (2007), 15% of the total area under soybean is irrigated. Most of the irrigation takes place in Mpumalanga and North West, while the majority of rainfed production occurs in Mpumalanga and the Free State.

Table 2.1: Seasonal production, area planted and yield of commercial soybean from 2013 to 2017 (DAFF, 2018c; DAFF, 2018d)

Season	2013/14	2014/15	2015/16	2016/17	2017/18*	Average
Area (ha)	502,900	687,300	502,800	573,950	787,200	595,108
Production (t)	948,000	1,070,000	742,000	1,316,370	1,430,300	1,048,528
Yield (t ha^{-1})	1.89	1.56	1.48	2.29	1.82	1.76

* Estimated figures provided for the 2017/18 season

Crop yields from commercial farms are typically higher than those from smallholder farms due to several factors, e.g. cultivar selection, use of irrigation, planting density and other management activities such as seed inoculation and use of fertilizers. The average yield in South Africa ranges from 1.5 to 2 t ha^{-1} (1.5 t ha^{-1} and 2.4 t ha^{-1} for dryland and irrigated conditions, respectively). However, for smallholder farmers, the average yield is 1.6 to 1.7 t ha^{-1} (Schulze and Maharaj, 2007b).

Coleman (2017) noted that, due to the steady increase in new farmers producing soybean, it will take a while for the country to achieve an average rainfed yield in excess of 2 t ha^{-1}. The Biofuel Regulatory Framework indicated that the average soybean yield is 2 t ha^{-1}. In addition, 60% of annual production is utilised for animal feed, followed by 30% for cooking oil, 7% for direct human consumption and 3% for industrial purposes (DMRE, 2020).

Coleman (2017) listed a number of other factors that have affected soybean production in South Africa. For example, maize producers took far too long to accept soybeans as "a complementary and supporting commodity, rather than a competing commodity". However, increased awareness among grain farmers of the benefits of rotating maize with soybean resulted from the emphasis on conservation tillage. Thus, there is growing appreciation of soybean's value as a rotational crop to potentially increase maize yields. Overall, the soybean industry is aiming for a crop ratio of 70% maize to 30% soybean, an improvement of the present ratio of 82:18 (maize:soybean), compared to about 50:50 in the USA and 18:82 in Argentina. However, sandy soils in the western Free State remain a challenge due to nematodes, which make farmers in these areas reluctant to plant soybean

Soybean is not commonly grown on smallholder farms due to the lack of farmers' willingness and knowledge to grow this crop. Hence, less is known about expected yields and water use of soybean at this farming scale, as well as the recommended management practices to improve yields, e.g. inoculation and fertilization (Letete and Von Blottnitz, 2012; Maonga et al., 2015). Furthermore, little information exists on the water use efficiency of soybean produced in South Africa. The yield and water use of soybean was measured on a commercial pig farm at Baynesfield during the 2012/13 season as part of another WRC-funded project (K5/2066) (Mengistu et al., 2014). Kunz et al. (2015a) reported a per hectare yield and water use of 3.52 t ha^{-1} and 4,690 m^3 ha^{-1}, respectively, which results in a WUE of 0.75 kg m^{-3}. The authors recommended that a second season of measurements should be undertaken at Baynesfield. However, no information on the WUE of soybean produced by smallholder farmers was found in the available literature.

2.3 GRAIN SORGHUM

Grain sorghum (*Sorghum bicolor* L. Moench) is a C4 grass crop that belongs to the Poaceae family. It is indigenous to Africa and originated in Ethiopia (DAFF, 2009b; El Bassam, 2010) and/or Sudan (ACCI, 2018). It is considered to be the fifth-most important cereal in the world (DAFF, 2010b; PANNAR, 2013b) and the second-most grown crop in sub-Saharan Africa (Modi and Mabhaudhi, 2017). The USA contributed 16.1% (9.2 million tons) to world production, followed by Nigeria at 11.4% (6.6 million tons), India at 8.2% (4.7 million tons), Mexico at 8.1% (4.6 million tons) and Sudan at 6.5% (3.7 million tons). The balance of 28.6 million tons (49.8%) was produced by various other countries (USDA, 2018).

Sorghum can be grown for human consumption (i.e. sorghum meal and sorghum rice) and is therefore produced at a smallholder scale. In addition, sorghum is suitable to drier conditions as it is more drought tolerant than other crops (e.g. maize). Therefore, it is highly suitable for smallholder farmers (DAFF, 2010b). In Limpopo, smallholder farmers produce 20,000 tons of sorghum on 25,342 ha of land (average yield of 0.8 t ha^{-1}) and mainly consume what they grow (Reddy et al., 2008; DAFF, 2010b).

Annual production of grain sorghum varies considerably due to farmers planting more profitable crops such as maize and soybean (Table 32.2). The national average yield varies between 2.6 and 3.6 t ha^{-1} (DAFF, 2013), which is more than the 2.1 t ha^{-1} (dryland) and 2.6 t ha^{-1} (irrigated) reported by Statistics SA (2007).

However, only approximately 5% of the total area planted to sorghum is irrigated. In marginal areas (drier or clayey soils), sorghum yields range from 2 to 4 t ha^{-1}, increasing to 8 t ha^{-1} in higher potential sites (wetter regions) and up to 12.5 t ha^{-1} under irrigation with a recommended row spacing of 75 cm (PANNAR, 2013b). The Biofuel Regulatory Framework indicated that the average sorghum yield is 2.8 ha^{-1}. In addition, 40% of annual production is utilised for animal feed, followed by 26% for human consumption, 22% for beverages and 12% for industrial purposes and exports (DMRE, 2020).

Table 2.2: Seasonal production, area planted and yield of commercial grain sorghum from 2013 to 2018 (DAFF, 2018c; DAFF, 2018d)

Season	2012/13	2013/14	2014/15	2015/16	2016/17	2017/18*	Average
Area (ha)	62,620	78,850	70,500	48,500	42,350	28,800	55,270
Production (t)	147,200	265,000	120,500	70,500	152,000	83,070	139,712
Yield (t ha^{-1})	2.35	3.36	1.71	1.45	3.59	2.88	2.56

*Estimated figures provided for the 2017/18 season

The yield, water use and water use efficiency of grain sorghum from the literature is given in Table 42.3. Kunz et al. (2015a) measured the water use and yield of grain sorghum over two seasons at two different sites (Ukulinga and Hatfield), whereas Hadebe (2015) considered the water use of different sorghum genotypes at two study sites. These studies highlight the large range in water use efficiencies estimated for grain sorghum in South Africa.

Table 2.3: Yield, water use, water use efficiency results of grain sorghum from the available literature

Source	Study sites	Yield (t ha^{-1})	Water use (m^3 ha^{-1})	WUE (kg m^{-3})
Kunz et al. (2015a)	Ukulinga Hatfield	2.10-5.70	4,360-5,020	0.41-1.02
Hadebe (2015)	Ukulinga Umbumbulu	1.90-4.82	2,580-3,730	1.16-2.67

2.4 OTHER FEEDSTOCKS

The suitability of various feedstocks for biofuel production in South Africa was assessed by Jewitt et al. (2009a), Khomo (2014), Kunz et al. (2015a) and Lembede (2017) and is thus not duplicated in this section. The Biofuel Industrial Strategy (DME, 2007) recommended two bioethanol feedstocks (sugarcane and sugarbeet) and three biodiesel feedstocks (soybean, canola and sunflower) for biofuel production. Kunz et al. (2015a) measured the water use and yield of sugarbeet, sweet sorghum and grain sorghum, and modelled the water use of other feedstocks, including sugarcane and canola. The water use and yield of soybean was obtained from another WRC-funded project (K5/2066).

The finalised Biofuel Regulatory Framework (DMRE, 2020) reiterated that maize (both white and yellow) is prohibited as a bioethanol feedstock for food security concerns. The use of other staple crops (e.g. wheat and potatoes) is also not supported. Jatropha is excluded as a biodiesel feedstock due to its alien invasiveness and toxicity threat to local birds and animals. The regulatory framework listed other “well-known” feedstocks not mentioned in the national Biofuel Industrial Strategy, such as grain sorghum, cassava and sweet sorghum for bioethanol production and groundnuts for biodiesel production.

A number of proposed biofuel manufacturers have applied to the former Department of Energy for licences to produce biofuel. The preferred feedstocks are listed in Table 2.4, which highlights why soybean and sorghum were selected as reference feedstocks in the draft Biofuel Regulatory Framework.

Table 2.4: Licence applications that have been processed by the Controller of Petroleum Products for biofuel production (after DoE, 2014)

Company	Biofuel	Feedstock	Capacity (Mℓ an^{-1})	Location
Mabele Fuels	Bioethanol	Sorghum	158	Bothaville, Free State
Arengo 316	Bioethanol	Sorghum	180	Cradock, Eastern Cape
Ubuhle RE	Bioethanol	Sugarcane	50	Jozini, KwaZulu-Natal
			388	**Subtotal**
Phyto Energy	Biodiesel	Canola	455	Port Elizabeth, Eastern Cape
Rainbow Nation	Biodiesel	Soybean	288	Port Elizabeth, Eastern Cape
Basfour	Biodiesel	Soybean	170	Berlin, Eastern Cape
			913	**Subtotal**

2.5 BIOFUEL PRODUCTION

2.5.1 Biodiesel

In August 2012, the former Department of Energy (DoE) published regulations regarding the mandatory blending of biofuel in the Government Gazette (DoE, 2012). The mandatory biodiesel blending rate is B5 (i.e. 5% biodiesel v/v), which equates to a minimum blending of ~465 million litres of biodiesel. Two of the four proposed biodiesel plants will produce sufficient biofuel to satisfy the B5 blending rate (cf. Table 2.4 in Section 2.4), provided both plants operate at full capacity (DoE, 2014). Soybean is the preferred feedstock, and an annual supply of ~2.51 million tons (from ~1.23 million ha) is required for the B5 blending. Therefore, the Biofuel Regulatory Framework (DoE, 2014) highlighted soybean as the reference feedstock to represent the production of biodiesel from vegetable oil. South Africa currently imports soybean oil cake for animal feed. Since oil cake is a by-product of the biodiesel manufacturing process, imports should reduce (DMRE, 2020).

2.5.2 Bioethanol

The mandatory ethanol blending rate is E2 (2% ethanol v/v), which equates to a minimum blending of ~238 million litres of ethanol (DoE, 2012). Two of the four proposed ethanol plants will produce sufficient ethanol to satisfy the E2 blending rate (Table 2.4; cf. Section 2.5.1), provided that both plants operate at full capacity (DoE, 2014). Grain sorghum is the preferred feedstock and an annual supply of ~571,000 tons (from ~204,000 ha) is required for the E2 blending (Kunz et al., 2015c). Therefore, the Biofuel Regulatory Framework (DoE, 2014) highlighted grain sorghum as the reference feedstock to represent the production of bioethanol from starch.

2.5.3 Biofuel Regulatory Framework

On 13 December 2019, Cabinet approved the draft Biofuel Regulatory Framework published in 2014 (DoE, 2014), which allows for the implementation of the 2007 Biofuel Industrial Strategy (DME, 2007). Amendments to the framework were completed in January 2020 and the document was published on 7 February 2020 (DMRE, 2020). The framework provides the following five areas to be regulated:

- Feedstock protocol, which mitigates the risk of the biofuel programme towards food security
- Mandatory blending regulations, which create certainty of biofuel demand
- Cost recovery mechanism for blending of biofuel
- The biofuel subsidy mechanism to support feedstock farmers and biofuel manufacturers
- The selection criteria for biofuel projects requiring a subsidy

The intention of the feedstock protocol is to help guide stakeholders (government, biofuel manufacturers and farmers) with regard to feedstock production and procurement. The goal is the sustainable production of feedstock with minimum risk to food security. National Treasury will need to provide the DALRRD with an annual budget allocation to fund the farmer support programme. The revised regulatory framework acknowledges that sugarcane should represent bioethanol production from sugar crops. In addition, it recognises the important role of the biofuel industry in utilising surplus sugarcane for bioethanol production once the local demand for sugar has been satisfied (DMRE, 2020).

Regarding the way forward, amendments are required to the mandatory blending regulations published on 23 August 2012 (DoE, 2012) to include second- and third-generation biofuel technologies. The Department of Mineral Resources and Energy (DMRE) will then convene a meeting of the Interdepartmental Biofuel Task Team to agree on an implementation plan for the framework. Thereafter, government will seek to implement a pilot biofuel programme starting in 2020. It is envisaged that the information and knowledge presented in this document will help government with its implementation plans.

In addition, a Biofuel Implementation Committee, comprising the petroleum industry, biofuel manufacturers and other stakeholders (e.g. Transnet), has been established to address matters pertaining to the practical issues of blending biofuel with conventional petroleum products (e.g. challenges resulting from the hydroscopic nature of bioethanol). Costs incurred by the petroleum industry to blend biofuel (infrastructure and operating costs) will be covered by government, which means blending will remain cost-neutral. All subsidy-related costs will be covered by a biofuel levy added to the fuel levy (DMRE, 2020).

Each biofuel manufacturer will submit their feedstock supply plan to the DALRRD for approval. Biofuel manufacturers will compete for the government subsidy, which only covers first-generation biofuel. In addition, preference will be given to the following:

- Biofuel manufacturers that utilise multiple-use feedstocks
- The use of arable land in the former homelands, land reform farms and/or commercial farms that have been fallow for at least three consecutive years
- The involvement of black farmers (emerging, smallholder and commercial farmers)
- The sustainability of feedstock supply
- Rainfed (not irrigated) crops

With regard to sustainability issues, the Biofuel Task Team will regularly monitor feedstock production. Farmers are also required to keep records of yield and harvest volumes. Government-appointed resource auditors will visit feedstock-producing areas and report back to the Biofuel Task Team to facilitate the monitoring of subsidised biofuel manufactures and the payment of subsidies (DMRE, 2020).

2.6 SUMMARY AND CONCLUSIONS

Policy related to biofuel production in South Africa strongly supports the cultivation of biofuel feedstocks under rainfed conditions, as well as the inclusion of black farmers in the biofuel value chain. In this section, it was noted that more studies have been conducted on grain sorghum than on soybean in South Africa. Based on this, this project aimed to assess the water use efficiency of two biofuel feedstocks at both the smallholder and commercial farming scale, but with an emphasis on soybean.

The knowledge gained from the field trials facilitated the development of agronomic guidelines for feedstock production, particularly for smallholder farmers, and the validation of the modelling approach to estimate the water use and yield of these two feedstocks.

CHAPTER 3: PRODUCTION GUIDELINES

This chapter presents an overview of production guidelines and best management practices that improve water use efficiency. Such practices promote an increase in harvestable yield and/or a decrease in crop evapotranspiration (accumulated over the growing season). It also gives enterprise budgets of income and costs.

3.1 INTRODUCTION

For rainfed farming systems in arid and semi-arid areas, water stress is the main factor limiting crop production. In sub-humid and humid areas, water deficit mainly affects crops grown in spring and/or on shallow soils. Due to, inter alia, increasing demand for water resources exacerbated by continuing population growth and the anticipated effects of climate change on rainfall magnitude and variability (Conway et al., 2009), the greatest challenge facing the emerging biofuel industry will be to increase crop production using less water, i.e. improve crop WUE. This can only be achieved by promoting management practices and cropping systems that improve water use efficiency by either increasing the harvested yield and/or reducing crop evapotranspiration accumulated over the growing season.

Debaeke and Aboudare (2004) suggested that farmers should select best management options that do the following:

- Increase the available soil water at planting (or during sensitive crop growth stages)
- Increase soil water extraction by the crop
- Reduce the contribution of soil evaporation to total water use
- Optimise the seasonal water use pattern between pre- and post-anthesis
- Select cultivars that tolerate water stress and recover after it has been alleviated

Each of these objectives is discussed in more detail. Certain management practices that influence each objective are also identified. Unless otherwise stated, the discussion presented in the following sections has mainly been synthesised from Debaeke and Aboudare (2004).

3.1.1 Improving available soil water content at planting

Increasing the available soil water at planting can be achieved by deep tillage (ripping) during the fallow period, which reduces runoff and increases infiltration, provided the soil is not high in clay content (especially those with high shrink:swell characteristics). In addition, a weed-free fallow period will increase moisture availability for spring-grown crops. Alternatively, rotating shallow rooted plants with deep rooted plants (e.g. canola) ensures that water is extracted at different depths of the soil profile (Kunz et al., 2015b). Singh and Singh (1995) stated that, in dry conditions, maize had the greatest water uptake from topsoil, whereas sorghum's water uptake was from the subsoil.

3.1.2 Increasing crop soil water extraction

The choice of planting density may influence weed growth. Weed control is thus vital in water-limited environments to retain sufficient water for crop growth. Suppressing (or preventing) weed growth early in the season helps to maximise soil water extraction by the crop. The selection of crop cultivars, characterised by deep roots, should also improve soil water extraction by the crop and thus increase plant growth. Soil tillage and/or fertilizer use also increase the soil volume explored by the crop's rooting system.

The application of nitrogen fertilizer generally improves leaf growth, thus promoting higher transpiration rates, while the application of phosphorus (if deficient) generally accelerates plant growth, thus reducing season length and improving transpiration efficiency. The application of nitrogen and phosphorus may increase root length and rooting depth, thus increasing soil water extraction by the crop.

3.1.3 Reducing soil water evaporation

Achieving high canopy cover is important in reducing soil evaporation water losses and improving biomass production by maximising transpiration (Mabhaudhi et al., 2013). The use of mulching will reduce soil water evaporation, as will the optimisation of plant density and row width. The selection of crop cultivars characterised by early vigour, or canopy growth that spreads laterally (rather than vertically), should also help reduce soil water evaporation.

The choice of planting density is based on soil water availability and the need to minimise soil water evaporation. In general, low plant populations are recommended when soil water availability is low, despite the increase in soil water evaporation (E_S). If the crop relies on stored soil water (i.e. autumn planting of canola), wide rows are appropriate because E_S will be small. On the other hand, if the crop relies mainly on rainfall, the objective is to minimise E_S by selecting a suitable plant density that maximises ground shading.

3.1.4 Optimising seasonal water use patterns

The adoption of early-maturing (or early-flowering) cultivars may help reduce water stress during the reproductive growth phase. Applying excess nitrogen in water-limited environments may result in a high LAI, leading to depleted soil water availability at grain/seed filling and thus a reduction in yield. In rainfed conditions, nitrogen is generally given at planting and placed at a depth to prevent nitrogen gaseous losses and maximise its uptake by the crop. The timing of a second dose of nitrogen is mainly related to rainfall, with the objective of minimising nitrogen leaching and ammonia volatilisation. Nitrogen efficiency at harvest may range from 20 to 80%, depending on fertilizer type, time and method of application, soil type and climatic conditions.

3.1.5 Reducing soil water stress

The degree to which water stress affects crop yield depends, inter alia, on the intensity and duration of the water deficit, the crop cultivar and the plant's development phase. Water stress affects several plant growth aspects, with obvious effects being the reduction of plant size and mass, leaf area and seed yield (WMO, 2012).

Rainwater harvesting and the use of mulch layers can improve soil water availability, thus making more water available for transpiration. In addition, cultivar selection aims to reduce risks by avoiding drought periods during the most critical growing stages of the plant growth, such as flowering and seed set. For sorghum, early drought before floral initiation can stop growth, whereas late drought stops leaf development, but not floral initiation (DAFF, 2009b; DAFF, 2010b; WMO, 2012). However, severe water stress in the vegetative and reproductive growth stages will reduce the plant's mass and leaf area development, which then affects grain yield. The effects of soil water stress can be reduced by planting drought-tolerant crops such as sorghum (cf. Section 3.2.3.5).

3.1.6 Summary and conclusions

The main factors that affect crop production can be grouped into the four general categories shown in Table 63.1. Although irrigation can be used to ameliorate low rainfall conditions, the other climatic factors listed below are more difficult, if not impossible, to modify or manipulate. Similarly, site preparation techniques can ameliorate certain physical properties of the soil deemed unfavourable for plant growth (e.g. ripping through root-impeding layers). Soil bunds ameliorate runoff loss and soil erosion, and thus increase infiltration of rainfall. However, farmers have the most control over the remaining factors listed in Table 63.1, in particular those related to cultivar selection and crop management.

Table 3.1: Categorisation of main factories affecting crop production (after WMO, 2012)

Category	Factors affecting crop production
Climate	Rainfall Solar radiation Air temperature Relative humidity Photoperiod
Soils	Physical soil properties Chemical soil properties Topography
Cultivar selection	Production potential Adaptability to the environment
Crop management	Site preparation Planting date Plant population Planting depth Fertilization Weed control Pest and disease control Mulching Inoculation

Cultivar choice strongly influences the crop's seasonal water use pattern, with the goal to reduce soil water stress at critical growth stages. Appropriate decisions regarding cultivar choice, plant density, weed control, as well as lime and fertilizer use will increase soil water extraction by the crop. Similarly, cultivar choice, plant density and mulching should reduce unproductive water use, i.e. soil water evaporation. Keeping the fallow period free of weeds or planting deep-rooted crops in autumn should improve the soil water available at planting for spring-sown crops. The final decision of cultivar choice and planting date often depend on the farmer's attitude to climatic and economic risks.

Information about cultivar choice is presented in Section 3.2. Production guidelines (cf. Section 3.3) and best management practices (cf. Section 3.4) for soybean and grain sorghum are presented according to the factors listed in the previous table. The agronomic requirements for each crop were obtained from the literature, in particular from the website of the DAFF website (e.g. DAFF, 2009a; DAFF, 2009b; DAFF, 2010a; DAFF, 2010b; DAFF, 2010c), which were mostly derived by the ARC in 1999, 2003 and 2008 (e.g. ARC, 1999; ARC, 2003; Du Plessis, 2008). Information was also obtained from the seed companies (e.g. PANNAR, 2006; PANNAR, 2013a; PANAR, 2013b; PANNAR, 2016; PANNAR, 2018; SEEDCO, 2018).

3.2 CULTIVAR SELECTION

3.2.1 Background

When making a particular cultivar choice, producers should consider characteristics such as length of growing season (which may differ for different climatic areas in South Africa), planting date and density, pod and plant height, standability, growth habits, row width, resistance against seed shattering and sensitivity to herbicides.

SEEDCO (2018) listed the following interrelated factors to consider when selecting a cultivar best suited to a particular area:

- Target yield
- Seed availability and quality
- Length of the growing season
- Rainfall amount and distribution over growing season

- Air temperature, altitude and frost risk
- Final use (consumption by human, animal or biofuel industries)
- Occurrence of pests and diseases

3.2.2 Soybean

3.2.2.1 Seed availability

According to the soybean cultivar recommendations published by the Grains Crop Institute of the ARC for 2019/20 (De Beer and Bronkhorst, 2019), 26 cultivars are conventional and 144 are genetically modified. The reader is referred to the ARC's latest publication on cultivar recommendations, which is not duplicated in this document due to the dynamic nature of the information. Approximately 85% of soybean cultivars are Roundup® Ready, and thus only a small percentage of conventional cultivars are available (PANNAR, 2018; ARC, 2018).

For the soybean trials conducted in this project, non-hybrid cultivars, as listed in the ARC's 2017/18 cultivar guide (De Beer and Bronkhorst, 2017), proved difficult to obtain from three seed companies (PANNAR, Link Seed and Capstone Seeds). Three cultivars that were sourced over the project's time span are listed in Table 73.2. They differ in relative maturity (i.e. the time taken for each cultivar to reach flowering and thus harvest maturity). LS6161R is an early-maturing cultivar (i.e. it takes ~128 to 160 days to mature), PAN1521R is an early- to medium-maturing cultivar (i.e. ~140 to 160 days) and CAPG3 is a late-maturing cultivar (i.e. ~160 to 180 days) (cf. Table 73.2). All three cultivars are genetically modified to have excellent pod height (i.e. the pods are formed much higher from the ground to reduce losses when harvesting with a combine harvester), standability (i.e. less susceptible to lodging) and shattering resistance, which is very important as it prevents early shattering of pods. All three cultivars are also genetically modified to withstand glyphosate (an active ingredient found in Roundup® herbicide) (PANNAR, 2006).

Table 3.2: Agronomic characteristics of the three cultivars (PAN1521R, LS6161R and CAPG3) grown under rainfed conditions and two inoculation treatments (PANNAR, 2006)

Agronomic characteristics	PAN1521R	LS6161R	CAPG3
Maturity group	5.7	6.1	6-6.2
Growth habit	Indeterminant	Semi-determinant	Indeterminant
Relative maturity	Early	Early-medium	Medium-late
Plant height (cm)	82	95-105	
Number of days to 50% flower	46-75	43-74	58-70
Number of days to 50% harvest maturity	128-160	140-160	160-170

3.2.2.2 Seed quality

In general, higher quality seeds are believed to have higher seed oil content. Factors that affect the oil content of soybean are discussed in Section 4.6. Oil content is provided in the soybean cultivar recommendations produced by the ARC (De Beer and De Klerk, 2014; De Beer and De Klerk, 2015; De Beer and Bronkhorst, 2016; De Beer and Bronkhorst, 2017). For example, seed oil content for 32 cultivars was provided by De Beer and Bronkhorst (2017), which ranged from 11 to 16% across three growing regions (cool to warm).

3.2.2.3 Maturity group

According to PANNAR (2018), South Africa has been divided into four climatic regions based on heat units and altitude, each suited to a particular maturity group:

- Cool: Maturity groups 4 and 5 (shortest growth period)
- Temperate: Maturity groups 5 and 6
- Warm: Maturity Group 6

- Hot: Maturity groups 6 and 7

Short-season cultivars (Maturity Group 4) require a relatively longer period of daylight to initiate flowering, whereas long-season cultivars (Maturity Group 7) require relatively shorter days before they will switch from vegetative to reproductive growth (DARD, 2016). Most cultivars being grown in South Africa currently fall within maturity groups 5 to 6 (Dreyer, 2017). The regions suited to each maturity group is shown in Figure 3.11. The same map (although copyrighted) was reproduced by PANNAR (PANNAR, 2018: 39). According to PANNAR (2018), cultivar PAN1521R is equally well suited to cool, moderate and hot regions.

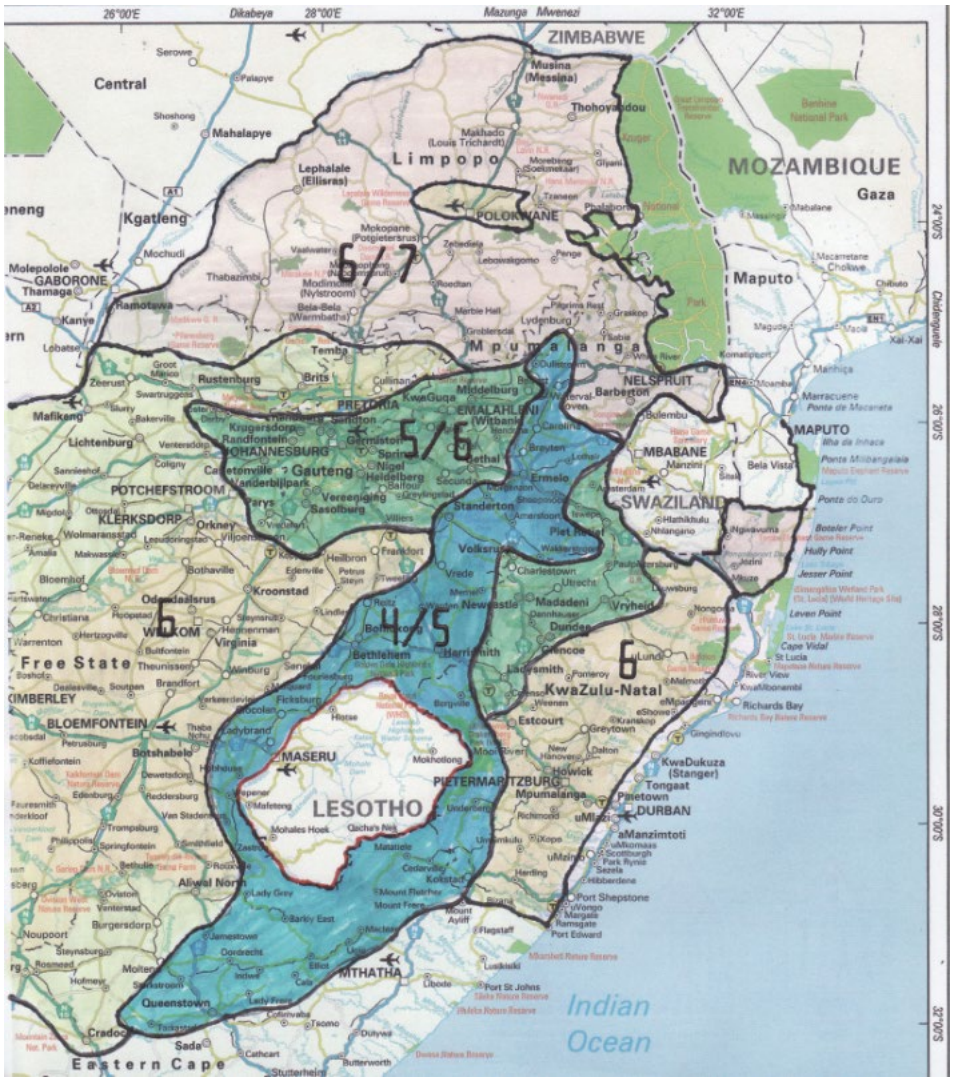

Figure 3.1: Regions suited to particular soybean maturity groups (Dreyer, 2017)

3.2.2.4 Growth habit

As noted in Table 3.2, there are two basic types of soybean cultivars related to the way the plant grows (SEEDCO, 2018):

- **Determinate:** These plants have a vegetative growth stage of about six weeks in which 10 to 12 leaves are produced, and then begin to flower. No further new leaves are produced on the main stem once flowering begins.

- **Indeterminate:** This plant type also grows for about six weeks, and then begins flowering when the main stem has about 10 leaves. However, the stem continues to grow for another three weeks or so, producing another five to seven leaves.

Thus, the vegetative and reproductive growth periods overlap in indeterminate cultivars, but not in determinate cultivars. Indeterminant crops continue to develop after flowering, which means they tend to grow taller than determinate plants. Determinate cultivars are better suited to warm, fast-growing environments (Lowveld areas, especially under irrigation), while in the Highveld areas, both types are suitable. Under drought conditions, indeterminates may have some advantage over determinates because they flower over a longer period (PANNAR, 2006; SEEDCO, 2018). There are several registered determinate and indeterminate cultivars in South Africa with suitability varying according to regions or provinces (DAFF, 2010c).

3.2.2.5 Growth type

Cultivars may be subdivided into two types: bushy with many side branches, and upright, mostly with a single stem (Dreyer, 2017).

3.2.2.6 Growing season length

The cultivar should have a growing season of four to five months. A fallow period of three to six months is recommended before planting to allow sufficient time to correct soil pH issues with lime. Depending on the cultivar, if the flowering period coincides with excessive moisture stress, only 25% of the flowers will set into pods, while the rest will abort (SEEDCO, 2018). PANNAR (2006) noted that water stress during the late grain-fill stage can reduce yields by as much as 30%. Hence, cultivar choice is important to avoid water stress coinciding with critical growth periods.

In general, soybean will mature later the further south it is planted in South Africa. If planted late, the crop will flower earlier due to the shorter day length. According to the Department of Agriculture and Rural Development (DARD) (2016), short-season cultivars (e.g. PAN1454R and LS6444R) were well suited to the cool climate experienced at Kokstad (602 mm; 1,340 growing degree-days (GDDs)). The medium-long season cultivars (LS6161R and LS6261R) obtained good yields at Cedara (666 mm; 1,616 GDDs) and Greytown (581 mm; 1,821 GDDs).

Short-season cultivars flower 30 to 35 days after planting and ripen within 75 to 105 days. These cultivars have low yields (Nieuwenhuis and Nieuwelink, 2005). The medium-duration cultivars also flower 30 to 35 days after planting and mature within 110 to 140 days, but give better yields (Nieuwenhuis and Nieuwelink, 2005). The long-season cultivars produce a large amount of leaf material (Nieuwenhuis and Nieuwelink, 2005). The duration from planting to maturity should be approximately 120 to 130 days for a well-adapted cultivar (DAFF, 2010c). For a crop taking about 125 days from planting to reach physiological maturity, the critical periods are as follows: germination: days 1-6; flowering: days 55-75; pod filling: days 95-125 (SEEDCO, 2018).

3.2.3 Grain sorghum

Cultivar selection aims to reduce risks by avoiding drought periods during the most critical growing stages of the plant growth, such as flowering and seed set (ARC, 2003; Du Plessis, 2008), as well as cold temperatures during the flowering stage (PANNAR, 2013b). Factors that should be considered when selecting a suitable cultivar include low-tannin cultivars, seed availability, growing season length, cold tolerance and drought tolerance.

3.2.3.1 Low-tannin cultivars

According to the South African list of cultivars (DAFF, 2018e), there are currently 23 registered grain sorghum hybrids and four open pollinated varieties. Seven of the 23 hybrids are sold by PANNAR. There are two types of sorghum: bitter and sweet sorghum. Bitter sorghum (high tannin) is planted in areas where birds are a major problem.

Kotze (2012) reported that PAN8625 is a tannin sorghum used mainly for malting and is not suitable for ethanol production. However, PANNAR supplies three grain sorghum hybrids suitable for ethanol production:

- PAN8816, a tannin-free sorghum currently used by 85% of the market for malting and milling
- PAN8906, a new hard-seed hybrid suitable for milling and ethanol
- PAN8909, which is similar to PAN8906 (Kotze, 2012)

Both PAN8816 and PAN8906 are bronze-grained, medium- to late-maturing, and low-tannin sorghum hybrids. Flowering occurs at approximately 80 days after planting (Table 83.3). The hybrids are well known for good leaf disease and head smut resistance. PAN8816 is used by 85% of the market for malting and milling, with yields ranging between 2-5 t ha^{-1} under optimum conditions. PAN894 is another zero-tannin cultivar and suitable for ethanol production (classified as genetically modified (GM), which indicates tannin-free, and good for malting and milling). This cultivar has a shorter growing season than PAN8816.

Table 3.3: Agronomic characteristics of grain sorghum hybrids available from PANNAR (PANNAR, 2018)

General characteristics	PAN8944	PAN8816	PAN8906	PAN8625
Growing season	Medium-early	Medium-late		Late
± days to 50% flowering	60-65	79-81	78-81	82-85
± days to harvest	120-130	135-142	135-142	140-145
Plant height (cm)	105-110	112-117	110-115	120-130
Uniformity (1 = excellent; 9 = poor)		2	1	3
Standability (1 = excellent; 9 = poor)		2	2	2
Threshability (1 = excellent; 9 = poor)		2	2	4
Head smut (1 = excellent; 9 = poor)		2	2	3
Plant colour		Purple	Purple	Purple
Grading	GM	GM	GL	GH
Seed colour	Red	Red	Red	Brown

Macia was developed by the International Crop Research Institute for the Semi-arid Tropics (ICRISAT). Macia is a low-tannin, open-pollinated variety. It is an early- to medium-maturing (60-65 days to heading and 115-120 days to maturity), semi-dwarf (1.3-1.5 m tall with thick stem) variety. However, Hadebe et al. (2017a) concluded that Macia is a late-maturing genotype with a consistently longer growing cycle compared to PAN8816. Macia has a wide growing rainfall range (250-750 mm) during the growing season, with stay green characteristics extending beyond harvest. However, the extractable starch content of Macia is much lower than that of PAN8816 and PAN8906, which is less desirable for ethanol production (cf. Section 12.2).

3.2.3.2 Seed availability

In order to meet the projected demand for ethanol production from sorghum, 60,000 to 70,000 bags of 25 kg seed will need to be supplied to the market, which is about five times that supplied in the 2012/13 season (Kotze, 2012). Due to various issues, including seed availability, South African farmers will not be able to realistically expand (“ramp up”) sorghum production to meet the immediate demand created

by biofuel manufacturers. Therefore, Lemmer and Schoeman (2011) noted that sorghum will initially be imported for a number of years to meet the increased demand. Over time, imports of sorghum are predicted to drop as local production increases.

3.2.3.3 Growing season length

Short-season cultivars take 90 to 110 days to mature and are best suited to areas where daily average temperatures exceed 20 °C. When the average daily temperature drops below 20 °C, the growth period is lengthened by 10 to 20 days for each 0.5 °C fall in temperature (Steduto et al., 2012; WMO, 2012). Medium-duration cultivars take 110 to 140 days to mature. At an average temperature of 15 °C, grain sorghum takes 250 to 300 days to mature. In cool climates, sorghum is grown mostly as a forage crop (Steduto et al., 2012).

3.2.3.4 Cold tolerance

There has been a shift in sorghum production from the drier, western areas to the wetter, eastern areas. This shift has resulted in the identification and development of cultivars that are more tolerant of lower temperatures (ARC, 2003; Du Plessis, 2008). After the flag leaf has emerged (during the reproductive stage, but after floral initiation) and before the developing ear becomes visible, the sorghum plant is sensitive to low temperatures. Temperatures of ~10 °C (for even two hours) will result in sterile pollen, and thus cold-tolerant cultivars should be selected for the cooler areas (PANNAR, 2013b). For example, PAN8944 is a short-season hybrid that exhibits high cold tolerance and can thus be planted in early spring.

3.2.3.5 Drought tolerance

According to the Biofuel Regulatory Framework, the government will promote the use of drought-resistant cultivars (DMRE, 2020). Sorghum's tolerance to drought (and waterlogging) makes it well suited to marginal sites and smallholder faming conditions (Modi and Mabhaudhi, 2017). Sorghum is typically grown in areas that are too dry for maize (DAFF, 2010b). In very dry areas, where water supply is deemed inadequate for sorghum, Singh and Singh (1995) recommended pearl millet. The crop enters a no-growth phase in response to water stress. The stems and leaves have a waxy layer that protects them from dehydration (PANNAR, 2018). Furthermore, sorghum leaves exhibit a row of motor cells along the mid-rib on the upper surface, which can roll the leaf during moisture-stressed conditions (DAFF, 2010b).

Sorghum's ability to tolerate water stress is also due to its dense and prolific root system, ability to maintain relatively high levels of stomatal conductance, maintenance of internal tissue water potential through osmotic adjustment and phenological plasticity (Tsuji et al., 2003). Sorghum is drought tolerant and adapts to dry conditions by deepening its root system (SEEDCO, 2018). Sorghum exhibits delayed leaf senescence when water stressed, which is referred to as the "stay-green" trait, i.e. the plant's ability to retain greenness (no reduction in chlorophyll content) during grain filling (Borrell et al., 2014). Delayed leaf senescence facilitates continued photosynthesis under drought conditions, which according to Tolk et al. (2013), can result in normal grain fill and larger yields when compared to senescent cultivars (e.g. maize).

Based on results for three sorghum genotypes grown over two seasons at Umbumbulu, Modi and Mabhaudhi (2017) reported the following:

- Lower water availability resulted in reduced plant growth (lower leaf number and plant height).
- Lower leaf numbers negatively affected canopy cover development and panicle yield.
- Chlorophyll content was not indicative of plant water stress, which was due to the "stay-green" trait of some sorghum genotypes.

- When water stressed, sorghum partially closes stomata to sustain reduced photosynthetic activity, thus ensuring “some” yield is produced, compared to no yield for other crops.
- Under low soil water availability, crops will often exhibit a shorter growth cycle as they try to escape drought.
- Water stress triggered plant dormancy, which resulted in delayed grain filling and reduced yield.

3.3 CROP MANAGEMENT

3.3.1 Soybean

3.3.1.1 Climate

Soybean is a relatively difficult crop to grow and not all areas are suitable for soybean cultivation. Soybean thrives in warm, fertile, clayey soil and is mainly cultivated under dryland conditions in South Africa (DAFF, 2018d). The crop can survive short periods of drought, mainly because its flowering period extends over three to five weeks, which is longer than other crops such as maize (10 to 14 days) (Smith, 1998; DAFF, 2010c). Although soybean can tolerate dry conditions prior to flowering, adequate soil moisture is important at the onset of flowering to ensure bud emergence and formation (Smith, 2006; DAFF, 2010c). Hence, the crop is susceptible to drought during the flowering and pod formation stages.

Climatic criteria for soybean growth were gleaned from the available literature by Kunz et al. (2015b) as part of the previous biofuel study. Additional sources of information have been added to Table D.1 in Appendix D. Soybean requires reliable rainfall, particularly from flowering to pod maturity. Soybean is best suited to areas that receive 700 mm or more rainfall over the growing period (Dreyer, 2017).

Optimum growth takes place at temperatures between 20 and 30 °C (Smith, 1994; DAFF, 2010c). Yields are adversely affected when temperatures rise above 30 °C, while temperatures lower than 13 °C for long periods during the flowering stage inhibit flower and seed formation. Young seedlings are easily damaged by excessively hot weather. Soil temperatures of at least 18 ºC favour rapid germination. High humidity before harvesting favours the incidence of diseases, which reduces vigour (PANNAR, 2006). The plant displays a medium tolerance to frost and recovers from frost damage if it occurs before flowering (Schulze and Maharaj, 2007b). However, frost can be fatal if it occurs during the early growth stages according to the Food and Agricultural Organisation (FAO) (2006).

3.3.1.2 Soil type and pH

Soybean is known for its deep rooting system, where Smith (2006) reported a maximum depth of 1.2 m and an effective rooting depth of 0.6 m. Nieuwenhuis and Nieuwelink (2005) observed rooting depths of 1 to 1.5 m in well-drained silt loam and clay loam soils. Waterlogged conditions have a negative effect on crop yield (Nieuwenhuis and Nieuwelink, 2005).

Soybean is suited to soils with relatively high clay content (better so than maize). When grown on sandy soils with a low organic matter content, the following risks need to be considered. Firstly, supplemental irrigation may be required at establishment, especially for shallow soils that dry out too rapidly. There is a high risk of nematode damage, which would need to be manged properly to ensure crop survival. The soil may be highly leached and exhibit low micro-nutrient levels, which would need to be corrected. The hypocotyl (or neck) of the seedling can easily break during emergence, and thus compacted soils or those that easily form a crust should be avoided or managed properly (PANNAR, 2006).

The crop is also sensitive to soil acidity (due to inoculation requirements) and does well when pH ranges from 5.5 to 6.5. Soils with high gravel content, and thus low moisture retention capabilities, should also be avoided (Dreyer, 2017; SEEDCO, 2018). SEEDCO (2018) listed many best management practices for grain and legume crops and highlighted the importance of providing plants with the required

nutrients. It states that “farmers must sample their soils for pH and fertility” and highlights the effect of acidic soils on uptake efficiency of macro elements (nitrogen, phosphorus and potassium). Soil pH between 6 and 6.8 is considered optimum for nutrient uptake. When soil pH is 4.5 to 5.5 or where the acid saturation is greater than 15%, uptake efficiency of nitrogen and potassium is only 30 to 77% and 23 to 48% for phosphorus. For inoculants to work properly, the soil pH should be 5.2 to 6. Molybdenum availability becomes limiting in soils with a low pH (less than 4.5), which could limit nitrogen fixation. Spraying sodium molybdate onto the foliage would help rectify the problem (Dreyer, 2017). SEEDCO (2018) strongly recommends that low pH is corrected using agricultural lime (either dolomite or calcite based) and provides many reasons for farmers to use lime regularly. The choice between dolomitic and calcitic lime depends on the magnesium content of the soil. Ideally, lime should be evenly applied at least two months before planting and mixed well into the soil (PANNAR, 2013b). A fallow period of three to six months is recommended before planting to allow sufficient time to correct soil pH issues with lime.

3.3.1.3 Inoculation

Nitrogen is an important macro-nutrient that is responsible for high growth rates in most crops (Nieuwenhuis and Nieuwelink, 2005). However, in many natural ecosystems, heavy losses of nitrogen occur due to crop uptake, soil erosion, leaching and denitrification processes (Khonje, 2016). A common technique that has been used worldwide to re-address this nutrient loss is the application of fertilizers in order to improve soil fertility, and thus improve crop yields (Khonje, 2016). Fertilizer treatments are often expensive and not readily available, especially for smallholder farmers, which therefore results in low crop yields (DAFF, 2010c). However, soybean can take up atmospheric nitrogen (N_2) by root-nodulating bacteria through a process known as biological nitrogen fixation (BNF) (Nieuwenhuis and Nieuwelink, 2005; Khonje, 2016). Hence, an inexpensive and environmentally friendly alternative to nitrogen fertilization is seed inoculation, which allows for N_2 to be fixed more readily by root-nodulating bacteria (e.g. *Rhizobium japonicum* or *Bradyrhizobium japonicum*) found in legume plants such as soybean (Salvagiotti et al., 2008; Khonje, 2016).

The amount of nitrogen that a plant can fix depends on the type of crop cultivar chosen, the type and productivity of the rhizobium bacteria selected, soil properties and climatic conditions (Chikowo et al., 2015; Leggett et al., 2017; Moretti et al., 2018). The factor that often has the greatest impact on BNF is the soil environment, where saturated soil profiles, highly acidic soils, poorly textured and structured soils can affect the ability of the rhizobium to fix nitrogen, which reduces the release of nitrogen into the soil (PANNAR, 2013a; Chikowo et al., 2015).

From the literature, rhizobium inoculation of soybean in combination with fertilizer use (such as phosphorus) is highly effective and can significantly increase soybean yield (refer to Figure 23.2), compared to no inoculation and/or only application of essential nutrients. Although soybean requires little or no nitrogen fertilizer, phosphorous is essential for high yields and improved seed quality (Malik et al., 2006).

However, the application of nitrogen to soybean that is already fixing nitrogen may limit yields, instead of boosting them (Abendroth et al., 2006; Salvagiotti et al., 2008). In the 2018/19 season at Swayimane (cf. Chapter 8), Reddy (2019) showed that inoculation, used in conjunction in PK fertilizer, significantly improved the canopy cover, stomatal conductance and chlorophyll content index of two soybean cultivars (LS6161R and CAPG3).

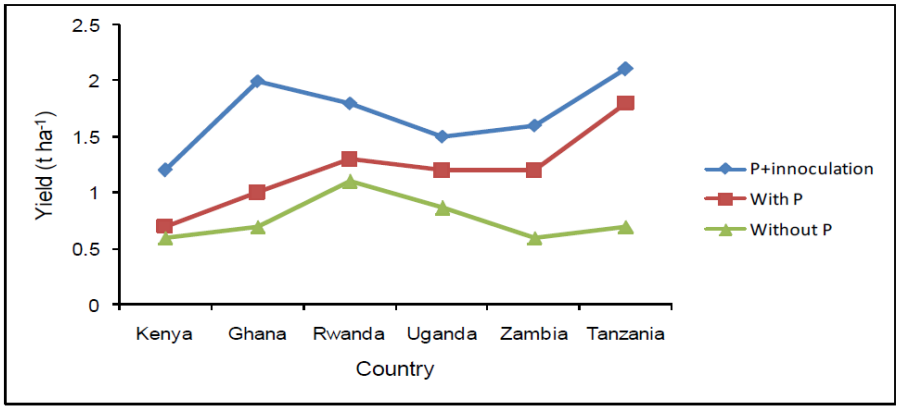

Figure 3.2: Soybean yield trend with and without phosphorus fertilization and inoculation, based on an average of three seasons from 2010 to 2012 (Mutegi and Zingore, 2014)

In many smallholder farming areas, there is often a lack of microbes present in the soil for soybean plants to develop active root nodules on their own. Therefore, the crop needs to be inoculated with a suitable rhizobium prior to planting (Khonje, 2016). Inoculation therefore offers a great opportunity for resource-poor farmers in South Africa to increase their crop yields, and thus improve food security (Salvagiotti et al., 2008). Inoculation should be used by smallholder farmers as it reduces fertilization costs. However, inoculation (and fertilization) is often not well understood by smallholder farmers. Therefore, promoting the awareness and training of local farmers will help enhance the production of soybean at the smallholder farming level. For these reasons, an inoculation guide has been developed, which is presented in Appendix E.

3.3.1.4 Fertilization

SEEDCO (2018) highlighted the stress that soybean production places on soil fertility when compared to other crops such as maize (Table 93.4). According to Dreyer (2017), soybean removes about 8 kg of phosphorus and 6 kg of sulphur from the soil per ton of grain produced, which differs to figures given in Table 3.4. PANNAR (2006) gave figures of 60, 7 and 19 kg (and 15, 3 and 3.5 kg for maize) of nutrient removal per ton of grain for nitrogen, phosphorus and potassium, respectively. Although soybean grows well with residual fertilizer or manure application, a general recommendation is to apply a pre-plant application of 150 to 300 kg ha^{-1} of either a basal fertilizer or Single Super Phosphate before planting, especially when fertility is low (SEEDCO, 2018). PANNAR (2006) recommends an application of approximately 200 kg of Single Super Phosphate, while 100 to 150 kg of potassium chloride per hectare (broadcasted and incorporated) is normally sufficient. Band placement of fertilizer is not recommended as soybeans do not readily respond to it and also because soybean seed is very sensitive to fertilizer burn.

Table 3.4: Nutrient removal per ton of harvested soybean seed in comparison to maize grain (SEEDCO, 2018)

Nutrient	Nutrient removal (kg per ton of grain)	
	Soybean	Maize
N	65	13
P	15	5.8
K	22	4.2
Ca	28	1.1
Mg	7.8	0.88
S	3	1.5
Zn	0.024	0.022

Provided that soybean seed is adequately inoculated, it does not need much nitrogen in the basal fertilizer. The crop binds its own nitrogen, which represents a saving of between 75 and 100 kg of nitrogen per ton of crop produced (Dreyer, 2017). However, SEEDCO (2018) recommends a starter-up nitrogen for the first six weeks after planting. Soils with poor to medium soil fertility require a small amount of fertilizer to sustain the crop for the first six weeks before effective nodulation occurs (Table 3.5).

Table 3.5: Average nutrient requirements of soybean (SEEDCO, 2018)

Nutrient (kg ha^{-1})	Nutrient status of soil		
	Poor	Medium	Good
N	30-40	20-30	Nil
P	40-60	20-30	Nil
K	40-60	20-30	Nil

3.3.1.5 Mulching

Continuous mono-cropping, over-utilisation of smallholder farming areas, and non-adoption of appropriate soil, water and nutrient management practices are increasingly deteriorating soil fertility and accelerating soil degradation (Ramakrishna et al., 2006). In order to address these issues, better soil management practices are needed to improve crop productivity (Ramakrishna et al., 2006). Mulching may be one such practice to help maintain an optimum soil moisture and thermal environment through reduction in soil evaporation (Chakraborty et al., 2008).

Mulching is generally defined as the covering of the soil surface between the crop plants with an organic (e.g. straw) or inorganic (e.g. plastic film) material (Pi et al., 2017). The more common mulches are organic material such as straw or hay that are cheap and easy to obtain, especially for smallholder farmers. Straw is regarded as one of the best mulches for improving water retention in the soil and reducing soil evaporation (Baumhardt and Jones, 2002; Zhang et al., 2009). Hence, mulching can improve soybean's water use efficiency by reducing soil water evaporation (Ramakrishna et al., 2006).

Under dryland conditions, surface mulch has been reported to have positive effects on the soil's hydrothermal regime, as well as crop evapotranspiration and yield (Thiagalingam et al., 1996; Hatfield et al., 2001; Li et al*.,* 2008; Wang et al*.*, 2009). For dryland soybean, mulching also increases leaf water potential and root length density, which, in turn, promotes high soybean development, allowing for early harvest and increased yields (Chakraborty et al., 2008; Zhang et al., 2009).

In the 2015/16 season at Swayimane (cf. Section 5.3.2), Lembede (2017) showed that, under 100% fertilization, hay-mulch treatment had higher soil water content (SWC) relative to no mulch (38.48% > 32.95%) for the 100% fertilizer treatment. Furthermore, significantly higher chlorophyll content under mulching during the vegetative growth stage indicated a higher photosynthetic rate. On the other hand, there were no significant differences observed for the stomatal conductance, LAI, biomass and yield of soybean under hay mulch when compared to the non-mulched treatment.

Mulching has other advantages, such as regulating soil temperature within the soil profile, reducing weed infestation by preventing light penetration or excluding certain wavelengths of light that are needed for weeds to grow (Ramakrishna et al., 2006). It also helps reduce surface runoff, which, in turn, reduces soil erosion (Pi et al., 2017). Therefore, mulch should be considered by smallholder farmers, especially under rainfed conditions where water is a major limiting factor.

3.3.1.6 Planting

For information on planting date and planting density, the reader is referred to Section 10.3.1 and Section 10.4.1, respectively. Soybean seed must be inoculated (cf. Section 3.3.1.3). In addition, a fungicide seed dressing with Flusilazole may help ensure good crop emergence and establishment. Treated seed helps to protect against diseases such as damping off (cf. Section 3.3.1.8) and sore shin.

Treated seeds should be planted into a fine tilth that ensures good seed-soil contact as follows: Create furrows 5 to 7 cm deep, then apply the basal fertilizer into the furrow; cover with 2 cm of soil, then plant the seed (this avoids direct contact between seed and fertilizer). Then, plant seeds 2 cm deep on clay soils and 5 cm deep on sandy soils (PANNAR, 2013a; SEEDCO, 2018). On the other hand, Dreyer (2017) recommends that fertilizer should be applied at least 5 cm below and 5 cm away from the seeds.

Rainfall at planting (or three to four days later) will encourage rapid germination and prevent possible crust formation. Emergence is expected within five to seven days after planting (PANNAR, 2013a). Six weeks after planting, it is important to cut young nodules in half to check if they are active (bright pink) or inactive (white). If nodules are inactive, a light top dressing of about 75 kg ha^{-1} of fertilizer may be recommended and should be applied before flowering.

3.3.1.7 Weed control

Weed control is vitally important to ensure maximum growth and yield of soybean (DAFF, 2010c). Weeds can dramatically reduce soybean yields because of serious impacts on crucial development stages, such as post-emergence and flowering (PANNAR, 2013a; DAFF, 2018d). Young seedlings are unable to compete with many fast-growing weeds. Therefore, controlling weeds at this growth stage is vitally important (Nieuwenhuis and Nieuwelink, 2005; Khonje, 2016). Ideally, the crop should be kept weed-free from planting until harvest, since weeds compete for the available light, nutrients and soil water. Weeds can also provide a safe habitat for insects that may damage the crop by eating it or via transmission of diseases (Nieuwenhuis and Nieuwelink, 2005). The greater the weed load, the higher the relative humidity between the plants, which increases the risk of fungi that can damage the crop (Nieuwenhuis and Nieuwelink, 2005; PANNAR, 2013a). Weeds also interfere with machine harvesters, which results in seed loss because they are damaged (DAFF, 2010c).

Weed control in soybean could be manual, chemical or both (FAO, 2006). Manual practices include using labour to manually remove weeds, which may be an effective approach for smallholder farms. However, manual weeding can be time consuming and labour intensive for larger commercial farms (Nieuwenhuis and Nieuwelink, 2005). Chemical weed control reduces the need for manpower. Therefore, it is highly effective for both commercial and smallholder farms (Nieuwenhuis and Nieuwelink, 2005; PANNAR, 2013a).

The choice of herbicide depends on the type of weed species and availability of herbicide. Hence, knowledge of weed problems and proper identification of weeds are essential when making herbicide decisions (Chikowo et al., 2015; Leggett et al., 2017; Moretti et al., 2018). Roundup® Ready Plus may be applied post-emergence to Roundup® Ready soybean cultivars from emergence through to flowering (Khonje, 2016). However, there are limitations (e.g. 6.7 ℓ ha^{-1}) to the total amount of Roundup® (e.g. glyphosate) that can be applied throughout the season.

3.3.1.8 Pest and disease control

Different pests and diseases can cause major damage to soybean crops, which can lead to stunted growth and reduction in the overall yield and quality of the seed (Nieuwenhuis and Nieuwelink, 2005; PANNAR, 2013a). Stink bugs and bollworm are known to attack the crop (Dreyer, 2017). Other common pests such as cutworms, snout beetle and nematodes occur naturally in the soil.

Root knot nematodes pose a serious problem in sandy soils of the western Free State and North West growing areas (Dreyer, 2017). During the seedling stage, plants are mainly attacked by cutworms and large false wireworms, which are often difficult to find. Therefore, identifying them and spraying them with appropriate insecticides during the early stages of growth is vitally important (FAO, 2006; PANNAR, 2013a).

Soybeans are also susceptible to various viral and fungal diseases caused by different organisms (Khonje, 2016). Soybean rust is a fungal disease spread mainly by wind that results in premature defoliation and can cause high yield loss. Infection results in fewer filled pods per plant, i.e. an approximate loss of 35% is common if the disease is left untreated (PANNAR, 2013a). Symptoms are usually only seen post-flowering (Nieuwenhuis and Nieuwelink, 2005; PANNAR, 2013a). Infected leaves have small dark brown to reddish brown lesions. Small raised bumps may occur on the lower leaf surface. Plants are most susceptible during the flowering stage when grown in areas with high humidity and air temperatures below 28 °C (SEEDCO, 2018). Fungicides from the triazole chemical group are very effective in controlling soybean rust (PANNAR, 2013a).

Sclerotinia stem rot can occur under wet and cold (11-15 °C) soil conditions that persist for longer than a week. Stem infection is optimal when the flower weaning stage coincides with high humidity and air temperatures (20-25 °C). Charcoal rot can occur in dry conditions and may result in significant losses in some seasons (Dreyer, 2017). Other diseases listed by SEEDCO (2018) are as follows:

- Downy mildew: In severe cases, infected leaves will die and fall off. The disease can also attack the pods and infect the seeds. Symptoms include yellowish-green areas with indefinite borders on the upper leaf surface. The infected areas can enlarge and become brown and papery.
- Damping off: This seed-borne disease causes seed rot before emergence or seedling mortality after emergence. Infected seedlings often have brown, sunken cankers on the leaves, which can become covered with pink spores in moist weather.
- Frogeye leaf spot: The fungus survives in infected crop residues and in infected seeds. Symptoms consist of brown, circular to irregular spots with narrow reddish-brown margins on the leaf surfaces. Lesions can also develop on stems and pods.
- Red leaf blotch: This disease will create dark red spots on the upper leaf surfaces and similar spots, with reddish-brown and dark borders on the lower leaf surfaces.
- Bacterial blight: The bacteria survive in infected crop residues and in infected seeds. It spreads during windy rainstorms and during cultivation if foliage is wet. Plants infected early in the season may be stunted and die. Symptoms in later growth stages include angular lesions, which begin as small water-soaked yellow to light brown spots on the leaves. The centres of the spots will turn a dark reddish-brown to black and dry out. Eventually, the lesions will fall out of the leaf (SEEDCO, 2018).

3.3.1.9 Harvesting

For smallholder famers, labour can be used for harvesting soybean, since the production area is often very small (DAFF, 2010c). It is vitally important that harvesting is done at the right time as a delay in harvesting can result in serious loss due to shattering (DAFF, 2010c). Harvesting is highly dependent on climatic conditions, as well as the choice of cultivar, i.e. early maturing vs late maturing cultivars (PANNAR, 2013a). Harvesting should occur when most of the leaves have been shed, the seed moisture content is 13 to 15%, yet stems are still pliable (FAO, 2006, PANNAR, 2013a). At this stage, only a few of the brown pods may shatter and the kernels will not be dry enough to break (PANNAR, 2013a; DAFF, 2010c). If plants ripen at different times, beans should be harvested from the plants that ripen first, while other plants are left standing to ripen further (Nieuwenhuis and Nieuwelink, 2005). For manual harvesting, ensure that there is sufficient capacity available to reduce the risk of shattering (Dreyer, 2017).

Many commercial farmers believe that soybean should not be harvested by hand, stacking or wind row techniques, since it is labour intensive and time consuming. The recommended harvesting method is to use a self-propelled combine harvester (PANNAR, 2013a). A slow drum speed (450-500 revolutions per minute) is required for soybean (Nieuwenhuis and Nieuwelink, 2005). The concaves must be set wider than for wheat and a slow ground speed (approximately 6 km/h) must be used. The faster the drum speed, the more splits will occur. To further minimise losses, the combine harvester head must be adjusted as low as possible (Nieuwenhuis and Nieuwelink, 2005) in order to cut the plants as close to the soil surface as possible, thus minimising the number of pods left behind (DAFF, 2010c). Pods that are below 12.5 cm from the soil surface cannot be collected by a combine harvester (Dlamini, 2015; DARD, 2016). Hence, cultivars that offer good pod height should be preferred.

3.3.1.10 Crop rotation

Soybean offers many advantages as a rotation crop, particularly in combination with maize in the medium and high potential areas (PANNAR, 2018). Soybean can carry over about 30 to 50 kg of available nitrogen per hectare to the following crop (PANNAR, 2006).

3.3.2 Grain sorghum

3.3.2.1 Rainfall

Climatic criteria for grain sorghum production were gleaned from the available literature by Kunz et al. (2015b) as part of the previous biofuel study. Additional sources of information have been added to Table 122D.2 in Appendix D. In general, sorghum is mainly cultivated in low and erratic rainfall areas, especially on shallow and heavy clay soils (DAFF, 2018d). Sorghum is typically grown in areas that are too dry for maize (DAFF, 2010b). According to Steduto et al. (2012), rainfall of 500-800 mm distributed evenly over the cropping season is normally adequate for cultivars maturing in three to four months. For season lengths of 110 to 130 days, the consumptive water use (evapotranspiration) of sorghum ranges from 450-750 mm, depending on evaporative demand. Optimum conditions occur when monthly rainfall distribution is proportional to monthly crop coefficients (Figure 3.3).

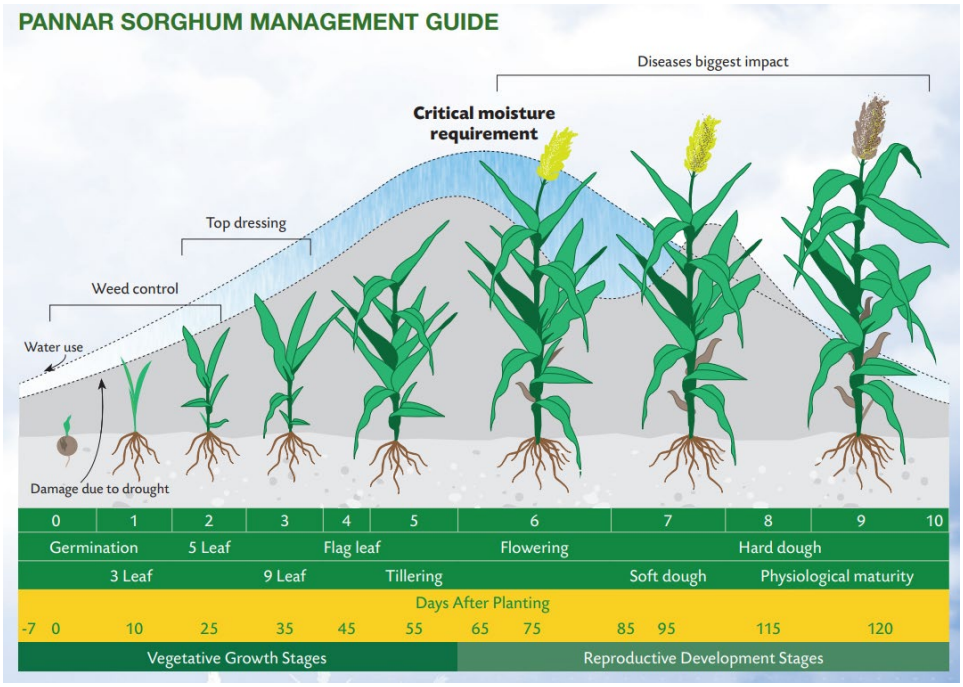

Figure 3.3: Phenological growth stage guide for grain sorghum (PANNAR, 2016)

3.3.2.2 Temperature

In general, sorghum prefers temperate to warm weather (daily maximums of 20 to 30 °C) and a frost-free period of approximately 120 to 140 days (ARC, 2003; Du Plessis, 2008). Sorghum is very sensitive to frost and does not grow well in shade (DAFF, 2009b). Sorghum is less tolerant to cold stress (Dhopte and Eastin, 1990; Rooney, 2004). Daily temperatures below 10 °C will inhibit growth, with 16 °C being the minimum temperature for all physiological processes to occur.

Vegetative stage

Germination: Sorghum's establishment is especially sensitive to cold temperatures, which results in a reduced plant population and grain yield (WMO, 2012). The absolute minimum temperature required for germination varies from 7 to 10 °C. The best time to plant is when there is sufficient moisture in the soil and the soil temperature is 15 °C (at a depth of 10 cm) or higher, considering that 80% of seeds should germinate within 10 to 12 days (ARC, 2003; Du Plessis, 2008; DAFF, 2010b; Steduto et al., 2012). However, other sources (e.g. Du Plessis, 2008; DAFF, 2009b; PANNAR, 2013b) stated that ~18 °C is the minimum temperature to ensure germination. The DAFF (2009b) reported that sorghum seed germinates at daily temperatures of between 20 and 35 °C. This is similar to the temperature range of 21 to 35 °C given by Steduto et al. (2012) and WMO (2012), with temperatures of 40 to 48 °C being lethal.

Three- to five-leaf growth phase: Sorghum plants older than three weeks are less tolerant to low temperatures and may die off at 0 °C. From one to three weeks, plants may recover if exposed to a temperature of -5 °C, but will die if the minimum temperature drops to -7 °C (Du Plessis, 2008; DAFF, 2010b).

Reproductive stage

After emergence, temperatures as low as 21 °C should not have a dramatic effect on growth and yield. However, a temperature range of 27 to 30 °C is recommended for optimum growth (ARC, 2003; Du Plessis, 2008; DAFF, 2010b).

PANNAR (2013b) reported similar ideal temperatures of 25 to 30 °C (with a minimum of 15 °C) and noted that, although the crop can withstand high temperatures better than most other crops, extremely high temperatures during flowering may be detrimental.

Flowering: According to Sorghum Trust (n.d.), the critical initial temperature for tiller formation is 18 °C (temperatures above 18 °C inhibit tiller formation). Reduction of soil temperature in the pollination and grain development periods reduces grain production (WMO, 2012). Hence, flowering occurs best when temperatures are between 22 and 26 °C, and less so when in the range of 17 to 20 °C (DAFF, 2009b). According to WMO (2012), a drop in soil temperature from 26 to 23 °C in the pollination and grain formation phases can result in decreased productivity. This is due to the negative influence of temperature on nutrient absorption and the translocation process. Low (< 15 °C) and high temperatures (> 35 °C) during flowering and grain formation cause reduced yields. Steduto et al. (2012) stated that pollination and fruit setting may fail when night temperatures fall below 12 to 15 °C at flowering. Pollen produced below 10 °C and above 40 °C is most likely non-viable. According to Nishiyama (1995), sorghum yield components are adversely affected when the crop is exposed to cold stress during the reproductive stage. When exposed to air temperatures ranging from 6.6 to 14.4 °C during flowering and grain formation, sorghum showed reduced panicle weight, seed weight and panicle harvest index (Krishnamurthy et al., 2014).

3.3.2.3 Photoperiod

Most sorghums are sensitive to the photoperiod and are classified as short-day plants, where the night must be longer than a critical minimum (WMO, 2012) as short nights retard flower formation. Sorghum plants are at their most sensitive to photoperiod during the flower initiation stage.

The optimum photoperiod that accelerates the start of flower formation is between 10 and 11 hours. Hence, photoperiods longer than 11 hours stimulate vegetative growth, but retard flowering (ARC, 2003; Du Plessis, 2008). However, some sorghum hybrids are not sensitive to the photoperiod (WMO, 2012).

3.3.2.4 Soil type and pH

Although sorghum can tolerate a wide range of soils and even waterlogged conditions, it is best suited to well-drained soils with a pH range of 5 to 8.5 (ARC, 2003; Du Plessis, 2008). PANNAR (2013b) reported a similar pH range of 4.5 to 7.5, whereas SEEDCO (2018) gave a narrower pH of 5.5 to 6.8. Furthermore, the crop is more sensitive to aluminium toxicity than maize and should not be planted on very acid soils, i.e. with an acid saturation of more than 15% (PANNAR, 2013b). However, sorghum is not well suited to sandy soils or long periods of waterlogging. The latter causes significant reductions in transpiration (65-78%) and LAI (69%) (Promkhambut et al., 2010). Land management strategies such as drainage furrows or raised beds can be employed to minimise the negative effects of waterlogging caused by high water tables (Modi and Mabhaudhi, 2017). Compacted soils can limit the plant's ability to survive drought by limiting the development of the rooting system (WMO, 2012).

If no soil impediments occur, roots can reach a lateral distribution of 1 m and a depth of up to 2 m early in the season (DAFF, 2010b; Steduto et al., 2012). The WMO (2012) noted that roots can extend to a depth of up to 1.5 m, even though the plant extracts 75% of its water from the upper metre of soil. Under dryland conditions, the maximum depth is generally reached at the time of flowering, but the roots continue to grow during the reproductive phase. When the soil profile is moist, most of the water is taken up from the top fifth of the rooting zone. As the upper part of the profile dries out, the uptake zone moves progressively downward (Steduto et al., 2012).

Sorghum prefers soils with a clay content of 10 to 30% (ARC, 2003; Du Plessis, 2008; DAFF, 2010b). Soils with a clay content of 25% or more facilitate the use of herbicides for chemical weed control (SEEDCO, 2018). According to PANNAR (2013b), grain sorghum during drought conditions will produce satisfactory yields on soils with a clay content of more than 50%, whereas maize will yield very little grain.

However, based on results for three sorghum genotypes grown over two seasons at Umbumbulu on a soil where the clay content exceeds 60%, Modi and Mabhaudhi (2017) concluded the following:

- Root growth is limited by increased clay content in soils, which results in less soil water extraction by crops.
- High clay contents can negatively affect plant available water due to high soil water retention.
- Clayey soils are susceptible to lower infiltration rates (more runoff loss) and higher risk of waterlogging (which sorghum will tolerate).

3.3.2.5 Fertilization

The nutrient requirements of grain sorghum are similar to those of maize, i.e. similar quantities of nitrogen, phosphorus and potassium are removed from the soil by these two crops. In order to maintain phosphorus and potassium levels in the soil, approximately 15 kg nitrogen, 3 kg phosphorus and 4 kg potassium should be added to the soil per ton of harvested crop (PANNAR, 2013b; Steduto et al., 2012). However, SEEDCO (2018) stated that 7 kg of phosphorus is removed from the soil per ton of grain produced (Table 3.6).

Table 3.6: Nutrient removal and uptake per ton of harvested sorghum grain (SEEDCO, 2018)

Nutrient	Removal	Uptake
Nitrogen	18 kg	30 kg
Phosphorus	7.2 kg	10 kg
Potassium	5.4 kg	30 kg

For the growth and development of sorghum, nitrogen is considered critical (Ruthrof et al., 2018). Soils with a low nitrogen content result in delayed crop development, thus increasing the risk of drought exposure and subsequent yield loss prior to physiological maturity (Buah et al., 2012). Recommendations for nitrogen application are usually based on the target yield, with more fertilizer required for sandy soils and for crops grown in the wetter (eastern) growing regions, when compared to the drier (western) regions. Buah et al. (2012) determined the response of grain sorghum to applications of nitrogen and found that an application of 40 kg nitrogen ha^{-1} resulted in yield increases of 47% relative to no nitrogen. Nitrogen increases early seedling vigour, LAI, chlorophyll concentration and plant height. In addition, nitrogen catalyses the conversion of carbohydrates into protein and protoplasm, resulting in increased biomass and grain yield (Buah et al., 2012).

In general, sorghum is sensitive to low phosphorus and potassium levels in the soil, which should thus be corrected with fertilizer application (DAFF, 2010b). Phosphorus is also usually applied in the band, except where the required quantity exceeds the amount applied in the fertilizer mixture. The optimal phosphorus concentration under conditions where 5-11 kg of phosphorus ha^{-1} is applied in the band at planting was determined as approximately 17 mg of phosphorus kg^{-1} for most regions. In order to raise the “phosphorus requirement” or soil phosphorus concentration by 1 mg phosphorus kg^{-1} (Bray 1 test), 5, 7 and 9 kg of phosphorus ha^{-1} should be applied on soils with clay contents less than 10%, 10-20% and 21-35%, respectively (PANNAR, 2013b).

For potassium, analyses should be undertaken to determine the status of the soil. The optimum concentration is at least 80 mg of potassium kg^{-1} of soil. If the topsoil potassium concentration is low (less than ~40 mg of potassium kg^{-1}), then 12-50 kg of potassium ha^{-1} is recommended. If the soil is sandy (less than 10% clay) and the topsoil potassium concentration is low, the subsoil potassium concentration should also be determined. Potassium is normally placed in the band using fertilizer mixtures.

However, high, mixed applications of potassium and nitrogen in the band should be avoided and should thus not exceed 70, 50 and 30 kg ha^{-1} for row widths of 0.9, 1.5 and 2.1, respectively. If potassium requirements are too high to place in the band, a portion can be spread before planting (PANNAR, 2013b).

Rotation with leguminous crops (e.g. soybean) may provide low-cost nitrogen addition and fertility build-up. Low grain protein can result when nitrogen deficiency occurs between anthesis and maturity. The crop thus responds well to nitrogen application (DAFF, 2009b; WMO, 2012). If fertilizer is applied in the band at planting, levels should not exceed the following (PANNAR, 2013b):

- 40 kg nitrogen ha^{-1} for 0.9 m row widths
- 30 kg nitrogen ha^{-1} for 1.5 m row widths
- 20 kg nitrogen ha^{-1} for 2.1 m row widths

Overall, sorghum responds well to a low application (100 to 300 kg ha^{-1}) of basal fertilizer, followed with a top dressing of 100 to 200 kg ha^{-1} of 28 to 34% nitrogen fertilizer. Before planting, the basal fertilizer is broadcast, then incorporated into the soil by disking (SEEDCO, 2018).

3.3.2.6 Planting

For information on planting date and planting density, the reader is referred to Section 10.3.2 and Section 10.4.2, respectively. Seeds should be planted to a depth of 1.5 to 5 cm (DAFF, 2009b). A planting depth of 5 cm is recommended for drier or sandy soils, compared to 2.5 cm for clayey soils (ARC, 2003; Du Plessis, 2008; DAFF, 2010b). The DAFF (2009b; 2010b) also recommends that when planting in dry soils, soil compaction may be necessary to ensure moisture absorption by the seed. After germination, thinning is required to establish an in-row spacing of 15 to 20 cm before tilling begins (usually four weeks after emergence). However, gap filling may be required if the seed does not germinate or seedlings are affected by disease.

3.3.2.7 Weed control

The sorghum plant grows very slowly in the early stages and is easily suffocated by weeds (PANNAR, 2013b). Hence, sorghum seedlings are very sensitive to weed competition, which should be avoided at all costs (PANNAR, 2018). Weed control during the first six to eight weeks after planting is crucial, as weeds compete vigorously with the crop for nutrients and water during this period (Du Plessis, 2008; DAFF 2009b; DAFF, 2010b). Grain sorghum is very sensitive to herbicides such as 2.4-D and Atrazine under certain conditions (PANNAR, 2013b).

Under low-input farming conditions (i.e. on smallholder farms), the root parasite *Striga asiatia* (L.) Kuntze (witchweed or rooiblom) can damage the crop. Most of the damage is done before the parasite emerges from the soil as a single-stemmed plant with bright red flowers. Sorghum will exhibit symptoms of water stress, which includes leaf wilt, leaf roll and leaf scorch, even though the soil has sufficient water. Striga's tiny seeds remain viable in the soil for 15 to 20 years and are dispersed by wind, water and animals. Rotation with cotton, groundnut, cowpea and pigeon pea will reduce the incidence of Striga. Manual weeding of the parasitic plant before it flowers is also recommended (ARC, 2003; Du Plessis, 2008; DAFF, 2010b). Research is currently underway in Tanzania to breed for resistance to Striga, combined with the use of a fungus (biological control agent). When applied to the seed, the fungus kills Striga when it attacks the roots of sorghum plants (ACCI, 2018).

3.3.2.8 Pest and disease control

According to Coleman (2012), the risk of planting sorghum is higher than that of maize in terms of possible damage by pests and diseases. Using disease-free or certified seed sources can reduce susceptibility to various diseases (DAFF, 2009b). For example, the choice of cultivars resistant to, inter alia, downy mildew, leaf spot, leaf blight, bacterial stripe, anthracnose and head smut offers the best preventative measures (PANNAR, 2013b).

The fungal disease that is possibly of greatest economic concern to the farmer is ergot or "sugary disease". Wet and cool conditions, as well as late plantings, favour infection and the spread of this disease. Hence, ergot is more prevalent in the higher rainfall and cooler production areas. Fungal spores spread to adjacent flowers by wind, rain and insects, which explains the rapid development of this disease (PANNAR, 2013b). Fungicide use is recommended if outbreaks becomes severe in order to avoid yield loss. Moderate air temperatures, wet conditions or heavy dew increase susceptibility to leaf blight (SEEDCO, 2018).

Grain crops such as sorghum and maize are susceptible to various insect pests such as stalk borers, with field infestations above 10% having economic impact (ARC, 2003; Du Plessis, 2008; DAFF, 2009b; DAFF, 2010b). According to PANNAR (2013b), the grain sorghum stalk borer (*Chilo partellus*) is more difficult to control than the maize stalk borer (*Busseola Fusca*) due to the higher number of life cycles per annum. Early October and especially late December/January plantings are most susceptible to infestation. Pesticide use is absolutely essential for the timely control of both pests. Stalk borer should be treated use Trichlorfon or Endosulfan granules applied in the funnels at three to six weeks after planting. Alternatively, spray into the funnels with Carbaryl (SEEDCO, 2018).

It is important to scout for aphids and bollworm during head emergence and grain-filling periods. Although timely control of aphids is very important, spraying is not necessary when the pest is first observed. When virtually all plants are infested (usually after a population explosion in December/January), spraying is necessary to ensure that the crop is aphid-free during the grain-filling stage (ARC, 2003; DAFF, 2010b). According to SEEDCO (2018), aphids can be sprayed with Dimethoate or Mercaptothion.

Sorghum is also prone to other pests such as maize beetle, spider mites and shoot fly. Spider mites should be treated with Acaricides, whereas hoot fly outbreaks on one- to four-week-old seedlings can be treated with Thionex and Carbaryl (SEEDCO, 2018). Hybrids with an open-type panicle (e.g. PAN8816) facilitate spraying, making it easier to control infestations. Since bollworm is resistant to most synthetic pyrethroids, two different chemical groups should be used in combination to control the pest (PANNAR, 2018). DAFF (2009b) recommends spraying when an average of two larvae are noticed per panicle.

3.3.2.9 Bird damage

Isolated or small areas of sorghum are prone to bird damage (ARC, 2003). The African Centre for Crop Improvement (ACCI, 2018) states that “birds love sorghum and are very problematic because they can decimate a field”. Kunz et al. (2015a) also noted that small stands of zero-tannin cultivars of grain sorghum are cause for concern due to possible bird damage. Grain sorghum trials conducted at Ukulinga and Hatfield in the 2012/13 season and at Ukulinga in the 2013/14 season were severely affected by feeding birds at both establishment and grain filling. Modi and Mabhaudhi (2017) stated that short genotypes (e.g. PAN8816) were susceptible to panicle destruction by large birds (e.g. guinea fowls) as the panicle was within reach. Rethman et al. (2007) also reported that sorghum grain was consumed by birds during the 1999/2000 season at Hatfield.

Possible damage from red-billed queleas (*Quelea quelea*) is a serious threat to grain crops in South Africa (Oschadleus and Underhill, 2006). Hence, queleas were declared pests in the Agricultural Pests Act, Act No. 36 of 1983. Steyn (2011) reported that queleas can eat around 10 g of grain per day, which means an average quelea flock can rapidly decrease sorghum yields from 5 to 1 t ha^{-1}. The birds have recently expanded into regions where previous sightings were uncommon. For example, Oschadleus (2015) recorded the first breeding of quelea in the Western Cape near Worcester. Coleman (2017) reported that all grain producers are urgently required to report quelea breeding and roosting spots to the Department of Agriculture, Land Reform and Rural Development.

3.3.2.10 Harvesting

When seeds reach the milk to dough stage, sorghum can be harvested manually (cutting by hand) or mechanically (with a combine harvester). Panicles are dried in heaps on the ground or threshing floor for 10 to 14 days. Sorghum grain can only be threshed when seed moisture is below 20 to 25%, even though the seed is physiologically mature at higher moisture levels of 30 to 35% (Steduto et al., 2012). Once the seed moisture content is 12 to 13% (or less), permanent storage in silos is recommended (DAFF, 2009b; DAFF, 2010b).

For seed drying, the absolute maximum air temperature is 40 °C. However, in order to reduce the risk of heat damage to the seeds, drying temperatures should be lower than 40 °C. If seed moisture is more than 18%, maximum drying temperature should be 32 °C, and if lower than 18%, 40 °C is the recommended temperature for drying (Reddy et al., 2008).

Sorghum’s harvest index is more variable than that of maize, mainly because of variable tilling in sorghum. Generally, reported harvest index values are low (0.3 to 0.4), but higher harvest index values (more than 0.5) have been observed and may be the result of vegetative (tiller) growth, which is affected by cultivar-specific water stress (Steduto et al., 2012).

3.3.2.11 Intercropping

Rethman et al. (2007) conducted trials at Hatfield over four seasons to determine the effects of competition between alley-cropped forage sorghum and *Leucaena leucocephala* hedgerows. Although the overall average yield of intercropped stands was lower than pure stands, central rows outperformed pure stands.

No statistical differences were obtained when sorghum yields were analysed relative to the previous crop (sweet potatoes or cowpeas), although intercropping reduced alley crop yields in most instances. The benefits of diversity often led to financial advantages when compared to pure stands. In rural, semi-arid areas, intercropping offers the community a safer and – in many cases – more lucrative alternative to monoculture (Rethman et al., 2007).

Modi and Mabhaudhi (2017) highlighted from their literature review (e.g. Zougmore et al., 2000) that intercropping may benefit rainfed production systems of sorghum due to a reduction in runoff when planted with cowpea. Based on a trial conducted at Ukulinga over two seasons, Modi and Mabhaudhi (2017) showed that intercropping with cowpea improved the following:

- Soil water availability by reducing soil water evaporation (i.e. live mulch)
- Water use efficiency of sorghum grain when compared to the sorghum-only treatment
- Plant height and leaf area of sorghum

Intercropping resulted in reduced tiller number since tilling in sorghum is more pronounced in conditions of low soil water availability. The authors concluded that intercropping of sorghum is beneficial, especially in regions with low and variable rainfall patterns. Hence, sorghum-cowpea intercropping should be recommended as a viable water management strategy in semi-arid regions or environments with low water availability.

3.3.2.12 Crop rotation

Sorghum is sensitive to nematodes (especially on sandy soils) and must therefore not be grown continuously or in close rotation with maize. A break of two to three years between sorghum crops is recommended by rotating with broadleaf crops such as soybean or groundnuts (SEEDCO, 2018).

3.4 BEST MANAGEMENT PRACTICES

3.4.1 Soybean

Based on the results from the Swayimane soybean trials (cf. Chapter 6 and Chapter 8) and other literature, the following best management practices for soybean are recommended:

- Farmers are encouraged to conduct germination tests to evaluate seed quality and viability prior to planting, considering that soybean seed is sensitive to high temperatures during storage.
- Inoculation did not result in significant differences in final biomass and yield of soybean. However, it significantly improved the stomatal conductance and chlorophyll content index of both soybean cultivars (LS6161R and CAPG3). Hence, farmers are encouraged to use inoculants. Smallholder farmers generally do not inoculate legumes due to the unaffordability of inoculants, as well as a lack of knowledge on how to use them. There is a need to also train farmers on how to use inoculants and to assist with this, a guide is provided in Appendix E.
- Inoculants reduce fertilizer costs by negating the need to apply nitrogen. This implies an economic benefit associated with inoculant use.
- Research has shown that inoculation use without application of PK fertilizers is not beneficial for growth. Furthermore, soil pH should be 5.2 to 6 for inoculants to work properly.
- Results from this project showed that mulching reduced the fluctuation in soil water content of the topsoil, as well as significantly improving chlorophyll content and leaf number. Although no significant differences were observed for stomatal conductance, LAI, biomass and yield of soybean under hay mulch, many studies have found positive benefits of mulching. For example, it helps reduce surface runoff, which in turn reduces soil erosion. Therefore, mulch should be considered by smallholder farmers, especially under rainfed conditions where water is a major limiting factor.

- Under rainfed conditions, rainwater harvesting and soil water conservation techniques such as those demonstrated in this project (e.g. mulching) would go some way in improving soil water availability. However, greater thought should be given to the selection of techniques as there may be negative trade-offs with crop yield.
- Under rainfed conditions, rainfall variability is an important determinant of crop yield. Thus, planting date selection is critical to ensure that critical growth stages do not coincide with dry spells. This would be completed by *in situ* rainwater harvesting and soil water conservation techniques to improve soil water availability.
- While results obtained in this project did not show any significant benefits of fertilization, farmers are still encouraged to apply optimum levels of fertilizers based on soil fertility recommendations. The lack of significant differences found in this project may be due to trade-offs between mulching and nitrogen mineralisation, as well as a fungal disease that may have been transferred from the hay mulch.
- Weeds are an important yield-limiting factor, especially during the early establishment stage before the plant canopy has closed. Thus, the use of pre-emergence herbicides prior to planting would be ideal and mitigate labour demands associated with weeding under smallholder conditions.
- In the 2015/16 season, a yield of 1.6 t ha^{-1} was obtained from the non-mulched treatment. This yield was not economically viable, since a break-even yield of 1.8 t ha^{-1} was calculated for soybean (cf. Section 3.5.1). However, the 2018/19 trial yielded 4.3 ha^{-1} for the same cultivar (LS6161R) at the same location. Both yields represented fully fertilized and non-inoculated conditions. The yield difference is due to planting density (266,667 vs 317,460 plants ha^{-1}), as well as better crop management in the latter season. Hence, smallholder farmers are encouraged to apply fertilizer at the start of the season, keep the plots completely weed-free (especially during the vegetative growth stage) and undertake preventative sprays for soybean rust after flowering.
- Results showed that there were significant differences (in chlorophyll content index, stomatal conductance, canopy cover and seed yield) between the two soybean cultivars tested. Agro-ecologies similar to Swayimane are better suited to an early-medium-maturing, semi-determinant cultivar (e.g. LS6161R), compared to a medium-late-maturing, indeterminant cultivar (e.g. CAPG3).
- The LS6161R cultivar is better suited to biofuel production due to its higher yield potential when compared to CAPG3. In addition, both mulching and inoculation improved the seed oil content of this cultivar, which means higher biodiesel yields.

3.4.2 Grain sorghum

Based on results from the Swayimane trial (cf. Chapter 7), the following best management practices for grain sorghum are recommended:

- Fertilizer use resulted in significant differences in stomatal conductance, but not in biomass accumulation, final biomass or grain yield, as well as harvest index. The soybean trial in the 2015/16 season also showed no significant differences due to fertilizer use. This could be due to the buffer capacity of the soil at Swayimane. Fertilization of sorghum is thus still recommended.
- Significant differences in leaf number, chlorophyll content index, time to physiological maturity, final biomass and grain yield (and harvest index) were found between the three sorghum genotypes. PAN8906 outperformed PAN8816 and Macia, and is thus highly recommended for biofuel production.
- The late (i.e. January) planting at Ukulinga resulted in cold and water stress, and is thus not recommended in similar agro-ecologies.
- The study demonstrated that grain yield is an important factor influencing biofuel production. Although PAN8816 had the highest extractable starch content and fermentation efficiency, PAN8906 produced a greater theoretical biofuel yield due to its higher yield. This again highlights the suitability of PAN8906 for biofuel production.
- Macia produced a relatively high proportion of biomass to grain, and may thus not be a suitable feedstock for biofuel production.

Based on results from Ukulinga (as part of another WRC project) (Modi and Mabhaudhi, 2017) and other literature, the following best management practices for grain sorghum are recommended:

- Best management strategies under rainfed agriculture optimise plot yield and crop water use efficiency. The Ukulinga study identified key efforts to better use variable rainfall received during and between planting dates. These include improved rainwater capture and infiltration, the reduction of water losses through evaporation, runoff and deep percolation, water use efficiency improvement by choice of water-efficient cultivars, and spatial and temporal arrangements (intercropping and rotations), and the reduction of transpiration through weed control or windbreaks.
- Current results showed that mid-season and early planting, respectively, are recommended for rainfed sorghum cultivation in similar agro-ecologies. Late-season planting risks increased rainfall variability and petering out of the rainy season, thus exposing the crop to frequent intermittent stress episodes. Late-season planting would be recommended in areas where farmers have access to irrigation to supplement rainfall.
- From a cultivar choice perspective, PAN8816 should be sown when planting early- and mid-season to attain early crop establishment, high emergence, and high canopy cover, as well as high, stable yields under variable rainfall. Planting an early-maturing cultivar (approximately 105 days to maturity) is recommended for late planting to escape terminal stress as the season comes to an end.
- Low and delayed emergence, and low canopy cover contribute to high unproductive water losses because of soil evaporation. Strategies to conserve soil moisture and increase soil cover should be applied at all planting dates to decrease unproductive water losses and reduce incidences of water stress at key developmental stages. Different types and levels of mulching and different low tillage strategies are recommended. Low cost mulching (e.g. dry grass) should be explored by subsistence farmers. In regions that experience high wind speeds, the growing of perimeter vegetation 3 m or higher should be explored as a long-term strategy to reduce transpiration.
- Different long- and short-term strategies should be explored to capture and better use excess rainfall from storm events. Rainfall must be retained by techniques that reduce storm-water runoff, improve infiltration and increase the water storage capacity of the soil. Strategies that can help reduce runoff through improved infiltration capacity and soil transmission characteristics include mulch farming, soil conditioning, the planting of cover crops, alley cropping, no-tillage farming practices and ploughing methods that keep the upper soil layers porous at least for a short time, especially in compact soils that restrict root development and infiltration. Of these recommendations, low-cost mulching and no-tillage practices are attractive, affordable strategies for subsistence farmers. Various strategies can also be explored to reduce runoff by controlling water movement over the surface. Examples include contour farming, ridge and mound tillage, strip farming and terrace farming. Ridging is particularly recommended for subsistence farmers with small land holdings. A recommended long-term strategy for water capture is rainwater harvesting for the supplementary irrigation of sorghum during dry spells. Rainwater water harvesting is beneficial, especially for the late planting of sorghum.
- Weather is known to vary between growing years, which affects the selection of planting dates. Access to seasonal weather forecasts is recommended to aid farmers' management practices, planning and selection of planting dates.

Based on the results from a scenario analysis reported by Modi and Mabhaudhi (2017) for two sorghum genotypes (PAN8816 and Ujiba) across 10 different planting dates and three agro-ecologies (Deepdale, Richards Bay and Ukulinga), the following best management practices for grain sorghum are recommended:

- Based on scenario analyses for the three agro-ecologies, production of sorghum is suited for Deepdale and Ukulinga agro-ecologies. At Richards Bay, high evaporation losses resulted in low yields. This area is thus unsuitable for sorghum production.

- Based on model simulations, optimal planting dates for sorghum at Ukulinga range from early September to late November (which produced high and stable yields). Planting in December and January resulted in less biomass, yield, water productivity and stability.
- Transpired water (less than 265 mm) for all planting dates and agro-ecologies was significant. Considerable yield improvement can be achieved through the effective capture, storage, supplementary irrigation and re-use of rainwater. Rainwater harvesting can be used to capture rainfall during and outside the growing season. Richards Bay sorghum farmers would benefit most from such strategies as transpiration was low throughout planting dates, since water scarcity-linked crop failure occurred frequently and the agro-ecology has a longer rainfall season.
- Sorghum farmers in Deepdale and Ukulinga can explore increasing planting population to exploit high evaporated water. Increasing planting population, however, increases demand for other resources such as soil nutrients and minerals. Therefore, appropriate soil fertilization mechanisms are recommended together with this strategy. In Richards Bay, farmers need to focus on strategies that maximise transpiration. Intercropping sorghum with a legume could be recommended to effectively use evaporated water in all three agro-ecologies. Ideally, the legume of choice should have low water requirements and a short growing season (≈90 days).
- Different levels of mulching and low tillage farming practices are suggested to conserve soil moisture and increase soil cover. The extent to which each strategy is used would largely depend on rainfall per growing season and evaporation, which differ per agro-ecology and planting date. This strategy is especially recommended when farming sorghum outside the optimal planting dates recommended by this study.
- Contour farming, ridge and mound tillage, strip farming and terrace farming are options that are suggested to reduce runoff during extreme rainfall events.

Based on scenario analyses conducted with the APSIM and AquaCrop models, Modi and Mabhaudhi (2017) suggested the following best management practices for a sorghum-cowpea intercrop system:

- To achieve high water use efficiency, early planting (15 September) and late planting (15 January) in low-rainfall and high-rainfall areas, respectively, is recommended.
- The ideal plant population of sorghum should be 39,000 plants·ha^{-1} in combination with 13,000 plants·ha^{-1} of cowpea.
- When yields of both crop species are desired, increasing the cowpea plant population to 19,500 plants·ha^{-1} is recommended.

3.5 ENTERPRISE BUDGETS

For this project, it was important to develop enterprise budgets (on a per-hectare basis) to determine the profitability of feedstock cultivation in communal farming areas. Hence, an economic analysis was undertaken for soybean and grain sorghum to determine the expected income, as well as the associated input costs (both fixed and variable).

It is important to note that the prices indicated in the following budgets are based on the following:

- General averages
- Interest at a rate of 5.25% per annum
- Costs applicable to 2016/17 (not updated to 2019)
- Casual labour costs as 2.5 labour hours per operation x six operations x R16.25 per hectare x 12.195, i.e. 10,000 m^2/820 m^2
- Certain information is obtained from http://www.grainsa.co.za/pages/industry-reports/production-reports

3.5.1 Soybean

The enterprise budget presents costs and income estimates for producing a hectare of soybean (Table 3.7). The estimated yield for the soybean crop ranges from 1.3 to 2.5 t ha^{-1}. Considering the 1.3 t ha^{-1} scenario, for example, the results show that the value of the gross production is R6,184 per hectare. The product price of R4,757 per ton in 2016/17 was offered for the best grade of the crop. As the estimated yields increase, the variable cost also increases, but the overhead costs remain constant.

Table 3.7: Enterprise budget of expected income and costs for soybean

Producer price framework for dryland soybean for the production year 2016/17							
Current product price for the best grade (minimum marketing cost) = R4,757 t^{-1}							**Field trial**
Estimated yields (t ha^{-1})	1.3	1.5	1.8	2.0	2.3	2.5	3.2
Gross production value (R ha^{-1})	6,184	7,136	8,563	9,514	10,941	11,893	15,222
Direct allocated variable costs (R ha^{-1})							
Seed	859	859	859	859	859	859	2,145
Fertilizer	732	853	973	1,093	1,214	1,334	1,411
Lime	355	355	355	355	355	355	
Fuel	772	783	793	804	814	824	
Preparation	615	617	619	621	622	624	
Herbicide	248	248	248	248	248	248	512
Pest control	201	201	201	201	201	201	327
Input insurance	116	139	162	186	209	232	
Grain hedging	316	337	358	380	401	422	
Contract harvesting – combine hire	-	-	-	-	-	-	-
Harvest insurance	800	959	1,119	1,279	1,439	1,599	
Land preparation	-	-	-	-	-	-	450
Transportation	-	-	-	-	-	-	272
Interest on production (R ha^{-1})	263	281	299	316	334	352	321
Total direct allocated variable cost (R ha^{-1})	**5277**	**5,631**	**5,986**	**6,341**	**6,695**	**7,050**	**6,439**
Total direct allocated variable cost (R t^{-1})	**4059**	**3,754**	**3,326**	**3,170**	**2,911**	**2,820**	**2,012**
Total overhead cost (R ha^{-1})	**2422**	**2,422**	**2,422**	**2,422**	**2,422**	**2,422**	**2,422**
Total cost before marketing cost (R ha^{-1})	**7698**	**7,698**	**7,698**	**7,698**	**7,698**	**7,698**	**7,698**
Total cost before marketing cost (R t^{-1})	**5922**	**5,132**	**4,277**	**3,849**	**3,347**	**3,079**	**2,406**
Total marketing cost (R t^{-1})	**63**	**63**	**63**	**63**	**63**	**63**	**63**
Expected minimum price, without profit	**5985**	**5,195**	**4,340**	**3,912**	**3,410**	**3,142**	**2,469**
Current price (R t^{-1})	**4820**	**4,820**	**4,820**	**4,820**	**4,820**	**4,820**	**4,820**

The trial yield of 3.2 t ha^{-1} was obtained for soybean cultivar LS6161R at Baynesfield in the 2016/17 season from 20 ha of land (cf. Section 6.3.2). Since the total direct allocated variable costs do not exceed the current price, it is possible to break even. The break-even figures in Table 3.8 show that target yield options of 1.3 t ha^{-1} and 1.5 t ha^{-1} do not have expected yields that exceed their break-even yields and are thus not commercially viable. From Figure 3.4, the break-even yield is 1.77 t ha^{-1}, which is based on a current price in 2016/17 of R4,820 per ton.

Table 3.8: Break-even analysis of soybean yields

Target yield (t ha^{-1})	1.30	1.50	1.80	2.00	2.30	2.50	3.20
Break-even yield at current price (R4,820 t^{-1})	3.47	2.42	1.69	1.53	1.31	1.25	0.88
Viable	**N**	**N**	Y	Y	Y	Y	Y

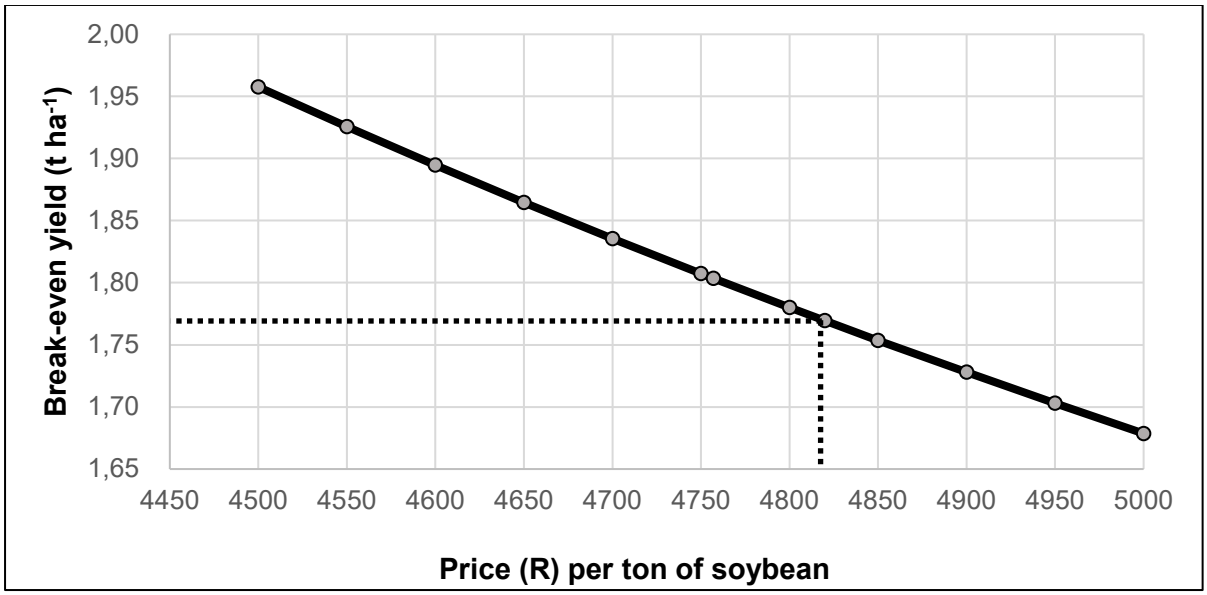

Figure 3.4: Break-even yield of soybean vs current price in 2016/17

3.5.2 Grain sorghum

The enterprise budget presents cost and income estimates for producing a hectare of sorghum (Table 3.9). The estimated yield for the sorghum crop ranges from 2 to 4 t ha^{-1}. The results show that the value of the gross production is R5,074 ha^{-1} for the minimum yield of 2 t ha^{-1}. The product price of R2,537 per ton in 2016/17 was offered for the best grade of the crop. The variable cost increases as the estimated yield increases. The overhead costs remain constant.

Table 3.9: Enterprise budget of expected income and costs for grain sorghum

Producer price framework for dryland grain sorghum for the production year 2016/17							
Current product price for the best grade (minimum marketing cost) = R2,537 t^{-1}						**Field trial**	
						No fertilizer	**With fertilizer**
Estimated yields (t ha^{-1})	2.0	2.5	3.0	3.5	4.0	1.6	2.6
Gross production value (R ha^{-1})	**5,074**	**6,343**	**7,611**	**8,880**	**10,148**	**4,130**	**6,561**
Direct allocated variable costs (R ha^{-1})							
Seed							
Fertilizer	309	347	386	386	425	309	347
Lime	809	928	**1,273**	**1,574**	1,944		809
Fuel	319	319	319	319	319		
Preparation	847	862	878	893	908		
Herbicide	618	622	626	630	635		
Pest control	565	565	565	565	565	565	565
Input insurance	543	543	543	543	543	576	576
Grain hedging	95	119	143	166	190		
Contract harvesting	351	371	409	441	482		
Harvest insurance	-	-	-	-	-		
Aerial spray	169	212	254	297	339		
Drying cost	-	-	-	-	-		
Packaging and packaging material	-	-	-	-	-		
Interest on production (R ha^{-1})	243	257	283	305	333	76	121
Total direct allocated variable cost (R ha^{-1})	**4,869**	**5,145**	**5,679**	**6,119**	**6,683**	**1526**	**2418**
Total direct allocated variable cost (R t^{-1})	**2,434**	**2,058**	**1,893**	**1,748**	**1,671**	**937**	**935**
Total overhead cost (R ha^{-1})	**2,641**	**2,641**	**2,641**	**2,641**	**2,641**	**2,641**	**2,641**
Total cost before marketing cost (R ha^{-1})	**7,510**	**7,787**	**8,320**	**8,760**	**9,324**	**4,167**	**5,059**
Total cost before marketing cost (R t^{-1})	**3,755**	**3,115**	**2,773**	**2,503**	**2,331**	**2,560**	**1,956**
Total marketing cost (R ha^{-1})	**63**	**63**	**63**	**63**	**63**	**63**	**63**
Expected minimum price, without profit	**3,818**	**3,178**	**2,836**	**2,566**	**2,394**	**2,623**	**2,019**
Current price (R t^{-1})	**2,600**	**2,600**	**2,600**	**2,600**	**2,600**	**2,600**	**2,600**

The trial yields of 1.63 (unfertilized) and 1.59 t ha^{-1} (fertilized) were obtained for sorghum cultivar PAN8906 at Swayimane in the 2017/18 season (cf. Section 7.3.2). Since the total direct allocated variable costs do not exceed the current price, it is possible to break even. The break-even figures in Table 3.10 show that target yield options of 2-3 t ha^{-1} do not have expected yields that exceed their break-even yields and are thus not commercially viable. Similarly, the trial yield obtained without fertilizer use was also not viable. From Figure 3.5, the break-even yield is 3.43 t ha^{-1}, which is based on a current price in 2016/17 of R2,600 per ton.

Table 3.10: Break-even analysis of sorghum yields

Fertilizer use (Y/N)?	Y	Y	Y	Y	Y	**N**	Y
Target yield (t ha^{-1})	2.00	2.50	3.00	3.50	4.00		
Field trial yield (t ha^{-1})						1.63	2.59
Break-even yield at current price (R4,600 t^{-1})	25.8	5.52	4.10	3.35	3.05	1.65	1.65
Economically viable (Y/N)?	**N**	**N**	**N**	Y	Y	**N**	Y

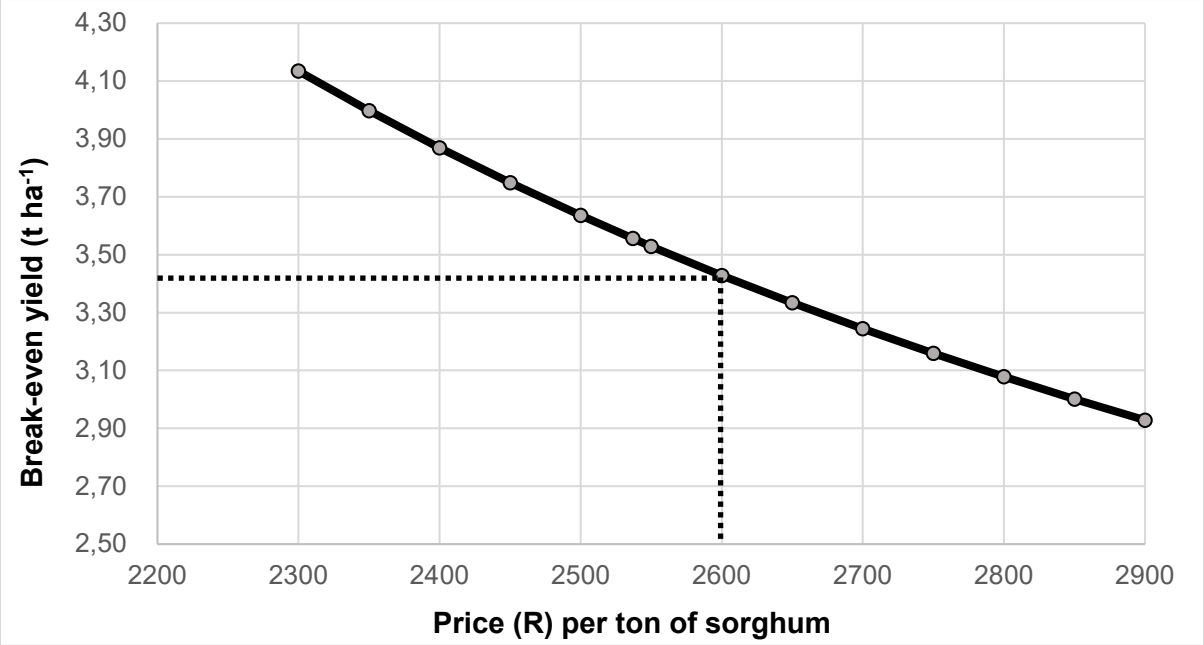

Figure 3.5: Break-even yield of sorghum vs current price in 2016/17

3.5.3 Summary and conclusions

The above enterprise budgets reflect the costs of production associated with the respective field sites (Baynesfield and Swayimane), based on the specific agronomic requirements of each crop. Using market-related data based on the prices obtained in each study area, improved costing of all the input and producer prices was achieved, thereby increasing the overall accuracy of the budgets for the field sites. However, the variation in costs for grain sorghum are due to the size of the field trial conducted at Swayimane. The figures shown in the table were scaled up from the plot size to a hectare for comparison purposes. Potentially, this can drastically distort the budget. As such, the trial would not be at the same economical level as conducting the same trial on a hectare of land. Furthermore, different technologies were used to produce and harvest the crop, i.e. casual labour vs machines for operations.

CHAPTER 4: FEEDSTOCK WATER USE EFFICIENCY

Global demand of domestic freshwater is constantly increasing due to population expansion (Ritchie and Basso, 2008). With limited water resources, efficient water use is essential (Gheewala et al., 2011). With an average rainfall of below 500 mm (Lynch, 2004), South Africa is considered a semi-arid country. Semi-arid regions are characterised by low average annual rainfall (400-600 mm), high temperatures and a crop-growing period ranging from 70 to 180 days (Palmer and Ainslie, 2006), with the rest of the year having higher evaporation than precipitation (Fischer et al., 2009). These growing conditions have adverse implications on rainfed agriculture as water availability for plant growth is limited and unreliable.

With limited water resources, efficient water use in agriculture is essential to maximise agricultural productivity (Gheewala et al., 2011). Improving WUE means that higher crop yields should be obtained using less and/or the same amount of water, i.e. “more crop per drop”. This can be achieved by ensuring that available water is used productively in a way that favours biomass accumulation and yield maximisation. Improving WUE can help contribute to economic growth and poverty reduction by narrowing yield gaps (Janda et al., 2012). In this section, the definition of water use efficiency is given, together with an explanation of how the term was derived.

4.1 INTRODUCTION

Since many different definitions of WUE exist in the literature, it is important to clarify the specific definition of WUE adopted in this project, as well as the methods (and units) used to quantify this term. The plethora of definitions of WUE is due, inter alia, to the many ways in which water use and yield can be defined.

4.2 WATER USE EFFICIENCY OF CROP PRODUCTION

Water use efficiency of crop production (WUE_C in kg m^{-3}) is defined as the ratio of dry crop yield (Y_C in kg ha^{-1}) pertaining to the utilisable portion of the total biomass to the accumulated water (evapotranspiration (ET) in m^{-3} ha^{-1}) from the crop over the growing season:

$$WUE_C = \frac{Y_C}{ET} \qquad \text{Equation 1}$$

The definition of yield is governed by the technology used to produce the biofuel. For example, first-generation technologies convert the utilisable portion of the biomass (i.e. stem, tuber, fruit, grain or seed) that contains sugar, starch or vegetable oil) into biofuel. On the other hand, second-generation technologies are interested in the entire above-ground biomass for biofuel production, and thus prefer to quantify feedstock yield in volumetric units.

Crop evapotranspiration (crop water use) refers to water lost through crop transpiration, soil water evaporation and canopy interception (Kunz et al., 2015a). These three processes occur simultaneously and are difficult to measure separately. Interception is the portion of water lost when the canopy or crop residue retains precipitation, which then evaporates into the atmosphere without recharging the soil’s water content. According to Molden et al. (2010), transpiration is the transfer of water vapour from plants to the atmosphere and is considered productive water use, since higher transpiration results in higher biomass production, and subsequently, higher crop yield. On the other hand, soil water evaporation is the transfer of water vapour from the soil surface to the atmosphere and is an unproductive loss because it reduces soil water that would otherwise be used for transpiration. The transpiration rate is related to canopy cover (number and leaf area), whereas soil water evaporation is proportional to the area of uncovered soil (Voloudakis et al., 2015)

4.3 WATER USE EFFICIENCY OF BIOFUEL PRODUCTION

Water use efficiency of biofuel production (WUE_B in ℓ m^{-3}) is defined as the ratio of the theoretical biofuel yield (Y_B in ℓ ha^{-1}) to the accumulated water (evapotranspiration in m^{-3} ha^{-1}) from the crop over the growing season:

$$WUE_B = \frac{Y_B}{ET} \qquad \text{Equation 2}$$

For soybean, Y_B represents the biodiesel yield estimated using the equation given in Section 12.1, which requires the seed oil content (measured in a laboratory at the University of KwaZulu-Natal). Similarly, Y_B also represents the bioethanol yield obtained from grain sorghum and was estimated using the equation given in Section 12.2, which requires the extractable starch content (measured in a laboratory at Stellenbosch University). Low crop yields result in low biofuel yield, and thus, low WUE_B is likely to occur.

Strictly speaking, the term “efficiency” implies that the numerator and dominator in the above equations have the same unit (i.e. m^3). However, agronomists prefer to express plant production in units of mass (kg or tons) and not volume (m^3), the latter requiring knowledge of the plant’s density. In this project, it is preferential to express Y_B in litres (not m^3) to avoid the calculation of small WUE_B values.

4.4 ESTIMATION OF CROP YIELD AND EVAPOTRANSPIRATION

From trials conducted over four seasons (2015/16 to 2018/19) at two locations (Swayimane and Baynesfield Estate), crop yield was measured at harvest. The harvested crop was then air dried to achieve a moisture content of 10 to 12%. In addition, dry crop yield for rainfed conditions was estimated using a crop simulation model for each relatively homogeneous response zone across South Africa (5,838 in total).

For the Baynesfield trial in 2016/17, crop evapotranspiration was estimated using a new surface renewal method (micrometeorological based) that does not require calibration against an eddy co-variance system. However, the method needs a fetch of approximately 80 to 100 m in all directions (equivalent to a hectare of cultivated crop). Since the crop was irrigated, crop evapotranspiration approached the maximum (i.e. potential) value as water stress was assumed to be minimal.

For the Swayimane trials, the SWB method was utilised as the trial area was insufficient for surface renewal to be used. Continuous monitoring of soil water content was done using different sensors. However, since the trials were rainfed, actual evapotranspiration (not potential evapotranspiration) was measured as rainfall was insufficient to meet the crop’s full water demand.

In addition, potential evapotranspiration was estimated using a crop simulation model for each relatively homogeneous response zone across that mentioned previously, from which crop (or water use) coefficients were determined for standard (non-stressed) conditions. It is important to note that simulated (modelled) crop evapotranspiration excluded the evaporation of intercepted water, as this process is not accounted for by the model. On the other hand, the surface renewal method measures all water loss from the surface.

4.5 INTERPRETATION OF WATER USE EFFICIENCY

Both the WUE metrics defined above should be interpreted with great caution and must be done with due consideration of other variables, in particular yield and season length. For example, certain crops (e.g. sugarcane) exhibit a higher WUE when stressed in comparison to non-stressed conditions. The WUE metric is most useful for determining if crops are grown in optimum (high-yielding) environments as opposed to those produced in sub-optimum areas (cf. Section 15.3.3). The WUE is sensitive to crop yield, which is influenced by crop management and is discussed next in more detail.

4.6 FACTORS AFFECTING WATER USE EFFICIENCY

By definition, WUE is strongly influenced by crop yield. The predominant factors that affect crop yield (and hence WUE) can be categorised into biotic (living) and abiotic (non-living) factors (Table 4.1). In the table, "yes" indicates the crop management options that can be implemented in order to effectively manage each factor.

Table 4.1: Environmental factors affecting crop yield and water use, as well as various farm management practices to help buffer the impacts (adapted from Oerke, 2006; Ritchie and Basso, 2008)

Abiotic factors	**Mulching**	**Cultivar selection**	**Planting date**	**Planting density**	**Crop rotation**	**Other**
Soil fertility	Yes			Yes	Yes	Intercropping
Radiation	Yes	Yes	Yes	Yes		Seed depth
Temperature	Yes	Yes	Yes	Yes		Irrigation
Soil water availability	Yes	Yes	Yes	Yes	Yes	Soil water
Soil nutrient status				Yes	Yes	Fertilizer
Biotic factors						
Weeds	Yes	Yes	Yes	Yes	Yes	Herbicide; cover crops
Insect pests		Yes	Yes		Yes	Pesticide
Plant diseases		Yes	Yes	Yes	Yes	Fungicide; bactericide
Animals and birds		Yes				Fencing; netting

Other crop management options are also listed. Crop yields can be improved by genetic modifications and appropriate crop management practices (Greiler, 2007), as discussed in Section 3.3 and Section 3.4. The most important and problematic factor that hinders optimal agricultural production in rainfed agriculture is low soil water availability (Molden et al., 2010). Soil water availability is affected by, inter alia, soil water evaporation, which can be reduced by implementing simple practices that aim to shade the ground, e.g. higher plant population density and crop breeding to enhance leaf expansion (Ritchie and Basso, 2008). Mulching and rainwater harvesting can also be used to improve soil water availability.

In terms of the WUE of biofuel production, the application of phosphorus and potassium to inoculated soybean can improve the seed oil content (Borges and Mallarino, 2000; Malik et al., 2006; Tanwar and Shakwat, 2003; Sawan et al., 2006; Win et al., 2010). Row spacing and applied irrigation can also impact on seed oil content (Bellaloui et al., 2015b). Additionally, early planting resulted in higher oil content, indicating an influence of temperature on seed oil content (Bellaloui et al., 2015a). In this study, Lembede (2017) showed that mulching improved the seed oil content of soybean grown in the 2015/16 season (cf. Section 12.1). Alsajri et al. (2020) tested the effect of five daily temperatures (21, 25, 29, 33 and 37 °C) on seed quality parameters on an indeterminate and determinate soybean cultivar. They found that seed oil concentration increased with temperature up to 26 °C for the indeterminate cultivar and 25 °C for the determinate cultivar (Figure 64.1).

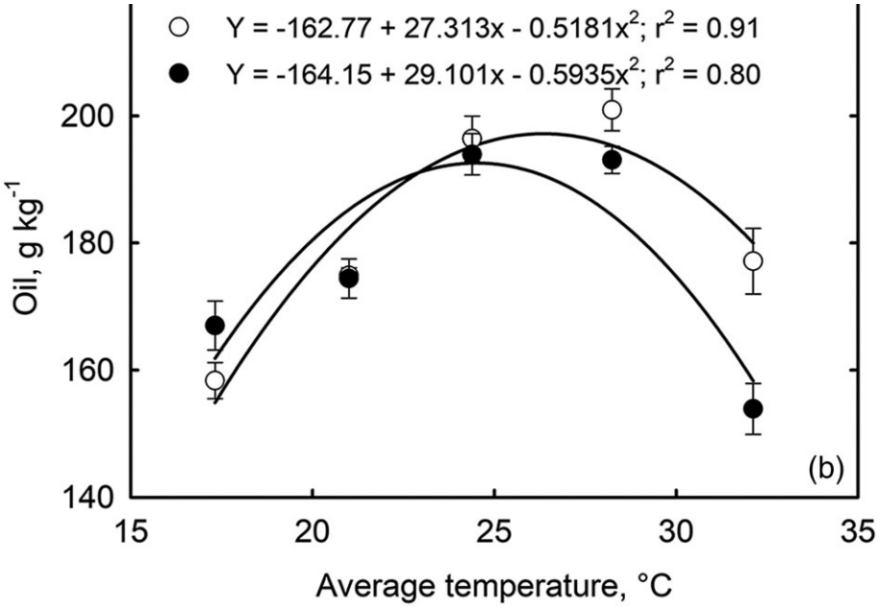

Figure 4.1: Temperature effects on the seed oil content of an indeterminate (white dot) and determinate (black dot) soybean cultivar (Alsajri et al., 2020)

4.7 NEED TO IMPROVE WATER USE EFFICIENCY

When sufficient water is available for vegetative growth, persistent yield gaps are attributed to poor agronomic practices (Fanadzo et al., 2010). A yield gap refers to the difference between actual and potential yield. Lack of knowledge, resources and poor support from extension officers are believed to contribute to low crop yields (and low water use efficiencies) in smallholder farming systems (Mendesil et al., 2007; Azadi and Ho, 2010; Fanadzo et al., 2010; Rossi, 2012). Knowledge regarding the causes of yield gaps can help to efficiently target efforts to improve crop production and narrow yield gaps (Lobell et al., 2009), thus improving WUE.

4.8 SUMMARY AND CONCLUSIONS

There is much potential for yield improvements by smallholder farmers. The exploitable yield gap describes the difference between 80% of the potential yield and the actual yield (Lobell et al., 2009). The exploitable yield may be achieved by commercial farmers, but smallholder farmers are likely to achieve only half of the exploitable yield due to the abovementioned limiting factors (Lobell et al., 2009).

For this project, research trials were conducted over four seasons to assess crop management options to improve yield. In the 2015/16 season, the impact of mulching and fertilization on soybean yield was assessed at Swayimane (cf. Chapter 5). In 2016/17, the water use and yield of soybean was measured for a second season (as recommended by Kunz et al., 2015a) at Baynesfield (cf. Chapter 6). The impact of fertilization and cultivar selection on sorghum yield was studied in the 2017/18 season at Swayimane (cf. Chapter 7). Finally, the impact of inoculation and cultivar selection on soybean yield was studied in the 2018/19 season at Swayimane (cf. Chapter 8).

CHAPTER 5: WATER USE AND YIELD OF SOYBEAN: 2015/16

5.1 INTRODUCTION

The overall aim of the field trial was to quantify feedstock water use and yield of soybean under various agronomic management scenarios (mulching vs fertilization). The field-based measurements contributed to the partial calibration of the SWB model for smallholder farming environments (e.g. Swayimane) under rainfed conditions.

5.2 MATERIALS AND METHODS

5.2.1 Site description

Swayimane High School (29°31'08.07"S; 30°41'39.86"E; 876 m above sea level) is situated near Wartburg in KwaZulu-Natal, South Africa (Figure 75.1). The school is situated about 56 km north-west of the University of KwaZulu-Natal. The area is located in the bioresource group called the moist midlands mist belt (Smith, 2006). The area is characterised by fertile clay loam soils. The region is well known for sugarcane and timber plantations, with about 75% of the local community actively involved in small-scale farming (Smith, 2006).

Figure 5.1: A satellite-derived image from Google Earth® (dated 15 March 2016) showing the location of the soybean trial within the Swayimane High School

The climate in Swayimane is hot, with relatively wet summers and cool, dry winters. Using monthly climate data provided by the South African Sugarcane Research Institute (SASRI) for Bruyns Hill (near Wartburg) from January 2001 to December 2016. Annual totals of daily rainfall for Swayimane vary between 580 and 1,080 mm, with an average of approximately 850 mm. The long-term mean annual temperature is 17.9 °C. Monthly averages of maximum and minimum temperatures were 24.0 and 11.8 °C, respectively (Table 5.1). The daily average of reference crop evaporation (FAO56 standard) is 3.3 mm d^{-1}, but varied between 2.8 and 4.1 mm.

Table 5.1: Long-term annual statistics derived from monthly values of certain climate variables measured by SASRI's automatic weather station situated at Bruyns Hill (Wartburg, KwaZulu-Natal)

Statistic	Total rainfall (mm)	Mean temperature (°C)	Total solar radiation (MJ m^{-2})	Mean relative humidity (%)	Mean wind speed (m s^{-1})	Total FAO56 evaporation (mm)
Minimum	578.5	16.5	5,098.3	56.9	1.20	1,030.1
Maximum	1,081.0	19.4	6,105.9	75.6	2.72	1,497.3
Average	848.2	17.9	5,550.3	63.3	1.76	1,206.3
Number of years	17	17	17	17	17	17

5.2.2 Planting material

The soybean cultivar planted at Swayimane was a Link Seed cultivar (LS6161R). As noted in Section 4.2.2.1, LS6161R is a Roundup® Ready, medium-growth class (semi-determinate growth type), narrow-leaf cultivar that is well adapted to both dryland and irrigated growing conditions (Link Seed, 2011). It is acknowledged that smallholder farmers cannot afford Roundup® Ready cultivars and it is cheaper to inoculate. A semi-determinate growth type means the crop continues leaf development (and higher transpiration) after flowering and pod development, with new pods being formed only if growing conditions are sufficiently warm and the soil is adequately moist. Hence, there is no clear distinction between the flowering and yield formation growth stages (Lembede, 2017).

5.2.3 Experimental design

The experimental design was a split plot arranged in randomised complete blocks, with sub-plots replicated three times. The main factor was allocated to mulching (i.e. mulching vs no mulching). The sub-plots comprised fertilizer treatments, which were designed to represent 0, 50 and 100% of the recommended fertilizer amounts. The trials measured 451 m^2 (or 0.0451 ha) in area, with individual plot sizes of 6 x 3 m (18 m^2), with 1 m spacing in between plots (Lembede, 2017). An inter-row spacing of 0.75 m and an intra-row spacing of 0.05 m were used.

5.2.4 Agronomic practices

Land preparation was done before planting by ploughing and disking. Hand hoes were then used to achieve a smooth tilth for planting. Land preparation and weeding were done manually by members of the community at a set fee. As noted earlier, the agronomic practices that were considered in the 2015/16 season included mulching and fertilization. Planting commenced on 6 November 2015. After planting, the trial was thinned to achieve the targeted planting density (266,667 plants ha^{-1}) and gap filling was done to account for seedlings that did not emerge (Lembede, 2017).

Soil samples from the top 0.15 m across the field were taken before planting for soil fertility analysis by the Soil Analytical Service Laboratory at the Cedara College of Agriculture, using recognised techniques as described by Manson and Roberts (2001). The recommended fertilizer application rate was 0 kg nitrogen ha^{-1}: 60 kg phosphorus ha^{-1}: 95 kg potassium ha^{-1}. This rate was adjusted accordingly for the 50% fertilizer level, while no fertilizer was applied in the 0% fertilizer plots. Based on soil fertility results, single superphosphate, namely phosphate (10.5%) and potassium chloride (0-0-60) were used to fertilize the trial. Fertilizer was added before planting by broadcasting. Kemprin (a/I cypermethrin) was applied twice after emergence as insect occurrence had been noticed.

Hay bales were used for mulch, which consisted of natural grassland obtained from the University of KwaZulu-Natal's research farm (Ukulinga). Ten hay bales were used throughout the growing season, each weighing approximately 25 kg, i.e. 250 kg of straw mulch in total. The mulch was applied to nine of the 18 sub-plots to form a uniform layer 5 cm thick. The mulch was applied after emergence to prevent the application from negatively impacting on crop establishment. Additional mulch was added when the ground cover became sparse due to natural decay (Lembede, 2017).

5.2.5 Data collection

The acquisition of climate data required as input by simulations models is described next. An automatic weather station (AWS) was installed at the trial site to measure rainfall, temperature, relative humidity, wind speed and solar irradiance. Measurements were recorded by a data logger in 15-minute intervals, then averaged to hourly and then daily values.

5.2.5.1 Climate

A 03101-L cup anemometer (RM Young Inc., USA) was used to measure wind speed at 2 m (Figure 85.2). All sensors were connected to a CR800 data logger (Campbell Scientific Inc., Logan, Utah, USA). The Swayimane weather station started recording data on 27 November 2015.

Figure 5.2: Automatic weather station installed at Swayimane during the 2015/16 season

However, soybean was planted on 6 November 2015. Hence, the climate record was extended using daily data obtained from the SASRI website for a nearby station (namely Bruyns Hill, approximately 4 km away). Daily meteorological data from 1 November 2015 until 31 March 2016 was used to develop the climate files required by each crop model. Table 5.2 presents the climate characterisation for the 2015/16 season at Swayimane.

Table 5.2: Monthly averages and totals of climate data measured by an AWS at Swayimane during the 2015/16 season

Month	T_{MAX} (°C)	T_{MIN} (°C)	RH_{MAX} (%)	RH_{MIN} (%)	u_2 (m s^{-1})	R (mm)	R_S (MJ m^{-2})	ET_O (mm)
	Mean	Mean	Mean	Mean	Mean	Total	Total	Total
November	25.7	16.6	74.1	62.2	1.8	126.7	540.9	125.1
December	27.2	16.4	74.3	55.5	1.7	64.5	531.8	122.3
January	26.0	16.7	73.5	58.2	1.4	160.3	466.9	104.5
February	24.7	14.3	73.0	51.6	1.3	37.6	352.4	79.1
March	22.5	11.3	65.5	43.3	1.3	41.4	345.5	70.7
April	21.6	10.0	62.4	34.9	1.7	6.6	289.6	71.0
May	23.4	12.7	65.9	54.1	2.2	73.8	522.7	123.1
June	26.0	16.3	73.5	60.5	2.1	114.3	556.7	132.7

5.2.5.2 Soil texture

At the beginning of the 2015/16 season, the Soil Analytical Service Laboratory performed a soil textural analysis on five samples taken from a soil survey pit at Swayimane. In addition, a soil fertility test conducted by the same laboratory provided the topsoil's organic carbon content of 3% (Table 5.3).

Table 5.3: Soil textural analysis for Swayimane as measured by the Soil Analytical Service Laboratory from samples derived from the drainage pit (Lembede, 2017)

Soil sample profile depth (m)	Clay %	Fine silt %	Coarse silt and sand %	Texture class	Organic carbon (%)
	(< 0.002 mm)	(0.002-0.02 mm)	(0.02-2 mm)		
0.2	36	15	49	Sandy clay	3
0.4	41	11	48		
0.6	47	7	46		
0.8	56	6	38	Clay	
1.0	54	6	40		

5.2.5.3 Soil water retention

Due to the unfortunate failure of the high-pressure air compressor in the soil water laboratory at the University of KwaZulu-Natal, the controlled outflow pressure method could not be used to determine the soil water retention parameters (at permanent wilting point, field capacity and saturation). These values, together with K_{SAT}, were then estimated using the Soil-Plant-Air-Water (SPAW) model, which was obtained from the United States Department of Agriculture's hydraulic properties calculator (USDA, 2009). This utility is based on a set of pedo-transfer equations described by Saxton and Rawls (2006), which are updated versions of the original equations presented by Saxton et al. (1986). The input values required by SPAW are the particle size distribution and organic matter content. The latter input was derived by multiplying the topsoil's organic carbon content (cf. Table 5.3) by a factor of 1.724 (Howard, 1965). Default values in SPAW for soil organic matter were used for the other three depths. Furthermore, compaction at the two lowest depths were reduced to account for the lower bulk densities at these depths. Soil salinity and gravel were not measured at Swayimane and were thus left at default values of zero in the SPAW model.

For Swayimane, the 1 m deep soil profile was divided into two soil horizons: a 0.60 m sandy clay and a 0.40 m clay (as per the soil texture results given in Table 5.3). The soil water retention characteristics determined for each depth were then averaged to represent these two horizons (Table 5.4).

Table 5.4: Soil parameters obtained for the Swayimane trial site

Soil texture	Thickness	θ_{PWP}	θ_{FC}	θ_{SAT}	K_{SAT}	ρ_b
	(m)	(%)			(mm d^{-1})	(g cm^{-3})
Sandy clay	0.6	25.9	37.6	46.0	46.1	1.41
Clay	0.4	32.9	44.3	47.3	1.5	1.33

5.2.5.4 Soil water content

At Swayimane, soil water content was monitored continuously at three depths (0.15, 0.30 and 0.60 m) using Watermark sensors (model A200SS-5, Irrometer, Riverside California, USA). Two additional Watermark sensors were installed at a depth of 0.80 and 1.0 m in a soil survey pit adjacent to the plots. The sensors were connected to a CR1000 data logger (Campbell Scientific Inc., Logan, Utah, USA) and readings of electrical resistance were taken every 15 minutes over the growing season.

Estimation of soil water tension

Watermark sensors measure the electrical resistance that results from the presence of soil water in each treatment plot. Electrical resistance values were then converted to soil water tension (i.e. soil matric potential) in kPa, considering the soil temperature (Chard, 2002). Lembede (2017) evaluated four different equations to calculate soil water tension (P in kPa) from sensor resistance (R_s in kΩ) and recommended the following quadratic equation developed by Allen (2000):

$$P = -2.246 - 5.239R_S\big(1 + 0.018(T_s - 24)\big) - 0.06756{R_S}^2(1 + 0.018(T_s - 24))^2 \quad \text{Equation 3}$$

where T_s is the soil temperature measured at the depth of each Watermark sensor using thermocouples. Allen (2000) developed the above equation with P ranging from -200 to -10 kPa for T_s at 24 ºC. The equation has a coefficient of determination (R^2) of 0.9996 and a standard error estimate of 1.07 kPa.

Estimation of volumetric water content

The conversion from soil water tension to volumetric water content was undertaken using a locally calibrated logarithmic equation as recommended by Varble and Chávez (2011). A logarithmic regression was developed for each soil depth as follows:

$$\theta_v = a \cdot \ln(h) + b \quad \text{Equation 4}$$

where θ_v is the volumetric water content ($cm^3\ cm^{-3}$), h is the soil pressure head (cm) and a and b represent the slope and the intercept, respectively (Shock et al., 2016). The pressure head (h) was calculated by multiplying the soil water tension matric potential (P) by -10.2.

An auger was used to obtain seven soil samples over the growing season at the depth of each Watermark sensor. The samples were weighed, then oven dried at 105 ºC for 24 hours and finally weighed again to calculate gravimetric water content. Estimates of bulk density, derived using the soil water characteristics programme (SPAW) (cf. Section 5.2.5.2), were then used to convert gravimetric to volumetric water content. The logarithmic equation θ_v = -8.339·ln(h) + 89.851 was developed for Watermark sensors installed at 0.60 m as shown in Figure 95.3. Equations for the other soil depths had R^2 values ranging from 0.77 to 0.87.

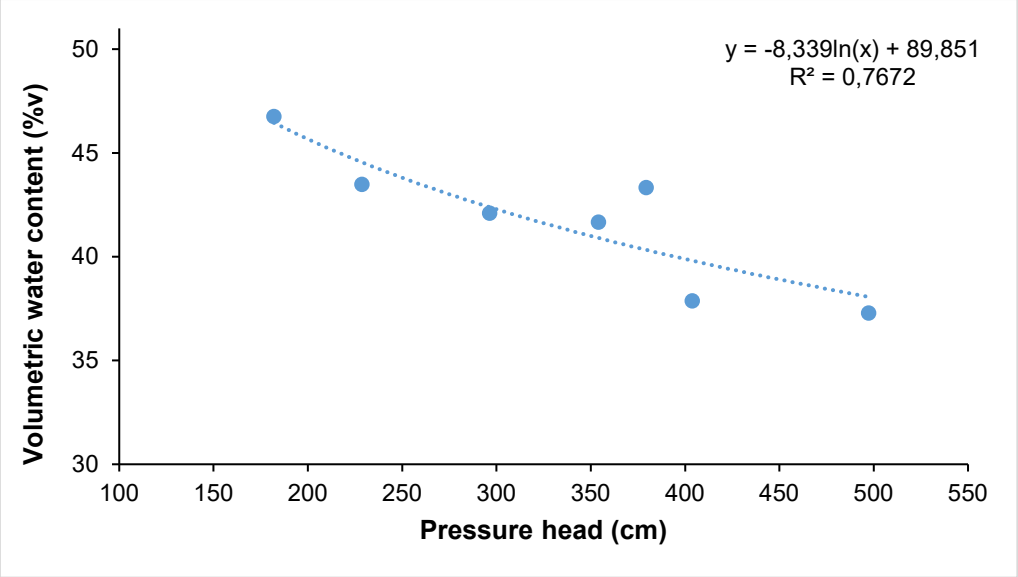

Figure 5.3: Logarithmic equation developed by comparing matric pressure head derived from the Watermark sensor with volumetric soil water content at the 0.6 m depth (dotted line represents the logarithmic trendline)

Profile water content

In order to estimate the soil profile water content for the control treatment at Swayimane, the three Watermark sensors (i.e. at 0.15, 0.30 and 0.60 m soil depths) represented a total of 0.60 m of the 1 m soil profile. To represent the bottom 0.4 m soil depth, the two sensors (i.e. at the 0.8 m and 1.0 m soil depths) installed in the adjacent soil survey pit were used. Therefore, the profile water content was estimated to 1 m depth, with each sensor representing approximately 0.2 m of the soil profile.

5.2.5.5 Crop growth and yield

During the 2015/16 season at Swayimane, the following crop parameters were measured (or observed) using the protocols given in Appendix F:

- Leaf Area Index
- Chlorophyll Content Index
- Stomatal conductance
- Biomass production

The following crop parameters were determined after harvest using the protocols given in Appendix F:

- Accumulated biomass
- Seed yield
- Harvest index

Six representative soybean plants were harvested from each plot at maturity, from which the average final biomass and yield were determined. Final biomass was estimated by measuring the total above-ground biomass, including pods. Thereafter, the pods were separated from the foliage and pod yield was determined. Following this, the pods were shelled and then the seed yield was determined.

5.2.5.6 Statistical analysis

Three statistical indicators (R^2, RMSE and d) were used to test each measured crop parameter. In general, a high R^2, low root mean square error (RMSE) and d approaching unity (i.e. 1) indicate a good fit between simulated and observed data.

5.2.6 Crop water use

At Swayimane, the SWB method was proposed for estimating crop evapotranspiration, since there was inadequate fetch to use any micrometeorological technique. However, runoff was not measured using runoff plots, and since the trial site is not relatively flat, it could not be assumed to be zero. Hence, soil water content was simulated using the SWB model (cf. Section 11.2.1).

5.2.7 Water Use Efficiency of crop and biofuel production

Two metrics were defined in Section 4.2 and Section 4.3: the water use efficiency of crop yield (WUE_C), and the water use efficiency of biofuel production (WUE_B). The theoretical biofuel yield was estimated using the equations given in Chapter 12.

5.3 RESULTS AND DISCUSSION

5.3.1 Observed weather

The average maximum and minimum temperature was 25.8 and 16.1 °C, respectively (Figure 5.4). The temperature ranged from 10.5 to 38.8 °C. Soybean is adversely affected at temperatures above 30 °C, while temperatures below 13 °C for long periods during the flowering stage inhibit flower and seed formation. For 27 days, soybean experienced intermediate stress due to exposure to high maximum temperatures above 30 °C that inhibit growth.

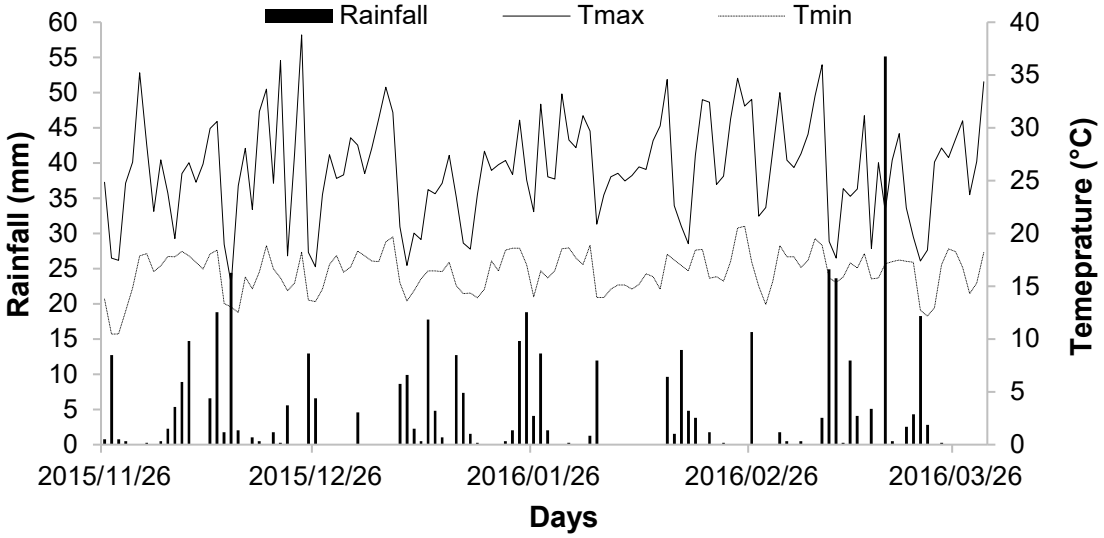

Figure 5.4: Climatic weather showing rainfall (mm), ET_O (mm), minimum and maximum temperature (°C) for Swayimane

During the growing period, soybean received 480.6 mm rainfall. Rainfall distribution was somewhat uneven during the growth periods. Between the reproductive and senescence growth stages, more rainfall (130 mm) was received than in any other growth stage. Reference crop evapotranspiration was 334 mm and it was less than the rainfall received, which was 480.6 mm.

5.3.2 Soil water content

Under 100% fertilization, the hay-mulch treatment had a higher SWC relative to no mulch (38.48% > 32.95%). From Figure 5.5 and Figure 5.6, the fluctuation in SWC at 15 cm (topsoil) is far less under hay mulch.

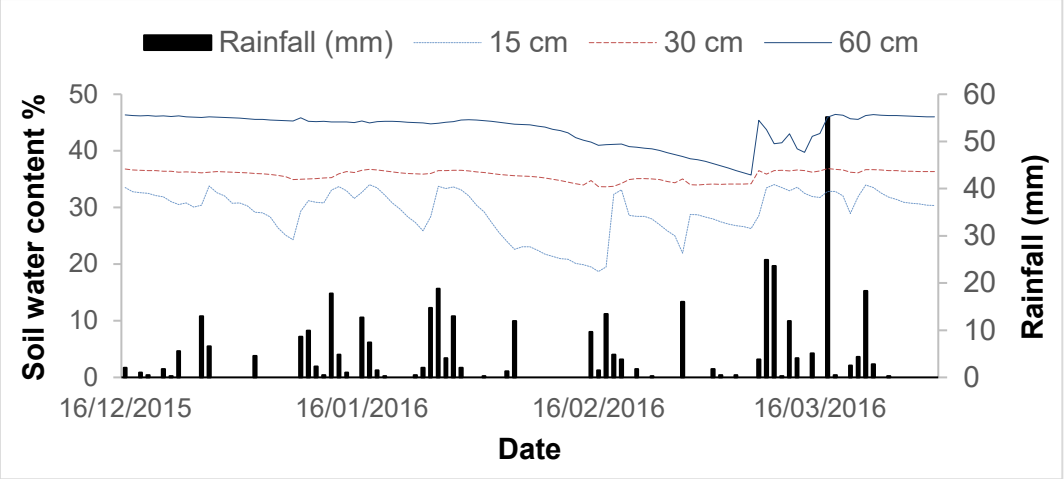

Figure 5.5: Volumetric soil water content at three depths with hay mulch over the 2015/16 season at Swayimane (Lembede, 2017)

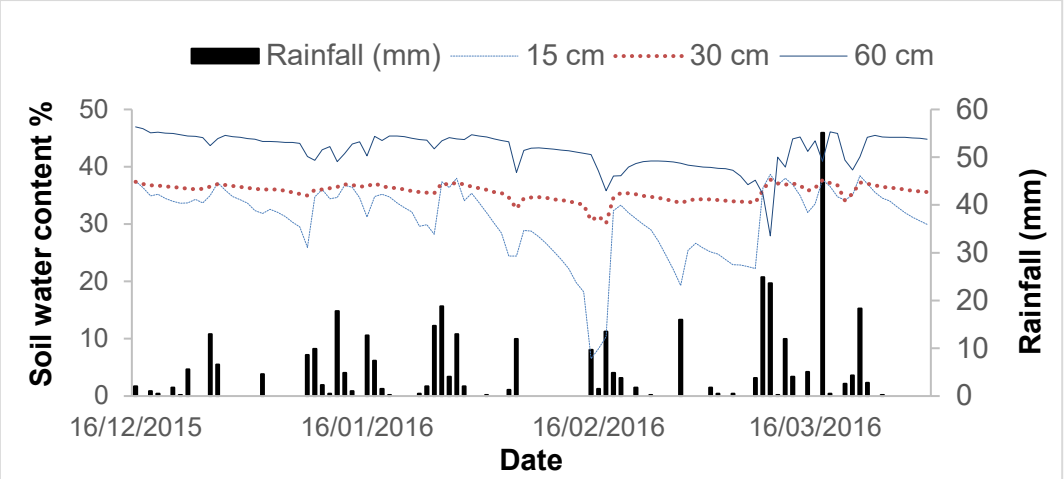

Figure 5.6: Volumetric soil water content at three depths with no mulch over the 2015/16 season at Swayimane (Lembede, 2017)

5.3.3 Crop growth and yield

5.3.3.1 Leaf Area Index

Leaf Area Index for Swayimane is shown in Figure 5.7. Soil fertility had a significant effect on soybean's LAI. The non-mulched, fully fertilized treatments exhibited the highest LAI, followed by the half-fertilized treatments. This was expected because of the known effects of phosphorus and potassium on several plant processes, such as enzyme activity, reproductive growth, uptake and transfer of certain nutrients, as well as the regulation of water vapour and carbon dioxide through stomatal control. However, no leaf analyses were conducted to confirm the benefits of fertilization.

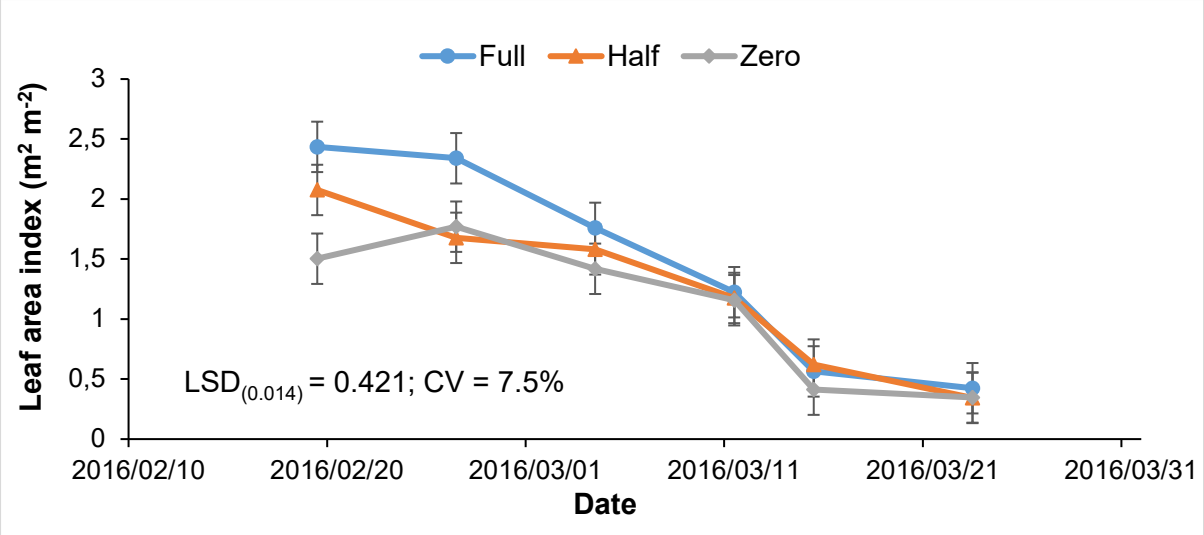

Figure 5.7: Impact of soil fertility on average leaf area index of soybean in the non-mulched treatments (Lembede, 2017)

As noted above, LAI measurements were not undertaken throughout the growing season. Due to this incomplete record, LAI values were then simulated using the SWB model. Since the model does not account for mulching or soil fertility, leaf development was only simulated for the control (i.e. non-mulched, fully fertilized) treatment (Lembede, 2017).

5.3.3.2 Chlorophyll Content Index

There were significant differences (P = 0.010) observed for the Chlorophyll Content Index (CCI) of soybean under hay mulch and no mulch (Figure 5.8). Hay mulch and no mulch had an average CCI of 46 and 39, respectively. The low CCI under no mulch could be an adaptive response to low water availability, thus minimising the production of reactive oxygen species and maintaining cellular integrity, relative to hay mulch. This means that plants capture less energy, which should be consistent with reduced stomatal conductance. Therefore, growing soybean under hay mulch can help maintain chlorophyll integrity, which can result in improved photosynthesis.

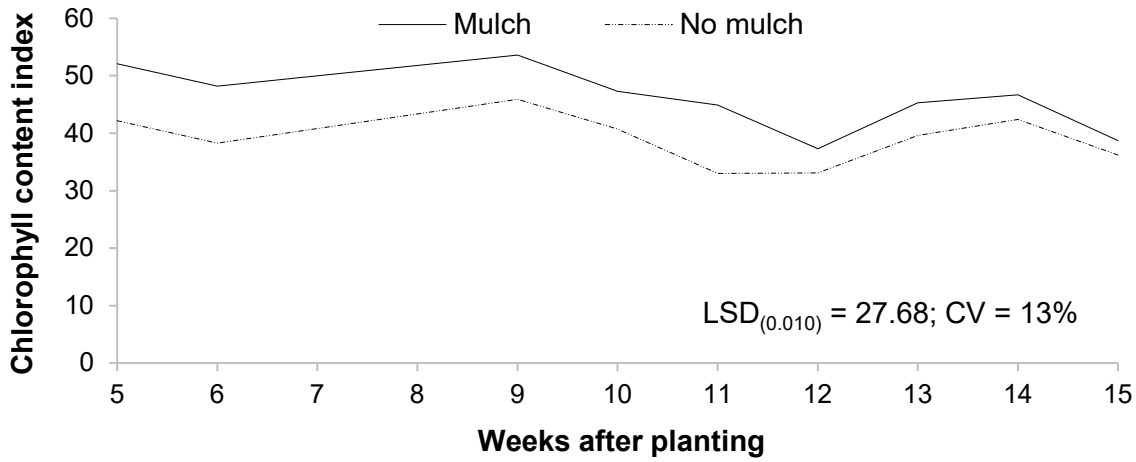

Figure 5.8: Soybean's chlorophyll content index in response to mulch treatments (hay mulch and no mulch) over time (Lembede, 2017)

5.3.3.3 Stomatal conductance

There were no significant differences (P = 0.057) for the stomatal conductance of soybean under hay mulch and no mulch (Figure 5.9). This sudden drop at nine weeks after planting was attributed to weather conditions, which were overcast with high relative humidity, low temperature and moderate rainfall.

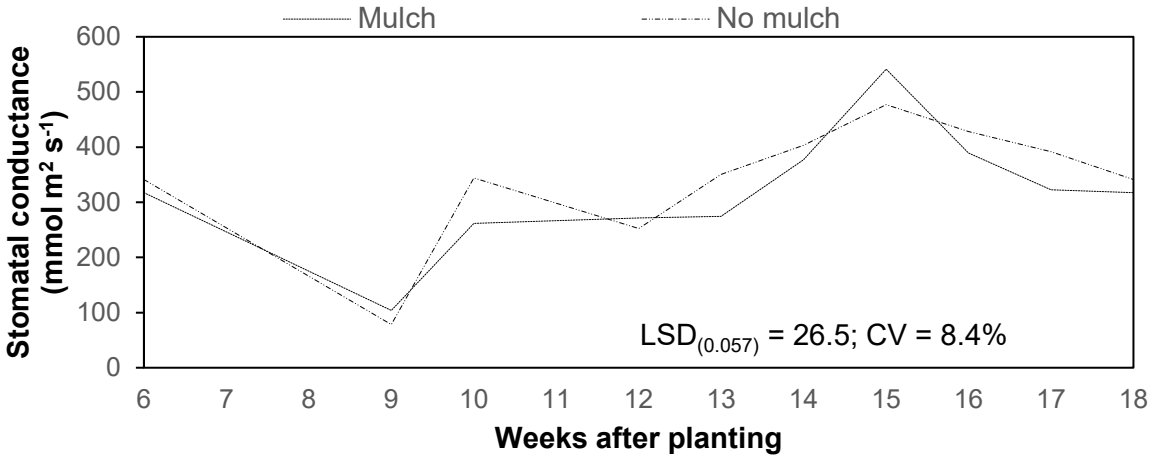

Figure 5.9: Soybean's stomatal conductance (mmol m^2 s^{-1}) in response to mulch treatments (hay mulch and no mulch) over time (Lembede, 2017)

5.3.3.4 Biomass production

Figure 5.10 shows the biomass accumulation for soybean at Swayimane. Soil fertility did not have a significant effect on biomass accumulation for the non-mulched treatments. It is unclear why the biomass accumulation on 20 February 2016 was higher for the non-fertilized treatment than for the half and full fertilized treatments. This may be attributed to erroneous measurements of biomass accumulation.

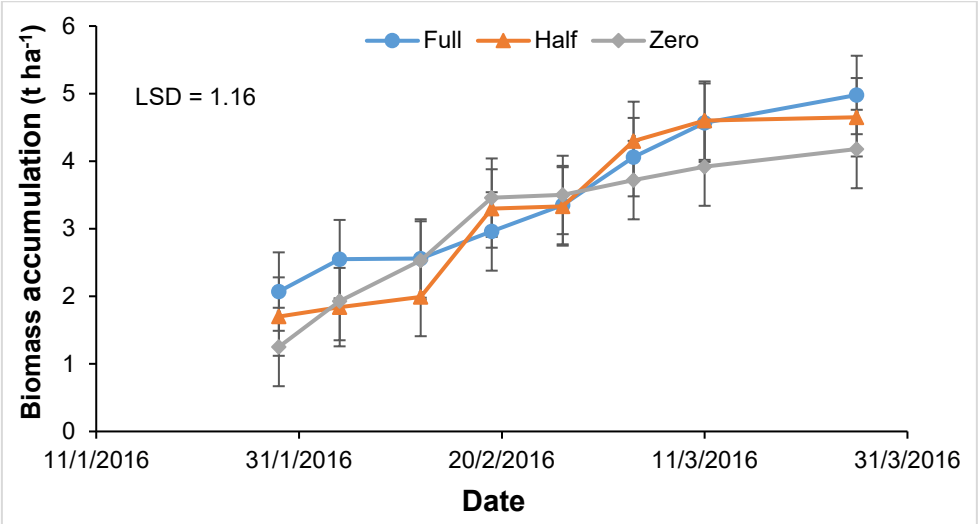

Figure 5.10: Impact of soil fertility on average biomass accumulation in the non-mulched treatments at Swayimane (after Lembede, 2017)

5.3.4 Final yields and Harvest Index

Figure 5.11 shows the soybean seed yield at Swayimane under the three fertilizer treatments for the non-mulched treatments. Soil fertility had no significant impact on the yield. As anticipated, the full fertilized treatments produced the highest yield. However, this was not statistically significant when compared to 0 and 50% fertilization.

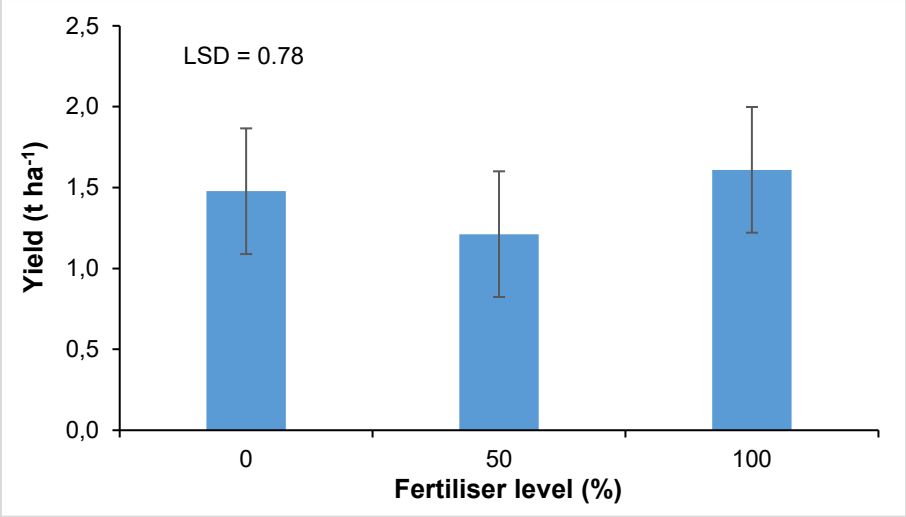

Figure 5.11: Impact of soil fertility on soybean seed yield at Swayimane for the non-mulched treatments (after Lembede, 2017)

The Harvest Index (HI) relates the final yield to the total biomass produced. Since HI is directly proportional to yield, high HI values indicate that a greater portion of the biomass is converted to yield. Soil fertility also had no significant impact on HI; the results of HI mirrored those of yield (Figure 5.12).

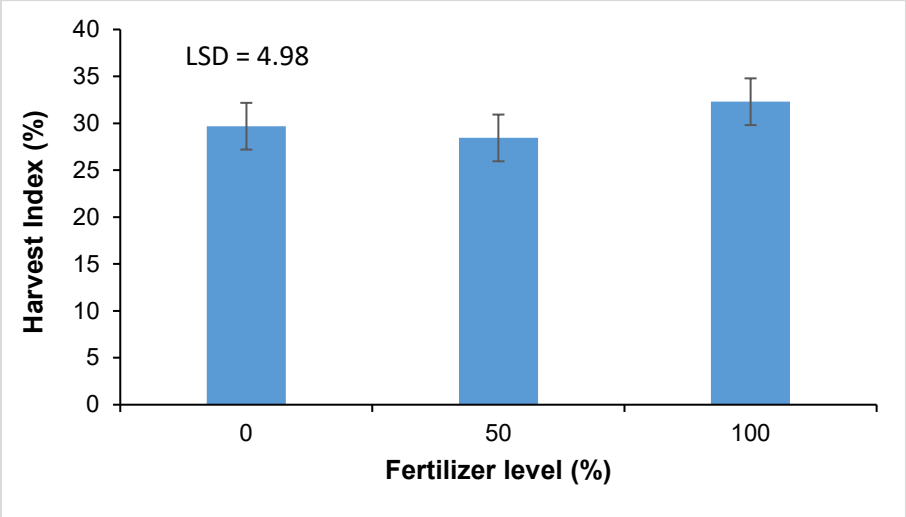

Figure 5.12: Impact of soil fertility on the Harvest Index of soybean at Swayimane for the non-mulched treatments (after Lembede, 2017)

5.3.5 Water Use Efficiency of crop and biofuel production

Crop water use was simulated using the SWB model as shown in Table 5.5. Biodiesel yield was determined from crop yield and a seed oil content of 18%. The WUE values for crop and biofuel production are low, due to the low yield of 1.6 t ha^{-1} that was measured and simulated at the site.

Table 5.5: Comparison of water and biofuel use efficiency derived from SWB model simulations for soybean (after Lembede, 2017)

Yield (kg ha^{-1})	Water use (m^3)	WUE_C (kg m^{-3})	Biofuel yield (L ha^{-1})	WUE_B (L m^{-3})
1,600	5215	0.31	297.4	0.06

5.3.6 Summary and conclusions

In the first season, the effects of fertilization and mulching on soybean growth and yield were assessed at Swayimane. Soil fertility had a significant effect on soybean's LAI, but not on biomass accumulation or final yield. Mulching not only improved the SWC, but also reduced fluctuations in the topsoil. Although chlorophyll content was significantly higher under mulching, there were no significant differences for stomatal conductance, LAI, biomass and yield of soybean. The overall yield of 1.6 t ha^{-1} was low, due partly to the lack of inoculation and a fungal disease that may have been transferred from the hay mulch. In addition, soil pH was low (4.2), which results in aluminium becoming soluble. Soluble aluminium retards root growth, restricting access to water and nutrients (Vanlauwe and Zingore, 2011).

CHAPTER 6: WATER USE AND YIELD OF SOYBEAN: 2016/17

6.1 INTRODUCTION

The overall aim of the field trial was to quantify feedstock water use and yield of soybean for a second season at Baynesfield, as recommended by Kunz et al. (2015a). The field-based measurements contributed towards the partial calibration of the AquaCrop model for commercial farming environments under irrigated conditions (e.g. Baynesfield).

6.2 MATERIALS AND METHODS

6.2.1 Site description

Baynesfield Estate (29°45'42.78"S; 30°20'35.82"E; 847 m above sea level) is situated in KwaZulu-Natal, about 25 km south of Pietermaritzburg. Field NR28 is adjacent to the main house as shown in Figure 6.1. The climate is classified as sub-humid, with dry and cool winters, but warm and rainy summers. Using monthly climate data provided by the ARC's Institute for Soil, Climate and Water (ISCW) from June 2009 to June 2017 (with missing data in 2014), annual totals of daily rainfall for Baynesfield vary between 600 and 765 mm, with an average of approximately 695 mm. The long-term mean annual temperature is 18.3 °C. Monthly averages of maximum and minimum temperatures were 25.4 and 11.1 °C, respectively (Table 6.1). The daily average of reference crop evaporation (FAO56 standard) is 2.7 mm d^{-1}, but varied between 2.6 and 2.9 mm.

Figure 6.1: A satellite-derived image from Google Earth® (dated 23 August 2016), showing the location of the soybean trial within field NR28 at the Baynesfield Estate

Table 6.1: Long-term annual statistics derived from monthly values of certain climate variables measured by the ARC's automatic weather station situated at Baynesfield (KwaZulu-Natal)

Statistic	Total rainfall (mm)	Mean temperature (°C)	Total solar radiation (MJ m^{-2})	Mean relative humidity (%)	Mean wind speed (m s^{-1})	Total FAO56 evaporation (mm)
Minimum	606.8	17.5	4,149.7	68.1	1.18	930.9
Maximum	764.3	20.1	5,061.6	70.2	1.64	1059.9
Average	693.9	18.3	4,685.8	68.7	1.37	992.3
Number of years	7	7	7	7	7	7

6.2.2 Planting material

During the 2016/17 season, the same soybean cultivar (LS6161R) planted at Swayimane was also planted at Baynesfield Estate. The reader is referred to Section 5.2.2 for a description of this cultivar. In addition, the results obtained in the 2016/17 season at Baynesfield were compared to those obtained in the 2012/13 season.

6.2.3 Experimental design

The Baynesfield site represents a commercial farming environment. Thus, there is no experimental design. However, an inter-row spacing of 0.76 m with a 0.032 m intra-row spacing was used to achieve a target population of 410,000 plants per hectare.

6.2.4 Agronomic practices

Soil samples, each representing 1 ha, were collected in early August 2016 and analysed for fertility. Thereafter, fallow land was mechanically ripped and disked, with an application of lime (unknown mass per ha) in between the ripping and disking. Soybean was planted on 21 October 2016 in a 27-ha field called NR28. Planting was conducted by drilling 31 seeds per metre at a depth of 0.6 cm (approximately 75 kg seed per hectare). After crop establishment (10 DAP), seedlings were not thinned to maintain the targeted population of 410,000 plants per hectare. A pre-emergence herbicide mix (Metagan: 1.2 ℓ ha^{-1}; classic: 30 g ha^{-1}; Roundup®: 5.0 ℓ ha^{-1}) was applied to control weeds prior to planting. Based on soil fertility recommendations, a basal fertilizer was applied using 1:2:3 (39) (specially blended fertilizer) at a rate of 230 kg ha^{-1}. A pesticide mix (Acanto: 0.300 ℓ ha^{-1}; Hit: 0.750 ℓ ha^{-1}) was applied was applied to control insect outbreaks one month after planting. A fungicide (Artea: 0.500 ℓ ha^{-1}) was also applied in January to prevent the outbreak of soybean rust.

6.2.5 Data collection

6.2.5.1 Climate

A Kipp and Zonen NR-Lite2 net radiometer (Delft, The Netherlands) was installed at Baynesfield to measure net radiation at 2 m above the ground surface. In addition, a two-dimensional sonic anemometer (DS2; Decagon Devices, Pullman, Washington, USA) was used to measure wind speed at 2 m to enable the calculation of reference grass evaporation, ET_O (Figure 6.2). All sensors were connected to a CR3000 data logger (Campbell Scientific Inc., Logan, Utah, USA).

Figure 6.2: NR-Lite2 net radiometer, LI200S pyranometer and Gill radiation shield housing a single air temperature and relative humidity sensor (HMP50), as well as a Texas Electronics tipping bucket rain gauge (Baynesfield Estate: 2016/17 season)

The Baynesfield weather station started recording data on 19 December 2016. However, soybean was planted on 21 October 2016. Hence, the climate record was extended using daily data obtained from SASRI's website for a nearby station (Thornville 134, approximately 5 km away). Daily meteorological data from 1 October 2016 until 31 May 2017 was used to develop the climate files required by each crop model. Table 6.2 presents the climate characterisation for the 2016/17 season at Baynesfield.

Table 6.2: Monthly averages and totals of climate data measured by an automatic weather station at Baynesfield during the 2016/17 season

Month	T_{MAX} (°C)	T_{MIN} (°C)	RH_{MAX} (%)	RH_{MIN} (%)	u_2 (m s^{-1})	R (mm)	R_S (MJ m^{-2})	ET_O (mm)
	Mean	Mean	Mean	Mean	Mean	Total	Total	Total
October	22.0	10.7	87.1	66.8	1.15	92.6	395.60	79.5
November	22.9	13.6	90.0	76.7	0.95	102.4	328.20	72.8
December	27.2	15.2	93.4	56.7	1.03	63.8	455.70	103.1
January	26.1	14.9	99.9	57.8	1.10	99.6	422.20	95.1
February	26.2	16.4	92.6	59.9	1.35	135.5	429.07	96.0
March	27.7	14.2	92.1	46.4	1.39	29.4	501.30	112.2
April	25.5	11.2	92.5	40.2	1.56	51.6	393.31	89.9
May	23.6	8.8	89.8	37.7	2.00	47.6	347.54	82.7

6.2.5.2 Soil texture

Mbangiwa et al. (2019) determined the soil texture at three depths in Baynesfield during the 2012/13 season (Table 6.3). Since their experimental site was situated within 100 m of the 2016/17 site (i.e. field NR28), the analysis was not repeated. The soil form is Hutton (Hu) as per the soil classification taxonomic system for South Africa (SCWG, 1991).

Table 6.3: Soil textural analysis for Baynesfield (Mbangiwa et al., 2019)

Soil sample profile depth (m)	Clay percentage	Fine silt percentage	Coarse silt and sand percentage	Texture class	Organic carbon percentage
	(< 0.002 mm)	(0.002-0.02 mm)	(0.02-2 mm)		
0.0-0.1	54	18	28	Clay	3.7
0.4-0.5	62	13	25		2.4
0.9-1.0	72	11	17		1.0

In August 2016, the Baynesfield farm manager sent 22 soil samples from field NR28 to the Soil Analytical Service Laboratory for soil fertility analysis. For one of the samples (due to budget limitations), mid-infrared estimates of organic carbon, nitrogen and clay content were estimated at 3.4, 0.23 and 47%, respectively. Soil pH levels (potassium chloride) ranged from 3.73 to 4.34 and acid saturation ranged from 4 to 20%. In addition, undisturbed soil cores were taken at Baynesfield on 12 July 2017 from an opened pit. Two cores, representing three soil profile depths (0-0.1, 0.4-0.5 and 0.9-1.0 cm), were oven dried to calculate dry bulk density (Table 6.4). These values differ to those reported by Mbangiwa et al. (2019) of 0.99, 1.03 and 0.98 g cm^{-3} for the three respective depths.

Table 6.4: Bulk density data for Baynesfield Estate obtained from samples taken in the 2016/17 season

Soil depth (m)	Bulk density (g cm^{-3})
0-0.1	1.11
0.4-0.5	1.25
0.9-1.0	1.23

6.2.5.3 Soil water retention

As noted in Section 5.2.5.2, the soil water retention parameters were estimated using SPAW. The SPAW estimates of permanent wilting point (PWP), field capacity (FC), saturation and K_{SAT} were used to derive soil parameters required by the simulation models (Table 6.5). Default values provided by Raes et al. (2017) for a clay soil are 39, 54 and 55% for θ_{PWP}, θ_{FC} and θ_{SAT}, respectively. These values for the PWP and saturation agree favourably with those shown in Table 6.5. Estimated bulk density for the topsoil was higher than measured values, whereas the value at 0.5 m agreed favourably with measurements.

Table 6.5: Soil parameters obtained for Baynesfield using the SPAW model

Soil texture	Thickness	θ_{PWP}	θ_{FC}	θ_{SAT}	K_{SAT}	ρ_b
	(m)	(%)			(mm d^{-1})	(g cm^{-3})
Clay	0.1	32.2	42.5	49.9	22.9	1.33
Clay	0.4	35.6	44.6	53.3	35.7	1.24
Clay	0.5	41.3	49.9	56.8	17.4	1.15

6.2.5.4 Soil water content

At Baynesfield, the approach used to determine crop water use did not require the measurement of soil water content at different depths. However, soil water content near the soil surface was measured for use with surface renewal measurements using two CS616 water content reflectometers (Campbell Scientific, Logan, Utah, USA).

6.2.5.5 Crop growth and yield

During the 2016/17 season at Baynesfield, the following crop parameters were measured (or observed) using the protocols given in Appendix F:

- Plant height
- Chlorophyll Content Index
- Leaf Area Index
- Canopy cover

The above measurements were conducted in three separate rows adjacent to the surface renewal system that measured crop water use. No destructive sampling of soybean biomass was undertaken at Baynesfield, and thus biomass production was not determined.

The following crop parameters were determined after harvest using the protocols given in Appendix F:

- Seed yield
- Harvest Index

At Baynesfield, the average attainable yield was measured from five 1 m^2 quadrants on 26 April 2017. All plant stems and attached pods were manually harvested in each quadrant, including those that were on the ground, as well as seeds that had already dispersed from shattered pods. Mechanical harvesting commenced on 10 May 2017, but stopped due to moist conditions. Harvesting resumed on 12 May and was completed using a combine harvester. A total of 20 ha was harvested and the average actual yield was obtained from weigh bridge readings.

6.2.5.6 Statistical analysis

The same statistical indicators described in Section 5.2.5.6 were used to evaluate the performance of AquaCrop for soybean grown at Baynesfield (a commercial farming environment).

6.2.6 Crop water use

Due to the adequate fetch at Baynesfield (at least 100 x 100 m of cropped area), crop water use (maximum evaporation, E_m) was estimated from the latent energy flux λE (W m^{-2}) derived as the residual of the shortened energy balance equation:

$$\lambda E = R_n - G - H \qquad \text{Equation 5}$$

Hence, this approach required measurements of net irradiance (R_n in W m^{-2}) (Section 6.2.5.1), soil heat flux (G in W m^{-2}), and sensible heat flux (H in W m^{-2}). Two Hukse flux plates (HFP01-15, Delft, The Netherlands) were used to measure soil heat flux density (G) at a depth of 80 mm. A system of parallel thermocouples was installed at depths of 20 and 60 mm to calculate the heat stored above the flux plates.

Sensible heat flux was estimated using an updated surface renewal (SR) method called SR2. It is similar to the classic (SR1) method used in the previous biofuel project (Kunz et al., 2015b) where high-frequency measurements of air temperature were made using unshielded fine-wire thermocouples at two heights above the soil surface (Figure 6.3a). However, SR2 requires the measurement of wind speed at canopy height using a two-dimensional sonic anemometer (DS2; Decagon Devices, Pullman, Washington, USA). The DS2 (Figure 6.3b) negates the need for calibration against the eddy co-variance method, as required by SR1. The SR2 also requires knowledge of canopy structure (especially LAI measurements). The SR2 datasets were analysed using two different methods based on Monin-Obukhov similarity theory (MOST) and dissipation theory (DT) to estimate scalar surface fluxes.

(a) (b)

Figure 6.3: Two fine-wire thermocouples installed at canopy height and 1 m above the canopy (left), as well as a two-dimensional sonic anemometer installed at canopy height (right) (Baynesfield Estate: 2016/17 season)

6.2.7 Water Use Efficiency of crop and biofuel production

The two WUE metrics listed in Section 5.2.7 were calculated for soybean in the 2015/16 season. Soybean seed oil content was determined using a hexane extraction process (Meyer et al., 2008) for each plot, then averaged. The seed oil content was then used to estimate the theoretical biofuel yield.

6.3 RESULTS AND DISCUSSION

6.3.1 Crop growth and yield

6.3.1.1 Leaf Area Index

As shown in Figure 6.4, weekly measurements of LAI were conducted during the 2016/17 season at Baynesfield for soybean from January to May 2017. These LAI measurements are larger than those reported by Kunz et al. (2015b) for soybean grown in the 2012/13 season at Baynesfield (Figure 6.5). The sharp decline in LAI in the 2012/13 season was not evident in the 2016/17 season.

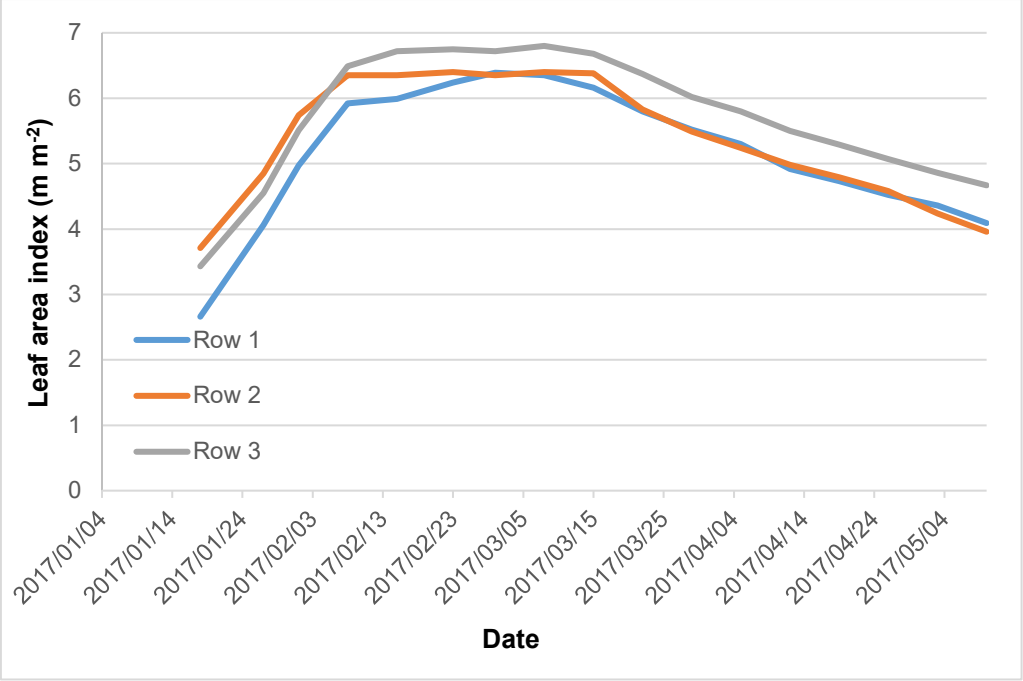

Figure 6.4: Weekly measurements of Leaf Area Index for soybean at Baynesfield from January to May 2017

Measurements of LAI obtained during the 2012/13 season are plotted in Figure 6.5. The LAI was low during the initial growth stage (< 1.0), but increased during the rapid growth stage and peaked at 5.35 during the mid-growth stage. Soybean loses all its leaves as the plant approaches physiological maturity, which is seen by the sharp decline in LAI towards the end of the season (final LAI of 0.44).

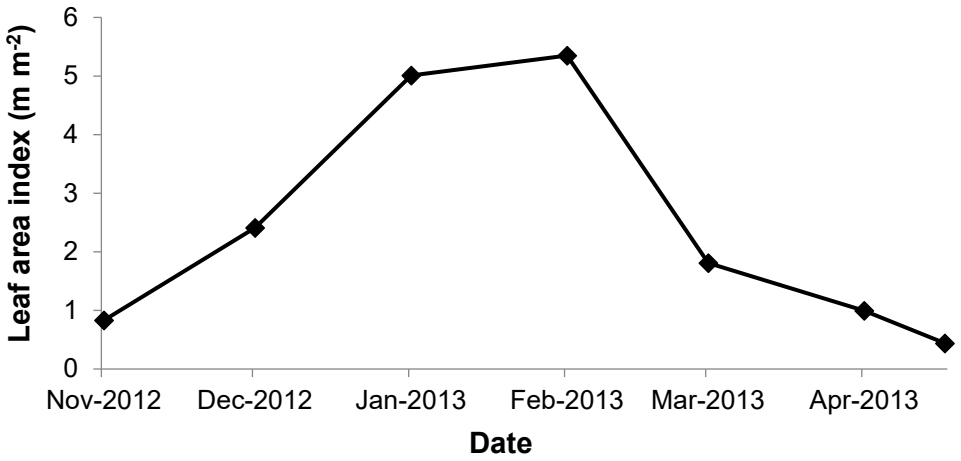

Figure 6.5: Leaf Area Index measured for soybean at Baynesfield during the 2012/13 growing season (Kunz et al., 2015b)

6.3.1.2 Plant height

Weekly measurements of plant height were made in three separate rows adjacent to the surface renewal system, as shown in Figure 6.6. Plant height peaked at about 95 cm, since soybean cultivar LS6161R averages 95-105 cm (Link Seed, 2011). Hence, the maximum plant height was set to 1 in the AquaCrop parameter file for soybean, as was done for Swayimane.

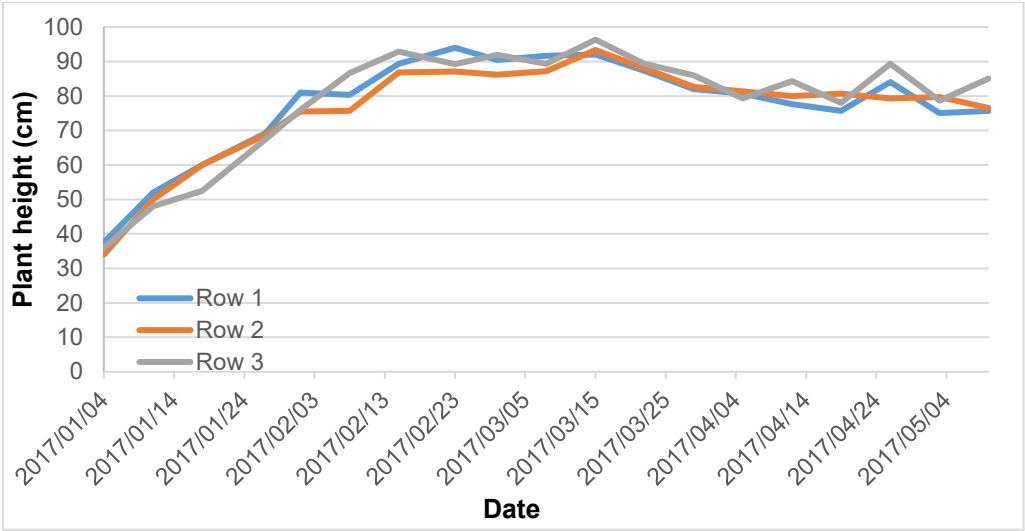

Figure 6.6: Weekly measurements of plant height for soybean at Baynesfield from December 2016 to May 2017

6.3.1.3 Chlorophyll Content Index

Figure 5.7 highlights the peak in CCI on 1 March 2017, which then declined steadily until the crop was harvested between 8 and 10 May 2017. It is important to note that CCI readings from 19 April 2017 onwards were no longer taken from the plant's top leaves (and same orientation) as these had been shed by the plants.

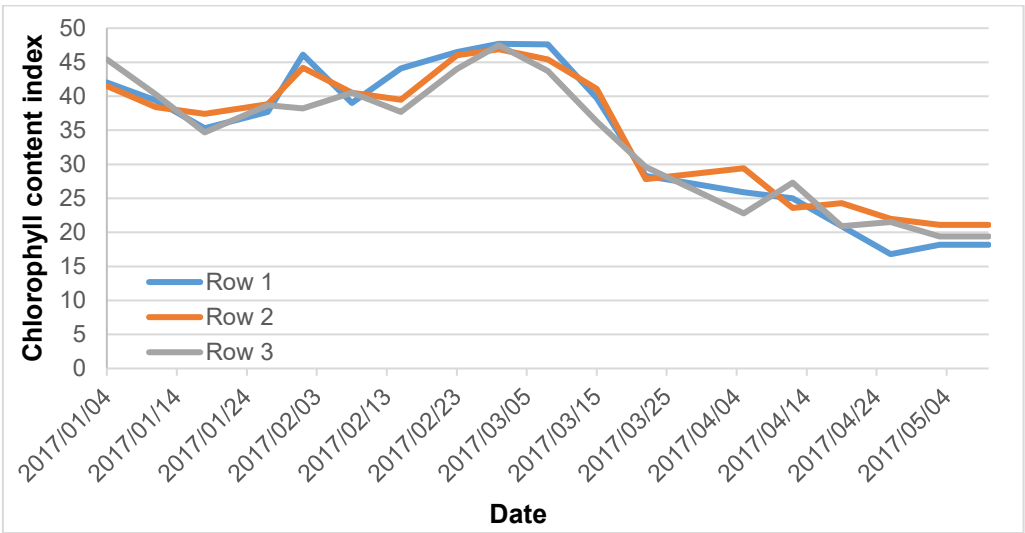

Figure 6.7: Weekly measurements of chlorophyll content for soybean at Baynesfield from January to May 2017

6.3.1.4 Canopy cover

The LAI measurements made in three rows were then averaged and used to calculate the canopy cover (CC) (in percentage) using the following equation:

$$CC_{soybean} = 1 - e^{(-0.46 \cdot LAI)}$$ Equation 6

The constant 0.46 represents the leaf extinction coefficient, which was also used by Adeboye et al. (2017) for soybean (cf. Section 17.3.2.4).

6.3.2 Final yields and Harvest Index

At Baynesfield, the farm authorities are not interested in biomass, and thus do not provide the total harvested biomass. However, a value of 8.75 t ha^{-1} was measured using five 1 m^2 quadrants at Baynesfield on 26 April 2017. No biomass values were reported by Mbangiwa et al. (2019) for the 2012/13 season. A measured seed yield of 5.14 t ha^{-1} was obtained from the quadrant approach. During the 2012/13 season, the measured seed yield was 5.28 t ha^{-1} (Table 6.6).

Table 6.6: Accumulated biomass accumulation and seed yield at Baynesfield (Masanganise, 2019; Mbangiwa et al., 2019)

Season	Biomass (t ha^{-1})	Final yield (t ha^{-1})		Harvest Index
	Measured	Measured	Harvested	Measured
2012/13		5.28	3.52	
2016/17	8.75	5.14	3.20	0.59

For the 2016/17 season, all plant stems and attached pods were manually harvested in each quadrant, including those that were on the ground, as well as seeds that had already dispersed from shattered pods. This explains the high final biomass and HI values that were measured. Furthermore, sampling error is likely to be high considering that 5 m^2 of crop was harvested manually and assumed to represent an entire field of 200,000 m^2.

As expected, the measured yield was higher than the average harvested value of 3.20 t ha^{-1} obtained from 20 ha in field NR28 between 8 and 10 May 2017. This highlights the yield loss that results from mechanical harvesting vs manual harvesting. Significant lodging was observed towards the end of the season. As noted by Dlamini (2015), pods that are below 12.5 cm from the soil surface cannot be collected by a combine harvester. The primary causes of lodging are high plant density, excessive soil water and excessive nitrogen. Excessive water and nitrogen was ruled out at Baynesfield since the crop was mainly rainfed (supplemental irrigation only) and the farm practices precision agriculture (it does not over-apply nutrients to the soil). Hence, the excessive lodging was probably a result of the high planting density.

6.3.3 Crop water use

6.3.3.1 Crop evapotranspiration

As noted in Section 6.2.6, crop water use was measured at Baynesfield using an updated surface renewal method (SR2), where the data was analysed using two different methods known as MOST and DT. Crop evapotranspiration figures were compared to those obtained in the 2012/13 season using different micrometeorological techniques as shown in Table 6.7. Although the crop was planted in October 2016, the SR2 system was only installed on 19 December. However, due to errors in the datalogger program, measurements for December were lost. Hence, data from early January to harvest (Day-of-year 5 to 129) was only available for analysis.

Table 6.7: Estimates of soybean crop evapotranspiration undertaken at Baynesfield for the 2012/13 and 2016/17 seasons

Season	Method	Crop ET (mm)	Length of measurement (days)	Reference
2012/13	SR1	469	189	Kunz et al. (2015a)
	EC-Residual LE	348	130	Mbangiwa et al. (2019)
	EC-Bowen ratio	336		
2016/17	SR2-MOST	378	125	Masanganise (2019)
	SR2-DT	384		

Mbangiwa et al. (2019) stated that the under-estimation of crop evapotranspiration using the eddy co-variance (EC) technique is mostly due to data exclusion by EddyPro quality assurance processing. Furthermore, occasional system failures and rainfall events reduced the evapotranspiration further. When compared to EC, the SR method is far less prone to data loss. Kunz et al. (2015a) measured crop evapotranspiration using the classic SR1 method for a longer period, where measurements were stopped just before the crop was mechanically harvested.

6.3.3.2 Crop coefficients

Crop coefficients are not necessarily transferrable from one region to another due to a number of factors, so they need to be adjusted to suit a location other than that in which they were developed. Although Allen et al. (1998) presented equations for adjusting crop coefficients for wind speed, humidity and plant height, the correction for mid-season K_C was problematic. Guerra et al. (2014) developed and tested an alternative equation that converts the tabulated mid-season K_C values in Allen et al. (1998), which mostly apply in the climate of Davis, California, USA. The mid-season K_C value of 1.15 (Allen et al., 1998) was adjusted to 0.99 using the Guerra et al. (2014) equation, while the late-season value was increased from 0.50 to 0.84 using the Allen et al. (1998) method. The K_C values of 0.99 and 0.84 were then used to calculate an accumulated crop evapotranspiration value of 368 mm. Masanganise (2019) also determined cumulate evapotranspiration values for the four stages of development shown in Table 296.8, from which crop coefficients were then calculated.

Table 6.8: Crop coefficients obtained from soybean evapotranspiration measurements undertaken at Baynesfield in the 2016/17 season (Masanganise, 2019)

Development stage	ET_O	ET_{CC}	K_C	$ET_{SR2\text{-}MOST}$	K_C	$ET_{SR2\text{-}DT}$	K_C
Flowering	64.5	63.8	0.99	81.4	1.26	78.4	1.22
Pod formation and seed filling	172.2	162.0	0.94	184.3	1.07	181.0	1.05
Senescence	50.7	42.8	0.84	39.4	0.78	41.2	0.81
Maturity	118.2	99.6	0.84	72.5	0.61	83.3	0.70
Total/average	**405.6**	**368.2**	**0.90**	**377.6**	**0.93**	**383.9**	**0.95**

Using measured soybean evapotranspiration, Mbangiwa et al. (2019) also determined crop coefficients in four developmental stages: emergence (nine days), vegetative (62 days), flowering (29 days) and yield formation and ripening (30 days). The K_C values for these were 0.19, 0.59, 0.73 and 1.12, respectively. Using AquaCrop, simulated values were 0.45, 1.03, 0.87 and 1.01 for these four stages, respectively. For the 2012/13 season at Baynesfield, Kunz et al. (2015a) provided crop coefficients derived from crop evapotranspiration estimated using the surface renewal method (Table 6.9).

Table 6.9: Crop coefficient values for soybean, derived from measured crop evapotranspiration at Baynesfield during the 2012/13 season (Kunz et al., 2015a)

Month	Crop coefficient	2012/13	FAO (2002)
November	K_{C_INI}	0.72	0.3-0.4
December	K_{C_DEV}	0.72	0.7-0.8
January/February	K_{C_MID}	1.03	1.0-1.2
March/April	K_{C_END}	0.84	0.4-0.5

During the initial crop growth stage, the predominant component of crop evapotranspiration is soil water evaporation. Therefore, the initial crop coefficient (K_{C_INI}) is largely influenced by the frequency and magnitude of rainfall and irrigation events.

Higher K_{C_INI} values are expected for Baynesfield since soybean is typically irrigated at the start of the season to help establish the crop. With the exception of the FAO K_{C_END} values, both measured and simulated crop coefficients remained high at maturity as reported by Kunz et al. (2015a), Masanganise (2019) and Mbangiwa et al. (2019).

6.3.4 Water Use Efficiency of crop and biofuel production

6.3.4.1 Crop Water Use Efficiency

Using the manually measured and mechanically harvested seed yields obtained in two seasons at Baynesfield, together with averaged crop water use (from two micrometeorological techniques), the water use efficiencies presented in Table 6.10 were calculated. These figures highlight the sensitivity of this metric to crop yield. The measured values represent the site's potential yield (i.e. it excludes mechanical harvesting losses), whereas the harvested values represent the actual yields. The WUE figures are also influenced by the fact that crop evapotranspiration was not measured over the entire season. Using a crop water use of 4,690 m^3 measured in 2012/13 (Kunz et al., 2015a), WUE_C for the mechanically harvested soybean decreases from 1.03 to 0.75 kg m^{-3}. Kunz et al. (2015a) (cf. Section 3.5.3.2) questioned whether WUE was a useful metric, considering its sensitivity to crop physiology (cultivar), agronomy (planting density), site conditions (climate and soils), and other management practices.

Table 6.10: Water use efficiency of crop yield for soybean grown at Baynesfield during the 2012/13 and 2015/16 seasons

Treatment	2012/13		2015/16	
Cultivar	**Measured**	**Harvested**	**Measured**	**Harvested**
Seed yield (kg ha^{-1})	5,280	3,520	5,140	3,200
Crop water use (m^3)	3,420	3,420	3,810	3,810
WUE_C (kg m^{-3})	1.54	1.03	1.35	0.84

6.3.4.2 Biofuel Water Use Efficiency

Using the equation given in Section 12.1, biofuel yield was calculated from the seed yields listed in the above table and an average seed oil content of 18%. The results presented in Table 6.11 highlight the sensitivity of the biofuel yield equation to crop yield. Using a crop water use of 4,690 m^3 measured in 2012/13 (Kunz et al., 2015a), WUE_B for the mechanically harvested soybean decreases from 0.19 to 0.0.14 kg m^{-3}.

Table 6.11: Biofuel yield and water use efficiency of biofuel production for soybean grown at Baynesfield during the 2012/13 and 2015/16 seasons

Treatment	2012/13		2015/16	
Cultivar	**Measured**	**Harvested**	**Measured**	**Harvested**
Biofuel yield (ℓ ha^{-1})	981.4	654.3	955.4	594.8
Crop water use (m^3)	3,420	3,420	3,810	3,810
WUE_B (ℓ m^{-3})	0.29	0.19	0.25	0.16

6.3.5 Summary and conclusions

The evapotranspiration of soybean was estimated using two micrometeorological methods: surface renewal combined with MOST (SR2-MOST), and surface renewal combined with DT (SR2-DT). However, the SR2-MOST method requires additional measurements of wind speed and canopy parameters.

In comparison to SR2-MOST, SR2-DT requires a relatively small number of input parameters and is more robust and less expensive. Evapotranspiration estimated using these two methods compared favourably to that obtained using the standard CC approach. The Guerra et al. (2014) procedure to correct the FAO56 mid-season K_C from 1.15 to 0.99 may be considered reliable. The cumulative evapotranspiration or the developmental stages was highest during the pod formation and seed filling stage compared to all other growth stages.

CHAPTER 7: WATER USE AND YIELD OF SORGHUM: 2017/18

7.1 INTRODUCTION

The overall aim of the field trial was to quantify feedstock water use and yield of grain sorghum under various agronomic management scenarios (cultivar choice vs fertilisation). The field-based measurements contributed to the partial calibration of the AquaCrop model for smallholder farming environments under rainfed conditions (e.g. Swayimane).

7.2 MATERIALS AND METHODS

7.2.1 Site description

The trial was conducted at the Swayimane High School (-29°31'08.07''S; 30°41'39.86''E; 876 m), which is located near Wartburg in KwaZulu-Natal, about 56 km north-west of the University of KwaZulu-Natal. Based on 19 years of observations at Bruyns Hill, the mean annual precipitation (MAP) is ~850 mm, mean annual temperature (MAT) is 17.9 °C and reference crop evaporation is ~1,200 mm per annum. Monthly averages of maximum and minimum air temperatures are 24.0 and 11.8 °C, respectively.

7.2.2 Planting material

Three sorghum genotypes were selected for the Swayimane trial during the 2017/18 season. The genotypes included two hybrids (PAN8816 and PAN8906) and an open-pollinated variety (Macia). The agronomic characteristics of each cultivar is given in Table 83.3 (cf. Section 3.2.3.1).

7.2.3 Experimental design

The trial design was similar to that used in the 2015/16 season at Swayimane (cf. Section 5.2.3). The experimental design was a split-plot design with fertilization (i.e. full vs no fertilization) as the main factor and genotype as the sub-factor, which was laid out in randomised complete blocks with three replications. There were 21 plants per row and each plot had five rows, i.e. 105 plants per experimental plot. The inter-row spacing was 0.75 m, while the intra-row spacing was 0.30 m. The three innermost rows were the experimental rows, with two rows for measurements and one row used for destructive sampling. Rows 1 and 5 were border rows to avoid edge effects.

7.2.4 Agronomic practices

Land preparation was completed before planting by ploughing and disking. Hand hoes were then used to achieve a smooth tilth for planting. Gramoxone, a pre-emergence herbicide was sprayed twice before planting using a dilution of about 15 ml per litre of water. Land preparation was done manually by members of the community at a set fee. Planting of the three genotypes commenced on 19 January 2018.

Planting rows were opened by hand hoes and seeds were hand sown to a depth of about 3 cm. On planting day, 50% of Gromor Accelerator (30 g kg^{-1} nitrogen, 15 g kg^{-1} phosphorus and 15 g kg^{-1} potassium), a slow-releasing organic fertilizer, was applied at the recommended rate of 1,000 kg ha^{-1} when placing the fertilizer in lines. The trial was thinned at crop establishment to achieve the planting density of 44,444 plants ha^{-1}. A top dressing was applied six weeks after emergence using Gromor Accelerator. Weeding was again done manually by members of the community.

7.2.5 Data collection

7.2.5.1 Climate

For the 2017/18 season, the AWS at Swayimane was upgraded using funds provided by the uMngeni Resilience Project (Figure 7.1). In addition, a modem was installed to gain access to the recorded weather data via a web interface. Table 7.1 presents the climate characterisation.

Figure 7.1: Automatic weather station installed at Swayimane in the 2017/18 season

Table 7.1: Monthly averages and totals of climate data measured by an automatic weather station at Swayimane during the 2017/18 season

Month	T_{MAX} (°C)	T_{MIN} (°C)	RH_{MAX} (%)	RH_{MIN} (%)	u_2 (m s^{-1})	R (mm)	R_S (MJ m^{-2})	ET_O (mm)
	Mean	Mean	Mean	Mean	Mean	Total	Total	Total
January	25.6	15.7	97.9	56.5	2.0	47.8	586.8	102.9
February	25.4	16.4	98.4	60.9	1.9	130.6	468.1	83.3
March	24.8	15.6	98.4	58.4	1.8	172.8	456.1	80.5
April	23.6	14.8	98.1	57.8	1.6	85.2	370.6	64.4
May	21.2	11.8	92.7	45.1	1.6	29.8	334.6	54.6
June	20.8	10.0	89.5	32.6	1.6	0.2	318.1	50.4

7.2.5.2 Soil texture

At the beginning of the 2017/18 season, the Soil Analytical Service Laboratory performed a soil textural analysis on eight samples taken from a soil survey pit. In addition, the same laboratory provided the topsoil's organic carbon content of 3.8 % (Table 7.2).

Table 7.2: Soil textural analysis for Swayimane as measured by the Soil Analytical Service Laboratory

Soil sample profile depth (m)	Clay percentage	Fine silt percentage	Coarse silt and sand percentage	Texture class	Organic carbon percentage
	(0.002 mm)	(0.002-0.02 mm)	(0.02-2 mm)		
0.15	34	17	49	Sandy clay loam	3.8
0.30	34	12	54		
0.60	36	12	52	Sandy clay	
1.00	43	09	48		

In addition, undisturbed soil cores were taken at Swayimane from an opened pit on 1 December 2017. Four cores, representing four soil profile depths (0.15, 0.30, 0.60 and 1.00 m), were oven dried in order to calculate dry bulk densities of 1.36, 1.37, 1.34 and 1.32 g cm^{-3}, respectively.

7.2.5.3 Soil water retention

Soil water retention parameters (PWP, FC and saturation) and K_{SAT} were estimated using SPAW (Table 7.3). Default values provided by Raes et al. (2017) for a sandy clay loam are 20, 32 and 47% for θ_{PWP}, θ_{FC} and θ_{SAT}, respectively. Similarly, the default values are 27, 39 and 50% for a sandy clay (Raes et al., 2017). These values agree favourably with those shown in Table 7.3. Estimated bulk density for the topsoil was higher than measured values, whereas the value at 0.5 m agreed favourably with measurements.

Table 7.3: Soil parameters obtained for Swayimane using the SPAW model

Soil texture	Thickness	θ_{PWP}	θ_{FC}	θ_{SAT}	K_{SAT}	ρ_b
	(m)	(%)			(mm d^{-1})	(g cm^{-3})
Sandy clay loam	0.15	23	36	50	164	1.32
	0.15	22	33	44	85	1.34
Sandy clay	0.30	23	34	44	64	1.33
	0.40	27	38	45	20	1.32

7.2.5.4 Soil water content

The majority of the Watermark sensors used in the 2015/16 season were left *in situ* in order to be re-used for the 2017/18 season. However, an additional Watermark sensor was installed at 100 cm in each plot so that soil water content could be monitored at four depths. Electrical resistance values measured by each Watermark sensor were then converted to soil water tension (i.e. soil matric potential) in kPa, as described in Section 5.2.5.4. Adjustments were made for soil temperature, which was measured at each of the four depths using thermocouples.

The conversion from soil water tension to volumetric water content was undertaken using a locally calibrated logarithmic equation (cf. Section 5.2.5.4). On 15 December 2017, Watermark sensors and CS650 soil water probes were installed in the opened soil pit at 10, 30, 60 and 100 cm. A PR2/6 access tube was also installed to facilitate weekly measurements of soil water content (using a PR2/6 profile probe; Delta-T, UK), and thus provided additional calibration data. Gravimetric soil samples were also taken on the day of planting to help validate the Watermark sensor calibration.

7.2.5.5 Crop growth and yield

During the 2017/18 season at Swayimane, the following crop parameters were measured (or observed) using the protocols given in Appendix F:

- Plant height and leaf number
- Chlorophyll Content Index
- Stomatal conductance
- Leaf Area Index
- Biomass production

The following crop parameters were determined after harvest using the protocols given in Appendix F:

- Accumulated biomass
- Grain yield
- Harvest Index

When the crop reached physiological maturity, the measured rows were harvested to determine the final biomass, yield and HI. Ten plants were harvested in each plot, five plants from each row. Harvesting was done sequentially since the crops matured at different times. PAN8906 was harvested first, followed by PAN8816 and lastly Macia. The harvested crops were air dried in a glasshouse for two weeks, after which each dry plant was weighed to determine total dry biomass. The panicle was then separated and weighed. The dry panicle was threshed to obtain the grains, which were then weighed.

7.2.5.6 Statistical analysis

Statistical analysis of crop growth, phenological development, final biomass and grain yield, and HI were performed using Genstat® (Version 18, VNS International, UK). An analysis of variance was performed to observe the difference between treatments. The least significant difference (LSD) and standard error of difference (SED) were used to separate means at 5% level of statistical significance.

7.2.6 Crop water use

The SWB method was proposed for estimating crop evapotranspiration. The SWB equation can be used to calculate actual crop evapotranspiration (*ET* in mm) as follows:

$$ET = P + I + U - R - D \pm \Delta S \qquad \text{Equation 7}$$

The above equation accounts for three positive fluxes of water (i.e. gains) into the root zone, such as precipitation (*P*), irrigation (*I*) and upward capillary rise (*U*). Negative fluxes (losses) include runoff (*R*), drainage (*D*), as well as changes in soil water content (ΔS).

Precipitation: Rainfall was measured using a tipping bucket rain gauge installed at the trial site (cf. Section 7.2.5.1).

Irrigation: The Swayimane trial was not irrigated to reflect typical smallholder farming conditions and thus, $I = 0$ mm.

Capillary rise: The assumption was made that the groundwater table is well below the root zone, and thus *U* is considered negligible (Dastorani and Poormohammadi, 2012).

Runoff: Due to the slope of the trial, runoff is not negligible. Three 1 x 1 m runoff plots were thus used to measure runoff.

Drainage: The wetting front at 1 m indicated that the soil water content was below field capacity throughout the growing period, and therefore deep percolation was zero.

Changes in soil water content: This variable was calculated as the difference between the initial (on planting day) and final (at physiological maturity) depth-averaged soil water content of the root zone.

7.2.7 Water Use Efficiency of crop and biofuel production

The two WUE metrics listed in Section 5.2.7 were calculated for sorghum in the 2017/18 season. Grain starch content was measured post-harvest at Stellenbosch University, then used to estimate the theoretical biofuel yield.

7.3 RESULTS AND DISCUSSION

7.3.1 Crop growth and yield

7.3.1.1 Plant height and leaf number

Plant height of all three sorghum cultivars increased gradually up to the flowering stage. Plant height increased mostly during the vegetative growth stage. Although Macia (semi-dwarf sorghum variety) reached a height of 95 cm compared to 87 and 80 cm for PAN8816 and PAN8906, respectively (Figure 7.2a), it can grow up to 150 cm tall. Neither of the two PANNAR cultivars reached their maximum height of approximately 115-117 cm. Statistical analysis of plant height revealed that there was a significant difference ($P < 0.001$) across cultivars, although data was statistically similar between fertility levels, as well as the interaction between factors. Although plant height showed no statistical difference with respect to fertility, all cultivars were taller when fertilized (Masanganise, 2019).

In Figure 7.2b, leaf numbers of all three sorghum cultivars increased gradually up to the end of the vegetative stage. All cultivars grew more leaves when fertilized, where the highest leaf number was observed for PAN8816 (11) at 89 DAP in the fertilized plots. The sharp decline in leaf number at 83 DAP in the unfertilized treatment occurred after a period of water stress, but may also be linked to deficient nutrients. Increased leaf number is desirable since it increases the surface area for radiation interception and transpiration (when necessary). It also reduces the amount of soil evaporation during dry periods. Leaf number was statistically similar ($P > 0.05$) between fertility and in the interaction between fertility and cultivar, but there was significant difference ($P < 0.001$) with respect to cultivar (Masanganise, 2019).

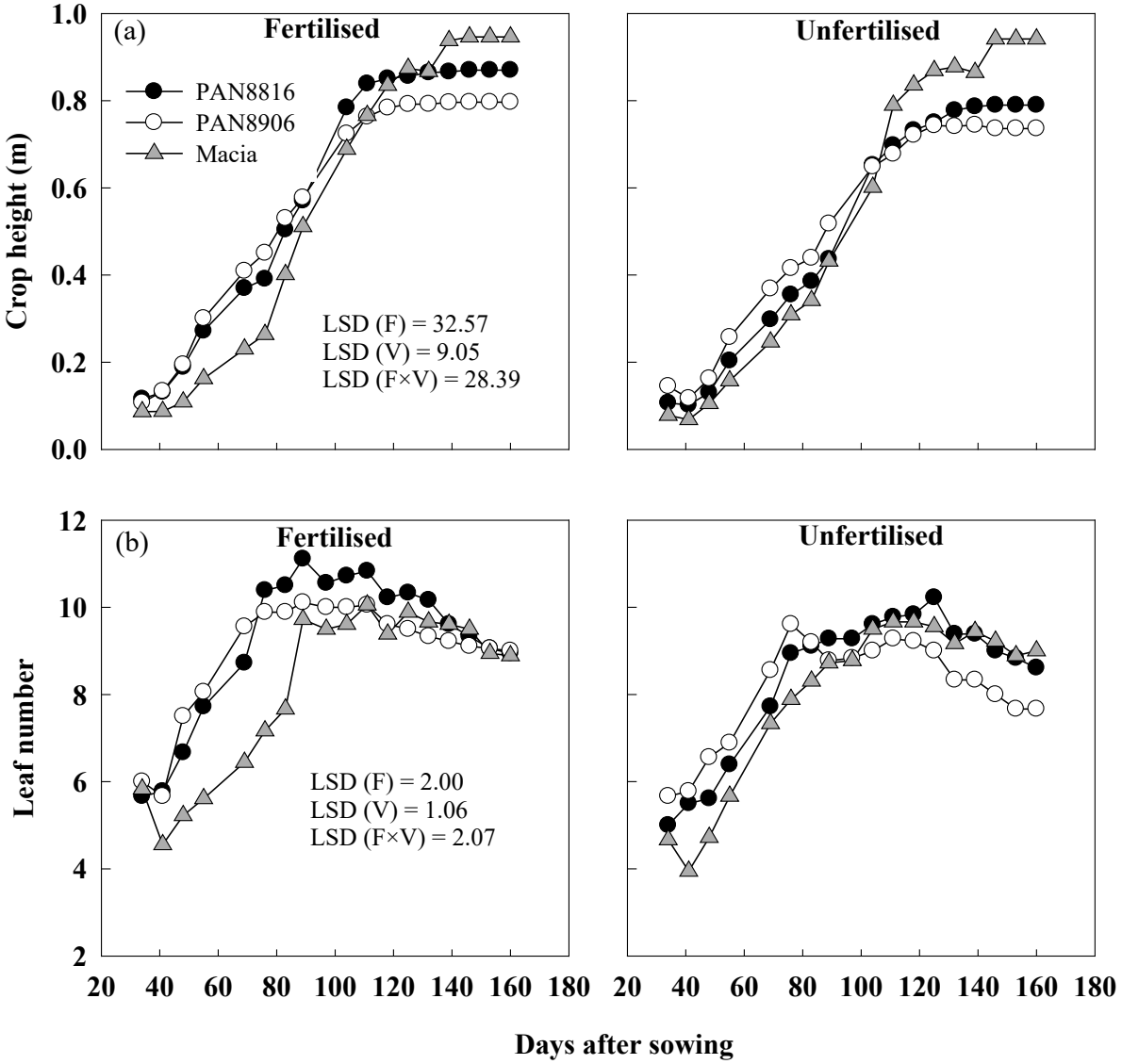

Figure 7.2: (a) Plant height and (b) leaf number for three grain sorghum cultivars (PAN8816, PAN8906 and Macia) grown under rainfed conditions and two fertility levels at Swayimane during the 2017/18 season (Masanganise, 2019)

7.3.1.2 Chlorophyll content and stomatal conductance

Stomatal conductance (SC) can provide an indicator of plant water stress. However, at around 80 and 120 DAP, low values resulted from measurements conducted during humid and overcast days. The SC was greatest on 97 DAP for all cultivars and under both fertilizer treatments. On average, SC was about 3% lower under 0% relative to 100% fertilizer. The SC was found to be significantly different $P < 0.001$) under fertility levels and neither significantly different across cultivars nor the interaction between fertility and cultivar (Figure 7.3a).

During periods of severe water stress, sorghum responds by closing leaf stomata to minimise water loss through transpiration. However, stomatal closure reduces intercellular gas exchange resulting in retarded metabolic processes. On the whole, cell development is inhibited resulting in decreasing plant growth and development (Pinheiro and Chaves, 2010). In a study to investigate the response of different sorghum genotypes to reduced soil water availability, Fracasso et al. (2016) reported that when the plants were water stressed, they allocated more biomass to roots than to leaves.

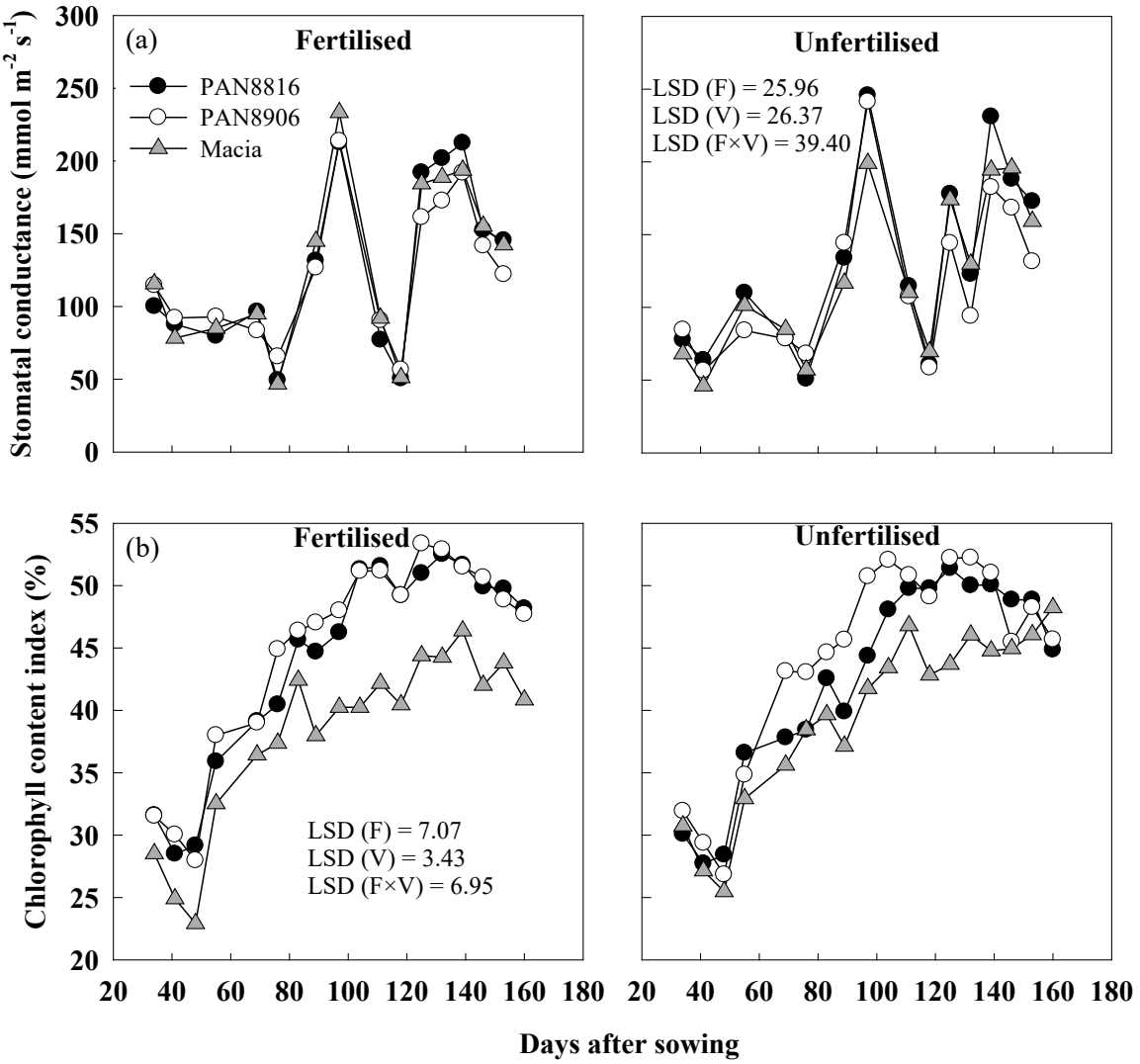

Figure 7.3: (a) Stomatal conductance and (b) Chlorophyll Content Index for three grain sorghum cultivars (PAN8816, PAN8906 and Macia) grown under rainfed conditions and two fertility levels at Swayimane during the 2017/18 season (Masanganise, 2019)

Chlorophyll Content Index is an indicator of plant health, as well as its ability to intercept photosynthetically active radiation. In Figure 7.3b, CCI decreased on Day 48 after planting, which coincided with a decrease in LAI (Figure 7.4a). Thereafter, CCI increased gradually and plateaued after floral initiation, with peak measurements exceeding 50. However, Hadebe et al. (2017a) reported a peak CCI of approximately 60 for PAN8816 and Macia grown at Ukulinga in the 2014/15 season. The average values were 43.4, 44.6 and 38.9% for PAN8816, PAN8906 and Macia, respectively. Although CCI for Macia was significantly lower than for both PANNAR cultivars for most of the season (especially in the fertilized treatment), its stay-green characteristics were evident as reflected in Figure 7.2b. The three cultivars were significantly different ($P < 0.001$) in terms of their CCI. However, the CCI was statistically similar under fertility levels, as well as in the interaction between fertility and cultivar.

7.3.1.3 Leaf Area Index and canopy cover

The LAI data shown in Figure 7.4a was measured using a LAI-2200 plant canopy analyser (LI-COR Inc., Nebraska, USA). Diffuse non-intercepted radiation (an output of the LAI-2200 canopy analyser) was then used to calculate canopy cover as described in Section F1.5 (Appendix F).

Due to the unexpected variation in LAI (and canopy cover) shown in Figure 7.4, the plant canopy analyser was returned to LI-COR in the USA, who confirmed the device as faulty, which was subsequently recalibrated and returned to South Africa.

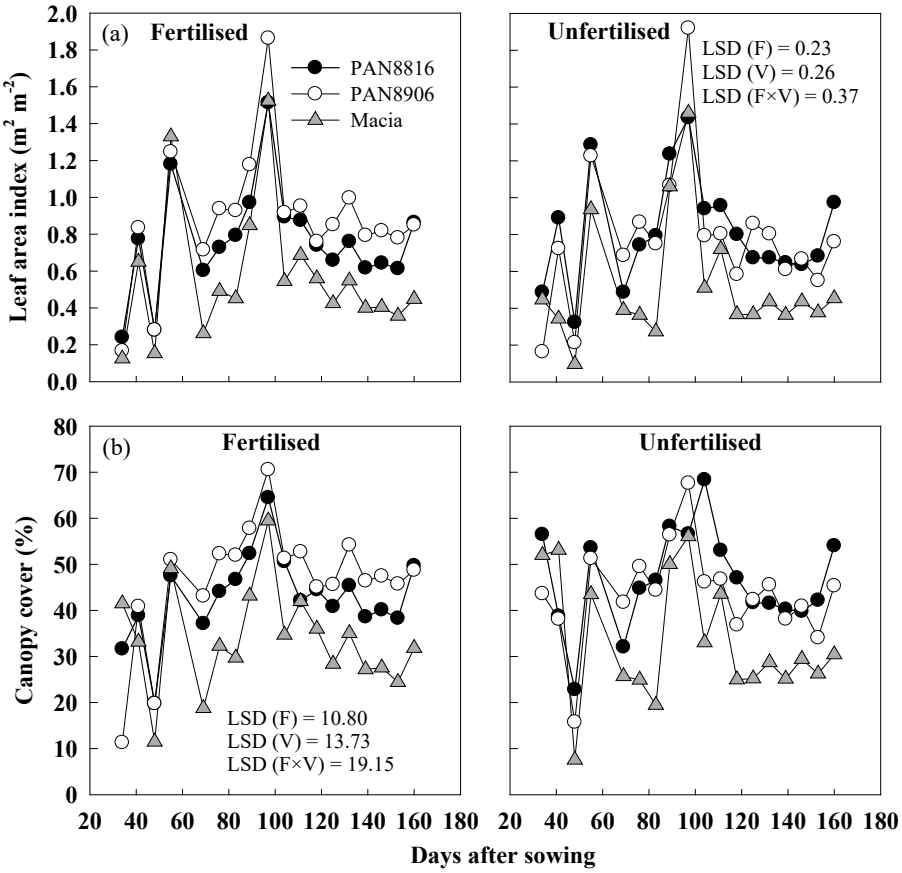

Figure 7.4: (a) Leaf Area Index and (b) canopy cover for three grain sorghum cultivars (PAN8816, PAN8906 and Macia) grown under rainfed conditions and two fertility levels at Swayimane during the 2017/18 season (Masanganise, 2019)

7.3.1.4 Phenological development

Time to establishment, expressed in GDDs, was significantly different ($P < 0.001$) across cultivars, but statistically similar between fertility levels, as well as in the interaction between fertility and cultivar. Time to flowering, the duration of flowering, as well as the time to start of grain filling and senescence were also significantly different ($P < 0.001$) with respect to cultivar, yet statistically similar with respect to fertility and the interaction between factors.

The cultivar significantly ($P < 0.001$) influenced the time to physiological maturity, while fertility and the interaction between fertility and cultivar did not. PAN8906 was the first to mature, followed by PAN8816 and lastly Macia. Similar trends in the phenological development of late-planted sorghum genotypes were reported by Hadebe et al. (2017a). In their study, they also found that Macia had a longer growing cycle than hybrids.

The authors explained that, under water stress, Macia adapts to irregular rainfall to a greater degree compared to hybrid genotypes. Therefore, its phenological stages are relatively longer. Macia demonstrated that it is more tolerant to harsh conditions in comparison to hybrids. These findings suggest that, to realise greater returns from late-planted sorghum, it is necessary to breed for improved cultivars that are tolerant to cold and water stress.

Table 7.4: Thermal time (in growing degree-days) to reach various phenological stages for three grain sorghum cultivars (PAN8816, PAN8906 and Macia) grown under 100% fertilizer at Swayimane during the 2017/18 season (Masanganise, 2019)

Phenological stage	Time in GDD for the fertilized treatment		
	PANN8816	PAN8906	Macia
Establishment	129	129	171
Flowering	993	979	1,133
Flowering duration	149	123	174
Grain filling	1,339	1,279	1,387
Senescence	1,544	1,518	1,574
Physiological maturity	1,634	1,616	1,707

7.3.1.5 Biomass production

Biomass accumulation for grain sorghum grown at Swayimane in the 2017/18 season is shown in Figure 7.5. In the fertilized treatment, PAN8906 produced significantly more above-ground biomass compared to the other two cultivars. Unfertilized Macia produced significantly lower biomass production. Generally, all cultivars showed increased biomass accumulation when fertilized. Biomass accumulation was not significantly different (P > 0.05) across cultivars, neither was it significantly different between fertility level or in the interaction between factors.

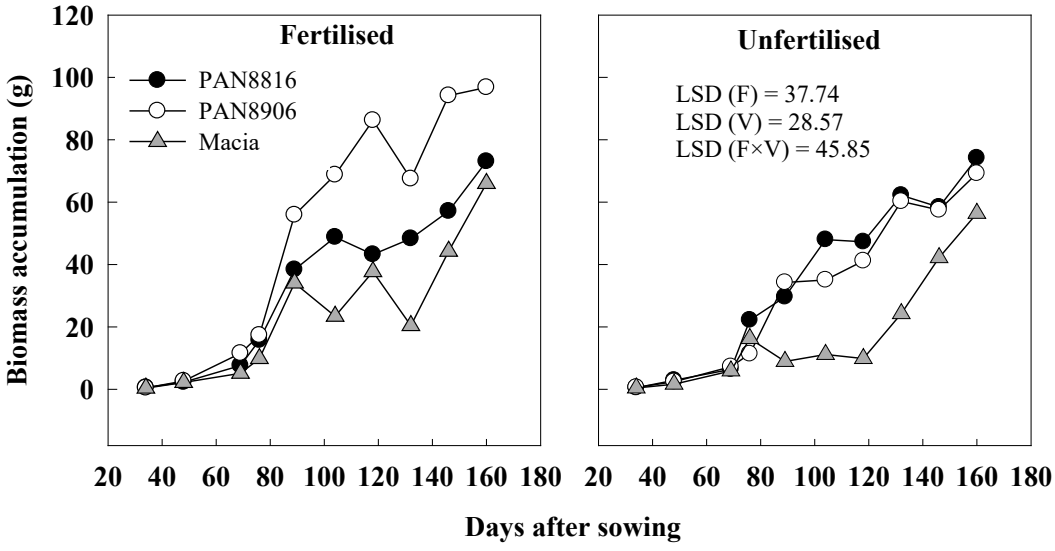

Figure 7.5: Biomass accumulation for three grain sorghum cultivars (PAN8816, PAN8906 and Macia) grown under rainfed conditions and two fertility levels at Swayimane during the 2017/18 season (Masanganise, 2019)

7.3.2 Final yields and harvest index

Harvesting of the 2017/18 trial at Swayimane commenced on 5 July 2018. The final biomass and grain yields obtained for the three grain sorghum cultivars are shown in Table 7.5, from which the HI was calculated. Across all factors, final biomass yield was not significantly different (P > 0.05). Grain yield was statistically similar (P > 0.05) under 0 and 100% fertilizer, as well as in the interaction between fertility and cultivar. However, it was statistically different (P < 0.05) across cultivars. The HI was statistically similar (P > 0.05) between fertility levels. However, it was statistically different (P < 0.05) across cultivars, as well as in the interaction between fertility and cultivar.

Table 7.5: Final biomass and grain yield, as well as Harvest Index values for three grain sorghum cultivars (PAN8816, PAN8906 and Macia) grown under 0 and 100% fertilizer at Swayimane during the 2017/18 season (Masanganise, 2019)

Treatment	Fertilized			Unfertilized		
Cultivar	PAN8816	PAN8906	Macia	PAN8816	PAN8906	Macia
Biomass (t ha^{-1})	4.64	6.41	5.32	4.06	4.13	3.35
Grain yield (t ha^{-1})	1.76	2.59	0.92	1.52	1.63	0.68
Harvest Index	0.38	0.40	0.17	0.37	0.39	0.20

Biomass yield for all cultivars was about 30% lower under 0% relative to 100% fertilizer. Notably, Macia produced more biomass than PAN8816 under 100% fertilizer. Grain yield for all cultivars was about 27% lower under 0% relative to 100% fertilizer. For PAN8816, grain yield was 13% lower, while it was 37 and 27% lower for PAN8906 and Macia, respectively. The increase in biomass and grain yield with fertility is expected. This is reported in many studies in the literature.

Since the average sorghum yield in South Africa is approximately 1.5 t ha^{-1}, PAN8906 is considered a high-yielding cultivar, especially when fertilized. However, the Swayimane yields were lower than those obtained at Ukulinga in two previous seasons. Hadebe et al. (2017a) reported yields of ~3.5 t ha^{-1} for PAN8816 and Macia planted in the 2013/14 season at Ukulinga, which were higher than those observed in the following season (2.71 and 3.26 t ha^{-1}, respectively).

Macia exhibited the lowest HI across cultivars and between fertility levels, due to the low grain yield observed for both treatments. Hadebe et al. (2017a) reported HI values of ~0.50 for PAN8816 and Macia from the 2013/14 season at Ukulinga. However, fertilization did not result in higher HI values, which was expected. Ideally, grain sorghum plants should achieve full canopy cover, avoiding high LAI since excessive vegetative growth tends to reduce the HI (Steduto et al., 2012). Furthermore, if there is no water stress during the vegetative period, some sorghum cultivars may tiller excessively. If a high portion of the tillers is barren, this results in high biomass produced, but with a low HI.

7.3.3 Crop water use

7.3.3.1 Crop evapotranspiration

As noted in Section 7.2.6, crop water use was estimated using the SWB equation. Runoff was measured from 15 March 2018 onwards, which means simulated values (using AquaCrop) were used before this date. Accumulated rainfall was higher for Macia as it reached physiological maturity 10 days after the two PANNAR hybrids. The SWC was based on measurements (at four depths) obtained from CS650 sensors installed in the unfertilized section of the trial; hence, the SWB in the fertilized block was assumed to be the same as for the non-fertilized block. Figures of 405, 410 and 400 mm were estimated for PAN8816, PAN8906 and Macia, respectively (Masanganise, 2019). Kunz et al. (2015a) reported similar seasonal ET values of 436 and 461 mm for grain sorghum grown under irrigated conditions at Ukulinga.

7.3.3.2 Crop coefficients

Crop coefficients were not determined as the trial was rainfed, and thus not conducted under standard (non-stressed) conditions. From the literature, Shenkut et al. (2013: 22) provided initial, development, mid-season and late-season K_C values of 0.45, 0.83, 1.18 and 0.78, respectively. Similarly, Kunz et al. (2015a) provided similar K_C values of 0.51, 0.89, 0.97 and 0.80 that presented averaged values obtained from two consecutive seasons at Ukulinga. Allen et al. (1998) provided a mid-season K_C value of 1.10 and 0.55 for the late season.

7.3.4 Water Use Efficiency of crop and biofuel production

7.3.4.1 Crop Water Use Efficiency

As noted earlier in Section 7.3.2, the grain yield was lower than expected. This resulted in low WUE across all cultivars (Table 7.6), due mainly to water stress experienced during the growing season. The growing season evapotranspiration and WUE were highest for PAN8906 and lowest for Macia for the two fertilizer treatments. This agrees with findings of Kunz et al. (2015a), who reported water use efficiencies of 0.572 and 0.405 kg m^{-3} for PAN8816. The low values of WUE exhibited by Macia may be explained in terms of low grain yield due to the distribution of assimilates. As mentioned earlier, Macia is thick-stemmed and was the tallest variety. During the vegetative phase when the conditions were relatively favourable, Macia partitioned more of its assimilates towards biomass production.

Table 7.6: Water use efficiency of crop yield for three grain sorghum cultivars (PAN8816, PAN8906 and Macia) grown under 100 and 0% fertilizer at Swayimane during the 2017/18 season (Masanganise, 2019)

Treatment	Fertilized			Unfertilized		
Cultivar	**PAN8816**	**PAN8906**	**Macia**	**PAN8816**	**PAN8906**	**Macia**
Grain yield (kg ha^{-1})	1,760	2,590	0,920	1,520	1,630	680
Crop water use (m^3)	4,050	4,100	4,000	4,050	4,100	4,000
WUE_C (kg m^{-3})	0.44	0.63	0.23	0.38	0.40	0.17

7.3.4.2 Biofuel Water Use Efficiency

Biofuel yield was calculated from the grain yields listed above, as well as the starch contents and fermentation efficiencies given in Section 12.2. PAN8906 produced the highest biofuel yield, followed by PAN8816 and lastly Macia under 100% fertilizer (Table 7.7). A hybrid, which has a greater grain yield, does not necessarily produce more biofuel. For example, the grain yield for PAN8816 was less than that of PAN8906 under 0% fertilizer (cf. Table 7.5), but this cultivar produced the highest biofuel yield under this treatment. This is explained by the highest grain starch content and the fermentation efficiency for PAN8816 across all cultivars and between the two fertilizer treatments (cf. Section 12.2). Wang et al. (2008) produced ethanol from seven different grain sorghum genotypes, whose grain starch content ranged between 64 and 74%, and reported that this difference in starch content could result in up to a 15% difference in ethanol volume per unit of grain used. Macia is less desirable for biofuel production because of the lower grain yield and higher biomass production. PAN8906 and PAN8816 were the most water use efficient hybrids in terms of biofuel production for the 100 and 0% fertilizer treatments, respectively.

Table 7.7: Biofuel yield and water use efficiency of biofuel production for three grain sorghum cultivars (PAN8816, PAN8906 and Macia) grown under 0 and 100% fertilizer at Swayimane during the 2017/18 season (Masanganise, 2019)

Treatment	Fertilized			Unfertilized		
Cultivar	**PAN8816**	**PAN8906**	**Macia**	**PAN8816**	**PAN8906**	**Macia**
Biofuel yield (ℓ ha^{-1})	707	941	291	618	560	270
Crop water use (m^3)	4,050	4,100	4,000	4,050	4,100	4,000
WUE_B (ℓ m^{-3})	0.18	0.23	0.07	0.15	0.14	0.07

7.3.5 Summary and conclusions

The 2017/18 trial was conducted to estimate the seasonal crop evapotranspiration, grain and biofuel yield, as well as the WUE of three grain sorghum cultivars grown under rainfed conditions and two fertility levels. The grain yield was mainly influenced by the climatic conditions that prevailed during the growing period. The decline in air temperature, solar irradiance and rainfall experienced before the end of the growing period point to the need for early planting if crops are to escape cold and water stress. The study demonstrated that grain yield and starch content are important factors influencing biofuel production from grain sorghum. PAN8906 showed potential to produce greater yields, and more biofuel with less water consumption than PAN8816. Macia produced a relatively high proportion of biomass to grain, and may thus not be a suitable feedstock for biofuel production.

CHAPTER 8: WATER USE AND YIELD OF SOYBEAN: 2018/19

8.1 INTRODUCTION

The overall aim of the field trial was to quantify feedstock water use and yield of soybean under various agronomic management scenarios (cultivar choice vs inoculation). The field-based measurements contributed towards the partial calibration of the AquaCrop model for smallholder farming environments under rainfed conditions (e.g. Swayimane).

8.2 MATERIALS AND METHODS

8.2.1 Site description

A description of the Swayimane trial site was provided in Section 5.2.1 and Section 7.2.1. Thus, it is not repeated here.

8.2.2 Planting material

In total, seven Roundup® Ready soybean cultivars were received from three suppliers (PANNAR, Link Seed and Capstone Seeds), of which two donated seed bags. Since the site is best suited to medium- to late-maturing cultivars, PAN1521R, LS6161R and CAPG3 were selected for planting. The agronomic characteristics of each cultivar is given in Table 73.2 (cf. Section 3.2.2.1).

8.2.3 Experimental design

Similar to the two previous trials at Swayimane, a split-plot design was selected, which was arranged in randomised complete blocks, with sub-plots replicated three times (Appendix H). The main factor was allocated to inoculant use. The sub-plots comprised three soybean cultivars. The trial measured 451 m^2 in area, with individual plot sizes of 6 m x 3 m (18 m^2). Each plot contained seven rows as follows: two inner (i.e. experimental) rows where all measurements were conducted over the growing season, one row for destructive sampling and two outer or border rows on either side (i.e. four rows in total), which were not considered due to edge effects.

Watermark sensors (Irrometer, Riverside, California, USA) were installed in plots 4 to 6 and 13 to 15 at depths of 0.15, 0.30, 0.60 and 1.00 m to monitor changes in soil moisture over the growing season (Appendix H). Four CS650 soil moisture sensors (Campbell Scientific, Utah, USA) were placed in Plot 14 at the same four depths as the Watermark sensors. This was done to calibrate the Watermark sensors, but due to budget constraints, CS650 sensors were not installed in any other plots. Soil thermocouples were also installed in plots 5 and 14 for soil surface temperature monitoring. All sensors were connected to a CR1000 data logger (Campbell Scientific Inc., Logan, Utah, USA) that was installed in the middle of the trial in a strong box (SB in Appendix H). Gravimetric samples were taken in plots 6 and 13 to represent both cultivars and treatments.

For surface runoff measurements, 1 m x 1 m aluminium square grids were placed down the slope of the trial in plots 4, 7 and 11, as well as to represent the three planted cultivars. An AWS is situated below the trial plots for the continuous monitoring of climatic parameters (i.e. rainfall, solar irradiance, air temperature, relative humidity, wind speed and direction) throughout the growing season.

8.2.4 Agronomic practices

8.2.4.1 Site preparation

Land preparation was completed in late October 2018. The site was sprayed with herbicide to kill the winter weed load. Fencing was installed around the experimental site to protect the plots from animals such as cows. Hand hoes were then used to achieve a smooth tilth in preparation for planting. The abovementioned tasks were completed with the help of staff from Ukulinga research farm, as well as contracted labour from the local Swayimane community. Prior to planting, the trial site was sprayed with Dual Gold, a pre-emergent herbicide, to control weeds. A dilution rate of 60 mℓ of herbicide per 16 ℓ of water was used. The trial site was sprayed at flowering using Kemprin insecticide (a/l cypermethrin) using a total dilution rate of 185 mℓ of insecticide to 16 ℓ of water.

8.2.4.2 Planting

Soybean is usually planted with a row spacing of 40 to 90 cm and 5 to 15 cm between the plants in each row to achieve a planning population of 200,000 to 400,000 plants per hectare. Planting was originally planned for 15 to 16 November, but was delayed due to the hot and dry conditions experienced since 10 November (Figure 8.1). Planting finally took place on Monday, 19 November, after 11.6 mm of rainfall had fallen over the weekend. This meant the inoculated seed was planted into moist soil (as desired).

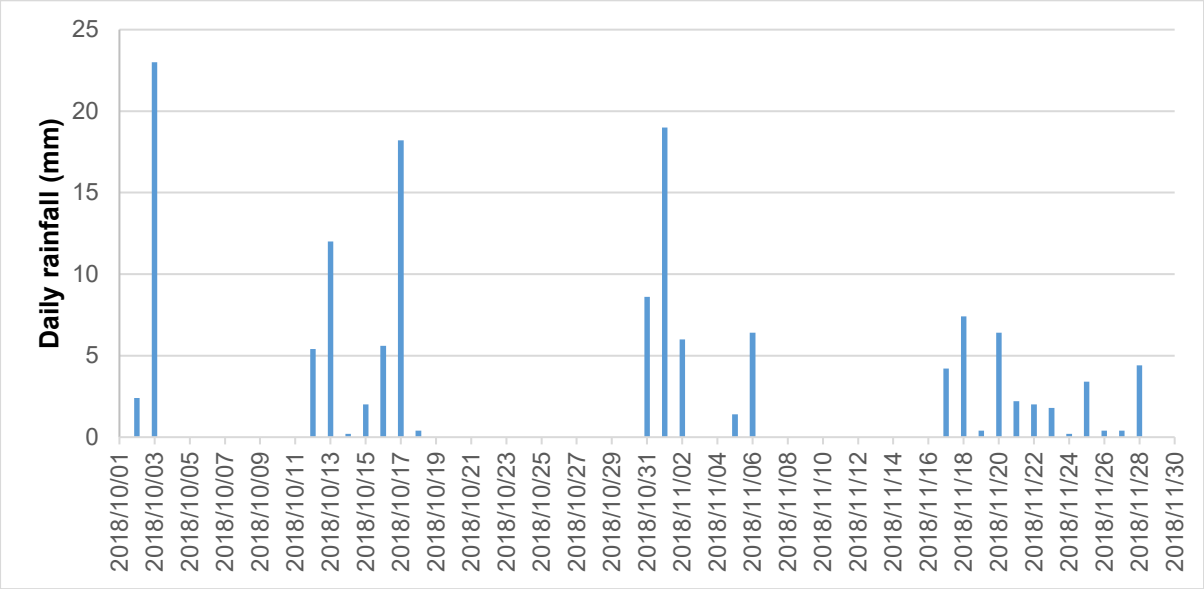

Figure 8.1: Daily rainfall measured with an automatic weather station at Swayimane during the month of planting

Planting was done with an inter-row spacing of 45 cm and an intra-row spacing of 7 cm to achieve a targeted planting density of ~317,460 plants ha^{-1}. Planting rows were opened using hand hoes and seeds were individually sown (not broadcasted) at a depth of 0.03 m. This negated the need to thin the trial after emergence, which can damage the establishing crop, and thus affect crop development (DAFF, 2010a). Unfortunately, six sub-plots planted to PAN1521R did not emerge. A germination test confirmed that the seed was not viable. Although PANNAR offered another bag of seed, the decision was made to leave these plots unplanted.

The immediate area surrounding the trial site was sprayed with Gramoxone (150 mℓ to 10 ℓ of water) to control weed growth during the growing season. To prevent an outbreak of soybean rust, the trial site was sprayed during floral initiation (February) using Artea fungicide spray at a dilution rate of 29 mℓ to 16 ℓ of water. A second application was applied 21 days later floral initiation.

8.2.4.3 Treatments

Seed planted in half of the trial plots was inoculated in accordance with the guideline published in Appendix E**.** In total, 50 mℓ of liquid inoculant (*Bradyrhizobium japonicum*), supplied by Link Seed, was added to a 16 ℓ knapsack and mixed thoroughly with water. The mixing was done in a cool shady place to prevent exposure of the bacterium to the elements. The inoculant was applied in the furrows with the seed and fertilizer to only one half of the trial. The furrows were then immediately covered to prevent the exposure of the bacteria to the climatic conditions, which could render the treatment ineffective over the growing period.

Nine topsoil samples were sent to Cedara Agricultural College on 18 September 2018 for fertility assessment. The clay content and organic carbon content of the topsoil samples varied from 26 to 37% and 1.3 to 4.6%, respectively. In addition, soil pH ranged from 4.11 to 4.23. The results showed that no nitrogen is required to achieve the optimum target yield, with phosphorus and potassium requirements ranging from 20 to 60 and 50 to 80 kg ha^{-1}. Single superphosphate (P; 10.5%) and potassium chloride (K; 50%) fertilizers were applied at optimum rates using a broadcasting method to all plots.

8.2.5 Data collection

For this study, variables related to the weather, crop water use, soil water content, as well as crop growth and phenology, were measured and monitored throughout the growing season. In this subsection, these variables are described in more detail.

8.2.5.1 Climate

As noted in Section 7.2.5.1, the AWS was upgraded in October 2016. Climate variables can be viewed online at http://agromet.ukzn.ac.za:5355/index.html.

8.2.5.2 Soil texture

Prior to planting, soil samples were taken at 0.15, 0.30, 0.60 and 1.00 m and sent to the Cedara Agricultural College for soil texture analysis. The soil textural analysis shown in Table 8.1 indicated that the top 0.3 m is dominated by sandy clay loam, which transitions into a sandy clay for the next 0.7 m.

Table 8.1: Soil particle size distribution and textural classes for the different depths at the experimental site

Soil profile depth	Coarse silt and sand (0.02-2 mm)	Fine silt (0.002-0.02 mm)	Clay (< 0.002 mm)	Soil textural class
m	Percentage	Percentage	Percentage	
0.15	48	19	33	Sandy clay loam
0.30	51	16	33	Sandy clay loam
0.60	49	17	34	Sandy clay
1.00	47	12	41	Sandy clay

8.2.5.3 Soil water retention

Soil water retention (i.e. porosity, FC and PWP) parameters and saturated hydraulic conductivity were estimated using the SPAW model and compared to measured values. The organic carbon content of the nine topsoil samples ranged from 1.3 to 4.6% (average 2.8%). Four undisturbed soil cores were obtained from an opened pit and used to determine soil dry bulk density, from which saturation was calculated. The undisturbed soil cores were also used to determine field capacity (at -33 kPa) using the controlled outflow pressure method in the soil water laboratory at the University of KwaZulu-Natal.

Data from the outflow pressure apparatus was also used to create soil water retention curves via the Van Genuchten equation (Van Genuchten, 1980), from which PWP (at -1,500 kPa) was estimated.

The results given in Table 8.2 show that the SPAW model tends to over-estimate dry bulk density and certain soil water retention parameters. Thus, values determined from the laboratory were used in this study. However, there is an error in the PWP value at 1 m that was obtained from the soil water retention curves (see difference of 11.5% when compared to the 0.60 m value). The error is due to the increasing clay content with depth and the high clay content of 41% at 1 m. The K_{SAT} decreased from 152.4 mm d^{-1} at 0.15 m to 31.7 mm d^{-1} at 1.00 m due to increasing clay content with depth. In addition, bulk densities should rather be measured and not estimated using SPAW.

Table 8.2: Estimation of soil water retention parameters using two methods (Reddy, 2019)

Method	Soil water characteristics	Depth (mm)			
		150	**300**	**600**	**1000**
SPAW model	θ_{SAT} (%)	48.2	44.3	44.6	45.0
	θ_{FC} (%)	34.4	32.6	33.1	36.9
	θ_{PWP} (%)	22.0	21.3	21.5	25.4
	ρ_B (g m^{-3})	1.4	1.5	1.4	1.4
	K_{SAT} (mm d^{-1})	152.4	94.6	89.9	31.7
Outflow pressure	θ_{SAT} (%)	58.5	58.4	57.9	52.8
	θ_{FC} (%)	36.7	38.9	40.5	38.1
	θ_{PWP} (%)	12.4	14.6	15.2	*26.7*
	ρ_B (g m^{-3})	1.1	1.1	1.2	1.2

8.2.5.4 Soil water content

The Watermark sensors from the 2017/18 season were left *in situ* to be re-used in 2018/19. Hence, soil water content was monitored at four depths in six plots. Soil temperature monitored by thermocouples at four depths, as well as by the CS650 probes, was used to adjust soil water tension readings obtained from the Watermark sensors. The Watermark sensors were re-calibrated using continuous measurements of volumetric water content obtained from four CS650 probes. In addition, periodic gravimetric samples were taken over the growing season to validate the Watermark sensor calibration.

8.2.5.5 Crop growth and yield

During the 2018/19 season at Swayimane, crop parameters listed in Section 7.2.5.5 were measured (or observed) using the protocols given in Appendix F. There were seven rows of plants in each treatment plot. Since the two outer rows were ignored due to edge effects, crop measurements were made on the two inner rows (Appendix H). When the crop reached physiological maturity, the two measured rows were harvested to determine the final biomass, yield and HI. Ten plants were harvested in each plot, five plants from each row. Harvesting was done sequentially since the two cultivars matured at different times. The LS6161R was harvested first, followed by CAPG3. The harvested crops were air dried in a glasshouse for two weeks, after which each dry plant was weighed to determine total dry biomass.

8.2.5.6 Statistical analysis

The same statistical analysis outlined in Section 7.2.5.6 was used in the 2018/19 season.

8.2.6 Crop water use

Total evaporation (actual evapotranspiration) was determined using the SWB equation as detailed in Section 7.2.6.

8.2.7 Water Use Efficiency of crop and biofuel production

The two WUE metrics listed in Section 5.2.7 were calculated for soybean in the 2018/19 season. Soybean seed oil content was determined using a hexane extraction process (Meyer et al., 2008) for each plot, then averaged for both soybean cultivars grown under the two inoculation treatments. The seed oil content was then used to estimate the theoretical biofuel yield.

8.3 RESULTS AND DISCUSSION

8.3.1 Crop growth and yield

8.3.1.1 Plant height and leaf number

As shown in Figure 8.2, the inoculated cultivars were slightly taller than the non-inoculated cultivars. Furthermore, CAPG3 was taller than the LS6161R cultivar for both inoculation treatments. However, there were no statistical differences ($P > 0.05$) in plant height between cultivars, inoculation treatments and the interaction between these factors. This suggests that the inoculation treatment did not significantly influence the plant height of both cultivars. Since LS6161R is a semi-determinant cultivar, plant height stops increasing once flowering to pod formation (i.e. approximately 71 to 88 DAP) is reached. The CAPG3 is a determinant cultivar that continues to develop after flowering pod formation and should thus be taller than LS6161R (cf. Section 3.2.2.1).

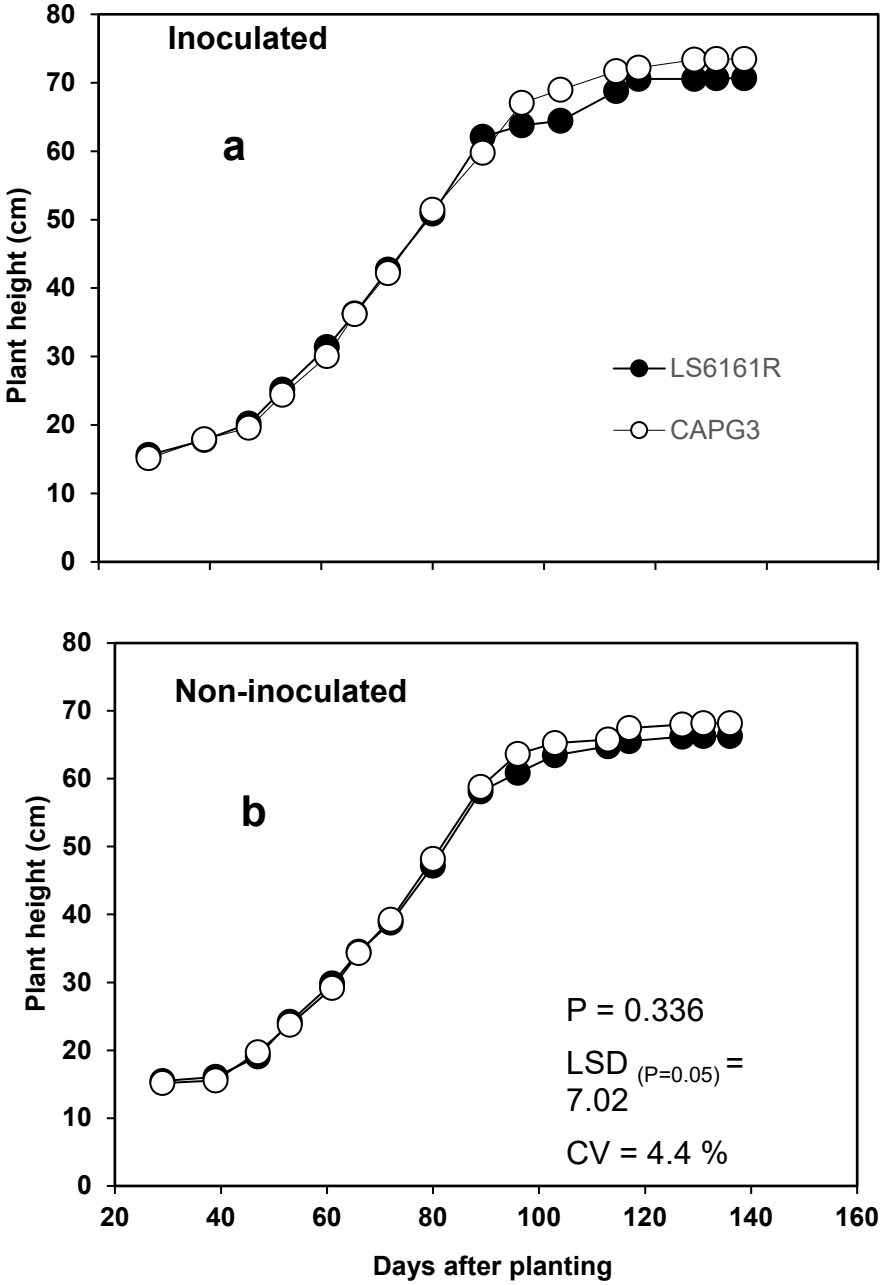

Figure 8.2: Plant height for two rainfed soybean cultivars (LS6161R and CAPG3) grown under (a) inoculated and (b) non-inoculated treatments at Swayimane during the 2018/19 season (Reddy, 2019)

From Figure 8.3, it is evident that CAPG3 produced more leaves than LS6161R under both treatments. Under inoculation, maximum measured values were 139 and 157 at 89 DAP for LS6161R and CAPG3, respectively. The maximum leaf number values measured were 128 and 138 at 89 DAP for LS6161R and CAPG3 respectively under non-inoculation treatment. The lower leaf number for LS6161R could be due to the difference in maturity date for each cultivar, since LS6161R is an early-maturing cultivar, which will produce less leaves as it develops faster, when compared to the later-maturing CAPG3 cultivar. Although there is a slight difference in leaf number between inoculation treatments, leaf number was not significant ($P > 0.05$) between cultivars, inoculation treatments and the interaction between these factors.

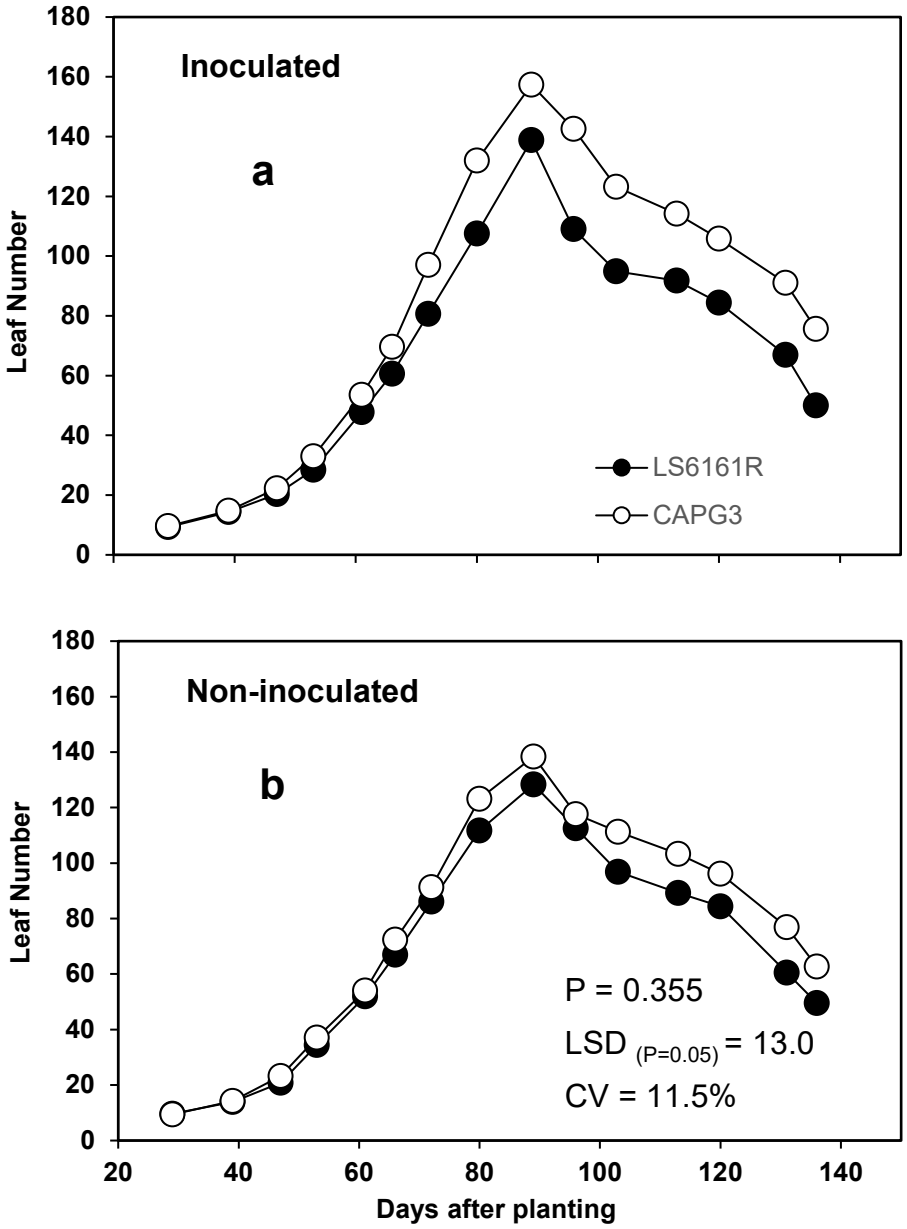

Figure 8.3: Leaf number for two rainfed soybean cultivars (LS6161R and CAPG3) grown under (a) inoculated and (b) non-inoculated treatments at Swayimane during the 2018/19 season (Reddy, 2019)

8.3.1.2 Chlorophyll content and stomatal conductance

Chlorophyll content index was measured as an indicator of both plant health and its ability to capture photosynthetically active chlorophyll (Devnarain et al*.,* 2016). The statistical analysis of CCI showed a significant difference ($P < 0.05$) between cultivars, but no significant difference ($P > 0.05$) between inoculation treatments. However, there were also significant differences ($P < 0.05$) in the interaction between cultivars and inoculation treatments. Both cultivars and inoculation treatments had a similar CCI trend, as shown in Figure 8.4.

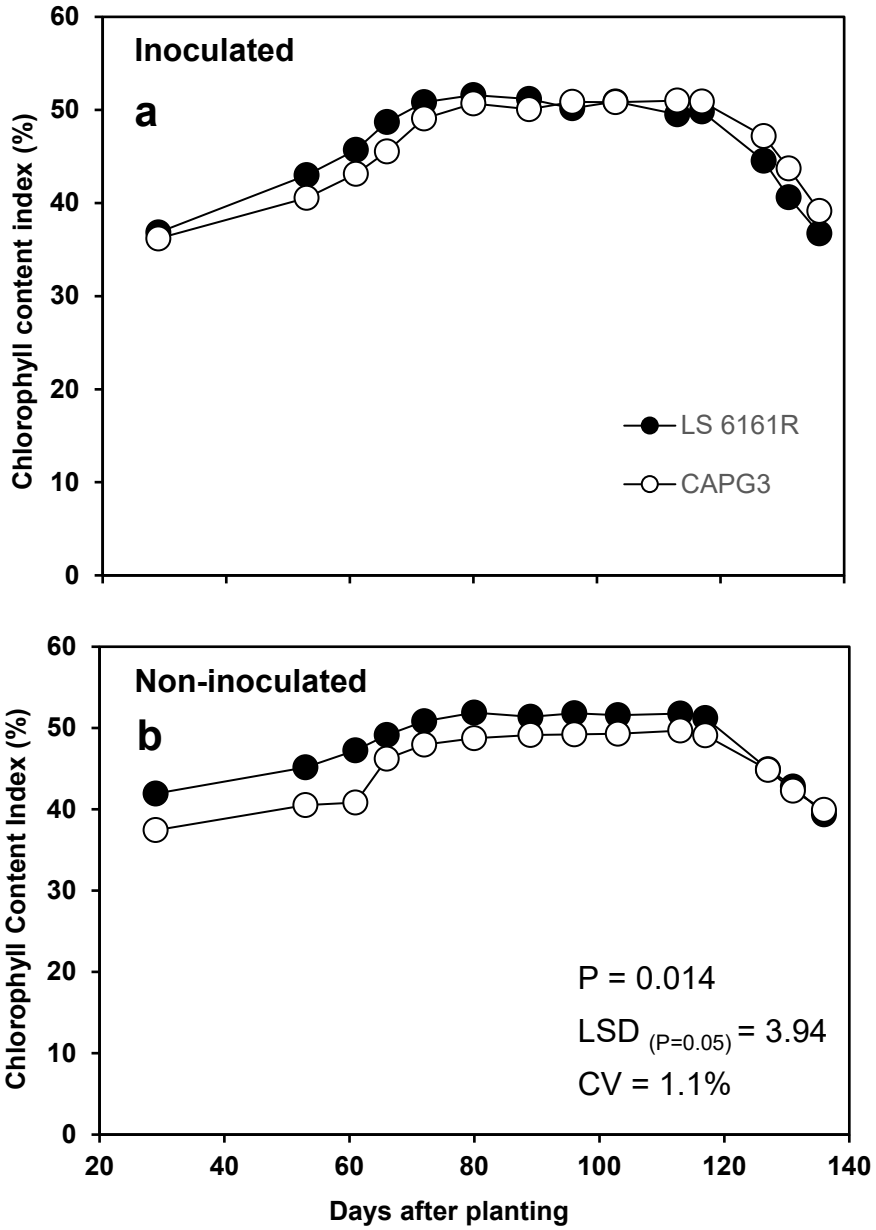

Figure 8.4: Chlorophyll content index for two rainfed soybean cultivars (LS6161R and CAPG3) grown under (a) inoculated and (b) non-inoculated treatments at Swayimane during the 2018/19 season (Reddy, 2019)

The LS6161R cultivar exhibited a slightly higher CCI than CAPG3, in particular for the non-inoculated treatment (cf. Figure 8.4b). This may indicate that the latter cultivar was affected more by nitrogen deficiency. In addition, LS6161R may be better adapted to nitrogen deficient conditions, which is deemed an attractive adaptation mechanism for smallholder farming. A healthy crop would indicate high transpiration or productivity (i.e. higher stomatal conductance), which results in higher biomass and crop yields, which was observed for both cultivars under the inoculation treatment.

Stomatal conductance was significantly different ($P < 0.05$) between cultivars and between inoculation treatments. However, the interaction between the two inoculation treatments and cultivars was not significantly different ($P > 0.05$). From Figure 8.5a and Figure 8.5b, SC was lowest on approximately 47 and 103 DAP for both cultivars and inoculation treatments, which coincided with high relative humidity levels that were close to 80% (i.e. the air was saturated); hence, there was no gradient for transpiration.

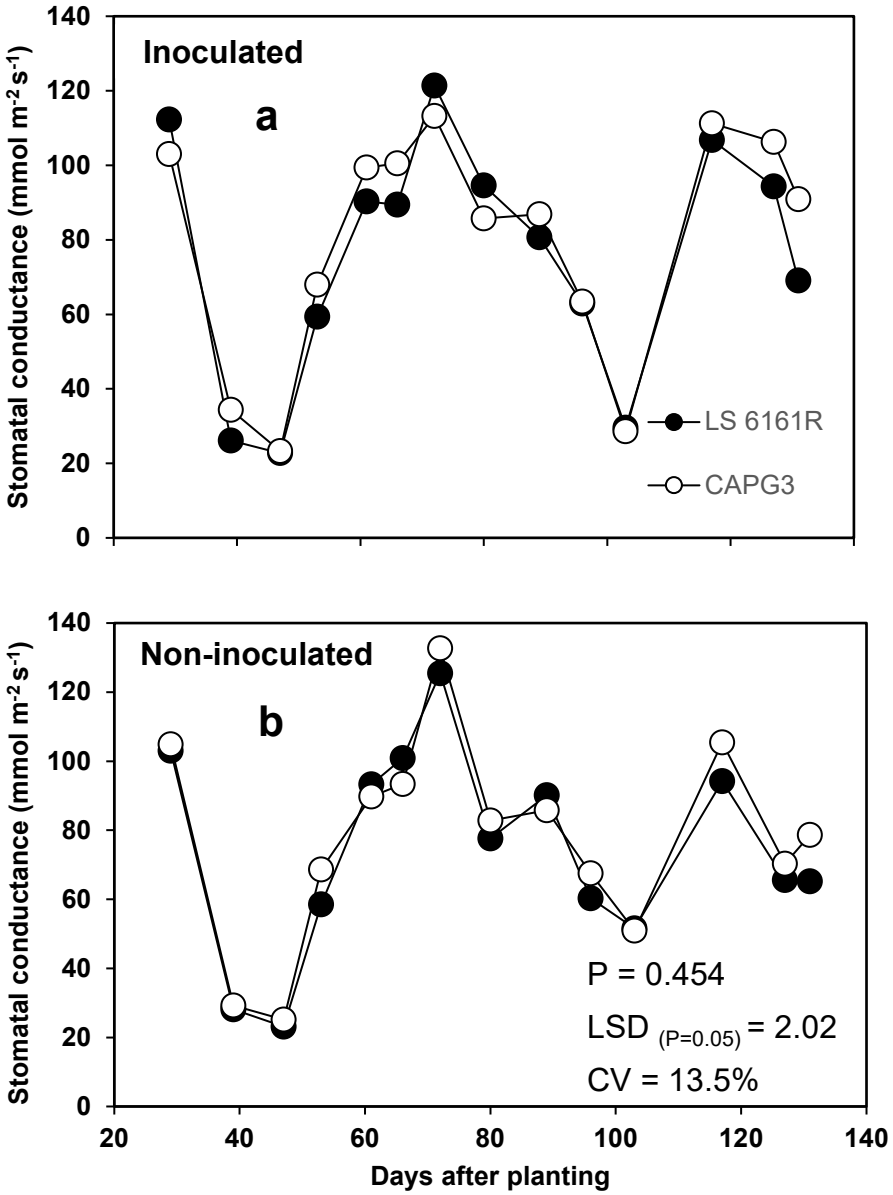

Figure 8.5: Stomatal conductance for two rainfed soybean cultivars (LS6161R and CAPG3) grown under (a) inoculated and (b) non-inoculated treatments at Swayimane during the 2018/19 season (Reddy, 2019)

8.3.1.3 Leaf Area Index and canopy cover

As shown in Figure 8.6, the LAI for both LS6161R and CAPG3 was not significantly different ($P > 0.05$) between cultivars and inoculation treatments. The interaction between the two inoculation treatments and cultivars was also not significantly different ($P > 0.05$). For the inoculated treatment, maximum LAI was 5.8 (at 103 DAP) and 4.6 m^2 m^{-2} (at 96 DAP) for CAPG3 and LS6161R, respectively. The LAI values for both cultivars and inoculation treatments followed a similar trend with low values at planting, which peaked from flowering to pod formation and decreased after senescence.

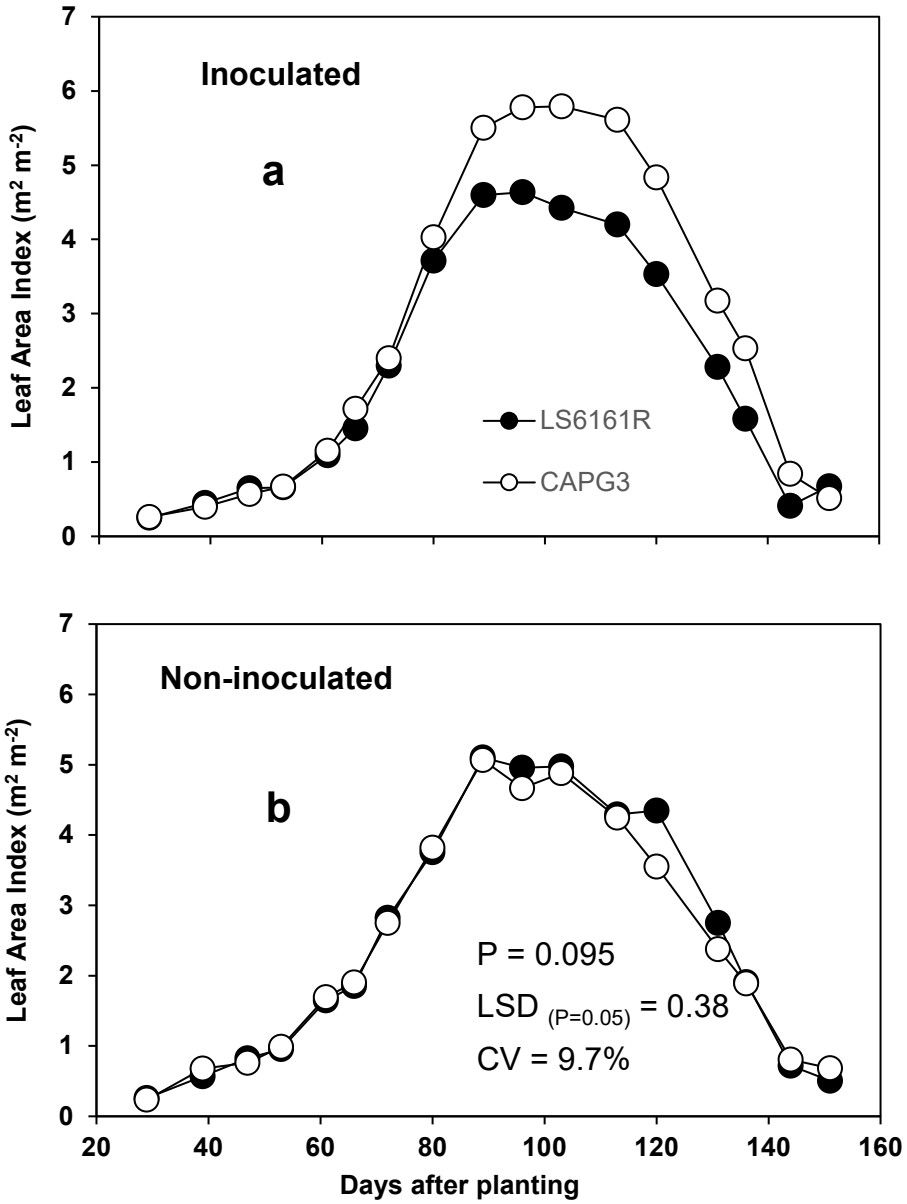

Figure 8.6: Leaf Area Index for two rainfed soybean cultivars (LS6161R and CAPG3) grown under (a) inoculated and (b) non-inoculated treatments at Swayimane during the 2018/19 season (Reddy, 2019)

The CAPG3 cultivar produced more leaves at 89 DAP (cf. Figure 8.3a) when compared to LS6161R, and will thus have a higher LAI. The higher LAI will also influence crop evapotranspiration, which, in turn, affects biomass and seed yield. There may be other reasons why LS6161R did not respond as expected to the combined inoculation and fertilizer application, such as the following:

- Ineffective application of inoculant at planting: Since the inoculant was sprayed via knapsack, it could have been rendered inactive by wind drift and/or failing to cover the seed with soil immediately after spraying.
- Possible human error when measuring the LAI of LS6161R under inoculation.

With respect to canopy cover for both LS6161R and CAPG3, there were no significant differences ($P > 0.05$) across all factors (cf. Figure 8.7). Maximum CC values approached 100% for both cultivars under the two inoculation treatments.

It is important to note that since CC is derived from LAI (cf. Section F1.5 in Appendix F), the two variables are directly proportional to one another. Hence, they follow similar trends with low values at planting, which peaked from flowering to pod formation, then decreased after senescence. Canopy cover can also be influenced by planting density (i.e. inter- and intra-row spacing). The planting density in 2018/19 was 317,460 plants ha^{-1}, compared to 266,667 plants ha^{-1} for the 2015/16 season (cf. Section 5.2.4). This helps to explain the large difference in biomass and seed yields obtained in the two seasons.

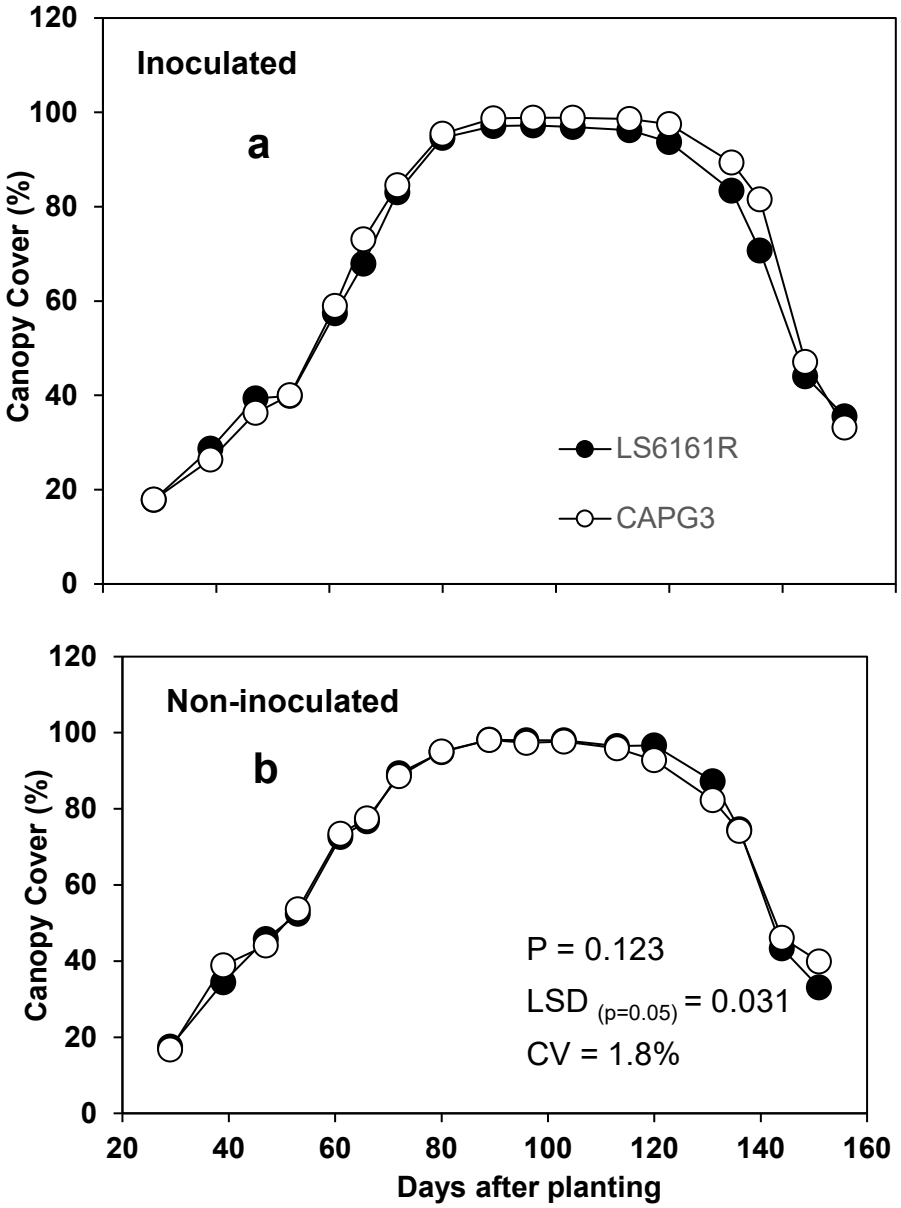

Figure 8.7: Canopy cover for two rainfed soybean cultivars (LS6161R and CAPG3) grown under (a) inoculated and (b) non-inoculated treatments at Swayimane during the 2018/19 season (Reddy, 2019)

8.3.1.4 Phenological development

Due to labour constraints, phenological dates were not observed on a per-plot basis. Therefore, the statistical analysis to determine significance between cultivars, inoculation treatments and the interaction between these factors was not performed. The phenological dates shown in Table 8.3 were observed for both cultivars in calendar days throughout the growing season, then converted to GDDs using the AquaCrop model.

The results indicated that LS6161R developed faster (by approximately one week) from flowering to maturity when compared to CAPG3. The faster crop development of LS6161R is due to its genetic makeup, considering it is an early-maturing cultivar when compared to CAPG3 (which is late maturing) (cf. Table 3.2 in Section 3.2.2.1).

Table 8.3: Thermal time (in GDD) to reach various phenological stages for two inoculated soybean cultivars (LS6161R and CAPG3) grown at Swayimane using the 2018/19 season

Parameters	Cultivar		Units
	LS6161R	CAPG3	
Time to 90% emergence	105	105	GDD
Time to maximum canopy cover	1440	1335	GDD
Time to flowering	1065	1185	GDD
Duration of flowering	255	240	GDD
Time to senescence	1950	2025	GDD
Time to maturity	2025	2145	GDD
Time to maximum rooting depth (Zr_{max})	1680	1680	GDD
Maximum rooting depth (Zr_{max})	0.62	0.62	m

8.3.1.5 Biomass production

Accumulated biomass, shown in Figure 8.8, represents the total above ground biomass of each cultivar measured bi-weekly for both inoculation treatments. The inoculated cultivars produced higher accumulated biomass when compared to the non-inoculated cultivars. In addition, CAPG3 produced more biomass than LS6161R, mainly due to its high leaf number (and thus greater leaf area). A greater LAI means more stomata, and thus higher transpiration rates leading to increased biomass production.

At 117 DAP, biomass growth peaked at 65.0 and 77.4 g for inoculated LS6161R and CAPG3, respectively. In comparison, the non-inoculated treatment produced values of 52.1 and 69.6 g for LS6161R and CAPG3, respectively. Furthermore, Figure 8.8 highlights a rapid increase in biomass growth for CAPG3 from 103 to 117 DAP, which is due to the cultivar forming pods. For LS6161R under both treatments, a lower biomass resulted from the lower leaf number. However, this shows that pod mass makes up most of the biomass at the same development stage, since LS6161R matured earlier (resulting in leaf drop) when compared to CAPG3. Overall, there was no statistically significant difference ($P > 0.05$) across cultivars and inoculation treatments, or in the interaction between these factors. The coefficient of variation obtained for biomass measure for both cultivars and inoculation treatments is slightly high, which may be due to inconsistency in selecting individual plants for destructive sampling across the season.

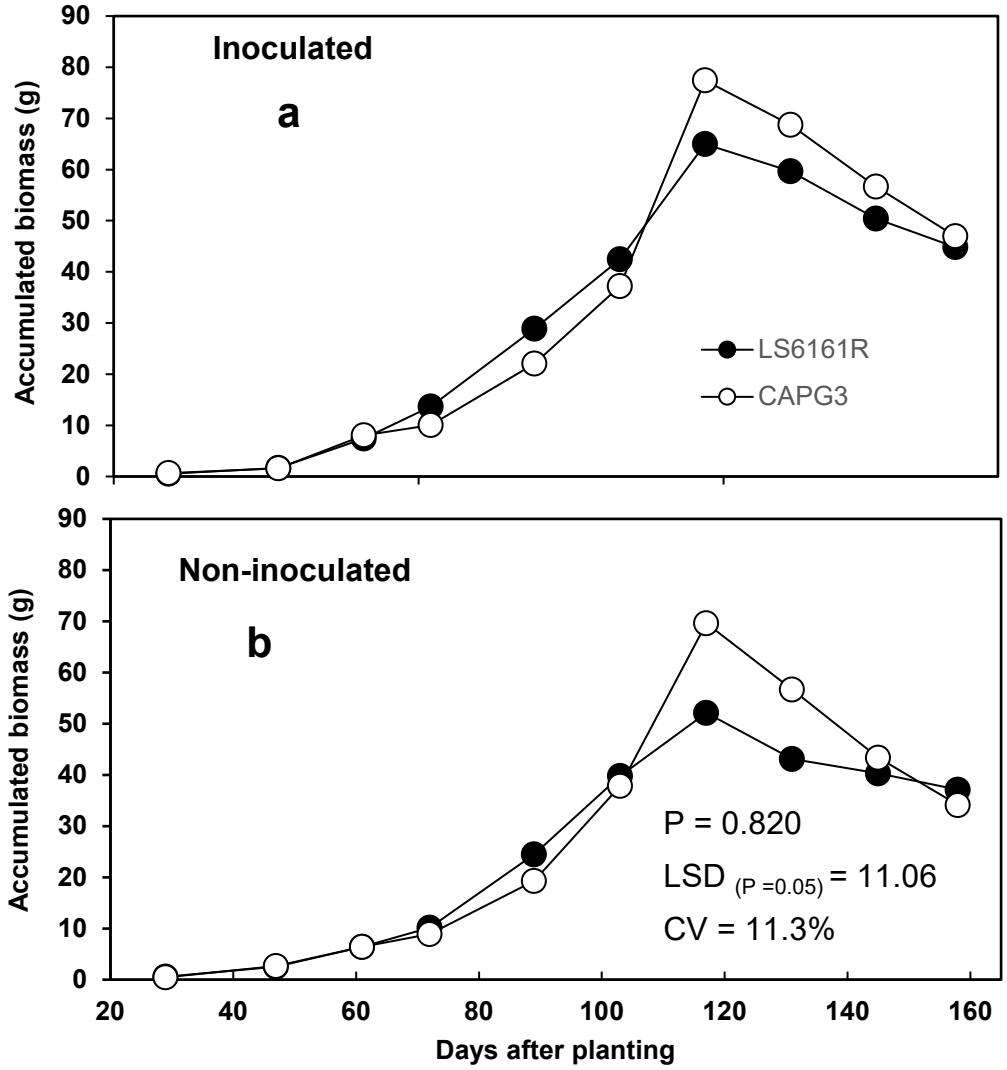

Figure 8.8: Accumulated biomass for two rainfed soybean cultivars (LS6161R and CAPG3) grown under (a) inoculated and (b) non-inoculated treatments at Swayimane during the 2018/19 season (Reddy, 2019)

8.3.2 Final yields and harvest index

Since only the pods and stem contribute to the final biomass, it is lower than the accumulated biomass, which includes the leaf mass. At harvest, the average number of pods per plant in the inoculated treatment is higher than the non-inoculated treatment. The higher number of pods, combined with the heavier pod mass, as shown in Table 8.4, produced more biomass under inoculation. The LS6161R cultivar produced heavier pods, which is reflected in the higher biomass produced for this cultivar. However, CAPG3 responded better to inoculation than LS6161R did. The increase in pod mass, pod numbers and final biomass as a result of the inoculation treatment correlates well with studies undertaken by Singh (2005), Schulz et al. (2005), Mokoena (2013) and Siyeni (2016). The statistical analysis of final biomass across all factors was not significantly different ($P > 0.05$).

Table 8.4: Final biomass and grain yield, as well as Harvest Index values for two soybean cultivars (LS6161R and CAPG3) grown under two inoculation treatments at Swayimane during the 2017/18 season (Reddy, 2019)

Variable	Inoculation		Non-inoculation	
	LS6161R	CAPG3	LS6161R	CAPG3
Pod mass (g plant^{-1})	27.68	25.61	26.72	21.97
Pod number (per plant)	58	51	55	48
Final biomass (t ha^{-1})	8.68	8.48	8.33	7.40
Seed yield (t ha^{-1})	4.59	4.35	4.28	3.72
Harvest Index	0.51	0.51	0.48	0.50

The high yields obtained in this study were due to the harvesting method (cf. Section 8.2.5.5), where only 10 plants from two experimental rows were harvested due to labour constraints. Ideally, all plants in both experimental rows should have been harvested, which would have increased the accuracy of the estimated seed yields. Therefore, it is not ideal to compare the statistical significance of yields between cultivars and inoculation treatments based on only ten plants per plot. Seed yield was significantly different ($P < 0.05$) between cultivars, but not significantly different between inoculation treatments, nor the interaction between these factors. As expected, the inoculated treatment produced higher soybean yields at harvest for both cultivars. Inoculation, together with the application of phosphorus and potassium nutrients, should increase crop yields, as was observed in this trial.

The seed yields obtained at Swayimane in 2018/19 were higher than the average soybean yields reported by DAFF (2010a) for South Africa, which range from 2.5 to 3 t ha^{-1}. The final yields were significantly higher than those obtained in the 2015/16 season at Swayimane (cf. Figure 5.11 in Section 5.3.4), mainly due to the higher planting density (266,667 vs 317,460 plants ha^{-1}) and better land management practices (e.g. higher level of weeding; use of preventative fungicide). However, the yields were lower than those reported by Masanganise (2019) and Mbangiwa et al. (2019) for Baynesfield (cf. Table 6.6 in Section 6.3.2), due to differences in planting density and the use of irrigation at Baynesfield.

Soybean's HI ranges from 25 to 40% owing to the relatively low yields of soybean in comparison to its high biomass production (Donatelli et al., 1997; Cui and Yu, 2005; Steduto et al., 2012; Islam et al., 2018; Raes et al., 2017). In this project, however, much higher values of 48 to 51% were obtained, although differences were not significantly different ($P > 0.05$). According to Donatelli et al. (1997), HI is generally used as an indicator of sampling error with respect to crop yield and biomass production. The large HI values obtained in 2018/19 are mainly due to the high yields that resulted from the sampling of too few plants.

8.3.3 Crop water use

8.3.3.1 Soil water content

The Watermark sensors were calibrated using regression equations that converted matric potential (expressed as a pressure head in cm) to volumetric water content (VWC in percentage). These regression equations were obtained by plotting VWC (CS650 probes) against corresponding pressure head (Watermark sensors) for each depth. However, poor correlations were obtained due to large periods of missing Watermark data, which occurred at each of the four depths due to damaged wires connecting sensors to the power unit. The damage occurred when hand hoes were used to initially prepare the trial site for planting and during frequent weeding sessions over the growing season. For this reason, only the VWC data measured by the CS650 probes is presented.

The soil water content measured by the CS650 soil moisture probe at four depths, together with daily rainfall measured during the growing season, is shown in Figure 8.9. The plotted PWP and FC lines represent the minimum PWP of the topsoil (12.4%) and the maximum FC of the subsoil (40.5%).

The figure highlights the largest variation in soil water content at 0.15 m, which is due to the frequent wetting and drying cycles resulting from interactions of soil water evaporation and rainfall at the soil surface. The initial soil moisture content at planting was low, which could have influenced seed germination. Several seeds from both cultivars did not germinate fully, therefore gap filling was undertaken to achieve the desired plant density.

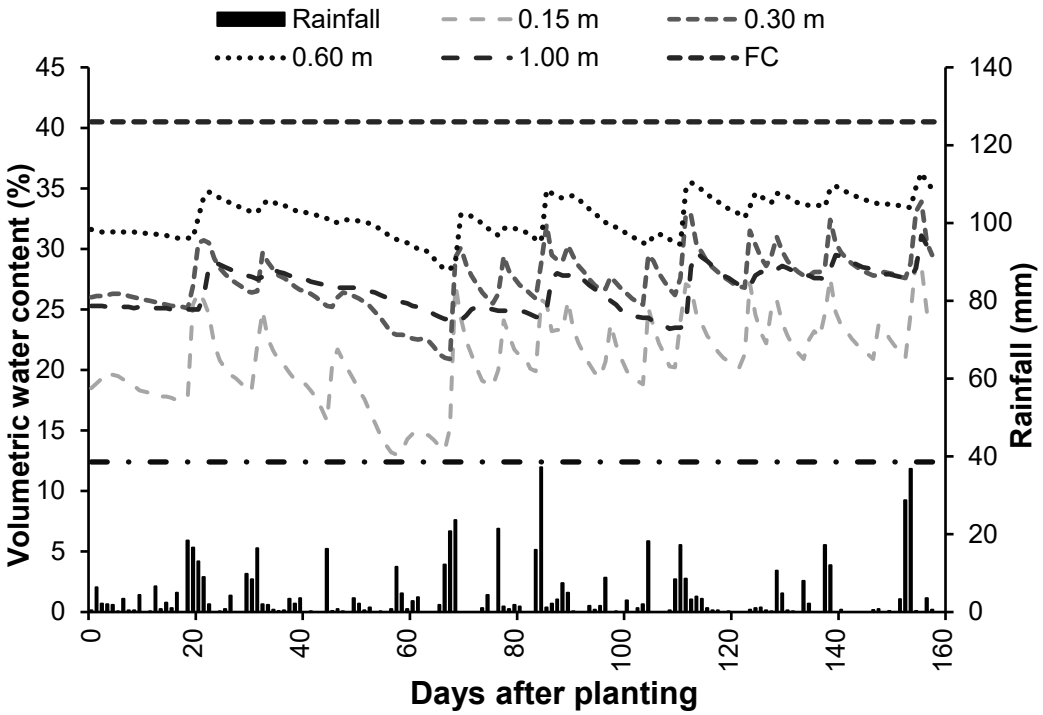

Figure 8.9: Soil water content measured by the CS650 at four depths over the 2018/19 growing season at Swayimane

8.3.3.2 Crop evapotranspiration

Crop evapotranspiration was estimated using the SWB method, with inputs of P and R assumed to be constant for the two treatments. The ΔS represents the difference between the SWC measured at planting (initial soil moisture) and at physiological maturity (final soil moisture), which was different for both cultivars as they matured at different times. The evapotranspiration values obtained for both cultivars and inoculation treatments are given in Table 8.5. The higher water use of CAPG3 is also due to its longer crop cycle of 143 vs 135 days for LS6161R. Therefore, it is difficult to compare crop evapotranspiration between cultivars due to their differences in crop season lengths (also highlighted in Table 6.7 in Section 6.3.3.1). The values were not significantly different ($P > 0.05$) across cultivars and between the two inoculation treatments.

Table 8.5: Actual crop evapotranspiration determined for two soybean cultivars (LS6161R and CAPG3) grown under rainfed conditions and two inoculation levels at Swayimane during the 2018/19 season (Reddy, 2019)

Treatment	Soybean cultivar	Crop evapotranspiration (mm)
Inoculation	LS6161R	481.0
	CAPG3	508.3
Non-inoculation	LS6161R	482.1
	CAPG3	519.3

8.3.3.3 Crop coefficients

The K_C values were calculated using weekly estimates of crop evapotranspiration derived using the SWB method and ET_O derived from the FAO's ET_O Calculator Utility. Monthly K_C values for both cultivars and inoculation treatments under rainfed conditions are shown in Table 8.6. For rainfed conditions, CAPG3 generally exhibits higher crop coefficients than LS6161R for both inoculation treatments. It is worth noting that April K_C values for both cultivars and inoculation treatments are higher than expected. This is difficult to understand considering that soybean typically drops its leaves once senescence begins. However, similar high end-season values were noted at Baynesfield (cf. Section 6.3.3.2). It is important to note that both cultivars reached physiological maturity on 2 and 10 April for LS6161R and CAPG3, respectively. Therefore, K_C in April is not based on 30 days of data, which may have contributed to the high value.

Table 8.6: Monthly observed crop coefficients determined for two soybean cultivars (LS6161R and CAPG3) grown under rainfed conditions and two inoculation levels

Treatment	Variety	Monthly crop coefficients					
		November	December	January	February	March	April
Inoculation	LS6161R	0.44	0.97	0.93	0.99	0.82	0.92
	CAPG3	0.33	0.85	0.95	1.03	0.87	1.05
Non-inoculation	LS6161R	0.32	0.96	0.94	1.01	0.91	0.97
	CAPG3	0.43	0.87	0.97	1.02	0.95	1.08

8.3.4 Water Use Efficiency of crop and biofuel production

8.3.4.1 Crop Water Use Efficiency

The WUE_C values calculated for inoculated LS6161R and CAPG3 were 0.95 and 0.86 kg m^{-3}, respectively. For the non-inoculated treatment, figures of 0.89 and 0.72 kg m^{-3} were obtained for LS6161R and CAPG3, respectively. Hence, LS6161R is more water use efficient than CAPG3 for both inoculation treatments. The CAPG3 produced less yield and used more water when compared to LS6161R. Hence, LS6161R is better suited for biodiesel production at both smallholder- and commercial-scale farming. As noted, it is clear that the WUE metric is sensitive to crop yield, which, in turn, is strongly influenced by various land management practices.

The WUE_C values obtained in previous seasons (cf. Table 6.10 in Section 6.3.4.1) ranged from 0.75 to 1.54 kg m^{-3} for soybean, depending on the method of yield determination and the technique used to measure crop water use. Demirtas et al. (2010) reported values of 0.41 to 0.64 kg m^{-3} for rainfed to fully irrigated conditions. According to Kunz et al. (2015a), the comparison of WUE_C values is very difficult, due to the different techniques used to measure crop water use and yield, as well as differences in the scale of each study. This comment is supported by the findings of this study, which questions the usefulness of this metric.

8.3.4.2 Biofuel Water Use Efficiency

Biofuel yield was calculated from seed yield and oil content. The seed oil content determined for both cultivars under the two inoculation treatments is shown in Table 8.7. According to Nolte (2007), the oil content of soybean seed is typically 18%. Lembede (2017) reported similar figures for the 2015/16 season, ranging from 16.7 to 21.

The CAPG3 cultivar exhibited a higher oil content than LS6161R for both treatments. The CAPG3 cultivar is known for its high seed oil content and quality (De Beer and Bronkhorst, 2017). Biodiesel yields given in Table 8.7 illustrate how higher seed oil contents can "offset" lower yields, considering that CAPG3 produced a similar quantity to LS616R under inoculation.

Therefore, CAPG3 may be better suited for animal feed production, since it produced more biomass and a higher oil content, whereas LS6161R produced more crop yield, making it better suited to biodiesel production.

Table 8.7: Biodiesel yield and Water Use Efficiency of biodiesel production for two soybean cultivars (LS6161R and CAPG3) grown under rainfed conditions and two inoculation levels (Reddy, 2019)

Treatment	Cultivar	Seed oil content	Biodiesel yield	Water use (evapotranspiration)	WUE_B
		Percentage	L ha^{-1}	m^3 ha^{-1}	L m^{-3}
Inoculation	LS6161R	17.9	850	4810	0.18
	CAPG3	18.8	845	5083	0.17
Non-inoculation	LS6161R	17.1	756	4821	0.16
	CAPG3	17.5	673	5193	0.13

8.3.5 Summary and conclusions

On smallholder farms, low yields are attributed to the incorrect application and concentration of fertilizers, no seed inoculation and poor land management practices. Although the yields obtained in this study are considered high, they show that, with better land management practices (e.g. inoculation, fertilization, weeding, as well as the application of herbicides, insecticides and fungicides), smallholder farmers should produce higher yields, thus reducing the yield gap between smallholder and commercial farms. Inoculation significantly improved canopy cover, stomatal conductance and the CCI of two soybean cultivars (LS6161R and CAPG3). However, smallholder farmers should use inoculation as it reduces fertilization costs and can be beneficial for rotational crops such as maize. However, emphasis must be placed on the correct application of the inoculant, which should be done in conjunction with phosphorus and potassium application. The LS6161R cultivar is better suited to biofuel production due to its higher yield potential when compared to CAPG3.

CHAPTER 9: MODEL SELECTION, DESCRIPTION AND COMPARISON

9.1 MODEL SELECTION

For this project, a review was undertaken of hydrological and crop yield models commonly used in South Africa. Thereafter, an overview of the different types of models was given, with the conclusion drawn that deterministic models are required to meet the objectives of this research project.

9.1.1 Water use

For ungauged catchments, the ACRU hydrological model was selected to assess the hydrological impacts of biofuel feedstock production on downstream water availability. In addition, this model was the preferred choice in previous studies (e.g. Jewitt et al., 2009a; Jewitt et al., 2009b; Warburton et al., 2010; Warburton et al., 2012; Kunz et al., 2015a; Kunz et al., 2015c), which considered the hydrological impacts of land use change, because the model does not require extensive parameterisation. A brief description of the ACRU model is given in Section 9.2.1.

9.1.2 Crop yield

Of the three different types of crop growth engines, water-driven models are considered more robust and less complex, with fewer input requirements. Based on this, the AquaCrop model was selected to estimate the attainable yield of strategic biofuel feedstocks. The model has also been successfully linked to the quinary subcatchment database, which facilitates crop yield estimates at the national scale. A summarised description of AquaCrop is given in Section 9.2.2. The SWB, another locally developed model was also used in this project to simulate crop growth and yield at the field scale (cf. Section 9.2.3).

9.1.3 National runs

Kunz et al. (2015b) successfully linked both AquaCrop and ACRU to the quinary subcatchment database, which facilitates the assessment of crop yield and water use at the national scale. Furthermore, this procedure was computationally automated, allowing a national run using ACRU to be completed within nine hours. However, the SWB model can only be used to simulate crop growth and yield at field scale, not at national level.

9.2 MODEL DESCRIPTION

9.2.1 Agricultural Catchments Research Unit model

The ACRU model (Schulze, 1995; Smithers and Schulze, 1995) was developed locally at the University of KwaZulu-Natal (Pietermaritzburg). The ACRU is primarily a catchment-scale, daily time-step hydrological rainfall runoff model. It is a physical-conceptual, multi-level and multi-purpose model, with various outputs that have been widely verified against observations in many countries and conditions (Warburton Toucher et al., 2010). The ACRU is an integrated agro-hydrological model that has been frequently used to assess the impacts, inter alia, of land use change and climate change on the following:

- Daily storm flows, base flows and total runoff
- Accumulated daily stream flows from all upstream subcatchments
- Peak discharge, sediment yields and recharge to groundwater
- Daily soil water content and evapotranspiration

9.2.2 AquaCrop

AquaCrop (Raes et al*.,* 2009; Steduto et al*.,* 2009) was developed by the FAO and initially designed to simulate the daily growth, productivity and water use of 16 crops, as affected by changing water availability and environmental conditions (Steduto et al., 2012). The model is particularly suited to simulating yield response to water as it is a water-driven model. Hence, AquaCrop is an engineering-type water productivity model that represents a simplified interpretation of the effects of water stress on crop productivity. According to Steduto et al*.* (2012), AquaCrop can be used to do the following:

- Assess the effect of water deficits on crop production
- Compare the results of several water allocation plans
- Optimise irrigation scheduling
- Enhance management strategies for increased water productivity and water savings
- Assess crop response to different climate change scenarios in terms of altered soil water content, temperature regimes and elevated atmospheric CO_2 concentration

9.2.3 Soil Water Balance model

The SWB is a mechanistic, real-time, soil water balance model, which was originally developed by Annandale et al. (1999) as an irrigation scheduling tool. However, SWB is also a field-scale crop growth model that has been developed for a number of crops (Jovanovic and Annandale, 1999; Jovanovic et al., 1999), as well as different irrigation systems and management options. The model's "scenario generator" allows multiple crop and irrigation scenarios to be easily configured. The SWB performs a soil water balance calculation and estimates crop growth using three components, which are weather, soil and crop related. Jovanovic and Annandale (2000) developed a newer version of the model (SWBPro).

9.3 MODEL COMPARISON

A comparison was undertaken to determine similarities and differences between the selected models. The criteria used for the comparison included how the models calculate accumulation of biomass, soil water content, and penalties on crop growth due to water deficit and/or temperature stress. The comparison is presented in three tables as shown in Appendix I, with similarities and differences between the models highlighted next.

9.3.1 Climatic and soil inputs

All three simulation models operate at the daily time step and require daily rainfall, as well as temperature (maximum and minimum) as climatic input. The FAO developed the ET_O Calculator Utility (Version 3.2) (FAO, 2012) to assist AquaCrop users to calculate reference crop evaporation, which is required as input. However, the SWB computes ET_O from inputs of measured irradiance, temperature (maximum and minimum), relative humidity (maximum and minimum), as well as wind speed.

The ACRU uses the A-pan as its reference evaporation standard, with evaporimeter readings used as input. Alternatively, A-pan equivalent evaporation can be computed from inputs of temperature via the Hargreaves and Samani (1985) equation, or via the Penman (1948) equation if average relative humidity and wind run measurements are also provided. The ET_O values can also be used in ACRU once they have been adjusted from reference crop to A-pan equivalent evaporation. Kunz et al. (2015a; 2015b) recommended using ACRU's CORPAN monthly input parameter for this adjustment, with values ranging from 1.17 to 1.51, particularly in the winter months.

The minimum soil input parameters required by models such as AquaCrop, SWB and ACRU are soil texture (textural class) and depth (in metres) for at least one (but preferably two) soil horizons. In addition, VWC at saturation (θ_{SAT} in percentage), FC (θ_{FC} in percentage) and PWP (θ_{PWP} in percentage) are also required, as well as saturated hydraulic conductivity (K_{SAT} in mm d^{-1}). Plant available water (PAW in mm d^{-1}) represents the soil water content (θ) between FC and PWP that is considered available for plant uptake, i.e. plant available water (PAW) = $\theta_{FC} - \theta_{PWP}$.

9.3.2 Soil water balance

All three models are based on a cascading soil water balance once canopy interception and surface runoff have been accounted for. However, AquaCrop does not account for canopy interception. It divides the soil profile into a maximum of 12 compartments, regardless of the number of soil horizons (from 1 to 5). Similarly, SWB considers up to 11 soil layers, compared to only two in ACRU. All three models calculate soil water evaporation based on the model of Ritchie (1972), which is divided into two stages. During the first stage, soil water evaporation occurs at a constant rate, i.e. at a maximum (potential) rate that is limited by the available energy. When the soil water content of the topsoil can no longer satisfy atmospheric demand, the second stage begins where soil water evaporation declines rapidly. For example, soil water evaporation occurs at the potential rate in SWB until the topsoil's water content reaches PWP. However, the potential rate is calculated differently in all three models. Capillary rise is not accounted for in SWB. The calculation of runoff is discussed in the section below.

9.3.3 Crop growth engine

The main difference between the models is their underlying crop growth engine. AquaCrop calculates biomass production as the product of transpired water (mm; normalised by ET_O) and a water productivity parameter, whereas SWB calculates dry matter (DM) production as the product of fractional intercepted solar radiation and a radiation use efficiency parameter. The canopy extinction coefficient for solar radiation (K_s), which is estimated from measurements of FI_{PAR} and LAI, is required by SWB (i.e. input parameter) in order to predict radiation-limited DM production.

Both AquaCrop and SWB calculate biomass accumulation from transpired water. However, transpiration is normalised by ET_o in AquaCrop, but is corrected for vapour pressure deficit (Tanner and Sinclair, 1983) in SWB. However, SWB also calculates radiation-limited growth (Monteith, 1977), then uses the lesser of the two daily DM yields (Jovanovic and Annandale, 2000). ACRU is considered an agro-hydrological model because it can estimate crop yields for maize, winter wheat and sugarcane. However, ACRU is not a crop growth model and only estimates yield based on transpired water (Schulze, 1995).

9.3.4 Partitioning

In AquaCrop, the portion of biomass that is partitioned to the harvestable organs to give yield is determined using the HI. It is important to note that, beyond the partitioning of biomass into yield, there is no other partitioning among the various plant organs (Steduto et al., 2012).

For SWB, specific leaf area (SLA) and the leaf-stem partitioning parameter (PART) must be known in order to calculate DM partitioning to different plant organs. The DM is first portioned into roots, then into leaves and finally to the stem. Partitioning depends on the phenology, which is calculated using thermal time (Annandale et al., 1999).

9.3.5 Thermal time

Both AquaCrop and SWB use the GDD concept to account for temperature effects on phenology. However, there are differences in the calculation of accumulated heat units as detailed in Appendix I.

9.3.6 Yield formation

Yield formation in AquaCrop is determined as the product of biomass accumulation and the HI. The HI is modified by water and temperature stresses as explained in the next section.

The SWB assumes that after flowering, DM is first partitioned to reproductive sinks, then to the other plant organs (as described above). Hence, when flowering commences, initial harvestable dry matter (HDM) is calculated as the product of the SDM follows and a crop-specific factor (input parameter) determining the translocation of dry matter from stem to grain. The HDM is then added to canopy dry matter (CDM) in order to include grain dry matter (Annandale et al., 1999).

In ACRU, primary production, maize, winter wheat and sugarcane yields are estimated from actual evapotranspiration (ET_a) accumulated over the growing season. For annual sugarcane yield, ACRU assumes a growing season from 1 July to 30 June for southern Africa. For maize and winter wheat, yield is estimated from the ratio of actual transpiration to maximum transpiration for three different growth stages (Schulze, 1995).

9.3.7 Stress effects

9.3.7.1 Water stress

Water stress affects early canopy cover senescence in AquaCrop and early leaf senescence in SWB. In AquaCrop, soil water stress affects biomass production by reducing canopy cover expansion, inducing both stomatal closure (i.e. reducing transpiration) and an early canopy senescence, and reducing pollination. The HI is also modified when water stress occurs both during and after flowering, which influences yield formation (Raes et al., 2012a). Although water stress often reduces HI, it can also increase it by inhibiting vegetation growth, i.e. more assimilates are available for grain/fruits (Vanuytrecht et al., 2014). A lack of aeration (due to water logging) reduces transpiration, and hence, biomass production. Crop growth in AquaCrop is also affected by soil fertility and salinity stress (Steduto et al., 2012).

The SWB calculates the daily increment in DM as being either transpiration-limited or radiation-limited, with water stress affecting the partitioning of assimilates to the different plant organs. Under conditions of water stress, half of the leaf DM is partitioned into roots, the other half into the stem. Leaf area development is reduced when actual transpiration is below potential transpiration (Annandale et al., 1999).

In ACRU, actual evapotranspiration (total evaporation) declines from the potential rate (maximum evaporation) when plant available water has been depleted by a certain percentage. This input parameter is called CONST and represents the fraction of plant available water at which total evaporation is assumed to drop below maximum evaporation, i.e. the onset of plant water stress. In the maize yield submodel, the crop's water use coefficient is reduced if transpiration falls below the maximum rate during the crop's vegetative growth stage (from emergence to onset of flowering). For winter wheat, maximum transpiration is estimated from the maximum crop coefficient, i.e. $0.9 \cdot K_{cm}$ during the reproductive growth stage (Schulze, 1995).

9.3.7.2 Temperature stress

Since AquaCrop and SWB use GDD as the thermal clock, temperature effects on phenology and crop growth are accounted for. Furthermore, temperature stress modifies the water productivity parameter and inhibits pollination in AquaCrop. Biomass production is affected by cold temperature stress, whereas hot or cold temperature stress inhibits pollination, which then reduces the HI. Thus, both biomass production and yield formation are affected by temperature stress (Vanuytrecht et al., 2014).

In the two sections that follow, a distinction is made between model inputs and model parameters. Model inputs include climate and soils data, as well as crop-specific inputs such a planting date and planting density. Model parameters have biophysical characteristics, which need to be understood before they are adjusted during the calibration process. Thus, parameters should be adjusted for a specific cultivar, but not for the site.

9.4 MODEL CALIBRATION

Model calibration involves the adjustment of certain parameters so that model simulations better match observations (Farahani et al., 2009). These adjustments account for specific cultivars, local growing conditions and management practices. In general, there are two levels of calibration: full and partial, which are described next.

9.4.1 Full vs partial calibration

A full calibration involves determining locally derived values for most of AquaCrop's input parameters. For example, Mabhaudhi (2012) adjusted 21 of the 35 parameters when calibrating AquaCrop for Bambara groundnut and taro. For a partial calibration, Steduto et al. (2012: 44) provided the following list of crop parameters that should be calibrated to reflect local conditions:

- Time to 90% emergence
- Maximum canopy cover (CC_X)
- Maximum rooting depth (Zr_{max})
- The time required to reach Zr_{max}
- Response to soil fertility
- Length of the crop cycle (time to maturity)
- Time to reach certain phenological growth stages (flowering, canopy senescence)

9.4.2 Partial calibration procedure

The calibration process typically begins with the finalisation and checking of climate and soil files required as input by the simulation model. Thereafter, experimental observations are used to calibrate certain crop parameters by fine-tuning default values to better represent local growing conditions. For example, since AquaCrop is a canopy-level model, simulated canopy cover values first need to be matched to observations.

The seedling leaf area (in cm^2) should be measured at emergence, and together with planting density as inputs, is used by the model to compute initial canopy cover (CC_O), as described by Raes et al. (2009). Measurements of LAI are used to compute diffuse non-intercepted radiation (DIFN), from which CC development (in percentage) is calculated (cf. Section F1.5 in Appendix F). Alternatively, CC is typically estimated from measured LAI using the Beer-Lambert equation, where the seasonal leaf extinction coefficient (k) is crop-specific (cf. Section 17.3.2.4). From this, maximum canopy cover (CC_X in percentage) and the time to reach CC_X can be determined as input parameters. AquaCrop then calculates the canopy growth coefficient (i.e. the increase in CC per degree-day) from CC_O, CC_X and the time taken to reach CC_X, and the canopy decline coefficient from observations of time to start of canopy senescence and maturity.

The next step involves adjusting parameters related to the thermal time required for the completion of various phenological growth stages. Observations are made in days, which are then converted to values in GDD using measurements of daily temperature at the location. Once good agreement between simulated and derived canopy cover has been obtained, agreement in soil water content, biomass, yield and HI is evaluated. Finally, an independent dataset (or other treatments) are used to test or evaluate (or validate) the model's performance.

In summary, the user should also ensure that the following is done:

- Rainfall data is collected at or nearby the experimental field.
- Evaporating power of the atmosphere (ET_O) is correctly determined.
- Air temperature is well defined (minimum, maximum and mean).
- Physical soil characteristics of the various soil horizons are well defined.
- Crop phenology and life cycle length are fine-tuned to the environment and the crop species.
- Moment of germination or transplanting is correctly specified.
- Moment and duration of flowering is specified for determinant fruit/grain crops.
- Field management practices that affect soil surface runoff, reduce soil water evaporation (mulches), and crop development and production (soil fertility) are specified correctly (FAO, 2015).

CHAPTER 10: MODEL INPUTS

This chapter describes the development of an updated quinary subcatchment climate database, which was used as input for the crop and hydrological models used in this study. Soil information required by the models is also discussed, as well as other model inputs (e.g. planting dates and densities).

10.1 CLIMATE DATA

The main differences in climatic input requirements of the two selected models are shown in Table I.1 in Appendix I. The main difference between the model inputs is reference evaporation. AquaCrop uses a hypothetical short grass as its reference evaporation, whereas ACRU uses the A-pan evaporimeter. As explained in Section 9.1.3, both models were run at a national scale using the quinary subcatchment climate and soils databases.

Kunz et al. (2015b) provided a summary of how the quinary subcatchments were delineated, as well as the development of the original climate database (cf. Section 5.4). For a more detailed description, the reader is referred to Schulze et al. (2011). In addition, Kunz et al. (2015b) described improvements to the climate database (cf. Section 5.5), in particular, the temperature and reference evaporation datasets. However, further improvements to the quinary subcatchment climate database were made in this project, which are described in the sections that follow.

10.1.1 Rainfall

Since mean annual runoff estimates are extremely sensitive to rainfall input, especially in high-intensity rainfall areas (Schulze, 1995), it cannot be over-emphasised that rainfall data used as input for ACRU must be as error-free as possible. Hence, effort then focused on improving the rainfall database, especially since hydrological and crop response is most sensitive to changes in this variable. The following improvements were made to the quinary rainfall database.

10.1.1.1 Driver stations

Since each of the three quinary subcatchments represent a subdivision of the quaternary catchment, driver stations that were originally selected to represent each quaternary catchment form the basis of the quinary rainfall database. Schulze et al. (2011) described the selection of 1,244 rainfall stations to “drive” the hydrology of the original 1,946 quaternary catchments. However, this total was reduced to 1,240 stations after the representative (or “driver”) station for 11 quaternary catchments was changed to improve the representation of rainfall in those catchments.

Although a list of driver stations existed, 317 errors in South African Weather Service (SAWS) ID numbers were discovered and corrected. For each station ID, a method was developed to automatically extract 50 years of daily rainfall data (from 1950 to 1999) from the rainfall database developed by Lynch (2004). This dataset was then compared to the quaternary driver rainfall to identify errors. When the daily rainfall did not match, it indicated an error in the SAWS’s ID numbers. Rainfall data from neighbouring stations was then extracted from the database of Lynch (2004), until an exact match was found. A total of 317 corrections was made to the list of driver stations, which affected 951 of the 5,838 quinary subcatchments. For example, the five first and last corrections to the station ID numbers are listed in Table 10.1.

Table 10.1: Corrections made to the list of South African Weather Service ID numbers, which identify each quinary rainfall driver station

Quinary subcatchment number	Old SAWS ID	New SAWS ID
0007-0009	0585056 W	0585016 W
0037-0039	0549358 W	0512481 W
0058-0060	0548280 W	0548165 W
0067-0069	0511672 W	0511573 W
0070-0072	0513382 W	0513677 W
.	.	.
.	.	.
5695-5697	0556020 W	0556110 W
5707-5709	0555567 W	0518759 W
5722-5724	0556088 W	0519077 W
5731-5733	0556020 W	0556110 W
5734-5736	0556898 W	0519572 W

This useful process not only identified the origin of the driver station rainfall, but also checked that the datasets were correct. Recently, the corrected list of driver stations proved most valuable to WRC Project K5/2833, which used the information to assign gridded Global Climate Model (GCM) data to the location of each rainfall driver station. The latter was then used to bias-correct the GCM's rainfall data for a 41-year baseline period (1961-1999). The number of driver stations per custodian is given in Table 10.2. It highlights the fact that SAWS owned the vast majority (93%) of stations in 2004.

Table 10.2: Missing rainfall values that were set to zero mm in the original quinary rainfall database

Custodian	SAWS ID	Number	Percentage of total
SAWS	W	1,158	93.4
ARC	A	34	2.7
SASA	S	22	1.8
SAWS/ARC	AW	14	1.1
SAWS/ARC	BW	1	0.1
Total		**1,240**	**100.0**

10.1.1.2 Missing data

Slight discrepancies between the driver station rainfall and that extracted from the database of Lynch (2004) were found. As shown in Table 10.3, these occurrences were few and resulted from rainfall data not patched by Lynch (2004) and was therefore missing (code -99.9). These missing values were simply set to 0.0 mm.

Table 10.3 Missing rainfall values that were set to zero mm in the original quinary rainfall database

Quinary subcatchment number	SAWS ID	Missing day/month
2248-2250	0351708 W	1999/07/31 1997/08/31
2383-2385	0134478 A	1995/04
0745-0747	0679608 W	1998/11/18

Quinary subcatchment number	SAWS ID	Missing day/month
1051-1053	0329166 W	1996/07/06 1996/07/07
4243-4245	0151351 W	1999/08/31
4366-4368	0207531 W	1999/08/29 1999/08/30 1999/08/31
4444-4446	0151351 W	1999/08/31

10.1.1.3 Extreme events

Using all 1,240 driver stations, a list of unique daily rainfall events was determined. A histogram of all 2,036 unique values (Table 10.4) shows that there are 13 events exceeding 400 mm as follows: 900.5, 585.5, 525.0, 520.7, 449.0, 440.0, 438.5, 435.0, 432.0, 425.5, 420.0, 415.5 and 407.2 mm.

Table 10.4: Histogram of 2,036 unique rainfall events from 1950 to 1999 obtained from all 1,240 driver rainfall stations

Class number	Rainfall range (mm)	Count	Percentage of total	Accumulated percentage
1	< 50	502	24.66	24.66
2	50-100	500	24.56	49.21
3	100-150	451	22.15	71.37
4	150-200	276	13.56	84.92
5	200-250	148	7.27	92.19
6	250-300	86	4.22	96.41
7	300-350	40	1.96	98.38
8	350-400	20	0.98	99.36
9	400-450	9	0.44	99.80
10	450-500	0	0.00	99.80
11	500-550	2	0.10	99.90
	550-600	1	0.05	99.95
	600-900	1	0.05	100.00
Total		**2,036**	**2,036**	**100.00**

For these extreme events, a method was developed to automatically extract daily rainfall for the 10 neighbouring stations from the rainfall database of Lynch (2004). A manual comparison was then performed to validate each rainfall event. A summary of adjustments made to high daily rainfall values is given in Table 10.5. For easy identification, each adjusted rainfall value was flagged with the letter "F" in the quinary subcatchment rainfall database. For more detail, the reader is referred to Appendix J.

Table 10.5: Adjustments made to extreme rainfall values that existed in the quinary rainfall database

Quinary subcatchment number	SAWS ID	Date	Daily rainfall (mm)	
			Original	Adjusted
4174-4175	0150620 W	1997/02/22	900.5	0.0
5119-5121	0304446 W	1980/12/14	585.5	85.5
2554-2556 2557-2559 2560-2562	0214485 W	1953/02/23	520.0	0.0
2626-2628	0022148 W	1991/06/23	440.0	44.0

Checking of daily rainfall totals by comparing them to observations from neighbouring stations is a time-consuming process, which therefore limited the number of events that could be checked manually. In the future, it is recommended that this process be automated as much as possible, so that daily rainfall events between 100 and 400 mm are also validated.

10.1.2 Daily temperature

In the previous biofuel project, the temperature data for each quinary subcatchment was interpolated from two temperature stations selected to best represent the centroid of each subcatchment. Each station was assigned a different weighting based on differences in distance and altitude between the station location and the quinary centroid. Adiabatic lapse-rate adjustments were made to account for the altitude difference between the stations and the quinary centroid. Quality control checks were then performed, inter alia, to ensure that maximum temperatures are non-negative and higher than minimum temperatures (Kunz et al., 2015b). For this project, the daily temperature dataset deemed representative of each quinary subcatchment was revised and is now based on observed data. In essence, a temperature station was selected for the driver rain gauge used for each quinary subcatchment. A detailed description of the methodology used is given next.

10.1.2.1 Exclusion of “duplicate” stations

Schulze and Maharaj (2004) developed a database of 973 temperature stations across South Africa. Duplicate stations where identified using the SAWS ID number (excluding custodian), as well as the location of the station. Duplicate stations were then ranked based on the percentage of observed (unpatched) records. The station with the highest ranking was selected, while the other stations were excluded. For example, there are four temperature stations situated at the same location and altitude in both Pretoria and Pietersburg that are managed by SAWS and the ARC (Table 10.6). The station ranked first (i.e. with the highest portion of reliable record) was selected to represent that location, meaning that the other stations were excluded. This process reduced the number of actual temperature stations from 973 to 819, i.e. 154 stations were excluded.

Table 10.6: Details of duplicate temperature stations located in two towns in South Africa

SAWS ID	Name	Lat (MMM)	Lng MMMM)	Altitude (m)	T_{MAX} observed (%)	T_{MIN} observed (%)	Ranking
0513314	Pretoria	1,544	1,691	1,300	52.8	52.6	1
0513314	Pretoria	1,544	1,691	1,300	22.6	22.7	2
0513314	Pretoria	1,544	1,691	1,300	15.0	15.0	3
0513314	Pretoria	1,544	1,691	1,300	10.0	10.0	4
0677802	Polokwane	1,432	1,767	1,250	55.8	55.7	1
0677802	Polokwane	1,432	1,767	1,250	44.9	44.8	2
0677802	Polokwane	1,432	1,767	1,250	14.2	14.2	3
0677802	Polokwane	1,432	1,767	1,250	8.5	8.4	4

The next step involved determining the difference in latitude, longitude and altitude between neighbouring stations. Stations located within a few minutes of a degree of one another and at a similar altitude (e.g. < 100 m) were further scrutinised. The best stations were selected manually, with the others excluded. For example, there were five temperature stations situated in Standerton (Table 10.7). The first two stations have identical coordinates and altitude, so the second station was eliminated due to its lower portion of reliable record. The remaining three stations were located with 1 minute of a degree and at a similar altitude, and were thus also excluded. Similarly, there are four stations located in Kokstad at the same altitude, of which two have the same coordinates; thus, one was excluded (i.e. rank of 2). However, the first station with the highest portion of reliable (observed) data was finally selected and the remaining three were excluded. This further reduced the number of actual temperature stations from 819 to 742. Hence, a further 77 stations were excluded, bringing the total to 231.

Table 10.7: Details of similar temperature stations located in two towns in South Africa

SAWS ID	Name	Lat (MMM)	Lng MMMM)	Altitude (m)	T_{MAX} observed (%)	T_{MIN} observed (%)	Ranking
0441416	Standerton	1,616	1,754	1,563	21.5	21.2	1
0441416	Standerton	1,616	1,754	1,563	14.0	12.2	2
0441385	Standerton	1,615	1,753	1,563	18.7	18.5	
0441446	Standerton	1,616	1,755	1,560	13.7	13.7	
0441447	Standerton	1,617	1,755	1,554	8.4	8.4	
0180721	Kokstad	1,831	1,765	1,354	44.5	44.5	
0180721	Kokstad	1,832	1,765	1,354	38.4	38.2	1
0180722	Kokstad	1,832	1,765	1,354	14.5	14.5	2
0180752	Kokstad	1,832	1,766	1,354	9.0	8.8	

The remaining 742 stations were sorted by latitude and longitude, as well as longitude and latitude to further identify similar stations. From this exercise, a further 88 stations were eliminated, especially those with a low percentage of observed record. Hence, the remaining 698 stations were deemed unique, with the portion of reliable record ranging from 8.2 to 99.2%.

10.1.2.2 Lapse rate regions

Kunz et al. (2015b) selected temperature stations in the same lapse rate region (LRR) as the quinary subcatchment. Hence, the LRR in which each temperature (and rainfall) station are located was determined using the geographic information system (GIS). This was achieved by first creating a point dataset using the geographical coordinates of each station, then intersecting this dataset with the LRRs. This process identified seven temperature (and three rainfall) stations outside South Africa's border, due to the coarseness of the coordinates in degrees and minutes (where 1 minute is approximately 1.6-1.8 km). Certain stations were directly located on the border between the LRRs. These were then checked, where one LLR was manually selected. A total of 12 LRRs were first determined for South Africa by Schulze and Maharaj (1994). The regions were then modified in 2004, where regions 6 and 11 were swopped and regions 8 and 9 were joined (Schulze and Maharaj, 2004).

10.1.2.3 Selection of temperature stations

The original quinary subcatchment climate database, as described by Schulze et al. (2011), contains daily estimates of maximum and minimum temperatures derived by Schulze and Maharaj (2004). These estimates were calculated using an algorithm that was based on two factors representing the altitude difference, and the distance between the temperature station and the point of interest. The algorithm selected two representative stations with the highest weightings. Kunz et al. (2015b) significantly improved the algorithm by assigning more emphasis to altitude difference than distance. In essence, the algorithm uses these two factors to identify the five most suitable temperature stations for a particular point of interest. In this study, the location of the quinary rainfall driver station was used as the point of interest, meaning that a "pseudo" temperature station was assigned to each rain gauge.

The distance from the rain gauge to each surrounding temperature station was first computed, followed by the altitude difference between the two locations. For simplicity, distances (*DIST*) were calculated in minutes of a degree (not kilometres) and altitude differences (*DALT*) in metres above sea level. Any temperature station more than 200 minutes of a degree (or 200 * 1.7 km = 340 km) away from the rain gauge was assigned the same distance factor (*DSTF*) of 0.1 (not suitable). A station located at the same location as the rain gauge was assigned a distance factor of 1.0 (ideal).

$$DSTF = 0.9 \cdot (1 - DIST/200) + 0.1 \qquad \text{Equation 8}$$

Similarly, all stations more than 1,500 m above or below the rain gauge altitude were assigned a factor (*ALTF*) of 0.1 (and 1.0 for zero altitude difference). This threshold was determined by comparing the automated station selection vs a manual selection process for a range of different rain gauges, until agreement was reached between both methods.

$$ALTF = 0.9 \cdot (1 - DALT/1500) + 0.1 \quad \text{Equation 9}$$

The distance threshold of 200 minutes was determined through a "trial and error" process where the algorithm was repeatedly run until it produced the same station section as was chosen manually. Setting a greater distance threshold (e.g. 250') placed too much emphasis on the altitude difference. For Rain Gauge 12 (0021809), the closest station (1.4' or 2.4 km) was selected when the threshold was set to 200', despite the large altitude difference of 338 m (Table 10.8). When the threshold was increased to 250', the closest station was ranked third, and the station with the smallest altitude difference (33 m) was chosen. Similarly, the temperature station located 12.4' away (*DALT* of 338 m) was selected for Rain Gauge 1161 when the threshold was 200. A threshold of 250 resulted in a station located 17.5' away (*DALT* of 149 m) being selected.

Table 10.8: Details of the two temperature stations selected for Rain Gauge 12 (SAWS ID 0021809) using a distance threshold of 200 and 250 minutes

Number		Rank	*DIST*	*DALT*	SAWS ID	
			(min)	(m)	RFL	TMP
12	200	10.30	1.4	338	0021809	0021778
		9.65	3.0	33		0021806
	250	12.07	3.0	33		0021806
		7.05	4.5	83		0005723

All temperature stations were then ranked (*RANK*) from "best" to "worst" using a method that is more sensitive to the distance factor (*DSTF*), than the altitude factor (*ALTF*). In other words, the distance factor is assigned a greater weighting than the altitude factor, as follows:

$$RANK = (10 \cdot DSTF) + (1 \cdot ALTF) \quad \text{Equation 10}$$

The importance of distance is best illustrated by Rain Gauge 355 (driver station for quinary subcatchments 1984-1986), where the closest temperature station (highest ranking of 13) was located four minutes (6.8 km) away at an altitude difference of 5 m (Table 10.9). However, the second temperature station is much further away (94 km), and is thus far less suited to represent the rain gauge location. This example highlights the sparseness of temperature stations relative to rain gauges.

Table 10.9: Details of the two temperature stations selected for Rain Gauge 355 (SAWS ID 0170099)

Number	Rank	*DIST*	*DALT*	SAWS ID	
		(min)	(m)	RFL	TMP
355	13.00	4.0	5	0170099	0170009
	2.51	55.2	81		0228420

The five identified temperature stations were then re-ranked relative to the station furthest away and the station with the greatest altitude difference. This ensures that the "worst" of the five stations exhibits the lowest ranking. The first (best) station with the highest ranking was then selected for each rain gauge location. However, more weighting was assigned to the altitude factor, as follows:

$$RANK = (10 \cdot DSTF) + (3 \cdot ALTF) \quad \text{Equation 11}$$

This allows for a temperature station slightly further away from the rain gauge to be selected if the altitude difference is much smaller than that for the closest station. This is best illustrated by Rain Gauge 186 (driver station for quinary subcatchments 3250-3252), where the closest temperature station was located 1' (1.7 km) away at an altitude difference of 100 m (Table 10.10). However, the second temperature station is only twice the distance away (3.4 km), but at a smaller altitude difference of 33 m. Hence, the second station was ranked higher (12.5 vs 12.3) and was thus selected for rain gauge ID 0028335.

Table 10.10: Details of the two temperature stations selected for Rain Gauge 186 (SAWS ID 0028355)

Number	Rank	*DIST*	*DALT*	SAWS ID	
		(min)	(m)	RFL	TMP
186	12.48	2.0	33	0028335	0028337
	12.31	1.0	100		0028365

The station rankings were also used to calculate weightings for the two best stations using the equations given below. These weightings were used to assess the difference in suitability between the best and second-best temperature stations.

$$WEIGHT_1 = RANK_1 / (RANK_1 + RANK_2)$$

$$WEIGHT_2 = 1 - WEIGHT_1$$

Equation 12

The weightings calculated for Rain Gauge 783 (0299700) indicate that both temperature stations are equally suitable (Table 10.11). However, the closest temperature station was chosen, simply because the altitude difference for the second station is not small enough to influence the selection process.

Table 10.11: Details of the two temperature stations selected for Rain Gauge 783 (SAWS ID 0299700)

Number	Rank	*DIST*	*DALT*	SAWS ID		Weight
		(min)	(m)	RFL	TMP	
783	11.459	6.3	131	0299700	0299646	0.500
	11.458	6.7	100		0299493	0.500

Ideally, the two selected temperature stations should be situated in the same LRR as the rain gauge. However, since there were almost half the number of temperature stations relative to rain gauges, the decision was made to ignore this criterion. As shown in Table 10.12, Rain Gauge 131 (SAWS ID 0100779) is located in LRR 8, while the best temperature station is located 5' (8.5 km) away at an altitude difference of 34 m in LRR 7. The closest temperature station in the same LRR (LRR 8) is situated much further away (42.2' or 72 km).

Table 10.12: Details of the four temperature stations that could be selected for Rain Gauge 131 (SAWS ID 0100779), depending on the lapse rate region in which they occur

Number	Rank	*DIST*	*DALT*	LRR		SAWS ID	
		(min)	(m)	RFL	TMP	RFL	RFL
131	13.00	5.0	34	8	7	0100779	0078872
	5.85	19.7	474				0101162
	11.70	42.2	354		8		0099415
	11.27	48.8	99				0122450

Furthermore, Table 10.13 indicates that fewer temperature stations are located in LLRs 5, 7, 10, 11 and 12 when compared to regions 1, 3, 4 and 8. This further justifies why the rule to select temperature stations in the same LRR as the rain gauge was not enforced. Similarly, 795 of the 1,240 rain gauges (64.1%) were located in LRRs 1, 3, 4 and 8. In total, only 103 selected temperature stations were located in a different LRR as the rain gauge.

Table 10.13: Histogram of lapse rate region in which each of the 698 unique temperature stations were located

Lapse Rate Region	Count	Percentage of total	Accumulated percentage
1	125	17.91	17.91
2	63	9.03	26.93
3	121	17.34	44.27
4	77	11.03	55.30
5	33	4.73	60.03
6	63	9.03	69.05
7	35	5.01	74.07
8/9	89	12.75	86.82
10	28	4.01	90.83
11	36	5.16	95.99
12	28	4.01	100.00
Total	**698**	**100.00**	

10.1.2.4 Outcome of station selection process

Of the 698 unique temperature stations, only 543 were chosen to represent all 1,240 rain gauges. This means that the same temperature station (e.g. SAWS ID 0145029) was selected for multiple rain gauges (e.g. 10 in total). Similarly, stations 0113025, 0125409, 0141264 and 0174723 were each chosen for nine rain gauges, while stations 0048383, 0096045, 0117495 and 0134478 were the best for eight rain gauges each.

Ideally, 114 rain gauges had a temperature station with the same SAWS station ID (ignoring the custodian), indicating their close proximity. For these gauges, the distance to the selected temperature station ranged from 0 to 2.8' (4.8 km), with the largest altitude difference being 272 m. Hence, the temperature station was considered a "perfect match" for the rain gauge. Furthermore, 184 temperature stations were within 1 minute (1.7 km) of the temperature station, with an altitude difference of 1 to 338 m.

In total, the temperature stations selected for 28.1% of the rain gauges were closer than 5 minutes of a degree (8.5 km), as indicated in Table 10.14. Of concern is the number of selected temperature stations that were more than 20 minutes (34 km) from the rain gauge. The temperature station furthest from a rain gauge was at a distance was 52.5 minutes (~89 km) for Rain Gauge 374 (representing quinary subcatchments 1978-1980).

Table 10.14: Histogram of distance from each rain gauge to the selected (best) temperature station

DIST (min)	Count	Percentage of total	Accumulated percentage
< 5	348	28.06	28.06
5-10	287	23.15	51.21
10-15	241	19.44	70.65
15-20	164	13.23	83.87
20-25	90	7.26	91.13
25-30	43	3.47	94.60
30-35	29	2.34	96.94
35-40	24	1.94	98.87
40-45	9	0.73	99.60
45-50	4	0.32	99.92
50-55	1	0.08	100.00
Total	**1,240**	**100.00**	

From the histogram given in Table 10.15, the altitude difference between the rain gauge and the selected (best) temperature station is less than 50 m for 42.3% of the gauges. Of concern is the number of selected temperature stations that are more than 250 m above (or below) the rain gauge. Rain Gauge 1157 (representing quinary subcatchments 0682-0684) has a temperature station with an altitude difference of 1,097 m that is 6.7' (11.4 km) away. Although the next best station exhibits an altitude difference of 442 m, it is located 9.4' (16 km) away. However, altitude differences can easily be adjusted for using adiabatic lapse rates, which explains why more emphasis is placed on the distance factor when selecting suitable temperature stations.

Table 10.15: Histogram of altitude difference from each rain gauge to the selected (best) temperature station

DALT (m)	Count	Percentage of total	Accumulated percentage
< 50	524	42.26	42.26
50-100	256	20.65	62.90
100-150	148	11.94	74.84
150-200	91	7.34	82.18
200-250	65	5.24	87.42
250-300	43	3.47	90.89
300-350	25	2.02	92.90
350-400	24	1.94	94.84
400-450	20	1.61	96.45
450-500	6	0.48	96.94
500-550	14	1.13	98.06
550-600	9	0.73	98.79
600-650	4	0.32	99.11
650-700	4	0.32	99.44
700-750	4	0.32	99.76
750-800	1	0.08	99.84
800-850	0	0.00	99.84
850-900	0	0.00	99.84
900-950	0	0.00	99.84
> 950	2	0.16	100.00
Total	**1,240**	**100.00**	

10.1.2.5 Lapse rate adjustments

Of the two most representative temperature stations selected for each rain gauge location, the best (first) station was chosen. The altitude difference between the temperature station and the average value for each quinary subcatchment was used to calculate “unique” temperature values for each subcatchment. This was achieved using the adiabatic lapse rates corresponding to the region in which the temperature station was located. For each of the 12 defined regions (cf. Section 10.1.2.2), Schulze and Maharaj (2004) developed monthly lapse rates for both maximum and minimum temperatures that represent the rate of change of temperature with altitude.

The average altitude across each quinary subcatchment was updated using the 90 m digital elevation model (DEM), then compared to values obtained from the 200 m DEM by Schulze and Horan (2011). Differences in average altitude ($DALT = ALT_{90} – ALT_{200}$) shown in Table 10.16 indicate that the values are within ±50 m for the majority (98.3%) of the quinary subcatchments, with the updated figures (ALT_{90}) being less than the older values (ALT_{200}). However, the altitude differences range from -168 to 273 m for 97 quinary subcatchments, which justified using the 90 m DEM.

Table 10.16: Histogram of differences in average altitude of each quinary obtained from the 90 and 200 m digital elevation models

DALT (m)	Count	Percentage of total	Accumulated percentage
< -150	1	0.02	0.02
-150 to -100	3	0.05	0.07
-100 to -50	71	1.22	1.28
-50 to 0	3,503	60.00	61.29
0 to 50	2,238	38.34	99.62
50 to 100	16	0.27	99.90
100 to 150	5	0.09	99.98
150 to 200	0	0.00	99.98
200 to 250	0	0.00	99.98
> 250	1	0.02	100.00
Total	**5,838**	**100.00**	

10.1.2.6 Quality control

Checks identical to those done on historical data by Schulze and Maharaj (2004) were then performed on the lapse rate adjusted temperatures. In other words, these checks were performed on daily maximum (T_{max}) and minimum (T_{max}) values after the lapse rate adjustment and included the following:

- $T_{max} \leq T_{min}$
- $T_{max} - T_{min} < 1.5$ °C
- $T_{max} < 0$ °C

The lapse rates were capped at -10 °C per 1,000 m to minimise occurrences of these anomalies, which were then corrected by calculating the following:

- $T_{ave} = (T_{max} + T_{min})/2$
- $T_{max} = T_{ave} + 0.75$
- $T_{min} = T_{ave} - 0.75$

In addition, daily temperature values for the 543 stations assigned to each of the rainfall driver rain gauges were scanned to determine the hottest and coldest temperatures recorded from 1950 to 1999, i.e. all infilled values were ignored. These extreme values were used to limit the altitude adjusted temperatures to a range of -10 to 50 °C. The reader is referred to Lumsden et al. (2011) for additional information on the methodology.

10.1.2.7 Thermal time

Growing degree-days were calculated from daily temperatures using a method described by McMaster and Wilhelm (1997), with the exception that no adjustment is made of the minimum temperature when it drops below the base temperature. This is believed to better represent the damaging or inhibitory effects of cold on plant processes. In AquaCrop, this method of calculating GDD is known as “Method 3”, which is detailed in Section I.5 in Appendix I.

10.1.3 Reference evaporation

Daily solar radiation, as well as relative humidity (maximum and minimum) values, was then generated from the revised temperature values using the method described by Schulze et al. (2011). Due to the lack of wind speed data, a daily default value of 2 m s^{-1} was used, as suggested by Allen et al. (1998). Daily reference evapotranspiration values (ET_O) were then calculated using the FAO56 version of the Penman-Monteith equation (Allen et al., 1998).

In addition, the method developed by Kunz et al. (2015b) to calculate monthly adjustment factors to derive unscreened A-pan equivalent evaporation from FAO56-based reference evaporation was again used in this project. The technique was based on a modified version of the PenPan equation, which was successfully applied in Australia to estimate A-pan equivalent evaporation. The adjustments suggest that A-pan equivalent evaporation exceeds FAO56 evaporation by a factor ranging from 16 to 51% for southern Africa. The reader is referred to Kunz et al. (2015b) for more detail on the PenPan method.

10.1.4 Generating a new quinary climate database

For each of the 1,240 quinary rainfall driver stations, daily rainfall from January 1950 to December 1999 was extracted from the rainfall database developed by Lynch (2004). This was done to obtain the data quality code, which indicates if the daily rainfall value is observed (code = “ ”), infilled (P) or missing (M). Missing data (flagged as -99.9M) was set to zero (as noted in Section 10.1.1.2) and extreme values (cf. Section 10.1.1.3) were adjusted downward. For all these adjustments, the rainfall code was changed to F, i.e. fixed. Using the updated list of rainfall driver stations (cf. Section 10.1.1.1), a new climate file for each quinary subcatchment was generated by combining daily rainfall (and code) with the lapse rate-adjusted temperatures (and codes). The ET_O data was added to the climate files, which were called *obstmp_xxxx.txt*, where *xxxx* represents the unique subcatchment identifier (*SUB_CAT*) that ranges from 0001 to 5838. These files are in ACRU-composite format and were used to estimate the hydrological impact of biofuel crop production.

10.1.5 AquaCrop climate files

According to Raes et al. (2017), the AquaCrop model requires a climate (.CLI) file, which contains the names of the daily rainfall (.PLU), air temperature (.TNX), reference evaporation (.ETo) and atmospheric CO_2 (.CO2) files. The format of the .PLU, .TNX and .ETo files are similar, with five header lines that provide station details, but more importantly, the start date of the climate record.

As noted earlier, the revised quinary subcatchment database consists of 5,838 climate files, each containing 50 years of daily climate data stored in the format required by the ACRU model.

In the previous biofuel project (Kunz et al., 2015b), a utility was developed to convert the climate files from ACRU's composite file format into that required by the AquaCrop model. This tool was modified to accommodate the change in the temperature file extension from .TMP to .TNX, which was done by FAO to avoid confusion with temporary files in Windows.

During this reformatting process, two additional files (.DSC and .DTA files) were created as required by FAO's ET_o calculator, which calculates ET_O data according to FAO standards (as described by Allen et. al., 1998). This tool was used to calculate daily ET_O values for 13 test quinary subcatchments, which were then compared to those stored in the ACRU composite files. Only slight differences of ±0.1 mm were found due to rounding issues, with the majority of daily values being identical.

In total, 35,028 (i.e. 5,838 * 6) climate-related files were created in order to run AquaCrop at national scale. Checks were conducted on 13 test quinary subcatchments to ensure that the AquaCrop climate files were correct and that the monthly adjustment factor (*PPTCOR*) had been applied to the daily rainfall values.

10.2 SOILS DATA

The minimum soil input parameters required by the simulation models used in this study (ACRU and AquaCrop) are depths of the A- and B-horizon, the volumetric water contents at saturation (θ_{SAT} in percentage), FC (θ_{FC} in FC in percentage) and PWP (θ_{PWP} in percentage), as well as saturated hydraulic conductivity (K_{SAT} in mm d^{-1}).

10.2.1 Soil water retentivity

Soil water retention parameters were obtained from the quinary subcatchment soils database (Schulze et al., 2011). Although this database has recently been updated, it was not available at the time the model runs commenced (cf. Section 17.3.4.3). A utility was developed to extract the soil water retention constants from the quinary soils database, and to output them in the format required by ACRU and AquaCrop. A total of 11,676 (5,838 * 2) soil-related files were produced to run the models at a national scale.

10.2.2 Saturated hydraulic conductivity

AquaCrop requires the saturated hydraulic conductivity (K_{SAT}) of each soil horizon. According to Raes et al. (2018), K_{SAT} represents the speed that soil water moves vertically through the saturated pore spaces in soil. Since this soil parameter is not required by ACRU, it was not available in the quinary subcatchment soils database. Hence, a pedo-transfer function was developed to estimate K_{SAT} for the soil water retention parameters. Saxton and Rawls (2006: 1571) provided a table of useful equations to estimate K_{SAT} (in mm h^{-1}) as follows:

$$K_{SAT} = 1930(\theta_{SAT} - \theta_{FC})^{[3 - \lambda]} \quad \text{Equation 13}$$

where θ_{SAT} and θ_{FC} are the soil water contents in m m^{-1} at saturation and field capacity, respectively. The term λ represents the inverse of the "slope of the logarithmic tension-moisture curve" and is calculated as follows:

$$\lambda = [ln(\theta_{FC}) - ln(\theta_{PWP})] / [ln(1500) - ln(33)] \quad \text{Equation 14}$$

where θ_{PWP} is the soil water content at the PWP (in m m^{-1}). The two constants, 33 and 1,500, represent the matric potentials (in kPa) at FC and PWP, respectively. A utility was developed to estimate K_{SAT} for each soil horizon in mm d^{-1} using the above two equations, with soil water retention parameters extracted from the quinary subcatchments soils database.

Typical particle size distributions (clay percentage and sand percentage) for 11 soil textural classes were used to calculate K_{SAT} for common South African soils using various equations provided by Saxton and Rawls (2006: 1571).

K_{SAT} ranged from 11 mm d^{-1} for a clay soil, to 3,292 mm d^{-1} for a sandy soil. A similar range of 35 to 3,000 mm d^{-1} was provided by Raes et al. (2018: 2-162) for 12 soil textures, with a proviso that the indicative values are not intended to replace measurements.

10.2.3 Readily evaporable water

Readily evaporable water (REW) expresses the maximum amount of water (mm) that can be extracted during Stage I evaporation from a "thin" soil surface layer (0.04 m). Raes et al. (2018) provided an equation to derive REW (in mm) from the A-horizon's soil water content at FC (θ_{FC} in volume percentage) and PWP (θ_{PWP} in volume percentage):

$$REW = 0.04(\theta_{FC} - \theta_{PWP} / 2) \cdot 10 \quad \text{Equation 15}$$

The REW values were derived for each quinary subcatchment and stored in the soils (.SOL file). The range of acceptable values was limited to 15 mm (and no values below 0 mm), based on recommendations by Raes et al. (2018).

10.2.4 Curve number

AquaCrop also requires the curve number (CN) for the simulation of surface runoff and its value refers to antecedent moisture class II (CNII). This parameter is stored in the model's soil (.SOL) file. Although the CN is a function of soil type, slope and relative wetness of the topsoil, it also depends on the land use and land cover. Raes et al. (2018: 2-166) provided default CNII values based on K_{SAT} of the A-horizon (using Equation 13) as given in Table 10.17.

Table 10.17: Default CNII values for various saturated hydraulic conductivities of the topsoil (Raes et al., 2018)

Hydrological soil group	Soil class	Typical soil texture	K_{SAT} (mm d^{-1})	CNII
D	Silty clayey	Silty clay loam, silty clay, clay	≤35	77
C	Sandy clayey	Sandy clay, sandy clay loam, clay loam	36-346	72
B	Loamy	Loam, silt loam, silt	347-864	61
A	Sandy	Sand, loamy sand, sandy loam	>864	46

The table shows that the soil's runoff-producing potential is highest (77) for silty, clayey soils, which conduct water slowly through the soil profile (i.e. more runoff production due to reduced infiltration). It is worth noting that the updated curve numbers derived for this project are different to those used in the previous biofuel study (Kunz et al. 2015b; cf. Table 10.13 in Section 10.1.2.3).

10.3 PLANTING DATE

Typical planting dates for each feedstock were obtained from a literature review. The fixed planting dates used in this study correspond to those used by Kunz et al. (2015a; cf. Table 10.2). The planting date was set to the beginning of the selected month and not mid-month so that the initial crop coefficients obtained from the modelling approach were averaged from 30 days of ET_C and ET_O data (not 15 days).

10.3.1 Soybean

Soybean's planting date is more critical than for maize, and has a significant influence on vegetative growth due to differences in day length (DAFF, 2010a). In general, a longer growing season (earlier planting date) will result in higher yields, as long as the climate remains optimal (Dreyer, 2017).

According to the cultivar recommendations developed by the ARC's Grain Crops Institute, soybean can be planted during October, as long as soil and air temperatures are suitable for germination (De Beer and De Klerk, 2014; De Beer and De Klerk, 2015; De Beer and Bronkhorst, 2016; De Beer and Bronkhorst, 2017; De Beer and Bronkhorst, 2019). DAFF (2010a) suggests that soybean is not planted before mean daily temperatures of 15 to 18 °C have been reached, but warns that early plantings stimulate excessive vegetative growth, which results in lodging problems without any yield advantages. However, planting dates from early to mid-November are mainly recommended for soybean in order to achieve optimum crop development and thus crop yield (Nieuwenhuis and Nieuwelink, 2005; DAFF, 2010a; Dreyer, 2017).

As a general guide, PANNAR (2006) recommends planting from the end of November to the end of December in very hot areas (Bushveld and Lowveld areas) and from mid-November to mid-December in warm areas. In cool areas, the end of October to the end of November is recommended. Shorter day lengths from February onwards affect the frame size and reduce the number of nodes and pods per plant, especially if shorter days coincide with vegetative growth, so planting should be done as early as mid-November (SEEDCO, 2018). Hence, the planting date in AquaCrop was set to 1 November for each of the 49 seasons (from 1950 to 1999). In relatively warm areas where high temperatures enhance growth rate, DAFF (2010a) noted that planting as late as the end of December can still produce satisfactory yields. Based on this, a second planting date of 1 December was chosen for the AquaCrop model runs. Furthermore, planting can be delayed up to the first week of January (De Beer and De Klerk, 2014).

10.3.2 Grain sorghum

Araya et al. (2016) found that planting date substantially affected biomass and grain yield simulations of grain sorghum using AquaCrop. Sorghum is typically planted in South Africa from mid-October to mid-December (DAFF, 2010d; Wani et al., 2012). This concurs with PANNAR (2013b), which stated that, in most areas, planting should take place during late October and November. In the drier, western regions, the best planting time is approximately mid-November. However, grain sorghum may still be grown successfully as late as January, depending on the climatic conditions, length of growing season and that required by the cultivar. It is important to choose a planting date that ensures that the period of ear initiation does not coincide with a drought period (ARC, 2003; Du Plessis, 2008; DAFF, 2010b).

Research was conducted at the Ukulinga research farm (Pietermartizburg, KwaZulu-Natal) in the 2014/15 season to assess the effects of three planting dates on the yield of four sorghum genotypes. The chosen planting dates were 3 November, 17 November and 26 January, which represented early, optimal and late options for sorghum. Sorghum planted late received approximately two-thirds of the rainfall received by the early planted crop. Water use efficiency for biomass production and grain yield were highest for the optimal planting date (30.5 and 9.2 kg mm^{-1}), followed by the early planting (25.2 and 8.3 kg mm^{-1}) and the late planting (23.1 and 8.7 kg mm^{-1}) dates. The authors noted that the trial should be repeated across environments different to Ukulinga to better understand the water use characteristics of the four genotypes (Hadebe et al., 2017a).

Chimonyo et al. (2016) assessed the effects of planting date and density on a sorghum-cowpea intercropped system across five sites in KwaZulu-Natal. The authors recommended a mid-November planting of a sorghum-cowpea intercrop for lower potential sites. For higher rainfall sites, planting around mid-December was recommended in shallower clay soils, but mid-October was recommended for deeper clay soils. Based on the above evidence, a planting date of 1 November was also selected for grain sorghum. A second planting date of 1 December was used for the AquaCrop model runs.

10.3.3 Generating planting dates

10.3.3.1 Background

As noted above, the fixed planting date approach was adopted in this study. Chimonyo et al. (2016) also tested another two methods for determining planting dates for sorghum: the trigger method and a modelling approach. For the trigger method, the start of the growing season occurs when monthly rainfall totals (R_{TOT}) exceed half of the monthly evaporative demand, i.e. $R_{TOT} \geq 0.5 \cdot ET_O$. The disadvantage of this method is access to reliable reference evapotranspiration data, especially for smallholder famers and agricultural extension service providers.

Most crop simulation models can generate suggested planting dates based on pre-defined criteria and inputs of climate data. For example, AquaCrop's criteria to determine the onset of the growing cycle are based on rainfall or temperature thresholds. The model cannot account for soil-related criteria, e.g. topsoil water content > 80% of field capacity (Chimonyo et al., 2016). Various rainfall criteria are provided in the model as follows (Raes et al., 2017; Raes et al., 2018):

- Cumulative rainfall since the start of the period is at least 80 mm.
- Total rainfall over a four-day period is at least 20 mm.
- Total rainfall over a 10-day period is at least 40 mm.
- Total rainfall over a 10-day period exceeds $0.5 \cdot ET_O$.

Similar temperature-based criteria are also provided in AquaCrop as follows (Raes et al., 2017; Raes et al., 2018):

- Cumulative growing degrees since the start of the period of at least 200 degree-days
- Minimum temperature over a three-day period of at least 5 °C
- Average temperature over a three-day period of at least 10 °C
- Cumulative growing degrees over a seven-day period of at least 30 degree-days

However, the process of generating planting dates using AquaCrop cannot be automated to run seamlessly for all suitable growing areas in the country. Hence, this approach could not be implemented in this study. In addition, Section 14.3.8.2 highlights the lengthy run times required to run the model at a national scale. Thus, a faster method for generating planting dates was developed.

Raes et al. (2004) evaluated the following three rainfall criteria for determining planting dates at the onset of the rainy season in Zimbabwe:

- Total rainfall over a seven-day period is at least 25 mm (used by Zimbabwe's Department of Agricultural, Technical and Extension Services)
- Total rainfall over a 15-day period is at least 40 mm (used by Zimbabwe's Department of Meteorological Services)
- Total rainfall over a four-day period is at least 40 mm (based on farmer practice)

The authors found that the first two criteria were highly susceptible to "false starts", resulting in the probability of crop failure being one in two years and two in five years, respectively. The third criterion resulted in the probability of crop failure of one year in four, which was deemed acceptable. However, the analysis was limited to the establishment stage (first 30 days after planting). Therefore, the rest of the growing season was not assessed (Raes et al., 2004).

Mhizha et al. (2014) used the latter criterion (40 mm within four days) to determine planting dates after 1 October of maize grown in Zimbabwe. Although they found that this criterion generated fewer possible planting dates (less than five per season), it was necessary as it did the following:

- Identified the start of the growing period

- Transformed a dry topsoil at wilting point to field capacity in order to sustain germination and seedling survival until the next rains were received

The authors then applied a second criterion (25 mm over seven days) to determine subsequent planting dates after the start of the growing season had been determined.

AquaCrop was then run for each planting date to estimate crop yields, from which planting guidelines were developed for different maize-growing regions in Zimbabwe.

Accumulated rainfall totals of 25 mm over 10 days, and 45 mm over four days were adopted by Tadross et al. (2009). They also created a third criterion by checking that once 25 mm of rainfall had fallen in a 10-day period, the next 20 days did not experience a long dry spell (defined as 10 consecutive “dry” days where daily rainfall ≤ 2 mm). The latter prevents false starts of the growing season, which could result in high probabilities of crop failure.

10.3.3.2 Methodology

Based on the above evidence, the following criteria were adopted in this study:

- Start of the growing season: ≥ 40 mm of total rainfall over four days (Mhizha et al., 2014); Raes et al., 2004)
- First planting date: ≥ 25 mm of total rainfall over seven days (Mhizha et al., 2014), with an average daily temperature exceeding 15 °C (DAFF, 2010a)
- Elimination of dry spells: At least one day of rainfall > 2 mm in each ten-day period over the next 20 days (Tadross et al., 2009).

Another criterion was added in this study where the first planting date must occur within 30 days of the start of the growing season. This prevents the soil from drying out completely after the initial rains (that mark the start of the growing period), but before the planting date. All these criteria should minimise the risk of crop failure to smallholder farmers wanting to produce biofuel feedstocks, especially for soybean, considering it is less drought tolerant than sorghum.

The elimination of dry spells involved a 10-day moving window from the possible planting date (Day 12 in Table 10.18) to 20 days thereafter (Day 31 in Table 10.18). For each of the 11 dekads (marked A to K in Table 10.18), a dry spell was defined when none of the 10 days received more than 2 mm of rainfall. If any of the 11 dekads was flagged as a dry spell, the possible planting date was rejected. The analysis was stopped when the dekad went beyond the 20-day period, e.g. dekad marked L in Table 10.18.

If the planting date occurred before 1 October, it was ignored to eliminate dates suitable for winter rainfall areas. Similarly, planting dates from February onwards were also ignored for obvious reasons. In most quinary subcatchments deemed suitable for crop production, multiple planting dates existed between October and January. Thus, only the first (or earliest) planting date was considered. The first planting date that met the above criteria was determined for all 49 seasons. The day value was ignored and the average and median planting month was calculated from the time series of month values. For the mean estimation, January’s cardinal value was changed from 1 to 13 to prevent this month from skewing the calculation. The results are presented in Section 15.3.1.

Table 10.18: Illustration of each dekad used to determine if a long dry spell occurred after a possible planting date

Day	A	B	C	D	E	F	G	H	I	J	K	*L*
12	1											
13	2	1										
14	3	2	1									
15	4	3	2	1								
16	5	4	3	2	1							
17	6	5	4	3	2	1						
18	7	6	5	4	3	2	1					
19	8	7	6	5	4	3	2	1				
20	9	8	7	6	5	4	3	2	1			
21	10	9	8	7	6	5	4	3	2	1		
22		10	9	8	7	6	5	4	3	2	1	
23			10	9	8	7	6	5	4	3	2	*1*
24				10	9	8	7	6	5	4	3	*2*
25					10	9	8	7	6	5	4	*3*
26						10	9	8	7	6	5	*4*
27							10	9	8	7	6	*5*
28								10	9	8	7	*6*
29									10	9	8	*7*
30										10	9	*8*
31											10	*9*
												10

10.4 PLANTING DENSITY

In general, short crops like soybean may be grown at a closer spacing than taller crops such as sorghum. In drier areas, wider spacing is preferable to provide more soil water for individual plants. In higher rainfall areas or under irrigation, closer spacing is recommended (SEEDCO, 2018). Planting densities at the lower end of the suggested ranges reported in the literature were selected for both feedstocks, which were deemed more representative of rainfed cultivation in smallholder farming environments.

10.4.1 Soybean

An inter-row of 0.40-0.90 m and an intra-row spacing of 0.05-0.15 m is recommended to achieve a planning population of 250,000 to 400,000 plants per hectare (Nieuwenhuis and Nieuwelink, 2005; PANNAR, 2006; DAFF, 2009a; DAFF, 2010a). PANNAR (2018) recommends a final plant population of 240,000-280,000 plants ha^{-1} (0.76-0.91 m wide rows) for most areas and climate conditions. In general, the higher the yield potential, the greater the plant population. However, Dreyer (2017) noted that plant density is determined by the type of cultivar, together with other specific cultivar characteristics. In addition, row widths should not exceed 0.75 m, especially where high-density plant populations are favoured. According to the ARC's Grain Crops Institute, soybean can be planted during October. Narrower rows, higher plant populations and shorter growing season cultivars are recommended for later plantings (De Beer and De Klerk, 2014). DAFF (2010a) states that, for drier climates, plant populations lower than 300,000 plants per hectare are recommended. For this study, a planting density of 250,000 and 300,000 plants ha^{-1} was selected for soybean, the latter being similar to that used at Swayimane in 2018/19.

10.4.2 Grain sorghum

According to DAFF (2009b), seeds are sown with a spacing of 0.75 to 1.00 m between rows and 0.30 m in the row at a plant density of 28,600 to 75,000 per ha under dryland conditions. However, a higher seeding rate can be adopted in relatively high rainfall areas. Under semi-arid conditions, Du Plessis

(2008) recommended a plant population of 26,666 plants ha^{-1} for sorghum grown in semi-arid areas, which is similar to the recommended dryland population for maize. Chimonyo et al. (2016) assessed the effects of planting date and density on a sorghum-cowpea intercropped system across five sites in KwaZulu-Natal. The authors recommended that, in order to achieve maximum WUE, the ideal plant population for sorghum should be 39,000 plants ha^{-1} in combination with 13,000 plants ha^{-1} for cowpea. For this study, a planting density of 44,444 plants ha^{-1} was selected, which corresponds to that used in the 2017/18 season at Swayimane (Masanganise et al., 2019) and at Ukulinga in 2013/14 and 2014/15 (Hadebe et al., 2017b).

However, PANNAR (2013b) stated that low populations (< 90,000 plants ha^{-1}) must be avoided because a poor canopy may lead to a weed problem. Hence, it recommended plant populations of 100,000 to 160,000 plants ha^{-1}, with a preference for higher populations when weed competition may be severe. In addition, Wani et al. (2012) recommended plant populations of 50,000 to 150,000 plants ha^{-1}, with low densities preferred in low rainfall areas. These plant populations are much higher than those recommended by DAFF (2009b) and Du Plessis (2008).

A general rule of thumb is that sorghum is typically planted in areas that are considered sub-optimal for maize production. For maize production in Zimbabwe, SEEDCO (2018) recommends a population of 36,000 to 60,000 plants ha^{-1}, depending on environmental potential (low vs high rainfall), the target yield and the selected hybrid (Figure 10.1). Based on this, a higher density of 60,000 plants ha^{-1} was also selected for grain sorghum in this study.

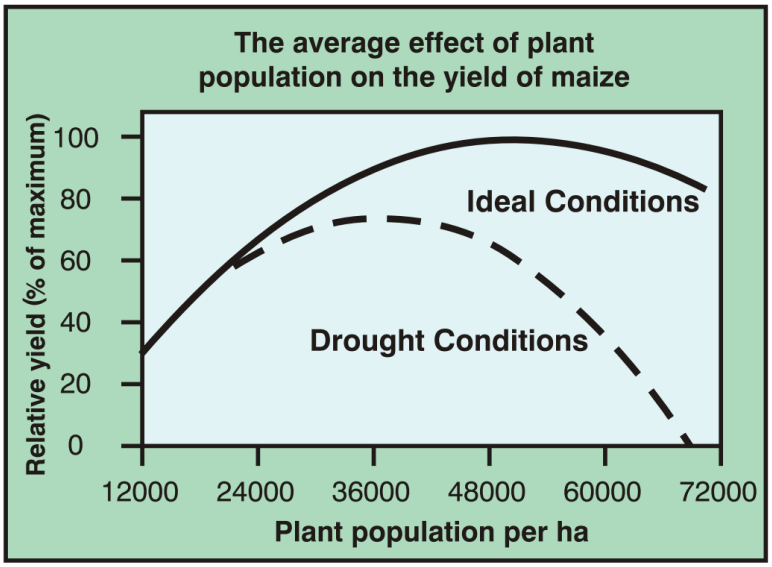

Figure 10.1: Impact of plant population on attainable yield of maize (SEEDCO, 2018)

10.5 SUMMARY AND CONCLUSIONS

The quinary climate database was revised and used for the first time in this project. Errors in extreme rainfall events (daily rainfall > 400 mm) were identified and corrected. Instead of using interpolated temperature data for each quinary subcatchment, observed daily data was assigned to each quinary subcatchment, from which reference evapotranspiration was estimated. No changes were made to the quinary soils database. Two planting dates and two planting densities deemed typical for soybean and sorghum production by smallholder famers in South Africa were used as model inputs. This meant four national model runs for each crop grown under rainfed conditions.

According to SEEDCO (2018), some commercial maize farmers in Zimbabwe are planting crops like maize at population densities higher than the recommendations in search of “compensatory yield

gains"'. These farmers then apply a growth regulator after emergence in an attempt to improve yields. However, this practice incurs additional costs (extra seed, growth regulator, compensatory fertilizer and spraying costs) and there is a risk of response failure when spraying times coincide with extended wet periods or dry spells. Further research is therefore required to ascertain whether the yield gains are significant. A cost-benefit analysis is also required to determine the profitability of this concept. As the practice becomes more popular, the breeding of short stature, high-yielding cultivars to accommodate these higher densities is also required.

CHAPTER 11: PARAMETERS USED FOR CROP MODELLING

This chapter provides a description of the input parameters required by the two crop models used in this study to simulate the water use and yield of soybean and grain sorghum. Hence, crop parameters are provided for both AquaCrop and SWB.

11.1 AQUACROP

According to Todorovic et al. (2009), the AquaCrop model requires about 35 parameters, compared to CropSyst, which requires 40. A full list of input parameters is provided in Table K.2 in Appendix K, of which 19 are conservative, and thus considered widely applicable. A summarised description of these conservative parameters was provided by Steduto et al. (2012: 44). Hence, the model does not require extensive calibration for a specific cultivar. Parameter values for soybean and grain sorghum were obtained from the available literature and are presented in this chapter.

11.1.1 Soybean

11.1.1.1 Default parameters

The original parameterisation of soybean was undertaken using data obtained from Patancheru (India) for June 1996, as described by Raes et al. (2012b; 2017). Default parameter values (for Version 4) are listed in Appendix K, together with an explanation of each parameter. However, Paredes et al. (2015) noted that the use of AquaCrop's default parameters for yield predictions is questionable (there is a clear tendency for under-estimation of biomass and yield), and thus a partial calibration (cf. Section 9.4) for local conditions is recommended. However, Battisti et al. (2017) showed that AquaCrop provided a poor estimation of soybean yield in southern Brazil using both default and partially calibrated crop parameters. Conversely, Vanuytrecht et al. (2014) noted that realistic simulations of maize yield were achieved in three different countries using default model parameter values with only minor adjustments.

It is worth noting that the crop parameter file for Version 6 of the model is different to that used previously in Version 4. Table K.3 in Appendix K highlights changes made by the model developers to three parameter values. One parameter has been slightly renamed from "minimum growing degrees required for full *biomass production*" to "minimum growing degrees required for full *crop transpiration*". In addition, the following two parameters are no longer used:

- Response of stomatal closure
- Shape factor for soil salinity stress coefficient

However, the following three parameters are new in Version 6:

- Calibrated distortion (percentage) of canopy cover due to salinity stress: Range of 0 (none) to +100 (very strong)
- Calibrated response (percentage) of stomata stress to EC_{sw}: Range of 0 (none) to +200 (extreme)
- Canopy size of individual plant (regrowth) on the first day (cm^2)

11.1.1.2 Serbia (1989/94)

In Serbia, soybean is mostly cultivated under rainfed conditions, with the growing season from April to September. Experimental data from 1989 to 1994 was used to calibrate and validate *AquaCrop*, with the crop (Maturity Group I) planted at 40,000 to 43,000 plants ha^{-1}. Over the six growing seasons, rainfall ranged from 140 to 415 mm and irrigation amounts of up to 140 mm were applied to the crop.

The final parameter values obtained using the 1994 dataset are given in Table K.4 in Appendix K. Although the upper temperature remained unchanged at 30 °C, the base temperature was changed to 8 °C. The initial canopy cover (CC_O) was 1.65%, but reached a maximum of 96% (CC_X). The normalised water productivity value was increased from 15 to 19 g m^{-2} and the HI was reduced to 35%. The observed phenological periods in calendar days are also given in Table K.4. For the calibration, the relative deviation between the simulated and observed dry yield was 2%. The 1989 to 1993 datasets were used for validation, where the relative deviation in yields ranged from 2 to 5%, except for 1989 (deviation of 12%). The coefficient of determination and correlation calculated for yield was 0.8529 and 0.9235 respectively. The study highlighted the robustness of AquaCrop, considering that only a few crop parameters were changed to achieve good agreement between simulated and observed yields.

11.1.1.3 China (2008/11)

As noted earlier, Paredes et al. (2015) suggested that the AquaCrop model developers should revise the default green canopy cover parameters for soybean. They used four years (2008-2011) of soybean experimental data observed at Daxing (North China Plain) to assess the ability of AquaCrop to predict soybean's final biomass and yield. Soybean cultivar Zhonghuang 13 was grown, which is a high-yielding, semi-determinate cultivar that belongs to Maturity Group II and takes an average of 96 days to reach full maturity. The model was calibrated using, inter alia, LAI, biomass and final yield data that were measured in 2008. The LAI was used to calibrate the CC curve, which results in four calibrated parameters: CC_O, CC_X, CGC and CDC. An accurate calibration of the CC curve was performed, with the lowest RMSE of 4.3% obtained using the 2010 dataset. The calibrated parameters are given in Table K.5 in Appendix K.

The averaged reference harvest index (HI_O) of 0.38 was obtained from yield observations performed in all seasons (without water stress). The value is within the range of 0.30-0.43 as reported by Donatelli et al. (1997). The normalised water productivity (WP*) value of 17 g m^{-2} was obtained using a trial-and-error procedure aimed at minimising differences between predicted and observed above-ground dry biomass. This value is within the range of values proposed by Steduto et al. (2012), i.e. 12-16 g m^{-2}. The model was validated using the 2009 to 2011 datasets. Simulations of final biomass and yield were considered excellent for 2009, with deviations from observed values of 3.4 and 2.0%, respectively. This was due to the satisfactory calibration of WP*. The worst estimates of biomass (17.8% deviation) and yield (12.9% deviation) were obtained for the 2010 and 2011 datasets.

11.1.1.4 Brazil (2013/14)

Battisti et al. (2017) compared the performance of five crop models, including AquaCrop, in simulating yield of soybean cultivar BRS 284 (Maturity Group 6.5; indeterminate growth habit; non-transgenic). Growth and yield data were obtained from different sites in Southern Brazil and divided into two sets for calibration and validation purposes. The initial soil water content was determined by the model's water balance initiated six months before planting, assuming prior fallow conditions.

The models were first run with default crop parameters, then partially calibrated using crop phenology only, followed by a full calibration to obtain the lowest RMSE and d values between simulated and observed values for the following: yield, total dry matter and harvest index (cf. Table K.6 in Appendix K). In addition, the parameter associated with determinacy linked to flowering was changed from 1 to 0. An analysis of LAI was not undertaken for AquaCrop, since the model does not estimate this variable (only canopy cover development). AquaCrop under-estimated total above-ground biomass (5,504 vs 6,090 kg ha^{-1}) after full calibration. When compared to the use of default parameters, the full calibration of the model reduced RMSE from 0.273 (72%) to 0.081 (21%). AquaCrop produced a poor correlation of HI, with simulated values almost not varying.

Only seed yield was used to validate the models. AquaCrop poorly estimated soybean yield when the default and partially calibrated parameters were used, and produced a negative bias of 1,700 kg ha^{-1}. The default parameters are for an unknown cultivar, probably for a higher maturity group, with a longer cycle and lower growth rate. The bias changed to 165 kg ha^{-1} when the fully calibrated parameters were used (R^2 = 0.71; RMSE = 536 kg ha^{-1}; d = 0.91). Hence, the model over-estimated the observed yield of 2,883 t ha^{-1}. Battisti et al. (2017) concluded that AquaCrop's performance may be due to its inability to simulate the crop life cycle, since it does not consider the effect of photoperiod on soybean development, resulting in an over-estimation of yield for early and late planting dates.

11.1.1.5 Brazil (2014/15)

Silva et al. (2017) calibrated AquaCrop for two soybean cultivars (TMG 1288 and MSOY 9144) grown in the Matopiba region in Brazil. Growth and yield datasets were obtained for both a dry and wet period. Treatments included rainfed production and seven irrigation schedules ranging from 25 to 100% of ET_O over the vegetative and reproductive growth phases, as well as the whole crop cycle. The wet period received 801 mm, and soil water stress was considered unlikely since 576 and 568 mm of irrigation were applied to the two cultivars, respectively, over the entire crop cycle for the 100% ET_O treatment. For the calibration, deviations from the observed yield were highest for the rainfed treatment and showed under-estimations of 13.4 and 25.7% for both cultivars. For the deficit irrigation treatments, predictions were better considered with deviations ranging from 0.3 to 3.1% for one cultivar (TMG 1288) and 1.0 to 16.2% for the other cultivar (MSOY 9144). For the validation, statistical measures of mean absolute error (MAE), normalised root mean square error (NRMSE), Nash-Sutcliffe efficiency index (NSE) and Willmott's index (d) revealed the following: 0.10 ≤ MAE ≤ 0.33 t ha^{-1}, 8.17 ≤ NRMSE ≤ 18.8%, 0.89 ≤ NSE ≤ 0.96 and 0.96 ≤ d ≤ 0.99. The authors concluded that AquaCrop performed best for soybean cultivar TMG 1288, which is more resistant to water stress than cultivar MSOY 9144 under the climatic conditions of tropical Brazil. The calibrated parameters for cultivar TMG 1288 are given in Table K.7 in Appendix K. For the other cultivar, the authors used the default value for the WP* during yield formation parameter (60%), but changed the length of the flowing stage to 62 days.

11.1.1.6 Nigeria (2013/14)

Adeboye et al. (2017) used two seasons (2013-2014) of soybean data from Ile-Ife (Nigeria) to assess the ability of AquaCrop to predict final biomass and yield of soybean. Cultivar TGX 1448 2^E was planted on 2 February (for calibration purposes) and on 8 November 2013 (for validation). The model was calibrated using, inter alia, LAI, biomass and final yield data. Green canopy cover was estimated from LAI using the Beer-Lambert equation with the seasonal leaf extinction coefficient (k) set to 0.46. The calibration of the CC curve was performed using the full irrigation treatment and near-optimal soil fertility. The results showed a tendency for the model to under-estimate the observed canopy cover (with regression coefficient b < 1.0). However, a strong correlation between measured and simulated canopy cover was obtained for calibration and validation (0.97 ≤ R^2 ≤ 0.99 for p < 0.05; 4.3% ≤ RMSE ≤ 5.9%; 0.93 ≤ NSE ≤ 0.99; d = 0.99). Since RMSE <10%, the evaluation was considered good.

The crop achieved a maximum canopy cover (CC_X) of 96%. The soil water depletion factors for canopy expansion and senescence were 0.14 and 0.70, respectively. These values are almost identical to the default parameters. The WP* was set to 16.7 g m^{-2}, which is within the range of 15-20 g m^{-2} for most C3 crops. Of concern is the calibrated reference HI (HI_O) of 62%, which is considerably higher than the default value of 40% (Raes et al., 2012b; Raes et al., 2017) and 38% used by Paredes et al. (2015). The calibrated parameters are given in Table K.8 in Appendix K.

The results showed a tendency for the model to under-estimate the observed canopy cover (with regression coefficient b < 1.0). However, a strong correlation between measured and simulated canopy cover was obtained for calibration and validation (0.97 ≤ R^2 ≤ 0.99 for p < 0.05; 4.3% ≤ RMSE ≤ 5.9%; 0.93 ≤ NSE ≤ 0.99; d = 0.99).

Although AquaCrop over-estimated biomass production from emergence until anthesis (regression coefficient b > 1.0) for the calibrated dataset, there was good agreement between simulated and measured values ($0.96 \leq R^2 \leq 0.99$; $0.08 \leq RMSE \leq 0.14$ t ha^{-1}; NSE = 0.99; $0.98 \leq d \leq 0.99$). Validation of the final biomass and seed yield showed excellent performance of the model, with only one in five predictions beyond 20 and 15% deviations, respectively. Simulated seed yields were significantly correlated with measurements ($R^2 = 0.99$; RMSE = 0.10 t ha^{-1}; NSE and d = 0.99).

11.1.1.7 Baynesfield (2012/13)

Mbangiwa et al. (2019) performed a partial calibration of soybean (cultivar PAN1666R) based on observations of crop growth at Baynesfield Estate (29°45'42.78"S; 30°20'35.82"E; 847 m above sea level) during the 2012/13 season. The estate is situated in KwaZulu-Natal, about 25 km south of Pietermaritzburg. Planting took place on 15 October 2012 at a density of 380,000 plants ha^{-1}. Although the phenological growth stages were observed in calendar days, the model performed the conversion to thermal time in GDD, as shown in Table 11.1.

Table 11.1: Time to and duration of each phenological developmental stage in growing degree-days for soybean (Mbangiwa et al., 2019)

Parameter	Cultivar
	PAN1666R
Time to emergence	112
Time to maximum rooting depth	951
Time to start of senescence	1476
Time to maturity	1881
Time to flowering	934
Duration of flowering	475

Only a few parameters were changed from the original parameterised values as shown in Table K.9 (cf. Appendix K), which emphasises the robustness of AquaCrop. The model calculates the canopy growth coefficient (i.e. the increase in CC per degree-day) from observations of the maximum canopy cover percentage (CC_X) and the time taken to reach CC_X (similar to time from planting to flowering). The default value of 98% for CC_X was used for Baynesfield. In addition, the model calculates the canopy decline coefficient from observations of time to start of canopy senescence and time to physiological maturity. The reference HI was increased by Mbangiwa et al. (2019) from 40 (default) to 45% to adjust for cultivar differences. However, Steduto et al. (2012) reported that the reference HI for soil seed crops ranges from 0.25 to 0.40. It is lower than that for grain crops because it takes approximately 2.5 times as much assimilate to make a gram of oil compared to sugar or starch. Results of model testing showed a good fit between the observed and simulated canopy cover under rainfed conditions (Figure 4111.1b).

During the 2012/13 season, the observed (manually harvested) seed yield was 5.28 t ha^{-1}, assuming no wastage due to pod shattering. AquaCrop simulated a seed yield of 4.79 t ha^{-1}, which was 90.7% of the observed yield and deemed satisfactory by Mbangiwa et al. (2019). Mechanical harvesting using a combine harvester produced a yield of 3.52 t ha^{-1} (Mbangiwa et al., 2019). This represents a high yield loss (38%) when compared to manual harvesting, which is probably due to lodging. As noted by Dlamini (2015), pods that are below 12.5 cm from the soil surface cannot be collected by a combine harvester. At Baynesfield, the farm authorities are not interested in biomass, and thus do not provide harvested total biomass.

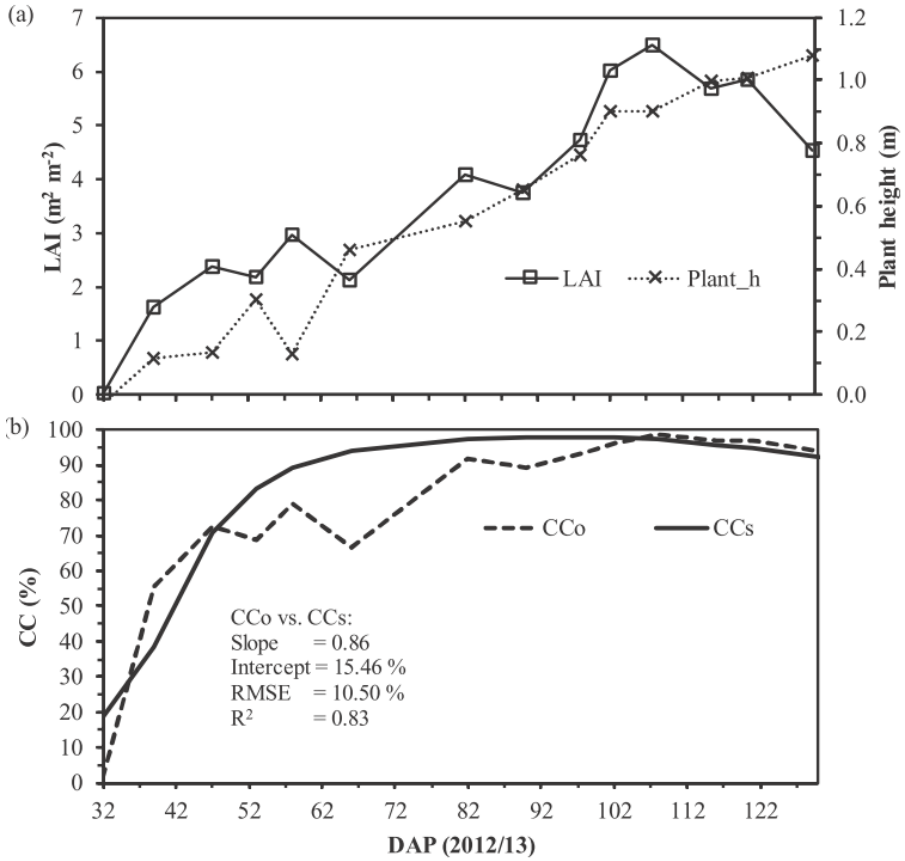

Figure 11.1: (a) Measured leaf area index and plant height, as well as (b) observed (CC_O) and simulated green canopy cover for the 2012/13 growing season at Baynesfield (Mbangiwa et al., 2019)

11.1.1.8 Swayimane (2015/16)

Crop parameters were determined for soybean cultivar LS6161R grown at Swayimane during the 2015/16 season using data from the control treatment (i.e. non-mulched, fully fertilized). However, 26 parameters were calibrated for non-standard conditions since the trial was not irrigated. For this reason, the crop parameters were not used in this study. A better approach would have been to identify non-stressed periods of crop growth, which should then have been used to calibrate the model.

In addition, the observed yield of 1.61 t ha^{-1} was relatively low, considering that the seasonal rainfall total was 540 mm (from November 2015 to March 2016), which was higher than the 16-year seasonal average of 518 mm obtained from an AWS at Bruyns Hill (Wartburg). A plot of accumulated rainfall shown in Figure 4211.2 does not suggest extended periods of low rainfall, considering that the longest period with no rainfall was eight days (91-98 DAP). Hence, the location does not appear to have been adversely affected by the 2015/16 drought.

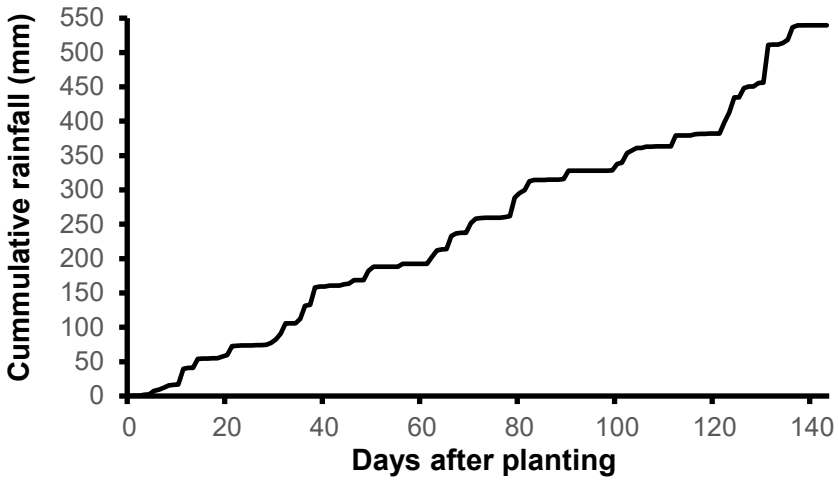

Figure 11.2: Accumulated rainfall from planting to maturity measured at Swayimane during the 2015/16 season

11.1.1.9 Swayimane (2018/19)

Reddy (2019) performed a partial calibration of AquaCrop for two soybean cultivars grown at Swayimane during the 2018/19 season. Planting took place on 19 November 2018 at a density of 317,460 plants ha^{-1}. The list of parameters for LS6161R and CAPG3 are given in Table K.10 and Table K.11 (in Appendix K). Parameters numbered 15, 41 and 42 were modified by the model developers in Version 6 (cf. Section 11.1.1.1).

Although the phenological growth stages were observed in calendar days (parameters 53-58 and 61), the model performed the conversion to thermal time in GDDs (parameters 70-75 and 78), as shown in Table 11.2. The maximum canopy cover attained was 97 and 98% for LS6161R and CAPG3, respectively.

Table 11.2: Time to and duration of each phenological developmental stage in growing degree-days for two soybean cultivars (Reddy, 2019)

No.	Parameter	Cultivar	
		LS6161R	CAPG3
70	Time to 90% emergence	105	105
71	Time to maximum rooting depth	1,680	1,680
	Time to maximum canopy cover	1,440	1,335
72	Time to start of senescence	1,950	2,025
73	Time to maturity	2,025	2,145
74	Time to flowering	1,065	1,185
75	Duration of flowering	255	240

As explained in Section 9.4.2, seedling leaf area should be measured at emergence, and together with planting density as inputs, is used by the model to compute initial canopy cover (CC_O) as shown in Table 11.3. Maximum canopy cover (CC_X in percentage; Parameter 51) and the time to reach CC_X were determined from measurements of LAI, which were then used to compute DIFN and CC development (cf. Section F1.5 in Appendix F). AquaCrop then calculates the canopy growth coefficient (i.e. the increase in CC per GDD; Parameter 75) from CC_O, CC_X and the time taken to reach CC_X, and canopy decline coefficient (Parameter 77) from observations of time to the start of canopy senescence and maturity. The maximum effective rooting depth (Parameter 39) was set to 0.62 m, based on observations from a pit dug in between two rows at the time the trial was harvested (Table 11.3).

Table 11.3: Adjustment of canopy cover and rooting depth parameters to represent both soybean cultivars grown at Swayimane in the 2018/19 season (Reddy, 2019)

No.	Parameter	LS6161R	CAPG3
44	Seedling leaf area (cm^2)	5.00	5.00
	Initial canopy cover (CC_O in %)	1.59	1.59
51	Maximum canopy cover (CC_X in %)	95	97
	Canopy growth coefficient (CGC):		
47	Percentage d^{-1}	7.4350	8.0960
76	Percentage GDD^{-1}	0.4957	0.5397
	Canopy decline coefficient (CDC):		
52	Percentage d^{-1}	0.6690	2.9860
77	Percentage GDD^{-1}	0.0485	0.1972
66	Maximum effective rooting depth (m)	0.62	0.62

Another important parameter (not listed in the tables in Appendix K) indicates whether crop determinancy is linked with flowering (or pod formation). For indeterminant crops (e.g. PAN1521R and CAPG3), crop determinancy is not linked to flowering (parameter value set to 0), meaning that the vegetative growth period stretches from planting until canopy senescence, as shown in Figure 11.3. In other words, the canopy continues to develop (i.e. increase in plant height) after flowering has occurred. For determinant or semi-determinant crops (e.g. LS6161R), crop determinancy is linked to flowering (parameter value set to 1), where canopy development occurs up to peak flowering (i.e. half of flower duration), but not thereafter (Figure 4311.3). If stresses reduce canopy expansion, then CC_X might not be reached at all (i.e. CC_X is delayed).

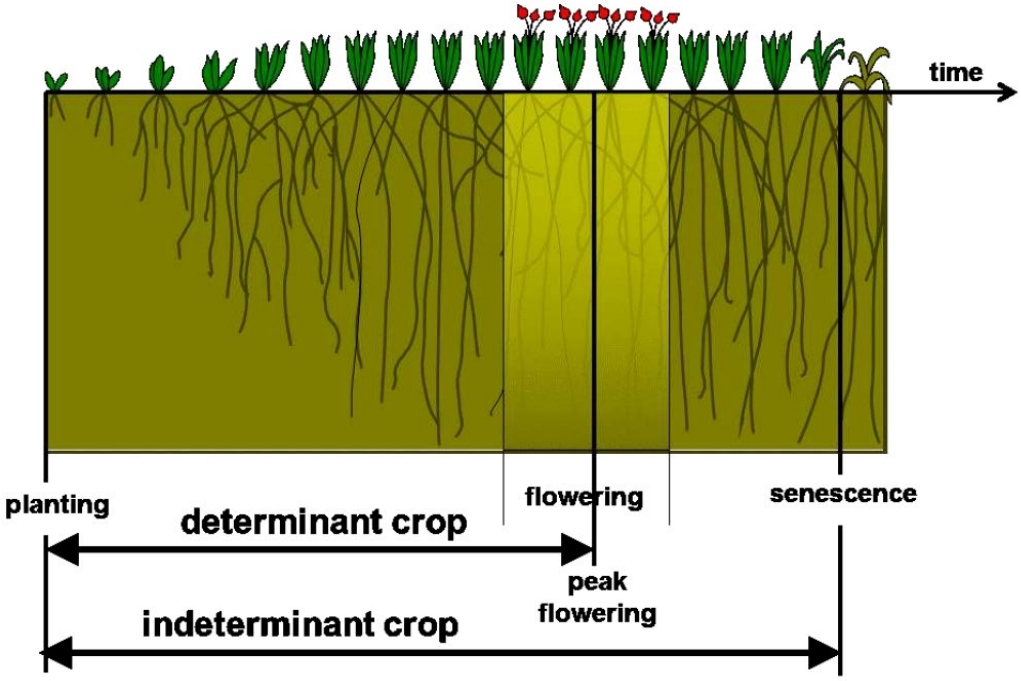

Figure 11.3: Period of potential vegetative growth for determinant and indeterminant crops (Raes, 2017a: 27)

As shown in Table K.10 and Table K.11 (Appendix K), only a few parameters were changed from the original parameterised values, which again emphasises AquaCrop's robustness. AquaCrop's soil fertility option was set to non-limiting to represent the inoculated treatment, whereas the moderate to near-optimal soil fertility option was selected to represent the non-inoculated treatment (since only nitrogen was deficient).

Crop evapotranspiration was determined from a weekly soil water balance, because runoff measurements were only recorded weekly at the site. Simulations of canopy cover and biomass growth for both soybean cultivars are shown in Figure 100L.1 and Figure 101L.2, respectively (cf. Appendix L). For final biomass and seed yield, as well as the HI, model simulations showed a good correlation between observed and simulated data, especially for the CAPG3 yield under the non-inoculated treatment (Table 11.4).

However, the model over-estimated biomass production of CAPG3 for both the inoculated (8.5 vs 9.8 t ha^{-1}) and non-inoculated (7.4 vs 9.6 t ha^{-1}) treatments. On the other hand, AquaCrop under-estimated biomass production of LS6161R for the inoculated (8.7 vs 8.1 t ha^{-1}) and non-inoculated (8.3 vs 8.0 t ha^{-1}) treatments. The over- and under-estimation may be due to the assumptions made to account for these treatments, as well as due to a partial calibration of the model.

Table 11.4: Observed versus simulated data of final biomass and seed yields, as well as the Harvest Index, for the two soybean cultivars grown under rainfed conditions and two inoculation levels at Swayimane in the 2018/19 season (Reddy, 2019)

Treatment	Variable	LS6161R		CAPG3	
		Observed	Simulated	Observed	Simulated
Inoculated	Final biomass (t ha^{-1})	8.7	8.1	8.5	9.8
	Seed yield (t ha^{-1})	4.6	3.2	4.4	3.8
	Harvest Index (%)	51.4	39.5	50.9	38.8
	Evapotranspiration (mm)	481	464	508	481
Non-inoculated	Final biomass (t ha^{-1})	8.3	8.0	7.4	9.6
	Seed yield (t ha^{-1})	4.3	3.1	3.7	3.7
	Harvest Index (%)	49.8	38.8	48.4	38.5
	Evapotranspiration (mm)	482	463	519	478

For the inoculated treatment, the model under-estimated the yield by 30.4 and 13.6% for LS6161R and CAPG3, respectively. Silva et al. (2017) reported deviations of -13.4 and -25.7% (for two cultivars) from the observed yield. It is important to note that, in each plot, only five plants in each of the two experimental rows were harvested, which may have resulted in higher yield estimates and HI values. Ideally, all the plants in each row should have been harvested, which was not done due to labour constraints experienced during the week of harvesting. From Table 11.4, the HI results are above the range of 25-45% reported in the literature. The model simulated HI well, as the default reference HI parameter value of 0.40 was used in this study.

AquaCrop simulations of crop water use correlated well with observed data for LS6161R under both treatments. Simulated values of crop evapotranspiration compared well with the figure of 469 mm reported by Kunz et al. (2015a) for the 2012/13 season at Baynesfield (measured using the surface renewal technique). The CAPG3 used more water than LS616R, which is likely due to the longer crop cycle (2,145 vs 2,025 GDD). Although there is some under-estimation of observed ET_C, these differences are not considered large. The model does not simulate the evaporation of intercepted water, which could explain the differences. As explained by Paredes et al. (2015), the over- and under-estimation of crop water use is due to the abandonment of the dual crop approach in AquaCrop. Similar findings were reported by Battisti et al. (2017). According to Mbangiwa et al. (2019), AquaCrop simulated a water use of 420 mm and a final yield of 4.79 t ha^{-1} for soybean grown at Baynesfield during the 2012/13 season.

Profile water content was simulated by AquaCrop for a 1 m soil comprising two horizons (i.e. 0.30 and 0.70 m thick). Simulations were compared to profile water content measured by CS650 probes and Watermark sensors installed at the four soil depths (Figure 4411.4).

However, the CS650s provided a more accurate and reliable estimate of soil water content than the Watermark sensors. The Watermark sensors had large periods of missing data, which were infilled using data from the CS650s. Hence, the Watermark data is not shown in Figure 11.4. Profile water content was under-estimated by the model in the early stages of development (i.e. 0 to 55 DAP), as well as in the late stages of development (i.e. approximately 115 to 135 DAP). The model over-estimated the soil water content during the mid-season growth stage (i.e. 55 to 95 DAP). Similar patterns were reported by Paredes et al. (2015) and Lembede (2017) for soybean, as well as in other studies for barley (Pereira et al., 2015) and maize (Paredes et al., 2014). According to Paredes et al. (2015), AquaCrop's abandonment of the FAO's dual crop coefficient approach has resulted in transpiration and soil water evaporation being too dependent on the CC curve.

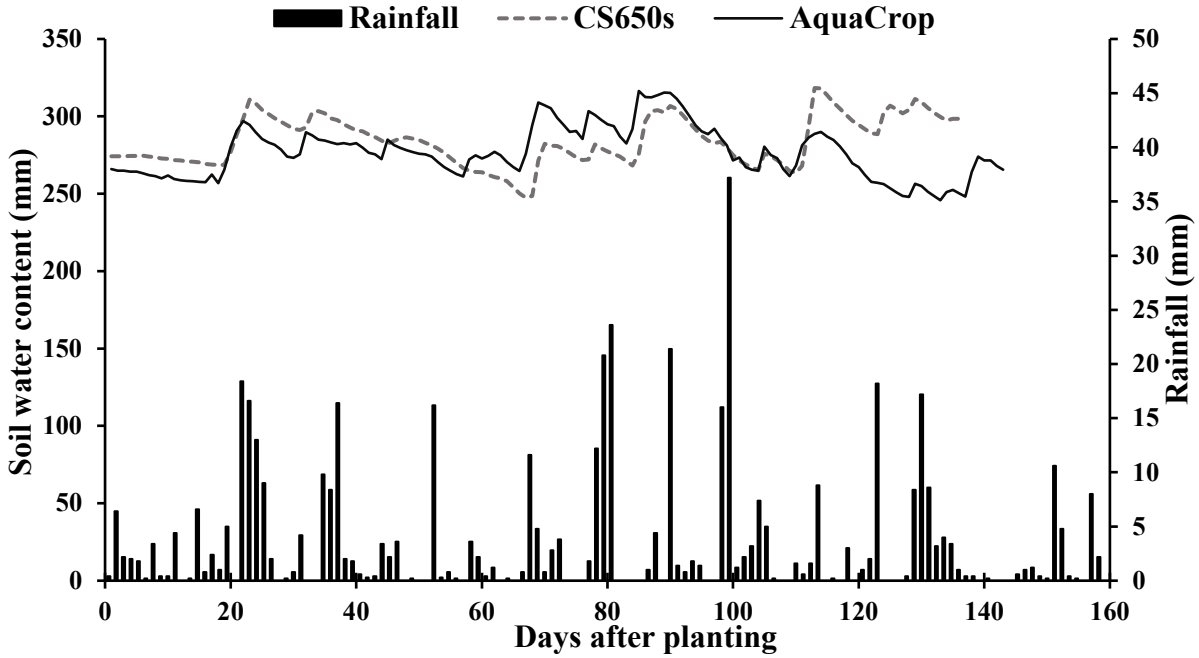

Figure 11.4: Comparison between soil water content simulated by AquaCrop and that observed by two different sensors (i.e. CS650s and Watermark) throughout the 2018/19 growing season at Swayimane (Reddy, 2019)

11.1.1.10 Discussion and conclusions

For the reasons given in Section 11.1.1.8, the crop parameter file developed by Lembede (2017) for soybean was not used for modelling purposes, i.e. to estimate the water use and yield of soybean at the national scale. Instead, the same approach adopted by Mbangiwa et al. (2019) and Reddy (2019) was used, whereby a partial calibration of the model was undertaken for soybean. The parameters shown in Table 141K.10 (Appendix K) for LS6161R were used in this project for modelling purposes. For the inoculated treatment, the model under-estimated the yield of LS6161R by 30.4%, as well as the final biomass by 6.9%. However, the model under-estimated the crop water use by 3.5%.

11.1.2 Grain sorghum

11.1.2.1 Default parameters

In this study, the majority of conservative crop parameters were those tabled by Raes et al. (2012b; 2017) for sorghum. The original parameterisation of grain sorghum was undertaken using data obtained from Bushland (Texas, USA) for May 1993. Default parameter values (for Version 4) are listed in Appendix K, together with an explanation of each parameter.

However, the crop parameter file for Version 6 of the model is different to that used previously in Version 4. Table K.12 in Appendix K highlights changes made by the model developers to four parameter values. As noted in Section 11.1.1.1, one parameter has been renamed, two parameters are no longer used and there are three new crop parameters.

It is worth noting that the base and cut-off temperatures for sorghum given in the crop parameter file are 8 and 30 °C. In South Africa, Du Plessis (2008) reported that the lower temperature threshold for sorghum was 7 °C, while the upper temperature threshold for sorghum grown in the semi-arid tropics was reported as 38 °C (Huda et al., 1984). The upper threshold was not altered in this study.

11.1.2.2 Kansas (2005)

Araya et al. (2016) conducted a study in Southwest Kansas to determine optimum limited-irrigation strategies for grain sorghum (unknown cultivar). Experimental datasets for grain sorghum were used to calibrate and validate AquaCrop. Calibration was done using growth and yield data measured in 2005 for the full and two deficit irrigation treatments. The inclusion of deficit irrigation treatments proved useful in estimating water stress factors. Hence, default values for canopy growth, stomatal conductance and canopy senescence were adjusted to 0.10, 0.45 and 0.45 for the respective stress factors. Steduto et al. (2009) indicated that canopy expansion is more sensitive to water stress when compared to stomatal conductance and canopy senescence. Crop phenological development was obtained from the field and is given in Table K.13 (Appendix K). Seedling leaf area was 3 cm^2, which matched the default value. Canopy cover was estimated from LAI measurements for optimal growing conditions using the Beer-Lambert equation and an extinction coefficient (k) of 0.416. Since biomass data were not collected, WP* was calibrated using stomatal conductance and canopy senescence. This value was reduced to 30 g m^{-2} to improve model predictions, which is within the range of 30 to 35 g m^{-2} for C4 plants (Raes et al., 2012b; Raes et al., 2017). The HI was set to 0.46, the most common value obtained under optimal growing conditions in 2005, which is within the range of 0.30-0.50 (Wani et al., 2012).

Experimental data from the full and deficit irrigation treatments measured during the 2007 and 2010 growing seasons was used to validate the model, and based on statistical goodness-of-fit measures for soil water and evapotranspiration, as well as final biomass and yield. The goodness-of-fit statistics for model validation showed that soil water was adequately simulated, with deviations of less than 15% ($0.71 \leq R^2 \leq 0.98$ for n = 6 in each season; $7.60 \leq$ RRMSE $\leq 12.20\%$; $0.66 \leq d \leq 0.94$). The other statistics obtained for evapotranspiration, biomass and yield are shown in Table 11.5. Araya et al. (2016) concluded that the goodness-of-fit values for both calibration and evaluation datasets indicated that AquaCrop can be used for simulating grain sorghum evapotranspiration, biomass and yield.

Table 11.5: Statistical goodness-of-fit test between measured and simulated evapotranspiration, biomass and yield for grain sorghum, based on evaluation datasets from two seasons in Kansas (Araya et al., 2016)

Year	Variable	R^2 (n = 6)	RRMSE (percentage)	d
2007	Evapotranspiration	0.91	2.00	0.96
	Biomass	0.44	5.20	0.79
	Yield	0.26	9.80	0.60
2010	Evapotranspiration	0.94	13.30	0.61
	Biomass	0.80	5.10	0.93
	Yield	0.85	10.70	0.77

11.1.2.3 Ukulinga (2013/14)

Hadebe et al. (2017b) performed a partial calibration of AquaCrop for three grain sorghum genotypes using data collected during the 2012/13 season at Ukulinga. They then validated the model with data from the following season. Planting took place on 17 January 2014 at a density of 44,444 plants ha^{-1}. The full list of changed parameters is given in Table 145K.14 (Appendix K).

Hadebe et al. (2017b) validated their calibration of grain sorghum using observations from field experiments conducted in the 2014/15 season at Ukulinga. Once canopy senescence had been triggered, AquaCrop simulated rapid canopy decline for three sorghum genotypes (with three different planting dates), whereas in reality, sorghum's canopy decline was moderate. This resulted in a slight over-estimation (≤ 7.8%) of time to physiological maturity by the model. Hadebe et al. (2017b) reported that AquaCrop significantly over-estimated the crop yield of all three genotypes. For the late planting (26 January 2015), where water stress was observed to be relatively high during field trials, biomass was over-estimated by 209 to 309%, while grain yield was over-estimated by 190 to 288%. Observed yields were low due to high water stress caused by low and erratic rainfall experienced over the late season.

They concluded that, since local sorghum genotypes differ significantly in growth and development characteristics from the default sorghum in AquaCrop, additional crop parameters should be calibrated. Hadebe et al. (2017b) suggested that the water productivity parameter, water stress coefficient, as well as the canopy sensitivity to water stress parameter, should be calibrated, which could potentially improve yield simulations.

11.1.2.4 Parameter evaluation

Araya et al. (2016) adjusted 11 crop parameters as shown in Table 11.6, which are compared to those used by Hadebe et al. (2017b). Similarly, Mhizha et al. (2014) calibrated AquaCrop for maize in Zimbabwe by adjusting the normalised biomass water productivity, reference HI, canopy growth and canopy decline coefficients. The authors reported satisfactory model performance after calibration.

Table 11.6: Grain sorghum crop parameters used by Araya et al. (2016) and Hadebe et al. (2017b)

Number	Parameter	Araya et al. (2016)	Hadebe et al. (2017b)
	Soil water depletion factors (upper thresholds) for:		
12	Canopy expansion	0.10	0.25
15	Stomatal control	0.45	0.70
17	Canopy senescence	0.45	0.70
	Soil water depletion factors (lower threshold) for:		
13	Canopy expansion	0.45	0.60
36	Crop transpiration coefficient (K_{CB})	1.02	1.07
39	Maximum effective rooting depth (m)	2.00	2.00
47	Canopy growth coefficient (in percentage d^{-1})	11.00	16.11
52	Canopy decline coefficient (in percentage d^{-1})	12.80	7.74
51	Maximum canopy cover (CC_X)	0.83	0.89
62	Normalised biomass water productivity (g m^{-2})	30.0	33.7
65	Reference HI (percentage)	46	45

The normalised biomass water productivity (WP*) is considered a conservative parameter. Raes et al. (2012b; 2017; 2018) used 33.7 g m^{-2} and noted that the parameter can vary between 30 and 35 g m^{-2}. Although Hadebe et al. (2017b) used the default value, Araya et al. (2016) reduced WP* to 30.0 g m^{-2} to improve their predictions for grain sorghum.

Wani et al. (2012) reviewed the HI for sorghum and found that the default value of 45 published by Raes et al. (2012b; 2017; 2018) is in the range of 45 ± 5. However, Araya et al. (2016) used a value of 46. They also adjusted the upper threshold of the water stress parameters, canopy expansion, stomatal closure and early canopy senescence to 0.10, 0.45 and 0.45, respectively, relative to the respective values of 0.25, 0.70 and 0.70 used by Hadebe et al. (2017b).

AquaCrop was run in GDD mode using the parameters listed in Table 11.6 to assess the model's performance in simulating canopy cover, biomass growth, final biomass and yield at Swayimane under rainfed conditions during the 2017/18 season. In addition, parameters 16, 41 and 42 were modified by the model developers in Version 6 (cf. Section 11.1.2.1). The maximum effective rooting depth (Parameter 39) was set to 0.60 m, based on observations from a pit dug in between two rows at the time the trial was harvested. No other crop parameter values were adjusted to represent the Swayimane trial, except for the phenological growth stages as shown in Table 11.7. The trial was planted on 19 January 2018 at a density of 44,444 plants ha^{-1}. Observations of phenological growth stages in days were converted to values in GDD using measurements of daily temperature from an on-site AWS. Soil water retention constants were derived from measured soil particle distributions at four depths using pedo-transfer functions developed by Saxton and Rawls (2006). The final set of parameters used for PAN8816 and PAN8906 are given in Table K.15 and Table K.16 (cf. Appendix K), respectively.

Table 11.7: Time to and duration of each phenological developmental stage in growing degree-days for sorghum grown in the 2017/18 season at Swayimane (Masanganise et al., 2019)

Number	Parameter	Cultivar		
		PAN8816	PAN8906	Macia
70	Time to 90% emergence	129	129	171
71	Time to maximum rooting depth	1,339	1,279	1,387
72	Time to start of senescence	1,544	1,518	1,574
73	Time to maturity	1,634	1,616	1,707
74	Time to flowering	9,93	979	1,133
75	Duration of flowering	149	123	174

Simulations of canopy cover and biomass growth using both crop parameter files for the three sorghum cultivars are shown in Figure 102L.3 (cf. Appendix L). AquaCrop's performance was evaluated using three statistical indicators: the RMSE, NSE and Willmott's index of agreement (d) (Table 11.8). According to De Jager (1994), d (and R^2) values above 0.8 indicate reliable model predictions. For all three cultivars, results showed that canopy cover was better simulated using the parameters derived by Araya et al. (2016) as opposed to those adopted by Hadebe et al. (2017b). The parameters of Araya et al. (2016) resulted in reduced RMSE, as well as increased mean error and d, thus suggesting a better simulation when compared to those obtained using parameter values from Hadebe et al. (2017b).

Table 11.8: Statistical measures used to evaluate the AquaCrop model in simulating canopy cover of sorghum grown at Swayimane in the 2017/18 season (Masanganise et al., 2019)

Canopy cover (percentage)						
Cultivar	Araya et al. (2016)			Hadebe et al. (2017b)		
	RMSE	NSE	d	RMSE	NSE	d
PAN8816	25.31	-3.11	0.55	49.57	-14.79	0.39
PAN8906	23.19	-0.66	0.73	43.06	-4.74	0.57
Macia	27.83	-2.76	0.42	49.01	-10.66	0.32

Across all cultivars, AquaCrop generally simulated biomass growth satisfactorily from planting until about mid-season (Table 11.9). Simulations were closer to observations when using the parameters obtained from Araya et al. (2016). From mid-season to the end of the growing period, simulations were higher than observations. Running the model with the parameters obtained from Hadebe et al. (2017b) resulted in increased RMSE as well as decreased mean error and d.

Table 11.9: Statistical measures used to evaluate AquaCrop's ability to simulate biomass growth of sorghum grown at Swayimane in the 2017/18 season (Masanganise et al., 2019)

Biomass growth (t ha^{-1})						
Cultivar	**Araya et al. (2016)**			**Hadebe et al. (2017b)**		
	RMSE	**NSE**	**d**	RMSE	**NSE**	**d**
PAN8816	2.73	-7.46	0.57	12.09	-165.35	0.18
PAN8906	2.50	-1.59	0.75	11.47	-53.64	0.29
Macia	2.07	-4.32	0.62	10.72	-142.19	0.19

Simulations of final biomass and grain yield using both crop parameters files for the three sorghum cultivars are shown in Figure 11.5. It is clear that the parameters used by Hadebe et al. (2017b) resulted in an over-estimation of both biomass and yield (by 190-288%) for all three cultivars, as was reported by the authors for Ukulinga.

Statistical measures of performance for observed vs simulated biomass and grain yield are listed in Table 11.10. The data indicates that AquaCrop generally over-estimated final biomass and grain yield across all three cultivars. However, the model simulated grain yield more accurately than biomass, in particular when the parameters of Araya et al. (2016) were used. For sorghum, comparisons were made against yield and biomass data from Ukulinga and Swayimane (2017/18 season). For example, the model over-estimated the yield of PAN8906 by 32.2%, as well as final biomass by 36.9%. The yield prediction accuracy shown in Table 11.10 is similar to that reported by Araya et al. (2016).

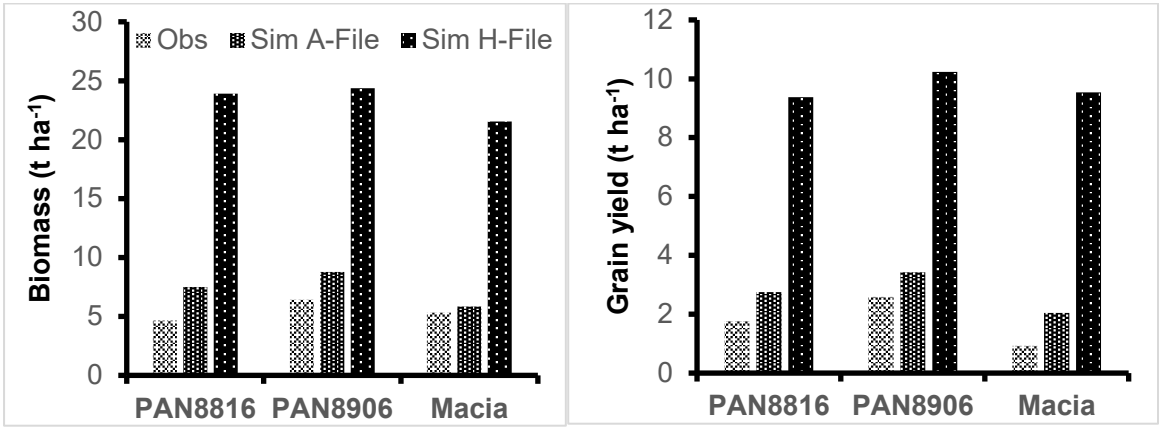

Figure 11.5: Observed and simulated final biomass and grain yield for three grain sorghum cultivars derived using two different crop files (A-file: Hadebe et al., 2017b; H-file: Araya et al., 2016) (Masanganise et al., 2019)

Table 11.10: Statistical measures used to evaluate the AquaCrop model in simulating final biomass and grain yield of sorghum grown at Swayimane in the 2017/18 season (Masanganise et al., 2019)

	Araya et al. (2016)			Hadebe et al. (2017b)		
	RMSE	**NSE**	**d**	**RMSE**	**NSE**	**d**
Final biomass (t ha^{-1})	2.16	-7.79	0.47	17.86	-599.45	0.07
Grain yield (t ha^{-1})	0.99	-1.12	0.65	7.97	-135.77	0.13

11.1.2.5 Discussion and conclusions

The AquaCrop model was used to simulate the canopy cover, final biomass and grain yield of three grain sorghum cultivars grown under rainfed conditions. Two crop files containing adjusted conservative crop parameters were evaluated. Masanganise et al. (2019) reported that, for the three sorghum cultivars, AquaCrop produced improved simulations of canopy cover, biomass growth, final biomass and grain yield using parameters suggested by Araya et al. (2016). Measurement of rainfall from an on-site AWS indicated that sorghum experienced water stress from mid-season to the end of the growing period (Figure 4611.6). This may explain why the water stress parameters used by Araya et al. (2016) produced better results than those adopted by Hadebe et al. (2017b).

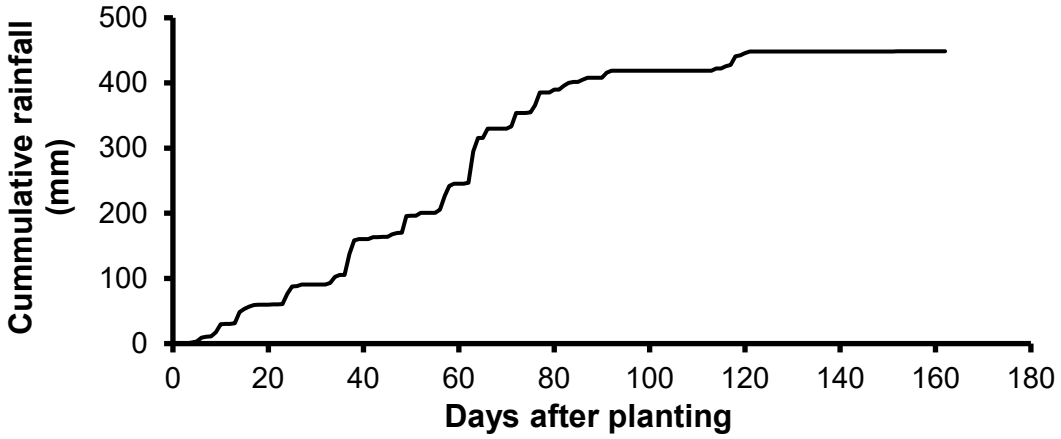

Figure 11.6: Accumulated rainfall from planting to maturity measured at Swayimane during the 2017/18 season (Masanganise et al., 2019)

The above findings highlight the need to adjust certain conservative crop parameters for local cultivars. In conclusion, eight parameters values, derived by Araya et al. (2016), were used in this study to estimate the water use and yield of grain sorghum, together with phenological growth stages in GDD for PAN8906 (cf. Table K.16 in Appendix K).

11.2 SOIL WATER BALANCE

11.2.1 Soybean

11.2.1.1 Model calibration

With assistance from the University of Pretoria, the SWB model was set up for soybean at Swayimane. The climate data for the 2015/16 season was converted into the format required by the model. The soil water retention parameters were estimated using the SPAW model, as described in Section 5.2.5.3. The SWB model does not account for mulching or soil fertility effects on crops. Hence, the model was then set up for the non-mulched, fully fertilized (i.e. control) treatment plot at Swayimane.

Some crop parameters required by the SWB model are considered to be conservative (i.e. those generally applicable to a wide range of growing conditions), such as the base temperature, optimum temperature, cut-off temperature, maximum rooting depth, stem to grain translocation, canopy storage, minimum leaf water potential, maximum transpiration, total dry matter at emergence and stress index. Hence, values for these parameters can be obtained from the SWB database or the literature. For example, Annandale et al. (1999) noted that the interception loss per rain event (canopy storage) is 1 mm for soybean. This default value was selected for cultivar LS6161R. Conservative parameters for cultivar PAN535R were selected to represent LS6161R. PAN535R is a determinate, early- to late-maturing cultivar, which is similar to LS6161R, i.e. a semi-determinate, medium-growth class cultivar. Determinate cultivars, which cease vegetative growth at flowering, have a fairly short transition period, compared to indeterminate cultivars that produce leaves and flowers during the flowering stage (Dlamini, 2015).

The SWB model requires several crop-specific growth parameters: canopy extinction coefficient for solar radiation, dry matter:water ratio, radiation use efficiency, plant height, and thermal time requirements for the completion of various phenological stages. The latter refers to the thermal time requirement from planting to crop emergence, completion of the vegetative growth stage, as well as the thermal time to leaf senescence, and finally maturity. Ideally, crop-specific parameters should be determined from field-based observations. Other parameters that are relatively simple to measure include the maximum plant height, transition period (period between vegetative and reproductive growth) and time to leaf senescence. Default values were selected for some of these parameters, which were obtained from Dlamini (2015) for soybean cultivar PAN535R. For the SWB model, the crop parameters determined for soybean grown at Swayimane in the 2015/16 season are presented in Table G.1 (cf. Appendix G).

The maximum plant height was changed to 1 m, considering cultivar LS6161R averages 95-105 cm (Link Seed, 2011). The maximum ET_O calculated for the growing season was 7.65 mm (1 December 2015; 5 January 2016). Assuming a basal crop coefficient of 1.10 (AquaCrop's default), maximum transpiration is 8.4 mm. Hence, maximum transpiration was adjusted slightly from 9 to 8 mm d^{-1}. The cut-off temperature was also changed from 32 °C (Dlamini, 2015) to 30 °C to match that used by AquaCrop (Steduto et al., 2012).

Although various sources suggest a base temperature of 10 °C for soybean (e.g. Knott, 1988; Kumar et al., 2008; Jescheke et al., 2017), the value was changed from 12 °C (Dlamini, 2015) to 5 °C. Most of the studies discussed in Section 11.1.1 (and Appendix K) used AquaCrop's default base temperature of 5 °C for soybean, except for Battisti et al. (2017) who used 10 °C. Since thermal time (i.e. GDDs) is sensitive to the base temperature, the difference in time taken to reach each phenological growth stage is different. This is highlighted in Table G.1 (cf. Appendix G) by the higher values in GDDs for each phenological growth stage.

11.2.1.2 Leaf Area Index

The SWB model was used to simulate the LAI of soybean at Swayimane. Although the model over-simulated leaf area index (Figure 11.7), model performance was considered adequate (R^2 = 0.87; d = 0.82; RMSE = 0.9). Dlamini (2015) obtained similar R^2 values for LAI, which ranged from 0.82 to 0.97.

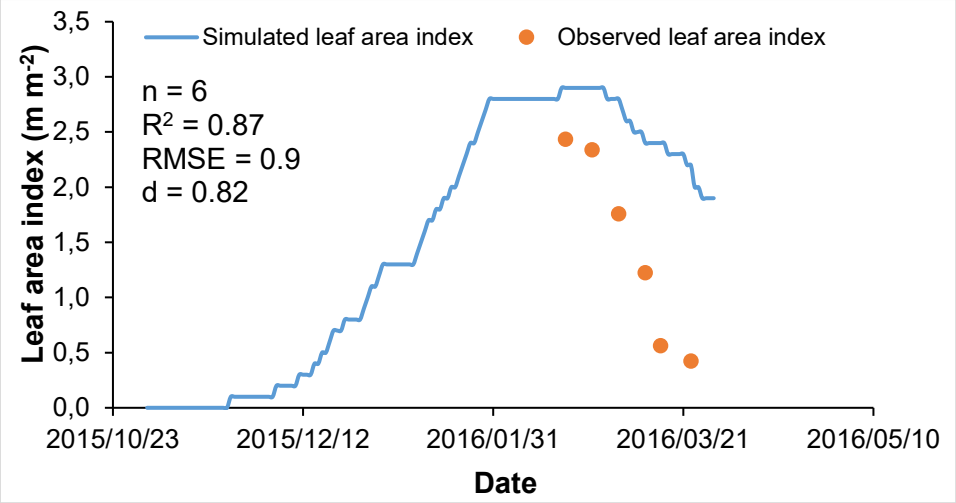

Figure 11.7: Leaf area index of soybean for the fully fertilized, non-mulched treatment as simulated by the SWB model (Lembede, 2017)

11.2.1.3 Accumulated biomass and yield

Although the SWB model over-simulated biomass accumulation (Figure 11.8), model performance was considerate adequate (R^2 = 0.94; RMSE = 1.4 kg m^{-2}; d = 0.56). Dlamini (2015) obtained similar R^2 values for harvestable dry matter yields, which ranged from 0.93 to 0.99. The model estimated a final dry yield of 1.6 t ha^{-1}, which agreed favourably with observations (1.61 t ha^{-1}). Overall, the calibration of the SWB model was deemed successful, as the simulated values generally correlated well with actual measured values. This may indicate that the model can be used to predict yields of soybean in other agro-ecological environments.

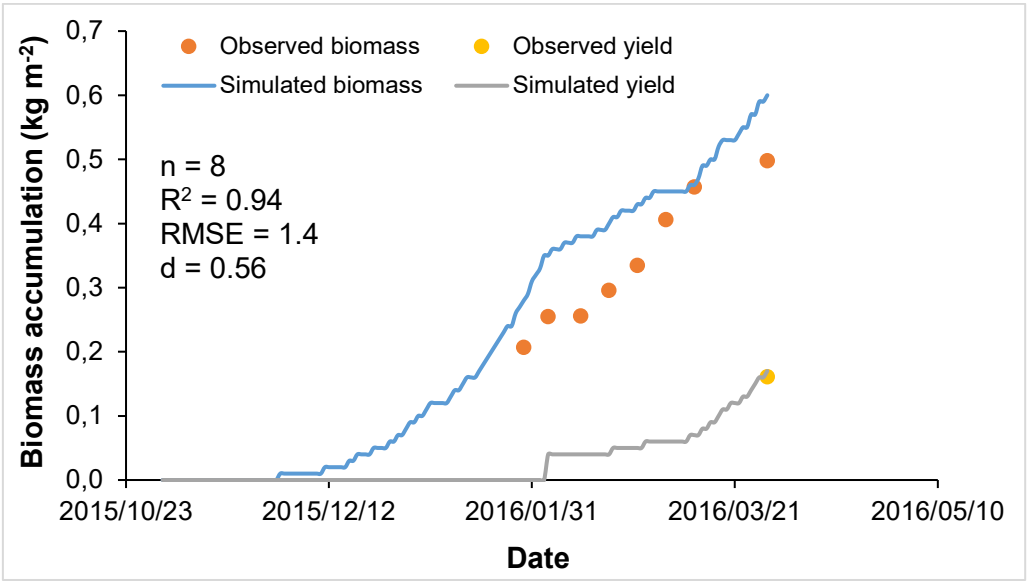

Figure 2.8: Biomass accumulation and final yield for the fully fertilized, non-mulched treatment as simulated by the SWB model (Lembede, 2017)

11.2.1.4 Soil water content

For the fully fertilized, non-mulched treatment, SWB did not adequately simulate the profile water content as shown in Figure 11.9. The SWB simulated a much drier soil profile, especially at mid-season and at harvest (29 March 2016).

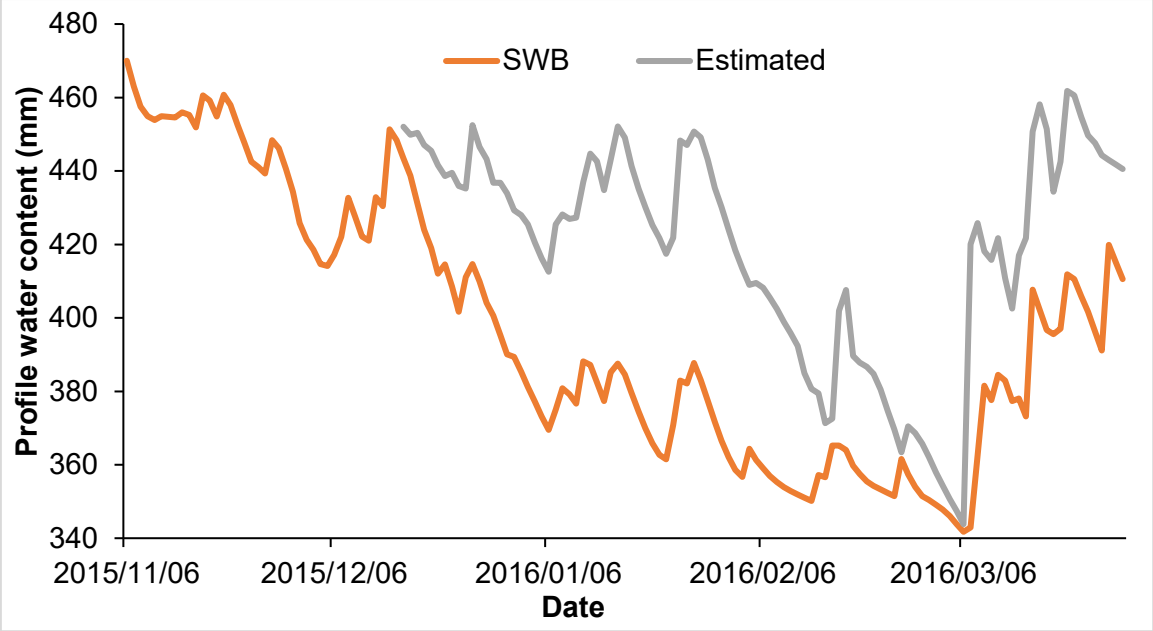

Figure 11.9: Comparison of profile water content between estimated (Watermark) and simulated (SWB) values for the non-mulched, fully fertilized treatment at Swayimane (Lembede, 2017)

11.2.1.5 Crop water use

The soil water balance simulated by the SWB model is given in Table 11.11, where the soil water evaporation (E) was much higher than crop transpiration (T). In the SWB model, the partitioning between transpiration and evaporation is mainly affected by the amount of energy reaching the crop canopy and the soil surface (Annandale et al., 1999). Therefore, the higher rate of soil water evaporation compared to transpiration may be attributed to higher radiation energy reaching the soil surface, due to the observed sparse canopy cover where a large portion of the soil surface was not shaded (Figure 11.10).

Table 11.11: Soil water balance simulated by SWB for soybean grown during the 2015/16 season at Swayimane (Lembede, 2017)

Soil water balance (mm)	*SWB*
Evaporation	321.1
Transpiration	200.4
Evapotranspiration	521.5
Drainage	16.0
Runoff	23.6
Interception	29.5
ΔS	-57.6

Note: ΔS is change in soil water content

Figure 11.10: Crop development in the hay-mulch (foreground) and no mulch (background) plots at Swayimane on 19 February 2016

11.2.1.6 Summary and conclusions

The LAI measurements were not undertaken throughout the growing season, and were thus simulated using the SWB model for the control (non-mulched, fully fertilized) treatment. Although the model over-simulated LAI, model performance was considered adequate. The SWB was also used to simulate biomass production, with a tendency to over-estimate observations. The SWB did not adequately simulate the profile water content and simulated a much drier soil profile, especially at mid-season and at harvest.

11.2.2 Grain sorghum

No modelling of grain sorghum, using the SWB model, was undertaken in this study. This was due to the fact that the grain sorghum trial conducted in 2017/18 was rainfed and not irrigated, and was thus water stressed. In addition, the measured LAI values were measured with a faulty LI-COR meter (cf. Section 7.3.1.3).

CHAPTER 12: PARAMETERS USED FOR BIOFUEL MODELLING

This chapter provides two equations to estimate the theoretical biodiesel and bioethanol yields that could be obtained from soybean and sorghum, respectively. The equations require dry crop yield, as well as the oil content of soybean seed or the extractable starch content of sorghum grain.

12.1 BIODIESEL YIELD

Theoretical biodiesel yield was estimated using the following equation:

$$biodiesel\ yield\ (L\ ha^{-1}) = OC * DY * 10 * 0.95 / 0.92 \quad \text{Equation 16}$$

where *OC* is the seed oil content (percentage) and *DY* is the dry yield (t ha^{-1}). The equation assumes that all bio-oil can be extracted from the seed; the conversion efficiency is 95% (Nolte, 2007); and soybean's oil density is 0.92 kg ℓ^{-1} (Atabani et al., 2013). Instead of using the average oil content from the available literature, actual values were determined in the laboratory by extracting it from seed using a technique described by Meyer and Terry (2008). Briefly, 1 g of ground lyophilised seed tissue was homogenised with hexane solvent and filtered under vacuum using Fisherbrand filter paper. The solvent was evaporated from the oil-containing filtrate under vacuum. The recovered oil was weighed using a scintillation vial and the seed oil content was calculated as a percentage (w/w).

The seed oil contents shown in Table 12.1 were measured for a soybean (cultivar LS6161R) grown at Swayimane in the 2015/16 season. De Beer and De Klerk (2014; 2015) reported an average oil content of 19.2% for a soybean cultivar (LS6161R) produced in warm environments (such as Swayimane). All these values are within the range of 15 to 22% given by Issariyakul and Dalai (2014).

Table 12.1: Seed oil content of soybean cultivar LS6161R obtained at Swayimane in the 2015/16 season (Lembede, 2017)

Main treatment	Fertilizer level (percentage)	Seed oil content (percentage)
Non-mulched	100	17.4
	50	17.4
	0	16.7
Mulched	100	20.5
	50	21.0
	0	21.8

The seed oil content was also determined for cultivar LS6161R for the 2016/17 season at Baynesfield. Oil content ranged from 17.2 to 19.8% (average 17.8%), with the default value of 18% used to derive a biodiesel yield. The seed oil content was also determined in the 2018/19 season at Swayimane for two soybean cultivars and two inoculation treatments as shown in Table 12.2. The inoculated treatment produced higher oil contents, especially for the CAPG3 cultivar.

Table 12.2: Seed oil content of soybean cultivar LS6161R and CAPG3 obtained at Swayimane in the 2018/19 season (Reddy, 2019)

Main treatment	Cultivar	Seed oil content (percentage)
Non-inoculated	LS6161R	17.1
	CAPG3	17.5
Inoculated	LS6161R	17.9
	CAPG3	18.8

The seed oil content presented in Table 12.1 and Table 12.2 for LS6161R and CAPG3 were averaged (18.6%) and used to estimate biodiesel production at the national scale. The previous biofuel project used a default value of 18% (Kunz et al., 2015b).

12.2 BIOETHANOL YIELD

Theoretical bioethanol yield was estimated using the following equation:

$$bioethanol\ yield\ (L\ ha^{-1}) = SC * AY * 10 * 1.11 * 0.511 * FE/0.79 \quad \text{Equation 17}$$

where *SC* is the extractable starch content (percentage), *AY* is the adjusted yield (t ha^{-1}), *FE* is the bioethanol fermentation efficiency and 0.79 is the density of bioethanol (kg ℓ$^{-1}$). The factor of 10 accounts for units. According to Kunz et al. (2015b), the equation is based on the hydrolysis of 1 g of starch into 1.11 g of glucose in which each gram of glucose yields 0.511 g of bioethanol. The equation requires the adjusted yield (*AY*), which is the dry grain yield (*DY*), excluding the moisture content (θ_g in percentage) as follows:

$$AY = DY(1 - \theta_g/100) \quad \text{Equation 18}$$

Sorghum grain is similar to maize grain and is usually dried to a moisture content of 10 to 12% (bulk density of 520 to 720 kg m^{-3}), which allows for efficient storage and transport (Turhollow et al., 2010). Based on this, a moisture content of 11% was used in this study.

Extractable starch content and fermentation efficiency were measured post-harvest at Stellenbosch University for three sorghum cultivars and two fertilization levels (Table 12.3). The table indicates the suitability of PAN8816 for bioethanol production, due to its high extractable starch content and fermentation efficiency when compared to other cultivars. The low values for Macia suggest that the crop is not well suited for biofuel production. For mapping purposes, the values shown in Table 12.3 were averaged.

Table 12.3: Extractable starch content and fermentation efficiency for three grain sorghum cultivars (PAN8816, PAN8906 and Macia) grown under 0 and 100% fertilizer treatments (Masanganise, 2019)

Fertility	Cultivar	Extractable starch (g/100g)	Fermentation efficiency
Fertilized	PAN8816	70.2	0.903
	PAN8906	62.6	0.883
	Macia	55.3	0.838
Unfertilized	PAN8816	68.1	0.935
	PAN8906	64.7	0.818
	Macia	52.6	0.875

Kunz et al. (2015b) reported similar values of extractable starch and fermentation efficiency for PAN8816, that were derived from grain samples taken at Ukulinga and Hatfield in 2012/13 and 2013/14, respectively (Table 12.4). The moisture content of the Ukulinga samples was 11.2% and 11.5% in 2012/13 and 2013/14, respectively, compared to 9.0% for Hatfield.

Table 12.4: Extractable starch content and fermentation efficiency for grain sorghum (PAN8816) grown at Ukulinga and Hatfield over two seasons (Kunz et al., 2015b)

Location	Season	Extractable starch (g/100g)	Fermentation efficiency (percentage)
Hatfield	2012/13	69.4	0.915
Ukulinga	2012/13	65.2	0.907
	2013/14	62.5	0.904

The extractable starch content and fermentation efficiencies presented in the above tables were averaged (i.e. 63.4% and 0.89) and used to estimate bioethanol production at the national scale.

CHAPTER 13: PARAMETERS FOR HYDROLOGICAL MODELLING

This section lists the parameters and variables used to model the water use of the two strategic feedstocks using the ACRU hydrological model. Since ACRU is a deterministic hydrological model, most of the input parameters have a physical meaning, and are thus measurable. These input parameters therefore represent the physical characteristics of the catchment (Smithers and Schulze, 1995), which implies that the model requires little calibration (Bergström, 1991). Thus, the ACRU hydrological model is not a model in which parameters are calibrated to produce a good fit between observed and simulated stream flow. However, the exception is a few critical parameters that are difficult to measure. Representative values for these parameters were obtained from the literature or derived from field-based evidence.

13.1 RAINFALL:RUNOFF PARAMETERS

Key parameters and variables that influence runoff generation in ACRU are shown in Table 13.1. The last five parameters are difficult to measure, and thus values that best represent the scale of the quinary subcatchments were obtained from the available literature.

Table 13.1: Key parameters and variables in ACRU that influence rainfall/runoff response

Variable	Definition
CORPPT	Monthly precipitation adjustment factors (e.g. to account for differences in monthly rainfall between the selected driver station and spatially averaged estimates for the subcatchment)
CORPAN	Monthly A-pan adjustment factors (e.g. to adjust Penman-Monteith evaporation estimates to A-pan equivalent evaporation)
EFRDEP	Effective soil depth for colonisation by plant roots
SMDDEP	Effective soil depth from which storm flow generation takes place (set to topsoil depth)
QFRESP	Storm flow response fraction for the catchment
COFRU	Base flow recession constant
COIAM	Coefficient of initial abstraction that accounts for vegetation, soil surface and climate influences on storm flow generation

13.1.1 Sensitivity analysis

A sensitivity analysis undertaken by Angus (1989), using the Cedara catchment (KwaZulu-Natal Midlands; altitude 1,067 m above sea level) revealed that stream flow output from ACRU is most sensitive to changes in rainfall input and highly sensitive to changes in certain soil-related parameters (e.g. *SMDDEP*). Schulze and Horan (2011) also noted that runoff response is most sensitive to rainfall, reference evaporation and certain soil characteristics. Since rainfall is the main driving factor in most hydrological models, most attention should be given to this input variable, especially in high intensity rainfall areas (Schulze, 1995). In other words, rainfall runoff models are particularly sensitive to rainfall input and any errors in rainfall are amplified in stream flow simulations (Schulze, 1995). This explains why effort was spent on correcting anomalies in the quinary subcatchment rainfall database as described in Section 10.1.1 and why error checking should continue in the future (cf. Section 17.3.4.1).

More recently, Warburton Toucher et al. (2019) conducted a similar sensitivity analysis using a small (14 km^2) grassland catchment situated in the Karkloof area (KwaZulu-Natal Midlands; altitude range 800-1,200 m above sea level). They concluded that stream flow generation in ACRU is insensitive to changes in *COIAM*. However, base flow simulated by the model is moderately sensitive to both increases and decreases in *COIAM*.

13.1.2 Rainfall adjustment

The *CORPPT* factors are applied to point rainfall data (observed at a rainfall recording station) to improve its representativeness of "average" catchment conditions (Schulze, 1995). The monthly rainfall adjustment factors used in this study were derived from the revised quinary subcatchment database and range from 0.50 to 2.00. The values were identical to those developed by Schulze et al. (2011), except for quinay subcatchments 4175-4177, where slight changes occurred due to the corrections made to extreme rainfall events (cf. Section 10.1.1.3).

13.1.3 Evaporation adjustment

Since ACRU uses the A-pan as its reference evaporation standard (cf. Section 10.1.2.7), monthly *CORPAN* factors are used to adjust reference crop evaporation to A-pan equivalent evaporation. In essence, *CORPAN* is the reciprocal of the pan factor (K_p) and represents the ratio of A-pan evaporation (E_p) to reference crop evaporation (ET_O). The adjustment factors were revised in this study, due to the new temperature dataset (cf. Section 10.1.3).

13.1.4 Effective rooting depth

The effective rooting depth (*EFRDEP*) is assumed to be the total soil depth (i.e. the sum of the A- and the B-horizon depths obtained from the quinary subcatchment soils database; cf. Section 10.2), with no impeding layer that restricts root growth (e.g. stone lines, plough or hard pans).

13.1.5 Soil moisture deficit depth

The soil moisture deficit depth (*SMDDEP*), also known as the critical storm flow generation depth, represents the soil depth that must be wetted before runoff can occur. This parameter accounts for the dominant runoff that produces mechanisms that may vary in different climates, as well as with land use, tillage practice, litter or mulch cover and soil conditions. Hence, stream flow generation is extremely sensitive to *SMDDEP*, particularly for sites with shallow soils and high rainfall intensities. If the parameter is under-estimated for drier sites, it results in over-estimated stream flow (Schulze, 1995).

For all hydrological simulations in this project, *SMDDEP* was set to the thickness of the topsoil, which is the suggested default value (Smithers and Schulze, 1995). Hence, the effective soil depth from which storm flow is generated is the topsoil depth. Schulze (2011) also set *SMDDEP* to the thickness of the topsoil, as did Kunz et al. (2015a) in the previous biofuel project.

13.1.6 Storm flow response fraction

The catchment's storm flow response fraction *(QFRESP)* influences the timing of stream flow leaving the catchment, but not the magnitude (or volume) of generated runoff. The value is dependent, inter alia, on topography in that catchments with steep slopes exhibit higher *QFRESP* values.

The *QFRESP* was increased from 0.21 (used in previous studies) to 0.30. Schulze (2011) recommended the latter value as being typical at the spatial scale of quinary subcatchments and is based on experimental evidence. For the uMngeni and Luvuvhu catchments, Warburton Toucher et al. (2010) also assumed that 30% of the storm flow generated from a rainfall event would exit the subcatchments on the same day.

13.1.7 Base flow recession constant

The base flow recession constant *(COFRU)* determines the fraction of daily groundwater store that is released as base flow, which then contributes to stream flow. Hence, this parameter controls the rate of base flow release from the groundwater store. A typical value is 0.009 (or 0.9%) for the quinary subcatchments (Schulze, 2011), compared to 0.010 used in previous studies. For example, Warburton Toucher et al. (2010) also assumed a value of 0.9% for *COFRU*, which has been found to be representative of large parts of southern Africa.

13.1.8 Coefficient of initial abstraction

The coefficient of initial abstraction *(COIAM)* takes cognisance of surface roughness (e.g. after ploughing) and initial infiltration before storm flow commences. It is affected by soil surface infiltrability, soil type and antecedent moisture conditions, as well as rainfall amount and intensity. This parameter is used to estimate the rainfall abstracted by interception, surface storage and infiltration before storm flow commences.

Warburton Toucher et al. (2019) noted that *COIAM* typically varies from 0 to 0.35, with the internationally used default value of 0.20. For dense natural forests and mulched crops, *COIAM* is normally set to 0.35. Schulze (2004) suggested various rules to determine *COIAM* from rainfall seasonality and distance from the sea as shown in Table 13.2.

Table 13.2: Suggested values for the coefficient of initial abstraction based on rainfall seasonality (after Schulze, 2004)

Rainfall seasonality	*COIAM*	
	Summer	Winter
All year; winter; very late summer	0.30	0.30
Early, mid- and late summer		
Coastal (< 100 km of the coastline)	0.25	0.30
Inland (> 100 km of the coastline)	0.15	0.30

This approach was used to obtain unique values of *COIAM* for each quinary subcatchment. Rainfall seasonality per quinary subcatchment was obtained from Schulze and Kunz (2010a), as shown in Figure 13.1. A GIS was used to determine if the entire quinary subcatchment is within 100 km of the coastline, and if so, it is considered to be a coastal subcatchment. For the fallow period, *COIAM* was set to 0.10.

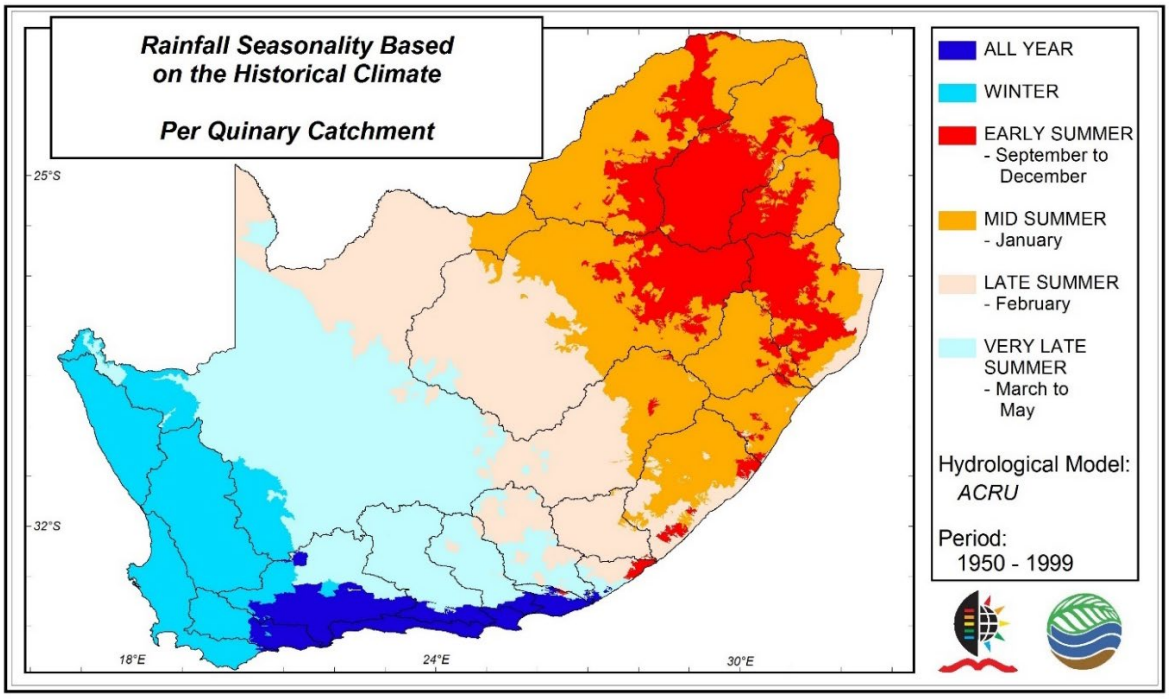

Figure 13.1: Rainfall seasonality classes over southern Africa obtained using historical climate data from 1950 to 1999 (Schulze and Kunz, 2010a)

In the two sub-sections that follow, a distinction is made between parameters and variables. A parameter is defined as a single value that remains constant during a simulation and is usually changed before the simulation to adjust model behaviour. A variable represents monthly values that can change during the simulation. In ACRU, variables can be changed during the model run via the dynamic input file.

During a simulation, changes in land cover or other agrohydrological responses can occur in a catchment, either gradually (e.g. afforestation) or more abruptly (e.g. deforestation). If such a "dynamic" change takes place in a subcatchment, ACRU has the option to change model variables during the simulation period. To invoke this option, the user sets the *DNAMIC* parameter to 1 (i.e. yes) and indicates the year a particular variable must change and its new monthly values via the dynamic input (.DYN) file.

13.2 LAND COVER PARAMETERS

Land cover and land use affect hydrological responses through canopy and litter interception, infiltration of rainfall into the soil and the rates of soil water evaporation and transpiration from the vegetation layer. The key parameters that account for land cover/use are shown in Table 13.3.

Table 13.3: Key parameters (single value) in ACRU that account for land cover/use (Smithers and Schulze, 1995)

Parameter	Definition
EVTR	Option for the estimation of total evaporation as an entity or by soil water evaporation and plant transpiration computed separately.
CONST	Fraction of plant available water at which plant stress sets in. The plant's physiological characteristics determine the onset of wilting in response to drier soil conditions.

13.2.1 Partitioning of evapotranspiration

For most situations, Schulze (1995) recommended that transpiration and soil water evaporation are calculated as separate components (i.e. *EVTR* = 2). Variables such as *PCSUCO* and *COLON* are only valid when *EVTR* = 2. This means that soil water evaporation is higher for *EVTR = 1* as there is no suppression due to the presence of soil cover (i.e. crop residue).

13.2.2 Onset of water stress

The *CONST* represents the onset of plant water stress and indicates the plant's susceptibly to water or drought stress. Schulze (2011) noted that *CONST* is typically set to 0.50 for most vegetation types. Similarly, Allen et al. (1998: 163-164) provided values for the depletion fraction (*p*) for a range of crops, which represents the fraction of plant available water that can be depleted before moisture stress occurs. A value of 0.50 for *p* is commonly used for many crops. Hence, *p* is equivalent to 1 – *CONST*. The values for *CONST* used in this study are shown in Table 13.4.

Table 13.4: Values of CONST used in ACRU to model feedstock water use, together with suggested values for the depletion fraction (p) from the literature

Feedstock	*CONST*	*p* (Allen et al., 1998)
Soybean	0.50	0.50
Grain sorghum	0.45	0.55

According to DAFF (2010a), soybean seed yield is maximised when water in the root zone is kept above 50% of plant available water. Hence, *CONST* was set to 0.50 for soybean, which corresponds to the value suggested by Allen et al. (1998). However, grain sorghum is able to withstand water deficit better than most other grain crops. This can be attributed to its relatively small leaf area, which limits transpiration, the waxy leaf coating that suppresses transpiration and improves desiccation, and the ability of the stomata to close rapidly, which limits water loss (ARC, 1999). Hence, *CONST* was set to 0.45 to account for its drought tolerance.

Although *CONST* is a single parameter in ACRU, Allen et al. (1998) noted that the fraction is a function of the evaporation demand of the atmosphere and also varies with soil type. The authors provided an equation for adjusting *p* based on the crop's evapotranspiration rate (ET_c) as follows:

$$p = p + 0.04(5.0 - ET_C) \quad \text{Equation 19}$$

The values of *p* given in Table 13.4 apply to an ET_C of 5 mm d^{-1} and can be adjusted using the above equation, but with *p* limited to the range of 0.1 to 0.8. Hence, *p* is up to 20% higher than the values listed in Table 13.4 when ET_C is low (i.e. < 3 mm d^{-1}) and 10-20% lower when ET_c is high (i.e. < 8 mm d^{-1}). The above approach could be used to determine unique values of *CONST* for each quinary subcatchment.

13.3 LAND COVER VARIABLES

The key variables that account for land cover/use are shown in Table 13.5. *ROOTA*, *CAY (or ELAIM)* and *VEGINT* represent the minimum set of parameters specified for each land use type. Values for these variables were derived from field-based observations or from the available literature. In addition, some parameters were obtained via modelling as explained in the subsections that follow.

Table 13.5: Key variables (monthly values) in ACRU that account for land cover/use (Smithers and Schulze, 1995)

Variable	Definition
PCSUCO	The fraction (expressed as a percentage) of the soil surface covered by a mulch or litter layer. This layer suppresses soil water evaporation. However, 20% of the soil water evaporation still takes place with 100% cover. Default in ACRU: 0%.
COLON	Extent of colonisation of plant roots in the B-horizon. Determines the amount of water that may be extracted by the plant from the B-horizon. Hence, this variable reflects the extent to which the subsoil is "colonised" by roots. Total evaporation from the B-horizon is suppressed by the fraction *COLON*/100. Default in ACRU: 100%.
ROOTA	The fraction of plant roots that are active in extracting soil moisture from the A-horizon in a given month. This fraction is linked to root growth patterns during a year and periods of senescence brought on, for example, by a lack of soil moisture or by frost.
ELAIM	Monthly LAI values. Can be used to calculate monthly interception losses and/or to determine the crop's consumptive water use.
VEGINT	Monthly interception loss values, which can change during a plant's annual growth cycle. They estimate the magnitude of rainfall that is intercepted by the plant's canopy on a rainy day.
CAY	A monthly consumptive water use (or "crop") coefficient, which reflects the ratio of water use by vegetation under conditions of freely available soil water to the evaporation from a reference surface (e.g. A-pan equivalent).

13.3.1 Sensitivity analysis

As mentioned in Section 13.1.1, a sensitivity analysis undertaken by Angus (1989) revealed that stream flow output from ACRU is highly sensitive to changes in *CAY* and slightly sensitive to changes in both *ROOTA* and *VEGINT*. Similar results were obtained by Warburton Toucher et al. (2019), where initial values for each input variable shown in Table 13.5 were changed by ±50% to better understand the impact on stream flow and base flow generation.

The results shown in Table 13.6 again highlight the importance of inputting accurate crop coefficients in ACRU. Based on this evidence, considerable effort was spent on deriving suitable crop coefficients for the two selected feedstocks (cf. Section 13.4).

Table 13.6: Sensitivity of stream flow and base flow output in ACRU to increases (↑) and decreases (↓) in land cover input variables (after Warburton Toucher et al., 2019)

ACRU output	Sensitivity to change in land cover variable									
	CAY		*VEGINT*		*ROOTA*		*COLON*		*PCSUCO*	
	↑	↓	↑	↓	↑	↓	↑	↓	↑	↓
Stream flow	H	H	S	S		S	I	I	M	S
Base flow	H	E	S	S		S	S	S	M	M

Extremely (output change > 20%) Due to a 10% change in input
Highly (10% < output change ≤ 20%) **M**oderately (5% < output change ≤ 10%)
Slightly (1% < output change ≤ 5%) **I**nsensitive (output change ≤ 1%)

13.3.2 Surface cover fraction

The percentage surface cover (*PCSUCO*) variable in ACRU is used to suppress soil water evaporation losses using a linear relationship such that complete cover (*PCSUCO* = 100%) allows for 20% soil water evaporation. The variable accounts for the surface cover, which includes mulch, plant litter and stone/rock. Warburton Toucher et al. (2019) suggested the following relatively linear relationship (Figure 13.2) between the crop coefficient (*CAY;* cf. Section 13.3.7) and percentage surface cover (*PCSUCO*) that was adopted in this study:

- $0.20 < CAY \leq 0.28$: $PCSUCO = 10\%$
- $0.28 < CAY \leq 0.90$: $PCSUCO = 140 \cdot CAY - 28$
- $0.90 < CAY < 1.40$: $PCSUCO = 100\%$

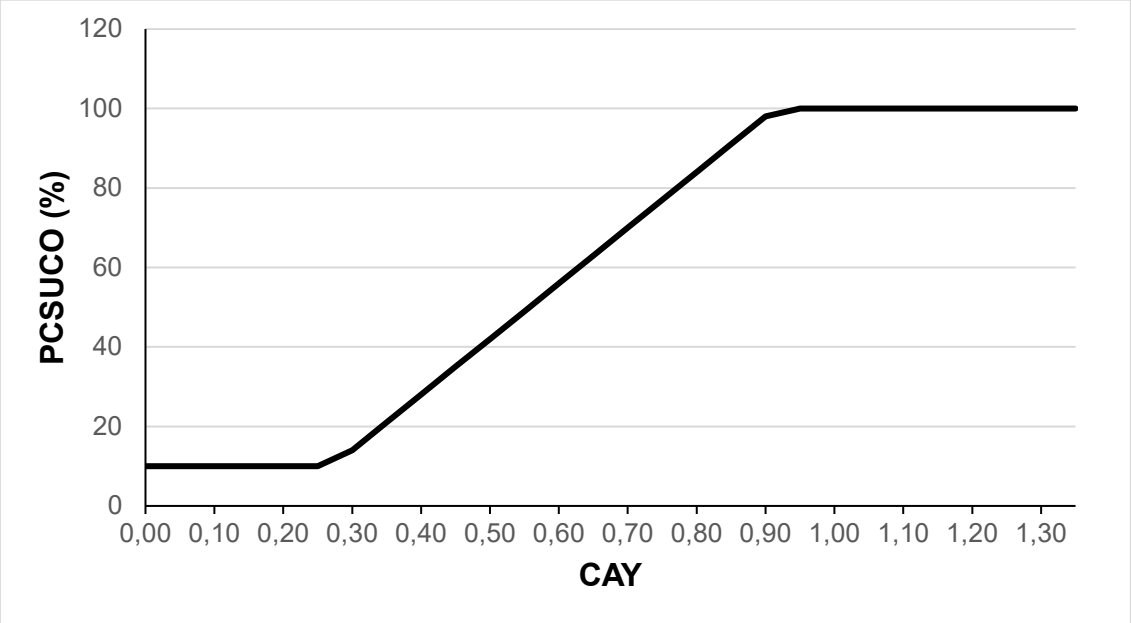

Figure 13.2: Relationship between surface cover (*PCSUCO* in percentage) and crop coefficient values, CAY (Warburton Toucher et al., 2019)

13.3.3 Root colonisation

In ACRU, it is assumed that the topsoil is 100% colonised by roots, i.e. roots can extract all available soil water in the A-horizon. Therefore, *COLON* reflects the extent to which the subsoil is colonised by roots. In ACRU, total evaporation from the B-horizon is suppressed by the fraction *COLON*/100. When *ROOTA* is set to 1 (e.g. during the fallow period), *COLON* is ignored as total evaporation occurs from the topsoil only. As a general rule, *COLON* increases as *ROOTA* decreases.

Colonisation of the subsoil is difficult to characterise given the paucity of root data under farming conditions in South Africa. Based on recommendations by Kunz et al. (2015a), *COLON* was set to 25% for soybean in each month. However, the value was increased to 70% to account for grain sorghum's drought tolerance.

13.3.4 Rooting distribution

ACRU requires monthly values of the fraction of active roots in the topsoil horizon (*ROOTA*), from which the fraction in the lower soil horizon is computed internally (i.e. 1 – *ROOTA*). These monthly values account for various genetic and environmental factors that affect transpiration, e.g. planting date, growth rates, senescence, winter dormancy and spring re-growth (Schulze, 1995). However, the fine roots (not the tap roots) are responsible for the uptake of water and nutrients (Ruark et al., 1982; Schulze et al., 1995). Hence, *ROOTA* reflects the distribution of fine roots (≤ 2 mm diameter) in the A-horizon, rather than coarse roots. Since rooting distribution was not observed at the experimental sites, representative values were obtained from the available literature.

In most environments, the majority of crop roots occur within the upper 30 cm of the soil profile, demonstrating a decrease in root density with increasing distance from the plant stem (Jackson et al., 1996; Schenk and Jackson, 2002; Raz-Yaseef et al., 2013). Similarly, Ruark et al. (1982) noted that numerous investigators report that 60-80% of the root volume (in particular fine roots) is found in the top 20 cm of soil. Kunz et al. (2015a) reported that approximately 30, 90 and 98% of sweet sorghum's rooting distribution was found at 0-10, 11-20 and 21-30 cm of the soil profile, respectively. However, this distribution may have been influenced by the drip irrigation system. Soybean plants stop root development at the "green bean" stage, when the first pod containing a single green seed is produced. Although soybean's tap root can extend to 1.5 m, the majority of the plant's extensive lateral root system occurs within 30 cm of the soil surface (DAFF, 2010a).

Based on this evidence, *ROOTA* was therefore set for each month across the growing season to:

- 0.70 if the topsoil depth (*DEPAHO*) is ≤ 20 cm
- 0.90 if the topsoil depth is > 20 cm

For 393 of the 5,838 quinary subcatchments (or 6.73%), the topsoil is 12 to 20 cm deep, and hence *ROOTA* was set to 0.70. For the remaining quinary subcatchments, *ROOTA* was set to 0.90, with the maximum topsoil depth being 31 cm.

During the fallow period (six months prior to planting), *ROOTA* was set to unity, which indicates that soil water evaporation takes place from the topsoil only. However, Warburton Toucher et al. (2019) noted that setting *ROOTA* to 1 resulted in large increases in the simulated stream flow and greater increases in the simulated base flow.

13.3.5 Leaf Area Index

In ACRU, it is optional (although hydrologically desirable) to utilise LAI as a growth/consumptive water use parameter, rather than the crop coefficient. ACRU requires daily LAI values (*ELAID*) via the input composite file or monthly values of LAI (*ELAIM*) via the model's input menu. ACRU then converts monthly values to daily values using Fourier analysis.

In this study, LAI values measured at Swayimane and Baynesfield were used to represent soybean and grain sorghum. In addition, LAI could be modelled using SWB or AquaCrop, and then used as input for ACRU.

13.3.5.1 Soybean

Measurements of LAI for soybean were conducted at the following places:

- Swayimane in the 2015/16 season from 19 February to 23 March 2016 for cultivar LS6161R (Lembede, 2017)
- Baynesfield in the 2016/17 season from 18 January to 10 May 2017 for cultivar LS6161R (Masanganise, 2019)
- Swayimane in the 2018/19 season for cultivars LS6161R and CAPG3

Only six LAI measurements were taken in the 2015/16 season. Thus, these values were not used for modelling. For the 2016/17 season, LAI measurements for three rows were averaged, then extrapolated "backwards" to 21 October 2016 when the crop was planted. This was done using LAI data measured by Mbangiwa et al. (2019) in the 2012/13 season at Baynesfield for cultivar PAN1666R (cf. Figure 4111.1a). These values were then averaged with those obtained by Mbangiwa et al. (2019). However, the most comprehensive set of LAI data was obtained at Swayimane during the 2081/19 season for two cultivars (LS6161R and CAPG3) for both inoculated and non-inoculated treatments (Figure 13.3). The decision was made to use these values for modelling the interception loss of soybean across South Africa.

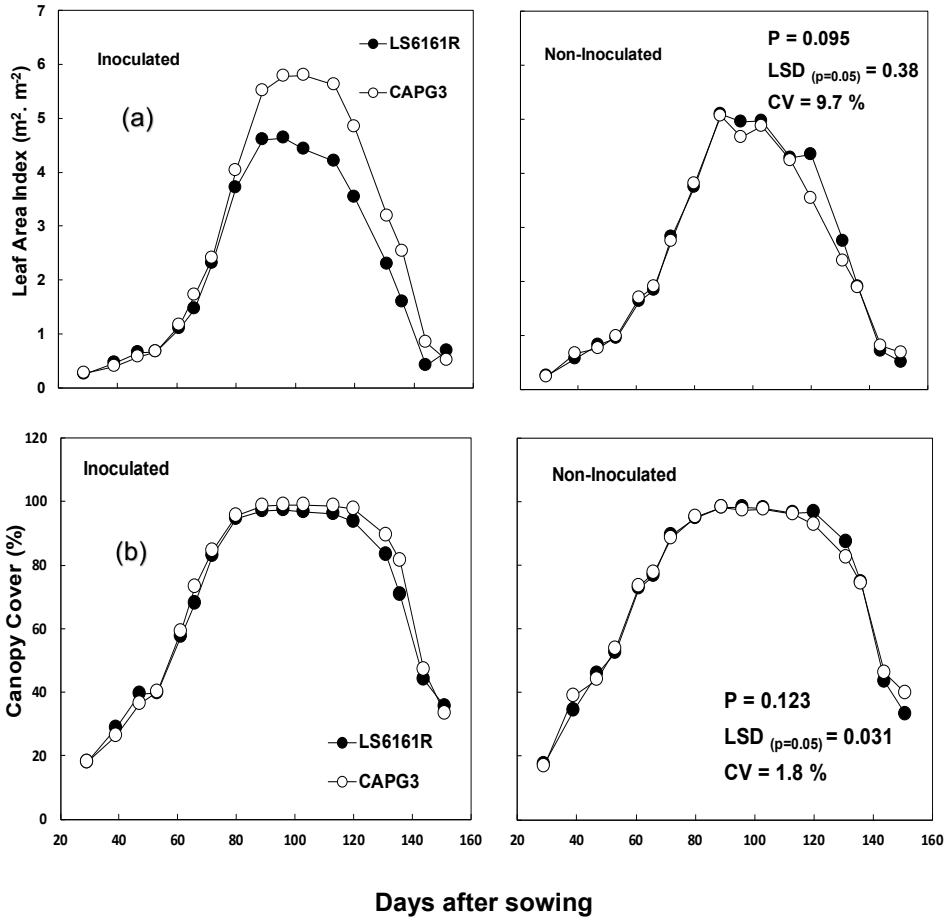

Figure 13.3: Influence of inoculation on (a) leaf area index and (b) canopy cover for two soybean cultivars (LS6161R and CAPG3) grown at Swayimane during the 2018/19 season (Reddy, 2019)

13.3.5.2 Grain sorghum

Weekly measurements of LAI were undertaken using a LI-COR LAI-2200 plant canopy analyser for three sorghum genotypes planted in January 2018 at Swayimane (Figure 13.4). The LAI was statistically similar ($p > 0.05$) across all factors (fertilization vs cultivar). The variation in LAI shown in the figure was not expected. Further investigation revealed that the LAI-2200 device used for measurements was faulty. The device was sent to the manufacturers in the USA (LI-COR, Lincoln, Nebraska, USA), where it was recalibrated and returned. Nevertheless, the decision was made to use these values for modelling the interception loss of grain sorghum across South Africa (Masanganise, 2019). The low values recorded on Day 48 were excluded and the remaining values were used to calculate monthly averaged LAI values.

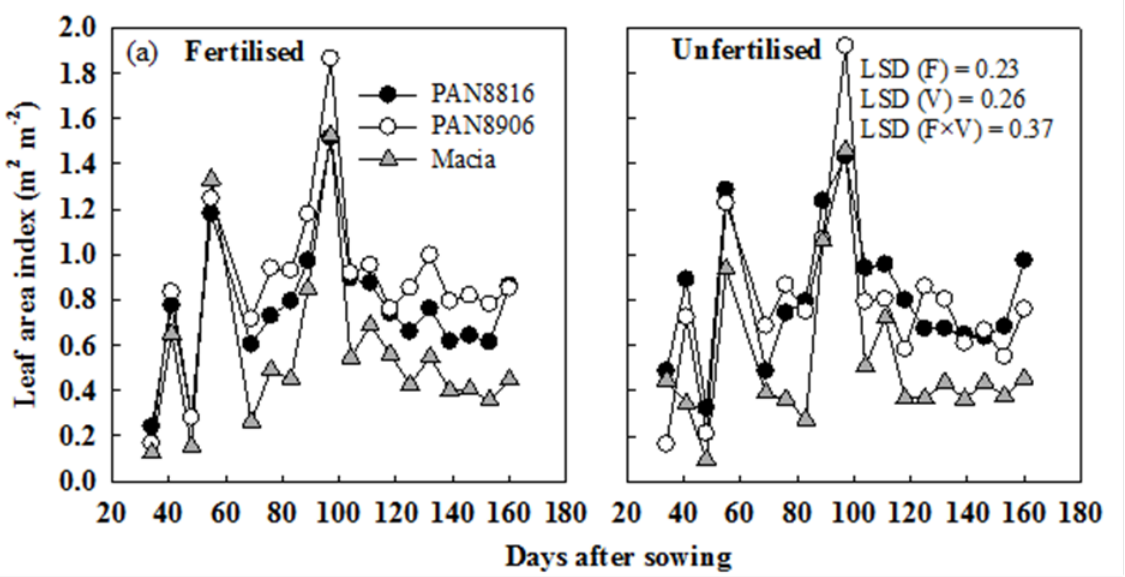

Figure 13.4: Leaf area index and for three grain sorghum genotypes (PAN8816, PAN8906 and Macia) grown under rainfed conditions and two fertility levels at Swayimane in 2018 (Masanganise, 2019)

13.3.6 Canopy interception

13.3.6.1 Background

The ACRU model requires monthly values of interception loss (*VEGINT*) by the vegetation canopy in mm per rain day. On every day on which rainfall occurs, the interception loss is set to *VEGINT* for that month (unless rainfall is less than *VEGINT*). Realistic values of monthly interception loss were estimated using the Von Hoyningen-Huene (1983) equation, as well as the modified Gash equation.

13.3.6.2 Von Hoyningen-Huene method

Monthly canopy interception values required as input by ACRU can also be estimated from LAI using the Von Hoyningen-Huene (1983) equation:

$$I_C = 0.30 + 0.27P_g + 0.13LAI - 0.013P_g^2 + 0.0285P_g \cdot LAI - 0.007LAI^2 \quad \text{Equation 20}$$

However, this method is only "stable" for gross rainfall (P_g) amounts up to 18 mm. Hence, P_g is "capped" at 18 mm, and thus produces lower estimates of I_C during the summer months when compared to the modified Gash model. For example, typical values of interception loss per rain day are shown in Figure 13.5 for events ranging from 0 to 18 mm and LAI from 1 to 8 m m^{-2}.

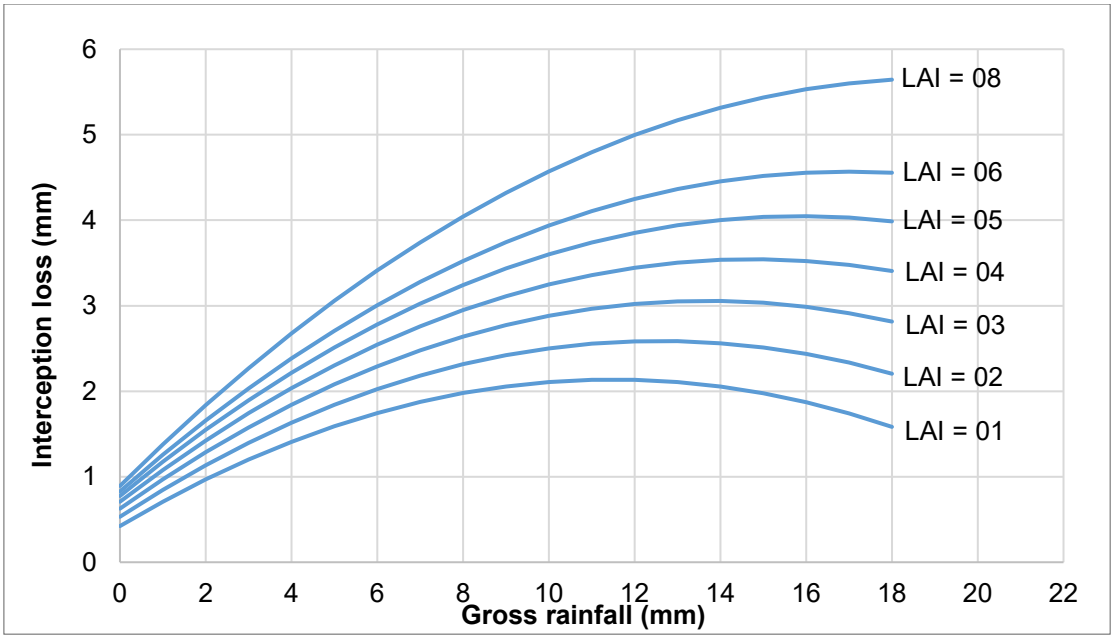

Figure 13.5: Canopy interception loss estimated from gross rainfall and Leaf Area Index using the Von Hoyningen-Huene equation

13.3.6.2 Variable storage Gash model

The Von-Hoyningen-Huene method does not consider rainfall intensity, which has been found to be an important parameter in modelling canopy interception. However, rainfall intensity data is very scarce in South Africa, making it a difficult parameter to derive when required as a model input. In a comprehensive review of 15 rainfall interception models by Muzylo et al. (2009), they showed that the original and revised Gash models were the most extensively applied models, and to a slightly lesser extent, the original and revised Rutter models.

As an alternative to the Gash and Rutter-type models (e.g. Rutter et al., 1975), Calder (1986; 1996) developed a stochastic model that accounted for varying canopy storage capacity with rainfall intensity. This highlighted a controversy over whether the canopy storage capacity should be treated as a variable or a fixed parameter (Roberts et al., 2004), which has not been resolved. However, Bulcock and Jewitt (2012) showed that canopy storage capacity varies with rainfall intensity. Based on these studies, the well-recognised Gash model was adapted to account for a variable storage capacity with a varying rainfall intensity by incorporating the methods developed by Calder (1996). The variable storage Gash model (Bulcock and Jewitt, 2012) was developed and successfully tested in South Africa against observed data. A detailed description of the model is given in Appendix M. The method has also been used to estimate interception losses for natural vegetation as part of WRC Project No. K5/2437, “Resetting the baseline land cover against which stream flow reduction activities and the hydrological impacts of land use change are assessed” (Warburton Toucher et al., 2019).

13.3.6.3 Methodology

The equations representing the Von Hoyningen-Huene (1983) model (cf. Section 13.3.6.2), as well as the variable storage Gash model (cf. Section M2 in Appendix M), were programmed using the Fortran language to develop a computationally efficient software utility. The utility acquires daily rainfall and reference crop evaporation data from the quinary climate database. It then applies a monthly adjustment factor to the rainfall to make it more representative of each quinary subcatchment.

Using monthly averaged LAI values for soybean from the 2018/19 trial at Swayimane (cf. Section 13.3.5.1), daily interception loss values were determined for the inoculated treatment of cultivar LS6161R.

Similarly, daily interception losses were determined for grain sorghum using monthly averaged LAI values from the 2017/18 trial at Swayimane (cf. Section 13.3.5.2) for the fertilized treatment of cultivar PAN8906. The monthly averaged LAI values were then "shifted" to correspond to the planting dates selected in this study (cf. Section 10.3). For the fallow period, the monthly LAI value was set to 0.13 m^2 m^{-2}.

The daily interception loss values were summed to a monthly level, and then divided by the number of rain days in that month to determine the average interception loss per rain day. This was repeated for all rainfall events from 1950 to 1999 (i.e. 50 years of climatic data input). From the annual time series of averaged interception values, all non-zero values were used to generate a range of statistics (e.g. mean, median and coefficient of variation) for each month. Hence, a unique set of monthly averaged interception loss values was derived for each quinary subcatchment for both crops.

13.3.6.4 Results and discussion

Soybean

For illustrative purposes, mean monthly interception losses were generated for soybean from averaged LAI values and 50 years of daily rainfall for quinary subcatchments 4697, 4699 and 4757, which represent Ukulinga, Swayimane and Baynesfield, respectively. Values for the fallow period are highlighted in italics in the tables below.

Table 13.7: Mean monthly interception loss (mm per rain day) calculated using the Von-Hoyningen-Huene method for soybean cultivar LS6161R planted in December

Quinary	Jan	Feb	Mar	Apr	May	Jun	Jul	Aug	Sep	Oct	Nov	Dec
4697	1.30	1.62	2.83	2.49	1.37	*1.14*	*1.10*	*1.02*	*1.13*	*1.20*	*1.23*	1.24
4699	1.12	1.43	2.33	1.96	1.33	*0.93*	*0.93*	*1.00*	*0.98*	*1.05*	*1.10*	1.10
4757	1.09	1.36	2.17	1.91	1.25	*1.01*	*1.01*	*0.92*	*0.99*	*1.05*	*1.07*	1.09

Table 13.8: Mean monthly interception loss (mm per rain day) calculated using the variable storage Gash model for soybean cultivar LS6161R planted in December

Quinary	Jan	Feb	Mar	Apr	May	Jun	Jul	Aug	Sep	Oct	Nov	Dec
4697	0.02	2.29	2.96	1.98	1.54	*0.02*	*0.02*	*0.01*	*0.02*	*0.01*	*0.01*	0.02
4699	0.01	1.48	1.84	1.14	1.04	*0.01*	*0.00*	*0.01*	*0.02*	*0.01*	*0.01*	0.01
4757	0.01	1.24	1.76	1.15	0.99	*0.01*	*0.02*	*0.01*	*0.02*	*0.00*	*0.00*	0.01

Grain sorghum

Using 50 years of daily rainfall for quinary catchments 4697 (Ukulinga), 4699 (Swayimane) and 4757 (Baynesfield), mean monthly interception losses were generated from averaged LAI values for grain sorghum.

Table 13.9: Mean monthly interception loss (mm per rain day) calculated using the von-Hoyningen-Huene method for sorghum cultivar PAN8906 planted in December

Quinary	Jan	Feb	Mar	Apr	May	Jun	Jul	Aug	Sep	Oct	Nov	Dec
4697	1.23	1.44	1.66	1.52	1.34	*1.14*	*1.10*	*1.02*	*1.13*	*1.20*	*1.23*	1.24
4699	1.07	1.28	1.44	1.27	1.30	*0.93*	*0.93*	*1.00*	*0.98*	*1.05*	*1.10*	1.10
4757	1.04	1.23	1.37	1.23	1.23	*1.01*	*1.01*	*0.92*	*0.99*	*1.05*	*1.07*	1.09

Table 13.10: Mean monthly interception loss (mm per rain day) calculated using the variable storage Gash model for sorghum cultivar PAN8906 planted in December

Quinary	Jan	Feb	Mar	Apr	May	Jun	Jul	Aug	Sep	Oct	Nov	Dec
4697	0.02	2.29	2.96	1.98	1.54	*0.02*	*0.02*	*0.01*	*0.02*	*0.01*	*0.01*	0.02
4699	0.01	1.48	1.84	1.14	1.04	*0.01*	*0.00*	*0.01*	*0.02*	*0.01*	*0.01*	0.01
4757	0.01	1.24	1.76	1.15	0.99	*0.01*	*0.02*	*0.01*	*0.02*	*0.00*	*0.00*	0.01

From the results, it is clear that monthly interception losses derived using the modified Gash model are higher in the summer months, but considerably lower in the fallow period (e.g. from 1.2 to 0 mm per rain day). For the Von Hoyningen-Huene method (Equation 2020), daily rainfall (P_g) is "capped" at 18 mm, and thus produces lower estimates of interception loss (I_C) during the summer months when compared to the modified Gash model.

13.3.6.5 Conclusions

In this study, the variable storage Gash model was used to generate mean monthly interception loss values for both biofuel crops across all 5,838 quinary subcatchments. This model is far more complex than the simpler Von-Hoyningen-Huene method described in Section 13.3.6.2. The variable storage Gash model has been developed and applied in South Africa (Warburton Toucher et al., 2019) and the USA (Van Stan et al., 2016). In both instances, the model produced adequate results, and is thus considered to be an improvement on the original Gash model, as well as an improvement on the current canopy interception routine in the ACRU model. The latter uses either the Von Hoyningen-Huene equation or fixed "interception per rain day" values.

13.3.7 Crop coefficient

The crop coefficient (K_C) is expressed as the ratio of maximum evaporation (E_m) from the plant at a given stage of plant growth to reference evaporation, E_r (Schulze, 1995). It accounts for differences in the canopy and aerodynamic resistances of the crop being simulated, relative to the reference surface. In other words, K_C serves as an aggregation of the physical and physiological differences between crops and considers canopy properties, as well as the aerodynamic resistance of the crop (Taylor et al., 2008). ACRU requires average monthly crop coefficients (*CAY*) for the dominant vegetation type in each subcatchment or hydrological response zone or unit. If crop coefficients are estimated using reference crop evaporation (i.e. hypothetical short grass), monthly values must be adjusted to reflect the A-pan as the reference standard.

13.3.7.1 Fallow conditions

Kunz et al. (2015a; cf. Section 8.3.1.3) recommended that the water use of soybean should be measured for a second season at Baynesfield. They also recommended that the evapotranspiration from bare soil be determined, which will help determine K_C values for the fallow period (i.e. non-growing season).

After the soybean crop was mechanically harvested from field NR28 at Baynesfield in May 2017, evapotranspiration measurements were continued to determine crop coefficients for the fallow period. However, the farm manager decided to plant white oats as a fodder crop. Thus, the surface renewal system was moved on 26 June 2017 to a nearby fallow maize field (Figure 13.6). Measurements of evapotranspiration continued throughout the winter months and weed growth became significant at the site, mainly due to the rainfall experienced since August. The field was then replanted to maize in October 2017. The surface renewal system was thus finally removed.

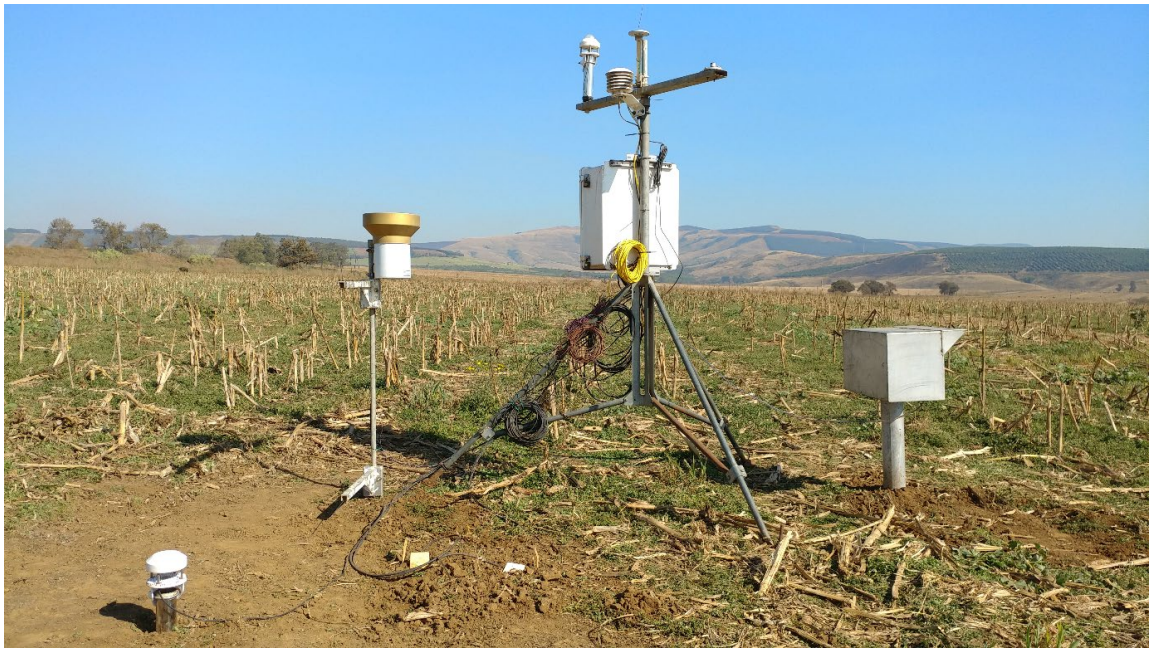

Figure 3.6: Surface renewal system and automatic weather station moved on 26 June 2017 to a fallow maize field at Baynesfield

Sensible heat flux was derived from the surface renewal data. Evapotranspiration was then determined from the shortened energy balance equation, from which daily and monthly crop coefficients representing fallow conditions were calculated (Table 13.11). From June to September, these values are similar to the range (0.10-0.20) suggested by Allen et al. (1998) for bare soil. This is despite the fact that the Baynesfield farm manager did not keep the field weed-free over the winter period. Most smallholder farmers also leave the land fallow after harvesting a summer crop, thus allowing weeds to grow, which shed seeds that increase the seed bank prior to planting.

Table 13.11: Monthly crop coefficients (K_C) estimated for the fallow period from 10 May to 31 October 2017 at Baynesfield Estate, then adjusted (K_{C_ADJ}) for Quinary Subcatchment 4757

Variable	May	Jun	Jul	Aug	Sep	Oct
K_C	0.26	0.15	0.10	0.18	0.22	0.40
CORPAN	1.44	1.46	1.45	1.40	1.36	1.32
K_{C_ADJ}	*0.20*	*0.20*	*0.20*	*0.20*	*0.20*	0.30

The K_C values were divided by monthly *CORPAN* factors for each quinary subcatchment to adjust them from grass to A-pan equivalent values, as required by ACRU. The example shown in Table 13.11 is for Quinary Subcatchment 4757, in which Baynesfield Estate is located. From May to September, adjusted crop coefficients (K_{C_ADJ}) were lower than the minimum value of 0.20, as suggested by Allen et al. (2011), and were thus set to 0.20. The values shown in Table 13.11 are lower than the value of 0.25 used by Kunz et al. (2015a) in the previous biofuel project, and 0.30 as suggested by Schulze (1995). These crop coefficients were used to represent fallow conditions for both soybean and grain sorghum for all quinary subcatchments.

13.3.7.2 Soybean

For Baynesfield, Mbangiwa et al. (2019) and Mengistu et al. (2014) calculated crop coefficients for the 2012/13 season. In addition, K_C values were determined for a second season at Baynesfield in 2016/17 as part of this project, based on the recommendation by Kunz et al. (2015a).

2012/13 season (Baynesfield: Study 1)

The water use of soybean was studied at Baynesfield during the 2012/13 season as part of WRC-funded project K5/2066 (Mengistu et al., 2014). From this research, Mbangiwa et al. (2019) published crop coefficients for soybean as shown in Table 13.12. Average single-crop coefficients were computed by dividing daily totals of residual and modelled evapotranspiration (using AquaCrop) by reference evapotranspiration (ET_O). Residual evapotranspiration was determined from sensible heat flux measurements (06:00 to 18:00) obtained from an eddy co-variance system, assuming closure of the shortened energy balance equation. The number of days per growing stage used for K_C calculations is also shown in Table 13.12. Modelled evapotranspiration was derived from AquaCrop simulations using crop parameters described in Section 11.1.1.7.

Table 13.12: Measured and modelling crop coefficients obtained for soybean during the 2012/13 season at Baynesfield (Mbangiwa et al., 2019)

Variable	Soybean development stages (1-4)			
	Emergence	Vegetative	Flowering	Yield formation
Length (days)	9	62	29	30
K_C (measured)	0.19	0.59	0.73	1.12
K_C (modelled)	0.45	1.03	0.87	1.01

It is important to note that residual evapotranspiration values were under-estimated, mostly due to data exclusion by EddyPro quality assurance processing. Furthermore, occasional system failures and rainfall events reduced evapotranspiration totals. This explains the relatively low evapotranspiration total of only 347.5 mm (over 130 days) and why residual evapotranspiration was consistently lower than modelled evapotranspiration from emergence to flowering (i.e. growth stages 1-3). A large discrepancy in residual evapotranspiration was observed during the transition from vegetative to flowering stage, where simulated evapotranspiration remained consistently higher than residual evapotranspiration, probably due to the high rainfall received. Rainfall events caused signal loss between the sonic anemometer transducers, resulting in no output for the turbulent energy fluxes (H and LE).

The crop was planted to soybean on 15 October 2012, and green canopy cover over the next nine days (Stage 1) was almost 0%, making soil water evaporation the major contributor to evapotranspiration. Hence, K_C for Stage 1 largely represents bare soil conditions, but only for a nine-day period. The value of 0.41 mentioned in the previous section for a 31-day period is more representative of conditions prior to planting.

2012/13 season (Baynesfield: Study 2)

Mengistu et al. (2014) also measured crop evapotranspiration derived using a surface renewal technique that was calibrated by the eddy co-variance system. Measurements were discontinued on 22 April 2013 when most of the seed pods were dry and ready for harvest. The crop was harvested mechanically using a combine harvester in the second week of May. Over the 189-day period, a total of 469 mm of evapotranspiration was accumulated, which is much higher than the 348 mm reported by Mbangiwa et al. (2019) for the 130-day period. Daily crop coefficients were also calculated (Table 13.13), and then averaged to produce monthly values as required by ACRU. These values were used by Kunz et al. (2015c) to quantify the hydrological impact of soybean production on downstream water availability.

Table 13.13: Crop coefficient values for soybean, derived from measured crop evapotranspiration at Baynesfield during the 2012/13 season (Kunz et al., 2015b)

Month	Growth stage	Length (days)	K_C	FAO (2002)
November	Initial	20-25	0.72	0.30-0.40
December	Development	25-35	0.72	0.70-0.80
January/February	Mid-season	45-65	1.00-1.03	1.00-1.20
March/April	Late season	20-30	0.84	0.70-0.80
April/May	Harvest		0.72	0.40-0.50

2016/17 season (Baynesfield)

For this project, half-hourly evapotranspiration measurements for soybean were determined at Baynesfield for the period January to April 2017 using a new surface renewal method. These values were summed during daylight hours (when R_n was positive) to derive daily evapotranspiration estimates. The seasonal water use of the crop was then estimated by summing the daily evapotranspiration values over the growing season. Furthermore, monthly crop coefficients were calculated for the five-month period. AquaCrop was then used to model evapotranspiration with applied irrigation to minimise crop water stress, from which K_C values from October 2016 to April 2017 were derived. From Table 13.14, AquaCrop's ability to adequately simulate crop coefficients is demonstrated.

Table 13.14: Crop coefficients for soybean at Baynesfield in the 2016/17 season, derived from crop evapotranspiration measured by a new surface renewal system and simulated using AquaCrop

Month	Crop coefficient (K_C)	
	Measured	Modelled
October		0.98
November		1.00
December		1.09
January	0.98	0.99
February	0.77	0.73
March	0.76	0.72
April	0.52	0.35
May	0.30	0.30

2015/16 season (Swayimane)

Runoff from the soybean trial was not measured during the 2015/16 season. Due to the slope of the trial site, runoff cannot be assumed to be negligible. Hence, crop water use could not be estimated using the SWB equation, and was thus simulated using AquaCrop and SWB for the control (non-mulched, fully fertilized) treatment. Crop coefficients (K_C) were calculated as the ratio of simulated crop evapotranspiration to FAO56 reference crop evaporation (Table 13.15). AquaCrop simulated higher evapotranspiration at the beginning of the season, whereas SWB simulated higher evapotranspiration at the end of the season. According to Allen et al. (1998), K_{C_INI} is expected to approximate 0.35, which is a typical value for legumes such as soybean.

Table 13.15: Crop coefficients for soybean at Swayimane in the 2015/16 season, derived from crop evapotranspiration simulated by AquaCrop for the control treatment (Lembede, 2017)

Crop coefficient (K_C)	AquaCrop	SWB	FAO (2002)
K_{C_INI}	0.53	0.41	0.30-0.40
K_{C_DEV}	0.80	0.81	0.70-0.80
K_{C_MID}	0.91	0.97	1.00-1.20
K_{C_END}	0.40	0.56	0.40-0.50

2018/19 (Swayimane)

Monthly estimates of crop evapotranspiration for dryland conditions were determined for soybean grown at Swayimane in the 2017/18 season. However, monthly crop coefficients were calculated from modelled evapotranspiration using AquaCrop*,* with applied irrigation to relieve water stress and no fertility stress (Table 13.16). Model simulations were performed from planting (19 November 2018) to harvest (3 April 2019). As shown in Table 13.16, the estimated values are comparable to the range suggested by FAO (2002).

Table 13.16: Crop coefficients for soybean estimated by AquaCrop for the 2018/19 season at Swayimane

Month	Growth stage	Length (days)	K_C (2018/19)
November	Initial	20-25	0.42
December	Development	25-35	0.74
January/February	Mid-season	45-65	1.02-1.11
March/April	Late season	20-30	0.89
April/May	Harvest		

13.3.7.3 Grain sorghum

For Ukulinga, Kunz et al. (2015a) calculated crop coefficients for the 2012/13 and 2013/14 seasons. In addition, K_C values were determined for Swayimane during the 2017/18 season. The abovementioned crop coefficients are given next for comparative purposes.

2012/13 and 2013/14 (Ukulinga)

During the 2012/13 and 2013/14 seasons, the seasonal water use for grain sorghum at Ukulinga was measured at 436 and 461 mm, respectively, using the surface renewal technique (Kunz et al., 2015b). This figure is lower than the range of 481 to 533 mm reported by Piccinni et al. (2009) for irrigated sorghum in Texas, USA. These values were derived from lysimeter measurements from 2006 to 2008. Monthly crop coefficients were also calculated as shown in Table 13.17 and compared to those suggested by FAO (2002).

Table 13.17: Crop coefficients for grain sorghum, derived from measured crop evapotranspiration at Ukulinga during the 2012/13 season (Kunz et al., 2015b)

Month	Growth stage	Length (days)	K_C (2012/13)	K_C (2013/14)	FAO (2002)
November	Initial	20-25	0.52	0.50	0.30-0.40
December	Development	30-40	1.00	0.78	0.70-0.80
January/February	Mid-season	40-45	1.05	0.89	1.00-1.10
March/April	Late season	30	0.90	0.80-0.87	0.70-0.80
April/May	Harvest		0.79	0.58	0.40-0.50

For PAN8816, Hadebe et al. (2017b) noted that the initial, canopy development, mid-season and late-season growth stages were 36, 29, 61 and 14 days in length, respectively. From Piccinni et al. (2009), values of 0.40, 0.73, 0. 97 and 0.73 were determined for the initial, development, mid-season and late-season growth stages. These values are lower than those reported by Shenkut et al. (2013: 22) of 0.45, 0.83, 1.18 and 0.78, respectively.

2017/18 (Swayimane)

Monthly estimates of crop evapotranspiration for dryland conditions were not determined for grain sorghum grown at Swayimane in the 2017/18 season. Seasonal crop water use was determined via the SWB equation using the difference between soil water contents at planting and harvest. However, monthly crop coefficients were calculated from modelled evapotranspiration using AquaCrop, with applied irrigation to relieve water stress (Table 13.18). Model simulations were performed from planting (19 January 2018) to harvest (28 June 2018). The estimated values are comparable to the range suggested by FAO (2002).

Table 13.18: Crop coefficients for grain sorghum estimated by AquaCrop for the 2017/18 season at Swayimane

Month	Growth stage	Length (days)	K_C (2017/18)
January	Initial	20-25	0.52
February	Development	30-40	0.82-0.85
March/April	Mid-season	40-45	0.94-0.98
May	Late season	30	0.68-0.73
June	Harvest		0.37

13.3.7.4 Discussion and conclusions

Crop coefficients are typically determined under “standard” conditions. This implies that no limitations are placed on crop growth or crop evapotranspiration, which may result from soil water and salinity stress, crop density, pests and diseases, weed infestations or low soil fertility (Taylor et al., 2008). The K_C values calculated for Swayimane for soybean and grain sorghum do not represent stress-free growing conditions as recommended by the FAO, since the trials were not irrigated. Furthermore, it is not ideal to calculate crop coefficients from evapotranspiration estimated using the SWB approach. A suitable micrometeorological technique or lysimeter is recommended for evapotranspiration estimation. Hence, the presence of water stress in each season, together with the reliance on the SWB approach, means that the crop coefficients obtained at Swayimane may not be easily transferable or applicable to other locations.

On the other hand, the Baynesfield site was irrigated, especially to establish the soybean crop. The crop coefficients published by Mbangiwa et al. (2019) for the 2012/13 season were not considered in this study, due to the low evapotranspiration measurements. For example, K_C at emergence using measured evapotranspiration data accumulated over nine days (16-24 October 2012) was 0.19. This value is lower than the simulated K_C value of 0.45. In addition, Piccinni et al. (2009) used lysimeters to calculate K_C values of 0.35 and 0.40 at emergence for irrigated maize (8 DAP) and sorghum (7 DAP), respectively. However, Mbangiwa (2018) reported an evapotranspiration total of 29.6 mm (range: 0.02 to 2.38 mm d^{-1}) for the period 25 September to 24 October 2012 (i.e. 31 days prior to emergence). From this, a crop coefficient of 0.41, representing bare soil conditions, was determined using a reference crop evaporation of 71.5 mm. During the initial crop growth stage, the predominant component of crop evapotranspiration is soil water evaporation. Therefore, the initial crop coefficient (K_{C_INI}) is largely influenced by the frequency and magnitude of rainfall and irrigation events. Higher K_{C_INI} values are expected for Baynesfield since soybean is typically irrigated each year to help establish the crop.

For the 2016/17 season, the new surface renewal system was only installed in December 2016, but initial problems resulted in data loss. Hence, crop coefficients for the entire growing season could not be determined. However, modelled K_C values derived from AquaCrop were comparable to measured K_C, especially for January to March. Hence, modelled K_C could be used to infill missing observed values from October to December.

13.4 MODELLING OF K_C VALUES

Kunz et al. (2015a) used the same monthly crop coefficients determined from measurements of evapotranspiration made at Baynesfield (for soybean) and Ukulinga (for grain sorghum) to represent all quinary subcatchments, with no adjustments made for different growing conditions. This approach assumed that K_C values at the experimental sites were applicable to all other areas deemed suitable for crop production. The authors concluded that this assumption represented a weakness in the methodology, which should be addressed in future studies. As noted in the previous section, crop coefficients derived from AquaCrop output were comparable to measured values. The option of using AquaCrop to derive monthly crop coefficients was explored further, as described next in more detail.

13.4.1 Methodology

The methodology is described in detail in Appendix N, with a summary provided here for convenience:

- Measured crop evapotranspiration was obtained for irrigated grain sorghum grown at Ukulinga during the 2012/13 season (Kunz et al., 2015a).
- The AquaCrop model was configured to simulate crop evapotranspiration for irrigated sorghum in the 2012/13 season.
- Simulated evapotranspiration was then compared to measured values, which showed that the model adequately estimated crop evapotranspiration.
- Crop coefficients were calculated from the measured and simulated evapotranspiration datasets and compared.
- Runoff was generated using the ACRU model with both the measured and simulated crop coefficients for the quinary subcatchment in which Ukulinga is located (Quinary Subcatchment 4697).
- Crop coefficients were then simulated for another quinary (Quinary Subcatchment 4325) to demonstrate the effect of cooler temperatures on crop growth, with the season length being more variable when compared to Quinary Subcatchment 4697.
- The results of this exercise are given next, which were compared to those obtained in the previous biofuel project by Kunz et al. (2015c).

13.4.2 Results

13.4.2.1 Original runoff estimates

Assuming a land use change from natural vegetation to grain sorghum production from November to March (a five-month crop cycle), Kunz et al. (2015a) simulated a reduction in mean annual runoff (MAR) to 120.91 and 48.47 mm for quinary subcatchments 4697 and 4325, respectively. This represented a percentage reduction relative to the baseline of 12.1 and 24.1% for quinary subcatchments 4697 and 4325, respectively. These reductions are above the 10% threshold suggested by Jewitt et al. (2009b). Thus, the land use change may be considered a potential stream flow reduction activity.

Table 13.19: The ACRU simulations of reduced mean annual runoff in two quinary subcatchments (4697 and 4325) that may result from grain sorghum planted in November using crop coefficients derived from measured evapotranspiration (Kunz et al., 2015c)

Quinary subcatachment	Mean annual runoff		Reduction in mean annual runoff		Potential stream flow reduction activity	Low flow period
	Baseline (mm)	Land use (mm)	Absolute (mm)	Relative (percentage)		
4697	137.56	120.91	16.65	12.1	Yes	6-8
4325	63.88	48.47	15.41	24.1	Yes	7-9

These reductions were based on observed K_C values derived from evapotranspiration measurements of grain sorghum planted at Ukulinga in the 2012/13 season. The monthly crop coefficients were used for both quinary subcatchments, with no adjustments made for the cooler growing conditions experienced in Quinary Subcatchment 4325.

13.4.2.2 New runoff estimates

Using the revised crop coefficients generated from evapotranspiration measurements from January to May 2013, and infilled with AquaCrop simulated evapotranspiration for December (cf. Table N.9 in Appendix N), the potential change in annual runoff generation was re-estimated for Quinary Subcatchment 4697. The results showed that a five-month (December to April) sorghum-growing season, followed by a seven-month fallow period (May to November) produced very similar runoff to natural vegetation. The simulated reduction in MAR of 2.5% is well below the suggested 10% threshold and is much lower than the 12.1% reduction estimated by Kunz et al. (2015a). The low-flow period remained unchanged as June to August.

Table 13.20: The ACRU simulations of reduced mean annual runoff that may result from grain sorghum planted in December for Quinary Subcatchment 4697, using crop coefficients derived from both measured and simulated evapotranspiration

K_C	Mean annual runoff		Reduction in mean annual runoff		Potential stream flow reduction activity	Low flow period
	Baseline (mm)	Land use (mm)	Absolute (mm)	Relative (percentage)		
Observed	137.56	134.16	3.40	2.5	No	6-8
Simulated	137.56	134.21	3.35	2.4	No	6-8

The ACRU model was re-run using monthly crop coefficients generated from ET_C estimates derived by AquaCrop for grain sorghum planted on 1 December. On average, they reached physiological maturity approximately 115 days later (in April), based on crop growth driven by thermal time (i.e. in GDD mode). The MAR calculated from 49 years of rainfall data (from 1950 to 1998) was 134.21 mm, which represents a 2.4% reduction from the baseline MAR of 137.56 mm. This highlights AquaCrop's ability to generate crop coefficients for use in ACRU.

The ACRU model was run using K_C values derived from 49 seasons of monthly evapotranspiration values estimated by AquaCrop from irrigated (i.e. non-stressed) growing conditions in Quinary Subcatchment 4697 and Quinary Subcatchment 4325. When compared to the baseline, a small reduction in MAR was simulated for Quinary Subcatchment 4697, which is much lower than the 12.1% reduction estimated by Kunz et al. (2015a). The low-flow period remained unchanged as June to August. As shown in Table 13.21, a 13.8% reduction in MAR was simulated for Quinary Subcatchment 4325, which again is less than the 24.1% estimated by Kunz et al. (2015a).

Table 13.21: The ACRU simulations of reduced mean annual runoff in two quinary subcatchments (4697 and 4325) that may result from grain sorghum planted in November using crop coefficients derived from simulated evapotranspiration under non-stressed conditions

Quinary Subcatchment	Mean annual runoff		Reduction in mean annual runoff		Potential stream flow reduction activity	Low flow period
	Baseline (mm)	Land use (mm)	Absolute (mm)	Relative (percentage)		
4697	137.56	135.55	2.01	1.5	No	6-8
4325	63.88	55.07	8.81	13.8	Yes	7-9

13.4.3 Discussion and conclusions

The relative reduction in MAR changed from 12.1 to 1.5% in Quinary Subcatchment 4697 and from 24.1 to 13.8% in Quinary Subcatchment 4325 due to using crop coefficients estimated with AquaCrop. This new approach simulated a much lower impact of crop production on runoff generation in both of the two subcatchments that were tested. This project has showed that AquaCrop adequately simulated ET_C measured above grain sorghum using the surface renewal technique. Furthermore, the model can be used to infill missing ET_C measurements. However, AquaCrop does not simulate the evaporation of intercepted water, only transpiration and soil water evaporation. Hence, AquaCrop estimates of ET_C will be lower than those measured using micrometeorological techniques such as surface renewal and eddy co-variance.

CHAPTER 14: SPATIAL APPLICATION OF MODELS

In Chapter 11 and Chapter 13, parameters used to run both simulation models were given for each strategic feedstock. This section focuses on changes made to the versions of AquaCrop and ACRU used in the previous biofuel project. In addition, the logistics of running the models at a national scale are discussed, as well as the significant improvements that were made for the models to run significantly faster.

14.1 AQUACROP

14.1.1 Model improvements

In AquaCrop Version 6, the following improvements and new features have been made to the model:

- Improved simulation of crop performance in dry environments
- Improved water thresholds for stomatal closure for certain crops
- Effects of gravel in the soil profile
- Simulation of weed infestation on crop production
- Inclusion of dry beans as a new crop

In addition to the above, the ratio of initial abstraction (I_a) to storage (S) has been decreased from 20% to 5%. Hence, AquaCrop Version 6 produces more runoff than Version 4 (cf. Section I3 in Appendix I for more detail). The default curve numbers have also been updated in Version 6 (cf. Table 10.17 in Section 10.2.4), due to the coefficient of initial abstraction changing from 20 to 5%. However, only the first two updates listed above are discussed next in more detail. This is due to their greater impact on simulated output from AquaCrop in this study.

14.1.1.1 Simulations in dry environments

Kunz et al. (2015b) noted that AquaCrop Version 4 was particularly sensitive to the availability of soil moisture in the first growth stage. They found that water stress at the start of the second growth stage reduced leaf expansion to such an extent that the crop died, and thus no biomass or yield was produced. A workaround was to set the initial soil water level to field capacity, which is the default option in AquaCrop, although it is unrealistic for rainfed farming conditions in South Africa.

This issue has been addressed in Version 6, which now assumes that sufficient reserves are available in the seed for leaf expansion to occur at its maximum rate just after germination. Any reduction of leaf expansion due to water stress is not considered until canopy cover is 25% above the initial value (CC_O). This protection of the seedling avoids an instantaneous killing of the seedling too soon after germination (FAO, 2017), as noted by Kunz et al. (2015b).

The improvement in simulating early development of the canopy cover under water stress was the main motivation to use Version 6 of the model in this project. Kunz et al. (2015b) selected a crop yield of 0.00 t ha^{-1} to represent crop failure and counted the number of times this occurred over the 49-season simulation period from 1950 to 1998. It is expected that the number of crop failures simulated by Version 6 of the model will be somewhat less than that outputted by Version 4.

Another improvement to the model allows for light rain to reduce the water stress of deep-rooted crops. This was achieved by comparing the depletion in the total root zone with that in the topsoil. Hence, the degree of water stress is influenced more by the wettest portion of the soil profile. Furthermore, root deepening slows down if the soil water content at root depth is near the permanent wilting point, which results in a smaller root zone in drier subsoils, and thus reduced soil water stress.

If the maximum canopy cover is not reached, the model will slow down the rate of canopy cover decline, allowing for the crop to recover if rain or irrigation occurs during early senescence. Lastly, there is less crop transpiration during cold periods in Version 6, which means the root zone is relatively wetter, resulting in reduced water stress (FAO, 2017).

14.1.1.2 Water thresholds for stomatal closure

The FAO (2017) reported that updates were made to crop parameters related to soil water thresholds for soybean, sorghum, potato and cotton. In particular, changes were made to the upper threshold for soil water depletion at which the stomata start to close, as well as the shape factor for the stress-depletion relationship. These updated parameter values were discussed in Section 11.1.1.1 (soybean) and Section 11.1.2.1 (sorghum).

14.1.2 Improved modelling approach

In the previous biofuel project, considerable effort was spent on linking AquaCrop to the quinary subcatchment climate and soils database. Over 5,000 lines of computer code were written to facilitate and automate this process (Kunz et al., 2015b). Although a similar procedure was followed in this study, the time required to run the model at a national scale was significantly reduced, which is discussed in Section 14.3. However, a number of changes made to the modelling approach developed by Kunz et al. (2015b) are discussed next.

14.1.2.1 Crop coefficients

As discussed in Section 13.4, a new approach involving the use of AquaCrop to derive monthly crop coefficients for ACRU was used in this study. Using the 50-year quinary climate database, AquaCrop simulated up to 49 seasons of monthly ET_C totals, with irrigation invoked to relieve water stress. From the model output, K_C values were calculated for months, exhibiting 48 to 49 seasons of data. The crop coefficients were then averaged to produce a single set of monthly crop coefficients deemed representative of each quinary subcatchment, which ACRU then used to determine the hydrological impact of biofuel crop production on stream flow generation.

14.1.2.2 Effective rooting depth

When comparing simulations of soil profile water content (*WCtot*) against observations, AquaCrop over-estimated the total because the roots grew to the maximum rooting depth defined in the crop parameter file, e.g. 1.8 m for grain sorghum, despite the soil depth being 0.6 m at Ukulinga. To correct this anomaly, the parameter for effective rooting depth (i.e. depth of restrictive soil layer inhibiting root zone expansion) in the AquaCrop soils (.sol) file was set to the total depth of the A- and B-horizons.

14.1.2.3 Low first season yield

Kunz et al. (2015b; cf. Section 6.5.12.2) highlighted lower crop yields being simulated in the first season (1950/51) in each quinary subcatchment when compared to subsequent seasons. Further investigation identified an error when determining the length of the first season, which caused a shorter crop cycle, and thus a lower simulated yield. This error was fixed and resulted in a slightly higher average yield simulated for each quinary subcatchment.

14.1.2.4 Model runtime error

When Kunz et al. (2015b) ran AquaCrop Version 4 at the national scale in the previous biofuel project, they noted that the model would stop running (reason unknown), and thus required user intervention to close the error dialog box, and to manually restart the model runs (cf. Section 6.5.12.3). Kunz et al. (2015b) developed a procedure to automatically restart the model after each “crash”.

Importunely, this problem has not been fixed in Version 6 and results in an “invalid floating-point operation” error (likely due to a division-by-zero error). For this study, the procedure to restart the model was significantly improved, which reduced the overall time required to execute AquaCrop at the national scale.

14.1.2.5 Maximum season length

Kunz et al. (2015b; cf. Section 6.5.12.4) set an upper limit of 730 days for the season length calculated using thermal time, based on a maximum two-year cycle for sugarcane. This addressed a problem with Version 4 of the model that would continue to run until sufficient growing degree-days had accumulated for the crop to reach physiological maturity. Using Quinary Subcatchment 4489 (average altitude 2,755 m) as an extreme example of a high altitude (i.e. cold) subcatchment, the model ran for an unrealistic season length of 29 years and simulated little to no yield.

This issue has not been corrected in Version 6 of the model and, for this study, crop cycles longer than a year were deemed economically non-viable for soybean or sorghum production. Hence, the upper limit was set to 365 days in order to reduce computational expense when running the model in cold regions of the country. When analysing the average crop cycle determined from 49 consecutive seasons, values exceeding 365 days were not expected. For example, Quinary Subcatchment 3169 produced a crop cycle of 1,447 days in Season 15, where the cropping period started on 1 December 1964. Although the cropping period was limited to a year (ending on 30 November 1965), the model outputted zero biomass and yield production, but did not reset (i.e. reinitialise) the crop cycle at the start of the next season (i.e. 1 December 1965). AquaCrop continued with the previous value of 352 days and finally reported a season length of 1,447 days that ended in November 1968. For mapping purposes, all season lengths longer than a year were limited to 365 days.

14.2 THE ACRU MODEL

14.2.1 Modifications to ACRU

In the previous biofuel project, Kunz et al. (2015b) used ACRU Version 3.37 to assess the hydrological impact of a land use change from natural vegetation to biofuel feedstock production. In this study, Version 3.41 of the model was used. The changes made to the model from Version 3.37 to Version 3.41 are briefly highlighted below.

14.2.1.1 Version 3.38

The Fortran version of ACRU was run for 24 quinary subcatchments (Basin M; cf. Section 14.2.2.1) to simulate runoff response from a land cover of natural vegetation. The model simulation was analysed using various tools developed by Intel, which showed that 100 of the 179 subroutines were executed during the run. However, ACRU spends most of its run time reading and writing data (i.e. it is a disk-intensive model). For example, four daily variables are stored in the DIRECT file for each subcatchment, which accounts for 33% of total run time. In addition, creating the total evaporation and water balance files accounts for a further 23%. Reading in user input from the menu and daily climate data accounts for 20 and 8%, respectively. In order to improve the model’s performance, modifications were made to 64 of the 100 subroutines, ranging from small changes to completely rewritten code. The end result is Version 3.38, which runs eight times faster when compared to the previous version.

14.2.1.2 Version 3.39

Changes were made to two subroutines to change the year from a two- to a four-digit number in the dynamic file. However, a decision was made not to input monthly crop coefficients derived using AquaCrop for each year via the dynamic input file.

14.2.1.3 Version 3.40

Kunz et al. (2015a) highlighted differences in stream flow generated by the Fortran version of ACRU when compared to that from the Java version. One of the reasons for the runoff differences is due to the way in which the two versions adjust the daily crop coefficient within the model. The Fortran version was programmed to reset the daily crop coefficient (K_C) value to that of the monthly input value at the beginning of every month. However, this monthly "resetting" procedure was removed in the Java version, thus allowing the daily K_C value to continue decreasing until recovery from stress begins when the soil water content rises above a threshold value. Kunz et al. (2015a) concluded that the Fortran version of the model should be modified to mimic the Java version.

Based on the above recommendation, changes were made to Version 3.40 of ACRU to prevent the resetting of the daily K_C value at the beginning of each month. In ACRU, 12 monthly crop coefficients are converted to 366 daily values using Fourier analysis. At the beginning of the simulation (i.e. the first day of Year 1), K_C is set to the daily (i.e. Fourier) value and not the monthly value, which mimics the Java version of ACRU. In addition, daily adjustments made to K_C are limited to Fourier values and not monthly values, which again mimics the Java version.

14.2.1.4 Version 3.41

For research of transpiration suppression due to elevated CO_2 levels conducted by a PhD student, five additional suppression values (i.e. 5, 10, 20, 25 and 30%) were added to the two existing values of 15 and 22%. This modification has no impact on the stream flow reduction assessment required in this study.

14.2.1.5 Compiling the model

The ACRU model was compiled using the latest version of Intel's Fortran compiler software (Version 18) to produce a 64-bit executable program. The Intel compiler was used to create eight 64-bit versions of the model, each optimised for a particular Intel CPU instruction set as shown in Table 14.1. The more features supported by a particular CPU, the faster the program's execution time.

Table 14.1: Features of each instruction set supported by Intel processors

Instruction set	Intel CPU features						
	SSE	**SSE3**	**SSE4.x**	**AVX**	**SMEP**	**AVX2**	**AVX-512**
SSE3	√	√					
SSE4.2	√	√	√				
AVX	√	√	√	√			
Sandy Bridge	√	√	√	√			
Ivy Bridge	√	√	√	√	√		
CORE-AVX2	√	√	√	√	√	√	
CORE-AVX512	√	√	√	√	√	√	√
COMMON-AVX512	√	√	√	√	√	√	√

SSE = Streaming SIMD Extensions
SIMD = Single Instruction, Multiple Data
SMEP = Supervisor Mode Execution Prevention
AVX = Advanced Vector Extensions
AVX2 = Advanced Vector Extensions 2
AVX-512 = Advanced Vector Extensions 512-bit

The version optimised for COMMON-AVX512 instruction sets runs slightly faster than the SSE3 version. More importantly, slight differences were found in the statistics generated from the model's output. The most significant difference was a change of 11.31% (428.48 – 417.17) in the coefficient of variation (CV) calculated in January for the saturated drainage from B-horizon to groundwater zone (*SUR2*) for Quinary Subcatchment 2137 (Basin D). This difference is not considered significant, considering the very large CV percentages that reflect the high variability in monthly totals for *SUR2*. Other minor differences in statistics ranged from 0.01 to 3.20.

14.2.2 Implications of ACRU modifications

14.2.2.1 Model test configuration

There are 22 primary drainage regions that cover southern Africa, numbered alphabetically from A to X, with letters I and O excluded. Of these, seven were selected (Table 14.2) to assess the modifications made to ACRU from Version 3.37 onwards and the impact of runoff (*SIMSQ*) generation. These basins were chosen because they have the smallest number of quinary subcatchments, thus reducing the computational time required to perform the required tests. In addition, Basin G exhibits highly erratic rainfall, which results in statistics with high values for kurtosis, as well as the CV, especially for ACRU output variables such as sediment yield (*SEDYLD*) and soil moisture deficit in the B-horizon (*DEF2*). The 28 ACRU variables shown in Table 14.3 were used for testing.

Table 14.2: Number of subcatchments for each of the seven drainage basins used for testing the ACRU model

Basin	Number of quinary subcatchments
M	24
P	48
R	90
F	105
N	108
K	120
G	174
Total	**669**

Table 14.3: Description of each ACRU output variable (all units in mm, except for CAYD)

Variable	Description	AGG.*
AET	Total evaporation (actual evapotranspiration)	Sum
AET1	Total evaporation (actual evapotranspiration) from A-horizon	Sum
AET2	Total evaporation (actual evapotranspiration) from B-horizon	Sum
APAN	A-pan equivalent reference evaporation	Sum
ASOEV	Actual evaporation from the soil surface	Sum
ATRAN1	Actual transpiration from the A-horizon	Sum
ATRAN2	Actual transpiration from the B-horizon	Sum
CAYD	Crop coefficient	Ave
CELRUN	Total streamflow from subcatchment including upstream contributions	Sum
DEF1	Soil moisture deficit in A-horizon in relation to drained upper limit	Ave
DEF2	Soil moisture deficit in B-horizon in relation to drained upper limit	Ave
DPE	Maximum evaporation (potential evapotranspiration)	Sum
EFRL	Effective rainfall (rainfall available for plant growth)	Sum

Variable	Description	AGG.*
PERC	Unsaturated drainage from the B-horizon to intermediate/groundwater zone	Sum
POSOEV	Maximum (potential) evaporation from the soil surface	Sum
POTR1	Maximum transpiration from the A-horizon	Sum
POTR2	Maximum transpiration from the B-horizon	Sum
PP1	Maximum evaporation (potential evapotranspiration) from the A-horizon	Sum
PP2	Maximum evaporation (potential evapotranspiration) from the B-horizon	Sum
QUICKF	Storm flow leaving catchment outlet on a given day	Sum
RFL	Input rainfall, adjusted by monthly *CORPPT* values	Sum
RUN	Base flow	Sum
RUNCO	Base flow store	Ave
SIMSQ	Simulated runoff (storm flow + base flow) from the subcatchment, excluding upstream contributions	Sum
STO1	Soil water content in A-horizon	Ave
STO2	Soil water content in B-horizon	Ave
SUR1	Saturated drainage from A-horizon to B-horizon	Sum
SUR2	Saturated drainage from B-horizon to groundwater zone	Sum

*Sum = Daily values are summed
Ave = Daily values are averaged

14.2.2.2 Version 3.38

For Basin M, ACRU Version 3.38 ran in half the time required by Version 3.37. This represents a significant speed improvement. Kienzle (2019) implemented the same code changes (i.e. moved the direct access file from the hard disk into memory as an array) in his version of ACRU, which handles snowmelt in Alberta, Canada. He reported that the model ran 30 times faster than the old version on an “average” PC, completing 1,722 subcatchments with 68 years of climate data in one hour instead of 33 hours.

Version 3.38 of the model produced the same statistics as Version 3.37 for the seven test basins, except for Subcatchment 2647, which produced a negligible difference in July's CV of soil moisture deficit in the B-horizon (*DEF2*) of 2.87%. This implies that the significant changes made to the code to improve model performance had no impact on model computation.

14.2.2.3 Version 3.39

Since the dynamic file option will not be used to input changing monthly crop coefficients on an annual basis, this version of the model was not tested.

14.2.2.4 Version 3.40

The changes made to the Fortran version of the model to mimic the Java version had an impact on the mean monthly crop coefficients (*CAYD*). Of the 669 subcatchments tested (cf. Table 14.2), 174 exhibited changes in *CAYD* ranging from 0.01-0.29. Quinary Subcatchment 2644 (Basin G) showed the largest decreases, especially in winter compared to the summer months. Since daily K_C is not reset to the monthly value at the beginning of each month, K_C continues to decrease due to soil water stress, which results in lower values.

Table 14.4: Differences in average crop coefficients for Quinary Subcatchment 2644, which resulted from changes made to ACRU Version 3.40

Version	Jan	Feb	Mar	Apr	May	Jun	Jul	Aug	Sep	Oct	Nov	Dec	Ann
3.37	0.36	0.37	0.38	0.46	0.56	0.58	0.60	0.57	0.59	0.49	0.41	0.38	0.48
3.40	0.27	0.25	0.26	0.28	0.30	0.30	0.31	0.31	0.32	0.33	0.32	0.30	0.30
Difference	**0.09**	**0.12**	**0.12**	**0.18**	**0.26**	**0.28**	**0.29**	**0.26**	**0.27**	**0.16**	**0.09**	**0.08**	**0.18**

In total, 169 quinaries reflected changes in monthly *SIMSQ,* ranging from 0.01 to 5.84 mm. Changes in annual runoff (MAR_{base}) ranged from 0 to 31.5 mm (or 0 to 48.5%). Again, Quinary Subcatchment 2644 (Basin G) exhibited the largest absolute difference (Table 14.5), with MAR_{base} increasing by 31.5 mm (or 8.5%), followed by Quinary Subcatchment 2638 (23.8 mm or 5.8% increase). However, Quinary Subcatchment 2661 exhibited the largest relative increase in MAR_{base} of 48.5%, resulting from only a 1.3 mm change in annual runoff. These increases in runoff are due to lower crop coefficients, which means less maximum evaporation from the vegetation layer, and thus more moisture in the topsoil. The latter results in increased runoff from the subcatchment. The largest decrease in mean annual maximum evaporation (*DPE*) was 248 mm for Quinary Subcatchment 2731, which resulted in a negligible increase in MAR_{base} of only 1.7 mm.

Table 14.5: Differences in simulated monthly and annual runoff resulting from changes made to ACRU Version 3.40

Version	Jan	Feb	Mar	Apr	May	Jun	Jul	Aug	Sep	Oct	Nov	Dec	Ann
3.37	8.9	5.7	5.6	6.8	21.4	54.3	76.0	77.7	49.9	28.3	21.2	13.5	368.6
3.40	9.5	6.0	5.9	7.3	23.9	59.9	81.8	82.5	53.9	31.7	23.4	14.7	400.1
Difference	**0.6**	**0.3**	**0.4**	**0.5**	**2.5**	**5.6**	**5.8**	**4.8**	**4.0**	**3.5**	**2.2**	**1.2**	**31.5**

14.2.2.5 Version 3.41

Changes made to ACRU to accommodate transpiration suppression due to elevated CO_2 levels will not affect the outcome of this project, and thus this version was not tested. However, stream flow was simulated using this (i.e. latest) version of the ACRU model. As noted earlier, the previous biofuel project (Kunz et al., 2015b) used Version 3.37.

14.2.3 New ACRU utilities

The PRINT Version 3.23 utility (called *PRN323*) converts ACRU's output files in binary (BIN) format into formatted, flat ASCII files that contain monthly time-series data. The statistics Version 3.24 utility (called *STA324*) then produces statistics from the monthly data files. On a fast PC that uses a RAM drive, it takes approximately 12 minutes to generate monthly data files for a national model run (5,838 quinary subcatchments), plus an additional minute to produce the statistics files. These two utilities, originally developed by Steve Lynch in the 1990s, last underwent minor changes in 2008. In this project, effort was spent on creating faster utilities to generate monthly data and statistics files from ACRU's output (i.e. BIN) files.

14.2.3.1 Improved PRINT utility

For this project, the *PRN323* utility was completely rewritten in Fortran to improve its computational performance and output format. The new utility (Version 3.25, called *PRN325*) runs approximately 1.7 and 15.3 times faster than Version 3.23 when creating daily and monthly data files, respectively.

Additional modifications were made to the PRINT utility to further improve its computational performance, and thus reduce the time required to produce statistics. The new utility also takes full advantage of multi-core CPUs by dividing the number of binary files to be analysed equally between each core. However, hyper-threading is a technology that is used by some Intel CPUs that allows a single core to act like two separate processors. Instead of analysing 5,838 binary files sequentially, a 10-core CPU with hyper-threading would subdivide the task into 20 smaller processes, each analysing 292 files simultaneously. Theoretically, this should equate to a 20-fold increase in speed. However, modern PC disk drives are unable to store the statistics files at the speed at which the multi-core CPU is creating them, thus creating a “bottleneck” in the process. With multi-threading enabled, the new utility (*PRN325*) runs approximately 12.6 and 129.3 times faster than Version 3.23 when creating daily and monthly data files, respectively. This represents a significant speed improvement, which means that ACRU users will spend less time wating for the required output files to be generated.

14.2.3.2 Improved statistics utility

The statistics utility (called *STA324*) was also completely rewritten in Fortran to improve its computational performance and output format. For example, each ACRU variable is now written out with two decimal places in a comma-separated file. The subcatchment number is given in the first column, together with an abbreviation of the ACRU variable in the second column. These improvements make it far easier to post-process the statistics using a line extraction utility.

The new utility has also been multi-threaded, and thus takes full advantage of multi-core CPUs. The new utility (*BIN2STA*) is now 121.3 times faster when producing both monthly and statistical files in one step. However, the new utility can read ACRU's output (i.e. BIN) files directly and produce statistical files only (i.e. no monthly data files), a process that takes about 3.6 seconds, equating to a speed improvement of 211.4 times. If only monthly data files are required, the improved utility is 129.2 times faster than *STA324*. Again, this represents a significant speed improvement for ACRU users.

Additional tests were undertaken to determine how performance is affected by the number of cores used by the improved statistics utility. There is an exponential relationship between the number of threads (i.e. twice the CPU cores) used and the speed of the statistics utility. When the number of threads used was reduced from 20 (maximum on test PC) to 10, the utility ran 1.14 times (14%) slower (Figure 14.1). Hence, the speed gain from running the utility on a CPU with more than 10 threads is minimal. Based on Figure 14.1, it is recommended that the utility is run on a PC with six to ten threads. There is a linear relationship between the number of threads and the CPU cost. The test CPU had 20 threads, which cost R17,500, compared to a CPU with 36 threads that cost R35,500 (prices as at August 2019). Hence, the performance gained from using more than 20 threads does not justify the substantial increase in the cost of the CPU.

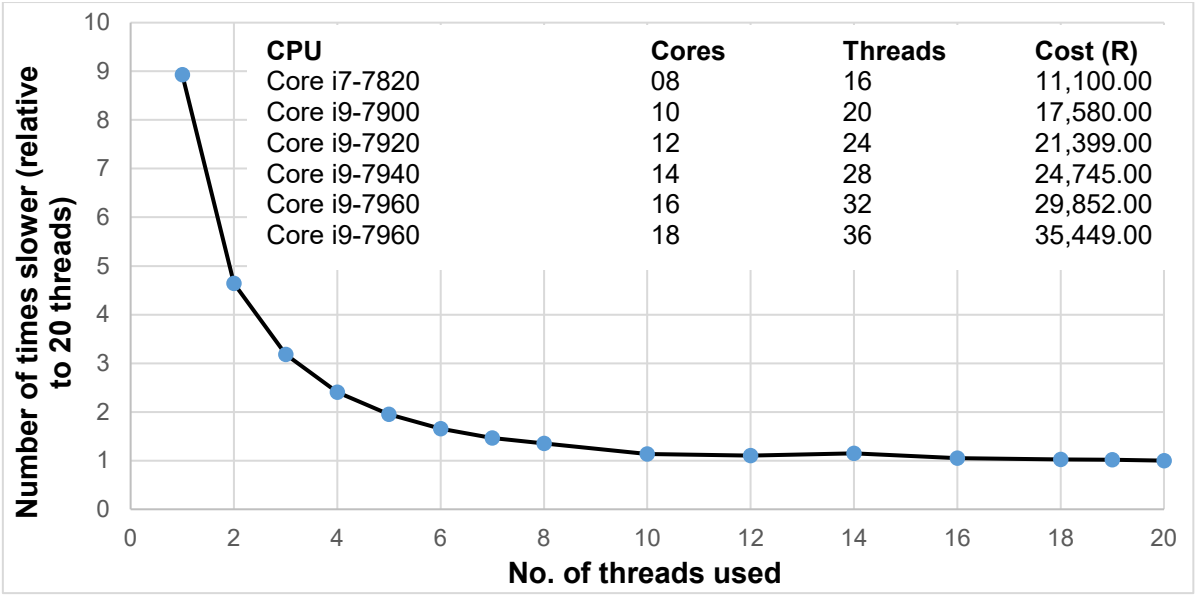

Figure 14.1: Number of times slower the new BIN2STA utility ran when the number of threads was reduced from 20 to one

Differences were found when comparing statistical output between the old utility (*STA324*) and the new and improved utility (*BIN2STA*). For example, *STA324* does not calculate annual averages for certain variables (Table 14.6), but instead calculates annual sums. Similarly, *STA324* does not calculate the annual maximum of the estimated peak discharge (*QPEAK*), but rather the annual sum. These differences are not deemed critical, as annual averages (or sums) of these variables are meaningless.

Table 14.6: Differences in annual statistics for certain ACRU output variables produced by the new statistics utility (BIN2STA) when compared to the old utility (STA324)

Variable description	Name	*STA324*	*BIN2STA*
Crop coefficient	*CAYD*	Sum	Average
Soil moisture deficit in A-horizon	*DEF1*	Sum	Average
Soil moisture deficit in B-horizon	*DEF2*	Sum	Average
Baseflow store	*RUNCO*	Sum	Average
Soil moisture content in A-horizon	*STO1*	Sum	Average
Soil moisture content in B-horizon	*STO2*	Sum	Average
Soil water content of the irrigated field	*SW_MAX*	Sum	Average
Estimated peak discharge	*PEAK*	Sum	Maximum

The *STA324* calculates statistics from monthly totals or averages of each ACRU output variable that is generated by the *PRN323* utility. The level of precision (i.e. number of decimal places) for each variable is determined by the dictionary file (DIC002.OUT). For example, *PRN323* reads the binary ACRU output file, which stores seven to eight decimal places for each daily value, then generates, for example, monthly averages of soil water content of the A- and B-horizons in mm to one decimal place (i.e. *STO1* and *STO2*). The latter values are then used to calculate monthly statistics using *STA324*. However, the *BIN2STA* utility reads the .BIN file directly, generating monthly totals or averages in memory, retaining all seven to eight decimals of precision.

Tests were conducted to determine which statistics and variables were most affected if all decimal values were used to generate statistics. Primary Catchment F, which comprises 421 quinary subcatchments, was selected as it produces highly variable data due to erratic rainfall. It was found that the coefficient of variation (expressed as a percentage) is mostly influenced, especially for the ACRU variables listed in Table 14.7.

Table 14.7: Differences in annual statistics for certain ACRU output variables produced by the new stats utility (BIN2STA) when compared to the old utility (STA324)

Variable description	Name
Unsaturated drainage from the B-horizon to groundwater	*PERC*
Estimated peak discharge	*QPEAK*
Storm flow	*QUICKF*
Sediment yield from catchment	*SEDYLD*
Storm flow from irrigated area	*STQIR*
Saturated drainage from A-horizon	*SUR1*
Saturated drainage from B-horizon	*SUR2*

14.3 MINIMISING COMPUTATIONAL EXPENSE

14.3.1 Background

This study required a relatively large number of model simulations to be performed, which is time consuming without access to a high-performance computing system. Thus, model runs were mostly conducted on a high-end computer running the MS Windows operating system. The PC has a single NVMe drive, two 7,200 RPM drives and another two 5,400 RPM drives for backup purposes. This PC has a core i9 CPU with 10 cores (20 threads) that are capable of handling AVX-512 instruction sets. This CPU can process twice the number of data elements as an Intel AVX2 CPU and four times that of an SSE-based CPU. The PC has 32 GB of RAM, which is adequate for working with a RAM drive (cf. Section 14.3.4). Due to interruptions related to loadshedding in December 2019 and January 2020, final model simulations were also performed on an older PC with a core i7 CPU (six cores; 12 threads).

According to Jones (2018), model execution speed can be dramatically increased on most computers by means of the following:

- Dividing the simulation run into smaller tasks
- Spreading the smaller tasks across several processing cores on the computer
- Instructing the model to read inputs from and write outputs to a small virtual disk drive defined in the computer's random-access memory (RAM drive)
- Running the model on a desktop PC as opposed to a laptop computer, the latter being typically slower due to cooling issues
- Post-processing model output, while it is temporarily stored on the RAM drive
- Executing large runs in "batch" mode using scripts designed for Windows- or Linux-based PCs

In the previous biofuel project, Kunz et al. (2015b) developed a methodology designed to speed up ACRU and AquaCrop model simulations, which incorporated some of the suggestions listed above. In this project, further improvements were made, which vastly reduced the time required to perform large model runs. A detailed explanation is provided next, which, to date, has allowed researchers working on other WRC-funded projects to implement and benefit from similar speed improvements.

14.3.2 Derivation of smaller tasks

14.3.2.1 The ACRU model

Kunz et al. (2015a) reported that Version 3.37 of ACRU could not simulate runoff for all 5,838 quinary subcatchments in a single national run, because the model ran too slowly. Hence, ACRU was run at the primary drainage basin level. However, Basin C and Basin D are run together, as Quinary Subcatchment 1431 (Basin C) flows into Quinary Subcatchment 1929 (Basin D).

In the past, a national run was completed in approximately 19 hours on a Core 2 Duo PC. Hence, considerable effort was spent on automating this process to minimise the computational time required to complete a national run. This approach vastly improved the time required to complete all 5,838 quinary subcatchments, which took approximately 8.5 hours (510 minutes) on a Core i7 PC (Table 14.8). Furthermore, the automation allows for a scenario to be re-run if errors are discovered during the analysis, or if model parameters are refined based on new evidence. For this project, ACRU was also run for each primary catchment (or drainage basin), as this approach subdivided a national run into 21 smaller tasks.

Table 14.8: The time required (in minutes) to run the ACRU model for each primary drainage basin (Kunz et al., 2015a)

Primary catchment	Start Quinary Subcatchment	End Quinary Subcatchment	Number of quinary subcatchments	Run time (minutes)
A	1	417	417	31
B	418	852	435	32
CD	853	2295	1,443	255
E	2296	2520	225	11
F	2521	2625	105	4
G	2626	2799	174	8
H	2800	3006	207	10
J	3007	3282	276	15
K	3283	3402	120	5
L	3403	3576	174	8
M	3577	3600	24	1
N	3601	3708	108	4
P	3709	3756	48	2
Q	3757	3969	213	10
R	3970	4059	90	3
S	4060	4233	174	8
T	4234	4635	402	29
U	4636	4821	186	8
V	4822	5079	258	14
W	5080	5526	447	34
X	5527	5838	312	18
Total			**5,838**	**510**

14.3.2.2 AquaCrop

In the previous biofuel project, a national run involving AquaCrop was also subdivided into 19 smaller tasks, where the model was run sequentially for each primary catchment. However, the order in which each task was run did not matter as each quinary subcatchment was equivalent to a single “standalone” simulation of crop response.

For this project, a better approach was developed where a national run was still divided into smaller tasks, and where the number of jobs depended on the PC’s CPU capability. A small utility (called cpuinfo.exe) was run to report the number of individual threads available on the PC. Two threads of the PC’s operating system were set aside to use, while the remaining threads were used to run AquaCrop. For a 10-core CPU with 20 threads, 18 simultaneous AquaCrop runs were completed, each involving ~324 quinary subcatchments. Similarly, each thread of a six-core CPU ran ~584 (5838/10) subcatchments. Hence, a national run is completed faster on PCs with more cores and threads.

14.3.3 Grouping of tasks

The speed improvements made to ACRU Version 3.38 allow for the model to be run for the first time for all 5,838 quinaru subcatchments in a sequential manner. However, both ACRU and AquaCrop will run faster in parallel mode, as explained next.

14.3.3.1 The ACRU model

An analysis of Table 14.8 revealed that, although the approach took 255 minutes to complete Basin C and Basin D (1,443 quinary subcatchments), the remaining 20 basins (i.e. 4,395 quinary subcatchments) were completed in the same time. Hence, a decision was made not to run the basins in a sequential manner, but rather to run a number of basins in parallel (i.e. simultaneously). Since Basin C and Basin D are run sequentially, an iterative procedure was developed to find which basins should be run together in order to finish at the same time as Basin C and Basin D.

It was noted that basins G, L and S have the same number of subcatchments (i.e. 174) and should be run together. Basins F, K and N also exhibit a similar number of quinary subcatchments, as do basins E, H and Q. Basins U and V have 444 quinary subcatchments, which is similar to basins B and W. Furthermore, basins R and X have 402 quinary subcatchments, which is similar to basins A and T. The remaining basins (P, M and J) were then added to another grouping to balance the computational load. Table 14.9 highlights the final grouping that was obtained after tests involving 16 national runs were completed.

Table 14.9: Seven tasks, each representing a particular grouping of drainage basins that, if run in parallel, take similar times for ACRU to complete

Task number	Sequence		Number of quinary subcatchments			
1	C		579			
	D		864			
2	G			174		
	S				174	
	L					174
3	F			105		
	K				120	
	N					108
4	E			225		
	Q				213	
	H					207
5	U	V		444		
	B				435	
	W					447
6	R	X		402		
	A				417	
	T					402
7	J			276		
	P				48	
	M					24
Total			**1,443**	**1,626**	**1,407**	**1,362**

14.3.3.2 AquaCrop

Initial national runs of the model on the high-end PC (with 20 threads) showed that each of the 324 individual tasks were completed in different times, ranging from 482 to 634 minutes. Further investigation revealed that this range was related to the following:

- Season length (crop cycle)
- The number of times the model "crashed"

For example, the average crop cycle varied from 92 days to 264 days for grain sorghum planted in December at a density of 60,000 plants ha^{-1} (Table 14.10). Hence, model runs for quinary subcatchments numbered 1297 to 1620 should take approximately three times longer than those for quinary subcatchments 1 to 324. However, since the crop cycle was limited to a year (cf. Section 14.1.2.5), Task 18 takes 30% longer (equivalent to 152 minutes) than Task 1.

Table 14.10: Variation in crop cycle as simulated by AquaCrop for grain sorghum (PAN8906) planted in December at a density of 60,000 plants ha^{-1}, together with the number of times AquaCrop crashed during the rainfed model run

Task number	Quinary subcatchment number		Crop cycle (days)			Model crashes
	Start	End	Min	Max	Ave	
1	0001	0324	49	154	92	7
2	1945	2268	45	730	115	14
3	0325	0648	60	287	115	4
4	0649	0972	57	309	115	1
5	5509	5838	50	328	118	1
6	5185	5508	51	291	121	2
7	4861	5184	75	597	122	0
8	0973	1296	66	519	123	8
9	4537	4860	75	612	126	2
10	3565	3888	74	569	136	15
11	3889	4212	84	560	151	14
12	1621	1944	49	672	167	14
13	4213	4536	89	569	172	3
14	3241	3564	81	756	173	15
15	2269	2592	63	865	178	16
16	2917	3240	67	866	186	14
17	2593	2916	72	863	203	20
18	1297	1620	62	807	264	21

The national run for grain sorghum planted in December at a density of 60,000 plants ha^{-1} crashed 171 times for the rainfed scenario, but only 14 times for the irrigated scenario. Hence, the "floating point operation error" (cf. Section 14.1.2.4) is related to model runs for quinary subcatchments that are actually too dry for rainfed crop production. With the exception of Task 2 and Task 13, the number of model crashes is also related to season length and more crashes occur in the colder areas of the country.

14.3.4 Disk storage performance

The ACRU model is a disk-intensive program, which reads and writes (i.e. creates) a large number of data files. Table 14.9 shows that the model will run faster if seven jobs are started concurrently as opposed to running the model in a sequential manner.

AquaCrop is also a disk-intensive model that creates a number of temporary files in the SIMUL folder. Based on this, a utility called CrystalDiskMark (Version 5.5.0; https://crystalmark.info/en/) was used to test the write (and read) performance of different storage disks. The test involved measuring the rate in MB per second for sequentially writing a 500 MB file to disk, then reading the same file from disk. The test was repeated numerous times, from which average rates were calculated. Table 14.11 indicates that although NVME drives are 4.4 times faster than SSDs when writing data, RAM drives are 2.8 times faster than a NVMe drive. The NVMe drives are solid state drives that are very expensive when compared to spinning disk drives, but are capable of writing data at a theoretical maximum of 2,500 MB s^{-1}. A RAM drive (or RAM disk) is a block of random-access memory (RAM) that is treated as temporary disk storage. A 7,200 RPM drive can write data at about 230 MB/s, which decreases to 145 MB/s for a 5,400 RPM drive.

Table 14.11: Sequential read and write rates in MB per second for different types of storage devices

Drive type	Drive connection	Sequential rate (MB s^{-1})	
		Read	Write
RAM	FSB	6113	6446
NVMe	PCI x4	3210	2333
SDD	SATA	556	532
SDD	USB 3	435	432
HDD (7,200 RPM)	SATA	237	228
HDD (5,400 RPM)	SATA	195	145

RAM = Random Access Memory
NVMe = Non-volatile Memory express
SDD = Solid-state Drive
HDD = Hard Disk Drive
RPM = Revolutions per minute

FSB = Front Side Bus
PCI = Peripheral Component Interconnect
SATA = Serial AT Attachment
USB = Universal Serial Bus

Based on the above findings, the possibility of running ACRU and AquaCrop in a RAM drive was conducted. A utility called OSFMount (Version 3.0.1005; http://www.osforensics.com/) was used to create multiple RAM drives to support concurrent model runs. However, the utility can only create a maximum of eight RAM drives, which is sufficient for running ACRU as seven concurrent tasks (Table 14.9) and insufficient for the 18 parallel tasks to run AquaCrop (Table 14.10). The developers of OSFMount recommended the running of each task in a separate folder on a single RAM drive, which provides the same speed improvements as creating multiple RAM drives that mimicked physical disks.

14.3.5 Disk space requirements

14.3.5.1 The ACRU model

The next step involved determining the total amount of disk space required to store all the data files for a particular basin. The storage of 28 output variables for 50 years (1950-1999) in binary (.BIN) format requires 2,042 KB of disk space. Similarly, ACRU creates separate files to store interception loss and other water balance information that requires 3,068 and 2,854 KB, respectively. This equates to 7,964 KB of files created by the model for each quinary subcatchment, plus an additional 6 KB for crop yield output. If the interception loss and water balance files are compressed and moved after each basin has been completed, there is sufficient storage space to create daily and monthly data files, as well as statistics files. Hence, 11.2 GB of storage is required to run ACRU for basins C and D and about 3.5 GB for basins W, B, A and T. The remaining basins require between 0.2 and 2.5 GB of storage.

This was a significant finding. Based on the groups shown in Table 14.9, it meant that 12 GB of storage is sufficient for Group 1 basins (i.e. basins C and D) and 4 GB for each of the remaining three groups. Hence, 24 GB of total storage space is required to run ACRU in four parallel sessions. In addition, 12.1 GB of storage is required for the 5,838 climate files containing 50 years of daily data from 1950-1999. The decision was made to store the climate files on the fast NVMe drive, since there was insufficient RAM to copy the climate files into memory.

14.3.5.2 AquaCrop

For each quinary subcatchment, AquaCrop's input climate files require 968 KB of disk space and a file of 57 KB that instructs the model when to start and end each of the 49 seasonal simulations. In addition, 220 KB is required for the monthly or seasonal output file (limited to 12 months for each season) and 132 KB for the generated statistics. Hence, a national run involving all 5,838 quinary subcatchments requires a total of 7.67 GB (i.e. 5,838 * 1377 KB). The decision was therefore made to copy the climate files into memory (RAM) in order to speed up the model runs.

14.3.6 Load balancing

14.3.6.1 The ACRU model

As shown in Table 14.12, Basin C and Basin D are run in the first folder on the RAM drive (called F1), while basins G, S and L are run simultaneously in three other folders (called F2 to F4). Hence, Task 1 and Task 2 start at the same time, and Task 3 begins as soon as Task 2 has completed. Finally, Task 7 finishes at the same time as Task 1. If there was no need to run Basin C and Basin D sequentially, a national run of ACRU could be subdivided into more parallel tasks for faster execution.

Table 14.12: Load balancing of 22 drainage basins allowing seven concurrent runs of ACRU in four separate folders in a single RAM drive to finish at the same time

Task number	RAM drive folder			
	F1	F2	F3	F4
1	C and D			
2		G	S	L
3		F	K	N
4		E	Q	H
5		U and V	B	W
6		R and X	A	T
7		J	P	M

14.3.6.2 AquaCrop

As noted in Section 14.3.3.2, AquaCrop took slightly different times to complete all 18 tasks, each involving 324 runs. Although all 18 tasks are started concurrently, Task 18 finished 152 minutes after the first task. The time that each of the 5,838 output files was written to the RAM drive was analysed to determine which quinary subcatchments could be grouped together, so that all 18 tasks would complete in the same time. Hence, Task 18 was assigned 267 quinary subcatchments, which takes a similar time to run as the 381 quinary subcatchments in Task 1 (Table 14.13).

Table 14.13: Load balancing of 5,838 quinary subcatchments, allowing 18 concurrent runs of AquaCrop in separate folders in a single RAM drive to finish at the same time

Task number	Quinary Subcatchment number		Number of runs
	Start	End	
1	0001	0381	381
2	1981	2304	324
3	0382	0715	334
4	5508	5838	331
5	5172	5507	336
6	4514	4840	327
7	4841	5171	331
8	0716	1057	342
9	1058	1383	326
10	3568	3889	322
11	2305	2634	330
12	3890	4209	320
13	2936	3248	313
14	3249	3567	319
15	2635	2935	301
16	4210	4513	304
17	1651	1980	330
18	1384	1650	267

14.3.7 Automation procedure

Kunz et al. (2015b) reported that considerable effort was spent on automating the procedure whereby ACRU runs non-stop for all 21 basins in a sequential manner. The automation procedure was developed in 2015 using a UNIX scripting language that runs in a “UNIX for Windows” (UWIN) emulator developed by AT&T. However, the UWIN emulator is not compatible with MS Windows 10, and thus failed to start. Owing to this setback, much effort was spent on finding a similar UNIX emulator that is compatible with a Windows 10-based PC. After months of research and testing, “Windows Subsystem for Linux” (WSL) was selected as a suitable replacement for UWIN.

A number of differences between WSL and UWIN became apparent, which meant that thousands of lines of UNIX scripting would not work without modification and re-testing. For example, files created in the UWIN environment are not case sensitive, whereas they are in WSL. In addition, UWIN interpreted both Windows and UNIX paths seamlessly, whereas WSL uses a utility called WSLpath to convert Windows to UNIX paths. Hence, the automation procedure was first modified to work properly in WSL, then adapted to run ACRU in four parallel sessions as opposed to sequentially. In order to automate the national model runs, approximately 8,600 and 10,000 lines of code (in UNIX and Fortran) were developed for AquaCrop and ACRU, respectively. In addition, over 1,400 lines of code were written to convert the climate input files from ACRU format to that required by AquaCrop.

14.3.8 Model run time

14.3.8.1 The ACRU model

ACRU was run for baseline conditions to simulate runoff generation from a land cover of natural vegetation for all 5,838 quinary subcatchments. The national run took approximately 51 minutes to complete, which represents a significant reduction in computational expense when compared to the run time of 510 minutes obtained in the previous biofuel project (cf. Table 14.8). This means that ACRU users now spend far less time waiting for model runs to complete, which allows them to consider additional scenarios.

The “load balancing” highlighted in Table 14.9, where the model is run simultaneously in seven folders in one RAM drive, worked very well, with Basin C and Basin D taking 3,063 seconds (51 minutes) to complete and finishing only five seconds before all other basins were completed. Table 14.14 shows that the majority of the time (81.5%) is spent actually running the model for all 1,443 quinary subcatchments, followed by the amount of time required to compress ACRU’s binary and daily output files.

Table 14.14: Time in seconds to run the ACRU model for Basin C and Basin D, and to create all other output files

Task	Number of seconds	Percentage of total
Copy files to RAM drive	10	0.3
Run ACRU model	2,497	81.5
Compress ACRU output (except .BIN) files	245	8.0
Create daily output files	43	1.4
Compress daily output files	158	5.2
Create monthly output files	7	0.2
Compress monthly output files	6	0.2
Create statistic files	6	0.2
Compress statistic files	4	0.1
Compress .BIN files	70	2.3
Compress ACRU menu and other input files	2	0.1
Copy files to permanent storage disk	15	0.5
Total	**3,063**	**100.0**

To date, other WRC-funded projects at the University of KwaZulu-Natal have benefitted from these speed improvements, most notably WRC Project No. K5/2560. This project required the running of ACRU at quaternary catchment scale to assess the impact of numerous land use change scenarios on runoff generation. Other projects that will benefit in the future include WRC projects K5/2791, K5/2792 and K5/2833.

14.3.8.2 AquaCrop

In the previous biofuel project, Kunz et al. (2015a) (cf. Section 6.3.4) reported that sequential runs of AquaCrop at the national scale for soybean took 89.3 hours to complete and 61.8 hours for grain sorghum. The approach developed in this project to execute the model simultaneously in multiple folders in a single RAM drive has reduced the run time to approximately 25 hours. Again, this represents a significant reduction in computational expense, which was further reduced to 16 hours when run on the faster PC.

14.3.9 Further optimisation of national runs

14.3.9.1 The ACRU model

Table 14.14 highlights the time spent creating daily and monthly output files from ACRU, the latter being essential for calculating statistics. As noted in Section 14.2.3.2, a new statistics utility was developed for this project to calculate statistics directly from ACRU’s output (BIN) files. With the new *BIN2STA* utility, there is no longer a need to generate daily and monthly data files, which represents another significant time saving. This reduced the national run time from 51 to 38 minutes.

Kunz et al. (2015a) reported that disabling the PC’s anti-virus software considerably reduced the time to complete a national run of ACRU. Hence, additional tests were carried out to assess the impact of the antivirus software scanning each file created by ACRU and its utilities. With the antivirus software disabled, Version 3.38 ran 7.9 times faster on a hard disk drive when compared to Version 3.37.

This highlights the importance of disabling the antivirus when running ACRU on slower hard drives. On a fast NVMe or RAM drive, only a slight performance increase was observed when the antivirus software was disabled. Other tests were conducted to test if the ACRU executable optimised for a CORE-AVX512 instruction set ran faster than a COMMON-AVX512 CPU (Table 14.1). Again, no significant differences were found.

No further optimisation is deemed necessary. Thus, the current automation procedure is considered efficient (i.e. computational expense is minimised). Although a multi-threaded version of the model would significantly improve its performance, it would require a complete restructuring of the Fortran code, which is a process that would take months to complete.

14.3.9.2 AquaCrop

Similar to ACRU, the AquaCrop model runs as a single process in a single core (i.e. not multi-threaded). Hence, running the model as multiple instances on a RAM drive offers significant reductions in computational expense. However, it is highly recommended that the model developers produce a multi-threaded version of AquaCrop. Alternatively, the reader should investigate an open-source version of the model called AquaCrop-OS, developed by Foster et al. (2017). The authors re-coded Version 5 and Version 6 of AquaCrop in Matlab, which facilitates parallel execution of the model.

Based on the above outcomes, it is recommended that the simulation models are run on a RAM drive. The computer should have sufficient RAM (> 24 GB is suggested). If this is not possible, then run the simulation models on a NVME or SSD drive. If the models are run on slower (e.g. spinning) hard drives, it is important to disable the antivirus software to prevent scanning of all model input and output files. Alternatively, configure the antivirus program to prevent the model executable and its output from being scanned.

CHAPTER 15: MODELLING OF CROP WATER USE AND YIELD

15.1 INTRODUCTION

As noted in Section 9.1.2, FAO's AquaCrop model was selected to estimate the attainable yield of each strategic biofuel feedstock. A brief description of the model is provided in Section 9.2.2. For the previous biofuel project, the model was successfully linked to the quinary subcatchment database. This effort facilitated the use of a deterministic crop model to derive crop yields at the national scale for the very first time. Prior to this, simple empirical crop models based on monthly climate input (e.g. those developed by Smith, 2006) had been used to estimate crop yields for each quinary subcatchment. However, Kunz et al. (2015a) reported that the model took days to complete a national run. The model's computational expense was significantly reduced (cf. Section 14.3.8.2), allowing multiple scenarios to be run (i.e. for different planting dates and densities). A summary of the approach used to estimate attainable crop for each quinary subcatchment is given next.

15.2 APPROACH

The crop modelling approach followed in this project is similar to that used by Kunz et al. (2015b) in the previous biofuel project. A summary of the approach used to model the water use efficiency of both soybean and sorghum is given next, together with a list of significant improvements that were made.

- Since the field trials undertaken in this project were rainfed and not irrigated, the measured crop water use and yield data collected over four seasons could not be used to calibrate AquaCrop.
- Default values provided by the model developers (FAO) were used for most of the crop parameters (cf. Section 11.1.1.1 for soybean; Section 11.1.2.1 for sorghum), except for 11 parameters where more representative values were obtained from the literature for sorghum.
- For both crops, a partial calibration of the model was undertaken to adjust certain parameters related to the thermal time required for the completion of various phenological growth stages. Observations were made in days, and then converted to GDD within the model.
- The parameters shown in Table K.10 (Appendix K) for soybean cultivar LS6161R were used in this project for modelling purposes. Similarly, parameters given in Table I.16 (Appendix K) were used for grain sorghum (PAN8906).
- From a review of the available literature, typical planting dates for both crops were obtained (cf. Section 10.3.1 and Section 10.3.2). Due to the range in planting windows, two dates (1 November and 1 December) were selected for each crop.
- An algorithm was used to estimate the first planting date in each year, based on certain rainfall and air temperature criteria (cf. Section 10.3.3). From the 50 planting dates determined for each quinary subcatchment, the mean and median months were calculated. For the majority of the quinary subcatchments, the first planting date occurred in November and December, with a few subcatchments suited to October or January plantings.
- Typical planting densities deemed suitable for smallholder farmers were obtained from the literature. The following two plant populations were selected for each crop: 250,000 and 300,000 plants ha^{-1} for soybean, and 44,444 and 60,000 plants ha^{-1} for sorghum.
- The quinary subcatchment climate database was revised for this study (cf. Section 10.1), where corrections were made to extreme rainfall events and observed temperatures were selected to represent each quinary subcatchment. The climate database was then converted into the format required by AquaCrop as described in Section 10.1.5.
- For the model runs, the simulation period was linked to the growing cycle of the crop.

- The initial soil water content was assumed to be at field capacity.
- The model was run with irrigation invoked to determine the net irrigation water requirement in order to relieve crop water stress when soil water content reached 50% of plant available water, so that monthly crop coefficients could be derived for standard conditions.
- The model was then re-run to estimate crop water use and yield for rainfed conditions, from which water use efficiency was estimated.
- AquaCrop was run at the national scale for all 5,838 quinary subcatchments, regardless of whether the feedstock could be successfully grown in the quinary subcatchment.
- Eight national runs were performed for this project, i.e. two crops x two planting dates x two planting densities x two systems (rainfed and irrigated).
- Significant improvements were made to optimise model runs at the national scale in order to reduce computational expense. This was achieved by the following:
  - Starting 18 parallel (i.e. simultaneous) simulations, each handling approximately 324 quinary subcatchments
  - Restricting the maximum season length to 365 days (i.e. reduced model run times in areas that are too cold for crop production)
  - Configuring the PC's antivirus software to not scan output files created by AquaCrop
  - Running the model on two PCs

15.3 RESULTS AND DISCUSSION

15.3.1 First planting date

The algorithm used to determine the first suitable planting date in each year (50 in total) for each quinary subcatchment is given in Section 10.3.3.2. The histogram in Figure 15.1 shows that no planting dates could be determined for 1,527 quinary subcatchments (or 26.2%), indicating that these regions are not suited to crop production. The dominant planting months, whether determined using the mean or median statistic, were November and December. For approximately 42.7 and 32.5% of all quinary subcatchments, the first planting date occurred in December based on the mean and median statistic, respectively. This finding supports the decision to use fixed planting dates of 1 November and 1 December in this project.

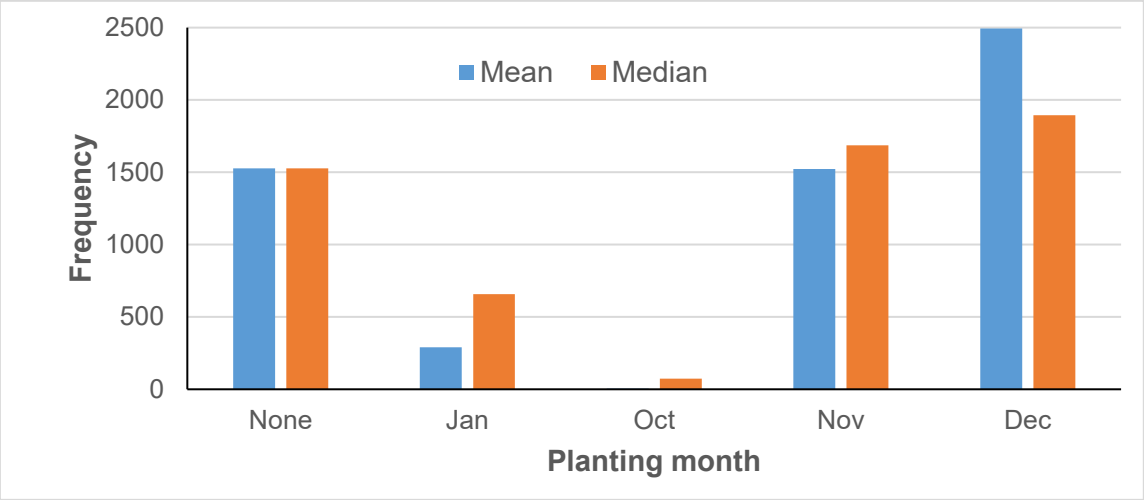

Figure 15.1: Histogram showing the mean and median planting month determined from 50 years of climate record for each of the 5,838 quinary subcatchments

Very few quinary subcatchments exhibit an October planting month, which is possibly due to the average temperature criterion that was used, as well as the consideration of long dry spells. The analysis also showed that few quinary subcatchments are suited to late plantings in January.

From the 2017/18 trial undertaken at Swayimane, planting on 19 January resulted in a decline in air temperature, solar irradiance and rainfall experienced before the end of the crop growing period (cf. Section 7.3.5), indicating that an earlier planting was preferred to avoid cold and water stress. Hadebe et al. (2017a) also found that a January planting at Ukulinga in the 2014/15 season produced a lower leaf number, canopy cover development, chlorophyll content index and stomatal conductance, which indicated that sorghum was subjected to significant water stress (due to lower seasonal rainfall). Phenological development was hastened in order to escape both pre- and post-anthesis water stress, which resulted in early flowering, decreased biomass and grain yields, and thus lower water use efficiency.

15.3.1.1 Mean vs median

Figure 15.2 and Figure 15.3 show the mean and median planting dates, respectively. Areas highlighted in white represent 1,527 quinary subcatchments where no planting date could be determined, and are thus deemed unsuitable for crop production (too dry and/or too cool). No planting dates were determined in the winter rainfall region of the country, since the algorithm only considered dates from 1 October to 31 January. Both maps show the same general pattern where the planting date moves from November in the eastern regions to January in the western regions in response to rainfall seasonality (cf. Figure 13.1 in Section 13.1.8).

However, the median statistic is less influenced by "outliers" and highlights more quinary subcatchments along the eastern coastline where the first planting date occurs in October. Parts of the Northern Cape and the western regions of the Free State and North West reflect a possible late planting window in January. However, this does not imply that sufficient rainfall will occur from January onwards to support the remainder of the crop season. Furthermore, neither map shown below provides any indication of variability in planting dates from year to year, which is discussed next.

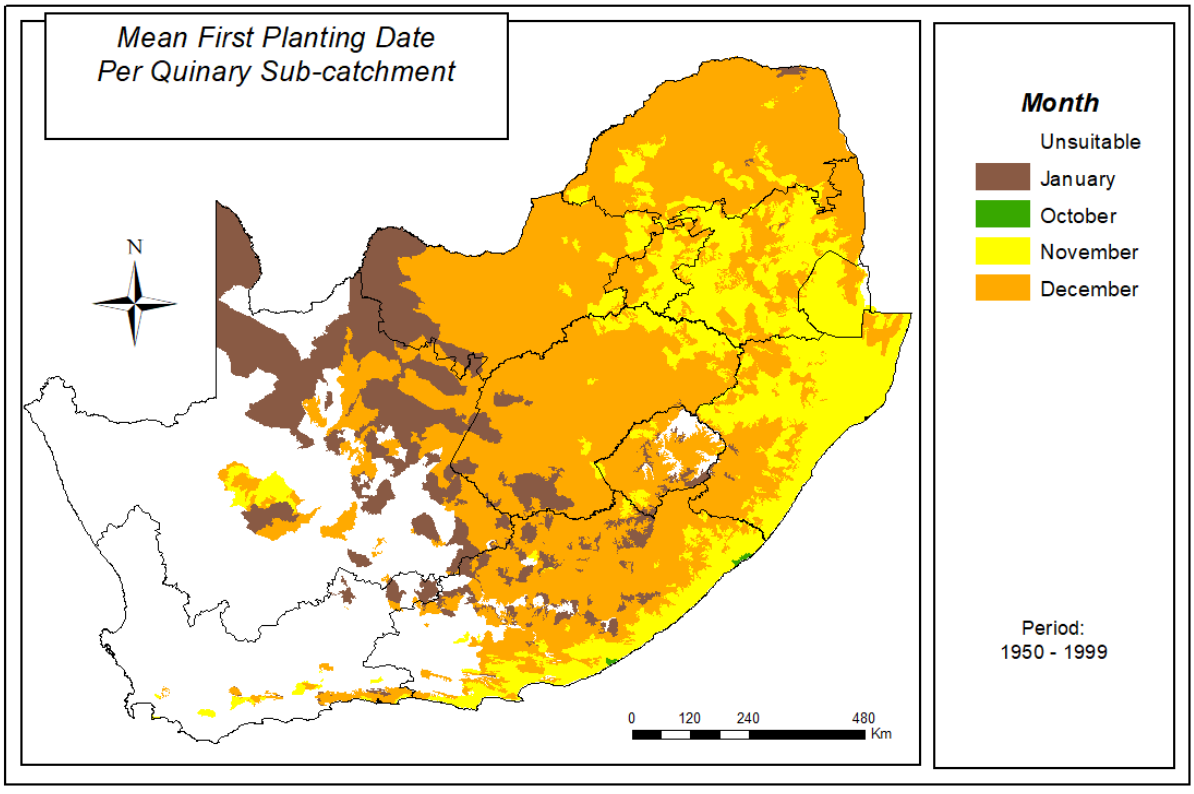

Figure 15.2: Mean planting date obtained from 50 years of historical climate data

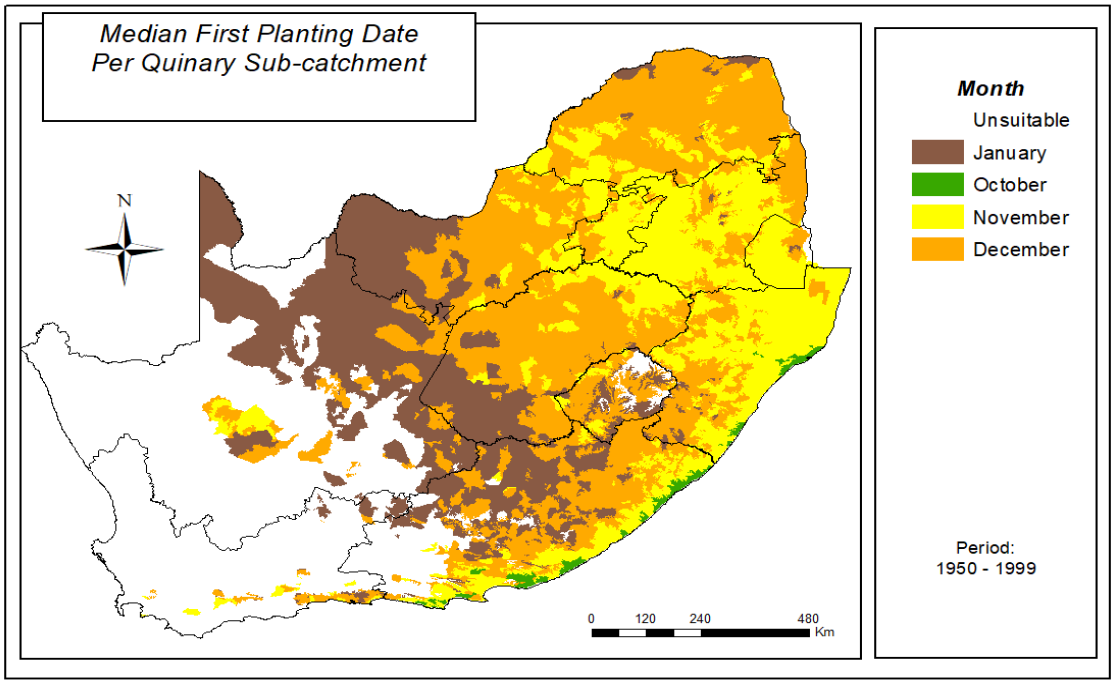

Figure 15.3: Median planting date obtained from 50 years of historical climate data

15.3.1.2 Inter-annual variability

From Figure 15.4, the standard deviation is approximately one month for the majority of areas where the first planting date occurs in either November or December. This means that a November planting varies from October to December over the 50-year period. Similarly, a December planting ranges from November to January. The higher the deviation, the more variable the climate, which results in a "fluctuating" first planting date in each year. This inter-annual variability highlights the fact that possible planting dates should be generated from climate forecasts and not historical climate records.

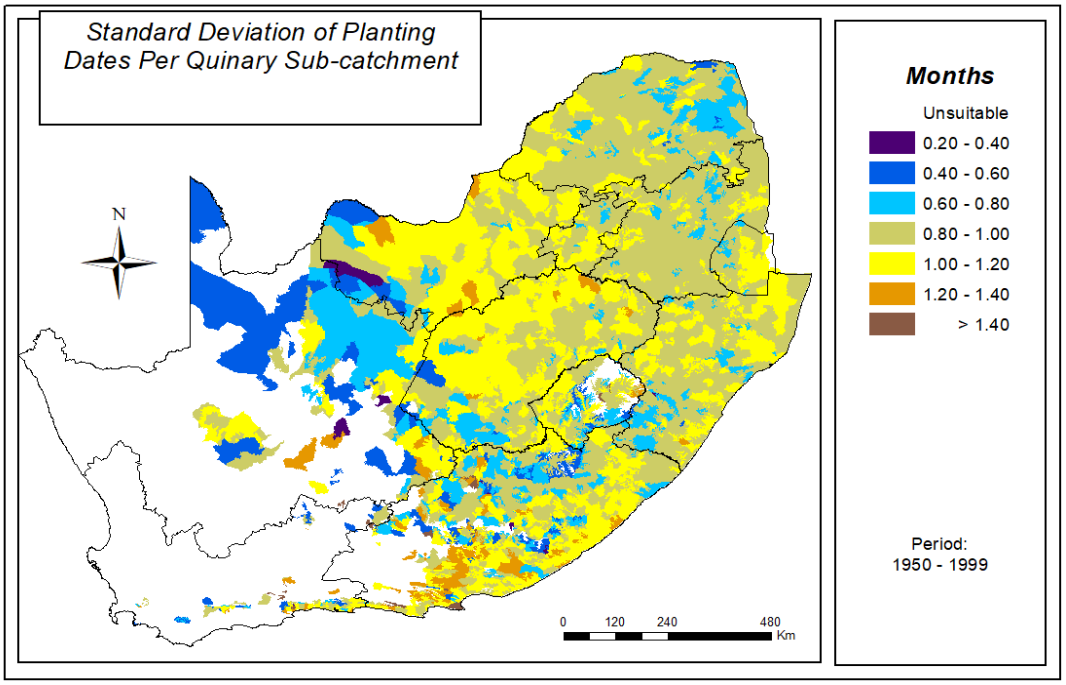

Figure 15.4: Standard deviation of first planting date obtained from 50 years of historical data

15.3.1.3 Risk of crop failure

It is important to highlight that statistics (mean, median, standard deviation) were only generated when the number of years with planting dates exceeded four out of 50 (i.e. 1,527 quinary subcatchments were excluded and deemed unsuitable for crop production). The histogram in Figure 15.5 indicates the suitability of all quinary subcatchments to crop production. For example, only four to six planting dates out of 50 were calculated for 183 quinary subcatchments, which indicates their unsuitability for crop production, due to the high risk of crop failure. On the other hand, 48 to 50 planting dates were determined from the 50-year climate record for 250 quinary subcatchments, which highlights their suitability for crop production. For a one in four-year probability of crop failure, all quinary subcatchments with more than 38 annual planting dates would be deemed suitable for crop production, i.e. 1,961 (or 33.6%) of the 5,838 subcatchments.

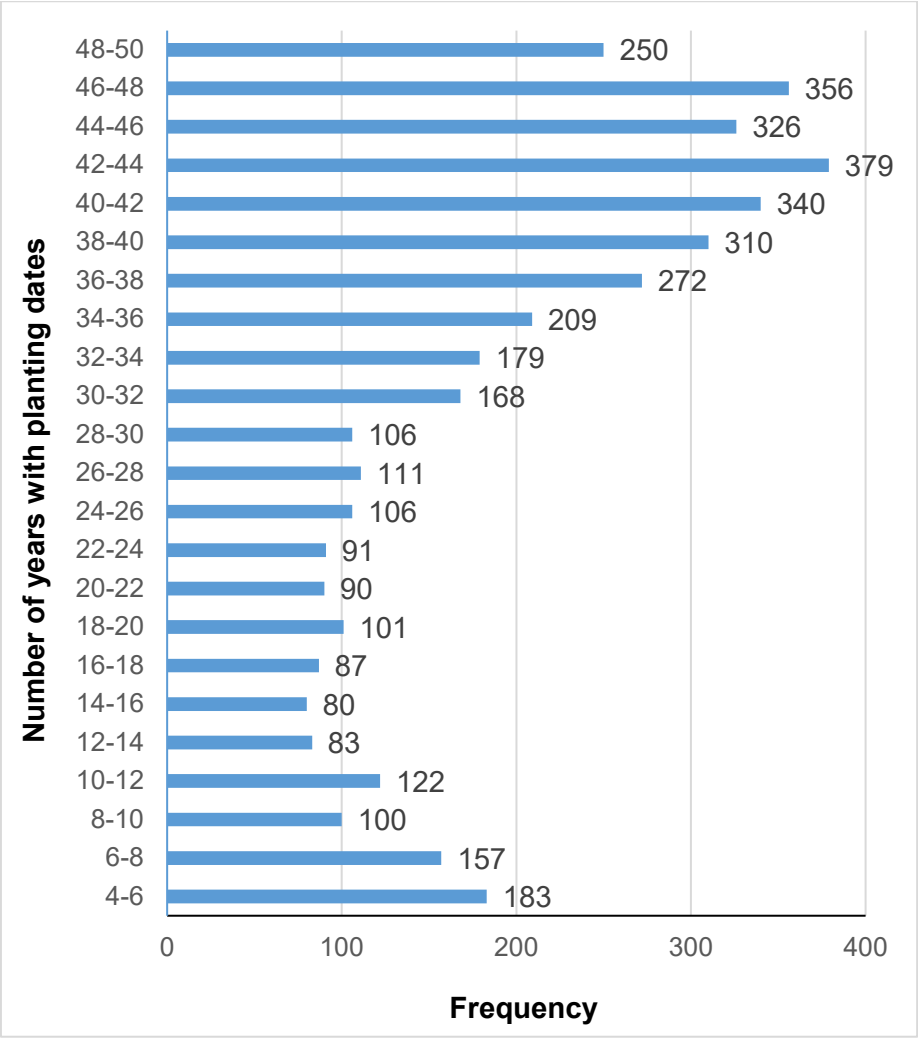

Figure 15.5: Histogram showing the number of years with planting dates for all 5,838 quinary subcatchments

The number of years (maximum 50) with planting dates from which the mean and median were calculated is shown spatially in Figure 15.6. Unsuitable as noted, 1,527 quinary subcatchments with no planting date occur in the western areas (too dry for rainfed crop production) and in high altitude areas (too cold for crop growth). Hence, areas shown in white are considered totally unsuitable for rainfed crop production. Similarly, the lower the number of years with planting dates, the higher the risk of crop failure. Blue and purple areas (i.e. > 38 years) are better suited to crop production, where the risk of crop failure due to insufficient rainfall is relatively low.

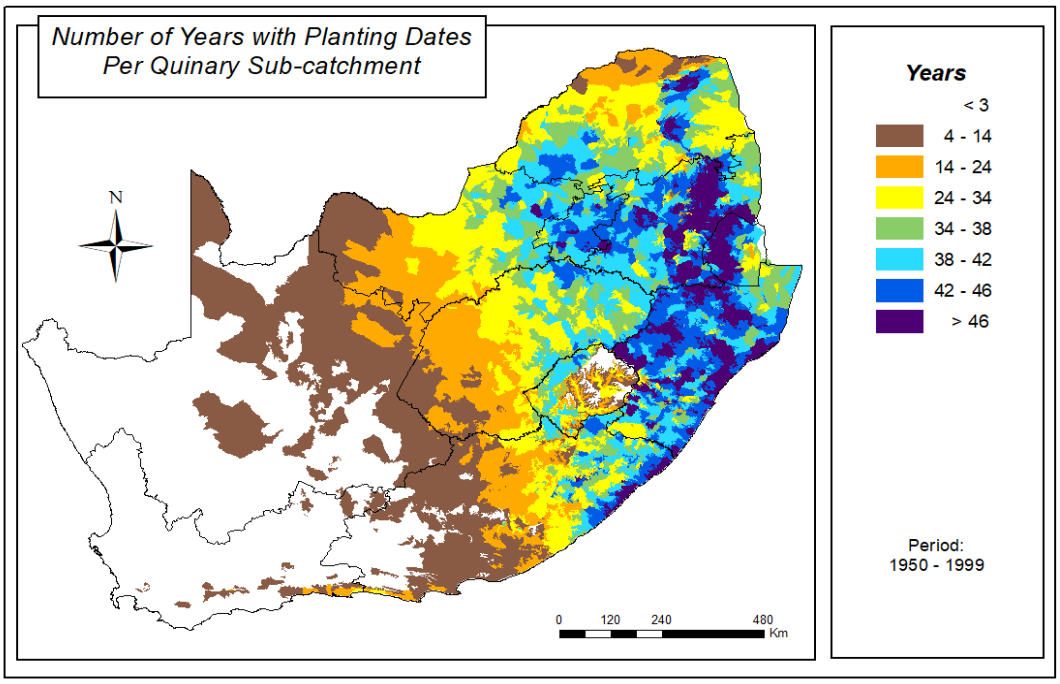

Figure 15.6: Number of years with planting dates from which the mean and median were calculated

15.3.1.4 Summary and conclusions

Although the analysis was conducted using historical climate record, it is acknowledged that planting dates should be determined using climate forecasts. Since the quinary climate database ends in 1999, it does not reflect the climate variability from 2000 to 2019, within which anthropogenically induced changes in extreme climatological events have occurred. For example, 2019 is likely to be the hottest year on record, as was 2018, which superceded 2017, and so on. Hence, the variability in inter-annual planting dates is likely to increase in the latter 20-year period. Hence, the quinary climate record should preferably be extended by 20 years.

15.3.2 Crop yield

The mean seasonal yield was determined for two planting dates (i.e. November and December) and two planting densities, i.e. four maps per crop. Yield estimates in dry tons per hectare (dry t ha^{-1}) were derived using AquaCrop (run in GDD mode) for each of the 5,838 quinary subcatchments. The mean yield was calculated from up to 49 seasonal estimates for rainfed growing conditions. Areas in white indicate low yields (< 0.50 dry t ha^{-1}), and are thus considered unsuitable for crop cultivation under rainfed conditions. All four maps produced for each crop highlight the suitability of the eastern seaboard for rainfed crop production.

Although an average yield was simulated for each subcatchment, the entire quinary subcatchment is not suited to crop production, for example, due to urban and protected areas, as well as existing land use, e.g. commercial forestry. In general, the higher planting density should produce higher yields, particularly in areas with sufficient rainfall. However, such increases are only visible when the mean yield crosses a mapping range of say between < 0.5 and > 0.5 t ha^{-1}.

15.3.2.1 Soybean

Figure 15.7 to Figure 15.10 show mean soybean yield for different planting densities (i.e. 250,000 and 300,000 plants ha^{-1}) and dates (1 November and 1 December). Based on the break-even analysis shown in Section 3.5.1, a yield of 1.77 t ha^{-1} was estimated as being economically viable.

Hence, all regions with an average yield of 1.5 t ha^{-1} or less, may not be suited to biodiesel production from soybean. These maps are very different to those produced in the previous project (Kunz et al., 2015c), which showed that most areas could produce yields exceeding 3 t ha^{-1}. These yield differences are due, inter alia, to a higher planting density (365,500 plants ha^{-1}) and the use of AquaCrop's default soybean parameters, as well as using an earlier version (Version 4) of the model (cf. Section 14.1).

The higher planting density in November resulted in more areas (i.e. quinary subcatchments) with a yield exceeding 1 t ha^{-1}, particularly in the western parts of Limpopo. A comparison of the maps highlights larger changes due to the planting date. Irrespective of the planting density, there is a general increase in yield due to the later planting, most notably in the western parts of Limpopo. However, the yields simulated for the majority of Limpopo are below the break-even value calculated for soybean. As shown in Table 2.4 (cf. Section 2.4), three major biodiesel manufacturers plan to locate processing plants in the Eastern Cape, two of which will be in Port Elizabeth. The high yielding areas near the Eastern Cape's coastline (south of KwaZulu-Natal) appear to be a better option for locating a processing plant and seed crushing facility. In addition, this region should be ideally suited to smallholder cultivation of soybean.

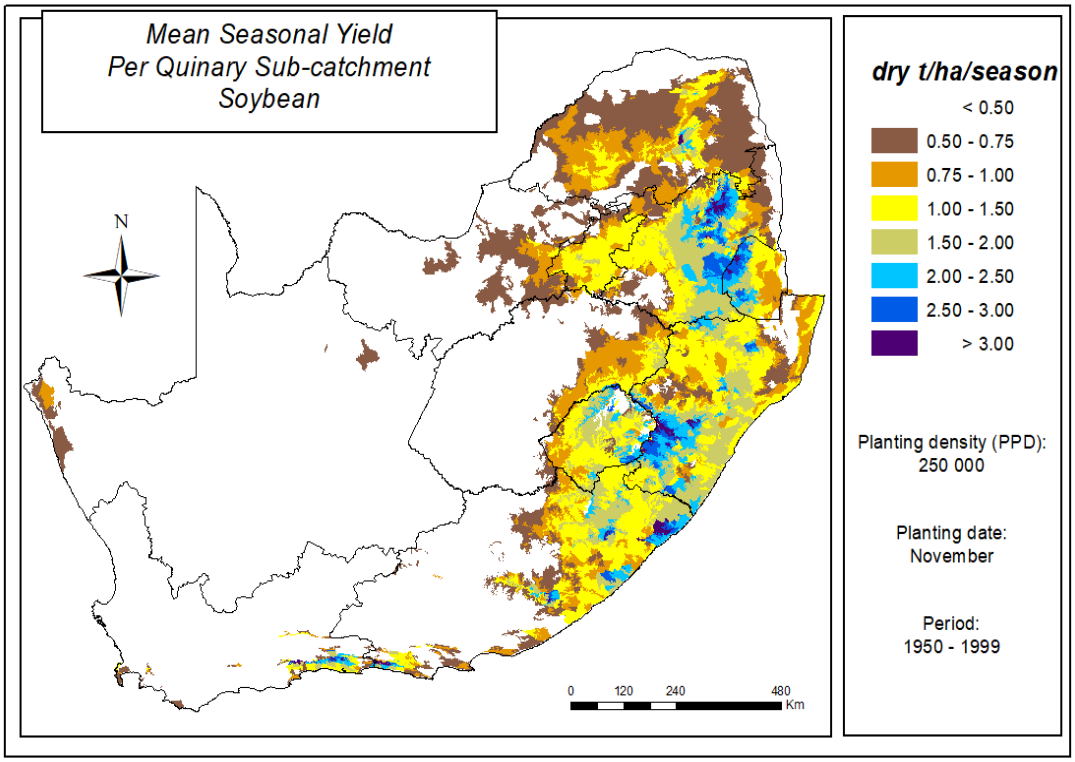

Figure 15.7: Mean seasonal yield per quinary subcatchment for soybean planted in November at a density of 250,000 plants ha^{-1}

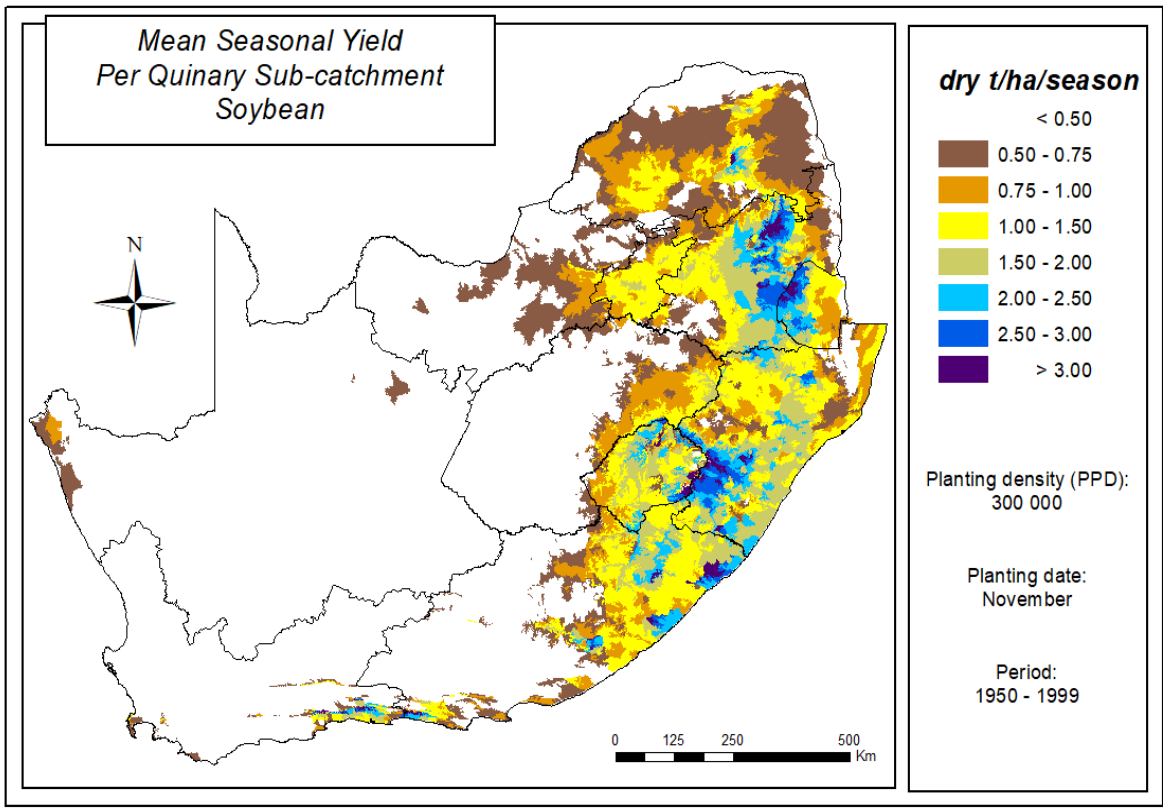

Figure 15.8: Mean seasonal yield per quinary subcatchment for soybean planted in November at a planting density of 300,000 plants ha^{-1}

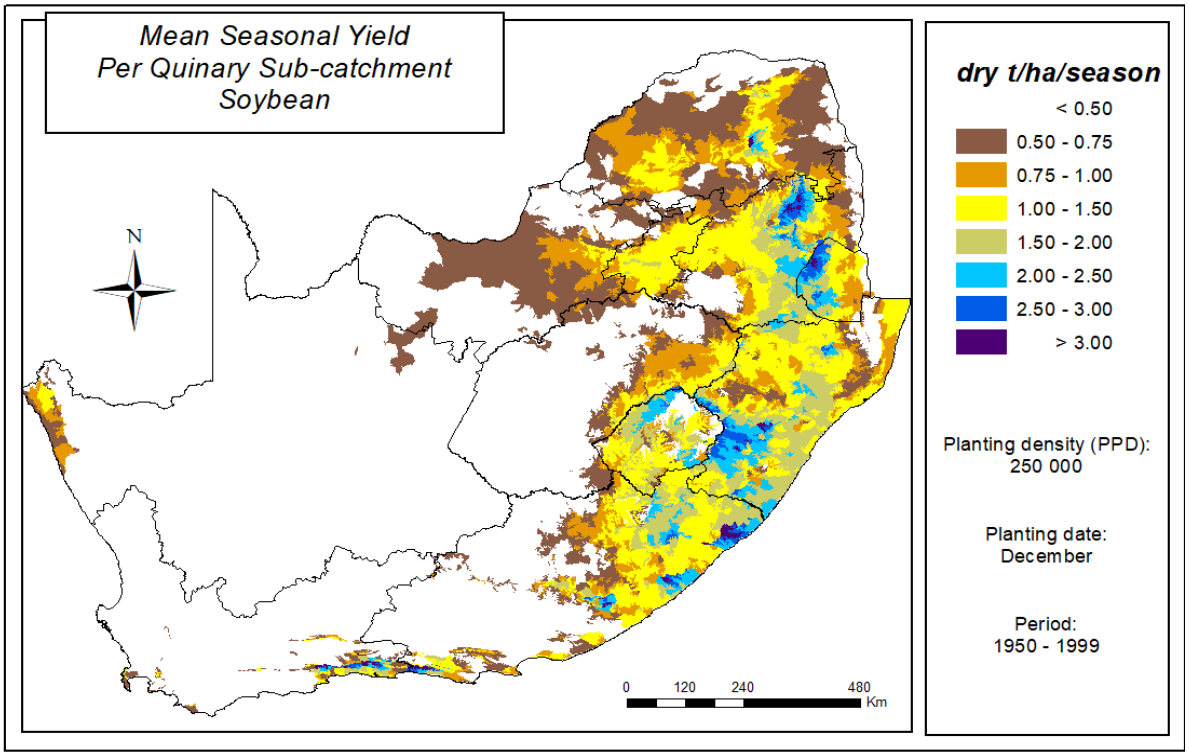

Figure 15.9: Mean seasonal yield per quinary subcatchment for soybean planted in December at a density of 250,000 plants ha^{-1}

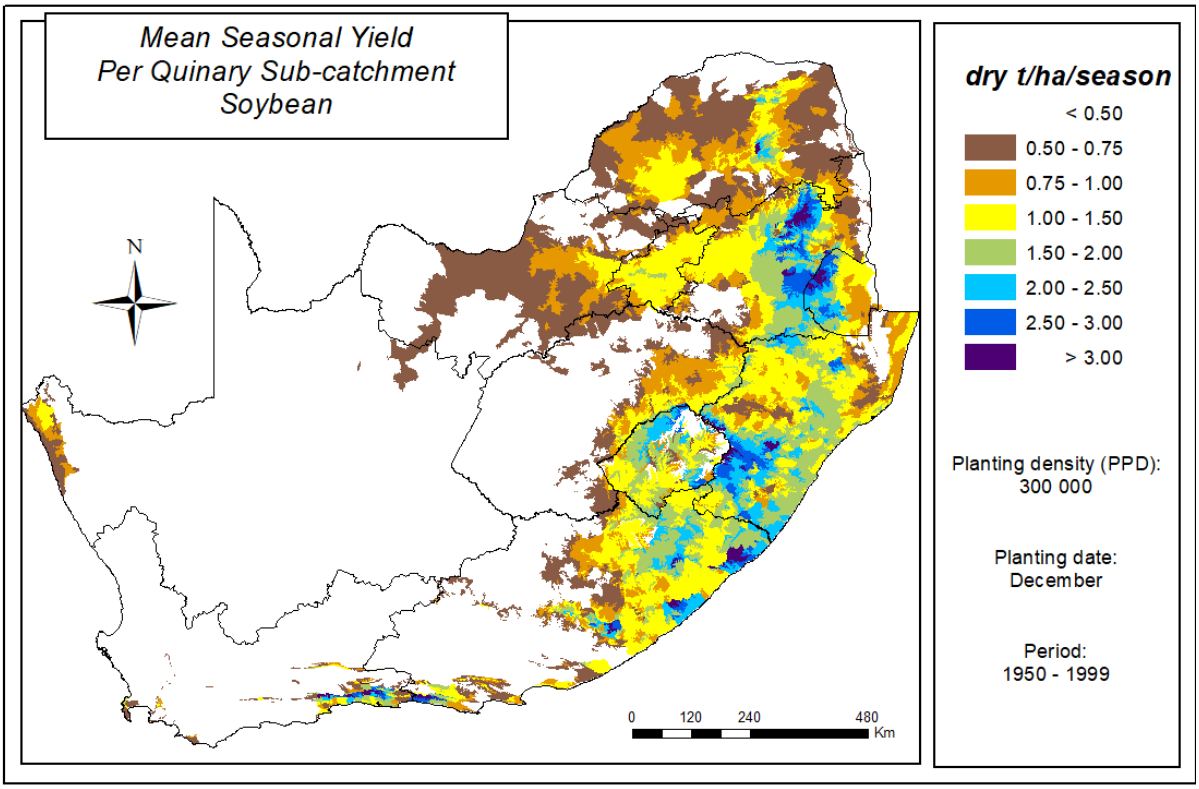

Figure 15.10: Mean seasonal yield per quinary subcatchment for soybean planted in December at a planting density of 300,000 plants ha^{-1}

15.3.2.2 Grain sorghum

Figure 15.11 to Figure 15.14 show mean sorghum yield for different planting densities (i.e. 44,,444 and 60,000 plants ha^{-1}) and dates (1 November and 1 December). According to PANNAR (2013b), average grain yields expected for sorghum vary from 2.5 to 4 t ha^{-1}. Based on the break-even analysis shown in Section 3.5.2, a yield of 3.43 t ha^{-1} was estimated as being economically viable. Hence, regions with an average yield of 3 t ha^{-1} or less, may not be suited to bioethanol production from grain sorghum. These maps are very different to those produced in the previous project (Kunz et al., 2015c), which showed that most areas could produce yields exceeding 6 t ha^{-1}. These yield differences are due, inter alia, to a higher planting density (65,000 plants ha^{-1}) and the use of AquaCrop's default sorghum parameters, as well as using an earlier version (Version 4) of the model (cf. Section 14.1).

The higher planting density resulted in more areas (i.e. quinary subcatchments) with a yield exceeding 2.50 t ha^{-1}. A comparison of the maps highlights larger yield changes due to the planting date. Irrespective of the planting density, there is an increase in areas where the model simulated a mean yield of < 0.75 t ha^{-1}, particularly in North West. However, these yields are below the break-even value calculated for sorghum. As shown in Table 2.4 (cf. Section 2.4), one major bioethanol manufacturer plans to locate its processing plant at Cradock in the Eastern Cape. Again, the high yielding areas near the Eastern Cape's coastline (south of KwaZulu-Natal) appear to be a better option for locating the processing plant.

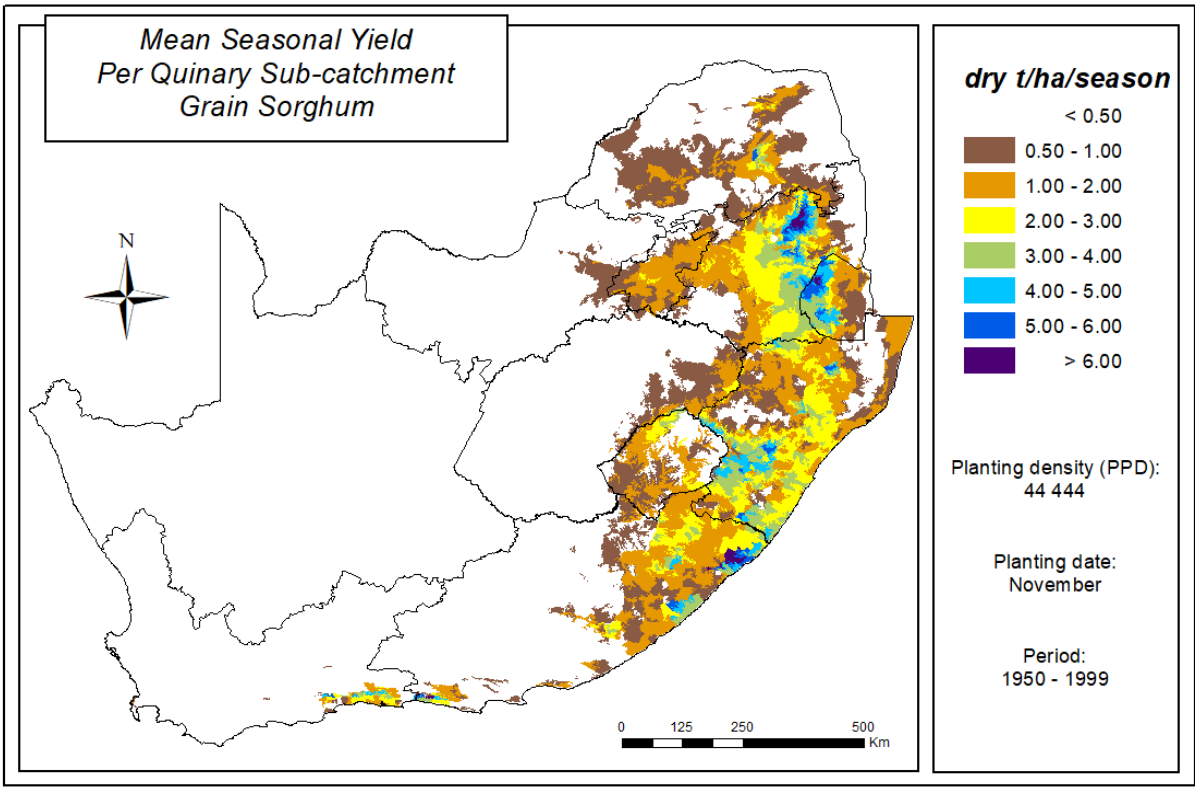

Figure 15.11: Mean seasonal yield per quinary subcatchment for grain sorghum planted in November at a planting density of 44,444 plants ha^{-1}

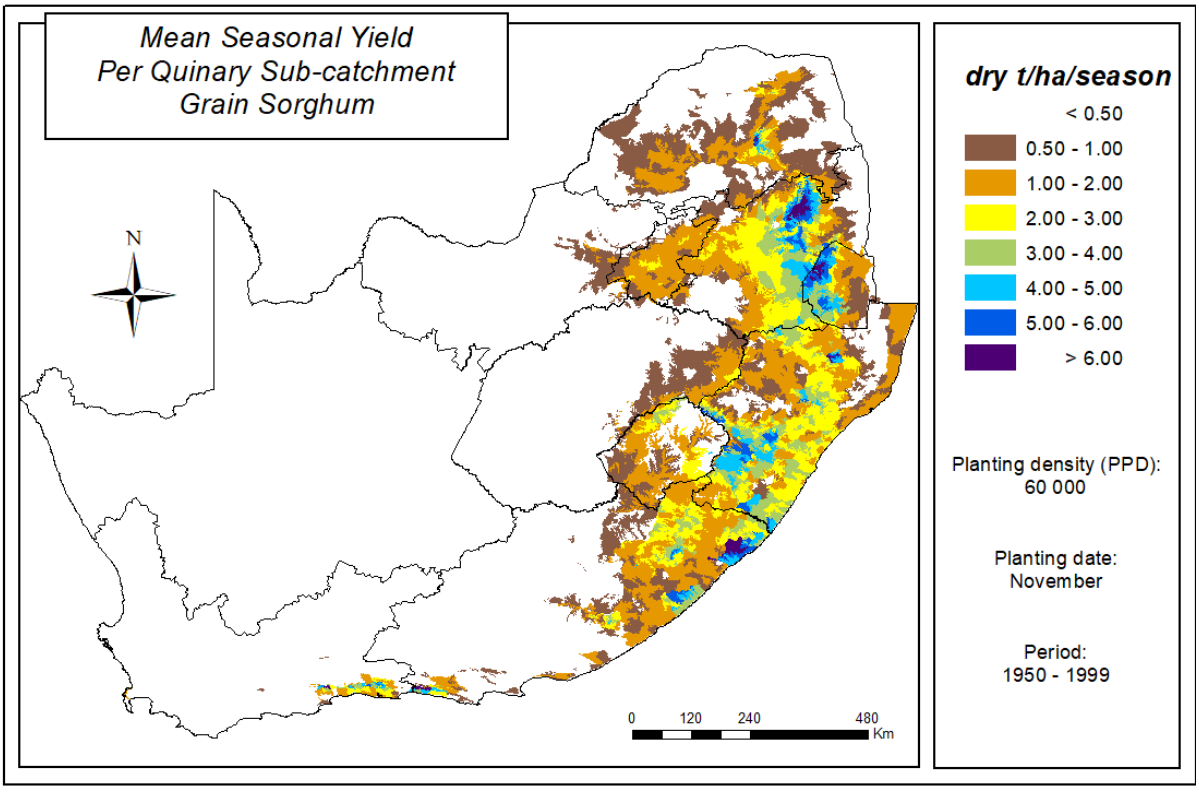

Figure 15.12: Mean seasonal yield per quinary subcatchment for grain sorghum planted in November at a planting density of 60,000 plants ha^{-1}

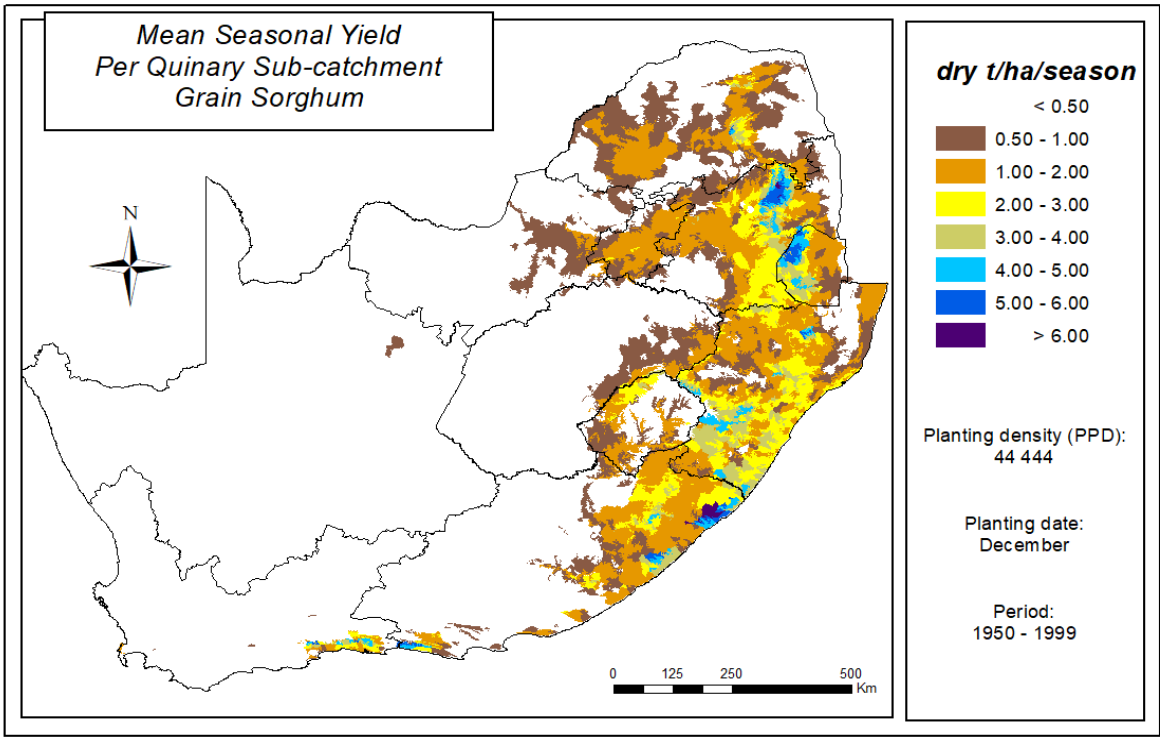

Figure 15.13: Mean seasonal yield per quinary subcatchment for grain sorghum planted in December at a planting density of 44,444 plants ha^{-1}

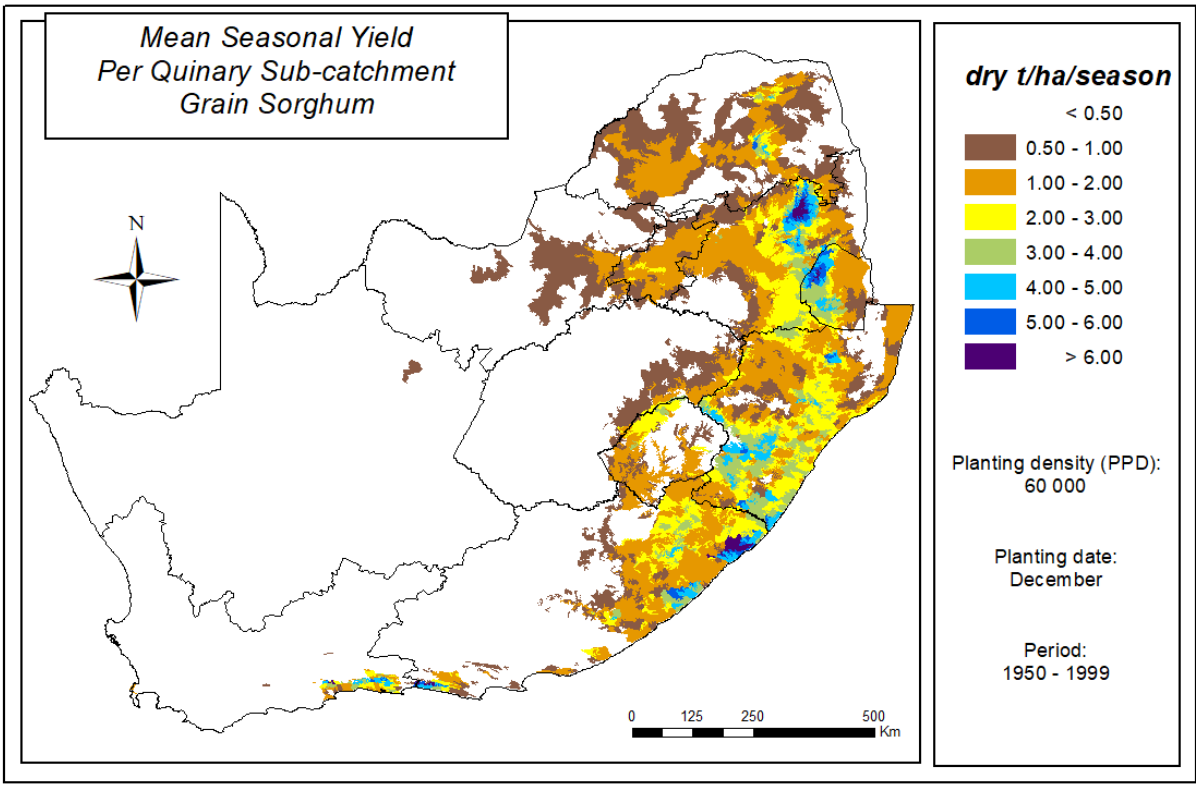

Figure 15.14: Mean seasonal yield per quinary subcatchment for grain sorghum planted in December at a planting density of 60,000 plants ha^{-1}

15.3.2.3 Summary and conclusions

The yield maps clearly highlight low and high potential production areas for soybean and sorghum. Large parts of the country's interior region, especially towards the western areas, are too dry for crop cultivation under rainfed conditions. Of concern is the northern Free State (the central to eastern parts in particular) where soybean is produced (Figure 15.15), yet AquaCrop simulated no yield for either crops. For soybean, this problem is probably due to the partial model calibration undertaken for cultivar LS6161R, which is best suited to warm areas (Maturity Group 6). The Free State is better suited to Maturity Group 4/Maturity Group 5 (cool/temperate) cultivars. Similarly, the model was partially calibrated for sorghum cultivar PAN8906, which may not be suited to the northern Free State. Although partial model calibrations were undertaken for other cultivars (soybean CAPG3 and sorghum PAN8816), national model runs were not done due to time constraints.

Figure 15.15: Soybean production areas based on yields extracted from the Producer-Independent Crop Estimate System (Blignaut and Taute, 2010)

The map shown above was based on rainfed and irrigated areas under commercial soybean production during the 2008/09 season. However, it does not highlight where soybean is irrigated. For example, the soybean production area along the Northern Cape and Free State border is mostly irrigated, and this region also grows a specific soybean cultivar suited to this region only. For this region, AquaCrop would need to be fully calibrated for this specific cultivar, and then used to estimate crop yields.

15.3.3 Crop Water Use Efficiency

The Water Use Efficiency of crop production is the attainable yield (in dry kg ha^{-1}), relative to crop water use (i.e. actual evapotranspiration in m^{-3}), accumulated from planting to physiological maturity. The mean seasonal WUE under rainfed conditions was determined for each planting date and density scenario, i.e. four maps per crop. Estimates of average WUE (in dry kg m^{-3}) were derived using AquaCrop from up to 49 seasons. The WUE maps follow similar trends evident in the yield maps, which highlights the sensitivity of this metric to yield input.

15.3.3.1 Soybean

The WUE maps for soybean (Figure 15.16 to Figure 15.19) highlight the same trend of higher WUE along the eastern seaboard, compared to the western regions. Areas in white indicate low WUEs (< 0.20 kg m^{-3}) and thus, should be considered too dry or too cold for rainfed crop production. However, the maps show that the crop is most water use efficient in small parts of Limpopo and Mpumalanga, but more noticeably along the Eastern Cape coast. In these areas, the model simulated the highest yields, which again highlights this part of the country where feedstock cultivation by smallholder famers should be encouraged.

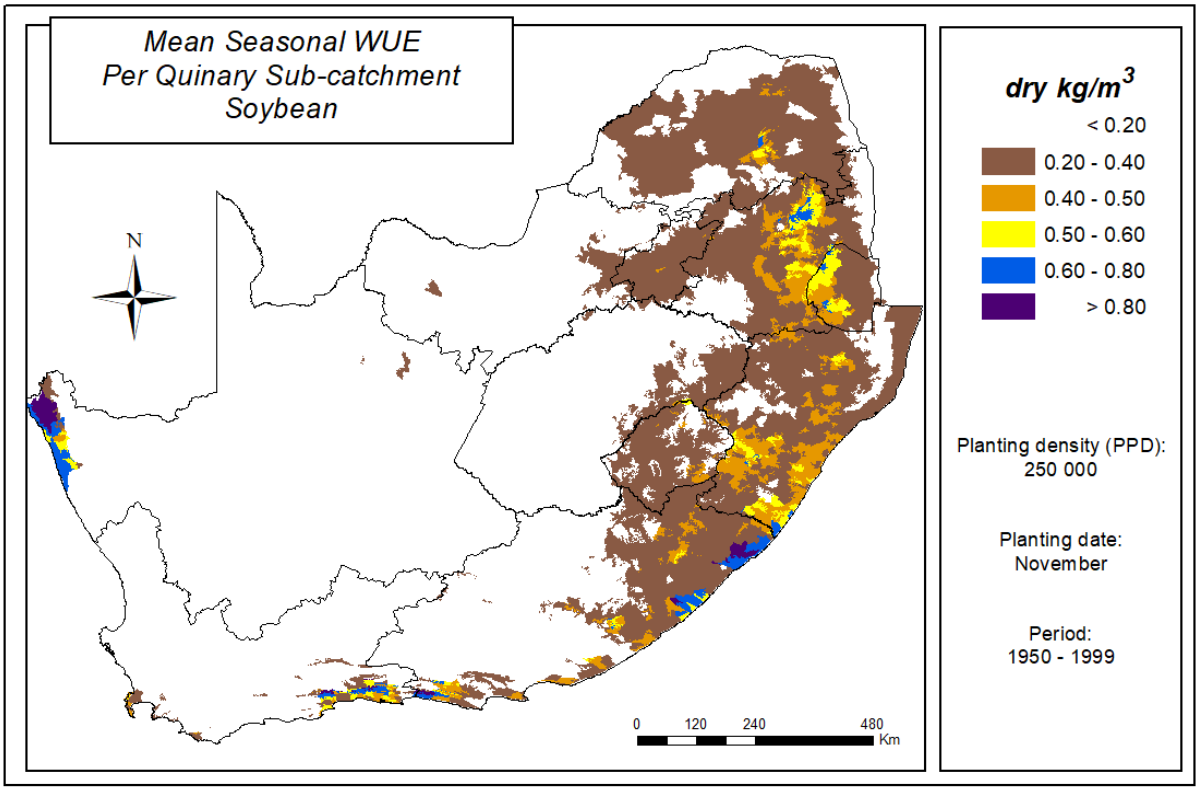

Figure 15.16: Mean seasonal water use efficiency per quinary subcatchment for soybean planted in November at a planting density of 250,000 plants ha^{-1}

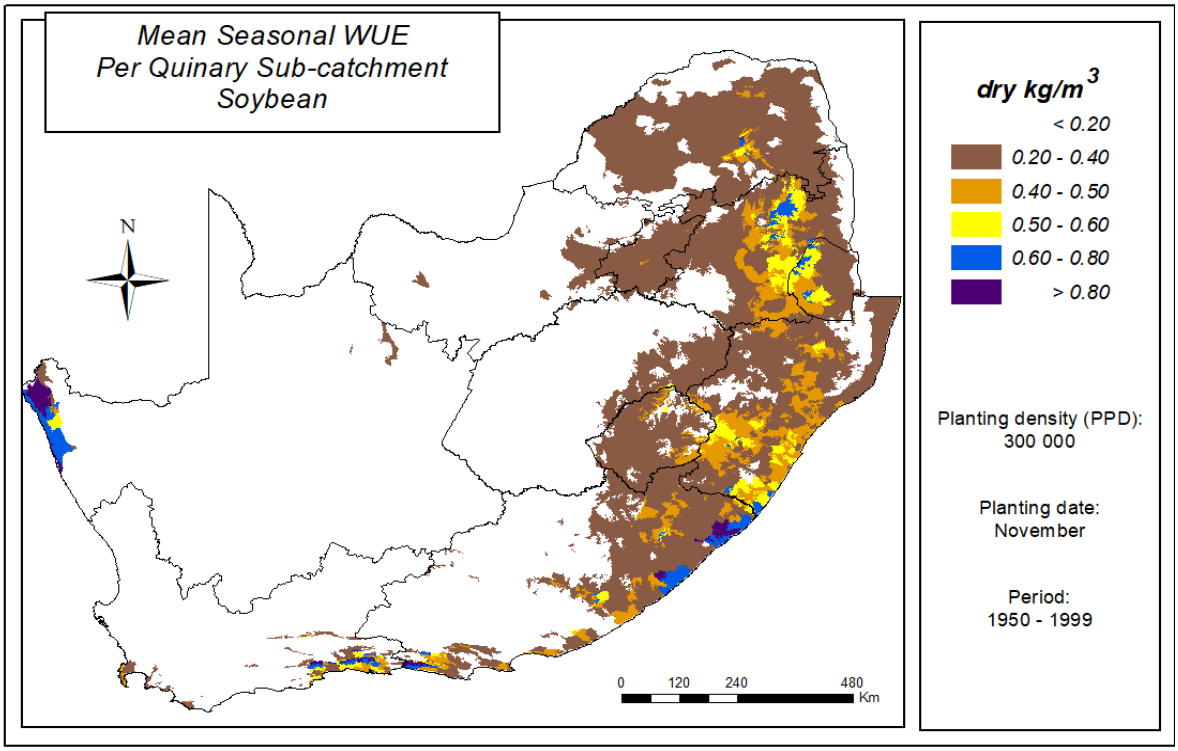

Figure 15.17: Mean seasonal water use efficiency per quinary subcatchment for soybean planted in November at a planting density of 300,000 plants ha^{-1}

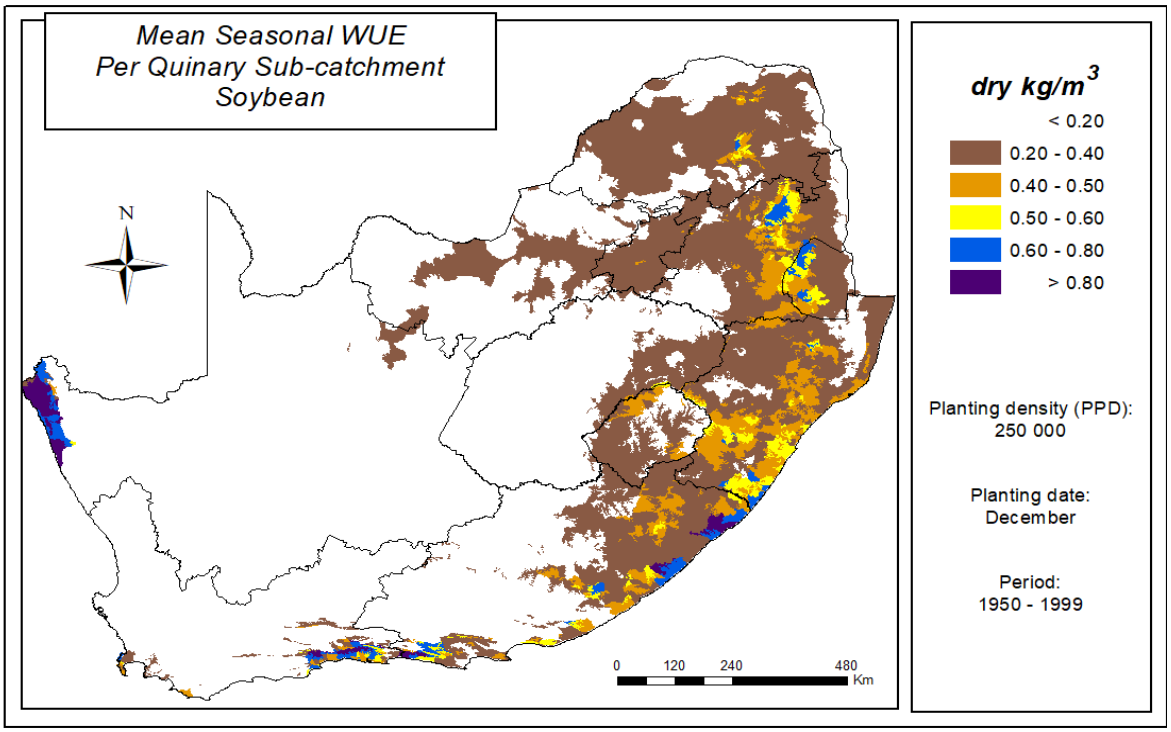

Figure 15.18: Mean seasonal water use efficiency per quinary subcatchment of soybean planted in December with a planting density of 250,000 plants ha^{-1}

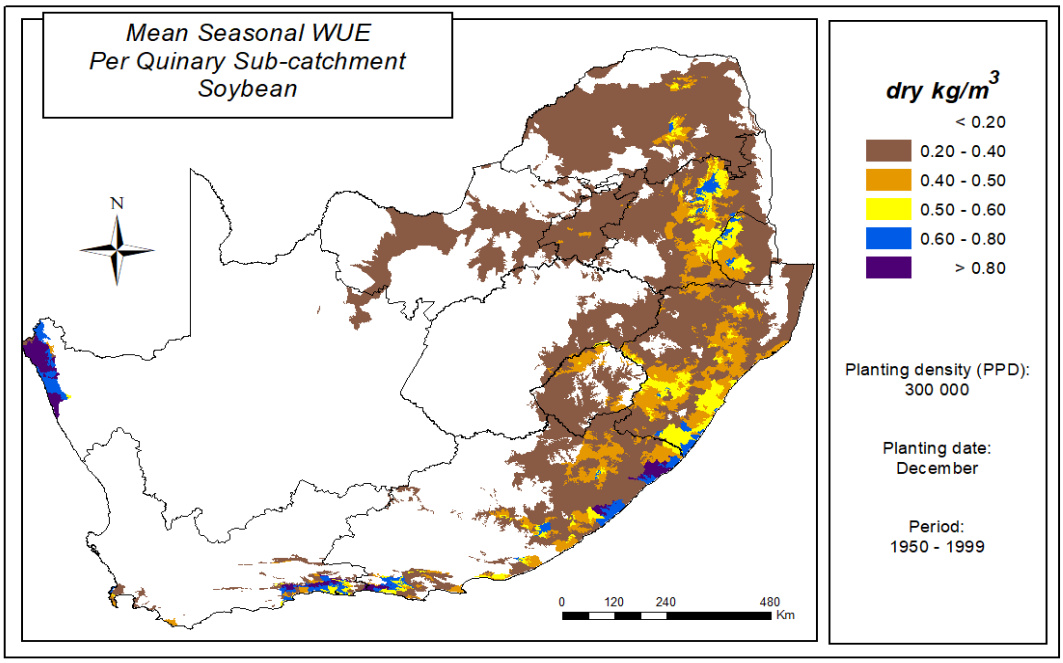

Figure 15.19: Mean seasonal water use efficiency per quinary subcatchment for soybean planted in December at a planting density of 30,0000 plants ha^{-1}

15.3.3.2 Grain sorghum

Maps of mean seasonal WUE for grain sorghum cultivation based on different planting dates and planting densities are presented in Figure 15.20 to Figure 15.23. Unsuitable areas (shown as white) indicate a mean WUE < 0.50 kg m^{-3}. Such areas are therefore too dry or too cold for grain sorghum cultivation under rainfed conditions. The maps show that grain sorghum is most water use efficient when cultivated along the coastal areas of southern KwaZulu-Natal and the Eastern Cape, with a December planting producing more “crop per drop” than the November planting at a higher planting density (i.e. 60,000 plants ha^{-1}). This trend was also highlighted by Kunz et al. (2015c) in the previous project.

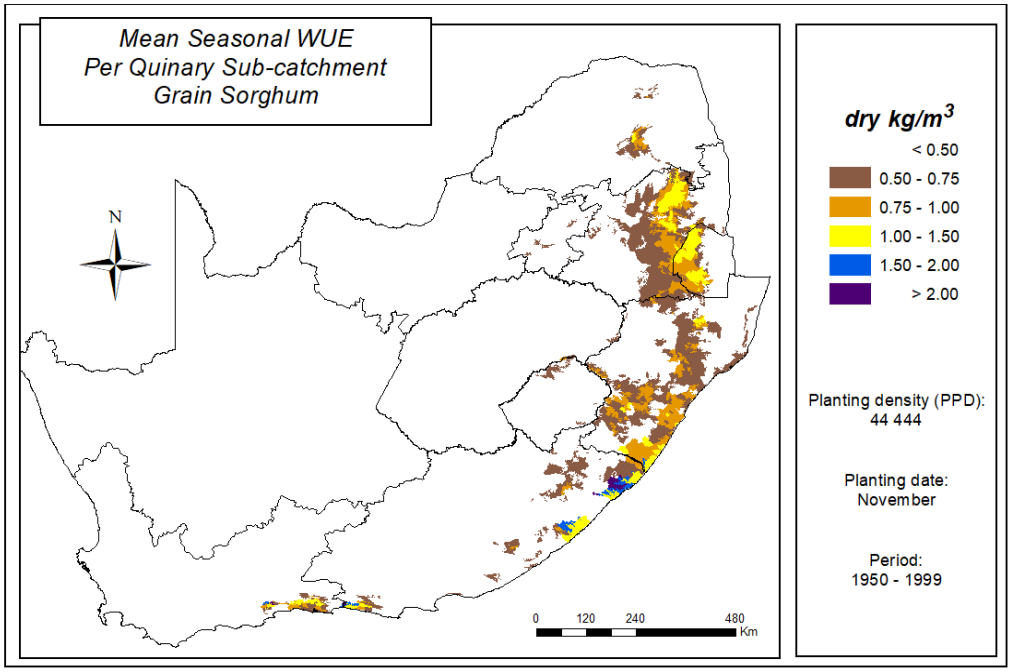

Figure 15.20: Mean seasonal water use efficiency per quinary subcatchment for grain sorghum planted in November at a planting density of 44,444 plants ha^{-1}

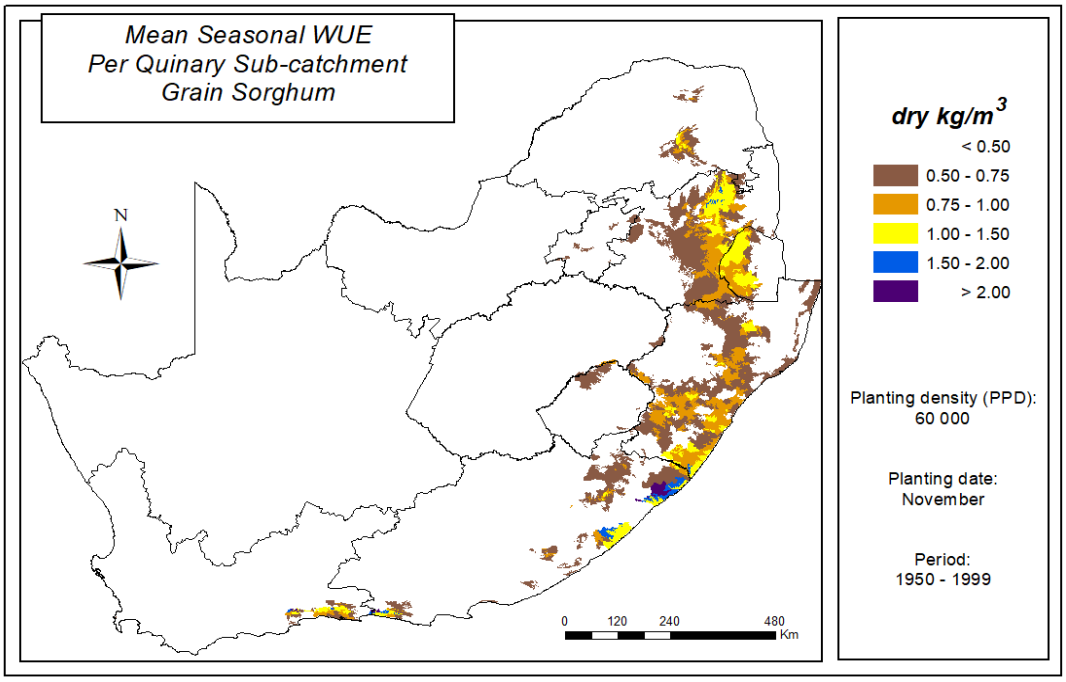

Figure 15.21: Mean seasonal water use efficiency per quinary subcatchment for grain sorghum planted in November at a planting density of 60,000 plants ha^{-1}

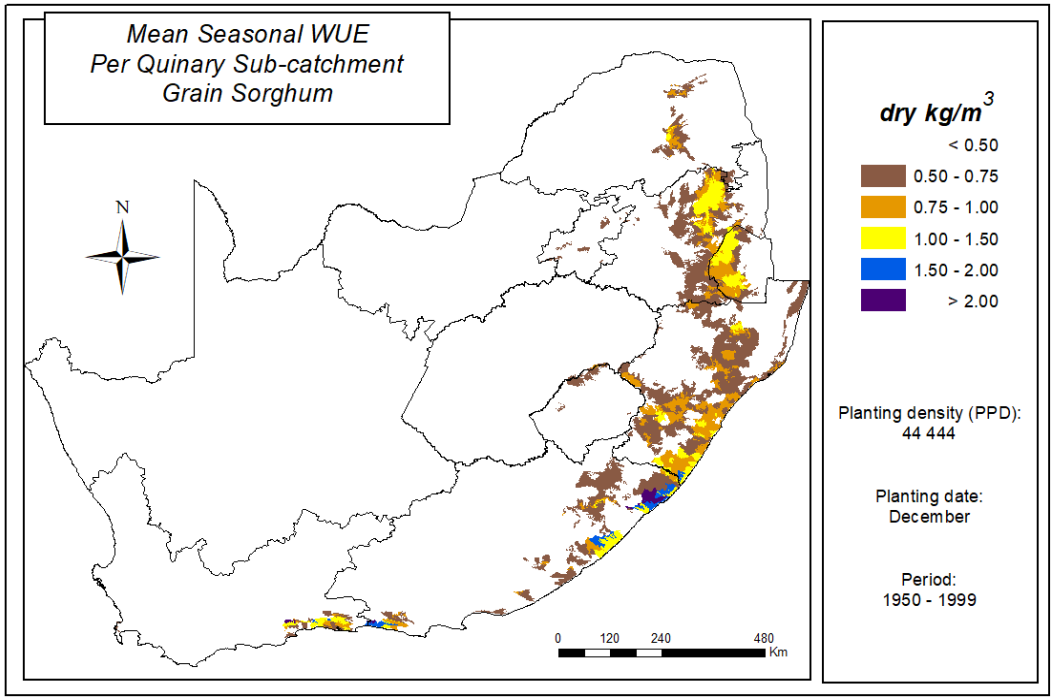

Figure 15.22: Mean seasonal water use efficiency per quinary subcatchment for grain sorghum planted in December at a planting density of 44,444 plants ha^{-1}

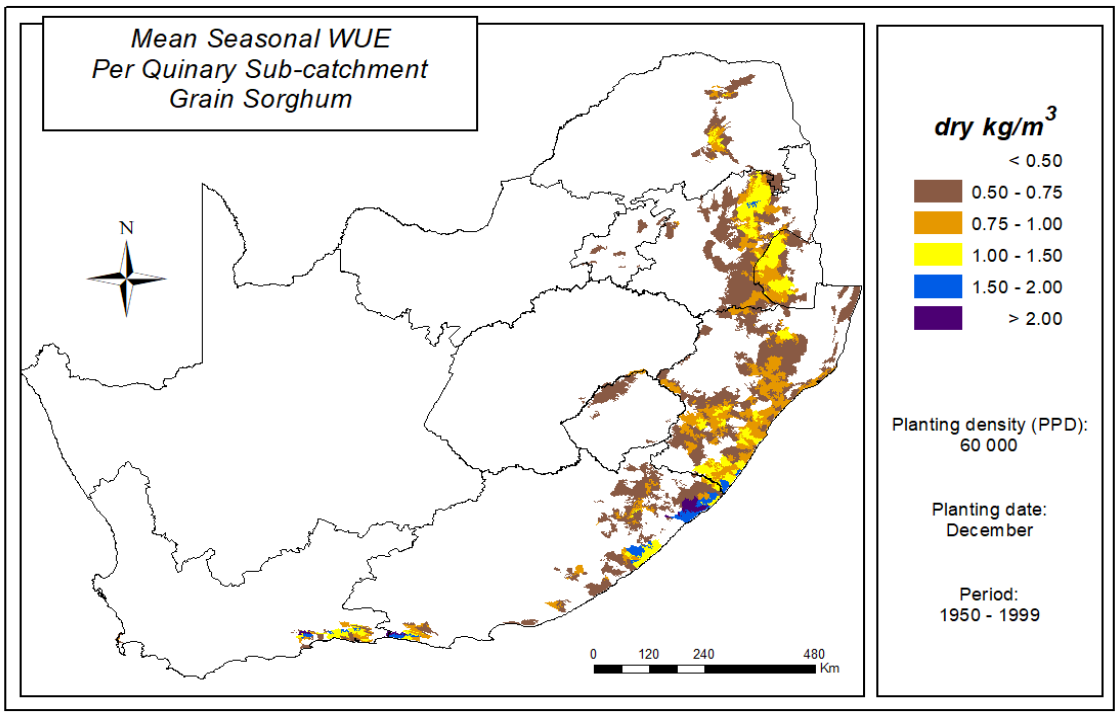

Figure 15.23 Mean seasonal water use efficiency per quinary subcatchment for grain sorghum planted in December at a planting density of 60,000 plants ha^{-1}

15.3.3.3 Summary and conclusions

The analysis showed that the WUE of sorghum is greater than that of soybean, due to higher grain (sorghum) yields when compared to seed (soybean) yields. The map show that changes in the planting date had a greater impact on crop production than the changes in planting density.

Since soybean cultivar LS6161R is semi-determinate, it continues to form new leaves after flowering. AquaCrop will struggle to accurately simulate the crop evapotranspiration of indeterminate crops, considering the model will reduce transpiration as the leaves dry out and mature towards the end of the season. Hence, the model is likely to under-estimate measured crop water use, and thus over-estimate crop WUE.

It is important to note that the WUE maps can be misinterpreted. A relatively high WUE may be calculated due to low crop evapotranspiration. For example, soybean exhibited relatively high WUE along the west coast in the Northern Cape. However, the yield estimates were below 1.5 t ha^{-1}, and thus high WUE resulted from low crop evapotranspiration. It is therefore recommended that the WUE maps are interpreted in conjunction with the yield and season length maps.

15.3.4 Biofuel yield

Theoretical biofuel yield was estimated using the equations provided in Chapter 12, with inputs of average crop yield and average seed oil content or starch content. An analysis of which planting date and density scenario produced the highest biofuel yield is shown in Table 15.1. For example, the highest bioethanol yield was obtained for a December planting of sorghum at 60,000 plants ha^{-1} in 3,974 of the 5,838 quinary subcatchments (i.e. 68.1%), when compared to the other three scenarios. For both crops, it is clear that the higher planting density produced more biofuel yield, due to the higher attainable crop yield. In addition, The December planting produced more biofuel yield than the November planting. However, it is important to note that the analysis was done for all quinary subcatchments, regardless of their suitability to crop production. The variability in biofuel yield for the later planting at the higher density is discussed next for both crops.

Table 15.1: Portion of quinary subcatchments that exhibited the highest biofuel production potential

Planting date (month)	Planting density (plants ha^{-1})		Quinary subcatchment portion (percentage)	
	Soybean	Sorghum	Soybean	Sorghum
11	250,000	44,444	1.1	16.7
	30,0000	60,000	33.1	45.2
12	250,000	44,444	3.8	17.5
	300,000	60,000	72.3	68.1

15.3.4.1 Biodiesel

According to DMRE (2020), soybean should produce a theoretical biodiesel yield of 185 ℓ per ton of crop, assuming a seed oil content of 18%. In this project, a value of 192 ℓ t^{-1} was used, based on a seed oil content of 18.6% (cf. Section 12.1). For soybean, 59 quinary subcatchments produced no biodiesel yield, i.e. mean seasonal crop yield is 0 t ha^{-1} (Figure 15.24). A break-even yield of 1.77 t ha^{-1} (cf. Section 3.5.1) equates to approximately 300 ℓ ha^{-1} of biodiesel. Only 18.5% of all quinary subcatchments may yield more than 300 ℓ ha^{-1} of biodiesel. Quinary Subcatchment 3361 produced the highest biodiesel yield of 848.3 ℓ ha^{-1} from a crop yield of 4.65 t ha^{-1}.

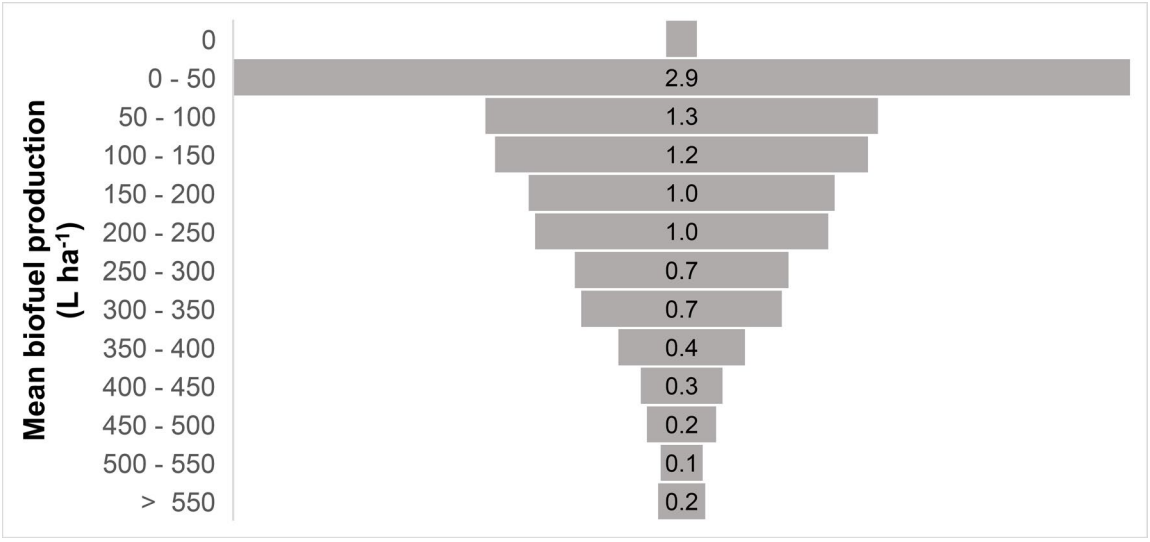

Figure 15.24: Funnel chart showing the mean season biodiesel yield from soybean planted in December at a density of 300,000 plants ha^{-1}

15.3.4.2 Bioethanol

Sorghum should produce a theoretical bioethanol yield of 417 ℓ per ton of crop (DMRE, 2020). In this project, a value of 361 ℓ t^{-1} was used, based on a moisture content of 11%, an extractable starch content of 63.4 and a fermentation efficiency of 89% (cf. Section 12.2). Similar figures of 370 and 372 ℓ t^{-1} were reported by BFAP (2008) and Smith and Frederiksen (2000), respectively. It is believed that the biofuel task team does not account for the moisture content of the crop, which explains its higher value. For sorghum, 1,010 quinary subcatchments produced no bioethanol yield, i.e. had a mean seasonal crop yield of 0 t ha^{-1} (Figure 15.25). A break-even yield of 3.43 t ha^{-1} (cf. Section 3.5.2) equates to approximately 1,200 ℓ ha^{-1} of bioethanol. Only 7.1% of all quinary subcatchments may yield more than 1,200 ℓ ha^{-1} of bioethanol. Quinary Subcatchment 4573 had the highest bioethanol yield of 2,590.2 ℓ ha^{-1} from a crop yield of 7.21 t ha^{-1}.

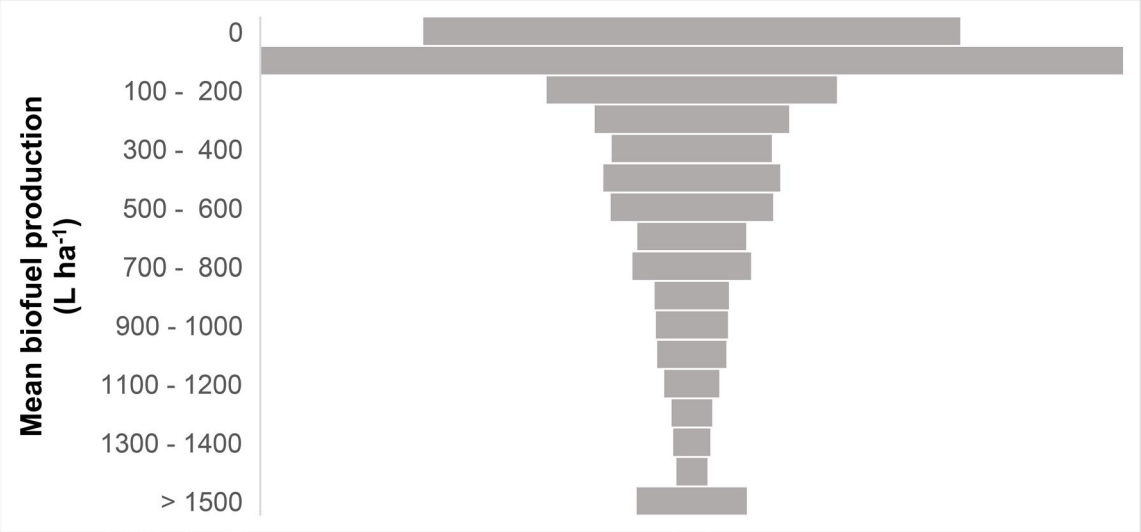

Figure 15.25: Funnel chart showing the mean season bioethanol yield from sorghum planted in December at a density of 60,000 plants ha^{-1}

15.3.4.3 Summary and conclusions

Biofuel yield is sensitive to crop yield and oil or starch content. The later planting date (i.e. December) at the higher planting density produced a greater biofuel yield, due to the higher attainable crop yield. However, it is important to note that the analysis was done for all quinary subcatchments, regardless of their suitability to crop production. A histogram showing the variability in biofuel yield showed that many quinary subcatchments are unsuited to crop production (especially sorghum), and thus produced low biofuel yields. Biofuel yields are higher for sorghum than for soybean, because one ton of sorghum produces 361 ℓ of bioethanol, compared to 192 ℓ of biodiesel from soybean. In addition, the sorghum yield was higher than the soybean yield in 2,012 quinary subcatchments.

15.3.5 Crop cycle

AquaCrop defines the length of the crop cycle from the number of days after emergence to when yield peaks, i.e. physiological maturity. It is different to the growing season length, which is the number of days from planting to physiological maturity. Hence, the crop cycle is always shorter than the season length. Maps of crop cycle are useful to identify areas too cold for crop production (shown in white) and in which crops should physiologically mature faster than others.

15.3.5.1 Soybean

It was expected that planting density would have no impact on the season length. In other words, soybean planted in November at 250,000 plants ha^{-1} would have the same crop cycle as that planted at 300,000 plants ha^{-1}. This was not the case for 136 quinary subcatchments where the difference in crop cycle was longer than a week. It is worth noting that, when compared to the higher planting density, the lower planting density exhibited longer crop cycles by up to 207 days. However, all these quinary subcatchments exhibited crop cycles longer than 180 days, indicating that they exist in areas too cold for soybean production.

For the December planting, 161 quinary subcatchments had differences in crop cycles longer than seven days, with the largest difference being 79 days. These results show that the later planting (i.e. December) reduced cold stress in the high-altitude quinary subcatchments, thus shortening the crop cycle. Such comparisons may prove useful in identifying areas that are unsuitable for crop growth. For soybean, only the later planting at the higher density map is shown, considering it is almost identical to the other scenarios.

Figure 15.26 clearly identifies areas that are deemed too cold to grow the crop in a reasonable crop cycle. For example, a crop cycle of six months or longer (i.e. more than 180 days) may not be considered viable for annual crops, which occurs mainly in the Lesotho Highlands and along the Drakensberg Escarpment. For either planting density, a change in planting date from November to December lengthened the crop cycle by 30 days or more in 554 quinary subcatchments. On the other hand, no quinary subcatchments exhibited a shortening of the crop cycle due to the later planting.

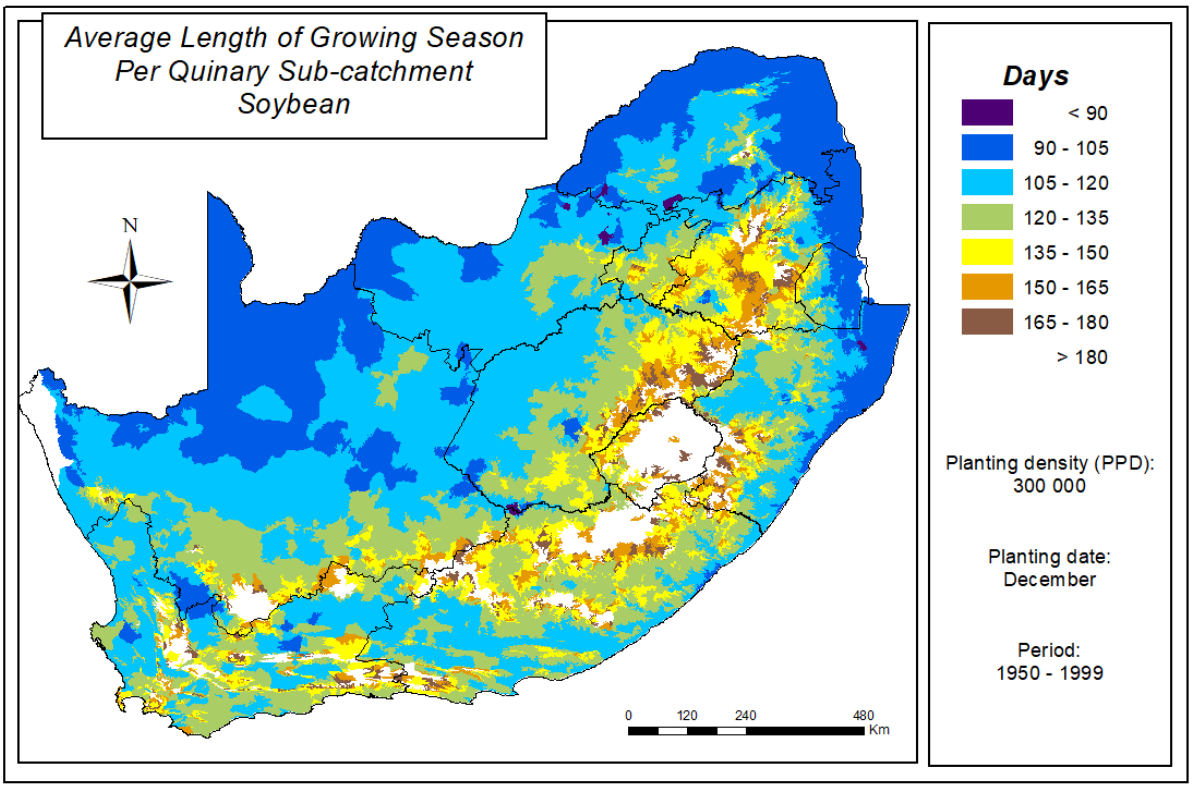

Figure 15.26: Average length of crop cycle for soybean planted in December at a planting density of 300,000 plants ha^{-1}

15.3.5.2 Grain sorghum

For the November planting, the change in planting density had a much larger impact on the crop cycle. A total of 51 quinary subcatchments experienced a lengthening of the crop cycle by seven to 77 days. For the majority (4,099) of the quinary subcatchments, changes in the crop cycle was small (i.e. ± seven days). For the remainder of the quinary subcatchments, the crop cycle shortened by up to 181 days. For example, Quinary Subcatchment 1838 experienced a reduction in crop cycle by 33 days (from 112 to 79 days).

For the December planting, the change in planting density had a much greater impact on the crop cycle. A total of 65 quinary subcatchments experienced a lengthening of the crop cycle by seven to 139 days. The majority (3,755) of the quinary subcatchments experienced small changes in the crop cycle by ± seven days. For the remainder of the quinary subcatchments, the crop cycle shortened by up to 95 days. For example, Quinary Subcatchment 3722 experienced a reduction in crop cycle from 240 (not viable) to 180 (viable) days, i.e. a reduction of 60 days. This example highlights that this subcatchment is better suited to a higher planting density when planted in December, However, the crop cycles were 125 and 112 days for the lower and higher planting densities, respectively. Such variations in crop cycle indicate that this quinary is not suited to grain sorghum production, with dry yields of only 0.05-0.11 t ha^{-1}. As for soybean, only the later planting at the higher density map is shown (Figure 15.27), considering that it is almost identical to the other scenarios for areas that can produce a viable yield.

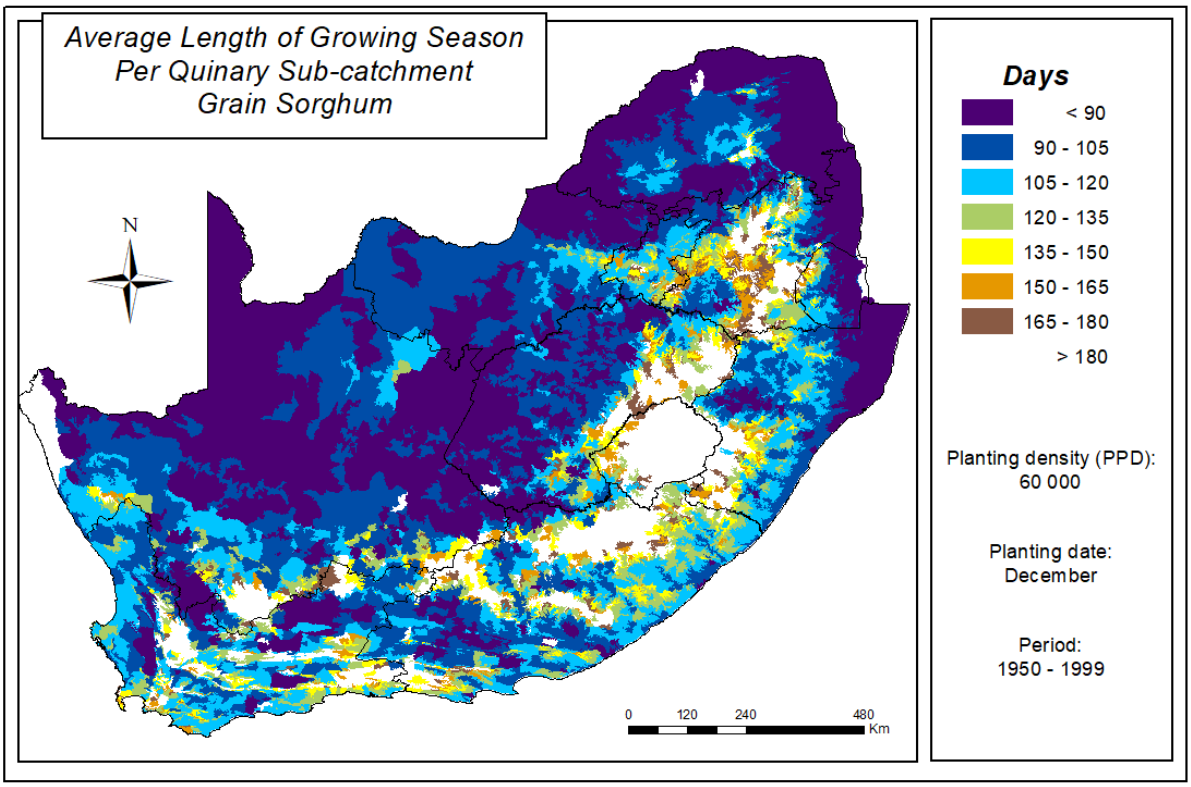

Figure 15.27: Average length of growing season for grain sorghum planted in December at a planting density of 60,000 plants ha^{-1}

15.3.5.3 Summary and conclusions

The above examples indicate that crop cycle should not be considered on its own. An analysis of crop cycle in conjunction with estimated yield revealed the following extreme cases for illustrative purposes:

- The highest yield of 3.04 t ha^{-1} for Quinary Subcatchment 1736 was generated for a December planting at 60,000 plants ha^{-1}, which represented a yield increase of 1.87 t ha^{-1} when compared to the November planting. However, the crop cycle increased from 148 to 273 days, indicating that November is the best planting date, despite the lower yield.
- The highest yield of 3.38 t ha^{-1} for Quinary Subcatchment 463 was generated for a December planting at 60,000 plants ha^{-1}, which represented a yield increase of 1.24 t ha^{-1} compared to the earlier planting. However, the crop cycles were relatively similar, which lengthened slightly from 122 (November) to 137 (December) days, indicating December to be the best planting date.
- For Quinary Subcatchment 4915, an earlier planting at a higher density produced the largest yield of 4.12 t ha^{-1}. The later planting resulted in a yield decline of 2.89 t ha^{-1}, indicating November to be the best planting date. However, the crop cycle is over 300 days, which means the quinary subcatachment is too cold for sorghum production.
- For Quinary Subcatchment 5665, the November planting at the higher density produced the largest yield of 5.91 t ha^{-1}. The later planting resulted in a yield reduction of 1.69 t ha^{-1}. The crop cycle also lengthened from 173 to 195 days, confirming November to be the best planting date.
- In Quinary Subcatchment 2911, a yield decline from 0.83 to 0.24 t ha^{-1} occurred when the planting density was increased from 44,444 to 60,000 plants ha^{-1}. However, crop cycles exceeded 400 days. Thus, this quinary subcatchment is not suited for crop production.
- Quinary Subcatchment 5434 produced a yield increase of 0.41 t ha^{-1} due to the higher density when planted in November. The crop cycle remained the same at 150 days. Thus, the higher planting density is recommended.

15.3.6 Summary and conclusions

Chimonyo et al. (2016) concluded that the APSIM crop model can be used as a tool to develop best management options for increased yield and WUE for intercropping under water-scarce agro-ecologies. This project has made excellent progress in reducing the computational expense associated with running AquaCrop (and ACRU) at a national scale for all 5,838 relatively homogeneous response zones (cf. Section 14.3). Although eight national runs were performed, the scene is set to run the model for other scenarios involving different planting dates and plant populations, as recommended by Chimonyo et al. (2016).

This project provided national scale maps of long-term attainable yields for soybean and grain sorghum, derived using AquaCrop driven with 50 years of daily climate record for 5,838 homogeneous response zones. Other maps also provide information on crop water use efficiency, crop risk failure (i.e. variation in seasonal yield) and season length. They provide valuable information for planning purposes, especially in areas where no (or insufficient) historical data exists on crop growth.

The maps showed that the higher planting density usually produced a greater crop yield as expected. Changes in the planting month had a larger impact on crop yield than increases in plant population. However, examples provided in this section clearly illustrate the danger of making decisions or drawing conclusions using one variable (e.g. crop yield), while ignoring others (e.g. crop cycle). Debaeke and Aboudare (2004) suggested that model output should support the decision-making process and not be used to derive absolute recommendations for best management.

CHAPTER 16: HYDROLOGICAL IMPACTS OF FEEDSTOCK PRODUCTION

16.1 INTRODUCTION

The South African National Water Act of 1998 requires reference flows to determine the ecological reserve, as well as to assess the impact of specific land uses on stream flow response (especially low flows). Section 36 of the National Water Act declares land that is used for commercial afforestation to be a stream flow reduction activity, and also makes provision for other activities (i.e. land uses) to be so declared if this should prove justified. This would be on the basis of such an activity being "likely to reduce the availability of water in a watercourse to the reserve, to meet international obligations, or to affect other water users significantly".

Crop "water use" in the context of SFRA assessments is defined as the difference in mean annual stream flow, resulting from a change in land use from the baseline (i.e. natural vegetation) to the cultivation of biofuel feedstock (or crop). This difference ($MAR_{BASE} – MAR_{CROP}$) is then expressed as an absolute difference and a percentage change from the baseline stream flow (MAR_{BASE}). This builds on the definition accepted for commercial forestry, i.e. the water used by afforestation is the reduction in stream flow compared with the stream flow that would have occurred from natural vegetation. Thus, in order to determine the hydrological impact of land use change to feedstock production, it is necessary to first define the baseline vegetation against which water use comparisons are made.

16.2 HYDROLOGICAL BASELINE

16.2.1 Background

Until recently, the South African Department of Human Settlements, Water and Sanitation supported and accepted the use of "natural vegetation" as depicted in the veld type map of Acocks (1988) as the reasonable standard or reference land cover against which impacts of land use change were assessed (Jewitt et al., 2009b). The veld types of Acocks were agriculturally based and defined as "an agro-ecological unit of vegetation whose range of variation is small enough to permit the whole of it to have the same farming potentialities" (Acocks, 1953).

A WRC-funded project (Project No. K5/2437), "Resetting the baseline land cover against which stream flow reduction activities and the hydrological impacts of land use change are assessed", was completed in October 2019 (cf. Warburton Toucher et al., 2019). In essence, the project's main objectives were as follows:

- Use the latest vegetation map, updated by the South African National Botanical Institute (SANBI) (2012) as the new hydrological baseline.
- Simplify the 435 vegetation types into 121 hydrologically relevant vegetation groupings (called clusters).
- Refine the hydrological parameters related to natural land cover using remotely sensed data (in particular, LAI).
- Determine the potential implications of using the revised baseline parameters for assessing the hydrological impact of potential stream flow reduction activities.

The project recommended that the 121 vegetation clusters be considered as the new hydrological baseline against which assessments are made. The DWS has recently expressed an interest in adopting the vegetation clusters as the new baseline against which all potential SFRAs should be assessed (Warburton Toucher, 2020). Hence, this work replaces the hydrological parameters associated with the vegetation layer in ACRU that were previously derived for each of the 72 Acocks veld types (Acocks, 1988). Since the WRC has not yet published the final report (Warburton Toucher et al., 2019), a brief summary of the work is given next.

16.2.2 Approach

16.2.2.1 Hydrological grouping of vegetation types

The SANBI (2012) vegetation map defines 435 vegetation units, where each unit is defined as “a complex of plant communities ecologically and historically (both in spatial and temporal terms) occupying habitat complexes at the landscape scale” (Mucina and Rutherford, 2006). For hydrological modelling purposes, it was not feasible (or practical) to adopt all 435 vegetation units as the baseline. Thus, the vegetation units were grouped into 121 clusters with a similar hydrological response that were reviewed and approved by vegetation experts. The hierarchical clustering was done by developing hydrological profiles for each of the vegetation units, which were then grouped to produce robust and compact clusters as shown in Figure 16.1.

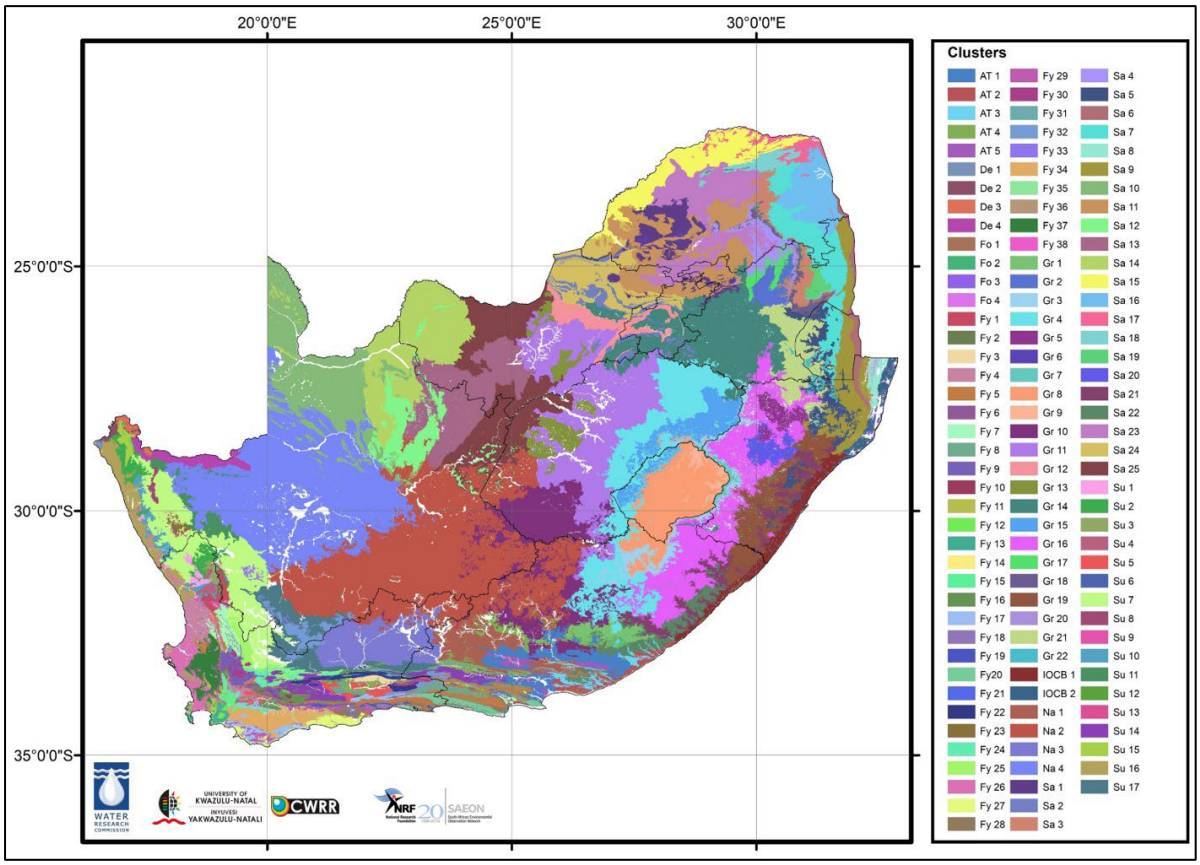

Figure 16.1: Vegetation clusters derived from the SANBI (2012) vegetation units (Warburton Toucher et al., 2019)

Due to the finer scale at which the SANBI (2012) vegetation units were mapped, the vegetation clusters provide a finer spatial resolution of natural vegetation when compared to the veld types of Acocks (1988). Although the number of vegetation units may not appear to be greatly improved (i.e. 72 to 121), the more detailed mapping provides the main advantage. In order to adopt the vegetation clusters as the new hydrological baseline, vegetation and water use parameters required by ACRU needed to be derived for each cluster.

16.2.2.2 Revised rainfall:runoff parameters

As described in Section 13.1, ACRU requires five parameters that determine rainfall:runoff response. Warburton Toucher et al. (2019) derived the following parameter values:

- Effective rooting depth (*EFRDEP*): The effective rooting depth of each vegetation cluster was estimated from mean annual precipitation via a regression equation developed by Schenk and Jackson (2002). However, this equation was not applied to trees or succulents, where respective values of 3.0 m and 0.25 m were used.
- Coefficient of initial abstraction (*COIAM*): The methodology described in Section 13.1.8 was used to determine representative monthly values for each vegetation cluster.

16.2.2.3 Revised land use variables

A database was developed of representative values for the six important vegetation variables (cf. Table 13.5 in Section 13.3) as follows:

- Surface cover fraction (*PCSUCO*): The methodology given in Section 13.3.2 was used to determine representative monthly values for each vegetation cluster.
- Rooting distribution (*ROOTA*): Representative values for each cluster were obtained from the available literature, as well as the use of equations and rules.
- Root colonisation (*COLON*): This monthly variable determined the relative proportion of roots that have access to soil moisture in the B-horizon. Due to the lack of information for natural vegetation types, the default value of 100% was used.
- Leaf Area Index (*ELAIM*): Monthly estimates of LAI for seven years (2012-2018) were derived from the remotely sensed MODIS product.
- Interception loss (*VEGINT*): Using the same methodology described in Section 13.3.6, monthly interception losses were derived for each vegetation cluster using both the Von Hoyningen-Huene (1983) equation and the modified Gash equation (Bulcock, 2011).
- Crop coefficient (*CAY*): Initially, crop coefficients for each of the vegetation clusters were determined from actual evapotranspiration derived from the Surface Energy Balance System (SEBS) model. However, the SEBS model tended to over-estimate the evapotranspiration from natural vegetation. In addition, evapotranspiration estimates for each cluster did not correspond to expected seasonal trends. Thus, the crop coefficients were not recommended for use. Instead, crop coefficients were derived from LAI via relationships published in the literature. However, none of the methods performed well, and thus an equation was fitted between K_C values produced for sites where evapotranspiration was observed over natural vegetation and the remotely sensed LAI of these sites. The derived relationship explained 75% of the variation in K_C using LAI.

16.2.3 Results and discussion

16.2.3.1 “New” vs “old” climate with “new” baseline

In order to better understand the implications of using the revised quinary climate database, the following analysis was undertaken in this study. The original (“old”) quinary climate database was used as input, together with the new baseline land cover, to simulate runoff response using ACRU as shown in Figure 16.2.

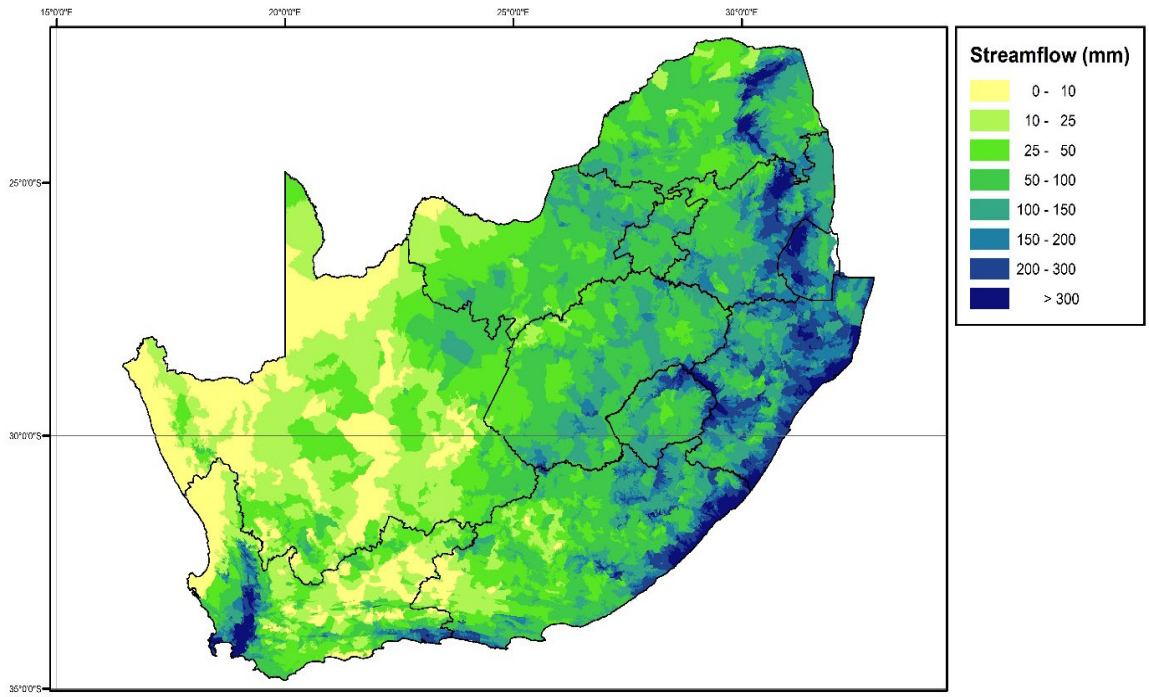

Figure 16.2: Mean annual stream flow response derived using ACRU, driven by the original quinary climate database as described by Schulze et al. (2011)

However, when using the revised ("new") quinary subcatchment climate database (cf. Section 10.1), the stream flow response shown in Figure 16.3 was produced. A visual comparison of the two figures below identifies where minor changes in runoff have occurred, especially in Limpopo and Free State. As noted in Section 10.1, the revised quinary climate database uses observed temperatures and not interpolated data, as well as numerous corrections to errors in extreme rainfall events. However, of more concern are changes in runoff response due to the new vegetation baseline.

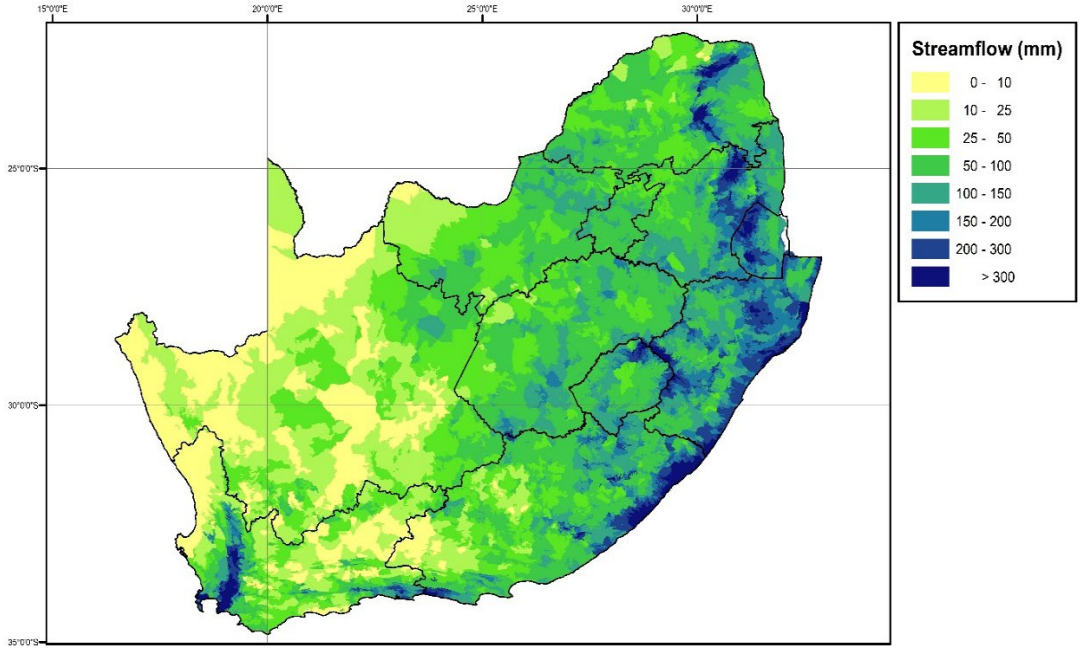

Figure 16.3: Mean annual stream flow response derived using ACRU, driven by the revised quinary climate database as described in Section 10.1

16.2.3.2 “New” vs “old” baseline with “old” climate

In order to better understand the implications of using the new baseline, Warburton Toucher et al. (2019) undertook the following analysis. Using the original quinary subcatchment climate database (Schulze et al., 2011) to drive ACRU and the new vegetation parameters and variables, the model produced more runoff along the east coast of South Africa, relative to that generated from the veld types of Acocks (Figure 16.4). The increased stream flows correspond to areas where the crop coefficients of the vegetation clusters are lower than those for the Acocks veld types.

In contrast, less runoff was produced for the interior region of the country (Figure 16.4), mainly due to larger K_C values and higher vegetation interception losses. The updated vegetation interception losses for each vegetation cluster are generally higher than those derived for each Acocks veld type. The revised crop coefficients are also larger, especially in the winter months. Crop coefficients representing the Acocks veld types reduce to 0.2 in winter as a result of senescence. Within each of the vegetation clusters, there are several vegetation types that are unlikely to senesce during winter, which explains the higher K_C values in winter.

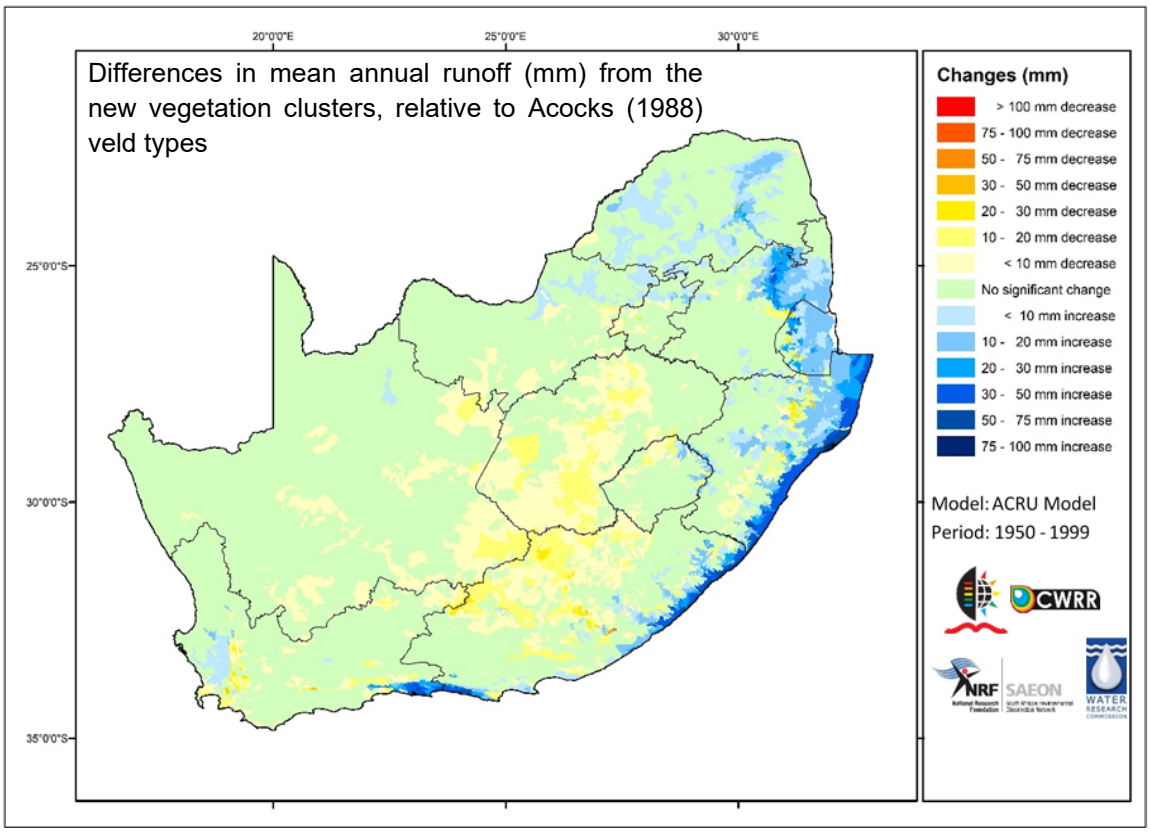

Figure 16.4: Changes in mean annual runoff, expressed in mm, that resulted from using the new hydrological baseline (Warburton Toucher et al., 2019)

Warburton Toucher et al. (2019) conducted further tests to determine the implication of changing the hydrological baseline from Acocks to the new vegetation clusters. This was done using the ACRU model configuration and input data developed by Jewitt et al. (2009b) in the SFRA project. On the national scale, the impacts of SFRAs were reduced slightly (< 5 mm change in MAR). Further tests were also conducted on the uMngeni catchment, where some quinary subcatchments produced changes in mean annual runoff under Eucalypts of up to 30 mm (greater) when compared to the Acocks veld types. To fully account for the improved spatial resolution of the new hydrological baseline, hydrological modelling needs to be undertaken on a spatial scale finer than the quinary catchments (Warburton Toucher et al., 2019).

16.2.3.3 “New” vs “old” baseline with “new” climate

As highlighted above by Warburton Toucher et al. (2019), the new vegetation baseline produced changes in runoff response that were determined using the original quinary climate database. In this study, the analysis was repeated using the revised (i.e. “new”) quinary climate database. A histogram of the difference in MAR from the new baseline (MAR_{NEW}) compared to that of Acocks (MAR_{OLD}) is shown in Figure 16.5. Approximately 66.3% of the quinary subcatchments exhibit a reduction in MAR when using the new baseline to represent natural vegetation. For the majority (56.1%) of these quinary subcatchments, the difference in MAR ranges from 0 to -10 mm. A total of 920 (15.8%) subcatchments exhibit a MAR difference of only ± 1 mm.

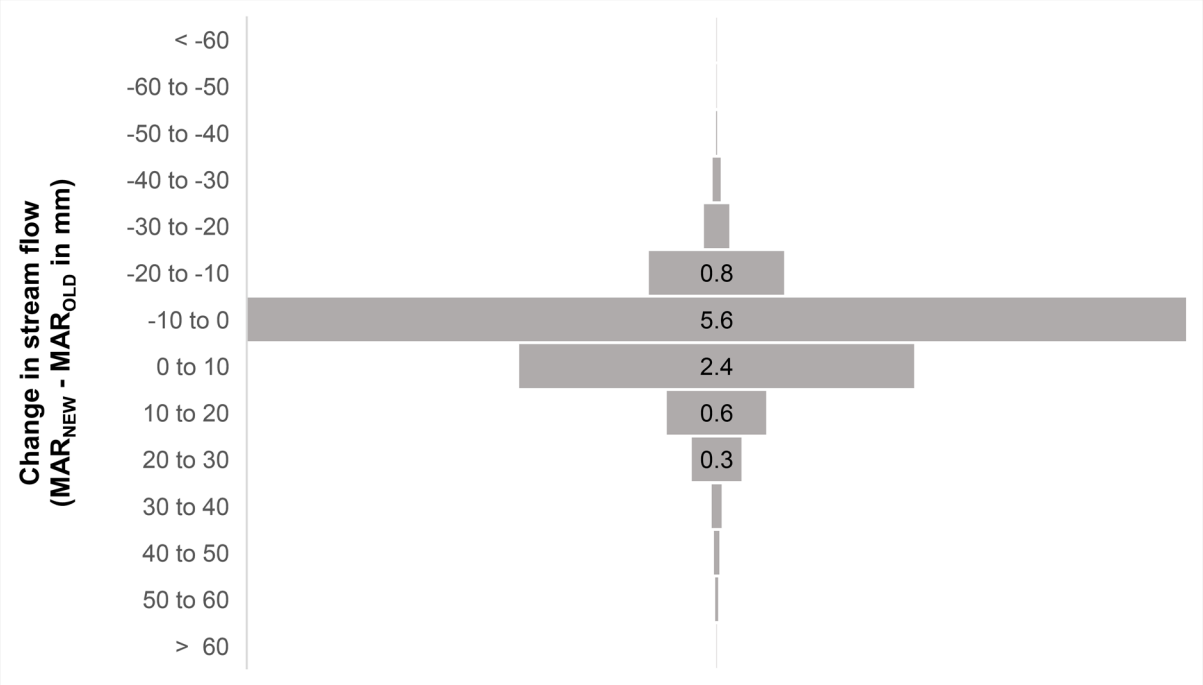

Figure 16.5: Funnel chart showing the difference in mean annual runoff produced from the new baseline (“new”) versus that of Acocks (“old”)

Of more concern should be the impact of land use change on stream flow during the low-flow period. The driest three-month period (or driest quartile) was determined using the monthly stream flow estimates produced by ACRU for the new baseline (i.e. natural vegetation), which was then compared to that produced using the Acocks veld types. This reduction in monthly runoff over the driest quartile was then determined and expressed as an absolute difference (MAR_{NEW} – MAR_{OLD} in mm in Figure 16.6), as well as a percentage change (data not shown). For the low-flow period (lowest quartile runoff), the difference ranged from -14.0 to 10.7 mm. For the majority (40.7%) of the quinary subcatchments, the difference in MAR ranges from 0 to -1 mm. A total of 2,875 (49.2%) subcatchments exhibit a MAR difference of only ± 1 mm.

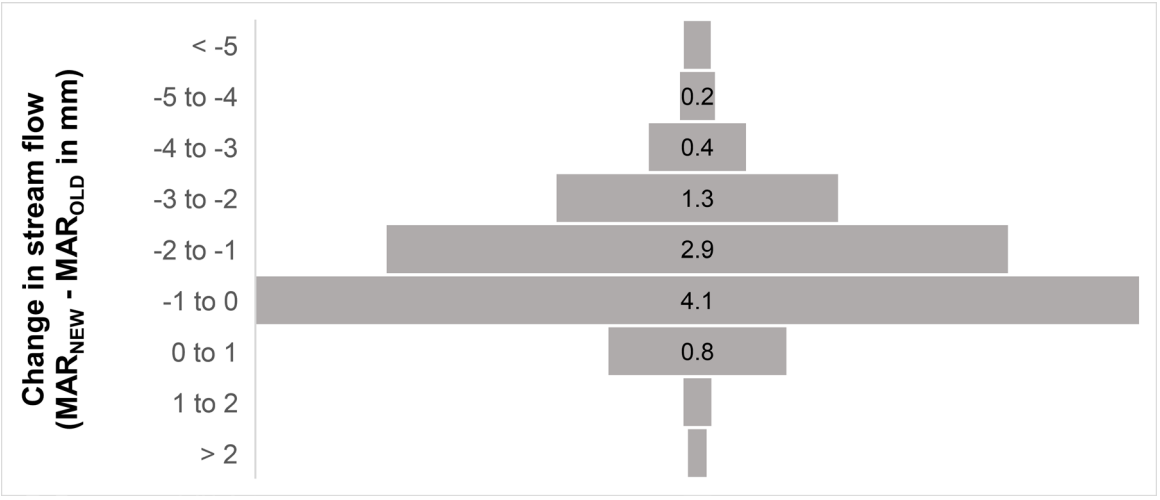

Figure 16.6: Funnel chart showing the difference in low flows produced from the new baseline ("new") versus that of Acocks ("old")

The relative change in MAR varied from -350% to +100%. The reduction of 350% occurred in Quinary Subcatchment 2205, where the low flow decreased by 0.14 mm from 0.18 mm (Acocks) to 0.04 mm (new vegetation clusters). Similarly, an increase of 100% occurred in Quinary Subcatchment 2235, where the low flow increased from 0 mm (Acocks) to 0.03 mm (new vegetation clusters). These two extremes highlight concerns when expressing differences in runoff in relative terms, as minor differences in small values result in large percentage changes.

16.2.4 Summary and conclusions

In conclusion, Warburton Toucher et al. (2019) provided an alternative hydrological baseline against which land use changes can be assessed. As noted, the DWS has recently expressed an interest in adopting the new baseline. The decision was therefore made to move forward in the best interests of research and use the updated parameters that represent an improved hydrological baseline to assess the impact of a proposed land use change from natural vegetation to biofuel feedstock production. In addition, another WRC-funded project (Project K5/2791) has also expressed an interest in using the new baseline to assess the hydrological impacts of commercial afforestation on stream flow. WRC Project K5/2833 will also use the updated baseline to assess the impacts of climate change on water yield.

16.3 CROP WATER USE

16.3.1 Background

Land cover and land use affect hydrological responses through, inter alia, canopy and litter interception, infiltration of rainfall into the soil and the rates of soil water evaporation and transpiration from the vegetation layer. It is virtually impossible to determine crop water use for all possible combinations of climate, soil and management conditions in South Africa. Hence, the ACRU model was selected to assess the hydrological impacts of a land use change from natural vegetation (the baseline) to feedstock production on downstream water availability.

16.3.2 Approach

The hydrological modelling approach followed in this project is consistent with the methodology used in previous studies that estimated the hydrological impact of a land use change from natural vegetation (as depicted by the Acocks veld type map) to the following:

- Selected biofuel feedstocks (biofuel scoping study; Jewitt et al., 2009a)
- Commercial forestry and sugarcane (SFRA project; Jewitt et al., 2009b)
- Other biofuel feedstocks (previous biofuel project; Kunz et al., 2015c)

All of these studies used ACRU to assess the impact of proposed land use changes on downstream water availability. A summary of the approach used in this project to assess the hydrological impact of biofuel crop production is as follows:

- The rainfall adjustment factors (*CORPPT* in ACRU) used in this study are those used in the previous biofuel project (Kunz et al., 2015c), which differ to values used in the SFRA (Jewitt et al., 2009b) and biofuel scoping (Jewitt et al., 2009a) studies.
- A number of errors in extreme daily rainfall values (> 400 mm) that existed in the quinary climate database were corrected (cf. Section 10.1.1.3). Hence, daily runoff response in the affected quinary subcatchments listed in Table 10.5 would be considerably less.
- A revised temperature dataset was developed for each quinary subcatchment (cf. Section 10.1.2), which is different to that used in previous land use change studies. This improved dataset was used for the first time in this project, from which reference evapotranspiration values were also calculated.
- Daily estimates of reference evapotranspiration for each quinary subcatchment were derived using the Penman-Monteith (FAO56) method as described by Kunz et al. (2105b), with wind speed assumed to be 2.0 m s^{-1} (cf. Section 10.1.3). These estimates are different to those used in the SFRA and biofuel scoping studies.
- The A-pan adjustment factors (*CORPAN* in ACRU) used in this study were derived using the PenPan method as described by Kunz et al. (2105b). Again, these estimates are different to those used in the SFRA and biofuel scoping studies.
- Regular measurements of LAI undertaken at Swayimane in 2017/18 for sorghum (PAN8906; fertilized treatment) and 2018/19 for soybean (LS6161R; inoculated treatment) were used to derive monthly interception loss values (*VEGINT*). Monthly values were derived for each of the 49 seasons, and then averaged to produce a set of unique figures for each quinary subcatchment. Although two different methods were used to calculate interception loss, values obtained from the modified Gash model were used as input for ACRU. The reader is referred to Appendix M for more detail.
- Crop coefficients for each feedstock were derived using the AquaCrop model. In total, monthly K_C values were derived for each of the 49 seasons, and then averaged to produce a set of unique values for each quinary subcatchment (*CAY* in ACRU). The crop was irrigated to artificially relieve water stress so that the derived crop coefficients represented standard conditions as suggested by the FAO (Allen et al., 1998). Thereafter, K_C was adjusted to A-pan equivalent values using the revised A-pan coefficients. This approach was not used in previous studies, and is thus considered a unique approach. The reader is referred to Appendix N for more detail.
- Crop coefficients representing the fallow period were derived from micrometeorological measurements undertaken at Baynesfield during the 2016/17 season (from May to October; cf. Section 13.3.7.1).
- A fallow period of six months was assumed, which ended one month prior to the selected crop planting dates (November and December).
- The long-term mean monthly crop coefficients were then used to estimate the surface cover fraction (*PCSUCO*) as described in Section 13.3.2.
- Constant monthly values of 25 and 75% were used to represent root colonisation of the B-horizon (*COLON*) for soybean and sorghum, respectively (cf. Section 13.3.3).
- The fraction of active roots in the topsoil horizon (*ROOTA*) was determined for the depth of the A-horizon (cf. Section 13.3.4).
- The coefficient of initial abstraction (*COIAM* in ACRU) was determined from rainfall seasonality and the distance from the coastlines as described in Section 13.1.8.
- Values for other rainfall:runoff parameters in ACRU are given in Section 13.1.
- Various changes were made to ACRU as described in Section 14.2 to improve the model's output and to reduce its run time.

- Significant improvements were made to optimise model runs at the national scale in order to reduce computational expense. A national run of ACRU for all 5,838 quinary subcatchments took approximately 37 minutes on a core i9 PC, which is considerably faster than 8.5 hours as was the case in the previous biofuel project (cf. Section 14.3).
- The ACRU model was run at the national scale for all 5,838 quinary subcatchments, regardless of whether the feedstock can be successfully grown in the quinary subcatchment.
- ACRU was run in "distributed" mode and not "lumped" mode, which allows for the estimation of stream flow that includes contributions from upstream subcatchments.
- For each quinary subcatchment, ACRU simulations were performed for the revised vegetation clusters (not the dominant Acocks veld type). This provided baseline stream flow depths for each subcatchment, from which estimated stream flow reductions resulting from a land use change to feedstock production were assessed.
- Feedstock water use was calculated relative to that of natural vegetation, i.e. water use is considered the difference between stream flow generated by the proposed land use and that of the revised vegetation clusters.
- Stream flow reductions were therefore assumed to be the difference between stream flow simulated for a quinary subcatchment where 100% of the natural vegetation is replaced by a biofuel feedstock. Reductions in mean annual stream flow totals and low flow indices (the driest three months) were calculated in this manner.
- Output was presented in a form compatible with the utilities and tools used for the management and assessment of existing SFRAs, i.e. for commercial forestry.

Since the models were run for all quinary subcatchments, the simulated crop water use and yield data could then be used to determine which quinary subcatchments are deemed suitable for feedstock production. The main advantage of running ACRU in "distributed" mode is to prevent duplication of effort in that other research projects could utilise the stored output.

16.3.3 Results and discussion

Histograms of simulated mean annual stream flow (MAR_{CROP} in mm) are shown in Figure 16.7 and Figure 16.8 for soybean and sorghum, respectively. Although both histograms are very similar, it appears that slightly more runoff is generated from a land cover of soybean when compared to that of grain sorghum. This is the case for 5,417 of the 5,838 quinary subcatchments. In other words, sorghum is more likely to reduce the availability of water to downstream users than soybean.

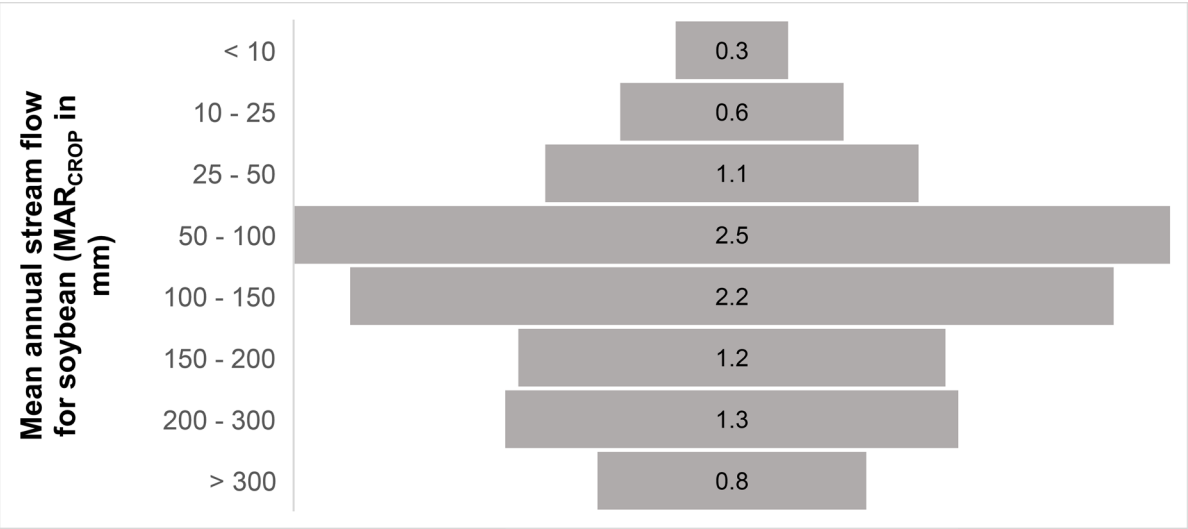

Figure 16.7: Funnel chart showing the mean annual runoff produced from a land cover of soybean planted in December (at 250,000 plants ha^{-1})

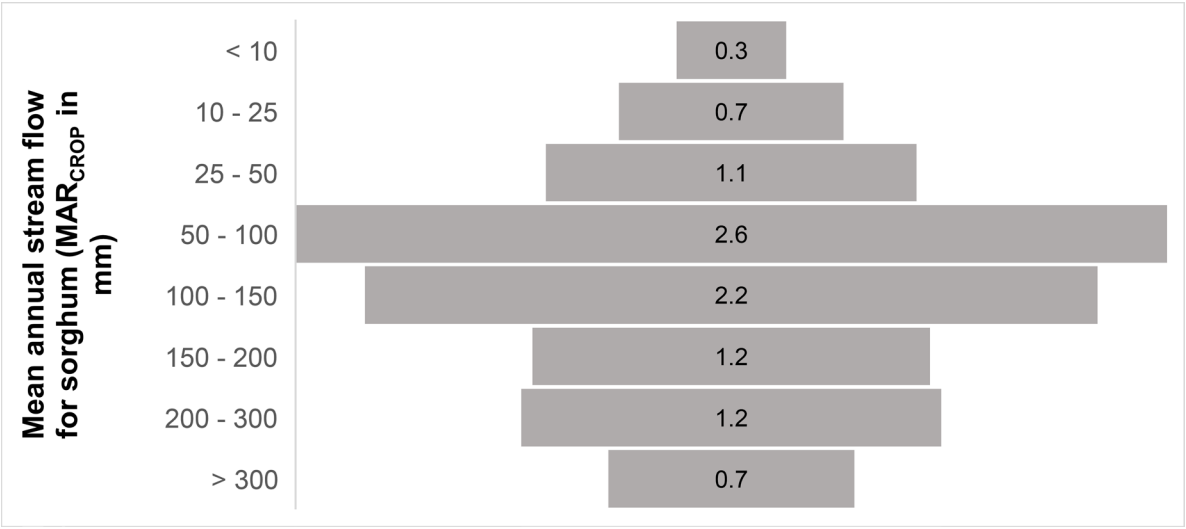

Figure 16.8: Funnel chart showing the mean annual runoff produced from a land cover of grain sorghum planted in December (at 44,444 plants ha^{-1})

The histogram representing the range in mean annual stream flow simulated for a land cover of natural vegetation (MAR_{BASE}) in shown in Figure 16.9. When compared to the two figures above, natural vegetation produces more quinary subcatchments with "lower" runoff (≤ 100 mm) and hence, less quinary subcatchments with "higher" runoff (> 100 mm). This indicates that crop production is unlikely to reduce the availability of water to downstream users. In the section that follows, an analysis of the absolute and relative reductions in runoff (i.e. MAR_{BASE} - MAR_{CROP}) is presented.

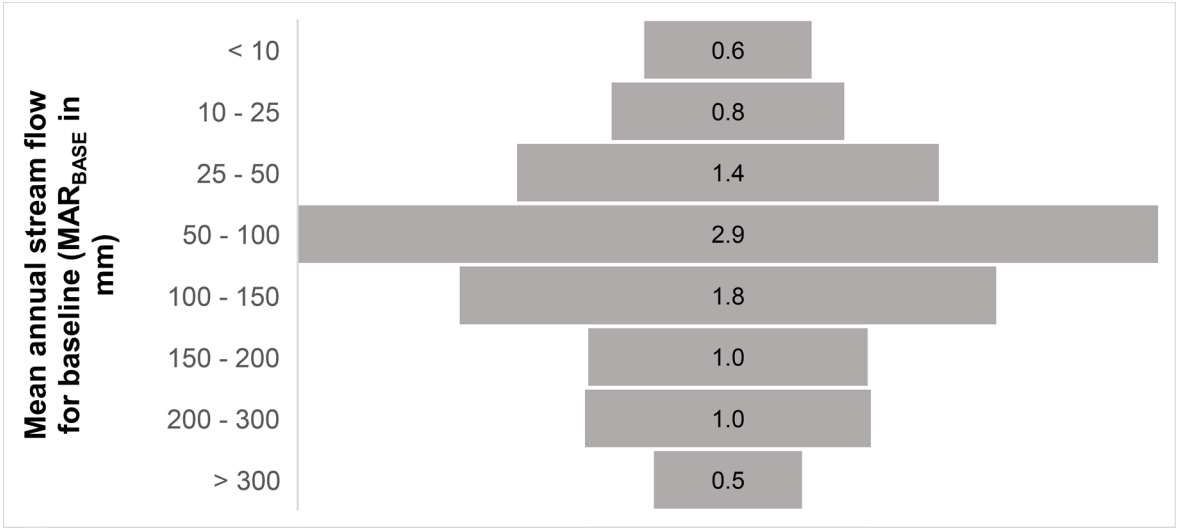

Figure 16.9: Funnel chart showing the mean annual runoff produced from a land cover of natural vegetation (MAR_{BASE})

16.4 STREAM FLOW REDUCTION

16.4.1 Background

Based on recommendations by Jewitt *et al*. (2009b), the reduction in runoff (relative to the baseline) is considered significant when the impact is ≥ 10% for annual runoff (i.e. extent of the impact). Jewitt et al. (2009b) also recommended that if the land-based activity's spatial extent is ≥ 10% of the catchment's area, the impact is considered significant (i.e. the extent of the impact). However, Scott and Smith (1997) highlighted the fact that stream flow reductions during low flow periods may be proportionately greater than for total annual flows. Based on recommendations by Jewitt et al. (2009b), the reduction in runoff (relative to the baseline) is considered significant when the impact is ≥ 25% for low flows.

16.4.2 Approach

Kunz et al. (2015c) recommended that the mean runoff statistic (and not the median) must be used to assess the impact of feedstock production on downstream water availability. Hence, feedstock water use was calculated as the difference between mean annual stream flow generated by the proposed land use (MAR_{CROP}) and that of natural vegetation (MAR_{BASE}) This difference in annual runoff ($MAR_{BASE} – MAR_{CROP}$) was then expressed as a percentage of the baseline stream flow (MAR_{BASE}). If the difference was above 10%, the crop may be flagged as a possible stream flow reduction activity.

16.4.3 Results and discussion

16.4.3.1 Soybean

For the two planting dates (November and December) and planting densities (250,000 and 300,000 plants ha^{-1}), the absolute reduction in MAR resulting from a proposed land use change from natural vegetation to soybean ranged from -131 to 35 mm (Table 16.1). The December planting produced a slightly wider range of impacts when compared to the November planting (-123 to 29 mm). The reduction in annual runoff appears insensitive to planting density, but sensitive to planting date.

Table 16.1: Absolute reduction in mean annual runoff resulting from a proposed land use change from natural vegetation to soybean production

Planting date (month)	Planting density (plants ha^{-1})	$MAR_{BASE} – MAR_{CROP}$ (mm)	$MAR_{BASE} > MAR_{CROP}$ (number of quinary subcatchments)
11	250,000	-123 to 29	22
11	300,000	-123 to 28	22
12	250,000	*-131 to 35*	27
12	300,000	-131 to 35	26

For the December planting at 250,000 plants ha^{-1}, Figure 16.10 shows that the reduction in runoff ($MAR_{BASE} – MAR_{CROP}$) ranges from -30 to -20 mm in 30.1% of the quinary subcatchments (for example). For the majority of the quinary subcatchments, this reduction is negative, indicating that more runoff is produced from the crop than for natural vegetation (i.e. $MAR_{CROP} > MAR_{BASE}$).

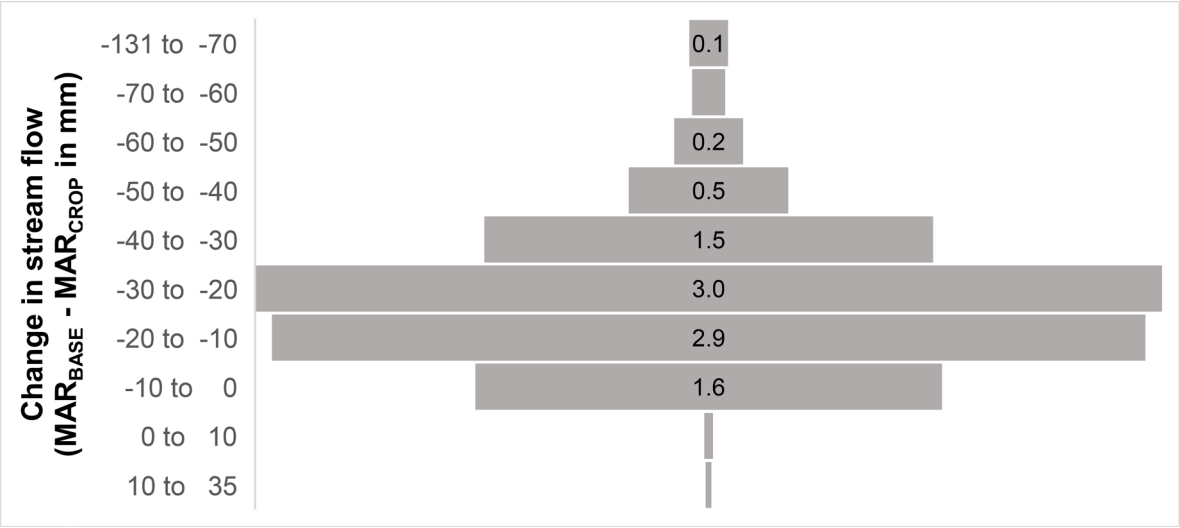

Figure 16.10: Funnel chart showing the difference in mean annual runoff produced from a land cover of soybean planted in December (at 250,000 plants ha^{-1}) compared to natural vegetation

When expressed as a relative change in percentage, only one quinary subcatchment (Quinary Subcatchment 3364) exhibited more than a 10% reduction in runoff for the November plantings (Table 16.2). Only eight quinary subcatchments (quinary subcatchments 2229, 2237, 2236, 2238, 2023, 3364, 3377 and 2015) produced reductions greater than 10% for the December planting, with the worst being ~26% (Quinary Subcatchment 2229). Quinary Subcatchment 3364 exhibits a reduction in MAR of 10% or more regardless of the planting date and density, whereas seven quinary subcatchments only exhibit SFRA potential if soybean is planted in December. In two quinary subcatchments (Quinary Subcatchment 2236 and Quinary Subcatchment 2238), the planting date has a significant effect on stream flow reduction potential. Overall, rainfed production of soybean does not appear to impact on downstream water availability to any great extent. Based on these results, it is unlikely to be declared a potential stream flow reduction activity.

Table 16.2: Impact of planting date and density on the stream flow reduction potential that may result from a land use change from natural vegetation to soybean production

Planting month	November		December	
Planting density (plants ha^{-1}) / Quinary Subcatchment	250,000	300,000	250,000	300,000
2015	7.3	7.4	**11.0**	**11.1**
2023	4.9	4.6	**13.8**	**13.1**
2229	7.0	6.9	***25.7***	***25.5***
2236	-12.6	-12.7	**17.3**	**17.1**
2237	-9.9	-9.9	**23.2**	**23.6**
2238	-23.1	-23.3	**14.4**	**14.4**
3367	9.3	9.1	**11.9**	**11.8**
3364	**10.7**	**10.2**	**12.9**	**12.8**

For low flows (the driest quartile), the December planting produced about nine quinary subcatchments with reductions above 10%, compared to 17 quinary subcatchments for the November planting. For the latter planting, a reduction greater than 25% only occurred in two quinary subcatchments (Quinary Subcatchment 3537 and Quinary Subcatchment 3666). However, Kunz et al. (2015b) raised concerns about possible shifts in the low-flow period that may result from the proposed land use change. The results showed that, for the majority (69%) of quinary catchments, a land use change to soybean production should not cause a shift in the low-flow period. However, it is interesting to note that, in 19% of the quinary subcatchments, the start of the low-flow period occurs from one to five months earlier. Similarly, in 714 (12%) of the quinary subcatchments, the low-flow period is shifted later by one to six months.

16.4.3.2 Grain sorghum

For the two planting dates (November and December) and planting densities (44,444 and 60,000 plants ha^{-1}), the absolute reduction in MAR resulting from a proposed land use change from natural vegetation to grain sorghum ranged from -126 to 44 mm (Table 16.3). The November planting produced a slightly wider range of impacts when compared to the December planting (-124 to 39 mm).

Table 16.3: Absolute reduction in mean annual runoff resulting from a proposed land use change from natural vegetation to grain sorghum production

Planting date (month)	Planting density (plants ha^{-1})	$MAR_{BASE} - MAR_{CROP}$ (mm)	$MAR_{BASE} > MAR_{CROP}$ (number of quinary subcatchments)
11	44,444	*-126 to 44*	34
11	60,000	-126 to 39	28
12	44,444	-124 to 39	35
12	60,000	-124 to 39	35

For the November planting at 44,444 plants ha^{-1}, Figure 16.11 shows that, for the majority of the quinary subcatchments, more runoff is produced from the crop than for natural vegetation (i.e. $MAR_{CROP} > MAR_{BASE}$). Hence, few quinary subcatchments exhibit stream flow reduction potential, i.e. $MAR_{CROP} < MAR_{BASE}$.

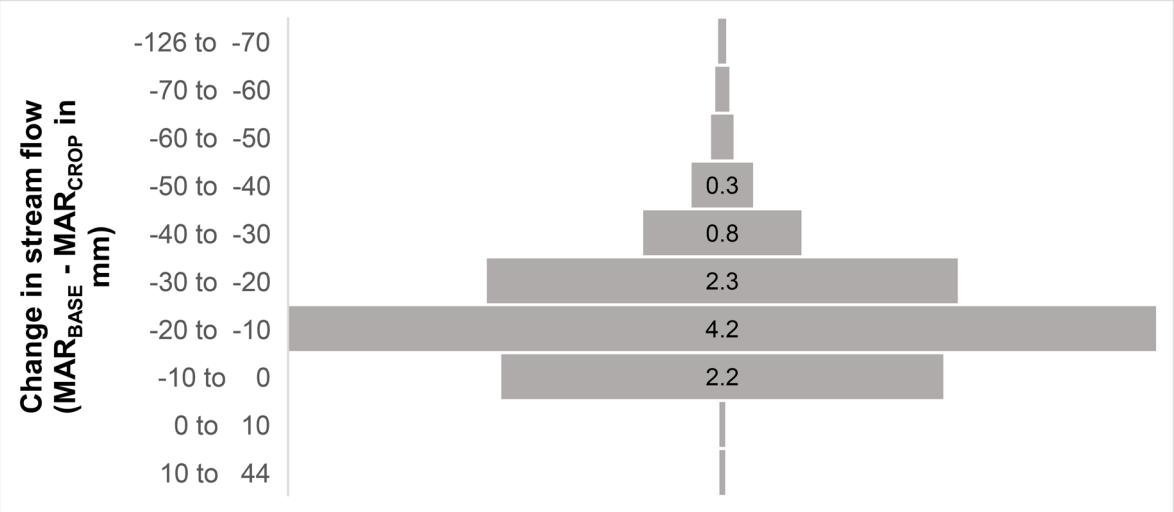

Figure 16.11: Funnel chart showing the difference in mean annual runoff produced from a land cover of grain sorghum planted in November (at 44,444 plants ha^{-1}) compared to natural vegetation

When expressed as a relative change in percentage, the December planting produced more quinary subcatchments with reductions greater than 10%, i.e. 12 and 11 quinary subcatchments for 44,444 and 60,000 plants ha^{-1}, respectively. Quinary Subcatchment 2229 has the worst reduction of 27%, followed by quinary subcatchments 2237, 2236, 2019, 2023, 3364, 2015, 2020, 3367, 2238, 3370 and 3340 (Table 16.4).

Table 16.4: Impact of planting date and density on the stream flow reduction potential that may result from a land use change from natural vegetation to sorghum production

Planting month	November		December	
Planting density (plants ha^{-1})	44,444	60,000	44,444	60,000
Quinary Subcatchment				
2019	-17.9	-18.6	**16.4**	9.9
2015	4.7	5.0	**12.7**	**13.0**
2020	8.2	8.3	**12.6**	**13.6**
2023	4.8	4.5	**16.2**	**16.1**

Planting month	November		December	
Planting density (plants ha^{-1}) / Quinary Subcatchment	44,444	60,000	44,444	60,000
2229	4.1	3.9	***26.8***	***26.7***
2236	-16.5	-16.9	**20.9**	**21.0**
2237	-16.2	-16.2	**21.9**	**21.7**
2238	-29.3	-29.3	**11.3**	**11.3**
3340	9.1	**10.1**	**10.7**	**10.7**
3364	**16.2**	**14.4**	**14.4**	**14.4**
3367	**14.1**	**12.1**	**12.4**	**12.4**
3370	**10.4**	**10.6**	**10.9**	**10.9**

Quinary subcatchments 3364, 3367 and 3370 exhibit a reduction in MAR of 10% or more regardless of the planting date and density, whereas eight quinary subcatchments only exhibit SFRA potential if sorghum is planted in December. In four quinary subcatchments (quinary subcatchments 2019, 2236, 2237 and 2238), the planting date has a significant effect on stream flow reduction potential. Overall, the rainfed production of grain sorghum has a slightly greater impact on downstream water availability than soybean.

For low flows (the driest quartile), the December planting produced 12 quinary subcatchments with reductions above 10%, compared to 24 quinary subcatchments for the November planting. For the latter planting, a reduction greater than 25% only occurred in five quinary subcatchments (quinary subcatchments 3537, 3666, 2622, 3664 and 3665). The results showed that, for the majority (69%) of quinary catchments, a land use change to sorghum production should not cause a shift in the low-flow period. However, it is interesting to note that in 20% of the quinary subcatchments, the start of the low-flow period occurs from one to five months earlier. Similarly, in 629 (11%) of the quinary subcatchments, the low-flow period is shifted later by one to six months. It is believed that such changes in the start of the low-flow period will have a greater impact on downstream water users than the reduction itself.

16.4.4 Summary and conclusions

With the exception of only a few quinary subcatchments, neither the cultivation of soybean nor grain sorghum for biofuel production is likely to significantly affect the quantity of water available to downstream users. Hence, these crops show little to no potential of being declared SFRAs. This outcome is very different to that obtained in the previous biofuel project, where Kunz et al. (2015c) noted that the number of quinary subcatchments that exhibited a 10% (or more) reduction in MAR was 2,423 (Figure 16.12) and 1,348 (Figure 16.13) for grain sorghum and soybean, respectively. The authors stated that, when compared to sugarcane, these two crops were ranked second and third in terms of their potential to reduce water availability to downstream users.

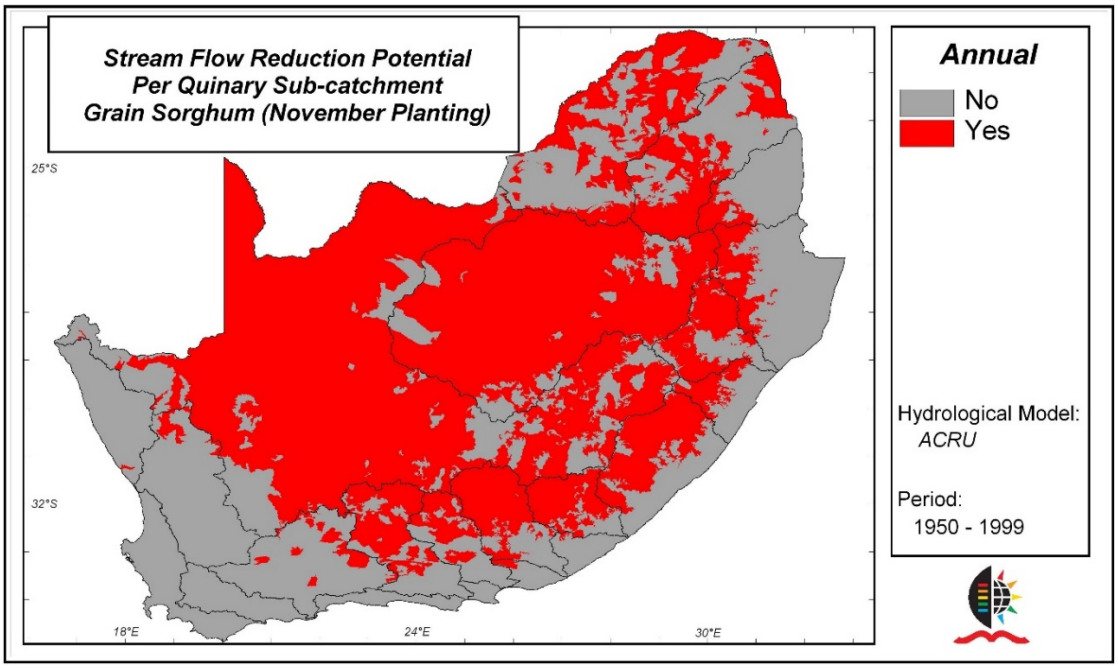

Figure 16.12: Subcatchments in which the reduction in mean annual runoff resulting from a land use change from natural vegetation to grain sorghum exceeds 10% (Kunz et al., 2015c)

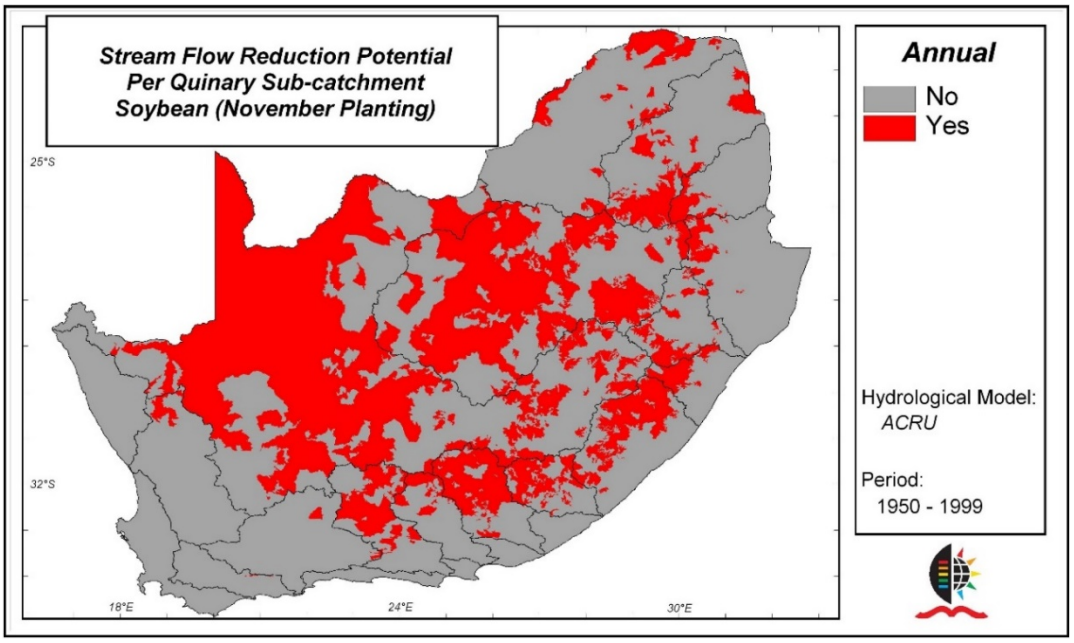

Figure 16.13: Subcatchments in which the reduction in mean annual runoff resulting from a land use change from natural vegetation to soybean exceeds 10% (Kunz et al., 2015c)

These differences in results are likely due to the modified approach adopted in this study, which is summarised as follows:

- The quinary climate database was revised where errors in numerous extreme rainfall events were corrected (cf. Section 10.1.1). In addition, observed temperature data and not interpolated data was used to represent each subcatchment (cf. Section 10.1.2).
- Changes were made to ACRU's code, which affected the way in which the model internally adjusted daily crop coefficients values due to water stress (cf. Section 14.2.1.3).

- Monthly interception loss values were derived using the modified Gash storage model, which produced higher values than those used in the previous biofuel project (cf. Section 13.3.6).
- A maximum season length of six months (i.e. 180 days) was assumed. As shown in Section 15.3.5, the crop cycle varied from two to six months (60-180 days). For quinary subcatchments with a hot climate and short crop cycles (< 90 days), the hydrological impact of crop production would be much less than that simulated in the previous project, which assumed a fixed (i.e. for all quinary subcatchments) season length of five and six months for soybean and sorghum, respectively.
- A new baseline was adopted in this study to represent natural vegetation (cf. Section 16.2).
- In the previous biofuel project, a crop coefficient of 0.25 was used for the fallow period. Based on actual measurements conducted in this project, a value of 0.20 was used.
- Monthly crop coefficients were calculated from simulations of accumulated reference evapotranspiration (ET_O) and water use (ET_C) for non-water stressed growing conditions derived using the AquaCrop model (cf. Section 13.4).

The first three difference listed above apply to both the baseline and crop model runs. Thus, there is a "cancellation" effect. Therefore, the latter point is responsible for the reduced impact of crop production on downstream water availability. The methodology that was followed to assess the impact of using AquaCrop-derived crop coefficients on runoff generation was described in detail in Appendix N (and summarised in Section 13.4.1), with the results presented in Section 13.4.2. Although only two quinary subcatchments were tested (Quinary Subcatchment 4697 and Quinary Subcatchment 4325), they both showed substantially lower impacts of land use change on runoff generation (cf. Section 13.4.3). These tests were not performed using the revised quinary climate database, nor the version of ACRU that handles K_C values differently, nor the new baseline. Hence, the lower impacts were solely due to the use of simulated crop coefficients.

CHAPTER 17: GENERAL CONCLUSIONS, RECOMMENDATIONS AND FUTURE RESEARCH

17.1 SUMMARY OF MAIN FINDINGS

17.1.1 Overview of biofuel feedstocks

The research focus of this project was largely guided by policy related to biofuel production in South Africa, in particular a policy paper released by DWS in 2016 (DWS, 2016), which strongly supports the cultivation of biofuel feedstocks under rainfed conditions. In addition, the draft Biofuel Regulatory Framework, published in 2014, highlighted soybean and sorghum as reference feedstocks to represent the production of biodiesel and bioethanol, respectively. It also strongly supports the inclusion of smallholder farmers in the biofuel value chain, and thus field-based research focused on the smallholder farming environment. On 13 December 2019, Cabinet approved the draft Biofuel Regulatory Framework, which allows for the implementation of the 2007 Biofuel Industrial Strategy. The framework was amended in January and published on 7 February 2020 (DMRE, 2020). The research presented in this document, together with that published by the previous project, will provide the government (in particular, the Biofuel Task Team) with valuable information and knowledge to assist with and hopefully guide the implementation process.

South Africa is a water-scarce country. The greatest challenge facing the emerging biofuel industry will thus be to increase crop production using less water (i.e. improve crop water use efficiency). From a literature review, more studies have been conducted on estimating the water use efficiency of grain sorghum compared to soybean in South Africa. Based on this, field-based research focused on soybean, rather than on sorghum. Research trials were conducted over four seasons. The knowledge gained facilitated the development of agronomic guidelines for feedstock production, particularly for smallholder farmers, and the validation of the modelling approach to estimate the water use and yield of these two feedstocks.

17.1.2 Production guidelines

Enterprise budgets of income and costs were developed pertaining to soybean and sorghum cultivation. For sorghum, costs were scaled up from the 2017/18 research trial to a hectare, which could potentially drastically distort the budget. Soybean production costs reflect a commercial farm. In addition, a break-even analysis was completed, with yields of 1.77 and 3.43 t ha^{-1} estimated for soybean and sorghum, respectively. Agronomic requirements and production guidelines for both crops were synthesised from the available literature and supplemented with knowledge gained from the field trials. For example, the application of mulch should be considered by smallholder farmers, especially under rainfed conditions where water is a major limiting factor. Smallholder farmers are also encouraged to inoculate soybean seed. An inoculation guide was developed to assist with this. In addition, smallholder farmers were encouraged to apply fertilizer at the start of the season, to keep the plots weed-free (especially during the vegetative growth stage) and to undertake preventative sprays to reduce the incidence of pests and diseases.

17.1.3 Field-based research

Crop water use, growth and yield were measured at trials conducted over four seasons (2015/16 to 2018/19) at two locations (Swayimane and Baynesfield). It is worth noting that, when compared to the non-fertilized treatment, fertilizer treatments during the 2015/16 and 2017/18 seasons did not significantly impact on crop yield or biomass production, which was not expected. A summary of the main findings from each trial are presented next.

17.1.3.1 The 2015/16 season

In the first season, the effects of fertilization and mulching on soybean growth and yield were assessed at Swayimane. Soil fertility had a significant effect on soybean's LAI, but not on biomass accumulation or final yield. Mulching not only improved soil water content, but also reduced fluctuations in the topsoil. Although chlorophyll content was significantly higher under mulching, there were no significant differences for stomatal conductance, LAI, biomass and yield of soybean. The overall yield of 1.6 t ha^{-1} was low, due partly to the lack of inoculation, a low pH of 4.2 (aluminium toxicity) and a fungal disease that may have been transferred from the hay mulch.

The LAI was simulated using the SWB model for the control (non-mulched, fully fertilized) treatment. Although the model over-simulated LAI, model performance was considered adequate. The SWB was also used to simulate biomass production, with a tendency to over-estimate observations. The SWB did not adequately simulate the profile water content and simulated a much drier soil profile, especially at mid-season and at harvest.

17.1.3.2 The 2016/17 season

During the second season, the water use and yield of soybean was measured at Baynesfield as recommended by the previous biofuel project. Crop evapotranspiration was estimated using a new surface renewal method (SR2) that does not require calibration against an eddy co-variance system. The SR2 data analysis was performed using MOST (SR2-MOST), and DT (SR2-DT). The SR2-MOST method requires additional measurements of wind speed and canopy parameters, compared to SR2-DT. The latter method needs a relatively small number of input parameters and is more robust and less expensive to implement.

Crop evapotranspiration accumulated over 125 days was estimated at 378 and 384 mm using the two methods. From the averaged water use of 381 mm, a WUE of 1.35 kg m^{-3} was calculated from a measured yield of 5.14 t ha^{-1}. Severe lodging occurred during the season, which is evident from the combine harvested yield of 3.2 t ha^{-1}. Using an average oil seed content of 18%, a biofuel yield of 955.4 ℓ ha^{-1} was obtained, which equates to a WUE for biofuel production of 0.25 ℓ m^{-3}.

17.1.3.3 The 2017/18 season

In the third season, a trial was conducted at Swayimane to estimate the crop water use, grain yield, WUE and biofuel yield of three grain sorghum genotypes grown under rainfed conditions and two soil fertility levels. Due to the late planting in January, grain yield was influenced by the decline in air temperature, solar irradiance and rainfall experienced towards the end of the growing period. This highlighted the benefit of planting early (November to December), which would have helped reduce cold and water stress. PAN8906 showed potential to produce greater yields, and more biofuel with less water consumption than PAN8816. Macia produced a relatively high proportion of biomass to grain yield and exhibited the lowest starch content. Thus, this open pollen variety may not be best suited to biofuel production. Based on these results, the crop model was partially calibrated for PAN8906 (not PAN8816 or Macia) due to its higher biofuel production potential.

17.1.3.4 The 2018/19 season

The fourth trial was conducted at Swayimane to estimate the crop water use and grain yield of three soybean cultivars grown under rainfed conditions and two inoculation treatments. Unfortunately, one cultivar (PAN1521R) failed to germinate, thus highlighting the importance of conducting germination tests (prior to planting) to assess viability. Inoculation significantly improved canopy cover, stomatal conductance and the chlorophyll content index of two cultivars (LS6161R and CAPG3). However, it did not significantly improve final biomass and grain yields.

Nonetheless, inoculation should be used by smallholder farmers as it reduces fertilization costs and can also be beneficial for rotational crops such as maize. However, emphasis must be placed on the correct application of the inoculant, which should be done in conjunction with phosphorus and potassium application. The LS6161R cultivar is better suited to biofuel production due to its higher yield potential when compared to CAPG3. Based on these results, the crop model was partially calibrated for LS6161R (not CAPG3) due to its higher biofuel production potential.

17.1.4 Model selection and description

The ACRU agro-hydrological model was selected to assess the hydrological impacts of biofuel feedstock production on downstream water availability. This model was the preferred choice in numerous other studies that assessed the impacts of land use change on runoff response, simply because ACRU does not require extensive parameterisation. The AquaCrop model was selected to estimate the attainable yield of each strategic biofuel feedstock. This model is ideally suited to performing multiple seasonal simulations of crop yield.

Both models have been successfully linked to the quinary subcatchment database, which facilitates simulations at the national scale. Each quinary subcatchment presents a relatively homogeneous response zone of similar altitude, and thus lower spatial variation in similar climate and soils. A brief description of each model was given, followed by a comparison of each one. Both models have similar climate and soil inputs, but differ in their calculation of runoff response. Although ACRU will produce more accurate estimates of runoff than AquaCrop, it cannot estimate soybean and sorghum yield (only sugarcane, maize and wheat).

17.1.5 Model inputs

17.1.5.1 Climate and soils

The quinary climate database contains daily climate data for a 50-year period (1950-1999). The climate database was revised and used for the first time in this project. Errors in extreme rainfall events (daily rainfall > 400 mm) were identified and corrected. Instead of using interpolated temperature data for each quinary subcatchment, observed daily data was assigned to each quinary subcatchment, and then adjusted to account for altitudinal differences between the temperature station and the quinary subcatchment. Daily reference evapotranspiration was then estimated from the adjusted temperatures, assuming a fixed wind speed of 2 m s^{-1}. No changes were made to the quinary soils database.

17.1.5.2 Planting date and density

At the request of the project's reference group, an algorithm was developed to determine the first planting date in each quinary subcatchment based on rainfall and temperature criteria gleaned from the literature. A total of 50 planting dates were determined for each quinary subcatchment, from which the mean and median dates were calculated. Of the 5,838 quinary subcatchments, no planting dates could be determined for 1,527 quinary subcatchments (or 26.2%), indicating their unsuitability for crop production. The dominant planting months, whether determined using the mean or median statistic, were November and December. Based on this finding, these two months were selected as fixed planting dates. Although the analysis was conducted using historical climate record, it is acknowledged that planting dates should be determined using climate forecasts. The day of planting was set to the beginning of the month and not mid-month. This was done because the crop model was used to generate monthly crop coefficients, and thus the initial value was averaged from 30 days of data (not 15 days).

Typical planting densities were obtained from a literature review. For this project, a planting density of 250,000 and 300,000 plants ha^{-1} was selected for soybean, the latter being similar to that used at Swayimane in 2018/19. For grain sorghum, a planting density of 44,444 plants ha^{-1} was selected, which corresponds to that used in the 2017/18 season at Swayimane.

As a general rule of thumb, sorghum is typically planted in areas that are considered sub-optimal for maize production and at the same planting density. Based on this, a higher density of 60,000 plants ha^{-1} was also selected for grain sorghum.

17.1.6 Model parameters

17.1.6.1 Crop yield

A full calibration of the crop model was not possible using data from the field trials as they were rainfed, and thus water stressed. Instead, a partial calibration was performed to adjust certain cultivar-specific parameters. For sorghum, certain crop parameter values were obtained from the literature. The calibration was then validated by comparing simulated against observed yields. With regard to parameterisation of the hydrological model, innovative approaches adopted in this project included the derivation of monthly crop coefficients from crop model output, and interception loss per rain day via a new method that required measured LAI. Furthermore, crop coefficients representing the fallow period were measured, which is also considered innovative.

17.1.6.2 Biofuel yield

Equations were provided to estimate theoretical biodiesel and bioethanol yield. Extractable starch content and fermentation efficiency were measured for three sorghum genotypes and pooled with data collected in the previous biofuel project. Hence, three seasons of data exists for PAN8816. The extractable starch contents (range: 62.5-70.2%) and fermentation efficiencies (range: 0.818-0.935) for PAN8816 and PAN8906 (Macia was excluded) were averaged (i.e. 66.1% and 0.90) and used to estimate bioethanol production at a national scale.

Similarly, seed oil content for two soybean cultivars was measured, with LS6161R measured over two seasons. The seed oil content ranged from 16.7-21.8%, and was then averaged (18.6%) and used to estimate biodiesel production at a national scale.

17.1.6.3 Runoff response

Parameters for the hydrological model were obtained from the literature and are mostly similar to those used in the previous biofuel project and other national studies involving the quinary subcatchments. However, a new algorithm was used to derive the coefficient of initial abstraction based on rainfall seasonality and distance from the coastline. In addition, surface cover fraction was estimated from monthly crop coefficients. The fraction of active roots in the topsoil horizon was estimated from the topsoil depth.

Using monthly averaged LAI values measured for soybean cultivar LS6161R during the 2018/19 trial at Swayimane, daily interception loss values were determined for the inoculated treatment. Similarly, daily interception losses were determined for grain sorghum (PAN8906) using monthly averaged LAI values from the 2017/18 trial at Swayimane for the fertilized treatment. The variable storage Gash model, which is far more complex than the simpler Von Hoyningen-Huene method, was used to generate mean monthly interception loss values using 50 years of daily climate input. Monthly interception losses derived using the modified Gash model are higher in the summer months, but considerably lower in the fallow period, where the monthly LAI value was set to 0.13 m^2 m^{-2}. A detailed methodology was provided to allow other researchers to utilise the modified Gash model.

AquaCrop's ability to simulate crop coefficients was tested against measured values derived for soybean using crop water use data obtained in the 2016/17 season at Baynesfield. Similarly, water use data obtained in the 2012/13 season at Ukulinga (as part of the previous biofuel project) was used to calculate monthly crop coefficients (K_C).

Simulated K_C values obtained from AquaCrop output compared favourably to measured K_C for both crops. Hence, AquaCrop was used to obtain monthly crop coefficients for each quinary subcatchment, where irrigation (to 50% of PAW) was used to artificially remove crop water stress. Monthly values were calculated for each of the 49 seasons, then averaged to produce a unique set of values for each quinary subcatchment.

Tests were performed on two quinary subcatchments (Quinary Subcatchment 4697 and Quinary Subcatchment 5325) where AquaCrop-derived crop coefficients were used as input for ACRU to estimate runoff response from sorghum, which was then compared to that generated from natural vegetation. The relative reduction in mean annual runoff that could result from a land use change to sorghum cultivation was then calculated and compared to results obtained in the previous biofuel study. The relative reduction in MAR changed from 12.1 to 1.5% in Quinary Subcatchment 4697 and from 24.1 to 13.8% in Quinary Subcatchment 4325. Hence, the use of AquaCrop-derived crop coefficients resulted in a much lower impact of crop production on runoff generation.

17.1.7 Spatial application of models

For this project, considerable effort was spent on reducing the computational expense associated with running both simulation models at the national scale. Firstly, major changes were made to ACRU's code to improve its execution speed. Secondly, significant improvements were made to utilities that post-process ACRU's output, especially the generation of statistics. Thirdly, in order to automate the national model runs, approximately 8,600 and 10,000 lines of code (written in UNIX and Fortran) were developed for AquaCrop and ACRU, respectively. Furthermore, over 1,400 lines of code were written to convert the climate input files from ACRU format to that required by AquaCrop. A national run involving ACRU and the new statistics utility took approximately 38 minutes to complete, which represents a significant reduction in computational expense when compared to the run time of 510 minutes obtained in the previous biofuel project. A detailed explanation of the methodology developed to run ACRU at the national scale is provided in this report, which, to date, has allowed researchers working on other WRC-funded projects to implement and benefit from similar speed improvements. A version of ACRU used in Alberta (Canada) to simulate snowmelt was also modified to improve its run time. This means that ACRU users will spend far less time waiting for model runs to complete, which allows them to consider additional scenarios.

17.1.8 Modelling of crop water use and yield

The national scale yield maps developed from AquaCrop output clearly highlight low and high potential areas for soybean and sorghum production. Large parts of the country's interior region, especially towards the western areas, are too dry for crop cultivation under rainfed conditions. Other parts in the Lesotho Highlands and along the Drakensberg Escarpment are too cold for crop production. Of concern is the northern Free State where soybean is produced, yet AquaCrop simulated no yield for both crops. This problem is probably due to the partial model calibration of cultivar LS6161R, which is best suited to warm areas (Maturity Group 6). The Free State is better suited to Maturity Group 4/Maturity Group 5 (i.e. cool/temperate) cultivars. Similarly, the model was partially calibrated for sorghum cultivar PAN8906, which may not be suited to the cooler parts of the northern Free State.

The maps of WUE indicate that sorghum is more water use efficient than soybean, due to higher sorghum yields. AquaCrop will under-estimate the crop evapotranspiration of indeterminate crops, considering that the model will reduce transpiration after flowering, but the crop will form new leaves and continue to transpire. Hence, the model is likely to over-estimate crop WUE. Water use efficiency maps must be interpreted in conjunction with the yield maps, considering low yields (and lower crop evapotranspiration) can result in relatively high WUE.

Eight national crop model runs were performed, which showed that changing the planting date had a greater impact on crop production than changing the planting density. The maps also showed that the higher planting density usually produced more crop yield as expected.

Due to the speed improvements made in running AquaCrop at the national scale, the scene is set to consider other scenarios involving different planting dates and plant populations. As noted in this project, model output should support decision-making processes and not be used to derive absolute recommendations for best management.

17.1.9 Hydrological impacts of crop production

Warburton Toucher et al. (2019) provided an alternative hydrological baseline against which land use changes can be assessed. Since DWS recently expressed an interest in adopting the new baseline, it was used in this project to assess the hydrological impact of land use changes from natural vegetation to biofuel feedstock production. With the exception of only a few quinary subcatchments, neither the cultivation of soybean nor the cultivation of grain sorghum for biofuel production is likely to significantly affect the quantity of water available to downstream users. Hence, these crops show little to no potential of being declared SFRAs. This is in contrast to results from the previous biofuel project, which showed that Quinary Subcatchment 2423 and Quinary Subcatchment 1348 exhibited SFRA potential for grain sorghum and soybean, respectively.

Compared to the previous WRC project, a revised (and improved) quinary climate database was used, as well as a new hydrological baseline. Changes were also made to ACRU's code that affects the way in which the model internally adjusts daily crop coefficient values due to water stress. However, the most significant change that was adopted was the derivation of monthly crop coefficients from AquaCrop simulations of accumulated ET_O and crop water use for non-water stressed growing conditions (ET_C). Hence, a unique set of monthly crop coefficients was derived for each quinary subcatchment, instead of using a fixed set of values derived at one location (Ukulinga) for all other quinary subcatchments.

17.2 LIMITATIONS AND ASSUMPTIONS

17.2.1 Single season trials

In this project, a number of best-management practices were based on results obtained in one season in different agro-ecologies (e.g. Swayimane, Baynesfield, Ukulinga, Umbumbulu, Deepdale and Richards Bay). This may offset the reliability of the conclusions drawn as results from multiple seasons would be more reliable. Hence, the guidelines may only apply to agro-ecologies similar to those where the trials were conducted. Ideally, such trials should be repeated across different agro-ecologies.

17.2.2 Measurements of sorghum LAI

Measurements of sorghum's LAI in the third season were averaged to produce monthly values, from which interception loss was estimated using the modified Gash model. However, LAI was measured using a faulty LAI-2200 plant canopy analyser. As a result of the unexpected variation in LAI, the device was returned to LI-COR in the USA for recalibration. Hence, the interception loss values should be considered unreliable.

17.2.3 Impacts of climate change

Since the quinary climate database ends in 1999, it does not reflect the climate variability from 2000 to 2019, within which anthropogenically induced changes in extreme climatological events have occurred. For example, 2019 was likely to be the hottest year on record, as was 2018, which superceded 2017, and so on. Hence, the variability in inter-annual planting dates, crop yields and WUEs is likely to increase in the latter 20-year period.

17.2.4 Fallow period crop coefficients

A single set of crop coefficients representing the fallow period was determined at Baynesfield. These values were then used to represent the fallow period in all other quinary subcatchments, which is not ideal. However, the monthly values were adjusted from FAO56 to A-pan equivalent crop coefficients, which produced a different set of values for each quinary subcatchment.

17.2.5 Crop model calibration

As noted in Section 15.2, the field trials undertaken in this project were rainfed and not irrigated, which meant the measured crop water use and yield data collected over four seasons could not be used to fully calibrate AquaCrop. Hence, default values provided by the model developers (FAO) were used for most of the crop parameters. Furthermore, a partial model calibration was undertaken to adjust certain parameters related to the thermal time required for the completion of various phenological growth stages. Observations were made in days, and then converted to GDDs within the model. Ideally, a full calibration of AquaCrop should have been undertaken for both crops using data collected in non-stressed environments.

17.2.6 Initial soil water content

For the national model runs, the initial soil water content was set to field capacity, which is AquaCrop's default option, but may be unrealistic for rainfed conditions. This was based on recommendations by Kunz et al. (2015b), who found that changing this setting to, for example, 50% of plant available water (ACRU's default option) resulted in a significant reduction in simulated yield (e.g. by 64-75% for sugarcane). As noted in Section 14.1.1.1, the sensitivity of seed germination to soil moisture has been addressed in Version 6, which now assumes that sufficient reserves are available in the seed for leaf expansion to occur at its maximum rate just after germination.

17.2.7 Simulation of crop evapotranspiration

Since soybean cultivar LS6161R is semi-determinate, it continues to form new leaves after flowering. It is expected that AquaCrop will struggle to accurately simulate crop evapotranspiration, considering that the model will reduce transpiration as the leaves dry out and mature towards the end of the season. Hence, the model is likely to under-estimate crop water use and hence, over-estimate WUE.

17.2.8 Crop yield maps

AquaCrop did not simulate crop yield in the northern Free State where both crops are produced. This problem is probably due to the partial model calibration of cultivar LS6161R, which is best suited to warm areas (Maturity Group 6). The Free State is better suited to Maturity Group 4/Maturity Group 5 (i.e. cool/ temperate) cultivars. Similarly, the model was partially calibrated for sorghum cultivar PAN8906, which may not be suited to the cooler parts of the northern Free State.

17.3 RECOMMENDATIONS FOR FUTURE RESEARCH

The various approaches developed and implemented in this study are by no means considered "exhaustive". Although much effort was spent on producing simulated output that is considered reliable and error-free, the following suggestions would further improve the accuracy of results. These suggestions pertain to the two main research thrusts: the crop water use and yield modelling, and the hydrological modelling.

17.3.1 Field-based research

From results obtained in the 2018/19 season at Swayimane (cf. Section 8.2.5.3), the SPAW model tends to over-estimate soil water retention parameters, and thus values should rather be determined using the outflow pressure method. Similarly, it is recommended that soil dry bulk density is measured and not estimated using SPAW.

The four trials conducted as part of this project were undertaken in one season and one location, which may offset the reliability of the results. For future research, a multi-season study replicated in different agro-ecologies is strongly recommended. In addition, soybean cultivar PAN1521R did not germinate in the 2018/19 trial at Swayimane. Since this cultivar is well adapted to all soybean growing regions (cool to warm), it should be considered in future trials to determine crop and biofuel yield, relative to its water use.

The new surface renewal method (SR2) implemented in this study is highly recommended for crop water use measurements. This micrometeorological technique is more accurate than the simple water balance approach for estimating crop water use. The SR2 method negates the need for calibration against the eddy co-variance method (in order to derive the alpha coefficient), as is required by the classic SR method (SR1) used in the previous biofuel project. Eddy co-variance is not only more expensive to implement, but is prone to data quality issues (and data loss), especially when it rains.

17.3.2 Modelling of crop yield

17.3.2.1 Model calibration

As noted in Section 17.2.5, a partial calibration of the crop productivity model was performed in this project. In the future, a full calibration should be undertaken for both soybean and sorghum. As a guideline, the model calibration and validation approach of Chibarabada et al. (2020) for groundnut should be followed. The authors used an extensive calibration dataset collected over two seasons at three acro-ecologies, with trials conducted under optimum irrigation, deficit irrigation and rainfed conditions.

17.3.2.2 Additional crop cultivars

The crop productivity model was run using partially calibrated crop parameters for soybean cultivar LS6161R and grain sorghum PAN8906. These two cultivars exhibited higher biofuel production potential than other cultivars tested, namely CAPG3 (soybean) and PAN8816 (sorghum). It is recommended that the crop model is run for the latter two cultivars in order to help derive best-management practices for specific areas.

17.3.2.3 Other planting dates

Results from this project showed that planting date had a greater impact on simulated yield than planting density. Owing to time constraints, only two planting dates were considered (November and December). However, knowledge of cultivar performance under different planting date scenarios is lacking. Therefore, it is recommended that the crop model is run with two other planting date scenarios: October and January.

For this project, an algorithm was developed to derive suitable planting dates in each quinary subcatchment based on historical climate record. However, planting dates should be determined using climate forecasts. Using a variable planting date approach for each quinary subcatchment is not recommended in future studies. Instead, the model should be run for a range of possible planting dates (e.g. October, November, December and January) in each quinary subcatchment, so that yield comparisons can be done to help derive best-management practices for specific areas.

17.3.2.4 Leaf Area Index from canopy cover

It is not ideal to use LAI values derived at one location to represent all other crop-growing regions in the country. Hence, the option to model LAI values is proposed. Although SWB was used to simulate LAI at Swayimane in the 2015/16 season, this approach is not feasible since the model cannot be run in “batch mode” to generate localised values for each quinary subcatchment. Alternatively, AquaCrop simulates daily canopy cover instead of LAI. A method is proposed in Appendix O to estimate LAI from simulated canopy cover.

17.3.2.5 Rooting depth

AquaCrop provides the rooting depth attained at each crop growth stage over the growing season. However, this daily output cannot be used to derive the monthly fraction of roots in the A-horizon (*ROOTA*), nor the colonisation of the B-horizon (*COLON*). Additional information of lateral root growth and mass is required, which the model does not output. Hence, further research is required to provide representative values for these two variables.

17.3.3 Modelling of crop water use

17.3.3.1 Simulation of crop evapotranspiration

Paredes et al. (2015) reported that, although AquaCrop adequately simulated soybean yield and biomass, poor estimates of crop evapotranspiration were obtained. The model under-estimated soil water evaporation when compared to measurements. The authors suggested that AquaCrop should be modified to calculate evapotranspiration using the dual K_C approach. This suggestion is strongly echoed in this project, considering that the model was used to derive monthly crop coefficients as input for ACRU.

17.3.3.2 Initial crop coefficient

As noted in Section 10.3, the planting date was set to the beginning of the month and not mid-month so that the initial K_C value was averaged from 30 days of ET_C and ET_O data (not 15 days). In the future, the cropping period in AquaCrop should start mid-month, but the simulation period should start 15 days earlier to simulate fallow conditions prior to planting. This means that the month crop coefficients are based on 30 days of data.

17.3.3.3 Initial soil water content

In the future, national model runs should be performed where the initial soil water content at planting is set to 50% of PAW in order to assess the impact of this setting on crop yield. This will determine if AquaCrop's sensitivity to initial soil moisture levels has been addressed by the model developers (cf. Section 14.1.1.1).

17.3.3.4 "Hot start" option in AquaCrop

The new "hot start" option in the model should be investigated where the simulated soil water content at the end of a previous season can be taken as the initial conditions for the following season. This option should replace the setting used in this project where the soil water content is assumed to be at field capacity at the start of the season.

17.3.4 Modelling of hydrological impacts

17.3.4.1 Extreme rainfall events

In Section 10.1.1.3, daily rainfall totals above 400 mm in the quinary subcatchment climate database were checked by comparing them to observations from neighbouring stations. In the future, it is recommended that this time-consuming process be automated as much as possible, so that daily rainfall events between 100 and 400 mm are also validated.

17.3.4.2 Updated climate data

The WRC recently approved a proposed project to update the quinary subcatchment climate database. This involves extending the daily record beyond 1999 up to 2019 (i.e. by an additional 20 years). In the past, this task has proven difficult due to the high costs involved in purchasing rainfall and temperature data from the SAWS and ARC.

National assessments of hydrological and agricultural responses to climate variability, based on the additional 20-year record (from 2000 to 2019), would provide a better assessment of risk. This is due to the anthropogenically induced changes in extreme climatological events that have occurred from 2000 onwards. Once this work has been completed, the simulation modelling undertaken in the biofuel project should be revised.

17.3.4.3 Updated soils information

Soil-related information in the current quinary soils database was derived from the land types dataset (SIRI, 1987) by Schulze and Horan (2007) using the *AUTOSOIL* decision support tool (Pike and Schulze, 1995). There are five terrain units (crest, scarp, midslope, footslope and valley bottom) within each land type, and each terrain unit has different soil types. As a by-product of the work reported by Schütte et al. (2019), the authors have sought to determine soil hydrological characteristics at terrain unit level. However, while much of the work has been completed, further work is required to refine the dataset of soil hydrological characteristics at terrain unit level for the whole country. Once complete, it will be possible to assign soil information for each terrain unit to a particular quinary subcatchment. This involves using a GIS to determine which terrain units exist in each quinary subcatchment, and then to area-weight the soils data accordingly. This endeavour will spatially improve the accuracy of the soils data and avoid the use of average soil characteristics. Once this work has been completed, the water use and yield estimates for each feedstock should be revised.

REFERENCES

ABENDROTH LJ, ELMORE RW and FERGUSON RB (2006) *Soybean inoculation. G06-1621 Soybean inoculation: Understanding the soil and plant mechanisms involved* (part one of a two-part series). Extension publication G1621, University of Nebraska-Lincoln, Lincoln, NE, USA.

ACOCKS JPH (1953) Veld types of South Africa. Memoirs of the Botanical Society **28**, Botanical Research Institute, Pretoria, South Africa.

ACOCKS JPH (1988) Veld types of southern Africa. Botanical Survey of South Africa Memoirs **57**, Botanical Research Institute, Pretoria, South Africa.

ADEBOYE OB, SCHULTZ B, ADEKALU KO and PRASAD K (2017) Modelling of response of the growth and yield of soybean to full and deficit irrigation by using AquaCrop. Irrigation and Drainage **66 (2)** 192–205. https://onlinelibrary.wiley.com/doi/full/10.1002/ird.2073.

AFRICAN CENTRE FOR CROP IMPROVEMENT (ACCI) (2018) *The new breed.* ACCI, University of KwaZulu-Natal, Pietermaritzburg, South Africa.

AGRICULTURAL RESEARCH COUNCIL (ARC) (1999) *Sorghum production guide*, Grain Crops Institute, ARC, Potchefstroom, South Africa.

AGRICULTURAL RESEARCH COUNCIL (ARC) (2003) *Sorghum production*, Grain Crops Institute, ARC, Potchefstroom, South Africa.
http://www.arc.agric.za/arc-gci/Fact%20Sheets%20Library/Sorghum%20Production.pdf.

AGRICULTURAL RESEARCH COUNCIL (ARC) (2018) *Sorghum production*, Crops Institute, ARC, Potchefstroom, South Africa. www.arc.agric.za/arc-gci/Documents/Soybeans/Soja17-18.pdf.

ALLEN R (2000) *Calibration for the Watermark 200SS soil water potential sensor to fit the 7-19-96 "Calibration #3" table from irrometer*.
http://www.kimberly.uidaho.edu/water/swm/calibration_watermark2.pdf.

ALLEN RG, PEREIRA LS, RAES D and SMITH M (1998) *Crop evapotranspiration – guidelines for computing crop water requirements.* Irrigation and drainage paper 56, Chapter 6, Food and Agricultural Organisation (FAO), Rome, Italy. http://www.fao.org/ag/agl/aglw/cropwater/docs/method.pdf.

ALLEN RG, PEREIRA LS, HOWELL TA and JENSEN ME (2011) Evapotranspiration information reporting: I. Factors governing measurement accuracy. Agricultural Water Management **98** 899–920. http://www.sciencedirect.com/science/article/pii/S0378377411000023.

ALSAJRI FA, WIJEWARDANA C, IRBY JT, BELLALOUI N, KRUTZ LJ, GOLDEN B, GAO W and REDDY KR (2020) Developing functional relationships between temperature and soybean yield and seed quality. Agronomy Journal 1–11.
https://acsess.onlinelibrary.wiley.com/doi/full/10.1002/agj2.20034.

ANGUS GR (1989) Sensitivity of ACRU model input. In*: ACRU: Background: Concepts and theory*, SCHULZE RE. WRC Report 154/1/89, Water Research Commission, Pretoria, South Africa.

ANNANDALE JG, BENADÉ N, JOVANOVIC NZ, STEYN M and DU SAUTOY N (1999) *Facilitating irrigation scheduling by means of the soil water balance model*. WRC Report No. 753/1/99, Water Research Commission, Pretoria, South Africa.

ARAYA A, KISEKKA I and HOLMAN J (2016) Evaluating deficit irrigation management strategies for grain sorghum using AquaCrop. Irrigation Science **34 (6)** 465–481. https://link.springer.com/article/10.1007/s00271-016-0515-7.

ARNAL L (2014) *An intercomparison of flood forecasting models for the Meuse River basin*. MSc dissertation, Deltares, Vrije Universiteit, Amsterdam, The Netherlands.

ATABANI AE, MAHLIA TMI, BADRUDDIN IA, MASJUKI HH, CHONG WT and LEE KT (2013) Investigation of physical and chemical properties of potential edible and non-edible feedstocks for biodiesel production, a comparative analysis. Renewable and Sustainable Energy Reviews **21** 749–755. http://www.sciencedirect.com/science/article/pii/S1364032113000580.

AZADI H and HO P (2010) Genetically modified and organic crops in developing countries: A review of options for food security. Biotechnology Advances **28 (1)** 160–168. https://www.sciencedirect.com/science/article/abs/pii/S0734975009001876.

BATTISTI R, SENTELHAS PC and BOOTE KJ (2017) Inter-comparison of performance of soybean crop simulation models and their ensemble in southern Brazil. Field Crops Research **200** 28–37. http://www.sciencedirect.com/science/article/pii/S0378429016304270.

BAUMHARDT RL and JONES OR (2002) Residue management and tillage effects on soil water storage and grain yield of dryland wheat and sorghum for a clay loam in Texas. Soil Tillage Research **68 (2)** 71–82. https://www.sciencedirect.com/science/article/pii/S0167198702000971.

BELLALLELOUI N, BRUNS HA, ABBAS HK, MENGISTU A, FISHER DK and REDDY KN (2015a) Agricultural practices altered soybean seed protein, oil, fatty acids, sugars, and minerals in the Midsouth USA. Frontiers in Plant Science **6 (31)** 1–14. https://www.frontiersin.org/articles/10.3389/fpls.2015.00031/full.

BELLALLELOUI N, BRUNS HA, ABBAS HK, MENGISTU A, FISHER DK and REDDY KN (2015b) Effects of row-type, row-spacing, seeding rate, soil-type, and cultivar differences on soybean seed nutrition under US Mississippi Delta condition. PLoS ONE **10 (6)** 1–23. https://journals.plos.org/plosone/article?id=10.1371/journal.pone.0129913.

BELLO ZA and WALKER S (2016) Calibration and validation of AquaCrop for pearl millet (*Pennisetum glaucum*). Crop and Pasture Science. **67** 948–960. http://www.publish.csiro.au/cp/CP15226.

BERGSTRÖM S (1991) Principles and confidence in hydrological modelling. Hydrology Research **22 (2)** 123–136.

BLIGNAUT C and TAUTE M (2010) *The development of a map showing the soybean production regions and surface areas of the RSA*. Produced for the Protein Research Foundation (PRF), Johannesburg, South Africa.

BORGES R and MALLARINO AP (2000) Grain yield and early growth and nutrient uptake of no-till soybean as affected by the phosphorus and potassium placement. Agronomy Journal **92 (2)** 380–388. https://acsess.onlinelibrary.wiley.com/doi/abs/10.2134/agronj2000.922380x.

BORRELL AK, MULLET JE, GEORGE-JAEGGLI B, VAN OOSTEROM E J, HAMMER GL, KLEIN PE and JORDAN DR (2014) Drought adaptation of stay-green sorghum is associated with canopy development, leaf anatomy, root growth, and water uptake. Journal of Experimental Botany **65** 6251–6263. https://academic.oup.com/jxb/article/65/21/6251/609700.

BUAH SSJ, KOMBIOK JM and ABATANIA LN (2012) Grain sorghum response to NPK fertilizer in the Guinea Savanna of Ghana. Journal of Crop Improvement **26 (1)** 101–115. https://www.tandfonline.com/doi/full/10.1080/15427528.2011.616625.

BULCOCK HH (2011) *An assessment of canopy and litter interception in commercial forest plantations and an indigenous forest in the KwaZulu-Natal Midlands, South Africa.* PhD thesis, School of Bioresources Engineering and Environmental Hydrology, University of KwaZulu-Natal, Pietermaritzburg, South Africa.

BULCOCK HH and JEWITT GPW (2012) Modelling canopy and litter interception in commercial forest plantations in South Africa using the variable storage Gash model and idealised drying curves. Hydrology and Earth Systems Science **16** 4693–4705. https://www.hydrol-earth-syst-sci.net/16/4693/2012/hess-16-4693-2012.pdf.

BUREAU FOR FOOD AND AGRICULTURAL POLICY (BFAP) (2008) *Impact analysis of the Biofuels Industrial Strategy on the South African agricultural and biofuel subsectors.* BFAP Biofuels Report 03/2008, BFAP, Pretoria, South Africa. http://www.bfap.co.za/reports/BFAP_Biofuels_report_no3.pdf.

CALDER IR (1986) A stochastic model of rainfall interception. Journal of Hydrology **89 (1–2)** 65–71. https://www.sciencedirect.com/science/article/pii/0022169486901435.

CALDER IR (1996) Dependence of rainfall interception on drop size: 1. Development of the two-layer stochastic model. Journal of Hydrology **185 (1–4)** 363–378. https://www.sciencedirect.com/science/article/pii/0022169495029982.

CHAKRABORTY D, NAGARAJAN S, AGGARWAL P, GUPTA VK, TOMAR RK, GARG RN and KARLA N (2008) Effect of mulching on soil and plant water status, and the growth and yield of wheat (*Triticum aestivum* L.) in a semi-arid environment. Agricultural Water Management **95 (12)** 1323–1334. https://www.sciencedirect.com/science/article/abs/pii/S0378377408001480.

CHARD J (2002) *Watermark soil moisture sensors: Characteristics and operating instructions*, Utah State University, Logan, UT, USA. https://www.researchgate.net/publications/237805713_WATERMARK_SOIL_MOISTURE_SENSORS_Characteristics_and_Operating_Instructions.

CHIBARABADA TP, MODI AT and MABHAUDHI T (2020) Calibration and evaluation of AquaCrop for groundnut (*Arachis hypogaea*) under water deficit conditions. Agricultural and Forest Meteorology **281** 1–8. https://www.sciencedirect.com/science/article/pii/S0168192319304666.

CHIKOWO R, SNAPP S, and HOESCHLE-ZELEDON I (2015) *Soybean: A versatile grain legume for smallholder farmers in Malawi.* Africa RISING Brief 38, International Livestock Research Institute Nairobi, Kenya. https://cgspace.cgiar.org/handle/10568/68094.

CHIMONYO VGP, MODI AT and MABHAUDHI T (2016) Assessment of sorghum-cowpea intercrop system under water-limited conditions using a decision support tool. Water SA **42 (2)** 316–327. https://www.ajol.info//index.php/wsa/article/view/134948.

COLEMAN A (2012) *R1,7 billion bio-ethanol plant in FS. Farmers Weekly*, 30 March 2012. http://www.farmersweekly.co.za/news.aspx?id=16363&h=Biofuels-Free-State.

COLEMAN A (2017) *Grain producers urged to report red-billed quelea outbreaks. Farmers Weekly*, 18 September 2017. https://www.farmersweekly.co.za/agri-news/south-africa/grain-producers-urged-report-red-billed-quelea-outbreaks/.

CONWAY D, PERSECHINO A, ARDOIN-BARDIN S, HAMANDAWANA H, DIEULIN C and MAHÉ G (2009) Rainfall and water resources variability in sub-Saharan Africa during the twentieth century. Journal of Hydrometeorology **10** 41–59. https://journals.ametsoc.org/doi/full/10.1175/2008JHM1004.1.

CUI SY and YU DY (2005) Estimates of relative contribution of biomass, harvest index and yield components to soybean yield improvements in China. Plant Breeding **124 (5)** 473–476. https://onlinelibrary.wiley.com/doi/full/10.1111/j.1439-0523.2005.01112.x.

DASTORANI MT and POORMOHAMMADI S (2012) Evaluation of water balance in a mountainous upland catchment using SEBAL approach. Water Resources Management **26** 2069–2080. https://link.springer.com/article/10.1007/s11269-012-9999-y.

DE BEER AS and BRONKHORST L (2016) *Soybean cultivar recommendations 2016/2017*. Grains Crop Institute, Agricultural Research Council, Potchefstroom, South Africa. http://www.arc.agric.za/arc-gci/Documents/Soybeans/Soybean%202016%202017.pdf.

DE BEER AS and BRONKHORST L (2017) *Soybean cultivar recommendations 2017/2018*. Grains Crop Institute, Agricultural Research Council, Potchefstroom, South Africa. https://www.arc.agric.za/arc-gci/Documents/Soybeans/Soja17-18.pdf.

DE BEER AS and BRONKHORST L (2019) *Soybean cultivar recommendations 2019/2020*. Grains Crop Institute, Agricultural Research Council, Potchefstroom, South Africa. https://www.arc.agric.za/Agricultural%20Sector%20News/Soybean%20Cultivar%20Recommendations%202019-2020.pdf.

DE BEER AS and DE KLERK N (2014) *Soybean cultivar recommendations*. Grain Crops Institute, Agricultural Research Council, Potchefstroom, South Africa. http://www.arc.agric.za/arcgci/Documents/Reports/Soybean%20Cultivar%20Recommendations%202013-2014.pdf.

DE BEER AS and DE KLERK N (2015) *Soybean cultivar recommendations*. Grain Crops Institute, Agricultural Research Council, Potchefstroom, South Africa. http://www.arc.agric.za/arc-gci/Documents/Soybeans/soyrecom14-15.pdf.

DE JAGER JM (1994) Accuracy of vegetation evaporation ratio formulae for estimating final wheat yield. Water SA **20 (4)** 307–317.

DEBAEKE P and ABOUDRARE A (2004) Adaptation of crop management to water-limited environments. European Journal of Agronomy **21 (4)** 433–446. https://www.sciencedirect.com/science/article/abs/pii/S1161030104000619.

DEMIRTAS C, YAZGAN S, CANDOGAN BN, SINCIK M, BŰYŰKCANGAZ H and GŐKSOY AT (2010) Quality and yield response of soybean (*Glycine max* L. Merrill) to drought stress in sub–humid environment. African Journal of Biotechnology **9 (41)** 6873–6881. https://www.ajol.info/index.php/ajb/article/view/130257.

DEPARTMENT OF AGRICULTURE AND RURAL DEVELOPMENT (DARD) (2016) *Soybean cultivar recommendations 2016.* DARD, Cedara, South Africa. https://www.kzndard.gov.za/images/Documents/researchandtechnologydevelopment/publications/Research_and_Technology_Bulletins/Soyabean-Cultivar-Recommendations.pdf.

DEPARTMENT OF AGRICULTURE, FORESTRY AND FISHERIES (DAFF) (2009a) *Soybeans*. DAFF, Pretoria, South Africa. http://www.nda.agric.za/docs/Brochures/soybean.pdf.

DEPARTMENT OF AGRICULTURE, FORESTRY AND FISHERIES (DAFF) (2009b) *Sorghum*. DAFF, Pretoria, South Africa. http://www.nda.agric.za/docs/Brochures/sorghum.pdf.

DEPARTMENT OF AGRICULTURE, FORESTRY AND FISHERIES (DAFF) (2010a) *Soya beans: production guideline*. DAFF, Pretoria, South Africa. http://www.nda.agric.za/docs/brochures/soya-beans.pdf.

DEPARTMENT OF AGRICULTURE, FORESTRY AND FISHERIES (DAFF) (2010b) *Sorghum: production guideline.* DAFF, Pretoria, South Africa. http://www.nda.agric.za/docs/Brochures/prodGuideSorghum.pdf.

DEPARTMENT OF AGRICULTURE, FORESTRY AND FISHERIES (DAFF) (2010c) *Soya beans production guideline.* DAFF, Pretoria, South Africa. http://www.nda.agric.za/docs/brochures/soya-beans.pdf.

DEPARTMENT OF AGRICULTURE, FORESTRY AND FISHERIES (DAFF) (2010d) *Grain sorghum market value chain profile.* National Department of Agriculture, Pretoria, South Africa. http://www.nda.agric.za/docs/AMCP/GrnSorghumMVCP2009-2010.pdf.

DEPARTMENT OF AGRICULTURE, FORESTRY AND FISHERIES (DAFF) (2013) *DAFF abstract of agricultural statistics.* DAFF, Pretoria, South Africa.

DEPARTMENT OF AGRICULTURE, FORESTRY AND FISHERIES (DAFF) (2018a) *Abstract of agricultural statistics 2018*. DAFF, Pretoria, South Africa. http://www.daff.gov.za/Daffweb3/Portals/0/Statistics%20and%20Economic%20Analysis/Statistical%20Information/Abstract%202018.pdf.

DEPARTMENT OF AGRICULTURE, FORESTRY AND FISHERIES (DAFF) (2018b) *Crops and markets: First quarter*. DAFF, Pretoria, South Africa. http://www.daff.gov.za/daffweb3/Home/Crop-Estimates/Statistical-Information/Crops-and-Markets.

DEPARTMENT OF AGRICULTURE, FORESTRY AND FISHERIES (DAFF) (2018c) *Crop estimates committee: Fourth forecast*. DAFF, Pretoria, South Africa. www.daff.gov.za/docs/Cropsestimates/Media%20May%202018.pdf.

DEPARTMENT OF AGRICULTURE, FORESTRY AND FISHERIES (DAFF) (2018d) *Trends in the agricultural sector: 2017*. DAFF, Pretoria, South Africa. http://www.daff.gov.za/Daffweb3/Portals/0/Statistics%20and%20Economic%20Analysis/Statistical%20Information/Trends%20in%20the%20Agricultural%20Sector%202017.pdf.

DEPARTMENT OF AGRICULTURE, FORESTRY AND FISHERIES (DAFF) (2018e) *South African varietal list as maintained by the registrar of plant improvement: Seed crops (December 2017)*. http://www.daff.gov.za/daffweb3/Branches/Agricultural-Production-Health-Food-Safety/Plant-Production/Verietal-Listing.

DEPARTMENT OF MINERALS AND ENERGY (DME) (2007) *The South African National Biofuels Industrial Strategy*. DME, Pretoria, South Africa. http://www.info.gov.za/view/DownloadFileAction?id=77830.

DEPARTMENT OF MINERAL RESOURCES AND ENERGY (DMRE) (2020) *South African Biofuels Regulatory Framework.* Government Gazette No. 43003, DMRE, Pretoria, South Africa. http://www.gpwonline.co.za/Gazettes/Gazettes/43003_7-2_Energy.pdf.

DEPARTMENT OF ENERGY (DoE) (2012*) Regulations regarding the mandatory blending of biofuels with petrol and diesel.* Government Gazette No. 35623, Amendment No. R.671 of the Petroleum Products Act of 1977, DoE, Pretoria, South Africa. http://www.info.gov.za/view/DownloadFileAction?id=173022.

DEPARTMENT OF ENERGY (DoE) (2014) *Position paper on the South African biofuels regulatory framework – the first phase of the implementation of the biofuels industrial strategy.* Government Gazette No. 538 of 2014, No. 37232, DoE, Pretoria, South Africa. http://www.gpwonline.co.za/.

DEPARTMENT OF WATER AND SANITATION (DWS) (2016) *Policy position on water use in bio-fuel production in South Africa*. DWS, Pretoria, South Africa.

DEVNARAIN N, CRAMPTON BG, CHIKWAMBA R, BECKER JVW and O'KENNEDY MM (2016) Physiological responses of selected African sorghum landraces to progressive water stress and re-watering. South African Journal of Botany **103** 61–69. https://www.sciencedirect.com/science/article/pii/S0254629915004007.

DHOPTE AM and EASTIN JD (1990) Response of sorghum to elevated night temperature imposed during floret differentiation under field conditions. In: *International Congress of Plant Physiology*, New Delhi, India, 15–20 February 1988, Volume 2, 929–934. Society for Plant Physiology and Biochemistry.

DLAMINI AP (2015) *Soybean (*Glycine max *L. Merr) productivity in varying agro-ecological zones.* MSc dissertation, Faculty of Natural and Agricultural Sciences, University of Pretoria, Pretoria, South Africa. http://repository.up.ac.za/handle/2263/50882.

DONATELLI M, STÖCKLE C, CEOTTO E and RINALDI M (1997) Evaluation of CropSyst for cropping systems at two locations of northern and southern Italy. European Journal of Agronomy **6 (1–2)** 35–45. https://www.sciencedirect.com/science/article/abs/pii/S1161030196020291.

DOORENBOS J and KASSAM (1979) *Guidelines for predicting crop water requirements*. FAO Irrigation and Drainage Paper 33, Food and Agriculture Organisation, Rome, Italy.

DREYER J (2017) *Soybeans – an exceptional crop*. Protein Research Foundation, Pretoria, South Africa. https://www.proteinresearch.net/poems/images/projects/0862/pamphlet/1-1-pp-pns-sojabone-skittergewas-prf-soybeans-exceptional-crop-2017.pdf.

DU PLESSIS J (2008) *Sorghum production*. National Department of Agriculture, Pretoria, South Africa. http://www.nda.agric.za/docs/Infopaks/FieldCrops_Sorghum.pdf.

EL BASSAM NE (2010) *Handbook of bioenergy crops: A complete reference to species, development and applications*, Earthscan, London, UK.

FANADZO N, CHIDUZA C, MNKENI PNS, VAN DER STOEP I and STEVENS J (2010) Crop production management practices as a cause for low water productivity at Zanyokwe Irrigation Scheme. Water SA **36 (1)** 27–35. https://www.ajol.info/index.php/wsa/article/view/50904.

FARAHANI HJ, IZZI G and OWEIS TY (2009) Parameterization and evaluation of the AquaCrop model for full and deficit irrigated cotton. Agronomy Journal **101** 469–476. https://dl.sciencesocieties.org/publications/aj/abstracts/101/3/469.

FISCHER G, VAN VELTHUIZEN H, HIZSNYIK E and WIDBERG D (2009) *Potentially obtainable yield in the semi-arid tropics. Global Theme on Agroecosystems*. Report No. 54. Patancheru 502 324, International Crops Research Institute for the Semi-Arid Tropics, Andra Pradesh, India. www.iwmi.cgiar.org/assessment/files_new/publications/ICRISATReport_54.pdf.

FOOD AND AGRICULTURAL ORGANISATION (FAO) (2002) *Crop water information*. http://ecocrop.fao.org/.

FOOD AND AGRICULTURAL ORGANISATION (FAO) (2006) *Ecocrop info*. FAO, Rome, Italy. http://ecocrop.fao.org/.

FOOD AND AGRICULTURAL ORGANISATION (FAO) (2012) *ETo calculator: Version 3.2.* Land and Water Digital Media Series No. 36. FAO, Rome, Italy. http://www.fao.org/land-water/databases-and-software/eto-calculator/en/.

FOOD AND AGRICULTURAL ORGANISATION (FAO) (2015) *AquaCrop new features and updates – Version 5.0*. FAO, Rome, Italy. http://www.fao.org/3/a-bc087e.pdf.

FOOD AND AGRICULTURAL ORGANISATION (FAO) (2017) *AquaCrop update and new features – Version 6.0.* FAO, Rome, Italy. http://www.fao.org/3/a-i7179e.pdf.

FOSTER T, BROZOVIĆ N, BUTLER AP, NEALE CMU, RAES D, STEDUTO P, FERERES E and HSIAO TC (2017) AquaCrop-OS: An open source version of FAO's crop water productivity model. Agricultural Water Management **181** 18–22. https://linkinghub.elsevier.com/retrieve/pii/S0378377416304589.

FRACASSO A, TRINDADE L and AMADUCCI S (2016) Drought tolerance strategies highlighted by two *sorghum bicolor* races in a dry-down experiment. Journal of Plant Physiology **190** 1–14. https://www.sciencedirect.com/science/article/pii/S017616171500245X.

GARCÍA-VILA M, FERERES E, MATEOS L, ORGAZ F and STEDUTO P (2009) Deficit irrigation optimization of cotton with AquaCrop. Agronomy Journal **101 (3)** 477–487. https://dl.sciencesocieties.org/publications/aj/abstracts/101/3/477.

GASH JHC (1979) An analytical model of rainfall interception by forests. Quarterly Journal of the Royal Meteorological Society **105 (443)** 43–55. https://rmets.onlinelibrary.wiley.com/doi/abs/10.1002/qj.49710544304.

GASH JHC, LLOYD CR and LACHAUD G (1995) Estimating sparse forest rainfall interception with an analytical model. Journal of Hydrology 170 (1–4) 79–86. https://www.sciencedirect.com/science/article/pii/002216949502697N.

GERRITS AMJ, PFSITER L and SAVENIJE HHG (2010) Spatial and temporal variability of canopy and forest floor interception in a beech forest. Hydrological Processes **24 (21)** 3011–3025. https://onlinelibrary.wiley.com/doi/full/10.1002/hyp.7712.

GHEEWALA SH, BERNDES G and JEWITT G (2011) The bioenergy and water nexus. Biofuels, Bioproducts and Biorefining **5** 353–360. https://onlinelibrary.wiley.com/doi/pdf/10.1002/bbb.295.

GREILER Y (2007) *Biofuels, opportunity or threat to the poor?* Swiss Agency for Development and Cooperation, Bern, Switzerland.

GUERRA E, VENTURA F, SPANO D and SNYDER RL (2014) Correcting midseason crop coefficients for climate. Journal of Irrigation and Drainage Engineering **141**. https://ascelibrary.org/doi/10.1061/%28ASCE%29IR.1943-4774.0000839.

HADEBE ST (2015) *Water use of selected sorghum (*Sorghum bicolor *L. Moench) genotypes*. PhD thesis. School of Agricultural, Earth and Environmental Sciences, University of KwaZulu-Natal, Pietermaritzburg, South Africa.

HADEBE ST, MODI AT and MABHAUDHI T (2017a) Water use of sorghum (*Sorghum bicolor* L. Moench) in response to varying planting dates evaluated under rainfed conditions. Water SA **43 (1)** 91–103. https://www.ajol.info//index.php/wsa/article/view/150827.

HADEBE ST, MODI AT and MABHAUDHI T (2017b) Calibration and testing of AquaCrop for selected sorghum genotypes. Water SA **43 (2)** 209–221. https://www.ajol.info/index.php/wsa/article/view/155168.

HALL RL (2003) Interception loss as a function of rainfall and forest types: Stochastic modelling for tropical canopies revisited. Journal of Hydrology **280** 1–12.

HARGREAVES GH and SAMANI ZA (1985) Reference crop evaporation from temperature. Journal of Applied Engineering in Agriculture **1** 96–99.

HATFIELD JL, SAUER TJ and PRUEGER JT (2001) Managing soils to achieve greater water use efficiency: a review. Agronomy Journal **93 (2)** 271–280. https://acsess.onlinelibrary.wiley.com/doi/abs/10.2134/agronj2001.932271x.

HOWARD PJA (1965) The carbon-organic matter factor in various soil types. Oikos **15 (2)** 229–236. https://www.jstor.org/stable/3565121.

HSIAO TC, LEE H, STEDUTO P, BASILIO RL, RAES D and FERERES E (2009) AquaCrop – the FAO crop model to simulate yield response to water: III. Parameterization and testing for maize. Agronomy Journal **101 (3)** 448–459. https://dl.sciencesocieties.org/publications/aj/abstracts/101/3/448.

HSIAO TC, FERERES E, STEDUTO P and RAES D (2012) AquaCrop parameterization, calibration and validation guide. Sorghum. In: *Crop yield response to water*, STEDUTO P, HSIAO TC, FERERES E and RAES D. Irrigation and Drainage Paper No. 66, Ch 3.3, 70–87, Land and Water Division, Food and Agricultural Organisation (FAO), Rome Italy. http://www.fao.org/docrep/016/i2800e/i2800e00.htm.

HUDA AKS, SIVAKURNAR MVK, VIRMANI SM, SEETHARARNA N, SINGH S and SEKARAN JG (1984) Modelling the effect of environmental factors on sorghum growth and development. Proceedings of the International Symposium 277–287. International Crops Research Institute for the Semi-Arid Tropics, Patancheru, India.

IRROMETER (2015) *Watermark soil moisture sensor – Model 200SS*. The Irrometer Company, Riverside, CA, USA. http://www.irrometer.com/pdf/sensors/403%20WATERMARK%20Sensor-WEB.pdf.

ISLAM MS, AHMED M, HOSSAIN MS, AKTER H and AKTAR S (2018) Response of soybean to Rhizobium biofertilizer under different levels of phosphorus. Progressive Agriculture **28 (4)** 302–315. https://www.banglajol.info/index.php/PA/article/view/36370.

ISSARIYAKUL T and DALAI AK (2014) Biodiesel from vegetable oils. Renewable and Sustainable Energy Reviews **31** 446–471. https://www.sciencedirect.com/science/article/pii/S1364032113007508.

JACKSON RB, CANADELL J, EHLERINGER JR, MOONEY HA, SALA OE and SCHULZE ED (1996) A global analysis of root distributions for terrestrial biomes. Oecologia **108 (3)** 389–411. http://link.springer.com/article/10.1007/BF00333714.

JANDA K, KRISTOUFEK L and ZILBERMAN D (2012) Biofuels: policies and impacts. Agricultural Economics **58 (8)** 372–386. https://www.agriculturejournals.cz/publicFiles/124_2011-AGRICECON.pdf.

JESCHEKE M, GASPAR A and VAN ROEKEL R (2017) *Effects of cold temperatures following soybean planting*. DuPont Pioneer Agronomy Sciences, Johnston, IA, USA. https://www.pioneer.com/home/site/us/agronomy/cold-temps-following-soybean-planting/

JEWITT GPW, KUNZ RP, WEN HW and VAN ROOYEN AM (2009a) *Scoping study on water use of crops/trees for biofuels in South Africa.* WRC Report No. 1772/1/09, Water Research Commission, Pretoria, South Africa. http://www.wrc.org.za/Knowledge Hub Documents/Research Reports/1772-1-09 Agricltural Water Management.pdf.

JEWITT GPW, LORENTZ SA, GUSH MB, THORNTON-DIBB S, KONGO V, WILES L, BLIGHT J, STUART-HILL SI, VERSFELD D and TOMLINSON K (2009b) *Methods and guidelines for the licensing of SFRAs with particular reference to low flows*. WRC Report No. 1428/1/09, Water Research Commission (WRC), Pretoria, South Africa. http://www.wrc.org.za/Knowledge%20Hub%20Documents/Research%20Reports/1428-1-09.pdf.

JONES MR (2018) *Fast DSSAT simulations with low-performance computers*. South African Sugarcane Research Institute, Mt. Edgecombe, South Africa.

JOVANOVIC NZ and ANNANDALE JG (1999) An FAO type crop factor modification to SWB for inclusion of crops with limited data: Examples for vegetable crops. Water SA **25 (2)** 181–189. http://www.wrc.org.za/Lists/Knowledge%20Hub%20Items/Attachments/4287/1999_April_apr99_p181_ABSTRACT.pdf.

JOVANOVIC NZ and ANNANDALE JG (2000) Calibration and validation of the SWB model for sunflower (*Helianthus annuus* L.). South African Journal of Plant and Soil **17 (3)** 117–123.

JOVANOVIC NZ, ANNANDALE JG and MHLAULI NC (1999) Field water balance and SWB parameters determination of six winter vegetable species. Water SA **25 (2)** 191–196. http://www.wrc.org.za/Knowledge%20Hub%20Documents/Water%20SA%20Journals/Manuscripts/1999/02/WaterSA_1999_02_apr99_p191.pdf.

KARUNARATNE S, AZAM-ALI SN, IZZI G and STEDUTO P (2011) Calibration and validation of FAO-AquaCrop model for irrigated and water deficient bambara groundnut. Experimental Agriculture **47 (3)** 509–527. http://dx.doi.org/10.1017/S0014479711000111.

KHOMO TL (2014) Spatial assessment of optimum and sub-optimum growing areas for selected biofuel feedstocks in South Africa. Unpublished MSc dissertation in Hydrology. School of Agricultural, Earth and Environmental Sciences, University of KwaZulu-Natal, Pietermaritzburg, RSA.

KHONJE DJ (2016) Adoption of the rhizobium inoculation technology for pasture improvement in sub-Saharan Africa. Utilization of Research Results on Forage and Agricultural By-Product Materials 780. FAO corporate document repository. http://www.fao.org/wairdocs/ilri/x5536e/x5536e1g.htm.

KIENZLE S (2019) Personal communication. Professor in Department of Geography, University of Lethbridge, Alberta, Canada, T1K 3M4, 12 July 2019.

KNOTT JE (1988) *Knott's handbook for vegetable growers*, 2nd ed., Wiley, New York, NY, USA.

KOTZE C (2012) DoE's mandatory blending regulations welcomed by grain producers. Engineering News **32 (6)**, Creamer Media, Johannesburg, South Africa. http://www.engineeringnews.co.za/article/does-mandatory-blending-regulations-welcomed-by-grain-producers-2012-09-21.

KOZAK JA, AHUJA LR, GREEN TR and MA L (2007) Modelling crop canopy and residue rainfall interception effects on soil hydrological components for semi-arid agriculture. Hydrological Processes **21 (2)** 229–241. https://onlinelibrary.wiley.com/doi/abs/10.1002/hyp.6235.

KRISHNAMURTHY L, DINAKARAN E, KUMAR AA and REDDY BVS (2014) Field technique and traits to assess reproductive stage cold tolerance in sorghum (*Sorghum bicolor* (L.) Moench). Plant Production Science **17** 218–227. https://www.tandfonline.com/doi/abs/10.1626/pps.17.218.

KUMAR A, PANDEY AM, SHEKH AM and KUMAR M (2008) Growth and yield response of soybean (*Glycine max* L.) in relation to temperature, photoperiod and sunshine duration at Anand, Gujarat, India. American-Eurasian Journal of Agronomy **1 (2)** 45–50.

KUNZ RP, MENGISTU MG, STEYN JM, DOIDGE IA, GUSH MB, DU TOIT ES, DAVIS NS, JEWITT GPW and EVERSON CS (2015a) *Assessment of biofuel feedstock production in South Africa: Synthesis report on estimating water use efficiency of biofuel crops*, Volume 1. WRC Report No. 1874/1/15, Water Research Commission, Pretoria, South Africa http://www.wrc.org.za/Pages/DisplayItem.aspx?ItemID=11673.

KUNZ RP, MENGISTU MG, STEYN JM, DOIDGE IA, GUSH MB, DU TOIT ES, DAVIS NS, JEWITT GPW and EVERSON CS (2015b) *Assessment of biofuel feedstock production in South Africa: Technical report on the field-based measurement, modelling and mapping of water use of biofuel crops*, Volume 2. WRC Report No. 1874/2/15, Water Research Commission, Pretoria, South Africa http://www.wrc.org.za/Pages/DisplayItem.aspx?ItemID=11674.

KUNZ RP, DAVIS NS, THORNTON-DIBB SLC, STEYN JM, DU TOIT ES and JEWITT GPW (2015c) *Assessment of biofuel feedstock production in South Africa: Atlas of water use and yield of biofuel crops in suitable growing areas*, Volume 3. WRC Report No. TT 652/15, Water Research Commission, Pretoria, South Africa. http://www.wrc.org.za/Pages/DisplayItem.aspx?ItemID=11698.

LAI-2200 (2010) *Instruction manual.* Publication No. 984-10633, LI-COR Biosciences, Lincoln, NE, USA.

LEGGETT M, DIAZ-ZORITA M, KOIVUNEN M, BOWMAN R, PESEK R, STEVENSON C and LEISTER T (2017) Soybean response to inoculation with *Bradyrhizobium japonicum* in the United States and Argentina. Agronomy Journal **109 (3)** 1031–1038. https://acsess.onlinelibrary.wiley.com/doi/pdf/10.2134/agronj2016.04.0214.

LEMBEDE LP (2017) *Estimating water use and yield of soybean (Glycine max.) under mulch and fertilizer in rainfed conditions in KwaZulu-Natal.* MSc dissertation, Centre for Water Resources Research, University of KwaZulu-Natal, Pietermaritzburg, South Africa.

LEMMER W and SCHOEMAN B (2011) *An assessment of the food security impact in South Africa and the world due to the South African Biofuels industry rollout.* Report by Grain SA, Bothaville, Free State, South Africa. http://www.mabelefuels.com/wp-content/uploads/2011/12/Sorghum.pdf.

LETETE T and VON BLOTTNITZ H (2012) Biofuel Policy in South Africa: A critical analysis. In: *Bioenergy for sustainable development in Africa,* JANSSEN R and RUTZ D, 191–199. Springer, Dordrecht, The Netherlands.

LI S, KANG S, LI F and ZHANG L (2008) Evapotranspiration and crop coefficient of spring maize with plastic mulch using eddy covariance in northwest China. Agricultural Water Management **95** 1214–1222. https://www.sciencedirect.com/science/article/abs/pii/S0378377408001169.

LINK SEED (2011) *Soya beans*. http://www.linkseed.co.za/products/soya-beans.html.

LOBELL DB and BURKE MB (2010) On the use of statistical models to predict crop yield responses to climate change. Agricultural and Forest Meteorology **150 1**443–1452. https://www.sciencedirect.com/science/article/pii/S0168192310001978.

LOBELL DB, CASSMAN KG and FIELD CB (2009) Crop yield gaps: Their importance, magnitudes and causes. *The Annual Review of Environment and Resources* 34: 179-204. https://www.annualreviews.org/doi/10.1146/annurev.environ.041008.093740

LUMSDEN TG, KUNZ RP, SCHULZE, RE, KNOESEN DM and BARICHIEVY KR (2011) Methods 4: Representation of grid and point scale regional climate change scenarios for national and catchment level hydrological impacts assessments. In: *Methodological approaches to assessing eco-hydrological responses to climate change in South Africa,* SCHULZE RE, HEWITSON BC, BARICHIEVY KR, TADROSS M, KUNZ RP, HORAN MJC and LUMSDEN TG, 89–99. WRC Report No. 1562/1/10, Water Research Commission, Pretoria, RSA. South Africa.

LYNCH SD (2004) *Development of a raster database of annual, monthly and daily rainfall for southern Africa*. WRC Report 1156/1/04, Water Research Commission, Pretoria, South Africa.

MABHAUDHI T (2012) *Drought tolerance and water-use of selected South African landraces of taro (*Colocasia esculenta *L. Schott) and bambara groundnut (*Vigna subterranea *L. Verdc).* PhD thesis, School of Agricultural, Earth and Environmental Sciences, University of KwaZulu-Natal, Pietermaritzburg, South Africa.

MABHAUDHI T and MODI AT (2013) Growth, phenological and yield responses of a bambara groundnut (*Vigna subterranea* L. Verdc) landrace to imposed water stress under field conditions. South African Journal of Plant and Soil **30 (2)** 69–79. https://www.tandfonline.com/doi/full/10.1080/02571862.2013.790492.

MABHAUDHI T, MODI AT and BELETSE YG (2013) Parameterization and testing of AquaCrop for a South African bambara groundnut landrace. Agronomy Journal **106 (1)** 243–251. https://dl.sciencesocieties.org/publications/aj/abstracts/106/1/243.

MABHAUDHI T, MODI AT and BELETSE YG (2014) Parameterisation and testing of the FAO AquaCrop model for a South African bambara groundnut landrace. Agronomy Journal **106** 243–251.

MALIK A, CHEEMA MA, KHAN HZ and WAHID MA (2006) Growth and yield response of soybean (Glycine Max L.) to seed inoculation and varying phosphorous levels. Journal of Agricultural Research **44 (1)** 47–53.

MANSON AD and ROBERTS VG (2001) *Analytical methods used by the soil fertility and analytical services section.* KZN AGRI-Report No. N/A/2001/04, KwaZulu-Natal Department of Agriculture and Environmental Affairs, Pietermaritzburg, South Africa.

MAONGA BB, MAGANGA AM and KANKWAMBA H (2015) Smallholder farmers willingness to incorporate biofuel crops into cropping systems in Malawi. International Journal of Food and Agricultural Economics **3(1)** 87–100.

MARSHALL JS and PALMER WM (1948) The distribution of raindrops with size. Journal of Meteorology **5** 165–166.

MASANGANISE J (2019) *Evapotranspiration of soybean and grain sorghum in a semi-arid climate.* PhD thesis, School of Agricultural, Earth and Environmental Sciences, College of Agriculture, Engineering and Science, University of KwaZulu-Natal, Pietermaritzburg, South Africa.

MASANGANISE J, KUNZ R, MABHAUDHI T and SAVAGE M (2019) *Testing of AquaCrop for simulating canopy cover, biomass, yield, crop evapotranspiration and water productivity of grain sorghum under rainfed conditions using two distinct crop files.* Manuscript in preparation.

MBANGIWA NC (2018) *Evapotranspiration over dryland maize and soybean using micrometeorological methods, modelling and remote sensing.* PhD thesis, School of Agricultural, Earth and Environmental Sciences, College of Agriculture, Engineering and Science, University of KwaZulu-Natal, Pietermaritzburg, South Africa.

MBANGIWA NC, SAVAGE MJ and MABHAUDHI T (2019) Modelling and measurement of water productivity and total evaporation in a dryland soybean crop. Agricultural and Forest Meteorology **266–267** 65–72. https://www.sciencedirect.com/science/article/pii/S0168192318303988?via%3Dihub.

MCMASTER GS and WILHELM WW (1997) Growing degree-days: one equation, two interpretations. Agricultural and Forestry Meteorology **87 (4)** 291–300. http://www.sciencedirect.com/science/article/pii/S0168192397000270.

MCNAUGHTON KG and JARVIS PG (1983) Predicting effects of vegetation changes on transpiration and evaporation. In: *Water deficits and plant growth,* KOZLOWSKI TT, Volume VII, 1–47. Academic Press, New York, NY, USA.

MENDESIL E, ABDETA C, TESFAYE A, SHUMETA Z and JIFAR H (2007) Farmers' perceptions and management practices on stored sorghum in southwestern Ethiopia. Crop Protection **26** 1817–1825. http://www.sciencedirect.com/science/article/pii/S0261219407000968.

MENGISTU MG, EVERSON CS, MBANGIWA NC and SAVAGE MJ (2014) The validation of the variables (evaporation and soil moisture) in hydrometeorological models. WRC Report No. 2066/1/13, Water Research Commission, Pretoria, South Africa. http://www.wrc.org.za/Knowledge%20Hub%20Documents/Research%20Reports/2066-1-13.pdf.

MEYER MD and TERRY LA (2008) Fatty acid and sugar composition of avocado, cv. Hass, in response to treatment with an ethylene scavenger or 1-methylcyclopropene to extend storage life. Food Chemistry **12** 1203–1210.

MEYER RF, STRAUSS PG and FUNKE T (2008) Modelling the impacts of macro-economic variables on the South African biofuels industry. Agrekon **47** 1–19.

MHIZHA T, GEERTS S, VANUYTRECHT E, MAKARAU A and RAES D (2014) Use of the FAO AquaCrop model in developing sowing guidelines for rainfed maize in Zimbabwe. Water SA **40** 233–244. https://www.ajol.info/index.php/wsa/article/view/102216.

MODI AT and MABHAUDHI T (2017) *Determining water use of indigenous grain and legume food crops.* WRC Report No. TT 710/17, Water Research Commission, Pretoria, South Africa. http://www.wrc.org.za/Knowledge%20Hub%20Documents/Research%20Reports/TT%20710-17.pdf.

MOKOENA TZ (2013) *The effect of direct phosphorous and potassium fertilization on soybean (Glycine max L.) yield and quality.* MSc dissertation, Faculty of Natural and Agricultural Sciences, University of Pretoria, Pretoria, South Africa.

MOLDEN D, OWEIS T, STEDUTO P, BINDRABAN P, HANJRA MA and KIJNE J (2010) Improving agricultural water productivity: between optimism and caution. Agricultural Water Management **97** 528–535. http://www.sciencedirect.com/science/article/pii/S0378377409000912.

MONTEITH JL (1977) Climate and efficiency of crop production in Britain. Philosophical Transactions of the Royal Society London **281** 277–294.

MORETTI LG, LAZARINI E, BOSSOLANI JW, PARENTE TL, CAIONI S, ARAUJO RS and HUNGRIA M (2018) Can additional inoculations increase soybean nodulation and grain yield? Agronomy Journal **110 (2)** 1–7. https://acsess.onlinelibrary.wiley.com/doi/10.2134/agronj2017.09.0540.

MUCINA L and RUTHERFORD MC (2006) The vegetation of South Africa, Lesotho and Swaziland. Strelitzia **19**, South African National Biodiversity Institute, Pretoria, South Africa.

MUTEGI J and ZINGORE SI (2014) *Boosting soybean production for improved food security and incomes in Africa.* The International Plant Nutrition Institute (IPNI), sub-Saharan Africa program, Georgia, USA.
http://ssa.ipni.net/ipniweb/region/africa.nsf/0/28600CA4712A18F685257BE100695F27/$FILE/Soybean%20production%20in%20SSA%20BMPs,%20Challenges%20and%20Opportunities.pdf.

MUZYLO A, LORENS P, VALENTE F, KEIZER JJ, DOMINGO F and GASH JHC (2009) A review of rainfall interception modelling. Journal of Hydrology **370 (1–4)** 191–206.
https://www.sciencedirect.com/science/article/pii/S0022169409001383.

NIEUWENHUIS R and NIEUWELINK J (2005) *Cultivation of soya and other legumes*. Agrodok 10, Agromisa Foundation, Wageningen, The Netherlands.
https://publications.cta.int/media/publications/downloads/1119_PDF.pdf.

NISHIYAMA I (1995) Damage due to extreme temperature. In: *Science of the rice plant,* MATSUO T, KAMAZAWA K, ISHII R, ISHIHARA H and HIRATA H, 769–793. Food and Agriculture Policy Research Center, Tokyo, Japan.

NOLTE M (2007) *Commercial biodiesel production in South Africa: A preliminary economic feasibility study.* MSc dissertation, Department of Process Engineering, University of Stellenbosch, Cape Town, South Africa. http://scholar.sun.ac.za/handle/10019.1/1797.

NUNKUMAR A (2006) *Studies on* Phakopsora pachyrizi*, the causal organism for soybean rust*. MSc dissertation, School of Biochemistry, Genetics, Microbiology and Plant Pathology, University of KwaZulu-Natal, Pietermaritzburg, South Africa
http://researchspace.ukzn.ac.za/xmlui/bitstream/handle/10413/4503/Nunkumar_Archana_2006.pdf.

OERKE EC (2006) Crop losses to pests. *Journal of Agricultural Science* 144(1): 31-43.
https://www.cambridge.org/core/journals/journal-of-agricultural-science/article/crop-losses-to-pests/AD61661AD6D503577B3E73F2787FE7B2

OERKE EC and DEHNE HW (2004) Safeguarding protection – losses in major crops and the role of crop protection. Crop Protection **23(4)** 275–285.
http://www.sciencedirect.com/science/article/pii/S0261219403002540.

OSCHADLEUS HD (2015) First red-billed quelea breeding record in the winter rainfall region of South Africa. Ostrich **86 (3)** 295–296. https://www.tandfonline.com/doi/pdf/10.2989/00306525.2015.1069413.

OSCHADLEUS HD and UNDERHILL LG (2006) Range expansion of the red-billed quelea, *Quelea quelea*, into the Western Cape, South Africa. South African Journal of Science **102** 12–14. https://open.uct.ac.za/handle/11427/28204.

PALMER T and AINSLIE A (2006) *Country pasture/forage resource profile*. Food and Agriculture Organization of the United Nations (FAO). http://www.fao.org/ag/agp/agpc/doc/counprof/PDF%20files/SouthAfrica_English.pdf.

PANNAR (2006) *Soybean production guide*. PANNAR SEED (Pty) Ltd, Greytown, South Africa. http://www.pannar.com/assets/documents/soybeans.pdf.

PANNAR (2013a) *Soybean production guide.* PANNAR SEED (Pty) Ltd, Greytown, South Africa. www.pannar.com/assets/countries/pannar_sa_PRODUCTCAT_eng.pdf.

PANNAR (2013b) *Grain sorghum production guide.* PANNAR SEED (Pty) Ltd, Greytown, South Africa. http://www.pannar.com/assets/documents/grain_sorghum_op.pdf.

PANNAR (2016) *Botswana farmer's guide*. PANNAR SEED (Pty) Ltd, Greytown, South Africa. http://www.pannar.com/assets/content/botswana-growsers-guide.pdf.

PANNAR (2018) *2018 Product Catalogue*. PANNAR SEED (Pty) Ltd, Greytown, South Africa. http://www.pannar.com/assets/documents/2018-catalogue-eng.pdf.

PAREDES P, DE MELO-ABREU JP, ALVES I and PEREIRA LS (2014) Assessing the performance of the FAO AquaCrop model to estimate maize yields and water use under full and deficit irrigation with focus on model parameterization. Agricultural Water Management **144** 81–97. https://www.sciencedirect.com/science/article/pii/S0378377414001784.

PAREDES P, WEI Z, LIU Y, XU D, XIN Y, ZHANG B and PEREIRA LS (2015) Performance assessment of the FAO AquaCrop model for soil water, soil evaporation, biomass and yield of soybeans in North China Plain. Agricultural Water Management **152** 57–71. https://www.sciencedirect.com/science/article/pii/S0378377414003916.

PENMAN HL (1948) Natural evaporation from open water, bare soil and grass. Proceedings of the Royal Society London **A (194) S** 120–145.

PEREIRA LS, PAREDES P, RODRIGUES GC and NEVES M (2015) Modelling barley water use and evapotranspiration partitioning in two contrasting rainfall years. Assessing SIMDualKc and AquaCrop models. Agricultural Water Management **159** 239–254. https://www.sciencedirect.com/science/article/pii/S0378377415300238.

PI X, ZHANG T, SUN B, CUI Q, GUO Y, GAO M and HOPKINS DW (2017) Effects of mulching for water conservation on soil carbon, nitrogen and biological properties. Frontiers **2**. http://journal.hep.com.cn/fase/EN/10.15302/J-FASE-2017136.

PICCINNI G, JONGHAN KO, MAREK T and HOWELL T (2009) Determination of growth-stage-specific crop coefficients (K_C) of maize and sorghum. Agricultural Water Management **96 (12)** 1698–1704. http://www.sciencedirect.com/science/article/pii/S0378377409001954.

PIKE A and SCHULZE RE (1995) *AUTOSOIL Version 3: A soils decision support system for South African soils*. Department of Agricultural Engineering, University of Natal, Pietermaritzburg, South Africa.

PIÑEIRO G, PERELMAN S, GUERSCHMAN JP and PARUELO JM (2008) How to evaluate models: Observed vs. predicted or predicted vs. observed? Ecological Modelling **216 (3–4)** 316–322. https://www.sciencedirect.com/science/article/pii/S0304380008002305.

PINHEIRO C and CHAVES MM (2010) Photosynthesis and drought: Can we make metabolic connections from available data? Journal of Experimental Botany **62 (3)** 869–882. https://academic.oup.com/jxb/article/62/3/869/478813.

PROMKHAMBUT A, YOUNGER A, POLTHANEE A and AKKASAENG C (2010) Morphological and physiological responses of sorghum (*Sorghum bicolor* L. Moench) to waterlogging. Asian Journal of Plant Sciences **9** 183–193. https://scialert.net/abstract/?doi=ajps.2010.183.193.

RAES D (2017a) *AquaCrop training handbooks – Book I: Understanding AquaCrop.* Food and Agriculture Organisation, Rome, Italy. http://www.fao.org/3/a-i6051e.pdf.

RAES D (2017b) *AquaCrop training handbooks – Book II: Running AquaCrop.* Food and Agriculture Organisation (FAO), Rome, Italy. http://www.fao.org/3/a-i6052e.pdf.

RAES D, SITHOLE A, MAKARU A and MILLFORD J (2004) Evaluation of first planting dates recommended by criteria currently used in Zimbabwe. Agricultural and Forest Meteorology **125** 177–185. https://doi.org/10.1016/j.agrformet.2004.05.001.

RAES D, STEDUTO P, HSIAO TC and FERERES E (2009) AquaCrop – the FAO crop model to simulate yield response to water: II. Main algorithms and software description. Agronomy Journal **101 (3)** 438–447. https://dl.sciencesocieties.org/publications/aj/pdfs/101/3/438.

RAES D, STEDUTO P, HSIAO TC and FERERES E (2012a) *AquaCrop Version 4.0 reference manual: Chapter 2 (users guide).* Land and Water Division, Food and Agricultural Organisation (FAO), Rome Italy. http://www.fao.org/nr/water/docs/aquacropv40chapter2.pdf.

RAES D, STEDUTO P, HSIAO TC and FERERES E (2012b) *AquaCrop Version 4.0 reference manual: Annex I (crop parameters).* Land and Water Division, Food and Agricultural Organisation (FAO), Rome Italy. http://www.fao.org/nr/water/docs/aquacropv40annexes.pdf.

RAES D, STEDUTO P, HSIAO TC and FERERES E (2017) *Reference manual AquaCrop (Version 6.0*). Land and Water Division, Food and Agriculture Organisation (FAO), Rome, Italy. http://www.fao.org/aquacrop/resources/referencemanuals/en/.

RAES D, STEDUTO P, HSIAO TC and FERERES E (2018) *Reference manual AquaCrop (Version 6.0–6.1).* Land and Water Division, Food and Agriculture Organisation (FAO), Rome, Italy. http://www.fao.org/aquacrop/resources/referencemanuals/en/.

RAMAKRISHNA A, TAM HM, WANJ SP and LONG TD (2006) Effect of mulch on soil temperature, moisture, weed infestation and yield of groundnut in northern Vietnam. Field Crops Research **95 (2–3)** 115–125. https://www.sciencedirect.com/science/article/abs/pii/S0378429005000560.

RAZ-YASEEF N, KOTEEN L and BALDOCCHI DD (2013) Coarse root distribution of a semi-arid oak savanna estimated with ground penetrating radar. Journal of Geophysical Research: Biogeosciences **118 (1)** 135–147. http://onlinelibrary.wiley.com/doi/10.1029/2012JG002160/full

REDDY KTC (2019) *Estimation of water use efficiency of soybean (Glycine max.) for biodiesel production in Kwazulu-Natal*. MSc dissertation, School of Bioresources Engineering and Environmental Hydrology, University of KwaZulu-Natal, Pietermaritzburg, South Africa.

REDDY BVS, RAMESH S, ASHOK KUMAR A and GOWDA CLL (2008) *Sorghum improvement in the new millennium*. International Crops Research Institute for the Semi-Arid Tropics, Patancheru, Andhra Pradesh, India. http://oar.icrisat.org/2160/.

RETHMAN NFG, ANNANDALE JG, KEEN CS and BOTHA CC (2007) *Water use efficiency of multi-crop agroforestry systems, with particular reference to small scale farmers in semi-arid areas.* WRC Report No. 1047/1/07, Water Research Commission, Pretoria, South Africa.

RITCHIE JT (1972) Model for predicting evaporation from a row crop with incomplete cover. Water Resources Research **24** 1121–1213.

RITCHIE JT and BASSO B (2008) Water use efficiency is not constant when crop water supply is adequate or fixed: The role of agronomic management. European Journal of Agronomy **28** 273–281. http://www.sciencedirect.com/science/article/pii/S1161030107000974.

ROBERTS J M, GASH JHC, TANI M and BRUIJNZEEL LA (2004) Controls of evaporation in lowland tropical rainforest. In: *Forest-water-people in the humid tropics,* BONELL M, BRUIJNZEEL LA and KIRBY C, 287–313. Cambridge University Press, Cambridge, UK.

ROONEY WL (2004) Sorghum improvement-integrating traditional and new technology to produce improved genotypes. Advances in Agronomy **83** 37–109. https://www.supagro.fr/ress-tice/ue1-ue2_auto/Etude%20cas%20sorgho/2004%20Rooney,%20Adv.%20Agron.pdf.

ROSSI A (2012) *Good environmental practices in bioenergy feedstock production – making bioenergy work for climate and food security.* FAO Environment and Natural Resources Working Paper 49. Food and Agriculture Organisation, Rome, Italy. http://www.fao.org/3/a-i2596e.pdf.

RUARK GA, MADER DL and TATTAR TA (1982) The influence of soil compaction and aeration on the root growth and vigour of trees – a literature review. Part 1. Arboricultural Journal **6 (4)** 251–265. http://www.tandfonline.com/doi/abs/10.1080/03071375.1982.9746581.

RUTHROF KX, STEEL E, MISRA S, MCCOMB J, O'HARA G, HARDY GESJ and HOWIESON J (2018) Transitioning from phosphate mining to agriculture: Responses to urea and slow release fertilizers for *Sorghum bicolor*. Science of The Total Environment **625** 1–7. https://www.sciencedirect.com/science/article/pii/S0048969717335301.

RUTTER AJ, MORTON AJ and ROBINS PC (1975) A predictive model of rainfall interception in forests II. Generalisation of the model and comparison with observations in some coniferous and hardwood stands. Journal of Applied Ecology **12** 367–384.

SALVAGIOTTI F, CASSMAN KG, SPECHT JE, WALTERS DT and WEISS A (2008) Nitrogen uptake, fixation and response to fertilizer N in soybeans: A review. Agronomy and Horticulture – Faculty Publications **133**. http://digitalcommons.unl.edu/agronomyfacpub/133.

SAVENIJE HHG (2004) The importance of interception and why we should delete the term evapotranspiration from our vocabulary. Hydrological Processes **18 (8)** 1507–1511. https://onlinelibrary.wiley.com/doi/abs/10.1002/hyp.5563.

SAWAN ZM, HAFEZ SA, BASYONY AE and ALKASSAS AR (2007) Cottonseed, protein, oil yields and oil properties as influenced by potassium fertilization and foliar application of zinc and phosphorus. International Journal of Fats and Oils **58 (1)** 40–48. http://grasasyaceites.revistas.csic.es/index.php/grasasyaceites/article/view/7/7.

SAXTON KE and RAWLS WJ (2006) Soil water characteristic estimates by texture and organic matter for hydrologic solutions. Soil Science Society of America Journal **70 (5)** 1569–1578. https://dl.sciencesocieties.org/publications/sssaj/abstracts/70/5/1569.

SAXTON KE, RAWLS WJ, ROMBERGER JS and PAPENDICK RI (1986) Estimating generalized soil-water characteristics from texture. Soil Science Society American Journal **50** 1031–1036.

SCHENK HJ and JACKSON RB (2002) Rooting depths, lateral root spreads and below-ground/above-ground allometries of plants in water-limited ecosystems. Journal of Ecology **90 (3)** 480–494. http://onlinelibrary.wiley.com/doi/10.1046/j.1365-2745.2002.00682.x/full.

SCHMIDT EJ and SCHULZE RE (1987) *Flood volume and peak discharge from small catchments in southern Africa, based on the SCS technique.* WRC Report No. TT/3/97, Water Research Commission, Pretoria, South Africa.

SCHULZ TJ, THELEN KD and WANG D (2005) Effect of *Bradyrhizobium japonicum* inoculant on soybean growth and yield. In: *The ASA-CSSA-SSSA International Annual Meetings*, 6–10 November 2005, Salt Lake City, UT, USA. https://scisoc.confex.com/crops/viewHandout.cgi?uploadid=757.

SCHULZE RE (1995) *Hydrology and agrohydrology: A text to accompany the ACRU 3.00 agrohydrological modelling system*. WRC Report TT 69/9/95, Water Research Commission, Pretoria, South Africa.

SCHULZE RE (2004) Determination of baseline land cover variables for applications in assessing land use impacts on hydrological responses in South Africa. In: *Development and evaluation of an installed hydrological modelling system,* SCHULZE RE and PIKE A. WRC Report No. 1155/1/04. 37-50, Water Research Commission, Pretoria, South Africa.

SCHULZE RE (2011) Methods 3: Modelling impacts of climate change on the hydrological system: Model requirements, selection of the ACRU model, its attributes and computations of major state variables and outputs. In: *Methodological approaches to assessing eco-hydrological responses to climate change in South Africa,* SCHULZE RE, HEWITSON BC, BARICHIEVY KR, TADROSS M, KUNZ RP, HORAN MJC and LUMSDEN TG, Chapter 8, 75–88. WRC Report 1562/1/10. Water Research Commission, Pretoria, South Africa.

SCHULZE RE and HORAN MJC (2007) Soils: Hydrological attributes. In*: South African Atlas of Climatology and Agrohydrology,* SCHULZE RE, Section 4.2. WRC Report 1489/1/06. Water Research Commission, Pretoria, South Africa.

SCHULZE RE and HORAN MJC (2011) Methods 1: Delineation of South African, Lesotho and Swaziland into quinary catchments. In: *Methodological Approaches to Assessing Eco-Hydrological Responses to Climate Change in South Africa,* SCHULZE RE, HEWITSON BC, BARICHIEVY KR, TADROSS M, KUNZ RP, HORAN MJC and LUMSDEN TG, Chapter 6, 55–62. WRC Report 1562/1/10. Water Research Commission, Pretoria, South Africa.

SCHULZE RE and KUNZ RP (2010a) Climate change 2010 and rainfall seasonality. In: *Atlas of climate change and the South African agricultural sector: A 2010 perspective*, SCHULZE RE, Chapter 3.10, 113–116. Department of Agriculture, Forestry and Fisheries, Pretoria, South Africa.

SCHULZE RE and KUNZ RP (2010b) Climate change and 2010 and sorghum yields. In: *Atlas of climate change and South African agricultural sector: A 2010 perspective,* SCHULZE RE, Chapter 5.3. Department of Agriculture, Forestry and Fisheries, Pretoria, South Africa.

SCHULZE RE and KUNZ RP (2010c) Climate change and 2010 and soybean yields. In: *Atlas of climate change and South African agricultural sector: A 2010 perspective,* Schulze RE, Chapter 5.4. Department of Agriculture, Forestry and Fisheries, Pretoria, South Africa.

SCHULZE RE and MAHARAJ M (1994) Monthly means of daily maximum and minimum temperatures for southern Africa. Unpublished documents and maps. Department of Agricultural Engineering, University of Natal, Pietermaritzburg, South Africa.

SCHULZE RE and MAHARAJ M (2004) *Development of a database of gridded daily temperatures for Southern Africa*. WRC Report 1156/2/04, Water Research Commission, Pretoria, South Africa.

SCHULZE RE and MAHARAJ M (2007a) Sorghum yield estimation. In: *South African atlas of climatology and agrohydrology,* SCHULZE RE, Chapter 16.4. WRC Report No. 1489/1/06, Water Research Commission, Pretoria, South Africa.

SCHULZE RE and MAHARAJ M (2007b) Soybean yield estimation. In: *South African atlas of climatology and agrohydrology,* SCHULZE RE, Chapter 16.8. WRC Report No. 1489/1/06, Water Research Commission, Pretoria, South Africa.

SCHULZE RE, JEWITT GPW and LEENHARDT D (1995) Forestry related responses: Hydrological impacts of afforestation and a timber yield model. In: *Hydrology and agrohydrology: A text to accompany the ACRU 3.00 agrohydrological modelling system,* SCHULZE RE, Chapter 20, AT20-1 to AT20-25. WRC Report TT69/95, Water Research Commission, Pretoria, South Africa.

SCHULZE RE, HORAN MJC, KUNZ RP, LUMSDEN TG and KNOESEN DM (2011) Methods 2: Development of the southern African quinary catchments database. In: *Methodological approaches to assessing eco-hydrological responses to climate change in South Africa,* SCHULZE RE, HEWITSON BC, BARICHIEVY KR, TADROSS M, KUNZ RP, HORAN MJC and LUMSDEN TG, Chapter 7, 63–74. WRC Report No. 1562/1/10, Water Research Commission, Pretoria, South Africa.

SCHÜTTE S, SCHULZE RE and PATERSON G (2019) *Identification and mapping of soils rich in organic carbon in South Africa as a climate change mitigation option*. Department of Environmental Affairs (DEA), Pretoria, South Africa.

SCOTT DF and SMITH RE (1997) Preliminary empirical models to predict reductions in annual and low flows resulting from afforestation. Water SA **23 (2)** 135–140. http://www.wrc.org.za/Knowledge%20Hub%20Documents/Water%20SA%20Journals/Manuscripts/1997/02/WaterSA_1997_02_1042%20abstract.pdf.

SEEDCO (2018) *Farmers guide – grain crops.* Seed Co Group, Harare, Zimbabwe. https://www.seedcogroup.com/sites/default/files/Agronomy%20Manual.pdf.

SHENKUT A, TESFAYE K and ABEGAZ F (2013) Determination of water requirement and crop coefficient for Sorghum (*Sorghum bicolor* L.) at Melkasa, Ethiopia. Science, Technology and Arts Research Journal **2 (3)** 16–24. http://www.starjournal.org/uploads/starjournal/3(2).pdf.

SHOCK CC, PEREIRA AB, FEIBERT EBG, SHOCK CA, AKIN AI and UNLENEN LA (2016) Field comparison of soil moisture sensing using neutron thermalization, frequency domain, tensiometer, and

granular matrix sensor devices: Relevance to precision irrigation. Journal of Water Resource and Protection **8** 154–167.

SILVA VPR, SILVA RA, MACIEL GF, BRAGA CC, SILVA JLC, SOUZA EP, ALMEIDA RSR, SILVA MT and HOLANDA M (2017) Calibration and validation of the AquaCrop model for the soybean crop grown under different levels of irrigation in the Motopiba region, Brazil. Ciência Rural **48 (1)** 1–8. http://www.scielo.br/scielo.php?script=sci_arttext&pid=S0103-84782018000100351&lng=en&tlng=en.

SINGH SP (1985) Sources of cold tolerance in grain sorghum. Canadian Journal of Plant Science **65** 251–257. https://www.mdpi.com/2073-4395/9/9/508/pdf.

SINGH MS (2005) Effect of bradyrhizobium inoculation on growth, nodulation and yield attributes of soybean. Agricultural Reviews **26** 305–308.

SINGH BR and SINGH DP (1995) Agronomic and physiological responses of sorghum, maize and pearl millet to irrigation. Field Crops Research **42 (2–3)** 57–67. https://www.sciencedirect.com/science/article/pii/037842909500025L.

SOIL CLASSIFICATION WORKING GROUP (SCWG) (1991) Soil Classification - Taxonomic System for South Africa. Soil Classification Working Group. Department of Agricultural Development, Pretoria, RSA. 257 pp.

SOIL AND IRRIGATION RESEARCH INSTITUTE (SIRI) (1987) *Land type series. Memoirs on the Agricultural Natural Resources of South Africa.* Soil and Irrigation Research Institute, Department of Agriculture and Water Supply, Pretoria, South Africa.

SOUTHERN AFRICAN GRAIN LABORATORY (SAGL) (2016) *South African soybean crop*. SAGL, Pretoria, South Africa http://www.sagl.co.za/Portals/0/Soya%20Crop%202014%202015/Soya%20Crop%20Report.zip.

SOUTH AFRICAN NATIONAL BIODIVERSITY INSTITUTE (SANBI) (2012) *Vegetation map of South Africa, Lesotho and Swaziland.* SANBI, Cape Town, South Africa http://bgis.sanbi.org/SpatialDataset/Detail/18.

SIYENI D (2016) Effects of rhizobia inoculation and phosphorus fertilizer on nodulation and yield of soybean (*Glycine max* (L.) Merril) in Dedza, Kasungi and Salima districts of Malawi. MSc dissertation, Bunda College of Agriculture, University of Malawi, Zomba, Malawi. https://www.n2africa.org/sites/default/files/MSc%20thesis%20Donald%20Siyeni_0.pdf.

SMITH B (2006) *The farming handbook*. University of KwaZulu-Natal Press, Pietermaritzburg, South Africa.

SMITH JMB (1994) *Crop, pasture and timber yield index*. Cedara Report N/A/94/4. Natal Agricultural Research Institute, Cedara, South Africa.

SMITH JMB (1998) *Handbook for agricultural advisors in KwaZulu-Natal*. KwaZulu-Natal Department of Agriculture, Cedara, South Africa.

SMITH CW and FREDERIKSEN RA (2000) *Sorghum: Origin, history, technology, and production*. Wiley, New York, NY, USA.

SMITHERS JC and SCHULZE RE (1995) ACRU agrohydrological modelling system: User manual Version 3.00. WRC Report TT 70/95. Water Research Commission, Pretoria, South Africa.

SMITHERS JC, ROWE TJ, HORAN MJC and SCHULZE RE (2018) Development and assessment of rules to parameterise the ACRU model for design flood estimation. Water SA **44 (10)** 93–104. https://www.ajol.info/index.php/wsa/article/view/166145.

SORGHUM TRUST (n.d.) *Cultivation*. http://www.sorghumsa.co.za/cultivation-climates.htm.

STATISTICS SA (2007) *Census of commercial agriculture.* Produced by Statistics South Africa for the Department of Agriculture, Forestry and Fisheries, Pretoria, South Africa.

STEDUTO P, HSIAO TC, RAES D and FERERES E (2009) AquaCrop – the FAO crop model to simulate yield response to water: I. Concepts and underlying principles. Agronomy Journal **101 (3)** 426–437. https://dl.sciencesocieties.org/publications/aj/abstracts/101/3/426.

STEDUTO P, HSIAO TC, FERERES E and RAES D (2012) Crop yield response to water. Irrigation and Drainage Paper No. 66, Food and Agriculture Organization, Rome, Italy. http://www.fao.org/docrep/016/i2800e/i2800e00.htm.

STEYN AJ (2011) *Farmers urged to report queleas. Farmers Weekly*, 16 November 2011. http://www.farmersweekly.co.za/article.aspx?id=10946&h=Farmersurgedtoreportqueleas.

TADROSS M, SUAREZ P, LOTSCH A, HACHIGONTA S, MDOKA M, UNGANAI L, LUCIO F, KAMDONYO D and MUCHINDA M (2009) Growing-season rainfall and scenarios of future change in southeast Africa: Implications for cultivating maize. Climate Research **40** 146–161. https://www.int-res.com/articles/cr_oa/c040p147.pdf.

TANNER CB and SINCLAIR TR (1983) Efficient water use in crop production: Research or re-search. In: *Limitations to efficient water use in crop production,* TAYLOR, HM, JORDAN, WR and SINCLAIR TR, 1–27. American Society of Agronomy, Madison, WI, USA.

TANWAR SPS and SHAKWAT MS (2003) Influence of phosphorus sources, levels and solubilizers on yield, quality and nutrient uptake of soybean – wheat cropping system in southern Rajasthan. Indian Journal of Agricultural. Sciences **73 (1)** 3–7. https://www.hindawi.com/journals/isrn/2012/234656/.

TAYLOR N, ANNANDALE J, ETISSA E and GUSH M (2008) *Draft report on potential evapotranspiration models.* Deliverable of Project K5/1770 to the Water Research Commission (WRC), Pretoria, South Africa.

TEKLEHAIMANOT Z, JARVIS PG and LEDGER DC (1991) Rainfall interception and boundary layer conductance in relation to tree spacing. Journal of Hydrology **123 (3–4)** 261–278. https://www.sciencedirect.com/science/article/pii/002216949190094X.

THIAGALINGAM K. DALGLIESH NP, GOULD NS, MCCOWN RL, COGLE AL and CHAPMAN AL (1996) Comparison of no-till and conventional tillage in the development of sustainable farming systems in the semi-arid tropics. Australian Journal of Experimental Agriculture **36 (8)** 995–1002. https://www.publish.csiro.au/an/EA9960995.

TODOROVIC M, ALBRIZIO R, ZIVOTIC L, ABI SAAB M, STOCKLE C and STEDUTO P (2009) Assessment of AquaCrop, CropSyst and WOFOST models in the simulation of sunflower growth under different water regimes. Agronomy Journal **101 (3)** 509–521.

TOLK JA, HOWELL TA and MILLER F (2013) Yield component analysis of grain sorghum grown under water stress. Field Crops Research **145** 44–51. https://www.sciencedirect.com/science/article/abs/pii/S0378429013000592.

TOVJANIN MJ, DJURDJEVIC V, PEJIC B, NOVKOVIC N, MUTAVDZIC B, MARKOVIC M and MACKIC K (2019) Modeling the impact of climate change on yield, water requirements, and water use efficiency of maize and soybean grown under moderate continental climate in the Pannonian lowland. Quarterly Journal of the Hungarian Meteorological Service **123 (4)** 469–486. https://www.met.hu/ismeret-tar/kiadvanyok/idojaras/index.php?no=2019.4.4.

TSUJI W, ALI MEK, INANAGA S and SUGIMOTO Y (2003) Growth and gas exchange of three sorghum cultivars under drought stress. Biologia Plantarum **46** 583–587. https://link.springer.com/article/10.1023/A:1024875814296.

TURHOLLOW AF, WEBB EG and DOWNING ME (2010) *Review of sorghum production practices: Applications for bioenergy.* ORNL/TM-2010/7. Oak Ridge National Laboratory, Oak Ridge, TN, USA. http://info.ornl.gov/sites/publications/files/Pub22854.pdf.

UNITED STATES DEPARTMENT OF AGRICULTURE (USDA) (2004) *Hydrologic soil-cover complexes*. In: *Hydrology, national engineering handbook*, Chapter 9 of PART 630. USDA, Washington, DC, USA. https://directives.sc.egov.usda.gov/OpenNonWebContent.aspx?content=17758.wba.

UNITED STATES DEPARTMENT OF AGRICULTURE (USDA) (2009) *Soil water characteristics: Hydraulic properties calculator.* USDA, Washington, CD, USA. https://hrsl.ba.ars.usda.gov/soilwater/Index.htm.

UNITED STATES DEPARTMENT OF AGRICULTURE (USDA) (2018) *Grain: World markets and trade*. USDA, Washington, DC, USA. https://apps.fas.usda.gov/psdonline/circulars/grain.pdf.

VAN DIJK AIJM and BRUIJNZEEL LA (2001a) Modelling rainfall interception by vegetation of variable density using an updated analytical model. Part 1. Model description. Journal of Hydrology **247 (3–4)** 230–238. https://www.sciencedirect.com/science/article/pii/S0022169401003924.

VAN DIJK AIJM and BRUIJNZEEL LA (2001b) Modelling rainfall interception by vegetation of variable density using an updated analytical model. Part 2. Model validation for a tropical upland mixed cropping system. Journal of Hydrology **247 (3–4)** 239–262. https://www.sciencedirect.com/science/article/pii/S0022169401003936.

VAN GENUCHTEN MTH (1980) A closed-form equation for predicting the hydraulic conductivity of unsaturated soils. Soil Science Society American Journal **44** 892–898.

VAN STAN JT, GUTMAN ED, LEWIS ES and GAY TE (2016) Modeling rainfall interception loss for an epiphyte-lade *Quercus virginiana* forest using reformulated static and variable storage Gash analytical models. Journal of Hydrometeorology **17** 1985–1997.

VANLAUWE B and ZINGORE S (2011) Integrated soil fertility management: an operational definition and consequences for implementation and dissemination. Better Crops **95 (3)** 4–7. http://www.ipni.net/publication/bettercrops.nsf/0/CA878688054B10C38525797C0078F394/$FILE/Better%20Crops%202011-3%20p4-7.pdf.

VANUYTRECHT E, RAES D, STEDUTO P, HSIAO TC, FERERES E, HENG LK, GARCÍA-VILA M and MORENO PM (2014) AquaCrop: FAO's crop water productivity and yield response model. Environmental Modelling and Software **62** 351–360. http://www.sciencedirect.com/science/article/pii/S136481521400228X.

VARBLE JL and CHÁVEZ JL (2011) Performance evaluation and calibration of soil water content and potential sensors for agricultural soils in eastern Colorado. Agricultural Water Management 101 (1) 93–106. https://www.sciencedirect.com/science/article/pii/S0378377411002484.

VOLOUDAKIS D, KARAMANOS A, ECONOMOU G, KALIVAS D, VAHAMIDIS P, KOTOULAS V, KAPSOMENAKIS J and ZEREFOS C (2015) Prediction of climate change impacts on cotton yields in Greece under eight climatic models using the AquaCrop crop simulation model and discriminant function analysis. Agricultural Water Management **147** 116–148. https://www.sciencedirect.com/science/article/pii/S0378377414002285.

VON HOYNINGEN-HUENE J (1983) Die Interzeption des Niederschlages in landwirtschaftlichen Pflanzenbeständen. Deutscher Verband für Wasserwirtschaft und Kulturbau. Schriften **57** 1–66. Verlag Paul Parey, Hamburg Germany.

WANG D, BEAN S, MCLAREN J, SEIB P, MADL R, TUINSTRA M, SHI Y, LENZ M, WU X and ZHAO R (2008) Grain sorghum is a viable feedstock for ethanol production. Journal of Industrial Microbiology and Biotechnology **35** 313–320. https://link.springer.com/article/10.1007/s10295-008-0313-1.

WANG Y, XIE Z, MALHI S, VERA C, ZHANG Y and WANG J (2009) Effects of rainfall harvesting and mulching technologies on water use efficiency and crop yield in the semi-arid Loess Plateau, China. Agricultural Water Management **96 (3)** 374–382. https://www.sciencedirect.com/science/article/abs/pii/S0378377408002072.

WANI SP, ALBRIZIO R and VAJJA NR (2012) Sorghum. In: *Crop yield response to water,* STEDUTO P, HSIAO TC, FERERES E and RAES D., Chapter 3.4, 144–151. Irrigation and Drainage Paper No. 66, Land and Water Division, Food and Agricultural Organisation, Rome Italy. http://www.fao.org/docrep/016/i2800e/i2800e00.htm.

WARBURTON ML, SCHULZE RE and JEWITT GPW (2010) Confirmation of ACRU model results for applications in land use and climate change studies. Hydrology and Earth System Sciences **14** 2399–2414. http://www.hydrol-earth-syst-sci.net/14/2399/2010/.

WARBURTON ML, SCHULZE RE and JEWITT GPW (2012) Hydrological impacts of land use change in three diverse South African catchments. Journal of *Hydrology* 414-415: 118-135. http://www.sciencedirect.com/science/article/pii/S0022169411007529

WARBURTON TOUCHER ML (2020) Personal communication. Hydrologist for the Grasslands-Wetlands-Forests Node, South African Environmental Observation Network, Pietermaritzburg, South Africa, 14 January 2020.

WARBURTON TOUCHER ML, RAMJEAWON M, MCNAMARA MA, ROUGET M, BULCOCK H, KUNZ RP, MOONSAMY J, MENGISTU M, NAIDOO T and VATHER T (2019) Resetting the baseline land cover against which stream flow reduction activities and the hydrological impacts of land use change are assessed. Draft report for WRC Project No. K5/2437, Water Research Commission, Pretoria, South Africa.

WEDDEPOHL JP (1988) *Design rainfall distributions for southern Africa.* MSc dissertation, Department of Agricultural Engineering, University of Natal, Pietermaritzburg, South Africa.

WIN M, NAKASATHIEN S and SAROBOL E (2010) Effects of phosphorus on seed oil and protein contents and phosphorous use efficiency in some soybean varieties. Kasetsart Journal (Natural Science) **44** 1–9. http://kasetsartjournal.ku.ac.th/kuj_files/2010/A1005061351011562.pdf.

WORD METEOROLOGICAL ORGANISATION (WMO) (2012) *Guide to agricultural meteorological practices*. Report WMO-No 134, WMO, Geneva, Switzerland. http://www.wmo.int/pages/prog/wcp/agm/gamp/documents/WMO_No134_en.pdf.

ZHANG S, LOVDAHL L, GRIP H, TONG Y, YANG X and WANG Q (2009) Effects of mulching and catch cropping on soil temperature, soil moisture and wheat yield on the Loess Plateau of China. Soil and Tillage Research **102 (1)** 78–86.
https://www.sciencedirect.com/science/article/pii/S0167198708001244.

ZOUGMORE R, KAMBOU FN, OUATTARA K and GUILLOBEZ S (2000) Sorghum-cowpea intercropping: An effective technique against runoff and soil erosion in the Sahel (Saria, Burkina Faso). Arid Soil Research Rehabilitation **14 (4)** 329–342.
https://www.tandfonline.com/doi/abs/10.1080/08903060050136441.

APPENDIX A

A1 DATA STORAGE

The project has generated over 50 GB of high-frequency temperature and wind speed data collected at Baynesfield Estate over a one-year period (January to December 2017). The data was analysed to estimate the evapotranspiration from a 20-hectare plot of soybean, as well as fallow conditions following the harvesting of maize. In addition, the project generated over 120 GB of compressed model output pertaining to the national water use and crop yield simulations. Data exists for eight national runs performed using AquaCrop and ACRU, i.e. two crops x two planting dates x two planting densities x two systems (rainfed and irrigated). In order to automate the national model runs, approximately 8,600 and 10,000 lines of code (written in UNIX and Fortran) were developed for AquaCrop and ACRU, respectively. In addition, over 1,400 lines of code were written to convert the climate input files from ACRU format to that required by AquaCrop. The biofuel assessment utility was used to disseminate the large database of daily stream flow simulations for natural vegetation, as well as for the selected feedstocks. All raw, processed and modelled data is stored and archived on a fileserver located in the ICS Server Room on the University of KwaZulu-Natal's main campus in Pietermaritzburg.

Contact person: Richard Kunz (kunzr@ukzn.ac.za).

APPENDIX B

B1 CAPACITY BUILDING

The WRC considers three levels of capacity building: postgraduate, institutional and community-based capacity building. Hence, reporting on capacity building is based on these three levels.

B1.1 Postgraduate capacity building

Details regarding the postgraduate students who benefitted from this project and contributed to it are given in Table B.1. As of April 2020, three honours students have graduated, as well as two MSc students and one PhD student. Another MSc student is likely to graduate at the end of 2020.

Table B.1: Individual capacity building: Postgraduate students

Name	Gender	Race	Degree	Discipline	Notes
Mr Ntuthuko Hadebe	Male	Black	BSc (Hons)	Hydrology	Awarded in 2017
Ms Lungile Lembede	Female	Black	MSc	Hydrology	Awarded in 2017
Ms Penisoh Metho	Female	Black	BSc (Hons)	Hydrology	Awarded in 2019
Ms Thivashnie Naidoo	Female	Indian	MSc	Hydrology	Fourth year
Mr Yadir Ramnarayan	Male	Indian	BSc (Hons)	Hydrology	Awarded in 2020
Mr Kyle Reddy	Male	Indian	MSc	Hydrology	Awarded in 2020
Mr Joseph Masanganise	Male	Black	PhD	Agrometeorology	Awarded in 2020

B1.1.1 Honours degree candidates

Mr Hadebe

This student evaluated the advantages of extending a 50-year daily rainfall record by an additional 15 years. He assessed the influence of record length on runoff generation using the ACRU model.

Title

Impacts of data availability on modelling rainfall:runoff response

Abstract

Limited data availability is a major problem in hydrology and a source of considerable uncertainty in any type of hydrological application. In this study, the main objective is to quantify the impact of artificially reducing the rainfall record length on the calculation of mean annual precipitation, as well as mean annual runoff, in order to determine the maximum record length beyond which no simulation improvement can be gained. The results help to justify if there is a need to update historical climate data used for modelling purposes at the catchment scale. A record of 65 years of daily rainfall data from Cedara was used to simulate runoff response using the ACRU hydrological model. The rainfall record was artificially reduced from 65 years to five years in 10-year increments, but also included a 50-year time series. The results show that there is no benefit in increasing the record length from 50 to 65 years, since the 50-, 55- and 65-year records produce similar MAP values. Although the recommended record length for MAP estimates is a minimum of 15 years, 20 years is suggested as the preferred minimum for Cedara. The simulations were then used to assess the “error” in simulated runoff that results from reduced input climate data, considering that changes in rainfall are amplified as larger changes in runoff. However, the 16 years of extended record from 2000 to 2015 produced little change in simulated MAR. However, 50 years of climate record is better than a 45-year record. The five-year reduction in record length results in a 2% change in MAP, which is amplified as an 8% change in MAR. There is a clear indication that sources of uncertainty (input data and parameter values) are substantially reduced with improved record length from five to 50 years.

Penisoh Metho

This student evaluated the use of AquaCrop to simulate crop evapotranspiration, from which monthly crop coefficients (K_C) were derived and used as input for the ACRU model (cf. Appendix N).

Title

Towards an updated methodology for estimating the hydrological impact of grain sorghum production

Abstract

Water availability determines the trajectory of water use, especially in water-limited environment. This is particularly true for water-limited regions with multiple competing water users. Moreover, crop coefficients (K_C) are underrated in their application to determine the downstream water availability. The current framework on evaluating the hydrological impact of a land use change (LUC) in South Africa acknowledges the green and blue water paradigm. However, emphasis is on the estimation of blue water flows, while green water flows are either neglected or inadequately quantified. To evaluate the variability and difficulties associated with field trials, modelled K_C was introduced as a pragmatic alternative, yielding an unbiased estimation on the subsequent in-stream water availability. Facilitated with light model linking, the results indicated a relationship between green and blue water flows at the field and catchment scale. More water use (green water flows) resulted in a reduction of water availability (blue water flows). Evapotranspiration and K_C were simulated with acceptable confidence for an observed growing season of grain sorghum in 2012/13, indicating the potential to derive site-specific K_C. The crop model output was validated by observed measurements and related fundamental indicator variables and related routines within the model including, soil water content, grain yield and evapotranspiration. A vegetational LUC required the description of the growing season in thermal time with locally derived crop parameters. Driving an agro-hydrological model with these crop water use parameters indicated the potential for application to deriving site-specific K_C databases for the country. Compared to existing K_C and SFRA ratings, the results generated by the AquaCrop-ACRU linked model were more modest and significantly different at the quinary catchment scale. The methodology applied has the potential to advance climate adaptation and mitigation strategies, as well as water availability based on the interplay identified between crop length and catchment climate inter-annual variability.

Yadir Ramnarayan

This student assessed the influence of wind speed on reference evapotranspiration. His work involved a comparison of an ultrasonic versus a cup anemometer to measure wind speed. The accuracy of the ultrasonic anemometer is crucial for the new surface renewal method that was utilised in this project (cf. Chapter 6).

Title

The influence of wind speed on reference evapotranspiration

Abstract

Reference evapotranspiration (ET_o) is an important component of the water cycle and is affected by various factors, including solar radiation, wind speed, air temperature and relative humidity. In order to quantify the effects of wind speed on ET_o, a mobile automatic weather station was positioned opposite a greenhouse exhaust fan, thus mimicking a wind tunnel experiment. Hourly weather data obtained over a 31-day period was inputted into a spreadsheet designed to calculate hourly and daily ET_o. Daily weather data was also inputted into a software utility to determine ET_o. Differences between hourly and daily calculations of ET_o were noted Weather data was also obtained from a nearby weather station and used to calculate hourly and daily reference evapotranspiration.

The ET_o estimates from both weather stations were then compared and highlighted differences between calculations of ET_o due to different sensors used to measure weather variables. More importantly, the study showed a 32% increase in reference evapotranspiration due to the higher wind speed caused by the exhaust fan. These findings should be of interest to Crop Science students, considering that higher rates of daily ET_o could enhance the growth and yield of irrigated crops grown in the vicinity of the greenhouse exhaust fan.

B1.1.2 Master's degree candidates

Lungile Lembede

This student conducted her research at Swayimane in the 2015/16 season. A summary of her work is presented in Chapter 5.

Title

Estimating water use and yield of soybean (*Glycine max*.) under mulch and fertilizer in rainfed conditions in KwaZulu-Natal

Abstract

South Africa is classified as a semi-arid country characterised by low and erratic rainfall. This poses major limitations to crop productivity, especially for smallholder farmers who rely on rainfed agriculture. This is worsened by a lack of knowledge regarding best management practices that can improve crop yields attained by smallholder farmers. In addition, smallholder farmers lack access to markets and do not participate in the agricultural value chain. The Biofuel Regulatory Framework (DoE, 2014) seeks to include smallholder farmers in the biofuel feedstock value chain. However, a prerequisite to their meaningful participation in the value chain would be to increase their current levels of crop and water productivity. The main aim of this study was to estimate the yield and water use of soybean (*Glycine max* L.) under rainfed and smallholder farming conditions using the AquaCrop model. Secondary to this, the effect of mulch and fertilizer on soybean water use efficiency was assessed. Lastly, a Soil Water Balance model was used to compare simulations made by AquaCrop for the non-mulched, full fertilizer treatment. Thereafter, the water use efficiency of soybean was calculated from crop water use and the final yield. The soybean trial was carried out at Swayimane, KwaZulu-Natal. The model simulations of crop water use and reference crop evapotranspiration were also used to calculate crop coefficients under non-standard conditions. Crop growth and yield parameters were measured to parameterise and evaluate model performance. Soil water content was monitored using Watermark sensors, along with climatic variables. An analysis of variance was used to detect significant interactions between treatments, while statistical indicators were used to evaluate the model performance of the AquaCrop and SWB models. Mulching improved soil water content and reduced soil water evaporation, although the final yield and total water use efficiency was reduced. The yield reduction in mulched plots was believed to be mostly affected by nitrogen immobilisation as a result of decaying straw mulch. Increasing soil fertility improved crop yield and water use efficiency in both mulched and non-mulched treatments. The AquaCrop model simulated the final yield and biomass fairly well, except in mulched treatments. The model simulated the highest yield in the mulched plots, which is contrary to what was observed. This is because the model only accounts for improved soil water content and does not account for the complex interactions between the soil and mulch residue that resulted in nitrogen deficiency. The SWB model simulated fairly similar crop water use and yield to AquaCrop. The water use efficiencies obtained in this study were compared to the water use efficiency of the same cultivar grown in a commercial environment by Mengistu et al. (2014) in Baynesfield, KwaZulu-Natal. In comparison to commercial farmers, smallholder farmers tend to produce lower water use efficiencies. However, implementing the best management practices narrowed the yield gap between commercial and smallholder farmers.

The modelled water use efficiency reported in Baynesfield was 1.277 kg m^{-3} with a biofuel use efficiency of 0.237 ℓ m^{-3}, while a water use efficiency of 0.359 kg m^{-3} and biofuel use efficiency of 0.067 ℓ m^{-3} was obtained in this study for the non-mulched, full fertilizer treatment. According to AquaCrop, the mulched, full fertilizer treatment had a water use efficiency of 0.485 kg m^{-3} and a biodiesel use efficiency of 0.103 ℓ m^{-3}. It is believed that the latter water and biofuel use efficiencies would have been achieved had enough nitrogen been available to the crop. In conclusion, implementing best management practices can help narrow the yield gap between smallholder and commercial farmers. It was evident from this study and others that agronomic practices have a significant impact on crop yield and ultimately, water use efficiency.

Thivashnie Naidoo

This student was tasked with using the *MaxEnt* model to identify regions suitable for soybean and sorghum production. She is expected to complete her degree in 2020.

Kyle Reddy

This student performed his field work at Swayimane in the 2018/19 season. A summary of his work is presented in Chapter 8.

Title

Estimation of water use efficiency of soybean (*Glycine max*.) for biodiesel production in KwaZulu-Natal

Abstract

The production of biofuel from crops is an alternative approach to that of fossil fuels, which is expected to increase in order to ensure both cleaner energy and energy security. Knowledge of water use and yield of biofuel crops under different crop management practices and rainfed conditions at a smallholder scale is scarce in South Africa. Therefore, the main aim of this study was to estimate the crop water use and yield of soybean (*Glycine max* L.), as well as the crop's response to inoculation. A field study was conducted at Swayimane in KwaZulu-Natal (South Africa) to estimate the seasonal water use, seed yield, water use efficiency (WUE_C) and biodiesel yield of two genetically modified soybean varieties (CAPG3 and LS6161R). The trial was grown under rainfed conditions with optimum fertilization (100%) and two inoculation levels (0 and 100%). Seasonal crop water use (m^3 ha^{-1}) was derived from actual crop evapotranspiration (ET_C in mm) that was estimated using the SWB method. Final biomass production and seed yield were measured at harvest, while biodiesel yield was determined post-harvest using measured seed oil content. The inoculated LS6161R variety consumed 4,810 m^3 ha^{-1} of water and produced 4.59 t ha^{-1} of seed, from which a WUE_C of 0.95 kg m^{-3} was calculated. For the CAPG3 variety, comparable figures of 5,083 m^3 ha^{-1}, 4.35 t ha^{-1} and 0.86 kg m^{-3} were obtained for water use, yield and WUE_C, respectively. Both varieties produced similar theoretical biodiesel yields of 845-850 ℓ ha^{-1}, based on a seed oil content of 17.9-18.9%. The non-inoculated treatment produced lower seed yields and WUE_C. However, there were no statistically significant differences between varieties and inoculation treatments for measured crop water use and yield. Observations of phenological growth stages were used to partially calibrate the AquaCrop model. The model was then used to simulate crop water use, yield and WUE_C, which was then compared to observations. Simulated values of WUE_C correlated poorly with observed data for both varieties and inoculation treatments. In conclusion, LS6161R is more water use efficient than CAPG3, and thus may be better suited for biodiesel production under rainfed conditions for both smallholder and commercial farming systems. CAPG3 produced a higher proportion of biomass instead of seed yield, and is thus less suited for biodiesel production. With the implementation of good crop management practices, the yield gap between smallholder and commercial farmers can be reduced as is evident in this study. Finally, a full calibration of AquaCrop under optimum (i.e. irrigated) growing conditions is recommended for both soybean varieties.

B1.1.3 Doctoral candidate

Joseph Masanganise

This student was responsible for the surface renewal measurements undertaken at Baynesfield in the 2016/17 season (cf. Chapter 6), as well as the measurements of water use and yield of grain sorghum at Swayimane during the 2017/18 season (cf. Chapter 7).

Title

Water use and yield of soybean and grain sorghum for biofuel production in South Africa

Abstract

In the last few decades, new methods were developed, while other existing methods have been improved for quantifying crop evapotranspiration. Some of the methods determine crop evapotranspiration from micrometeorological measurements of surface energy fluxes above crop surfaces. The surface renewal method for estimating sensible heat flux was introduced in the 1990s and has been refined over the years to produce sub-methods (commonly called SR2) that are relatively inexpensive and simpler to operate. The SR method can be combined with surface energy balance to determine the latent heat flux from which crop evapotranspiration is derived. Despite its numerous refinements, the SR method is still confined to a small research community, mainly the same groups of international researchers. This provides opportunities for further research to explore the utility of this method in a wide range of applications. The objective of the current study was to estimate crop evapotranspiration of soybean and grain sorghum produced under rainfed conditions. We track the evolution of SR as far back as the 1930s to date. Eight different versions of the SR method are reviewed. For each sub-method, the principles underlying its application are presented, highlighting the complexity in the mathematical formulations, as well as its accuracy and suitability. The adoption of the SR method in local and international studies is examined. Also highlighted is the sparsity of information regarding the performance of SR2, which makes it unclear in the literature. In this review, the following recommendations for future research are given: further refinement of the latest versions to simplify the methods to improve their adoption by potential users; the application of SR2 in varied environments and over a wide range of surfaces and stability conditions; and expanding the coverage of SR to determine fluxes other than sensible and latent heat. Two versions of the SR method (SR2) and the temperature variance method for estimating sensible heat flux were used to estimate the sensible heat flux (H) above a soybean canopy in KwaZulu-Natal, South Africa. One version combines surface renewal analysis with Monin-Obukhov similarity theory (SR-MOST). The other version is a combination of surface renewal analysis and dissipation theory (SR-DT). Prior to application, the performance of SR-MOST and SR-DT in estimating H over fallow land had been evaluated using the eddy co-variance method. For soybean, H was derived from air temperature measurements made above the canopy surface at a frequency of 10 Hz using two unshielded fine-wire thermocouples at 0.85 and 1.94 m above the soil surface. Net irradiance and the soil heat flux were also measured. A shortened surface energy balance equation was used to calculate the latent heat flux (LE) for SR-MOST and SR-DT. The evaluation of SR-MOST and SR-DT using eddy co-variance showed good performance. A comparison of H for SR-MOST vs SR-DT for unstable conditions using the time lag of 0.4 s showed good agreement with a slope of 0.73, intercept of 14.14 W m^{-2}, coefficient of determination (R^2) of 0.89 and RMSE of 25.42 W m^{-2} at 0.85 m. The corresponding statistics for the measurement height of 1.94 m were 1.18, 16.54 W m^{-2}, 0.90 and 38.21 W m^{-2}, respectively. Generally, the two methods, SR-MOST and SR-DT produced H estimates that are almost indistinguishable. The temperature variance method over-estimated H when compared to SR-MOST and SR-DT at both measurement levels. We found a good agreement between estimates of LE for SR-MOST and SR-DT at both measurement levels with a slope of 1.05, intercept of 7.58 W m^{-2}, R^2 of 0.96 and RMSE of 25.53 W m^{-2} at 0.85 m.

The corresponding statistical measures for the measurement height of 1.94 m were 0.88, -15.25 W m^{-2}, 0.97 and 38.11 W m^{-2}, respectively. The proportion of missing values of H was greater for SR-MOST compared to the SR-DT method. The SR-DT method requires a relatively small number of input parameters compared to SR-MOST and its application resulted in reduced loss of data. Therefore, it was more robust in estimating H. Using air temperature measurements obtained from the lower thermocouples, the values of LE for SR-MOST and SR-DT were used to compute evapotranspiration using the latent heat of evaporation of water. The evapotranspiration estimated using SR-MOST and SR-DT (ET_{SRMOST} and ET_{SRDT}), respectively, was compared to the evapotranspiration obtained using the standard crop coefficient (CC) approach (ET_{CC}). Comparison of the cumulative daily sums of evapotranspiration for the study period showed that ET_{SRMOST} was closer to ET_{CC}. However, both SR-MOST and SR-DT slightly overestimated the cumulative evapotranspiration by 2.4 and 4.2% respectively. During flowering, pod formation and seed filling, both SR-MOST and SR-DT slightly overestimated evapotranspiration obtained using canopy cover with an average RMSE of 1.35 mm and an average MAE of 0.39 mm for SR-MOST and 1.25 and 0.36 mm for SR-DT, respectively. The diurnal patterns of both ET_{SRMOST} and ET_{SRDT} were similar to that of ET_{CC}. During senescence and at maturity, the diurnal patterns of ET_{SRMOST}, ET_{SRDT} and ET_{CC} were similar. However, SR-MOST and SR-DT under-estimated evapotranspiration compared to canopy cover. The average statistical measures for SR-MOST were RMSE = 0.71 mm and MAE = 0.25 mm. Correspondingly, the statistics for SR-DT were 0.54 and 0.19 mm, respectively. Both SR-MOST and SR-DT methods produced good estimates of evapotranspiration and can be used as alternative methods in areas where crop coefficients are not available. Water use and yield of crops are necessary for selecting the best varieties to grow for a particular purpose. A wide range of grain sorghum varieties exist in South Africa, but very few have been recommended as potential biofuel feedstocks. A study was conducted to estimate the seasonal crop evapotranspiration, water use efficiency and biofuel yield of three grain sorghum varieties: PAN8816, PAN8906 and Macia grown under rainfed conditions and two fertility levels (0 and 100 %). Crop evapotranspiration was estimated using the SWB method. Biofuel yield was determined from measurements of grain yield, starch content, fermentation efficiency and a theoretical equation. When fertilized, PAN8816 consumed 405.3 mm of water and produced 1.8 $\pm$ 0.3 t ha^{-1} of grain, 707.4 ℓ ha^{-1} of biofuel, with a corresponding WUE of 0.4 kg m^{-3}. Mean values for PAN8906 were 410.0 mm, 2.6 $\pm$ 0.3 t ha^{-1}, 940.9 ℓ ha^{-1} and 0.6 kg m^{-3}. For Macia, the mean values were 399.8 mm, 0.9 $\pm$ 0.3 t ha^{-1}, 291.4 ℓ ha^{-1} and 0.2 kg m^{-3}. These findings suggest that PAN8816 and PAN8906 could be candidate feedstocks for biofuel production with potential to achieve greater biofuel yield if produced under optimal conditions. Macia produced a relatively high proportion of biomass to grain and this variety may not be a suitable feedstock.

B1.2 Institutional capacity-building

Postgraduate students benefit from various courses offered by the University of KwaZulu-Natal, which are designed to assist them in completing their degrees. Training is provided for free of charge on using the Microsoft Office (MS) suite of products (MS Word, MS Excel, MS PowerPoint, etc.), as well as bibliography managers (e.g. Endnote, RefWorks). Training on how to efficiently utilise the library is also provided. All postgraduate students working on this project were encouraged to attend the training sessions, which they did. In addition, the following more specialised courses were attended by researchers and students working on this project.

2017

In May, Mr Richard Kunz attended a five-day course on data analytics held at the University of KwaZulu-Natal's Durban Campus. The free course was offered by the University of KwaZulu-Natal's Teaching and Learning Office and was presented by four academics (three local and one international) with backgrounds in Chemical Engineering, Information Technology, Higher Education Research, Social Psychology and Statistics. Mr Kunz was exposed to Big Data structures, databases capable of handling Big Data and learnt how to inject scripts into a server database to analyse data.

In June, Mr Kunz, Dr Mabhaudhi and Mr Masanganise attended a two-day workshop on eddy co-variance organised by Prof Savage (Agrometeorology), with input from Dr Clulow, Prof Everson and a PhD student at the University of KwaZulu-Natal (Mr Mbangiwa). The workshop included both eddy co-variance theory, as well as a practical component on data analysis, which was held at the University of KwaZulu-Natal in Pietermaritzburg.

In December, Mr Kunz, Dr Mabhaudhi and Mr Masanganise attended a three-day training workshop on bio-economic modelling. The workshop was organised by the uMngeni Resilience Project and held at the University of KwaZulu-Natal in Pietermaritzburg. The course was given by Dr Marta Monjardino and Dr Brendan Brown from the Commonwealth Scientific and Industrial Research Organisation (CSIRO) (Agricultural and Food Division, Australia), with input from Dr Mabhaudhi. The workshop covered two useful tools: ADOPT and IAT. ADOPT predicts the likely adoption and diffusion of specific innovations within a smallholder environment, and IAT is a bio-economic model developed by CSIRO to explore the biophysical and economic impacts of innovations in smallholder farming systems.

2018

In July, Mr Masanganise attended a one-day workshop at the University of KwaZulu-Natal in Pietermaritzburg on surface renewal that was given by Prof Mike Savage (Agrometeorology). The workshop was the first of its kind and included both SR theory and a practical component on data analysis.

In July, Mr Kunz, Dr Mabhaudhi and Mr Masanganise attended a two-day Data Carpentry workshop on Python programming held at the University of KwaZulu-Natal in Pietermaritzburg. Data Carpentry is a sibling organisation of Software Carpentry, which is designed to teach fundamental concepts, skills and tools for working more effectively with data. The workshop was delivered by volunteer instructors: Katrin Tirok, Justin Pringle (University of KwaZulu-Natal's Civil Engineering Department) and San Emmanuel James (University of KwaZulu-Natal's Nelson Mandela School of Medicine).

In November, Mr Reddy and Mr Masanganise also attended an R statistics training workshop at the University of KwaZulu-Natal in Pietermaritzburg. The course was run over two days by Dr Sibiya.

2019

In July, Mr Masanganise attended a two-day workshop at the University of KwaZulu-Natal in Pietermaritzburg on sap flow measurements that was organised by Prof Mike Savage (Agrometeorology). The workshop was also the first of its kind and involved contributions from Dr Clulow, Prof Everson and Dr Scott-Shaw (a postdoctorate student). Presenters covered principles of sap flow on the first day, followed by practical aspects of measurements on the second day.

In September, Mr Masanganise attended a summer school in the Philippines on the topic: "Transformative changes in agriculture and food systems". The summer school was organised by the South-East Asian Regional Centre for Graduate Study and Research in Agriculture, together with the Food Security Centre of the University of Hohenheim in Germany. Mr Masanganise was one of only 17 applicants from Africa, Asia and Latin America to receive funding to attend the event, which covered travel, board and lodging expenses.

B1.3 Community-based capacity-building

Both teachers and learners at Swayimane High School were exposed to the research and instrumentation at the trial site, which was located on the school's property. In addition, members of the community were hired to assist with land preparation. The trial site was also showcased to municipality and government officials responsible for managing the uMgungundlovu District.

APPENDIX C

C1 TECHNOLOGY TRANSFER

Technology transfer in this project has mainly occurred via presentations at workshops, symposiums and conferences. The presentations are listed below in chronological order.

C1.1 Presentations

2015

In July, Ms Lembede presented her MSc project proposal presentation to staff and students at the University of KwaZulu-Natal.

In August, the following three presentations were given at the project's inaugural workshop held at the University of KwaZulu-Natal in Pietermartizburg:

Mr Kunz:	Overview of previous WRC-funded research related to the water use of biofuel crops
Dr Mabhaudhi:	Overview of the new project, highlighting the feedstocks to be considered in field experiments
Ms Lembede:	Summary of her MSc research proposal, focusing on the field work component

2016

Presentations were given at the following symposiums, which showcased the previous six-year biofuel project, as well as this five-year project:

May:	Howard Davis Memorial Ukulinga Symposium, Ukulinga Research Farm, Pietermartizburg (Presenters: Mr Kunz and Ms Lembede)
September:	South African National Committee of the International Association of Hydrological Sciences (SANCIAHS) Symposium (Presenters: Mr Kunz and Ms Lembede)
	Biofuel Dialogue (Presenter: Mr Kunz)
October:	South African National Committee on Irrigation and Drainage (SANCID) Symposium (Presenters: Mr Kunz and Ms Lembede).

A popular article emanated from the Ukulinga Symposium, which was published in *Farmers Weekly* on 5 August 2016.

2017

March:	Mr Kunz delivered a presentation titled "Assessing the hydrological impact of biofuel feedstock production" at the World Water Day Summit and Expo in Durban

2018

April:	Dr Mabhaudhi attended a conference titled "Sorghum in the 21st Century" in Cape Town.
May:	Mr Masanganise delivered a presentation titled "Water use and yield of soybean and grain sorghum for biofuel production in South Africa" at the Howard Davis Memorial Ukulinga Symposium held at the Ukulinga Research Farm, Pietermartizburg

In November, the following three presentations were given at the project's second workshop held at the University of KwaZulu-Natal in Pietermartizburg:

Mr Kunz: An overview of the project, including a summary of progress made to date

Mr Masanganise: Measurements of crop water use and yield obtained over three seasons

Mr Kunz: Proposed modelling approach using AquaCrop and ACRU

2019

October: Mr Masanganise delivered a presentation titled "Evapotranspiration estimates of soybean using surface renewal: Comparison with AquaCrop" at Waternet held in Johannesburg

C1.2 Popular articles

Since April 2015, three popular articles highlighting this project have appeared in the Farmer's Weekly (August 2016), AgriWater (August 2016) and the Water Wheel (November 2016). In addition, the biofuel project was mentioned in articles published on UKZN's website (Ndaba Online; April 2017) as well as the CWRR's website (October 2017). The latter article involved a drone flight at Baynesfield to obtain aerial photographs of the surface renewal system measuring actual evapotranspiration in a fallow maize field.

C1.3 Papers

As at February 2020, Mr Masanganise submitted a paper titled "Surface renewal approaches for estimating sensible heat flux: a review" to the *Physics and Chemistry of the Earth Journal*.

APPENDIX D

Table D.1: Growth criteria for soybean cultivation obtained from the literature (after Kunz et al., 2015b)

Source	Annual rainfall (mm)	Seasonal rainfall (mm)	T_{ave} (°C)	Frost tolerance	RH_{ave} (%)	HU (GDD) Base 10°C	Soil depth (mm)
Smith (1994)	> 700	450-700	18-35 Sub Jan > 19 Abs			1100-2400	
Smith (1998)	> 700	> 450 550-700		Medium			250-400
Smith (2006)		550-700					600-1,200
FAO (2006)	600-1500 Opt 450-1800 Abs		20-33 Opt 10-38 Abs				
Nunkumar (2006)					< 75		
PANNAR (2006)		550-850	13-30				
Schulze and Maharaj (2007b)	> 600		Jan > 18			> 1,500 1,000-2,600 (October to March)	
Jewitt et al. (2009a)		550-700 Opt	20-30 Opt 18-35 Sub			> 1,500	
Schulze and Kunz (2010c)	> 600		Jan > 18			10,00-2,600 (October to March)	
DAFF (2010a)		500-900	13-30 25 Opt				300-500
DAFF (2010a) - at planting			15-18				
El Bassam (2010)	500-750		24-25 Opt 20-25 Sub				300-400
Steduto et al. (2012)							
Dreyer (2017)		> 400 Abs > 700 Opt					
SEEDCO (2018)		550-650	18-30				

Table D.2: Growth criteria for grain sorghum cultivation obtained from the literature (after Kunz et al., 2015b)

Source	Annual rainfall (mm)	Seasonal rainfall (mm)	T_{ave} (ºC)	T_{min} (ºC)	T_{max} (ºC)	RH_{ave} (%)	Soil depth (mm)
Doorenbos and Kassam (1979)		450-650					
Singh (1985)			> 18				
Smith (1994)	650-800	450-650 Opt	> 10 Opt > 25 Ger Jan = 21 Ger Jul < 16 Ger	> 15 Flo	< 35 Flo	Not hot/humid	1,000-1,500
Smith (1998)	650-800	450-650	> 25 Opt Jan > 21	> 15 Flo	< 35 Flo	Not hot/humid	
Smith (2006)	650-800	450-650	> 25 Opt Jan > 21	> 15 Flo	< 35 Flo	Not hot/humid	
FAO (2006)	500-1 000 Opt 300-3 000 Abs	400-600 opt 300-700 abs	27-35 Opt 8-40 Abs	> 8	< 40		500-1,500
Schulze and Maharaj (2007a)	> 600	300-1200 600 OPT	25 Opt Jan > 21	> 15 Flo	< 35 Flo	< 60 Not hot/humid	
Du Plessis (2008)		> 400 dry > 800 wet	27-30 Opt 20-30 Sub > 21 Sub	7-10 Ger			> 250
Jewitt et al. (2009a)		450-650 Opt	20-25 Jan > 21				
DAFF (2009b)		500-600					
DAFF (2010b)		300-750	27-30 Opt 20-30 Sub > 21 Sub	7-10 Ger			> 250
El Bassam (2010)		400-600	27-30 Opt	8-10			
Schulze and Kunz (2010b)	600	300-1200	25 Opt Jan > 21	> 15 Flo	< 35 Flo	< 60 Not hot/humid	
PANNAR (2013b)		400-800	25-30 Opt > 15 Abs		25-30 Rip	Not cool/humid	Deep
Steduto et al. (2012)		500-800					
Hadebe et al. (2017a)		450-650					

Note: Min = Minimum criterion; Opt = Optimum criterion; Sub = Sub-optimum criterion; Abs = Absolute criterion; Dry = Ideal for drier regions; Wet = Ideal for wetter regions; Ger = ideal for germination; Flo = ideal for flowering; Rip = ideal for ripening; Jan = Month of January; Jun = Month of June; Jul = Month of July

APPENDIX E

E1 INOCULATION GUIDE

Nitrogen fixation is crucial in achieving the yield potential of soybean. Seed inoculation aids in establishing the nitrogen-fixing bacteria *Bradyrhizobia japonicum*. If this bacterium establishes functional root nodules, soybean can acquire up to 75% of its nitrogen requirements from the atmosphere. Yields of above 4 t ha^{-1} are attainable when soybean has been inoculated with the right inoculant. The potential benefits of inoculation outweigh the associated costs. Soybean inoculation should not be considered under the following circumstances:

- The field has no prior history of soybean planting in the previous three to four years.
- Soil pH falls outside the range of 5.5 to 6.5.
- Soil organic matter is below 1%.
- There was drought or flooding in the prior season.

Soybean grown on soils with a high sand content can still be inoculated, but via a leaf spray. On soils where soybean is being planted for the first time, it is recommended that the normal dose of bacterial inoculant is doubled. Inoculants can be purchased in the form of concentrated liquid or powdered peat. Concentrated liquid is generally preferred in large-scale commercial farming, while powdered peat may be recommended for smallholder farmers. Rhizobia in the inoculant is a living organism and shelf life typically varies from one week to three months, with some products lasting more than a year (depending on the manufacturer). Since it is a living organism, rhizobia can be killed by heat, desiccation and contact with some fertilizers or chemicals. Therefore, inoculants should be stored away from other chemicals. Where molybdenum seed treatment is also required, it must be applied in the form of sodium molybdate, which is less toxic to the bacterial inoculant. In addition, inoculants should be stored in a cool place where they are not exposed to direct sunlight (e.g. the fridge). The farmer needs to check the product label to ascertain what not to mix the rhizobia with. It is important to have rhizobia that is specific for soybean, since different legumes are inoculated with rhizobia specific to them. The effectiveness of the inoculation depends on the freshness and viability of the inoculant and the method of application.

E1.1 Peat or dry inoculum

i. Add soybean seed, preferably into a plastic container.
ii. For 100 kg of soybean, dissolve 100 g of inoculant in 1 litre of water.
iii. To make the solution adhesive (sticky), add one of the following: 100 g sugar, 100 ml vegetable oil, 100 g powdered milk or methyl cellulose.
NB: Use of water alone in the absence of other adhesive agents results in the seed absorbing most of the moisture, leaving the inoculant at risk of being blown away during planting.
iv. Pour the inoculant solution plus adhesive into the plastic container containing the soybean seed. The seed should be turned during the pouring to ensure adequate contact. Mix the seed and solution well until all the seed is visibly wet.
v. Alternatively, spread out the seed onto a clean plastic sheet placed in the shade, then sprinkle the inoculant onto the seed. Turn the seed gently to ensure that all are coated and look shiny wet.
vi. Seed should be planted soon after inoculation so as to prolong the viability of the rhizobia.
NB: The inoculated seed should be protected from direct sunlight. This may entail covering the plastic containers or storing them under a nearby tree.
vii. Seed should be planted in moist soils.

Some manufactures of powdered peat-based inoculum include a sticker that allows the inoculant to adhere better to the seed. Safeners that help protect rhizobial cells against toxic pesticides may also be included. It is important that the farmer follows the specific instructions on the label as application rates of inoculum will generally differ.

E1.2 Liquid inoculum

With liquid inoculum, the inoculant can either be diluted with non-chlorinated water or direct application to the seed can take place as per instructions on the label. Application is normally straightforward and entails applying the recommended dosage of the liquid inoculum to the seed. Although the amount of liquid inoculum is generally product-specific, it is approximately 270 ml for 100 kg of seed. Smaller-sized seed will generally require slightly more inoculant due to their larger specific surface area when compared to larger-sized seed.

NB: If a seed treater is being used, proper calibration should take place before use. Once treated, seed should be used within a period of less than four hours (the life span will differ depending on the manufacturer). Liquid inoculation should only be utilised on moist soil.

E1.3 In-furrow application

Both dry and liquid inoculants can be applied in furrows. It is important to ensure that spray rigs and tanks are clean. Clean water with neutral pH is ideal. The diluted inoculum should be applied to the planting furrows at recommended rates, usually around 50-100 ℓ ha^{-1}. Do not dilute the inoculant with too much liquid as it may cause the seed coat to shrink and burst.

NB: It is critical that the farmer follows specific instruction for the particular inoculant being used to achieve the best results.

E2 REFERENCES

ABENDROTH LJ, ELMORE RW and FERGUSON RB (2006) G06-1621 Soybean inoculation: Understanding the soil and plant mechanisms Involved (part one of a two-part series). Historical Materials from University of Nebraska-Lincoln Extension 2078. http://digitalcommons.unl.edu/extensionhist/2078/.

CHRISTMAS EP (2009) Update on soybean inoculant research. Purdue University, Department of Agronomy. https://www.agry.purdue.edu/cca/2008/proceedings/christmas.pdf.

DREW E, HERRIDGE D, BALLARD R, O'HARA G, DEAKER R, DENTON M, YATES R, GEMELL G, HARTLEY E, PHILLIPS L, SEYMOUR N, HOWIESON J and BALLARD N (2012) Inoculating legumes: A practical guide. Grains Research and Development Corporation.

HERRIDGE DF (2008) Inoculation technology for legumes. In: *Nitrogen-fixing leguminous symbioses,* pp. 77–115, Springer, Dordrecht.

IOWA STATE UNIVERSITY EXTENSION AND OUTREACH (2008) Seed Inoculation. https://crops.extension.iastate.edu/soybean/production_seedinoc.html.

N2AFRICA (2014) Better soybean through good agricultural practices.

PANNAR (2006) Soybean production guide. http://www.pannar.com/assets/documents/soybeans.pdf.

SEEDCO (2018) Farmers guide – grain crops. https://www.seedcogroup.com/sites/default/files/Agronomy%20Manual.pdf.

APPENDIX F

The protocols listed below were followed for all fieldwork conducted in each growing season.

F1 CANOPY CHARACTERISTICS

F1.1 Seedling leaf area

The mean leaf area of 20 seedlings sampled at 90% emergence was used to estimate the initial canopy size (cm^2 per plant).

F1.2 Leaf number

The number of fully formed leaves were counted over the growing season (from 90% emergence to maturity). A fully formed leaf is defined when the leaf collar is visible without dissecting the plant. The flag-leaf is counted as the first leaf upon full formation.

F1.3 Plant height

The height of a plant (from the base of the stem to the top of the canopy) was measured at regular intervals over the growing season.

F1.4 Leaf Area Index

Leaf Area Index is defined as the cumulative one-sided area of leaves per unit ground area. The LAI is a dimensionless value, typically ranging from 0 for bare ground to 6 for dense forest. The LAI was measured indirectly using a LAI-2200 plant canopy analyser (LI-COR Inc., Nebraska, USA). The LAI-2200 calculates LAI and other canopy structure attributes from solar radiation measurements made with a wide-angle optical sensor. Measurements above and below the canopy are used to determine canopy light interception at five angles, from which LAI is computed using a model of radiative transfer in vegetative canopies. A single measurement was taken above the canopy (i.e. A1 reading), and four measurements were taken below the canopy (at ground height) in a 1 m diagonal distance (i.e. B1 to B4 readings). The four below-canopy readings were taken at different positions: next to the row, slightly further away from the row, at the centre of the row and towards the next row. The sequence of taking measurements is shown in Figure F.1.

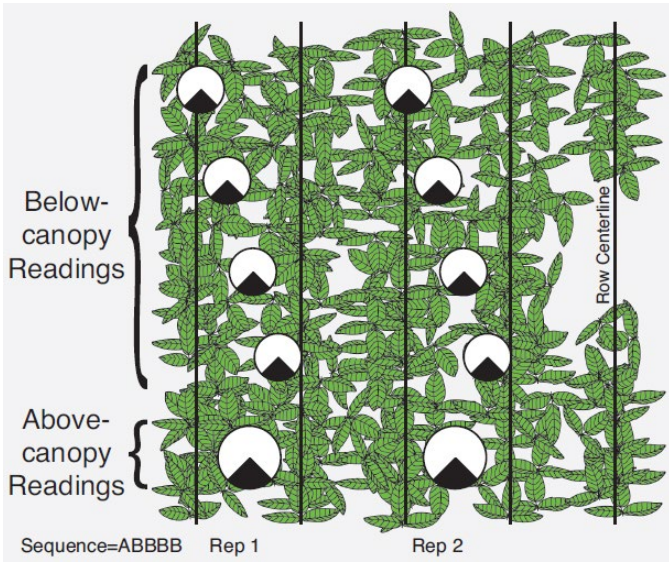

Figure F.1: Sequence of LAI measurements (adapted from LAI-2200, 2010

F1.5 Canopy cover

Since AquaCrop is a canopy-level model, simulated canopy cover values first needed to be matched to observations (Hadebe et al., 2017b). Canopy development is expressed through canopy cover and not via LAI. Canopy cover can be estimated from measurements of LAI using various equations as proposed by Garcìa-Vila et al. (2009), Hsiao et al. (2009), Raes et al. (2009) and Karunaratne et al. (2011). In this study, DIFN, an output of the LAI-2200 canopy analyser, was used to calculate canopy cover (as a percentage), which is a measure of the above-ground biomass, based on the following equation by Mabhaudhi et al. (2014):

$$CC = 1 - DIFN$$ Equation 21

The DIFN is indicative of the fraction of sky that is not obscured by the plant's canopy, with the value ranging from 0 (i.e. no sky visible) to 1 (i.e. no canopy obscuring the sun) (LAI-2200, 2010). Maximum canopy cover (CC_X) is the maximum achievable percentage of canopy cover, i.e. peak in weekly canopy cover values.

F2 PHYSIOLOGICAL PARAMETERS

F2.1 Chlorophyll Content Index

Chlorophyll Content Index was measured weekly (where possible) on dry, fully expanded and exposed leaves using a chlorophyll content meter (SPAD CCM-200 PLUS, Opti-Sciences, USA).

F2.2 Stomatal conductance

Stomatal conductance (flux of carbon dioxide entering, or water vapour exiting, through the stomata of a leaf) was measured weekly (around midday) using a steady state leaf porometer (Model SC-1, Decagon Devices, USA). In addition, diurnal measurements were also made when the plant reached the flowering stage.

F3 CROP PHENOLOGY

F3.1 Seedling emergence

The time to emergence was recorded as the time between planting and 90% emergence. An emerged seedling was defined as an exposed and fully expanded seed cotyledon, or when coleoptiles were visible at the soil surface. The time taken to reach each phenological stage was recorded in calendar days when ≥ 50% of the experimental plant population exhibited diagnostic signs of that particular growth stage.

F3.2 Other growth stages

The time taken to reach each phenological stage was recorded in calendar days when ≥ 50% of the experimental plant population exhibited diagnostic signs of that particular growth stage. Flowering was observed as the time taken for 50% of the experimental plant population to reach panicle bloom (or flower inflorescence). The duration of flowering was recorded as the time taken from flowering until 50% of the experimental population exhibited anthesis. The time to canopy senescence was observed when 50% of the experimental plant population exhibited no new leaf formation or appearance. The time to physiological maturity was recorded when dry matter accumulation (biomass and yield) ceased.

F3.3 Physiological maturity

The time to physiological maturity was recorded when visual observations of at least 50% of the experimental plants had a black layer at the base of the kernel (or a dark spot seed on the opposite side of the kernel from the embryo).

F3.4 Harvest maturity

Harvest maturity is defined as the time when seeds have attained less than 20% moisture content and can be stored without damage to the seed.

F4 CROP GROWTH AND YIELD

F4.1 Biomass production

Biomass is the mass (fresh and/or dry) of above-ground living matter per unit of ground. Fresh and dry mass was recorded as plant shoot and fruit mass (marketable biomass) weekly after emergence (90% emergence). Using destructive sampling, biomass accumulation (or total dry matter) was determined by measuring the weight of a representative plant (with the roots removed prior to weighing).

F4.2 Crop yield

Crop yield is defined as the mass of the fruiting body at harvest time.

F4.3 Harvest Index

Harvest Index is defined as the mass of a harvested product (grain or seed) to the total dry biomass, expressed as a percentage. Harvest Index was recorded as zero until the start of head/pod formation.

F5 ROOT PARAMETERS

F5.1 Initial root depth

The root length of 10 random seedlings at 90% emergence was measured. The root is defined as the section of plant below the soil surface, usually visible by change of stem colour from green to white or lighter colours.

F5.2 Maximum root depth

This represents the maximum attained root length achievable in the field. This was determined by carefully removing the plant from the soil to examine the rooting distribution. The time (in days) taken for the plant to reach maximum rooting depth was also recorded.

APPENDIX G

Table G.1: SWB crop parameters for soybean cultivar LS6161R grown at Swayimane in the 2015/16 season (Lembede, 2017), compared with PAN535R parameters derived by Dlamini (2015)

Crop parameter	LS6161R	PAN535R
Canopy extinction coefficient for solar radiation, K_{PAR}		0.65
Dry matter to water ratio, *DWR* (Pa)		5.0
Radiation use efficiency, *RUE* (kg MJ^{-1})		0.00120
Base temperature (°C)	5	12
Optimum temperature (°C)		25
Cut-off temperature (°C)	30	32
Emergence day degrees (d °C)	108	62
Flowering day degrees (d °C)	1,023	600
Maturity day degrees (d °C)	2,189	1,155
Transition period (d °C)	900	550
Leaf senescence (d °C)	1,714	1,012
Maximum plant height H_{max} (m)	1.00	0.66
Maximum root depth RD_{max} (m)		0.6
Stem to grain translocation		0.200
Canopy storage (mm)		1.0
Minimum leaf water potential (kPa)		-1,500
Maximum transpiration (mm d^{-1})	8	9
Specific leaf area (m^2 kg^{-1})		18
Leaf-stem partition (m^2 kg^{-1})		1.500
Total dry matter at emergence (kg m^{-2})		0.0030
Root fraction		0.010
Root growth rate		5.0
Stress Index		0.95

The SWB model parameters determined by Dlamini (2015) for six soybean cultivars grown at Hatfield (Pretoria) are given in Table G.2. The trials were conducted at Hatfield in Pretoria. All cultivars are genetically modified (i.e. Roundup® Ready) and exhibit different maturity groups and growth habits (determinate and indeterminate) as shown in Table G.3.

Table G.2: Six soybean cultivars of different maturity groups that were planted at the Hatfield experimental farm in Pretoria (Dlamini, 2015)

No.	Cultivar	Maturity Group	Growth habit
1	LS6162R	IV	Determinate
2	PAN535R	V	Determinate
3	PAN1664R	VI	Determinate
4	LS6164R	VI	Indeterminate
5	LS6150R	VI	Indeterminate
6	PAN737R	VII	Determinate

Table G.3: SWB crop parameters for six soybean cultivars (Dlamini, 2015)

Crop parameter	LS6150R	LS6162R	LS6164R	PAN535R	PAN737R	PAN1664R
Canopy extinction coefficient for solar radiation, K_{PAR}	0.50	0.50	0.45	0.65	0.70	0.60
Dry matter to water ratio, DWR (Pa)	6.0	5.5	6.0	5.0	4.0	5.5
Radiation use efficiency, RUE (kg MJ^{-1})	0.00150	0.00130	0.00140	0.00120	0.00130	0.00120
Base temperature (°C)	12	12	12	12	12	12
Optimum temperature (°C)	25	25	25	25	25	25
Cut-off temperature (°C)	32	32	32	32	32	32
Emergence day degrees (d °C)	45	50	45	62	62	62
Flowering day degrees (d °C)	650	530	900	600	890	720
Maturity day degrees (d °C)	1,200	1,120	1,280	1,155	1,550	1,266
Transition period (d °C)	550	590	380	550	660	546
Leaf senescence (d °C)	1,050	750	1,080	1,012	1,150	1,150
Maximum plant height H_{max} (m)	0.87	0.63	0.78	0.66	0.77	0.67
Maximum root depth RD_{max} (m)	0.7	0.6	0.6	0.6	0.7	0.5
Stem to grain translocation	0.220	0.200	0.210	0.200	0.230	0.200
Canopy storage (mm)	1.0	1.0	1.0	1.0	1.0	1.0
Minimum leaf water potential (kPa)	-1500	-1500	-1500	-1500	-1500	-1500
Maximum transpiration (mm d^{-1})	9	9	9	9	9	9
Specific leaf area (m^2 kg^{-1})	18	18	19	18	22	21
Leaf-stem partition (m^2 kg^{-1})	1.500	1.520	1.600	1.500	1.700	1.500
Total dry matter at emergence (kg m^{-2})	0.0030	0.0030	0.0030	0.0030	0.0030	0.0029
Root fraction	0.011	0.010	0.012	0.010	0.011	0.010
Root growth rate	6.0	5.0	5.0	5.0	5.5	4.0
Stress Index	0.95	0.95	0.95	0.95	0.95	0.95

APPENDIX H

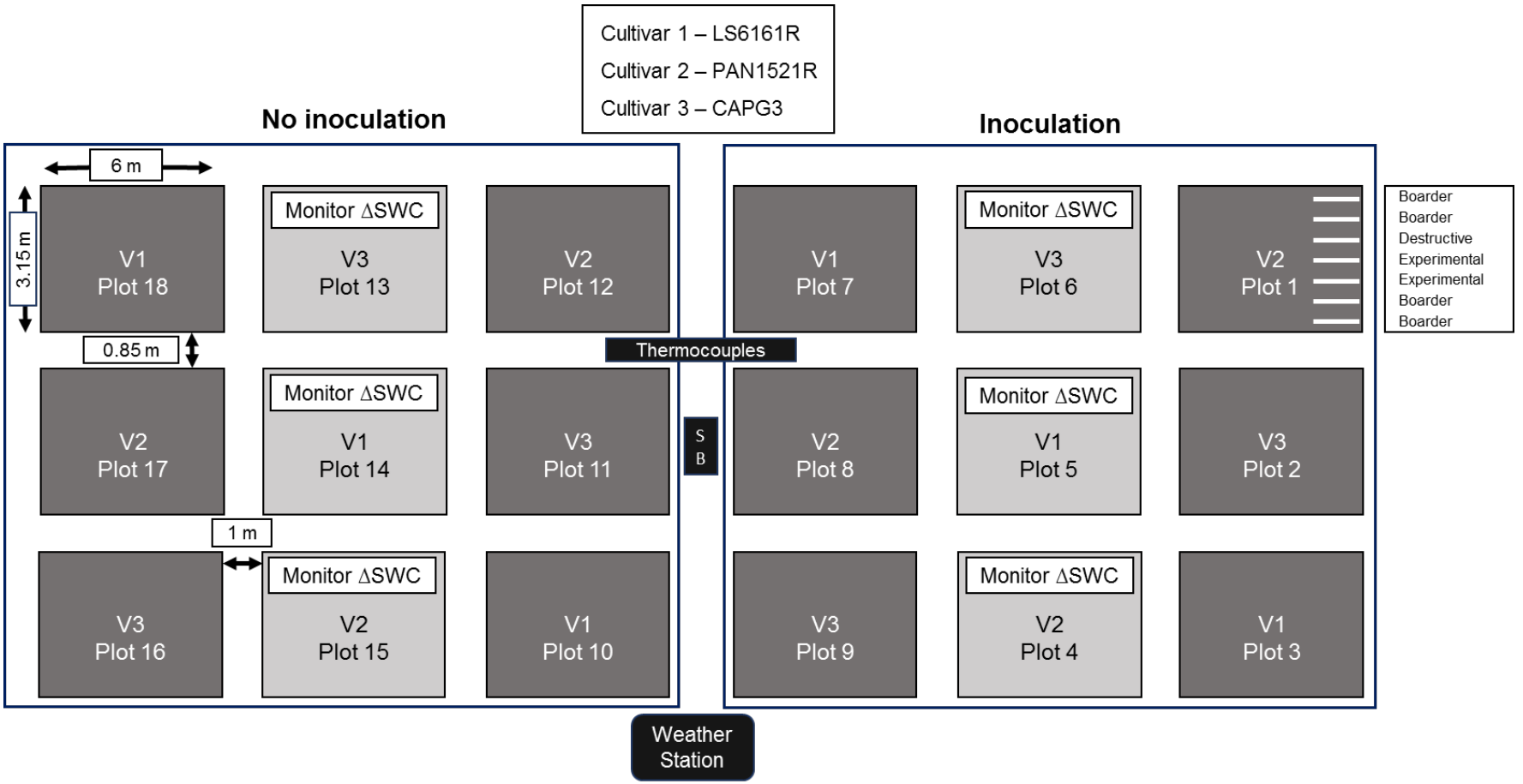

Figure H.1: Design for the 2018/19 soybean trial undertaken at Swayimane, where the main factor was inoculation and the sub-plots comprised of three cultivar choices (Reddy, 2019)

APPENDIX I

As noted in Section 9.3, the selected models were compared to determine similarities and differences in how the models calculate the accumulation of biomass, soil water content, and water deficit and/or temperature stress.

I1 CLIMATIC INPUTS

Differences in climatic input requirements between each model are shown in the table below.

Table I.1: Main differences in climatic inputs required by the selected models

Process	AquaCrop	SWB	ACRU
Rainfall	Input	Input	Input
T_{max}	Input	Input	Input
T_{min}	Input	Input	Input
ET_O/A-pan	Input/computed	Computed	Input/computed
R_S		Input	Input
RH_{max}		Input	
RH_{min}		Input	
RH_{ave}			Input
Wind speed		Input	
Wind run			Input

I2 SOIL WATER BALANCE

Differences in soil water balance calculations between each model are shown in the table below.

Table I.2: Main differences in the soil water balance used in each model

Process	AquaCrop	SWB	ACRU
Approach	Cascading	Cascading	Cascading
Soil horizons	12-layer	11-layer	2-layer
Reference evaporation	FAO56	FAO56	A-pan
Drainage	Empirical fn(K_{SAT}, TAW)	Empirical fn(SWD, D_f)	fn(θ_{SAT}, θ)
Upflow	If groundwater table is present	-	fn(θ_{SAT}, θ)
Soil evaporation	2-stage stage 1-energy limited fn(CC, K_{ex}, ET_O) stage 2-water limited fn(CC, K_{ex}, ET_O, K_r)	2-stage stage 1-energy limited fn(PE, PET) stage 2-water limited fn(PE, PET, θ, θ_{PWP})	2-stage stage 1-energy limited fn(α_S) stage 2-water limited fn(α_S, t_d)
Runoff	CN method fn(P, c, CN)	CN method fn(P, c, CN)	Modified SCS method fn(P, c, θ_{SAT} , θ)

Refer to the list of symbols at the beginning of the document for an explanation of the symbols.

I3 RUNOFF GENERATION

Both AquaCrop and SWB calculate runoff using the curve number approach as developed by the USDA as follows:

$$R = (P + I - cS)^2 / [P + I + S(1 - c)] \quad \text{Equation 22}$$

where

R = runoff in mm

P = precipitation in mm

I = irrigation in mm

c = coefficient of initial abstraction

I_a = infiltrated water in mm

= $c \cdot S$

S = potential maximum soil moisture retention in mm

= (1000/*CN*) - 10 (in *AquaCrop* and *SWB*)

CN = curve number

The coefficient of initial abstraction (c) is set to 0.2 in SWB and AquaCrop Version 4 or lower. Runoff is assumed to be zero if $P + I \leq 0.2S$. From Version 5 onwards (FAO, 2015), c was reduced in AquaCrop from 0.20 to 0.05 (i.e. $I_a = 0.05 \cdot S$). Furthermore, *CN* can now be increased or decreased by a set percentage value in order to account for changing field management or cropping conditions. The *CN* values can be derived for four hydrological soil groups (USDA, 2004) using the saturated hydraulic conductivity (K_{SAT}) of the topsoil (cf. Table 10.17 in Section 10.2.4).

In ACRU, although the above equation is also used to calculate storm flow, S is not computed from *CN*. Instead, ACRU calculates the soil water deficit (S) as the difference between water retention at saturation and the actual soil water content ($\theta_{SAT} - \theta$) prior to a rainfall event, but after total evaporation for the day has been abstracted. S is calculated for the critical storm flow response depth of the soil (*SMDDEP*). If *QFRESP* is less than 1, only that fraction of storm flow exits the catchment on the same day and the remainder is added to the storm flow for the following day. In addition, the coefficient of initial abstraction (*COIAM*) is a monthly input (Smithers et al., 2018).

I4 CROP GROWTH AND YIELD

The main differences in the calculation of crop growth and yield between the three selected models is shown in the table below.

Table I.3: Main differences in the crop growth engine used by each simulation model

Process	AquaCrop	SWB	ACRU
Growth engine	Water-driven	Radiation-driven	Water-driven
Canopy formation	CC	LAI	
LAI		fn(SLA, CDM, PART)	
Biomass accumulation	fn(WP, Tr, ET_O)	Tr or R_S limited fn(E_c, LAI, R_S)	
Yield formation	fn(B, HI)	fn(SDM, $Trans_g$)	fn(Tr, Tr_{max}, ET_a)

Process	AquaCrop	SWB	ACRU
Transpiration	fn(K_S, CC, K_{CB})	fn(K_{PAR}, LAI, Tr_{max}, Ψ_{LW}, θ, RD) fn(θ - θ_{PWP})	
Phenology	Thermal	Thermal	
Partitioning	Modified HI	root, leaf, stem	
Root growth		fn(RGR, RDM)	

Refer to the list of symbols at the beginning of the document.

I5 THERMAL TIME

AquaCrop

The GDD is calculated using a method described by McMaster and Wilhelm (1997), with the exception that no adjustment is made of the minimum temperature when it drops below the base temperature. This is believed to better represent the damaging or inhibitory effects of cold on plant processes. In AquaCrop, this method of calculating GDD is known as “Method 3”, which is detailed next.

The maximum air temperature (T_{max}) is adjusted to fall in the range T_{bse} to T_{upp}.

if $T_{max} \geq T_{upp}$ then $T_{max} = T_{upp}$

if $T_{max} < T_{bse}$ then $T_{max} = T_{bse}$

The minimum air temperature (T_{min}) is adjusted if above T_{upp}.

if $T_{min} \geq T_{upp}$ then $T_{min} = T_{upp}$

The minimum air temperature (T_{min}) is adjusted if below T_{bse} (not done in AquaCrop).

if $T_{min} < T_{bse}$ then $T_{min} = T_{bse}$

The average temperature (T_{ave}) is then calculated from T_{max} and T_{min}.

$T_{ave} = (T_{max} + T_{min})/2$

The average temperature (T_{ave}) is adjusted if below T_{bse} (to avoid negative GDDs).

if $T_{ave} < T_{bse}$ then $T_{ave} = T_{bse}$

The GDD is calculated as the difference between the average (T_{ave}) and base (T_{bse}) temperatures.

$GDD = T_{ave} - T_{bse}$

SWB

In *SWB*, no adjustments are made to T_{max} and T_{min} before the calculation to T_{ave}. However, T_{ave} is adjusted to fall in the range T_{bse} to T_{upp}.

The average temperature (T_{ave}) is calculated from T_{max} and T_{min}.

$T_{ave} = (T_{max} + T_{min})/2$

The average temperature (T_{ave}) is adjusted if below T_{bse} (to avoid negative GDDs).

if $T_{ave} < T_{bse}$ then $T_{ave} = T_{bse}$

The average air temperature (T_{ave}) is adjusted if above T_{upp}.

if $T_{ave} \geq T_{upp}$ then $T_{ave} = T_{upp}$

The GDD is calculated as the difference between the average (T_{ave}) and base (T_{bse}) temperatures.

$GDD = T_{avg} - T_{bse}$

APPENDIX J

Rain Gauge 0150620 W had a daily rainfall event of 900.5 mm on 22 February 1997. The three closest weather stations, 0150621 A, 0150257 W and 0150779 W, recorded 0, 3 and 4 mm, respectively. Based on this, the extreme rainfall value of 900.5 mm was adjusted to 0.0 mm. In addition, the FEWS ARC 2.0 remotely sensed dataset estimated very little rain over South Africa that day and zero rainfall at nearby rain gauges. Unfortunately, this extreme event influenced the rainfall patching technique used by Lynch (2004) and missing data on 22 February 1997 was patched with values of 900.5, 778.9 and 711.4 mm for gauges 0151080 W, 0150595 W and 0150288 W, respectively.

Similarly, Rain Gauge 0304446 W had a daily rainfall event of 585.5 mm on 14 December 1980. The closest gauge reported 84.0 mm and another nearby gauge showed 85.6 mm, if a one-day phase error is assumed. Hence, the large value of 585.5 was changed to 85.5 mm, which affects quinary subcatchments 5119, 5120 and 5121. This gauge was also used to patch several other gauges, but none of these gauges were used as drivers. Thus, it was not necessary to adjust any other rainfall values.

Rain Gauge 0305308 W, situated at Kwambonambi (Zululand coast in KwaZulu-Natal), which drives quinary subcatchments 5113, 5114 and 5115, recorded daily rainfall totals of 18.5, 208.0, 141.5, 525.0 and 6.8 mm from 25-29 September 1987. For neighbouring stations mostly located between Kwambonambi and Richards Bay, the September 1987 flood produced a number of record rainfall events as shown in Table J.1. Based on the 449 mm recorded at Rain Gauge 0339538 W, the value of 525.0 does not appear erroneous. However, the 12 mm recorded on 30 September 1987 for Rain Gauge 0305306 A is likely a phase error. These gauges were also used to patch several other gauges, with values ranging from 158.8 to 576.9 mm.

Table J.1: Record rainfall events captured by rain gauges situated along the KwaZulu-Natal coast and in the KwaZulu-Natal Midlands

Gauge	September 1987 flood (day)					
	25	26	27	28	29	30
0305308 W	18.5	208.0	141.5	525.0	6.8	0.0
0305306 A	0.0	16.0	192.0	164.5	0.0	12.0
0305128 S	18.2	103.0	260.2	300.0	71.8	0.0
0305211 S	0.0	90.0	95.0	425.0	10.0	0.0
0305037 W	0.0	70.0	125.0	260.0	12.5	0.0
0339538 W	17.0	115.0	119.0	449.0	12.0	0.0
0239133 W	0.0	18.0	225.0	435.0	10.0	0.0

Rain Gauge 0214485 W had a daily rainfall event of 520.7 mm on 23 February 1953. The three nearby gauges had no data for that day and were patched with values of 13.8, 0.0 and 0.0 mm. Neither this gauge nor the three nearby gauges had any rainfall in the latter half of February 1953. Based on this, the decision was made to adjust this value of 520.7 to 0.0 mm, which affected quinary subcatchments 2554 to 2562.

As shown in Table J.1, the high rainfall events of 449.0 and 435.0 mm were associated with the September 1987 flood, which mainly affected the northern coastal region of KwaZulu-Natal. Hence, these values were not downward adjusted. The 440.0 mm event appears in the historical record for Rain Gauge 0022148 W. However, the two neighbouring stations recorded far less rainfall, as indicated in Table J.2. Neighbouring gauges with patched data had values ranging from 22.3 to 130.3 mm on 23 June 1991. Hence, the decision was made to change the value from 440 to 44 mm, which affected quinary subcatchments 2626 to 2628.

Table J.2: Rainfall events obtained for three nearby rain gauges situated near Robertsvlei (Western Cape)

Gauge	June 1991 (day)			
	21	22	23	24
0022148 W	25.8	50.2	440.0	50.1
0022174 W	21.0	6.5	87.5	46.0
0022113 W	22.0	10.0	84.0	44.5

The next highest value of 438.5 mm was measured on 4 February 1993 by Rain Gauge 0723155 W (Goedehoop, Limpopo), which is used as a driver station for quinary subcatchments 0394-0396. Six neighbouring stations reported observed rainfall totals between 200 and 300 mm. Hence, there was no strong evidence to adjust this total.

Rain Gauge 0239133 W recorded a total of 435 mm on 28 January 1984. Most of the neighbouring stations recorded rainfall totals above 200 mm on Day 28. This major flood event was caused by cyclone Demoina, which formed on 16 January 1984. The gauges listed in Table J.3 were used to patch other stations, with values ranging from 163 to 435 mm. Again, there was no strong evidence to adjust this total.

Table J.3: Rainfall events obtained for three nearby rain gauges situated in KwaZulu-Natal

Gauge	January 1984 (day)			
	26	27	28	29
0239133 W	18.0	225.0	435.0	10.5
0239225 A	46.0	101.0	252.2	24.5
0239097 A	43.3	108.5	243.7	17.4
0239184 A	34.0	65.0	150.0	16.0
0239518 A	43.6	65.4	212.3	6.8
0239472 W	0.0	135.0	257.0	22.0
0239585 A	40.3	106.5	247.0	11.1
0238636 W	43.5	88.0	194.5	15.0
0239585 W	40.3	106.5	247.0	11.1
0239266 A	58.8	119.0	216.0	22.0
0238682 A	47.0	77.0	195.0	28.0

On 12 May 1971, a total of 432 mm was recorded by Rain Gauge 0339538 W, which is used to drive quinary subcatchments 5194-5196, as well as quinary subcatchments 5197-5199. Nearby gauges recorded totals ranging from 190.9 to 400 mm. Similarly, Rain Gauge 0305308 W (quinary subcatchments 5113-5115) experienced a daily rainfall total of 415.5 mm on the same day, while the nearest gauge (Rain Gauge 0305336 W) measured 400 mm and another gauge (Rain Gauge 0305043 W) reported 391.5 mm. Similarly, patched rainfall from surrounding gauges ranged from 181.4 to 398.2 mm. For quinary subcatchments 5087-5088 and 5116-5118, Rain Gauge 0272121 W had a daily rainfall value of 407.2 mm on 12 May 1971, with values of 125 to 531 mm from neighbouring statins. These three extreme values were not altered.

A total of 420.0 mm was measured on 20 August 1978 by Rain Gauge 0029624 W, which drives quinary subcatchments 3238-3240, as well as quinary subcatchments 3322-3324. The nearest Rain Gauge (0029683 W) recorded 364.3 mm on this day; hence, the value of 420 mm was not adjusted. Cyclone Demonia was responsible for another total of 420 mm recorded by this gauge on 31 January 1984. Two gauges near the St. Lucia Estuary recorded 497 and 542 mm, the latter presenting one of the highest single rainfall events ever recorded in South Africa's history.

The value of 425.5 mm on 30 January 1984 was measured by Rain Gauge 0337431 W, which drives quinary subcatchments 5143-5145 and 5164-5166. This event was also associated with Cyclone Demoina, with neighbouring gauges recording between 200 and 315 mm on the same day. Patched values for three other nearby stations ranged from 105 to 344 mm. With reference to DWA report TR122, the values at this gauge seem reasonable and also correlate well with the values reported in TR122 at Rain Gauge F7 (Langgewacht). Once again, this rainfall total was deemed reasonable.

APPENDIX K

A distinction is made between inputs (Table K.1) and parameters (Table K.2) as required by the AquaCrop model. The parameters listed in Table K.2 are generally representative of legume crops. Specific parameters may vary from crop to crop.

Table K.1: Inputs required by the AquaCrop model

Inputs	Comments
Weather data (daily): • Rainfall (mm) • T_{max}, T_{min} (°C) • ET_O (mm)	Needs solar radiation (MJ m^{-2} d^{-1}), wind speed (m s^{-1}) as well as RH_{max} and RH_{min} (%) to generate reference crop evaporation (ET_O)
Soil chemical properties: • Percentage nitrogen • Percentage phosphorus • Percentage potassium • Organic matter content	Data derived from soil analysis undertaken by the Soil Analytical Service Laboratory at Cedara
Soil physical properties: • Rooting depth (m) • Soil textural class • Bulk density (g cm^{-3})	Soil textural analysis obtained from soil samples submitted to the Soil Analytical Service Laboratory at Cedara
Soil water content values: • Saturation (SAT as a volume percentage) • Field capacity (FC as a volume percentage) • Permanent wilting point (PWP as a volume percentage) • Total available water (TAW as a volume percentage) • Saturated hydraulic conductivity (K_{SAT} in mm d^{-1})	Values for these parameters are determined in the Soil Water Laboratory at the University of KwaZulu-Natal or using the SPAW model
Crop-specific inputs: • Planting date • Planting density	Determined at time of planting

Table K.2: Parameters required by the AquaCrop model for legume crops

Parameter	Comments
Base temperature (T_{bse} in °C)	From the literature
Cut-off temperature (T_{upp} in °C)	From the literature
Time to emergence (GDD)	Observed from field trials
Seedling leaf area (cm^2)	From field observations
Initial canopy cover (CC_o in percentage)	AquaCrop requires observed seedling leaf area and plant density to compute CC_O. For details on algorithms used, refer to Raes et al. (2009)
Maximum canopy cover (CC_X in percentage)	Observations of LAI are converted to canopy cover as described by Mabhaudhi et al. (2014)
Time to CC_X (GDD)	Observed from field trial as time taken from planting to achieve maximum LAI
Canopy growth coefficient (CGC in percentage GDD d^{-1})	Calculated using the parameters of CC_O, CC_X and time to CC_X. For details on algorithms used, refer to Raes et al. (2009)
Canopy declining coefficient (CDC in percentage GDD d^{-1})	Calculated from time to reach canopy senescence and maturity. For details on algorithms used (see Raes et al., 2009).
Minimum rooting depth (Zr_{min} in m)	From field observations
Maximum rooting depth (Zr_{max} in m)	From field observations
Time to achieving Zr_{max} (GDD)	From field observations
Shape factor for root expansion	This is a model-derived parameter. For details on algorithms used (see Raes et al., 2009)
Water extraction pattern	From field observations
Time to flowering (GDD)	Time taken from planting to when at least 50% of the plants have started to flower. For detailed definitions, refer to Mabhaudhi and Modi (2013)
Start of yield (pod) formation (GDD)	Observed as the time taken from planting to when at least 50% of the plants have started to form pods. For detailed definitions, refer to Mabhaudhi and Modi (2013)
Duration of flowering (GDD)	Observed as the time from when flowering started to the time when flowering stopped. For detailed definitions, refer to Mabhaudhi and Modi (2013) and Mabhaudhi et al. (2014)
Length of Harvest Index build-up (GDD)	Defined as the time from when yield formation started, up to maturity (cf. Raes et al., 2009; Steduto et al., 2009)
Time to canopy senescence (GDD)	Observed as the time taken from planting to when at least 50% of the plants have started to senesce. For definitions of senescence, refer to Mabhaudhi and Modi (2013)
Maturity (GDD)	Observed as the time taken from planting to when at least 50% of the plants have reached harvest maturity. For detailed definitions of maturity, refer to Mabhaudhi and Modi (2013)
Upper limit of soil water depletion factor canopy expansion (p-leaf)	Stress factor derived using the AquaCrop model. For details on algorithms used, refer to Raes et al. (2009)
Lower limit of soil water depletion factor canopy expansion (p-leaf)	As above
Soil water depletion for stomatal control (p-stomatal)	As above
Soil water depletion for canopy senescence (p-senescence)	As above
Water stress during flowering (p-upper)	As above
Shape factor for water stress: leaf expansion	As above
Shape factor for water stress: stomatal control	As above
Shape factor for water stress: canopy senescence	As above
Biomass (B in kg)	Cumulative biomass measured by destructive sampling in-field. Final biomass determined at time of harvest

Parameter	Comments
Yield (Y in kg) • Pod yield • Seed yield	Determined as economic yield measured at time of harvest
Water productivity (WP in kg m^{-3})	From experiments conducted under well-controlled conditions (not done in this study)
Reference Harvest Index (HI_O in percentage)	Computed using measurements of Y and B at the time of harvest
Positive effect of HI as a result of limited growth in vegetative period	Requires observations from water-stressed pot trial or field trials with deficit irrigation (not done in this study)
Positive effect of HI as a result of water stress affecting leaf expansion	As above
Negative effect on HI as a result of water stress inducing stomatal closure	As above

Table K.3: Difference in crop parameters for soybean from Version 4 (Raes et al., 2012b) to Version 6 of AquaCrop (Raes et al., 2017)

No.	Parameter	Version 6	Version 4
9	Base temperature for no crop development (°C)		5
10	Cut-off temperature for no crop development (°C)		30
11	Crop cycle length (GDD)		2,700
	Soil water depletion factors for:		
12	Canopy expansion (upper threshold)		0.15
13	Canopy expansion (lower threshold)		0.65
15	Stomatal control	0.60	0.50
17	Canopy senescence		0.70
	Shape factor for:		
14	Water stress coefficient for canopy expansion		3
16	Water stress coefficient for stomatal control		3
40	Describing root zone expansion		15
	Shape factor for response of:		
23	Canopy expansion to soil fertility stress		25
24	Maximum canopy cover to soil fertility stress		25
25	Crop water productivity to soil fertility stress		25
26	Decline of canopy cover to soil fertility stress		25
36	Crop transpiration coefficient (K_{CB})		1.10
38	Minimum effective rooting depth (m)		0.30
39	Maximum effective rooting depth (m)		2.00
	Maximum root water extraction in:		
41	Top quarter of root zone	0.048	0.012
42	Bottom quarter of root zone	0.012	0.003
	Canopy growth coefficient:		
47	Fraction per calendar day		0.104250
76	Fraction per growing degree-day		0.005000
	Canopy decline coefficient:		
52	Fraction per calendar day		0.027780
77	Fraction per growing degree-day		0.001500
44	Seedling leaf area (cm^2)		5.00
51	Maximum canopy cover (CC_X)		0.98
	Calendar days from planting to:		
53	Emergence		10
54	Maximum rooting depth		93
55	Start of senescence		106
56	Maturity (length of crop cycle)		133
57	Flowering		72
	Growing degree-days from planting to:		
70	Emergence		200
71	Maximum rooting depth		1,934
72	Start of senescence		2,200
73	Maturity (length of crop cycle)		2,700
74	Flowering		1,500
	Length of the flowering stage:		
58	Calendar days		30
75	Growing degree-days		600
	Building up of Harvest Index		
61	Starting at flowering (days)		60
78	During yield formation (GDD)		1,180
62	Normalised water productivity WP* (g m^{-2})		15
63	WP* during yield formation (as percentage of WP*)		60
65	Reference Harvest Index (percentage)		40
	Possible increase (in percentage) of Harvest Index due to:		
66	Water stress before flowering		3

Table K.4: Crop parameters used for soybean (Maturity Group I cultivar) grown at Rimski Sancevi, Serbia (Tovjannin et al., 2019), plus default values from the original parameter file (Raes et al., 2012b; Raes et al., 2017)

No.	Parameter	Tovjannin et al. (2019)	Default
9	Base temperature for no crop development (°C)	8	5
10	Cut-off temperature for no crop development (°C)		30
11	Crop cycle length (GDD)		2,700
	Soil water depletion factors for:		
12	Canopy expansion (upper threshold)		0.15
13	Canopy expansion (lower threshold)		0.65
15	Stomatal control		0.50
17	Canopy senescence		0.70
	Shape factor for:		
14	Water stress coefficient for canopy expansion		3
16	Water stress coefficient for stomatal control		3
40	Describing root zone expansion		15
	Shape factor for response of:		
23	Canopy expansion to soil fertility stress		25
24	Maximum canopy cover to soil fertility stress		25
25	Crop water productivity to soil fertility stress		25
26	Decline of canopy cover to soil fertility stress		25
36	Crop transpiration coefficient (K_{CB})		1.10
38	Minimum effective rooting depth (m)		0.30
39	Maximum effective rooting depth (m)		2.00
	Maximum root water extraction in:		
41	Top quarter of root zone		0.012
42	Bottom quarter of root zone		0.003
	Canopy growth coefficient:		
47	Fraction per calendar day	0.102000	0.104250
76	Fraction per growing degree-day		0.005000
	Canopy decline coefficient:		
52	Fraction per calendar day	0.029000	0.027780
77	Fraction per growing degree-day		0.001500
44	Seedling leaf area (cm^2)		5.00
51	Maximum canopy cover (CC_X)	0.96	0.98
	Calendar days from planting to:		
53	Emergence	15	10
54	Maximum rooting depth	98	93
55	Start of senescence	109	106
56	Maturity (length of crop cycle)	135	133
57	Flowering	78	72
	Growing degree-days from planting to:		
70	Emergence		200
71	Maximum rooting depth		1,934
72	Start of senescence		2,200
73	Maturity (length of crop cycle)		2,700
74	Flowering		1,500
	Length of the flowering stage:		
58	Calendar days	13	30
75	Growing degree-days		600
	Building up of Harvest Index		
61	Starting at flowering (days)	59	60
78	During yield formation (GDD)		1,180
62	Normalised water productivity WP* (g m^{-2})	19	15
63	WP* during yield formation (as a percentage of WP*)		60
65	Reference Harvest Index (percentage)	35	40
	Possible increase (percentage) of harvest index due to:		
66	Water stress before flowering		3

Table K.5: Crop parameters used for soybean (cultivar Zhonghuang No. 13) grown at Daxing, North China Plain (Paredes et al., 2015), plus default values from the original parameter file (Raes et al., 2012b; Raes et al., 2017)

No.	Parameter	Paredes et al. (2015)	Default
9	Base temperature for no crop development (°C)		5
10	Cut-off temperature for no crop development (°C)		30
11	Crop cycle length (GDD)		2,700
	Soil water depletion factors for:		
12	Canopy expansion (upper threshold)		0.15
13	Canopy expansion (lower threshold)		0.65
15	Stomatal control		0.50
17	Canopy senescence		0.70
	Shape factor for:		
14	Water stress coefficient for canopy expansion		3
16	Water stress coefficient for stomatal control		3
40	Describing root zone expansion		15
	Shape factor for response of:		
23	Canopy expansion to soil fertility stress		25
24	Maximum canopy cover to soil fertility stress		25
25	Crop water productivity to soil fertility stress		25
26	Decline of canopy cover to soil fertility stress		25
36	Crop transpiration coefficient (K_{CB})	1.12	1.10
38	Minimum effective rooting depth (m)		0.30
39	Maximum effective rooting depth (m)		2.00
	Maximum root water extraction in:		
41	Top quarter of root zone		0.012
42	Bottom quarter of root zone		0.003
	Canopy growth coefficient:		
47	Fraction per calendar day		0.104250
76	Fraction per growing degree-day	0.007100	0.005000
	Canopy decline coefficient:		
52	Fraction per calendar day		0.027780
77	Fraction per growing degree-day	0.001040	0.001500
44	Seedling leaf area (cm^2)		5.00
51	Maximum canopy cover (CC_X)		0.98
	Calendar days from planting to:		
53	Emergence		10
54	Maximum rooting depth		93
55	Start of senescence		106
56	Maturity (length of crop cycle)		133
57	Flowering		72
	Growing degree-days from planting to:		
70	Emergence		200
71	Maximum rooting depth		1,934
72	Start of senescence		2,200
73	Maturity (length of crop cycle)		2,700
74	Flowering		1,500
	Length of the flowering stage:		
58	Calendar days		30
75	Growing degree-days		600
	Building up of Harvest Index		
61	Starting at flowering (days)		60
78	During yield formation (GDD)		1,180
62	Normalised water productivity WP* (g m^{-2})	17	15
63	WP* during yield formation (as a percentage of WP*)		60
65	Reference harvest index (%)	38	40
	Possible increase (%) of harvest index due to:		
66	Water stress before flowering		3

Table K.6: Crop parameters used for soybean (cultivar BRS 284) grown in southern Brazil (Battisti et al., 2017), plus default values from the original parameter file (Raes et al., 2012b)

No.	Parameter	Battisti et al. (2017)	Default
9	Base temperature for no crop development (°C)	10	5
10	Cut-off temperature for no crop development (°C)	35	30
11	Crop cycle length (GDD)		2,700
	Soil water depletion factors for:		
12	Canopy expansion (upper threshold)		0.15
13	Canopy expansion (lower threshold)		0.65
15	Stomatal control		0.50
17	Canopy senescence		0.70
	Shape factor for:		
14	Water stress coefficient for canopy expansion		3
16	Water stress coefficient for stomatal control		3
40	Describing root zone expansion	20	15
	Shape factor for response of:		
23	Canopy expansion to soil fertility stress		25
24	Maximum canopy cover to soil fertility stress		25
25	Crop water productivity to soil fertility stress		25
26	Decline of canopy cover to soil fertility stress		25
36	Crop transpiration coefficient (K_{CB})	1.15	1.10
38	Minimum effective rooting depth (m)		0.30
39	Maximum effective rooting depth (m)	1.10	2.00
	Maximum root water extraction in:		
41	Top quarter of root zone	0.024	0.012
42	Bottom quarter of root zone	0.004	0.003
	Canopy growth coefficient:		
47	Fraction per calendar day		0.104250
76	Fraction per growing degree-day	0.010000	0.005000
	Canopy decline coefficient:		
52	Fraction per calendar day		0.027780
77	Fraction per growing degree-day	0.014200	0.001500
44	Seedling leaf area (cm^2)		5.00
51	Maximum canopy cover (CC_X)		0.98
	Calendar days from planting to:		
53	Emergence		10
54	Maximum rooting depth		93
55	Start of senescence		106
56	Maturity (length of crop cycle)		133
57	Flowering		72
	Growing degree-days from planting to:		
70	Emergence	85	200
71	Maximum rooting depth	998	1,934
72	Start of senescence	1,580	2,200
73	Maturity (length of crop cycle)	1,800	2,700
74	Flowering	570	1,500
	Length of the flowering stage:		
58	Calendar days		30
75	Growing degree-days	356	600
	Building up of Harvest Index		
61	Starting at flowering (days)		60
78	During yield formation (GDD)	1,225	1,180
62	Normalised water productivity WP* (g m^{-2})		15
63	WP* during yield formation (as a percentage of WP*)		60
65	Reference Harvest Index (percentage)	45	40
	Possible increase (percentage) of Harvest Index due to:		
66	Water stress before flowering		3

Table K.7: Crop parameters used for soybean (cultivar TMG 1288) grown in Brazil (Silva et al., 2017), plus default values from the original parameter file (Raes et al., 2012b)

No.	Parameter	Silva et al. (2017)	Default
9	Base temperature for no crop development (°C)		5
10	Cut-off temperature for no crop development (°C)		30
11	Crop cycle length (GDD)		2,700
	Soil water depletion factors for:		
12	Canopy expansion (upper threshold)	0.30	0.15
13	Canopy expansion (lower threshold)	0.65	0.65
15	Stomatal control	0.70	0.50
17	Canopy senescence	0.35	0.70
	Shape factor for:		
14	Water stress coefficient for canopy expansion		3
16	Water stress coefficient for stomatal control		3
40	Describing root zone expansion		15
	Shape factor for response of:		
23	Canopy expansion to soil fertility stress		25
24	Maximum canopy cover to soil fertility stress		25
25	Crop water productivity to soil fertility stress		25
26	Decline of canopy cover to soil fertility stress		25
36	Crop transpiration coefficient (K_{CB})		1.10
38	Minimum effective rooting depth (m)		0.30
39	Maximum effective rooting depth (m)	0.60	2.00
	Maximum root water extraction in:		
41	Top quarter of root zone		0.012
42	Bottom quarter of root zone		0.003
	Canopy growth coefficient:		
47	Fraction per calendar day	0.111000	0.104250
76	Fraction per growing degree-day		0.005000
	Canopy decline coefficient:		
52	Fraction per calendar day	0.031000	0.027780
77	Fraction per growing degree-day		0.001500
44	Seedling leaf area (cm^2)		5.00
51	Maximum canopy cover (CC_X)	0.99	0.98
	Calendar days from planting to:		
53	Emergence		10
54	Maximum rooting depth	65	93
55	Start of senescence	102	106
56	Maturity (length of crop cycle)	115	133
57	Flowering	44	72
	Growing degree-days from planting to:		
70	Emergence		200
71	Maximum rooting depth		1,934
72	Start of senescence		2,200
73	Maturity (length of crop cycle)		2,700
74	Flowering		1,500
	Length of the flowering stage:		
58	Calendar days	61	30
75	Growing degree-days		600
	Building up of Harvest Index		
61	Starting at flowering (days)		60
78	During yield formation (GDD)		1,180
62	Normalised water productivity WP* (g m^{-2})	15.5	15
63	WP* during yield formation (as a percentage of WP*)	71	60
65	Reference Harvest Index (percentage)		40
	Possible increase (percentage) of Harvest Index due to:		
66	Water stress before flowering		3

Table K.8: Crop parameters used for soybean (cultivar TGX 1448 2E) grown at Ile-Ife, Nigeria (Adeboye et al., 2017), plus default values from the original parameter file (Raes et al., 2012b)

No.	Parameter	Adeboye et al. (2017)	Default
9	Base temperature for no crop development (°C)		5
10	Cut-off temperature for no crop development (°C)		30
11	Crop cycle length (GDD)		2,700
	Soil water depletion factors for:		
12	Canopy expansion (upper threshold)	0.14	0.15
13	Canopy expansion (lower threshold)		0.65
15	Stomatal control	0.58	0.50
17	Canopy senescence		0.70
	Shape factor for:		
14	Water stress coefficient for canopy expansion		3
16	Water stress coefficient for stomatal control		3
40	Describing root zone expansion		15
	Shape factor for response of:		
23	Canopy expansion to soil fertility stress		25
24	Maximum canopy cover to soil fertility stress		25
25	Crop water productivity to soil fertility stress		25
26	Decline of canopy cover to soil fertility stress		25
36	Crop transpiration coefficient (K_{CB})	1.15	1.10
38	Minimum effective rooting depth (m)	0.30	0.30
39	Maximum effective rooting depth (m)	0.80	2.00
	Maximum root water extraction in:		
41	Top quarter of root zone		0.012
42	Bottom quarter of root zone		0.003
	Canopy growth coefficient:		
47	Fraction per calendar day	0.132000	0.104250
76	Fraction per growing degree-day		0.005000
	Canopy decline coefficient:		
52	Fraction per calendar day	0.029100	0.027780
77	Fraction per growing degree-day		0.001500
44	Seedling leaf area (cm^2)		5.00
51	Maximum canopy cover (CC_X)	0.96	0.98
	Calendar days from planting to:		
53	Emergence	10	10
54	Maximum rooting depth	71	93
55	Start of senescence	97	106
56	Maturity (length of crop cycle)	112	133
57	Flowering	43	72
	Growing degree-days from planting to:		
70	Emergence		200
71	Maximum rooting depth		1,934
72	Start of senescence		2,200
73	Maturity (length of crop cycle)		2,700
74	Flowering		1,500
	Length of the flowering stage:		
58	Calendar days	12	30
75	Growing degree-days		600
	Building up of Harvest Index		
61	Starting at flowering (days)	69	60
78	During yield formation (GDD)		1,180
62	Normalised water productivity WP* ($g\ m^{-2}$)	16.7	15
63	WP* during yield formation (as a percentage of WP*)		60
65	Reference Harvest Index (percentage)	**62**	40
	Possible increase (percentage) of Harvest Index due to:		
66	Water stress before flowering		3

Table K.9: Crop parameters used for soybean (cultivar PAN1666R) grown at Baynesfield in 2012/13 (Mbangiwa et al., 2019), plus default values from the original parameter file (Raes et al., 2012b)

No.	Parameter	PAN1666R (Baynesfield)	Default
9	Base temperature for no crop development (°C)		5
10	Cut-off temperature for no crop development (°C)		30
11	Crop cycle length (GDD)	1,881	2,700
	Soil water depletion factors for:		
12	Canopy expansion (upper threshold)		0.15
13	Canopy expansion (lower threshold)		0.65
15	Stomatal control		0.50
17	Canopy senescence		0.70
	Shape factor for:		
14	Water stress coefficient for canopy expansion		3
16	Water stress coefficient for stomatal control		3
40	Describing root zone expansion		15
	Shape factor for response of:		
23	Canopy expansion to soil fertility stress		25
24	Maximum canopy cover to soil fertility stress		25
25	Crop water productivity to soil fertility stress		25
26	Decline of canopy cover to soil fertility stress		25
36	Crop transpiration coefficient (K_{CB})		1.10
38	Minimum effective rooting depth (m)		0.30
39	Maximum effective rooting depth (m)		2.00
	Maximum root water extraction in:		
41	Top quarter of root zone		0.012
42	Bottom quarter of root zone		0.003
	Canopy growth coefficient:		
47	Fraction per calendar day	0.104970	0.104250
76	Fraction per growing degree-day		0.005000
	Canopy decline coefficient:		
52	Fraction per calendar day	0.001900	0.027780
77	Fraction per growing degree-day		0.001500
44	Seedling leaf area (cm^2)		5.00
51	Maximum canopy cover (CC_X)		0.98
	Calendar days from planting to:		
53	Emergence	9	10
54	Maximum rooting depth	92	93
55	Start of senescence	104	106
56	Maturity (length of crop cycle)	130	133
57	Flowering	71	72
	Growing degree-days from planting to:		
70	Emergence	112	200
71	Maximum rooting depth	951	1,934
72	Start of senescence	1,476	2,200
73	Maturity (length of crop cycle)	1,881	2,700
74	Flowering	934	1,500
	Length of the flowering stage:		
58	Calendar days	29	30
75	Growing degree-days	475	600
	Building up of Harvest Index		
61	Starting at flowering (days)	59	60
78	During yield formation (GDD)	787	1,180
62	Normalised water productivity WP* ($g\ m^{-2}$)		15
63	WP* during yield formation (as a percentage of WP*)		60
65	Reference Harvest Index (percentage)	45	40
	Possible increase (percentage) of Harvest Index due to:		
66	Water stress before flowering		3

Table K.10: Crop parameters used for soybean (cultivar LS6161R) grown at Swayimane in 2018/19 (Reddy, 2019), plus default values from the original parameter file (Raes et al., 2012b)

No.	Parameter	LS6161R (Swayimane)	Default
9	Base temperature for no crop development (°C)		5
10	Cut-off temperature for no crop development (°C)		30
11	Crop cycle length (GDD)	2,025	2,700
	Soil water depletion factors for:		
12	Canopy expansion (upper threshold)		0.15
13	Canopy expansion (lower threshold)		0.65
15	Stomatal control	0.60	0.50
17	Canopy senescence		0.70
	Shape factor for:		
14	Water stress coefficient for canopy expansion		3
16	Water stress coefficient for stomatal control		3
40	Describing root zone expansion		15
	Shape factor for response of:		
23	Canopy expansion to soil fertility stress		25
24	Maximum canopy cover to soil fertility stress		25
25	Crop water productivity to soil fertility stress		25
26	Decline of canopy cover to soil fertility stress		25
36	Crop transpiration coefficient (K_{CB})		1.10
38	Minimum effective rooting depth (m)		0.30
39	Maximum effective rooting depth (m)	0.62	2.00
	Maximum root water extraction in:		
41	Top quarter of root zone	0.048	0.012
42	Bottom quarter of root zone	0.012	0.003
	Canopy growth coefficient:		
47	Fraction per calendar day	0.074350	0.10425
76	Fraction per growing degree-day	0.004957	0.00500
	Canopy decline coefficient:		
52	Fraction per calendar day	0.006690	0.027780
77	Fraction per growing degree-day	0.000485	0.001500
44	Seedling leaf area (cm^2)		5.00
51	Maximum canopy cover (CC_X)	0.95	0.98
	Calendar days from planting to:		
53	Emergence	7	10
54	Maximum rooting depth	112	93
55	Start of senescence	130	106
56	Maturity (length of crop cycle)	135	133
57	Flowering	71	72
	Growing degree-days from planting to:		
70	Emergence	105	200
71	Maximum rooting depth	1,680	1,934
72	Start of senescence	1,950	2,200
73	Maturity (length of crop cycle)	2,025	2,700
74	Flowering	1,065	1,500
	Length of the flowering stage:		
58	Calendar days	17	30
75	Growing degree-days	255	600
	Building up of Harvest Index		
61	Starting at flowering (days)	63	60
78	During yield formation (GDD)	945	1,180
62	Normalised water productivity WP* ($g\ m^{-2}$)		15
63	WP* during yield formation (as a percentage of WP*)		60
65	Reference Harvest Index (percentage)		40
	Possible increase (percentage) of Harvest Index due to:		
66	Water stress before flowering		3

Table K.11: Crop parameters used for soybean (cultivar CAPG3) grown at Swayimane in 2018/19 (Reddy, 2019), plus default values from the original parameter file (Raes et al., 2012b)

No.	Parameter	CAPG3 (Swayimane)	Default
9	Base temperature for no crop development (°C)		5
10	Cut-off temperature for no crop development (°C)		30
11	Crop cycle length (GDD)	2,145	2,700
	Soil water depletion factors for:		
12	Canopy expansion (upper threshold)		0.15
13	Canopy expansion (lower threshold)		0.65
15	Stomatal control	0.60	0.50
17	Canopy senescence		0.70
	Shape factor for:		
14	Water stress coefficient for canopy expansion		3
16	Water stress coefficient for stomatal control		3
40	Describing root zone expansion		15
	Shape factor for response of:		
23	Canopy expansion to soil fertility stress		25
24	Maximum canopy cover to soil fertility stress		25
25	Crop water productivity to soil fertility stress		25
26	Decline of canopy cover to soil fertility stress		25
36	Crop transpiration coefficient (K_{CB})		1.10
38	Minimum effective rooting depth (m)		0.30
39	Maximum effective rooting depth (m)	0.62	2.00
	Maximum root water extraction in:		
41	Top quarter of root zone	0.048	0.012
42	Bottom quarter of root zone	0.012	0.003
	Canopy growth coefficient:		
47	Fraction per calendar day	0.080960	0.10425
76	Fraction per growing degree-day	0.005397	0.00500
	Canopy decline coefficient:		
52	Fraction per calendar day	0.029860	0.027780
77	Fraction per growing degree-day	0.001972	0.001500
44	Seedling leaf area (cm^2)		5.00
51	Maximum canopy cover (CC_X)	0.97	0.98
	Calendar days from planting to:		
53	Emergence	7	10
54	Maximum rooting depth	112	93
55	Start of senescence	135	106
56	Maturity (length of crop cycle)	143	133
57	Flowering	79	72
	Growing degree-days from planting to:		
70	Emergence	105	200
71	Maximum rooting depth	1,680	1,934
72	Start of senescence	2,025	2,200
73	Maturity (length of crop cycle)	2,145	2,700
74	Flowering	1,185	1,500
	Length of the flowering stage:		
58	Calendar days	16	30
75	Growing degree-days	240	600
	Building up of Harvest Index		
61	Starting at flowering (days)	64	60
78	During yield formation (GDD)	960	1,180
62	Normalised water productivity WP* ($g\ m^{-2}$)		15
63	WP* during yield formation (as a percentage of WP*)		60
65	Reference Harvest Index (percentage)		40
	Possible increase (percentage) of Harvest Index due to:		
66	Water stress before flowering		3

Table K.12: Difference in crop parameters for grain sorghum from Version 4 (Raes et al., 2012b) to Version 6 of AquaCrop (Raes et al., 2017)

No.	Parameter	Version 6	Version 4
9	Base temperature for no crop development (°C)		8
10	Cut-off temperature for no crop development (°C)		30
11	Crop cycle length (GDD)		1,760
	Soil water depletion factors for:		
12	Canopy expansion (upper threshold)		0.15
13	Canopy expansion (lower threshold)		0.70
15	Stomatal control	0.75	0.70
17	Canopy senescence		0.70
	Shape factor for:		
14	Water stress coefficient for canopy expansion		3
16	Water stress coefficient for stomatal control	3	6
40	Describing root zone expansion		13
	Shape factor for response of:		
23	Canopy expansion to soil fertility stress		25
24	Maximum canopy cover to soil fertility stress		25
25	Crop water productivity to soil fertility stress		25
26	Decline of canopy cover to soil fertility stress		25
36	Crop transpiration coefficient (K_{CB})		1.07
38	Minimum effective rooting depth (m)		0.30
39	Maximum effective rooting depth (m)		1.80
	Maximum root water extraction in:		
41	Top quarter of root zone	0.048	0.016
42	Bottom quarter of root zone	0.012	0.004
	Canopy growth coefficient:		
47	Fraction per calendar day		0.143260
76	Fraction per growing degree-day		0.012001
	Canopy decline coefficient:		
52	Fraction per calendar day		0.119000
77	Fraction per growing degree-day		0.009862
44	Seedling leaf area (cm^2)		3.00
51	Maximum canopy cover (CC_X)		0.90
	Calendar days from planting to:		
53	Emergence		11
54	Maximum rooting depth		132
55	Start of senescence		132
56	Maturity (length of crop cycle)		147
57	Flowering		87
	Growing degree-days from planting to:		
70	Emergence		136
71	Maximum rooting depth		1,583
72	Start of senescence		1,579
73	Maturity (length of crop cycle)		1,760
74	Flowering		1,041
	Length of the flowering stage:		
58	Calendar days		26
75	Growing degree-days		306
	Building up of Harvest Index		
61	Starting at flowering (days)		60
78	During yield formation (GDD)		719
62	Normalised water productivity WP* (g m^{-2})		33.7
63	WP* during yield formation (as a percentage of WP*)		100
65	Reference Harvest Index (percentage)		45
	Possible increase (percentage) of Harvest Index due to:		
66	Water stress before flowering		4

Table K.13: Crop parameters for grain sorghum (unknown cultivar) grown at Garden City, Kansas (Araya et al., 2016), plus default values from the original parameter file (Raes et al., 2012b; Raes et al., 2017)

No.	Parameter	Araya et al. (2016)	Default
9	Base temperature for no crop development (°C)		8
10	Cut-off temperature for no crop development (°C)		30
11	Crop cycle length (GDD)		1,760
	Soil water depletion factors for:		
12	Canopy expansion (upper threshold)	0.10	0.15
13	Canopy expansion (lower threshold)	0.45	0.70
15	Stomatal control	0.45	0.70
17	Canopy senescence	0.45	0.70
	Shape factor for:		
14	Water stress coefficient for canopy expansion		3
16	Water stress coefficient for stomatal control		6
40	Describing root zone expansion		13
	Shape factor for response of:		
23	Canopy expansion to soil fertility stress		25
24	Maximum canopy cover to soil fertility stress		25
25	Crop water productivity to soil fertility stress		25
26	Decline of canopy cover to soil fertility stress		25
36	Crop transpiration coefficient (K_{CB})	1.02	1.07
38	Minimum effective rooting depth (m)		0.30
39	Maximum effective rooting depth (m)	2.00	1.80
	Maximum root water extraction in:		
41	Top quarter of root zone		0.016
42	Bottom quarter of root zone		0.004
	Canopy growth coefficient (CGC):		
47	Fraction per calendar day	0.110000	0.143260
76	Fraction per growing degree-day		0.012001
	Canopy decline coefficient (CDC):		
52	Fraction per calendar day	0.128000	0.119000
77	Fraction per growing degree-day		0.009862
44	Seedling leaf area (cm^2)		3.00
51	Maximum canopy cover (CC_X)	0.83	0.90
	Calendar days from planting to:		
53	Emergence	15	11
54	Maximum rooting depth	93	132
55	Start of senescence	100	132
56	Maturity (length of crop cycle)	120	147
57	Flowering	73	87
	Growing degree-days from planting to:		
70	Emergence		136
71	Maximum rooting depth		1,583
72	Start of senescence		1,579
73	Maturity (length of crop cycle)		1,760
74	Flowering		1,041
	Length of the flowering stage:		
58	Calendar days	16	26
75	Growing degree-days		306
	Building up of Harvest Index		
61	Starting at flowering (days)		60
78	During yield formation (GDD)		719
62	Normalised water productivity WP* ($g\ m^{-2}$)	30.0	33.7
63	WP* during yield formation (as a percentage of WP*)		100
65	Reference Harvest Index (percentage)	46	45
	Possible increase (percentage) of Harvest Index due to:		
66	Water stress before flowering		4

Table K.14: Crop parameters for grain sorghum (cultivar PAN8816) grown at Ukulinga (Hadebe et al., 2017b), plus default values from the original parameter file (Raes et al., 2012b; 2017)

No.	Parameter	Hadebe et al. (2017b)	Default
9	Base temperature for no crop development (°C)		8
10	Cut-off temperature for no crop development (°C)		30
11	Crop cycle length (GDD)	1,747	1,760
	Soil water depletion factors for:		
12	Canopy expansion (upper threshold)	0.25	0.15
13	Canopy expansion (lower threshold)	0.60	0.70
15	Stomatal control		0.70
17	Canopy senescence		0.70
	Shape factor for:		
14	Water stress coefficient for canopy expansion		3
16	Water stress coefficient for stomatal control		6
40	Describing root zone expansion		13
	Shape factor for response of:		
23	Canopy expansion to soil fertility stress		25
24	Maximum canopy cover to soil fertility stress		25
25	Crop water productivity to soil fertility stress		25
26	Decline of canopy cover to soil fertility stress		25
36	Crop transpiration coefficient (K_{CB})		1.07
38	Minimum effective rooting depth (m)		0.30
39	Maximum effective rooting depth (m)	2.00	1.80
	Maximum root water extraction in:		
41	Top quarter of root zone	0.010	0.016
42	Bottom quarter of root zone	0.003	0.004
	Canopy growth coefficient:		
47	Fraction per calendar day	0.161140	0.143260
76	Fraction per growing degree-day	0.011258	0.012001
	Canopy decline coefficient:		
52	Fraction per calendar day	0.077420	0.119000
77	Fraction per growing degree-day	0.007178	0.009862
44	Seedling leaf area (cm^2)		3.00
51	Maximum canopy cover (CC_X)	0.89	0.90
	Calendar days from planting to:		
53	Emergence	14	11
54	Maximum rooting depth	97	132
55	Start of senescence	126	132
56	Maturity (length of crop cycle)	140	147
57	Flowering	70	87
	Growing degree-days from planting to:		
70	Emergence	203	136
71	Maximum rooting depth	1,320	1,583
72	Start of senescence	1,596	1,579
73	Maturity (length of crop cycle)	1,747	1,760
74	Flowering	999	1,041
	Length of the flowering stage:		
58	Calendar days	21	26
75	Growing degree-days	247	306
	Building up of Harvest Index		
61	Starting at flowering (days)	70	60
78	During yield formation (GDD)	748	719
62	Normalised water productivity WP* ($g\ m^{-2}$)		33.7
63	WP* during yield formation (as a percentage of WP*)		100
65	Reference Harvest Index (percentage)		45
	Possible increase (percentage) of Harvest Index due to:		
66	Water stress before flowering		4

Table K.15: Crop parameters for grain sorghum (cultivar PAN8816) grown at Swayimane in 2017/18 (Masanganise et al., 2019), plus default values from the original parameter file (Raes et al., 2012b; 2017)

No.	Parameter	PAN8816 (Swayimane)	Default
9	Base temperature for no crop development (°C)		8
10	Cut-off temperature for no crop development (°C)		30
11	Crop cycle length (GDD)	1,634	1,760
	Soil water depletion factors for:		
12	Canopy expansion (upper threshold)	0.10	0.15
13	Canopy expansion (lower threshold)	0.45	0.70
15	Stomatal control	0.45	0.70
17	Canopy senescence	0.45	0.70
	Shape factor for:		
14	Water stress coefficient for canopy expansion		3
16	Water stress coefficient for stomatal control		6
40	Describing root zone expansion		13
	Shape factor for response of:		
23	Canopy expansion to soil fertility stress		25
24	Maximum canopy cover to soil fertility stress		25
25	Crop water productivity to soil fertility stress		25
26	Decline of canopy cover to soil fertility stress		25
36	Crop transpiration coefficient (K_{CB})	1.02	1.07
38	Minimum effective rooting depth (m)		0.30
39	Maximum effective rooting depth (m)	0.60	1.80
	Maximum root water extraction in:		
41	Top quarter of root zone	0.048	0.016
42	Bottom quarter of root zone	0.012	0.004
	Canopy growth coefficient:		
47	Fraction per calendar day		0.143260
76	Fraction per growing degree-day	0.008760	0.012001
	Canopy decline coefficient:		
52	Fraction per calendar day		0.119000
77	Fraction per growing degree-day	0.016103	0.009862
44	Seedling leaf area (cm^2)		3.00
51	Maximum canopy cover (CC_X)	0.83	0.90
	Calendar days from planting to:		
53	Emergence		11
54	Maximum rooting depth		132
55	Start of senescence		132
56	Maturity (length of crop cycle)		147
57	Flowering		87
	Growing degree-days from planting to:		
70	Emergence	129	136
71	Maximum rooting depth	1,339	1,583
72	Start of senescence	1,544	1,579
73	Maturity (length of crop cycle)	1,634	1,760
74	Flowering	993	1,041
	Length of the flowering stage:		
58	Calendar days		26
75	Growing degree-days	149	306
	Building up of Harvest Index		
61	Starting at flowering (days)		60
78	During yield formation (GDD)	644	719
62	Normalised water productivity WP* (g m^{-2})	30.0	33.7
63	WP* during yield formation (as a percentage of WP*)		100
65	Reference Harvest Index (%)	46	45
	Possible increase (percentage) of Harvest Index due to:		
66	Water stress before flowering		4

Table K.16: Crop parameters for grain sorghum (cultivar PAN8906) grown at Swayimane in 2017/18 (Masanganise et al., 2019), plus default values from the original parameter file (Raes et al., 2012b; Raes et al., 2017)

No.	Parameter	PAN8906 (Swayimane)	Default
9	Base temperature for no crop development (°C)		8
10	Cut-off temperature for no crop development (°C)		30
11	Crop cycle length (GDD)	1,616	1,760
	Soil water depletion factors for:		
12	Canopy expansion (upper threshold)	0.10	0.15
13	Canopy expansion (lower threshold)	0.45	0.70
15	Stomatal control	0.45	0.70
17	Canopy senescence	0.45	0.70
	Shape factor for:		
14	Water stress coefficient for canopy expansion		3
16	Water stress coefficient for stomatal control		6
40	Describing root zone expansion		13
	Shape factor for response of:		
23	Canopy expansion to soil fertility stress		25
24	Maximum canopy cover to soil fertility stress		25
25	Crop water productivity to soil fertility stress		25
26	Decline of canopy cover to soil fertility stress		25
36	Crop transpiration coefficient (K_{CB})	1.02	1.07
38	Minimum effective rooting depth (m)		0.30
39	Maximum effective rooting depth (m)	0.60	1.80
	Maximum root water extraction in:		
41	Top quarter of root zone	0.048	0.016
42	Bottom quarter of root zone	0.012	0.004
	Canopy growth coefficient:		
47	Fraction per calendar day		0.143260
76	Fraction per growing degree-day	0.008907	0.012001
	Canopy decline coefficient:		
52	Fraction per calendar day		0.119000
77	Fraction per growing degree-day	0.016158	0.009862
44	Seedling leaf area (cm^2)		3.00
51	Maximum canopy cover (CC_X)	0.83	0.90
	Calendar days from planting to:		
53	Emergence		11
54	Maximum rooting depth		132
55	Start of senescence		132
56	Maturity (length of crop cycle)		147
57	Flowering		87
	Growing degree-days from planting to:		
70	Emergence	129	136
71	Maximum rooting depth	1,279	1,583
72	Start of senescence	1,518	1,579
73	Maturity (length of crop cycle)	1,616	1,760
74	Flowering	979	1,041
	Length of the flowering stage:		
58	Calendar days		26
75	Growing degree-days	123	306
	Building up of Harvest Index		
61	Starting at flowering (days)		60
78	During yield formation (GDD)	644	719
62	Normalised water productivity WP* ($g\ m^{-2}$)	30.0	33.7
63	WP* during yield formation (as a percentage of WP*)		100
65	Reference Harvest Index (percentage)	46	45
	Possible increase (percentage) of Harvest Index due to:		
66	Water stress before flowering		4

APPENDIX L

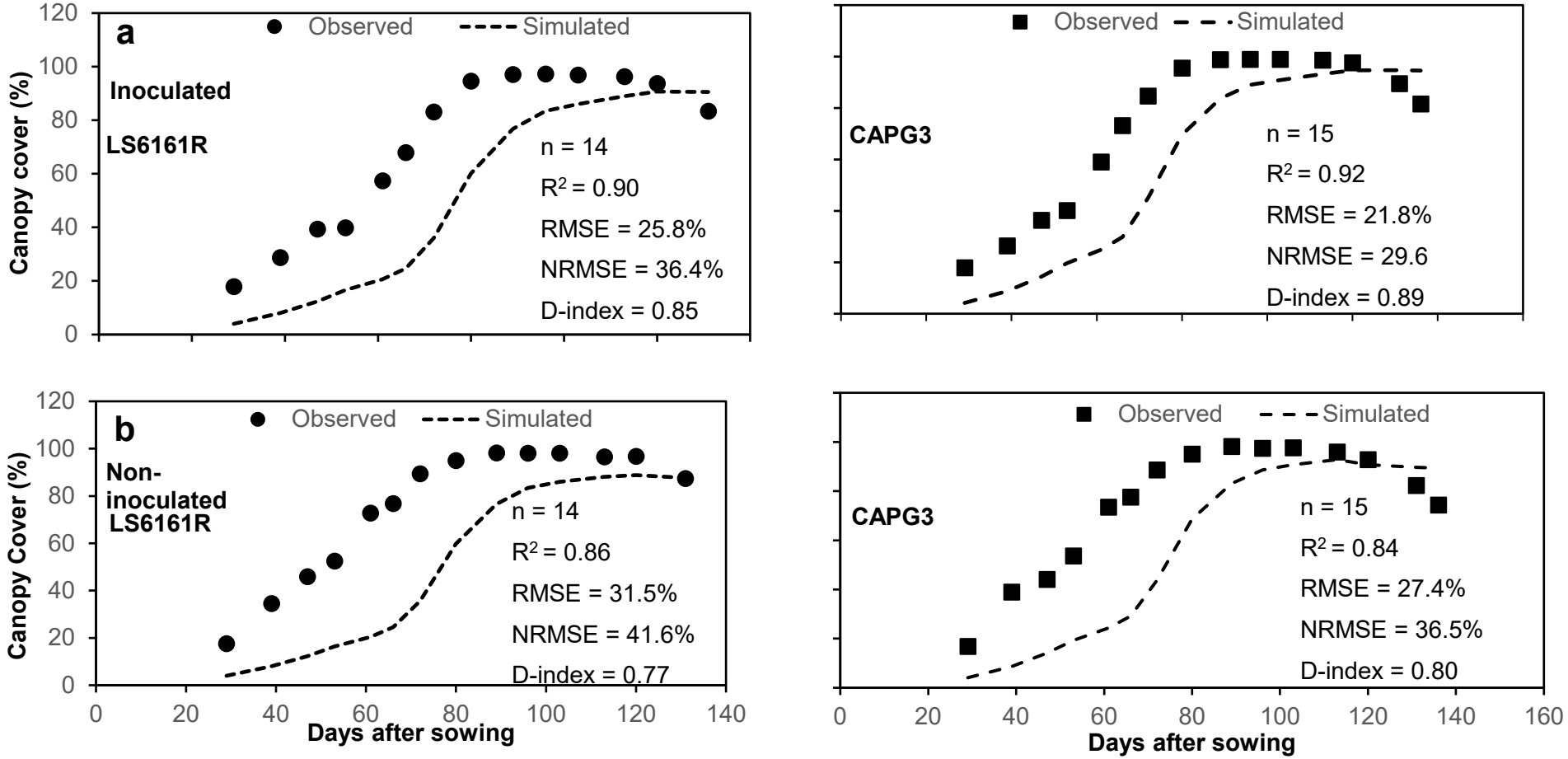

Figure L.1: Comparison between simulated and observed canopy cover for two rainfed soybean varieties grown under (a) inoculated and (b) non-inoculated treatments during the 2018/19 season at Swayimane (Reddy, 2019)

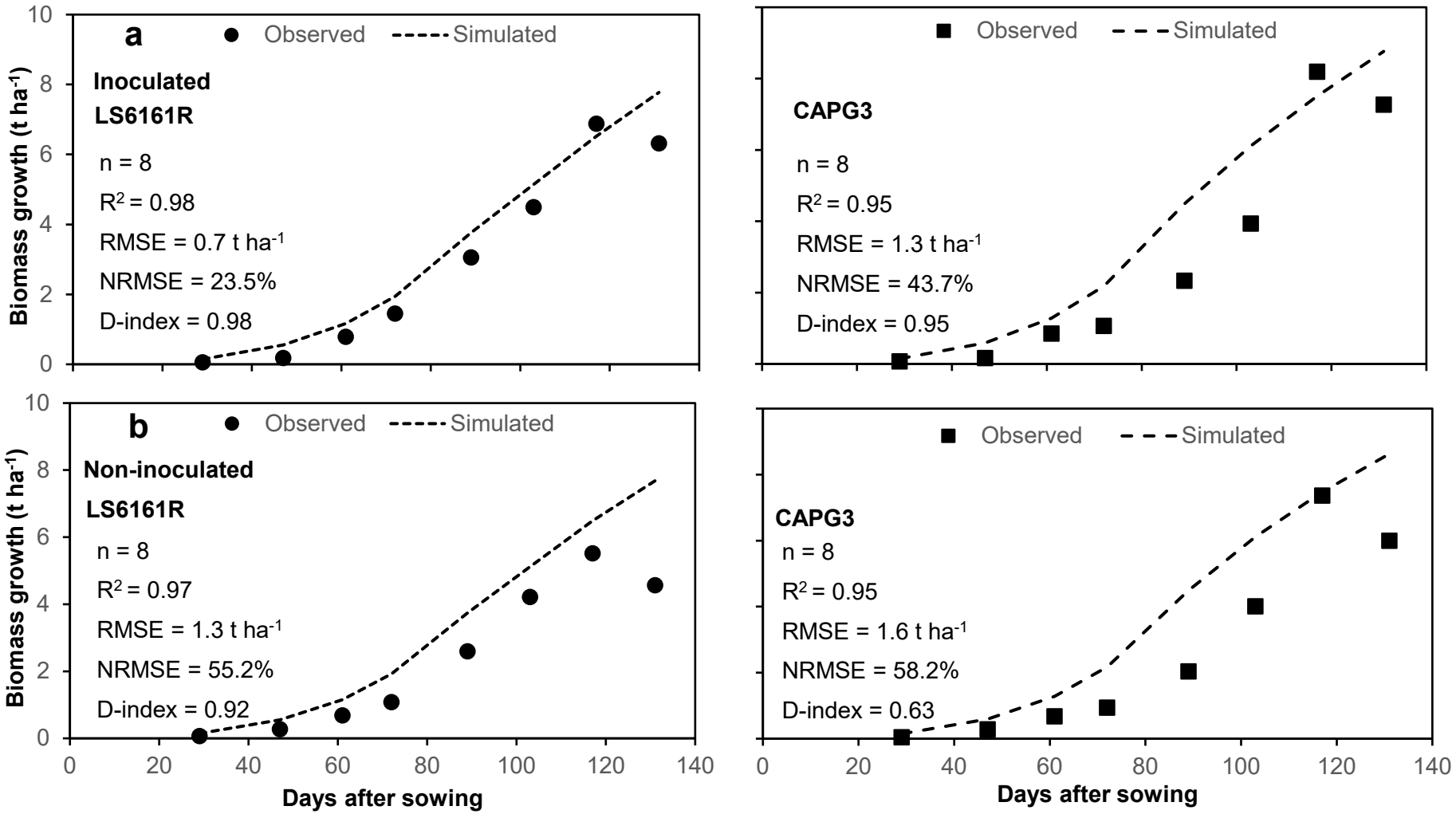

Figure L.2: Comparison between simulated and observed biomass growth for two rainfed soybean varieties grown under (a) inoculated and (b) non-inoculated treatments during the 2018/19 season at Swayimane (Reddy, 2019)

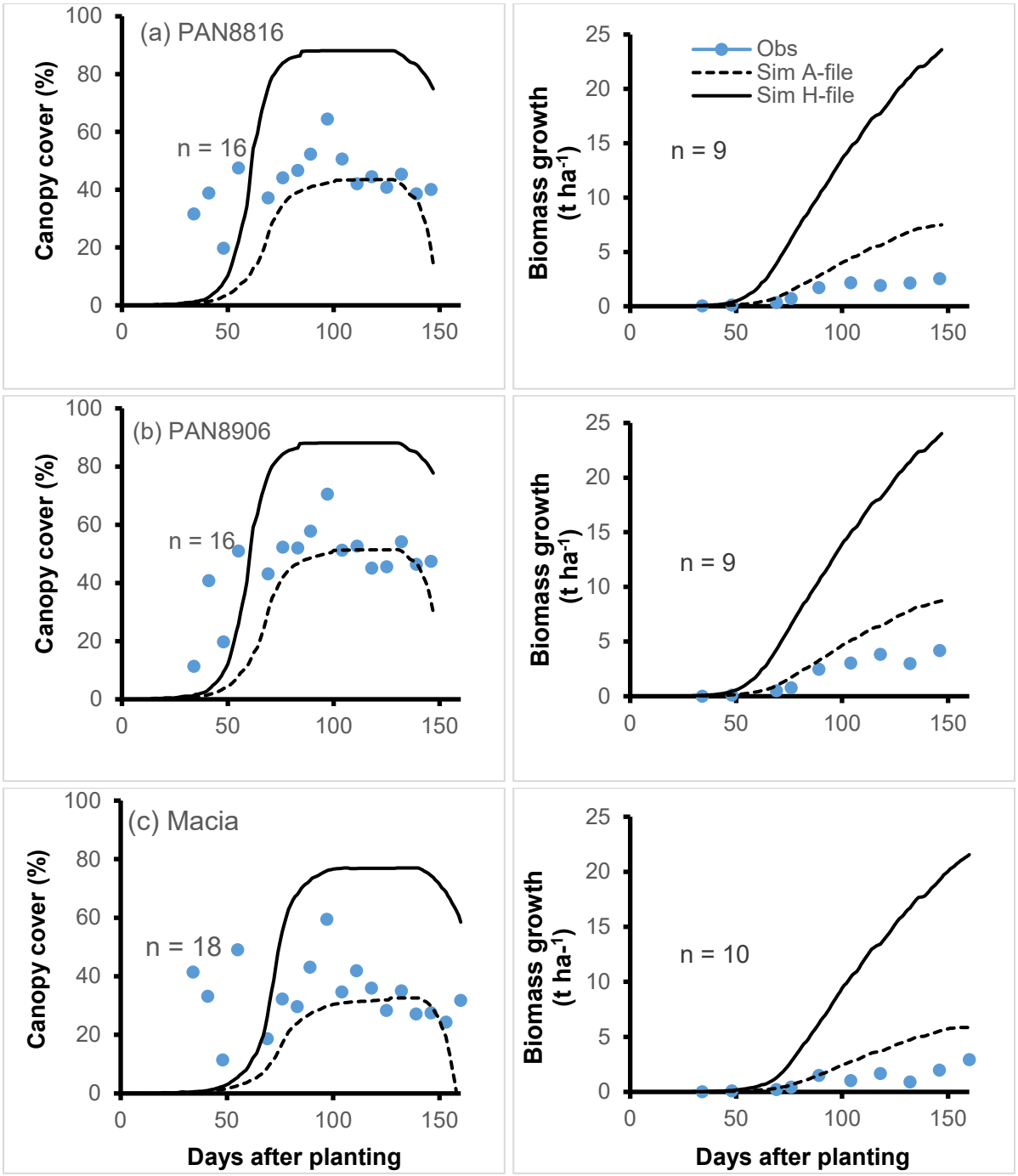

Figure L.3: **Observed and simulated canopy cover and biomass growth for three grain sorghum cultivars derived using two different crop files (A-file: Hadebe et al., 2017b; H-file: Araya et al., 2016) (Masanganise et al., 2019)**

APPENDIX M

M1 INTRODUCTION

Interception loss is typically considered to constitute only a small portion of total evaporation. In some models, it is disregarded completely (Gerrits et al., 2010) or merely lumped with total evaporation and not considered as a separate process (Savenije, 2004). Interception is a threshold process, so a certain amount of water is required to saturate the canopy storage before successive processes such as infiltration and runoff can take place (Bulcock and Jewitt, 2012), making it important to be included in hydrological models.

Interception may be defined as a stock, a flux or – more appropriately – a process. If interception is considered as interception storage (S_c), then it is defined as the rainfall that is temporarily stored on a surface. As a flux, interception is defined as water that has evaporated over a certain period both during and after an event. However, if interception is considered a process, then it is defined as being part of the rainfall flux that is intercepted by a surface and is subsequently evaporated back into the atmosphere. Interception may be expressed as the sum of the change in interception storage (S_c) and the evaporation from this stock (E_i) (Gerrits et al., 2010) as shown in Equation 23:

$$I_c = E_i + \frac{dS_c}{dt} \qquad \text{Equation 23}$$

This section describes the parameterisation of a canopy interception model and the estimation of rainfall intensity from daily rainfall data. This allowed for canopy interception to be adequately modelled in the absence of canopy storage capacity and rainfall intensity data.

M2 GASH INTERCEPTION MODEL

The original Gash (1979) and later the revised Gash et al. (1995) model are probably the best-known canopy interception models. Both the Gash (1979) and revised Gash et al. (1995) models classify storms according to the amount of gross rainfall (P_g) generated and then compute canopy interception (I_c), stemflow (S_f) and throughfall (T). The Gash (1979) and Gash et al. (1995) models and, subsequently, the variable storage Gash model, require canopy structure and interception parameters and climate forcing variables as input.

The variable storage Gash model (Bulcock and Jewitt, 2012) is based on following three assumptions, the first two being from the original Gash model:

- The rainfall distribution pattern may be represented as a succession of discrete storms, separated by sufficiently long periods to allow the canopy and trunks to dry (Gash, 1979; Gash et al., 1995).
- The rainfall and evaporation rates are constant during each storm and may be considered as constant between several storms during the same period (Gash, 1979; Gash et al., 1995).
- The maximum canopy storage capacity (S_c^{max}) is linearly related to *LAI* (Van Dijk and Bruinzeel, 2001a; Van Dijk and Bruinzeel, 2001b), but the storage capacity (S_c) varies with rainfall intensity (R).

The process of interception is a function of several properties of the tree, including branch, stem and crown characteristics, as well as the structure of the stand (Rutter et al., 1975). Widely spaced trees have larger spaces between them, therefore the ventilation within the stand increases and may result in more rainfall being intercepted and evaporated from the tree. However, tree spacing also affects the leaf area per unit of ground area and the spatial distribution of leaf area density. This will modify both the available energy and boundary layer conductance of the stand, and thus influence the rate of evaporation of intercepted water (McNaughton and Jarvis, 1983 in Teklehaimanot et al., 1991). In the variable storage Gash model, this has been accounted for using LAI as the primary parameter to describe the canopy structure.

The integrity of the original Gash model has not been jeopardised by the modifications made for the variable storage Gash model. The model requires the following input variables and parameters to describe canopy interception: gross precipitation, evaporation, rainfall rate, LAI and maximum storage capacity. For stemflow, the additional parameters are trunk storage capacity (S_t) and the stemflow partitioning coefficient (p_t).

M2.1 Interception parameters and variables

One of the most important parameters in all versions of the Gash model, including the variable storage Gash model, is the rain to fill canopy storage (P'_g) which is described by Equation 24 from the original Gash model (Gash, 1979):

$$P'_g = -\ln\left(1 - \frac{E}{R(1-p-p_t)}\right) \cdot S_c \left(\frac{R}{E}\right) \quad \text{Equation 24}$$

In this equation, the main term is $S_c(R/E)$, which is the amount of rain needed to fill the storage, given that most of the rain passes through the tree canopy. A check was implemented to ensure that E does not exceed $R(1 - p - p_t)$, else P'_g cannot be calculated. Gash et al. (1995) noted that $R(1-p-p_t)$ represents the rainfall mount intercepted by the canopy and, if less than the mean evaporation rate (E), the canopy fails to wet up, resulting in a negative logarithm which cannot be computed.

The rain to fill the trunk storage (P'_t) (Gash, 1979) is described by Equation 25:

$$P'_t = S_t / p_t \quad \text{Equation 25}$$

The stemflow partitioning coefficient (p_t) is the fraction of rain that runs down the stem of a tree during a storm and a constant value of 0.07 was used for all vegetation clusters in this study. The trunk storage capacity (S_t) is the total amount of water the trunk can hold. A constant value of 0.40 was used (Bulcock, 2011).

M2.2 Analytical model equations

The equations common to the original Gash (1979) and variable storage Gash models were used to distribute daily rainfall between the different storage terms as described below. Some are constant for all storms, while others depend on the actual rainfall amount.

Where the rainfall amount is insufficient to saturate the canopy (i.e. $P_g < P'_g$), the evaporation from the unsaturated canopy (I_c) during a small storm is described by Equation 26:

$$I_c = (1 - p - p_t) \cdot P_g \quad \text{Equation 26}$$

The term $(1 - p - p_t)$ is the intercepted coefficient and represents the fraction of rain held in the canopy during a storm. Another check was implemented to ensure that the evaporation from the unsaturated canopy (I_c) cannot exceed the daily evaporation rate (E). For large storms (i.e. $P_g > P'_g$), evaporation is considered in four phases as described by Equation 27 to Equation 31:

Evaporation during wetting phase:

$$I_w = (1 - p - p_t) \cdot P'_g - S_c \quad \text{Equation 27}$$

Evaporation from the saturated canopy:

$$I_s = \left(\frac{E}{R}\right) \cdot (P_g - P'_g) \quad \text{Equation 28}$$

Evaporation after rain ceases:

$$I_a = S_c \quad \text{Equation 29}$$

Evaporation from stems or trunks is dependent on whether gross rainfall is above or below the amount required to fill the trunk storage:

$$I_t = S_t \quad \text{if } P_g \geq P'_t \quad \text{Equation 30}$$

$$I_t = p_t \cdot P_g \quad \text{if } P_g < P'_t \quad \text{Equation 31}$$

Hence, the daily interception loss (I_c) was estimated as the sum of the above four components as follows:

$$I_c = I_w + I_s + I_a + I_t \quad \text{Equation 32}$$

However, the evaporation from the trunk (I_t) can be ignored if the vegetation type is not predominately trees (e.g. forest plantation or mixed forest), which was the approach in this study. For all storms, irrespective of size, the stemflow (S_f) and throughfall (T) are considered as:

$$S_f = p_t(P_g - P'_t) \quad \text{Equation 33}$$

$$T = P_g - I_c - S_f \quad \text{Equation 34}$$

The stemflow is the product of the stemflow partitioning coefficient (p_t) and the difference between gross precipitation (P_g) and rain to fill the trunk storage (P'_t). Throughfall is simply the difference of gross precipitation, interception loss (I_c) and stemflow (S_f).

M2.3 Canopy structure parameters

Gash et al. (1995) introduced the canopy cover fraction (c) to account for inadequacies in the simulation of sparse canopies in the original model. Van Dijk and Bruijnzeel (2001a; 2001b) then modified the revised Gash et al. (1995) model, allowing it to be applied to rapidly growing vegetation where the LAI is changing over time. The variable storage Gash model introduces a vegetation/species-specific parameter, termed the maximum elemental storage (S_e^{max}), which accounts for the water holding characteristics of the canopy and is described more fully in Section M2.4 below.

The LAI is defined as the cumulative one-sided area of leaves per unit area. The relationship between canopy cover and LAI is thus given by Equation 35, where the extinction coefficient (k) was obtained from the literature:

$$CC = 1 - e^{-k \cdot LAI} \quad \text{Equation 35}$$

The LAI and canopy cover are related to one another via the Beer-Lambert equation (Equation 35), which describes the attenuation of photosynthetically active radiation (PAR) as a function of LAI. Since PAR does not penetrate far through leaves, the Beer-Lambert equation may be expressed in terms of canopy cover fraction using similar parameters. For the extinction coefficient (k), a value of 0.416 was used for grain sorghum (Araya et al., 2016) and 0.460 for soybean (Adeboye et al., 2017). The latter compares favourably with a range 0.45-0.70 provided by Dlamini (2015) for various soybean cultivars (cf. Table G.3 in Appendix G).

The throughfall coefficient (p) is the fraction of rain that passes through a canopy during a storm without touching the canopy, and can be described as (Van Dijk and Bruijnzeel, 2001a):

$$p = 1 - CC \quad \text{Equation 36}$$

During the initial testing of the above equations, erroneous interception loss values were calculated for small LAI values, i.e. 0.10 ≤ *LAI* ≤ 0.12. This was due to the calculated canopy cover fraction (Equation 35) being smaller than the stemflow partitioning coefficient (p_t; constant), and thus the intercepted coefficient ($1 - p - p_t$) became zero (or negative). This was corrected by setting $CC = p$.

M2.4 Canopy storage capacity

The variable storage Gash model also requires the maximum canopy storage capacity (S_c^{max}), which represents the amount of rain required to wet the canopy with droplets of almost "zero" kinetic energy. According to Calder (1996), this can occur when the rainfall intensity is less than 0.36 mm h^{-1}. When the maximum storage capacity is reached, throughfall may begin.

In the absence of S_c^{max} data, Von Hoyningen-Huene (1983) developed a non-crop specific estimate of maximum storage capacity, which has been recognised by Kozak et al. (2007) as being accurate. The equation requires LAI data to estimate S_c^{max} and is decribed by the equation:

$$S_c^{max} = 0.935 + 0.498 \cdot LAI - 0.00575 \cdot LAI^2 \qquad \text{Equation 37}$$

The canopy storage capacity (S_c) for non-zero kinetic energy drops can be estimated from canopy cover fraction (c) using the following equation:

$$S_c = CC \cdot S_c^{max} \qquad \text{Equation 38}$$

However, storage capacity was derived in this study as follows:

$$S_c = S_c^{max} \quad \text{if R} \leq 0.36 \text{ mm h}^{-1} \qquad \text{Equation 39}$$

$$S_c = S_c^{max} \cdot (0.5 + 0.73e^{-5.5v}) \quad \text{if R} > 0.36 \text{ mm h}^{-1} \qquad \text{Equation 40}$$

where v is the raindrop volume (mm^3), which is estimated using the Marshall-Palmer (1948) equation:

$$v = a \cdot R^b \qquad \text{Equation 41}$$

In the above equation, R is the gross rainfall rate or intensity (mm h^{-1}) and both a (= 0.124) and b (= 0.63) are unitless parameters of a power function to scale mm h^{-1} to mm^3 (Hall, 2003).

M3 METHODOLOGY

The climatic forcing variables required for the variable storage Gash model are gross precipitation (P_g), gross rainfall rate or intensity (R in mm h^{-1}) and mean evaporation rate (E in mm d^{-1}) per event. The derivation of each input dataset required by the interception model is explained in the subsections that follow.

M3.1 Daily rainfall

The quinary climate database consists of, inter alia, daily rainfall, daily maximum and minimum temperature and reference crop evaporation (ET_O) estimated using the FAO56 Penman-Montieth procedure (Allen et al., 1998). This database provided the rainfall input for the modified Gash model.

M3.2 Rainfall intensity

As noted in Section M1, data on rainfall intensity is scarce in South Africa, making it a difficult parameter to derive when required as a model input. As a result, a surrogate method of using the EI_{30} multiplication factors to determine rainfall intensity from daily rainfall was derived, as detailed next.

Warburton Toucher et al. (2019) used rainfall intensity data from four diverse locations to derive median multiplication factors, which were then compared to those determined by Schmidt and Schulze (1987) as presented in Table M.1. The multiplication factors determined from the rainfall intensity data compare well with those derived by Schmidt and Schulze (1987), with a RMSE of 0.178 for all sites. For regions outside South Africa, a factor of 0.745 should be used (Smithers and Schulze, 1995).

Table M.1: Multiplication factors for the different rainfall intensity distribution zones of southern Africa (after Schmidt and Schulze, 1987)

Rainfall intensity distribution zone	1	2	3	4
Multiplication factor	0.430	0.664	0.974	1.236

The sites located close to the border of two zones exhibited the largest error. This is because the changes in rainfall patterns are not as abrupt as those shown in Figure M.1. This anomaly could be addressed by creating a transition zone along the boundary where two zones meet. In Figure M.1, Zone 1 is characterised by long duration, relatively uniform rainfall events, whereas zones 2 and 3 represent convective-type storms. In Zone 4, short cloudbursts with large rainfall amounts (i.e. high-intensity rainfall) typically occur (Smithers and Schulze, 1995).

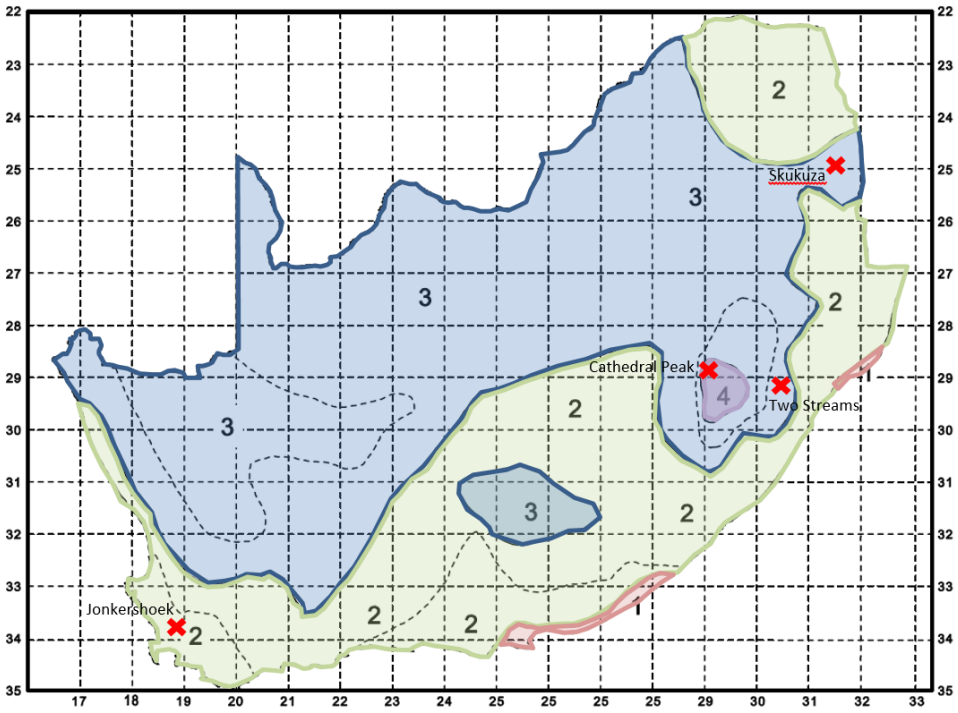

Figure M.1: Rainfall intensity distribution zones in southern Africa (after Weddepohl, 1988)

Unfortunately, the above map has not been digitised, and thus could not be used to derive zone numbers per quinary subcatchment. Since soybean and sorghum production occurs mainly in zones 2 and 3, the average correction factor of 0.819 was used in this project.

M3.3 Evaporation rate

In this study, Penman-Monteith reference crop evaporation (ET_O) was used to determine the mean evaporation rate (E in mm d^{-1}) per daily rainfall event. Daily values were obtained from the revised quinary subcatchment climate database (cf. Section 10.1.4).

M3.4 Leaf Area Index

The other input required to model canopy interception loss is an estimate of LAI, which is defined as the leaf area covering a unit of ground area and is expressed in m^2 m^{-2}. In this study, LAI was routinely measured using a plant canopy analyser at the respective experimental sites. Monthly averages were then obtained as used as input for the modified Gash model.

M3.5 Maximum canopy storage

For this project, maximum storage capacity (S_c^{max}) was estimated using a method depicted by the conceptual flow diagram shown in Figure M.2. In essence, S_c^{max} comprises two components representing the leaves and woody portion of the canopy. The method requres two parameters (*SI* and $S_c^{max}{}_{\_wood}$), for which values were determined from the *WFlow_sbm* model, a distributed hydrological model developed by Deltares in the Netherlands (Arnal, 2014).

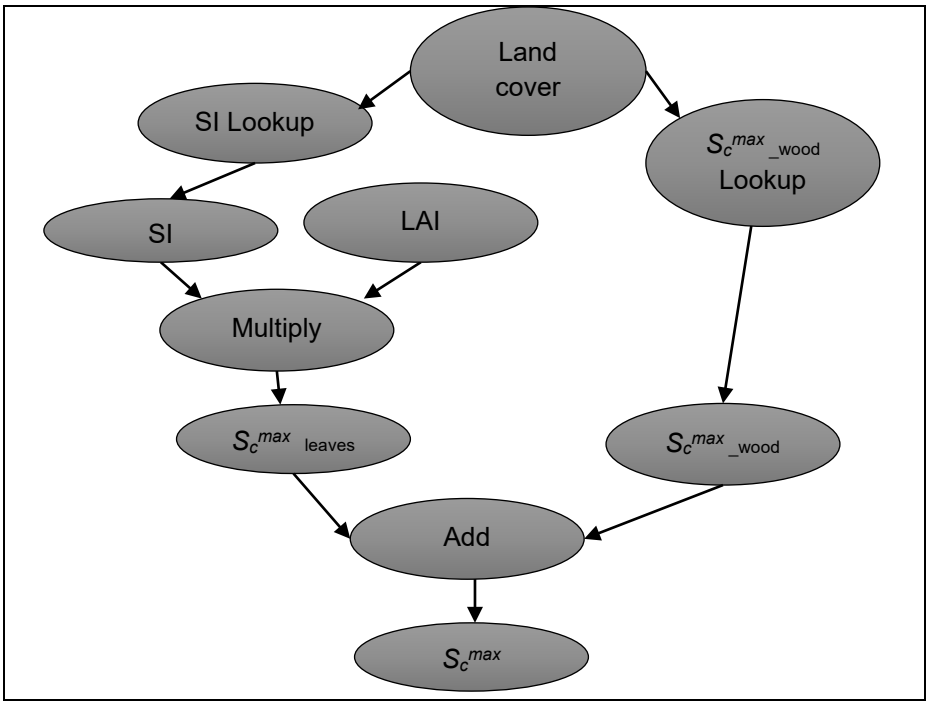

Figure M.2: Conceptual flow diagram to determine Scmax (Warburton Toucher et al., 2019)

The model's canopy intercepion routine requires the same storage capacity parameters as the variable storage Gash model. For croplands, the *Wflow_Sbm* model uses 0.127 for the specific leaf storage (*SI*) and 0 for the maximum storage capacity representing the woody portion of the canopy ($S_c^{max}{}_{\_wood}$).

APPENDIX N

The following methodology was used to validate the use of AquaCrop to simulate ET_C, from which monthly crop coefficients (K_C) were derived. The latter values are required as input for ACRU in order to assess the hydrological impact of biofuel crop production.

N1 MEASURED CROP ET_C

Daily observations of grain sorghum evapotranspiration from Ukulinga in the 2012/13 season were obtained from Kunz et al. (2015a), i.e. WRC Project No. K5/5221 (the previous biofuel project). Estimates of crop water use were derived using the surface renewal technique from 3 January to 10 May 2013. A total of 399 mm was accumulated over this period of 128 days.

N2 MODELLING OF CROP ET_C

The AquaCrop model was configured for the 2012/13 growing season at Ukulinga. Daily values of rainfall temperature (maximum and minimum) and ET_O were obtained from the ARC's weather station. Daily irrigation values were obtained from Kunz et al. (2015a) and converted from volumes to depths. The irrigation mode was set to 5 (drip irrigation), with the percentage of soil surface wetted to 20%. A total of 172 mm of supplemental irrigation was applied to the crop on 15 days from 24 December 2012 to 8 April 2013. The trial was well managed to minimise crop stress and reduced growth. The planting date was set to 27 November 2012 and the target planting density was 100,000 plants ha^{-1}.

N2.1 Reference crop evaporation (ET_O)

Daily values of reference evaporation for a short grass surface were obtained from the ARC's automatic weather station located at Ukulinga (-29.66765°S; 30.40602°E) at a height of 812 m above sea level.

N2.2 Soils data

Soil water retention parameters and saturated hydraulic conductivity (K_{SAT}) were obtained from Kunz et al. (2015a) for a predominately clay loam soil of 0.6 m in depth. The initial soil water content was set to field capacity, which is AquaCrop's default option when the value is unknown.

Table N.1: Measured soil water retention and saturated hydraulic conductivity values for three soil layers at Ukulinga (Kunz et al., 2015a)

Thickness (m)	SAT (%)	FC (%)	PWP (%)	TAW (%)	K_{SAT} (mm d^{-1})
0.2	36.5	29.3	15.7	13.6	184.4
0.2	36.5	30.0	17.5	12.5	228.0
0.2	36.1	32.0	20.8	11.2	108.0
0.6	**36.4**	**30.4**	**18.0**	**12.4**	**173.5**

N2.3 Calibrated crop parameters

Partially calibrated crop parameters for grain sorghum (PAN8816) were obtained from Hadebe et al. (2017b), which were developed for WRC Project No. K5/2274 (Modi and Mabhaudhi, 2017). A list of crop parameters that were calibrated is given in Table K.14 (Appendix K).

N2.4 Crop parameters in GDD

The crop parameters published by Hadebe et al. (2017b) had phenological growth stages expressed in calendar days, with a season length (crop cycle) of 140 days. These figures were converted to thermal time (in GDD) using AquaCrop, by loading Ukulinga's climate record for 2014 and setting the planting date to 17 January 2014 (cf. Table K.14 in Appendix K).

N2.5 Number of soil layers

Initial tests were done to determine if model output was influenced by the number of soil layers used in AquaCrop. The model was run in calendar mode using the calibrated crop parameters derived by Hadebe et al. (2017b). Hence, physiological maturity was reached on 16 April 2013 or 140 DAP. AquaCrop runs for a one- and three-layer soil showed negligible variation in model output. Hence, the decision was made to perform all model runs for a one-layer soil (i.e. averaged soil water retention values).

Table N.2: Difference in AquaCrop model output derived using a one and three-layered soil profile of 0.6 m in depth

Number of soil layers	Infiltration (mm)	Runoff (mm)	Drain (mm)	Evapotranspiration (mm)	Biomass (t ha^{-1})	Yield (t ha^{-1})
1	590	66	97	496	29.89	13.43
3	589	67	96	495	29.81	13.45

N2.6 Calendar vs thermal time

Using partially calibrated crop parameters and a one-layer soil 0.6 m deep, the model was run for the 2012/13 season at Ukulinga with crop phenology determined using both calendar (CAL) and thermal (GDD) time. In CAL mode, the crop matured on 16 April 2013 (140 DAP) and nine days earlier (131 DAP) in GGD mode. The shorter crop cycle resulted in less accumulated evapotranspiration (496 vs 487 mm), which resulted in lower biomass accumulation and final yield. The calibration was performed in the 2013/14 season at Ukulinga, which was then used to assess the water use and yield of grain sorghum in the 2012/13 season. Since 2012/13 was slightly warmer than the calibration season, the crop reached physiological maturity nine days earlier, which explains the difference in results between the CAL and GDD mode runs.

Table N.3: Difference in AquaCrop model output derived with crop development based on calendar and thermal time

Mode	Infiltration (mm)	Runoff (mm)	Drain (mm)	Evapotranspiration (mm)	Biomass (t ha^{-1})	Yield (t ha^{-1})
CAL	590	66	97	496	29.89	13.43
GDD	594	61	109	487	26.96	11.67

In GDD mode (i.e. crop cycles based on thermal time), much of the temperature effects on crops, such as on phenology and canopy expansion rate, are accounted for. For example, the model inhibits the conversion of transpiration into biomass at low temperatures when using thermal time (Steduto et al., 2012). In other words, running the model in GDD model invokes a number of functions within the model that incorporates temperature effects on phenology and transpiration. Hence, the model runs much slower in GDD mode than compared to CAL mode. Kunz et al. (2015a) reported that the model took 55.08 seconds to simulate 49 consecutive seasons of crop yield in GDD mode, compared to only 1.24 seconds in CAL mode. Furthermore, the model simulated lower yields in the cooler, higher latitude areas due to temperature stress effects. Hence, the decision was made to run the model in GDD mode as recommended by Steduto et al. (2012) and Kunz et al. (2015a).

N2.7 Effective rooting depth

Using default crop parameters for grain sorghum and a one-layer soil 0.6 m deep, AquaCrop was run with the effective rooting depth (ERD) set to no limit and 0.6 m. The model produced relatively similar output for accumulated evapotranspiration, biomass and final yield. Using thermal time to determine the crop cycle, physiological maturity was reached on 9 April 2013 or 133 DAP.

Table N.4: Difference in AquaCrop model output derived with the effective rooting depth set to 0.6 m using a one and three-layered soil profile of 0.6 m in depth

ERD (m)	Infiltration (mm)	Runoff (mm)	Drain (mm)	Evapotranspiration (mm)	Biomass (t ha^{-1})	Yield (t ha^{-1})
No limit	599	57	107	495	29.18	12.26
0.6	603	52	115	492	28.84	12.21

However, the simulated water content in the soil profile (WCtot) was very different. With the effective rooting depth not set (no limit), WCtot was simulated as 541 mm, based on a maximum rooting depth of 1.8 m (as per the default parameter value), even though the soil is 0.6 m deep. When the effective rooting depth was set to 0.6 m, WCtot was reduced to 160.9 mm, based on a maximum rooting depth of 0.6 m. Hence, the decision was made to set the effective rooting depth to 0.6 m for Ukulinga. For the national model runs, the effective rooting depth was set to the depth of the A- and B-horizons.

N2.8 Comparison of observed vs simulated ET

According to Piñeiro et al. (2008), the coefficient of determination (R^2) can be used as a measure of the proportion of the variance in observed values that is explained by the simulated (or predicted) values. The authors also recommend that the root mean square deviation (RMSD) is calculated, which represents the mean deviation of simulated values ($\hat{y}_i$) with respect to the observed ones (y_i), in the same units as the variable under evaluation. The RMSE will be always smaller than the RMSD, and thus represents an under-estimation of the real error between observed and simulated values (Piñeiro et al., 2008).

$$RMSD = \sqrt{\frac{1}{n-1}\sum_{i=1}^{n}(\hat{y}_i - y_i)^2} \qquad \text{Equation 42}$$

The Nash-Sutcliffe Efficiency coefficient was also used to evaluate model performance, where y_m is the mean of the observed values. The NSE is similar to R^2, where values range from 0 (poor fit) to 1 (perfect fit).

$$NSE = 1 - \frac{\sum_{i=1}^{n}(\hat{y}_i - y_i)^2}{\sum_{i=1}^{n}(\hat{y}_i - y_m)^2} \qquad \text{Equation 43}$$

Crop evapotranspiration was measured using the surface renewal technique from the 3 January 2013 (37 DAP) to harvest date (10 May 2013; 164 DAP). Using partially calibrated crop parameters (Hadebe et al., 2017b) and a one-layer soil profile with the ERD set to 0.6 m, the model was run in GDD mode to simulate crop ET_C from planting date (27 November 2012) to actual harvest date (10 May 2013). Based on the model run, physiological maturity was reached on 7 April 2013 (131 DAP). Hence, a comparison of observed vs simulated evapotranspiration was done from 37-131 DAP (i.e. n = 95). The regression statistics indicate a relatively good fit, and thus AquaCrop was successful in simulating the evapotranspiration of grain sorghum (Figure N.1).

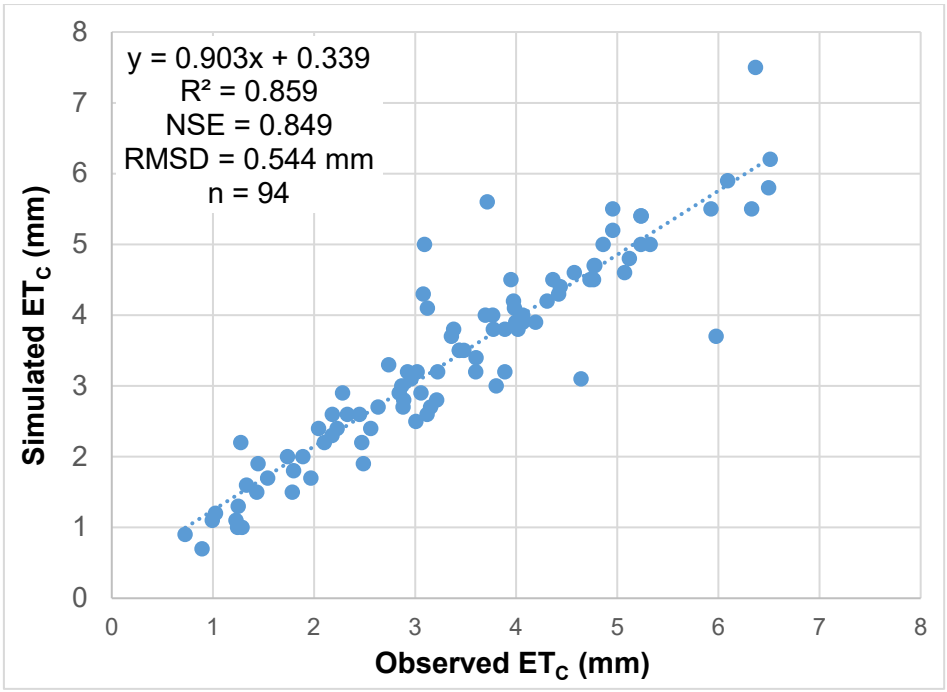

Figure N.1: Comparison of ET_C simulated by AquaCrop with ET_C measured using the surface renewal technique for grain sorghum grown in the 2012/13 season at Ukulinga

N2.9 Infilling of observed ET

The regression equation shown in the previous figure was used to infill missing evapotranspiration data from planting to 2 January 2013. Hence, the total water use over the entire crop season of 164 days was estimated at 513 mm (not 436 mm as reported by Kunz et al., 2015a). AquaCrop simulated a lower total of 488 mm for the same period. However, the model does not simulate evaporation of intercepted water, only transpiration and soil water evaporation. Hence, simulated evapotranspiration should always be lower than surface renewal-based measurements, considering that the evaporation of intercepted water is accounted for by this micrometeorological technique.

N3 GENERATING MONTHLY CROP COEFFICIENTS

N3.1 Observed values

Using daily values of crop evapotranspiration (i.e. ET_C) measured using surface renewal, monthly crop coefficients (K_C) were calculated using the following two methods:

- **Method 1**: Daily K_C values were calculated by dividing ET_C by ET_O. Values outside the acceptable range of 0.20-1.25 (refer to Allen et al., 2011) were considered outliers and omitted. Monthly crop coefficients were then calculated as the average of daily values.
- **Method 2**: Monthly crop coefficients were calculated by summing ET_C for each month, then dividing it by the monthly accumulated ET_O.

These two methods produced somewhat different results as shown in Table N.5. In general, calculating crop coefficients from monthly data produced lower values than averaged daily values, expect for April 2013. Although AquaCrop can produce daily output, this increases the model's run time, while it creates the daily files. For this reason, the decision was made to calculate K_C values using Method 2, i.e. from monthly totals of ET_C and ET_O. The K_C values were not determined for November 2012 and May 2013 considering the accumulated totals were only based on three and 10 days, respectively.

Table N.5: Monthly crop coefficients for grain sorghum, derived from measured ET_C using two methods for the 2012/13 season at Ukulinga

Year	Month	Crop coefficient (K_C)	
		Method 1	Method 2
2012	December	0.87	0.81
2013	January	0.93	0.92
2013	February	1.00	1.01
2013	March	0.99	0.98
2013	April	0.88	0.91

N3.2 Simulated values

The next step involved the calculation of monthly K_C value from estimates of ET_C for grain sorghum derived using AquaCrop over the 164-day crop cycle. Monthly totals of ET_C and ET_O were used to derive K_C. For December 2013, the observed and simulated crop coefficients are identical, simply because missing ET_C was infilled with simulated values derived from AquaCrop (cf. Section N2.9). Table N.5 shows good agreement between observed and simulated values of monthly crop coefficients, except for April 2013.

Table N.6 Monthly crop coefficients for grain sorghum, derived from both measured and simulated ET_C for the 2012/13 season at Ukulinga

Year	Month	Crop coefficient (K_C)	
		Observed	Simulated
2012	December	*0.81**	0.81
2013	January	0.92	0.94
2013	February	1.01	1.03
2013	March	0.98	0.97
2013	April	0.91	0.69

*Missing ET_C data infilled using simulated data

N3.3 Adjustment of observed K_C

Table N.6 shows a 28.9% decline in simulated K_C from March to April. This is expected considering the crop reached physiological maturity on the 7 April (131 DAP). For the remainder of the month, the model ceases transpiration (T) and only simulates soil water evaporation (E). In other words, simulated evapotranspiration from 132-164 DAP comprises E alone since T is zero.

However, the change in observed K_C from 0.98 (March) to 0.91 (April) only represents a 7.1% decrease. This is surprising since grain sorghum's LAI decreased from 3.05 to 1.90 (i.e. a 37.7% decline) from 7 March to 22 April 2013. Hence, the surface renewal evapotranspiration data did not show the expected decline as the crop approached physiological maturity. For this reason, the observed K_C value of 0.91 was adjusted downward by 28.9% to 0.65 in order to mimic the decline in simulated K_C value from March to April.

N3.4 Dryland vs irrigated K_C

The next step involved running AquaCrop for Quinary Subcatchment 4697, in which Ukulinga is located. The model was run using partially calibrated crop parameters and the ERD set to the combined depth of the A- and B-horizons. The quinary climate database, comprising 50 years of daily data, was used to simulate 49 consecutive seasons of crop evapotranspiration data. A statistical utility written in Fortran was modified to calculate crop coefficients from monthly accumulations of ET_A and ET_O, and then to determine averaged values from 49 seasons of data for each month.

However, Allen et al. (1998) recommended that crop coefficients should be obtained under standard (i.e. non-stressed) growing conditions. Hence, drip irrigation (with a 20% wetted surface) was invoked in the model to relieve plant stress assumed to occur when the soil water content dropped below 50% of total available water, i.e. between FC and PWP. Hence, a new set of monthly averaged K_C values was derived from 49 seasons of monthly ET_C values estimated by AquaCrop from irrigated (i.e. non-stressed) growing conditions.

Table N.7: Monthly crop coefficients for grain sorghum, derived from simulated ET_C by AquaCrop for both rainfed and irrigated conditions in Quinary Subcatchment 4697

Month	Crop coefficient (K_C)		
	Rainfed	Irrigated	Percentage increase
December	0.54	0.60	11.1
January	0.79	0.86	8.9
February	0.78	1.05	34.6
March	0.63	0.98	55.6
April	0.51	0.82	60.8

Crop coefficients derived for non-stressed (i.e. irrigated) growing conditions are obviously larger than those for rainfed conditions. The highest value of 1.05 (February) approaches the maximum value of 1.07, which represents K_{CB} when canopy cover is complete (i.e. prior to crop senescence). This value is an input parameter required by the model.

In order to demonstrate this new approach of deriving site-specific K_C values, the reduction in MAR simulated by ACRU using observed crop coefficients (similar to those given in Table N.6) was used to identify another subcatchment for testing purposes. Crop coefficients generated by AquaCrop for Quinary Subcatchment 4325 are given in Table N.8. The climate of Quinary Subcatchment 4325 is much cooler than that of Quinary Subcatchment 4697. Hence, the season length is longer. Thus, crop coefficients for May were generated.

Table N.8: Monthly crop coefficients for grain sorghum, derived from simulated ET_C by AquaCrop for both rainfed and irrigated conditions in Quinary Subcatchment 4325

Month	Crop coefficient (K_C)		
	Rainfed	Irrigated	Percentage increase
December	0.56	0.65	16.1
January	0.67	0.79	17.9
February	0.83	1.06	27.7
March	0.69	1.03	49.3
April	0.50	0.94	88.0
May	0.27	0.84	211.1

N3.5 Influence of crop cycle

AquaCrop was run in GDD mode in order to account for temperature stress effects on crop growth and yield. In this mode, the model determined the date the crop reached physiological maturity (i.e. after sufficient GDDs had accumulated). This date varied in each season, as well as in each quinary. Quinary Subcatchment 4325 was selected to demonstrate the effect of cooler temperatures on crop growth, with the season length being more variable than compared to Quinary Subcatchment 4697.

For non-stressed growing conditions, the crop cycle for Quinary Subcatchment 4697 varied from 106 to 126 days and averaged 115 days. The median crop cycle was also 115 days and the inter-seasonal variation was only 3.9% (coefficient of variation). These statistics highlight the low inter-seasonal variability in growing season length as shown in Figure N.2 for Quinary Subcatchment 4697. For most seasons, the crop reached physiological maturity in April, with only one season (1 December 1987) maturing in the previous month (30 March 1988). Hence, almost all monthly crop coefficients were calculated as the average of 49 seasons, except for April, which only exhibited 48 seasons.

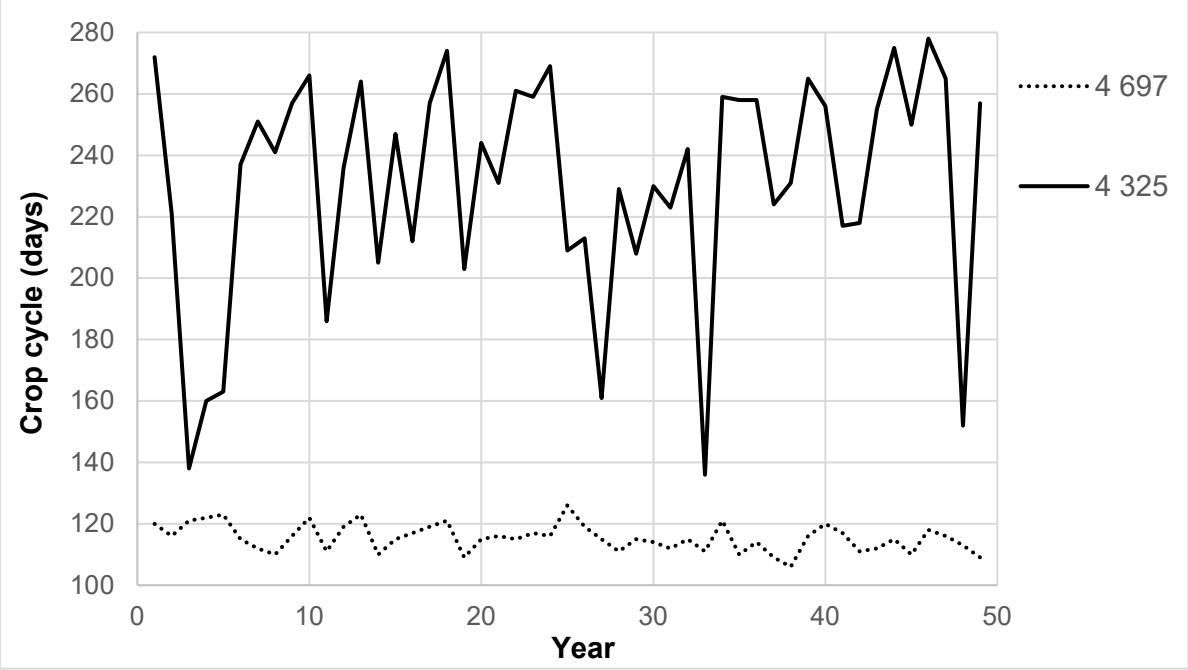

Figure N.2: Variation in crop cycle for grain sorghum as determined by AquaCrop over 49 seasons from 1950-1998

For Quinary Subcatchment 4325, the crop cycle varied from 136 to 278 days and averaged 231 days (Figure N.2), with an inter-seasonal variation of 16.1%. Averaged crop coefficients from December to May were derived from 49 seasons of data. However, crop coefficients in June, July, August and September were calculated from 43, 42, 32 and 19 seasons, respectively. This highlights the fact that although Quinary Subcatchment 4325 is suited to grain sorghum production, the crop takes much longer to mature compared to Quinary Subcatchment 4697. The decision was made to limit the season length for crop production to a maximum of six months.

N3.6 K_C adjustments for ACRU

As noted by Kunz et al. (2015a), ACRU is driven by A-pan reference evaporation, not grass reference evaporation. Hence, crop coefficients derived using ET_O (i.e. K_{C_ETO}) cannot be used in ACRU without adjustment. The methodology suggested by Kunz et al. (2015a) was adopted, where K_{C_ETO} is divided by a correction factor to calculate K_{C_PAN}. Since the correction factor ranges from 1.32-1.38 and 1.33-1.40 for Quinary Subcatchment 4325 and Quinary Subcatchment 4697, respectively, monthly K_{C_PAN} values are lower than K_{C_ETO}, as shown in Table N.9. For the fallow period (May to November), a crop coefficient of 0.25 was used as suggested by Kunz et al. (2015a). If the adjusted crop coefficient was below 0.25, it was set to this minimum value. This occurred in May for K_{C_PAN}, derived for rainfed conditions in Quinary Subcatchment 4325.

Table N.9: Monthly crop coefficients for grain sorghum, derived from simulated ET_C by AquaCrop for both rainfed and irrigated conditions in Quinary Subcatchment 4325

Month	Ukulinga		Quinary Subcatchment	
	Measured	Simulated	4697	4325
December	0.61	0.61	0.45	0.49
January	0.69	0.71	0.65	0.60
February	0.75	0.77	0.78	0.80
March	0.72	0.71	0.72	0.77
April	0.50	0.49	0.59	0.68
May				0.59

As noted in Chapter 6 of the ACRU Theory Manual (Schulze, 1995), monthly crop coefficients are converted to daily values by the model using Fourier analysis. However, for periods of sustained soil water stress, ACRU further reduces the crop coefficient based on an exponential decay function. When soil water stress is relieved through rainfall (or irrigation), a crop coefficient recovery curve based on the daily average temperature is used to increase the crop coefficient back to the allowed daily value. Table N.10 shows the change in K_C value used as model input and how the model adjusted the values based on soil water stress.

Table N.10: Adjustments made by ACRU to monthly A-pan equivalent crop coefficients representing irrigated grain sorghum for Quinary Subcatchment 4697 and Quinary Subcatchment 4325

Month	Quinary Subcatchment 4697		Quinary Subcatchment 4325	
	Input	Output	Input	Output
December	0.45	0.42	0.49	0.44
January	0.65	0.58	0.60	0.53
February	0.78	0.67	0.80	0.67
March	0.72	0.63	0.77	0.63
April	0.59	0.50	0.68	0.51
May	0.25	0.25	0.59	0.44
June	0.25	0.21	0.25	0.24
July	0.25	0.24	0.25	0.22
August	0.25	0.21	0.25	0.24
September	0.25	0.24	0.25	0.24
October	0.25	0.24	0.25	0.25
November	0.25	0.25	0.25	0.24

N3.7 ACRU configuration

The monthly crop coefficients given in Table N.10 were used as input for ACRU (for variable *CAY*) to estimate the reduction in runoff that may result from grain sorghum production. For all other ACRU parameters for grain sorghum (e.g. VEGINT, ROOTA, COIAM, CONST, COLON and *PCSUCO*), the same values derived by Kunz et al. (2015a) were used.

Since the planting date selected for grain sorghum by Kunz et al. (2015a) was 1 November, all values were shifted by one month to accommodate the new planting date of 1 December. Since planting of the crop at Ukulinga began on 27 November 2012 and was completed in early December, it was decided that a December planting date better mimicked actual conditions at Ukulinga. For the baseline (i.e. natural vegetation), the same ACRU configuration developed by Kunz et al. (2015a) was used.

ACRU Version 3.38 was used to generate runoff, which offers substantial speed improvements over Version 3.3.7 that was used by Kunz et al. (2015c) in the previous biofuel project (Kunz et al., 2015c). To ensure that Version 3.38 produced the same results as the previous version, it was re-run for the baseline (natural vegetation) and results were compared to those obtained in 2015 by Kunz et al. (2015c). The outcome showed that the faster version (Version 3.38) of the model produced identical results to those previously obtained.

APPENDIX O

For model calibration purposes, various equations have been used in the literature to calculate canopy cover from LAI. These equations, which are given next, could be re-arranged to derive LAI values from canopy cover simulations. The advantage of this approach is that monthly LAI values can be determined for each quinary subcatchment, which are deemed more representative of actual growing conditions, instead of using "constant" values measured at Swayimane or Baynesfield to represent all growing regions.

From the literature, the following Beer-Lambert type equations were used to estimate canopy cover from LAI measurements:

$CC_{cotton} = \frac{1-e^{(-0.833 \cdot LAI)}}{1+e^{(-0.769 \cdot LAI)}}$	Garcìa-Vila et al. (2009)	Equation 44
$CC_{sorghum} = 1 - e^{(-0.416 \cdot LAI)}$	Araya et al. (2016)	Equation 45
$CC_{soybean} = 1 - e^{(-0.46 \cdot LAI)}$	Adeboye et al. (2017)	Equation 46
$CC_{soybean} = 1.005\left[1 - e^{(-0.6 \cdot LAI)}\right]^{1.2}$	Hsiao et al. (2009)	Equation 47

The latter equation was developed by combining data for maize (several treatments and years) and soybean data. The curve shown in Figure O.1 was obtained by regression, with slight adjustments at the extreme low and high ends of values. The above four equations were used to estimate canopy cover from LAI ranging from 0.5 to 1 m^2 m^{-2}, as shown in Table O.1. The equation used by Adeboye et al. (2017) for soybean consistently provides lower canopy cover values than those obtained by the equation of Hsiao et al. (2009), especially in the LAI range of 2.5-4.0 m^2 m^{-2}. When the equations were re-arranged, only that provided by Garcìa-Vila et al. (2009) for cotton did not produce exact LAI values from inputs of canopy cover. For example, the largest deviation of 3.8% was obtained for a canopy cover of 99.93%, which yielded a LAI of 9.62 instead of 10 m^2 m^{-2}.

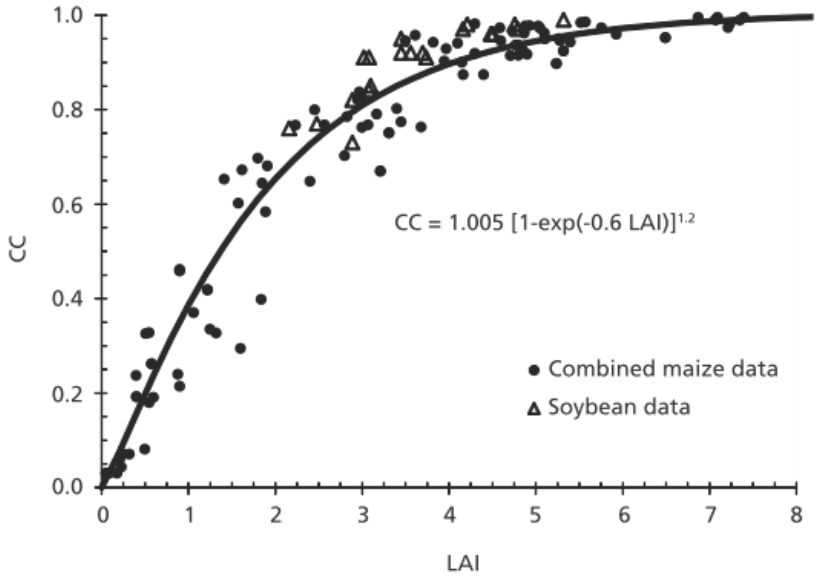

Figure O.1: Canopy cover in relation to Leaf Area Index derived from maize and soybean data (Hsiao et al., 2012)

Table O.1: Estimation of canopy cover fraction from LAI using various equations published in the literature

LAI	Araya et al. (2016)	Adeboye et al. (2017)	Hsiao et al. (2009)	Garcìa-Vila et al. (2009)
	Sorghum	Soybean	Soybean	Cotton
0.5	0.19	0.20	0.20	0.20
1.0	0.34	0.37	0.39	0.39
1.5	0.46	0.50	0.54	0.54
2.0	0.56	0.60	0.65	0.67
2.5	0.65	0.68	0.74	0.76
3.0	0.71	0.75	0.81	0.83
3.5	0.77	0.80	0.86	0.89
4.0	0.81	0.84	0.90	0.92
4.5	0.85	0.87	0.92	0.95
5.0	0.88	0.90	0.95	0.96
5.5	0.90	0.92	0.96	0.98
6.0	0.92	0.94	0.97	0.98
6.5	0.93	0.95	0.98	0.99
7.0	0.95	0.96	0.99	0.99
7.5	0.96	0.97	0.99	0.99
8.0	0.96	0.97	1.00	1.00
8.5	0.97	0.98	1.00	1.00
9.0	0.98	0.98	1.00	1.00
9.5	0.98	0.99	1.00	1.00